Aspects of E_6 Inspired Supersymmetric Models

Dylan Harries

Supervisors:
Prof. A. G. Williams
Dr. M. White

Department of Physics
School of Physical Sciences

THE UNIVERSITY
of ADELAIDE

Thesis submitted for the degree of
Doctor of Philosophy

May 2017

Contents

Abstract vii

Statement of Originality ix

Acknowledgements xi

List of Publications xiii

1 Introduction 1

2 The Minimal Supersymmetric Standard Model 9
- 2.1 Field Content and Interactions . . . 9
- 2.2 The Phenomenological MSSM . . . 13
- 2.3 The Constrained MSSM . . . 16
- 2.4 Electroweak Symmetry Breaking . . . 20
- 2.5 The Particle Spectrum of the MSSM . . . 25
  - 2.5.1 The MSSM Higgs Sector . . . 26
  - 2.5.2 The Neutralino and Chargino Sectors . . . 28
  - 2.5.3 The Sfermions . . . 30
- 2.6 Why Might the MSSM not be Enough? . . . 32

3 E_6 Inspired Supersymmetric Models 37
- 3.1 $U(1)$ Extensions of the MSSM . . . 37
- 3.2 The Exceptional Supersymmetric Standard Model . . . 42
- 3.3 Gauge Symmetry Breaking in the E_6SSM . . . 49
- 3.4 The Particle Spectrum of the E_6SSM . . . 52
  - 3.4.1 Exotic States . . . 54
  - 3.4.2 The E_6SSM Higgs Sector . . . 57
  - 3.4.3 The Neutralino Sector . . . 59

4 Extensions to Mass Spectrum Generators for BSM Models 63
4.1 Automated Tools for BSM Models: Benefits and Limitations 63
4.2 Semi-analytic RGE Solutions in General Models 67
4.2.1 SUSY Models 68
4.2.2 Non-SUSY Models 72
4.3 The Semi-analytic BVP Solver Algorithm 74
4.3.1 Review of the Two-scale Algorithm 75
4.3.2 Implementation of the Semi-analytic BVP Solver Algorithm . . 80
4.3.3 Tests and Comparisons of the BVP Solvers 84
4.4 Loop Induced Decays 90

5 Fine Tuning in the E_6SSM 99
5.1 A New Source of Fine Tuning 99
5.2 Measures of Fine Tuning 101
5.3 Calculating Fine Tuning in the E_6SSM 106
5.4 Naturalness Impact of Z' Limits in the E_6SSM 111
5.4.1 Stop Mass Fine Tuning 111
5.4.2 Fine Tuning at Low Energies 113
5.5 Benchmark Scenarios 117
5.6 Alternative E_6 Inspired Models 121
5.7 Conclusions 123

6 An E_6 Inspired Model with Exact Custodial Symmetry 127
6.1 An Alternative to the E_6SSM 127
6.2 The SE_6SSM and the CSE_6SSM 129
6.3 Gauge Symmetry Breaking in the SE_6SSM 134
6.4 Modifications to the Particle Spectrum 139
6.4.1 The Neutralino Sector 141
6.4.2 The Exotic Sector 143
6.4.3 The Higgs Sector 147

7 Dark Matter Scenarios in the CSE_6SSM 155
7.1 Dark Matter in BSM Models 155
7.1.1 Calculation of the Relic Density 156
7.1.2 Direct Detection of Dark Matter 158
7.2 Scanning the CSE_6SSM Parameter Space 160
7.3 Mixed Bino-Higgsino Dark Matter 166

7.4 Pure Higgsino Dark Matter . . . 173
7.5 Benchmark Scenarios . . . 177
7.6 Impact of Current and Future Searches . . . 181
7.7 Conclusions . . . 186

8 Summary **189**

A Review of SUSY Model Building **193**
A.1 The Super-Poincaré Algebra . . . 193
A.2 Superspace and Superfields . . . 196
A.3 Supersymmetric Lagrangians . . . 200

B Approximate RGE Solutions in the MSSM **205**

C Approximate RGE Solutions in the E_6SSM **209**

D SE_6SSM RGEs **235**
D.1 Gauge Couplings . . . 235
D.2 Superpotential Trilinear Couplings . . . 237
D.3 Superpotential Bilinear and Linear Couplings . . . 244
D.4 Gaugino Masses . . . 245
D.5 Soft-breaking Trilinear Scalar Couplings . . . 246
D.6 Soft-breaking Bilinear and Linear Couplings . . . 269
D.7 Soft Scalar Masses . . . 272

Bibliography **309**

Abstract

Supersymmetry (SUSY) is currently one of the best motivated extensions of the Standard Model (SM) of particle physics. Softly broken SUSY naturally stabilises the electroweak scale against large quantum corrections, without the unnatural fine tuning required in the SM. However, experimental searches for superpartners and the observed 125 GeV Higgs mass now imply that large corrections again arise in the minimal supersymmetric standard model (MSSM), reintroducing the need for fine tuning.

In this thesis, we study a class of non-minimal E_6 inspired SUSY models that are partially motivated by solving these and other problems of the MSSM. A unified E_6 gauge group at high energies is assumed to lead to a low-energy theory with one or more additional $U(1)$ gauge symmetries and extra matter content compared to the MSSM. To facilitate the study of these and other Beyond the Standard Model theories, we implement several extensions to existing automated tools, significantly improving their capabilities and range of applicability.

In the simplest E_6 inspired models, additional contributions to the Higgs mass reduce the need for large radiative corrections but introduce a new source of fine tuning associated with a massive Z' boson. By considering several such models at low energies, we show that experimental limits on the mass of this state imply a minimal amount of fine tuning is required to reproduce the electroweak scale. The severity of this fine tuning is also shown to depend strongly on the details of the gauge symmetry breaking.

We next consider an alternative E_6 model with a single, exact custodial symmetry. This custodial symmetry, combined with an automatically conserved matter parity, implies the existence of two dark matter candidates in the model. We explore the parameter spaces of constrained versions of this model and the MSSM in which one dark matter candidate is a MSSM-like mixed bino-Higgsino or pure Higgsino state. We find that the dark matter relic density may be reproduced while satisfying experimental constraints, and that light exotics may be discoverable at the Large Hadron Collider. We conclude by investigating the impacts of current and future direct detection searches on the parameter spaces of both models.

Statement of Originality

I certify that this work contains no material which has been accepted for the award of any other degree or diploma in my name, in any university or other tertiary institution and, to the best of my knowledge and belief, contains no material previously published or written by another person, except where due reference has been made in the text. In addition, I certify that no part of this work will, in the future, be used in a submission in my name, for any other degree or diploma in any university or other tertiary institution without the prior approval of the University of Adelaide and where applicable, any partner institution responsible for the joint-award of this degree.

I give consent to this copy of my thesis when deposited in the University Library, being made available for loan and photocopying, subject to the provisions of the Copyright Act 1968.

I also give permission for the digital version of my thesis to be made available on the web, via the University's digital research repository, the Library Search and also through web search engines, unless permission has been granted by the University to restrict access for a period of time.

I acknowledge the support I have received for my research through the provision of an Australian Government Research Training Program Scholarship

Signed _____ Date _____

Acknowledgements

This thesis would not have come about were it not for the many brilliant people who worked with and supported me. I would like to thank my supervisor Tony Williams, whose guidance and sage advice encompassed day-to-day questions about physics to all things academic, and more besides. Thanks also to my supervisor Martin White for his useful hints and ideas during my candidature. Special thanks are due to my collaborators, from whom I have learned a tremendous amount. To Peter Athron, for his keen insights and for allowing me to work on all sorts of interesting projects. To Roman Nevzorov, for his incredible knowledge and answers to all sorts of questions. Thank you both for your patience, kindness, and for countless enlightening and entertaining discussions. Further afield, thanks also to Alexander Voigt, for sharing his unsurpassed talents in coding and all kinds of awesome suggestions for improvements, new ideas and things to try.

I would also like to thank the staff and students of the CSSM and CoEPP for their help and support, and for the friendly environment in which to work. In particular, thanks to Alex Chambers, Taylor Haar, Filip Rajec, Michael Evans, Jake Forster and my office mates for the many shared laughs, and conversations ranging from the very helpful to the outright random.

During my candidature I was fortunate to be supported by the generosity of Peggy Barker through the Barker Tong Scholarship in Physics. I am very grateful for her support and encouragement, her interest in how our research progressed, and for reminding me to spend time out of the office as well as in it.

For this I can also thank my friends, for barbecues, book suggestions, and, occasionally, just for a much needed distraction.

Finally, thanks to my wonderful family, including my siblings Katie, Jordan and Emily, for always being there, even when I was not. Most especially, thank you to my parents Richard and Julia. Without their hard work and love I would not be where I am today.

List of Publications

The results of the research described in this thesis have appeared in the following publications, with the corresponding chapters also given:

- P. Athron, D. Harries, and A. G. Williams, Phys. Rev. **D91**, 115024 (2015), arXiv:1503.08929 [hep-ph] (Chapter 5)
- P. Athron, D. Harries, R. Nevzorov, and A. G. Williams, Phys. Lett. **B760**, 19 (2016), arXiv:1512.07040 [hep-ph] (Chapter 7)
- F. Staub, P. Athron, L. Basso, M. D. Goodsell, D. Harries, M. E. Krauss, K. Nickel, T. Opferkuch, L. Ubaldi, A. Vicente, and A. Voigt, Eur. Phys. J. **C76**, 516 (2016), arXiv:1602.05581 [hep-ph] (Chapter 4)
- P. Athron, D. Harries, R. Nevzorov, and A. G. Williams, JHEP **12**, 128 (2016), arXiv:1610.03374 [hep-ph] (Chapter 6 and Chapter 7)

Additionally, the work on a semi-analytic boundary value problem solver algorithm described in Chapter 4 forms one part of a major update to the public software package `FlexibleSUSY` (P. Athron, M. Bach, D. Harries, J.-h. Park, D. Stöckinger, A. Voigt, and J. Ziebell, in preparation).

Within the chapters presenting original work carried out during this thesis, the discussion naturally focusses on those parts of the research that I carried out. In particular, in Chapter 4 the generalisation of the semi-analytic boundary value problem solver to generic models and its implementation in `FlexibleSUSY`, along with the implementation of a fixed point root finding algorithm and the implementation of loop induced decays, is my own work. Although together with my co-authors I was also involved in the model validation and the documentation of the additional extensions to `FlexibleSUSY` described in the above publications, detailed discussions of these aspects of the work are omitted. Similarly, the numerical results presented in Chapters 5 and 7 are my own work.

Chapter 1

Introduction

In recent decades, extraordinary progress has been made in understanding the nature of the fundamental constituents of matter and their interactions. The theoretical framework that has been assembled, known as the Standard Model (SM) of particle physics [1–7], is a phenomenally successful description of the properties of matter at the energy scales probed so far. The SM is a four-dimensional renormalisable quantum field theory (QFT), in which the allowed interactions are determined by requiring that the model respects a certain set of symmetries. The continuous symmetries of the SM include invariance under spacetime transformations belonging to the Poincaré group and, separately, invariance under the action of local gauge transformations[1] belonging to the group

$$G_{SM} = SU(3)_C \times SU(2)_L \times U(1)_Y \,. \tag{1.1}$$

The gauge symmetries of the SM collectively describe all but one of the known interactions between elementary particles. In Eq. (1.1), invariance under $SU(3)_C$ describes the strong interactions, mediated by the gauge fields known as gluons. The corresponding gauge theory is referred to as quantum chromodynamics (QCD). The $SU(2)_L \times U(1)_Y$ symmetry unifies the electromagnetic and weak interactions into a single electroweak (EW) force, with the corresponding gauge bosons eventually giving rise to the photon and the Z and $W^{\pm}$ bosons.

The matter fields of the SM are not uniquely specified by this collection of symmetries. Empirically it is known [8–19] that these must include three generations of spin-1/2 charged leptons and neutrinos, and three generations of spin-1/2 up- and down-type quarks. All of these states interact via the electroweak interactions, but

[1] Hence, the SM is an example of a gauge theory.

only the quarks are strongly interacting. In the SM, these fermion fields are accompanied by one additional spin-0 particle, the Higgs boson. This state arises from an $SU(2)_L$ doublet of elementary scalar fields that is responsible for the breakdown of electroweak symmetry, $SU(2)_L \times U(1)_Y$, to the familiar electromagnetic interactions described by an Abelian $U(1)_{\rm em}$ gauge symmetry. Electroweak symmetry breaking (EWSB) occurs in the SM through the Higgs mechanism [20–25], in which a component of the Higgs doublet develops a non-zero vacuum expectation value (VEV) in the vacuum state. In this process non-zero masses for the Z and $W^{\pm}$ gauge bosons are generated, along with those for the SM fermions through Yukawa interactions with the Higgs field. Following the recent discovery of a new particle [26, 27] with a mass of $m_h^{\rm exp.} = 125.09 \pm 0.21 \pm 0.11$ GeV [28] and properties consistent with a SM Higgs [29–31] the existence of all of the constituents of the SM has now been established.

The prediction of the Higgs is just one of the many successes of the SM. The model is in excellent agreement with almost all available experimental results. Yet the SM as it currently stands must be incomplete. To start with, the observation of neutrino oscillations [32–51] implies that neutrinos must have small but non-zero masses [52–54]. Neutrinos are massless in the SM, however, and so the model must be modified to allow for massive neutrinos. Moreover, a satisfactory Beyond the Standard Model (BSM) theory should provide some explanation as to why the observed neutrino masses are so small. For instance, the SM can be extended with a set of massive right-handed neutrinos, which do not participate in gauge interactions, to generate small neutrino masses via a see-saw mechanism [55–59]. At least in this case, the incorrect prediction of the SM can be fixed with a relatively minor extension of the model.

Beyond this, though, there are also aspects of Nature about which the SM simply makes no predictions or provides no explanation for. The most obvious is the omission of gravity; the development of a consistent quantum theory of gravity is still an active area of research. In parallel with this, our classical understanding of gravity when applied to astrophysical observations, such as measurements of the rotation curves of galaxies [60–65] and gravitational lensing studies [66], indicates that much of the mass of the Universe must be in the form of non-luminous, non-baryonic matter, appropriately called dark matter (DM). The standard model of cosmology, known as "Λ Cold Dark Matter" or ΛCDM, provides a good fit to observations such as satellite measurements [67–70] of the cosmic microwave background (CMB) if DM presently accounts for approximately 26% [70] of the total mass-energy density of the Universe. By comparison, in this model ordinary baryonic matter amounts to only $\sim 5\%$, with the remainder corresponding to unknown dark energy. Currently, one of the favoured

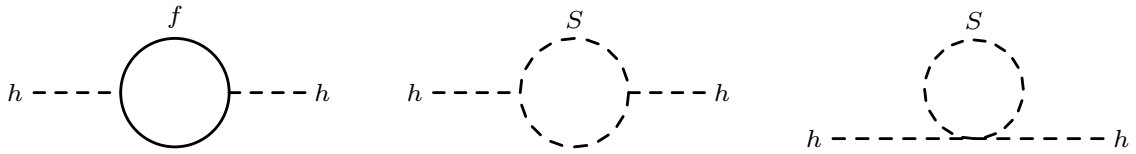

Figure 1.1: Examples of generic diagrams involving a fermion (left-most diagram) or scalar loop that contribute to the Higgs self-energy. Here h denotes the SM Higgs, while f and S denote general fermion or scalar fields, respectively.

explanations for DM is that it is composed of a new particle that does not interact electromagnetically, referred to as a weakly interacting massive particle (WIMP). The SM contains no viable WIMP candidate (for reviews of various DM candidates see, e.g., Refs. [71, 72]); thus, if DM is made up of a new particle or particles[2] then the SM encompasses only a very small fraction of the Universe indeed. A BSM theory is required to describe the rest.

One of the next areas in which further shortcomings of the SM might be revealed is in the Higgs sector responsible for EWSB. In the wake of the Higgs discovery, an important experimental task is to determine if the mechanism of EWSB is consistent with that predicted in the SM. Experimentally, this aspect of the SM is the least tested. Theoretically, it is one of the most puzzling. The conceptual problems associated with having a fundamental scalar in the theory have been known since shortly after the Higgs mechanism was proposed [77–81]. Unlike mass terms for fermions, which are protected by chiral symmetry[3], a scalar mass parameter receives quadratically divergent loop corrections from diagrams such as those shown in Figure 1.1. Upon introducing a naïve cutoff Λ_{NP} that is of the order of the scale at which any new BSM physics appears to regulate the loop integrals in Figure 1.1, the leading correction to the Higgs mass parameter m_H^2 is found to be proportional to Λ_{NP}^2. Since the SM must at least be extended to include gravity, Λ_{NP} may be of the order of the Planck scale, $M_{Pl} \sim 10^{18}$ GeV, at which gravitational interactions are expected to be relevant. The resulting value for the Higgs mass should then also be of the order of the Planck scale. Since m_H^2 sets the size of the Higgs VEV and hence also the physical gauge boson

[2]An alternative to postulating a particle physics origin for DM is to suppose that it has macroscopic astrophysical origins, such as being composed of the class of objects collectively known as massive compact halo objects (MACHOs), or that the laws of gravity are modified [73], as in modified Newtonian dynamics (MOND) [74]; however, it is for example challenging to explain cosmological data [75] with these solutions, and many scenarios can be tightly constrained [76].

[3]Chiral symmetry in a relativistic field theory, in which each fermion is accompanied by its antiparticle, implies that the radiative corrections to a fermion mass m_f are proportional to m_f, so that when $m_f \to 0$ chiral symmetry is restored at all orders in perturbation theory, see, e.g., Ref. [82]. Fermion mass terms are therefore "technically natural", in the sense of Ref. [81].

masses M_Z and M_W, this implies that these should also be similarly large. The fact that they are not implies that the bare mass parameter, $m^2_{H_0}$, must be very carefully fine tuned to cancel this correction to obtain $M_Z \sim 91$ GeV.

For the sake of illustration, Λ_{NP} has been introduced as a cutoff scale, which can be removed when the theory is renormalised. However, the problem remains that any new, heavy degrees of freedom in the model that couple directly or indirectly to the Higgs will generate substantial corrections to the Higgs mass. For example, the fact that the SM gauge couplings nearly unify at a scale $M_{GUT} \sim 10^{16}$ GeV may indicate that at this scale the SM can be embedded in a Grand Unified Theory (GUT) [83], in which a single unified gauge group G is broken near M_{GUT} down to G_{SM}. In this case, the heavy states associated with the breaking of G with masses that are $M_G \sim O(M_{GUT})$ should generate corrections to the Higgs mass that are proportional to $M_G^2 \gg M_Z^2$ [84]. The essential problem is that the Higgs mass is (quadratically) sensitive to the highest mass scale in the theory, and it appears that m_H should naturally be of the order of that scale. In the SM it is very difficult to maintain the observed hierarchy between the EW scale, characterised by M_Z for example, and any higher energy scales without resorting to extreme fine tuning. This is known as the hierarchy problem; resolving it without invoking unnatural cancellations is a key motivation for many BSM physics models.

One elegant possibility for stabilising the EW scale against corrections from heavy states is to consider BSM theories that possess a new spacetime symmetry known as supersymmetry (SUSY) [85–87]. According to the Haag-Łopuszánski-Sohnius (HLS) theorem [88], SUSY is the most general extension of the Poincaré group, which is otherwise forbidden from being non-trivially combined with the internal symmetries, e.g., G_{SM}, by the Coleman-Mandula (CM) theorem [89]. Amazingly, this extension of the spacetime symmetry of the theory also has the effect of protecting the EW scale from quadratic divergences. The diagrams shown in Figure 1.1 are each individually quadratically divergent, but the fermion and scalar diagrams contribute with opposite signs and can cancel provided appropriate relations exist between the relevant coupling constants. It is a consequence of SUSY that the number of fermionic and bosonic degrees of freedom in a SUSY invariant model must be equal. Therefore in a supersymmetric model, each fermion loop diagram such as that in Figure 1.1 is accompanied by the scalar loop diagrams, and vice versa. In fact, SUSY can do better than simply ensuring these diagrams are present so that some cancellation can occur. Exact SUSY automatically implies relations among the coupling constants of the theory such that the resulting correction to the Higgs mass completely vanishes [90–94].

Thus unbroken SUSY naturally solves the hierarchy problem without any fine tuning. Naturalness is therefore a major motivation for considering SUSY models.

Unfortunately, unbroken SUSY would also require that the fermions and their boson partners are degenerate in mass, but no such superpartners have been observed [95]. SUSY, if realised in Nature, must be a broken symmetry. A natural solution to the hierarchy problem can still be achieved provided that SUSY is only softly broken [96], i.e., broken only by operators in the Lagrangian with couplings having positive mass dimension. In this case, the worst quadratic divergences are still cancelled, leaving only much milder logarithmic divergences that are proportional to the splitting between the fermion and boson masses. Provided that this splitting is not too large, the EW scale remains low without substantial fine tuning. Phenomenologically viable models of SUSY are constructed from a set of SUSY preserving interactions, supplemented by some set of soft SUSY breaking interactions as required by experiment. The introduction of new fields and interactions also has many interesting consequences for some of the other problems of the SM; for example, many SUSY models are found to contain promising DM candidates.

In Chapter 2, we review the simplest such model, known as the minimal supersymmetric standard model (MSSM). While the MSSM successfully addresses the SM hierarchy problem, in light of the Higgs discovery and unsuccessful searches for superpartners the simplest versions of the MSSM also appear to suffer from a fine tuning problem known as the little hierarchy problem. This, along with some of the other shortcomings of the MSSM, is described in Section 2.6. Although the MSSM is the simplest viable model of low-energy SUSY, it is also possible to consider other non-minimal models, some of which have compelling motivations. In this thesis, we focus on one such class of models based on an underlying E_6 GUT group at high energies that lead to extensions of the MSSM with an additional $U(1)'$ symmetry. These E_6 inspired models can emerge naturally from theories of gravity based on superstring theory, and contain exotic matter that can potentially lead to spectacular signals at experimental facilities such as the Large Hadron Collider (LHC).

The low-energy properties of E_6 inspired models are reviewed in Chapter 3, with a focus on the specific example known as the exceptional supersymmetric standard model ($\mathrm{E_6SSM}$). In this chapter we describe how these models more easily accommodate a 125 GeV Higgs and so are able to solve the little hierarchy problem as well as other issues in the SM and MSSM, providing additional good reasons to study this type of model. In particular, the $\mathrm{E_6SSM}$ is also able to account for non-zero neutrino masses, as well as explain the observed asymmetry between matter and anti-

matter. The details of EWSB in the E_6SSM and the resulting particle spectrum are then summarised. We highlight the potential for a new source of fine tuning in the E_6SSM, associated with the presence of a heavy Z' boson, whose mass contributes to the prediction for the EW scale at tree-level.

One of the main challenges in studying non-minimal SUSY models such as the E_6SSM, and many other new BSM models for that matter, is in handling the many new states and interactions that may be introduced. Carrying out calculations at the level of precision needed to draw reliable conclusions is difficult. It is not uncommon, for example, for simplifying assumptions to be made to avoid having to implement a full numerical calculation by hand, which is a time consuming and error prone process even when only considering the lowest order in perturbation theory. However, these simplified calculations also risk missing important features of a model. Recently, new tools have become available that automate the process of performing fully general numerical calculations at one- and two-loop order. Before proceeding to study E_6 models in details, in Chapter 4 we describe work undertaken to extend one of these tools, a "spectrum generator generator" called `FlexibleSUSY`, to handle these and similar models. The work presented in this chapter forms one part of a large set of improvements to `FlexibleSUSY` that are to be publicly released as `FlexibleSUSY`-2.0 [97]. The implementation in `FlexibleSUSY` of a calculation of loop-induced diphoton and digluon decays in general BSM models [98], and its validation in a large number of models, is also described.

In Chapter 5, we report the results of applying some of these numerical tools to study the problem of fine tuning in the E_6SSM at low energies [99]. We show in this chapter that the usual sources of fine tuning responsible for the little hierarchy problem depend strongly on assumptions made about the model at high energies. The fine tuning associated with the Z' mass, on the other hand, is a tree-level effect that is unaffected by these assumptions. By defining both the MSSM and the E_6SSM at low energies, we minimise the model dependent contributions to fine tuning and demonstrate that experimental searches for the Z' can be used to set a conservative lower bound on the degree of fine tuning in these E_6 inspired models. The severity of this bound is set by the specific $U(1)'$ that is present at low energies. We also show that the competing effects of the reduced Higgs mass fine tuning and the new Z' contribution mean that exactly which model, out of the MSSM and the E_6SSM, is more fine tuned depends on high-scale assumptions. In the E_6SSM, where the limits on the Z' mass are by now quite high, the minimal fine tuning at low energies is already

quite significant, which poses a problem for naturalness in the simplest variants of this model.

The E_6SSM is notable for the particular $U(1)'$ symmetry that results at low energies, allowing to explain the neutrino masses and baryogenesis, and for its relative simplicity. Alternative E_6 inspired models with the same choice of $U(1)'$ can also be constructed in the context of orbifold GUT models. In Chapter 6, we review the construction of one such model, which we refer to as the singlet-extended E_6SSM (SE_6SSM). This model, in addition to retaining the successful features of the E_6SSM, has several attractive features, one of which includes suppressing the terms responsible for large fine tunings in the E_6SSM. A novel consequence of the construction of the model is that the SE_6SSM contains multiple possible DM candidates. We discuss some of its advantages before explaining the expected particle spectrum in a constrained version of the model at tree-level and its possible collider signatures.

In Chapter 7, we investigate in detail how the constrained SE_6SSM can address the major open question of DM [100, 101]. Using our improvements to `FlexibleSUSY`, in combination with other numerical tools, we study the regions of parameter space compatible with a 125 GeV SM-like Higgs and other constraints. The DM candidates in the model are studied and directly compared with analogous states in the constrained version of the MSSM. We find that, while DM can be explained in both models, results from direct detection experiments already impose rather stringent constraints. The so-called "well-tempered" neutralino scenario, in which the DM candidate is a mixture of the superpartners of the $U(1)_Y$ gauge boson and the neutral Higgs bosons, is found to already be excluded by the current limits. A heavier DM candidate, with a mass of ~ 1 TeV and composed purely of the neutral Higgs superpartners, can still explain the DM relic abundance despite the direct detection constraints. However, the next generation of experiments will also be able to explore a large portion of this part of the parameter space. The extended Higgs and exotic sectors of the SE_6SSM mean that this model has some interesting features compared to the MSSM. We find that, when other comparable parameters are matched between the two models, a lighter DM candidate can be viable in the SE_6SSM due to resonant annihilations with a pseudoscalar Higgs boson. These scenarios would evade direct detection searches but can be tested at the LHC. In general, direct detection searches stand posed to probe much heavier SUSY mass spectra, and null results from these experiments would push constrained MSSM and SE_6SSM into regions of their respective parameter spaces that are almost inaccessible at the LHC. However, we show that the exotic states in the SE_6SSM can

still be within reach, preserving a potentially distinctive discovery channel for this model.

Finally, in Chapter 8, we conclude by summarising our results and discussing the outlook for the E_6 inspired models discussed in the preceding chapters.

Chapter 2

The Minimal Supersymmetric Standard Model

2.1 Field Content and Interactions

The ordinary SM is not compatible with low-energy $N = 1$ SUSY. This can be seen, for example, by noting that SUSY would commute with the internal symmetries of the SM, and thus the components of each supermultiplet must have the same $SU(3)_C \times SU(2)_L \times U(1)_Y$ quantum numbers. However, the SM contains no colour octet fermion that could play the role of the superpartner of the gluon, and the same is true for the other gauge bosons as well. Similarly, attempts to construct supermultiplets by grouping existing SM states, such as might be formed from the left-handed leptons and Higgs scalars [102], are not phenomenologically viable [103]. Therefore acceptable SUSY models must extend the field content of the SM with new superpartners for all of the known SM fields, at least. The minimal such extension of the SM is achieved by promoting the matter fields of the SM to chiral superfields. Anomaly cancellation requires that the single $SU(2)_L$ doublet Higgs of the SM should be replaced by two chiral superfields $\hat{H}_u$ and $\hat{H}_d$ with opposite $U(1)_Y$ hypercharges [103]. Similarly, for each of the gauge fields a vector superfield is introduced. The resulting model [91, 92] is known as the MSSM[1]. The chiral and vector superfields of the MSSM are summarised in Table 2.1 and Table 2.2, respectively.

With the field content of the SM extended in this fashion, the required Yukawa and gauge interactions arise in the MSSM from the supersymmetric interactions of the chiral and vector superfields. A minimal superpotential for the MSSM, which retains

[1]Extensive reviews of the MSSM may be found in Refs. [103–105].

Supermultiplet	Spin-0	Spin-1/2	$SU(3)_C$	$SU(2)_L$	$\sqrt{\frac{5}{3}}Q_Y$	Z_2^M
$\hat{Q}_i$	$\begin{pmatrix}\tilde{u}_L \\ \tilde{d}_L\end{pmatrix}_i$	$\begin{pmatrix}u_L \\ d_L\end{pmatrix}_i$	**3**	**2**	$\frac{1}{6}$	$-$
$\hat{u}_i^c$	$\tilde{u}_{iR}^*$	u_{iR}^c	**3**	**1**	$-\frac{2}{3}$	$-$
$\hat{d}_i^c$	$\tilde{d}_{iR}^*$	d_{iR}^c	**3**	**1**	$\frac{1}{3}$	$-$
$\hat{L}_i$	$\begin{pmatrix}\tilde{\nu}_L \\ \tilde{e}_L\end{pmatrix}_i$	$\begin{pmatrix}\nu_L \\ e_L\end{pmatrix}_i$	**1**	**2**	$-\frac{1}{2}$	$-$
$\hat{e}_i^c$	$\tilde{e}_{iR}^*$	e_{iR}^c	**1**	**1**	1	$-$
$\hat{H}_d$	$\begin{pmatrix}H_d^0 \\ H_d^-\end{pmatrix}$	$\begin{pmatrix}\tilde{H}_d^0 \\ \tilde{H}_d^-\end{pmatrix}$	**1**	**2**	$-\frac{1}{2}$	$+$
$\hat{H}_u$	$\begin{pmatrix}H_u^+ \\ H_u^0\end{pmatrix}$	$\begin{pmatrix}\tilde{H}_u^+ \\ \tilde{H}_u^0\end{pmatrix}$	**1**	**2**	$\frac{1}{2}$	$+$

Table 2.1: Summary of the chiral superfields of the MSSM, showing their representations under $SU(3)_C$ and $SU(2)_L$ and their $U(1)_Y$ charges. The transformation property of each under the discrete symmetry Z_2^M, defined in the text, is also shown. Here and throughout this thesis, Roman indices $i, j, \ldots = 1, 2, 3$, while Greek indices $\alpha, \beta, \ldots = 1, 2$.

the usual set of SM Yukawa couplings and is phenomenologically viable, reads

$$\hat{W}_{\rm MSSM} = y_{ij}^U \hat{u}_i^c \hat{H}_u \cdot \hat{Q}_j + y_{ij}^D \hat{d}_i^c \hat{Q}_j \cdot \hat{H}_d + y_{ij}^E \hat{e}_i^c \hat{L}_j \cdot \hat{H}_d + \mu \hat{H}_d \cdot \hat{H}_u \,. \tag{2.1}$$

Here and below we denote superfields with hats, and adopt the convention $\hat{A} \cdot \hat{B} \equiv \epsilon_{\alpha\beta} \hat{A}^\alpha \hat{B}^\beta = \hat{A}^2 \hat{B}^1 - \hat{A}^1 \hat{B}^2$ for the $SU(2)$ dot product. Of the terms in Eq. (2.1), the first three lead to the SM Yukawa interactions between the SM fermions and Higgs scalars, as well as corresponding trilinear and quartic interactions involving the superpartners of these states. Note that the requirement that the superpotential is a holomorphic function of the chiral superfields[2] implies that $\hat{H}_u$ may not have Yukawa interactions with both the up-type quarks and down-type quarks and leptons; this is an additional reason for why the MSSM must contain two Higgs doublets. Moreover, the neutral components of both Higgs scalar doublets must develop VEVs to generate masses for all of the SM fermions[3]. The last term in Eq. (2.1), generally referred to as the μ-term, furnishes a supersymmetric mass term for the superpartners of the Higgs

[2] A brief review of this and similar restrictions in supersymmetric model building is given in Appendix A; further details can be found in, e.g., Ref. [84].

[3] Assuming that the masses are generated at tree-level, which is not necessarily the case [106, 107].

Supermultiplet	Spin-1/2	Spin-1	$SU(3)_C$	$SU(2)_L$	$\sqrt{\frac{5}{3}}Q_Y$	Z_2^M
$\hat{G}$	$\tilde{g}$	g	**8**	**1**	0	+
$\hat{W}$	$\tilde{W}^{\pm}$, $\tilde{W}^0$	$W^{\pm}$, W^0	**1**	**3**	0	+
$\hat{B}$	$\tilde{B}$	B	**1**	**1**	0	+

Table 2.2: Summary of the vector superfields of the MSSM and their transformation properties under the gauge symmetries and Z_2^M.

scalars, the Higgsinos. A non-zero value of μ is required for successful EWSB and to avoid unacceptable axions in the particle spectrum [108].

The superpotential Eq. (2.1) is not the most general allowed by gauge and SUSY invariance. Unlike in the SM, additional terms may be written down that are consistent with all of the gauge symmetries but that violate conservation of baryon number, B, or lepton number, L. These read [109, 110]

$$\hat{W}_{\text{MSSM}}^{\not{R}} = -\epsilon_i \hat{L}_i \cdot \hat{H}_u + \frac{1}{2}\rho_{ijk}\hat{L}_i \cdot \hat{L}_j \hat{e}_k^c + \rho'_{ijk}\hat{L}_i \cdot \hat{Q}_j \hat{d}_k^c + \frac{1}{2}\rho''_{ijk}\hat{u}_i^c \hat{d}_j^c \hat{d}_k^c \,. \tag{2.2}$$

Simultaneous non-negligible values for the couplings ρ'_{ijk} and ρ''_{ijk} would result in a proton lifetime far shorter than current experimental limits [111] due to new squark[4] mediated decays [112, 113]. It is therefore common to forbid all of these dangerous terms by imposing an exact discrete Z_2 matter parity [91, 114–116], Z_2^M, defined by

$$Z_2^M = (-1)^{3(B-L)} \,. \tag{2.3}$$

This may alternatively be expressed at the level of the component fields in terms of invariance under R–parity [117], where the R–parity of a field Φ is given by

$$R_\Phi = (-1)^{3(B-L)+2s} \,, \tag{2.4}$$

where s is the spin of the component field Φ. All of the terms in Eq. (2.2) that would lead to rapid proton decay are then forbidden by the assumed matter- or R–parity invariance. In the R–parity conserving MSSM, to which we restrict ourselves in this thesis, the allowed terms are therefore simply those given in Eq. (2.1). It should be kept in mind, however, that R–parity conservation is an additional assumption imposed

[4]The names of the superpartners of the SM fermions follow from prepending an "s" to the name of the corresponding SM state; hence the scalar partners of quarks are squarks, those of leptons are sleptons, and so on. The superpartners of the SM scalar and vector bosons are named by adding the suffix "-ino", leading to gauginos and Higgsinos.

on the MSSM. R–parity violating models, in which the problematic combinations of couplings are suppressed by other means, may also be considered [118–124].

The presence of a discrete Z_2 symmetry has important consequences for the phenomenology of the model. By construction, the R–parity odd states in the MSSM correspond to the as-yet unobserved superpartners of the SM particles. Invariance of the Lagrangian under R–parity implies that these R–parity odd states would be pair produced at colliders, and that an R–parity odd state must decay into an odd number of R–parity odd states. In particular, this means that the lightest R–parity odd state must be absolutely stable. If this state, called the lightest supersymmetric particle (LSP), is also electrically neutral, then it would be a very attractive candidate for DM [125]. Under the assumption of a standard thermal history of the Universe, a weakly interacting, stable LSP would be expected to have been in thermal equilibrium with the SM states in the early Universe. Due to its stability, a sufficient number should then remain at present times to account for the observed relic abundance of DM provided that the LSP mass is less than a few hundred TeV [126]. Thus R–parity has the benefit of providing a natural DM candidate in the MSSM, as well as preventing rapid proton decay.

The details of the particle spectrum in the MSSM, including the identity of the LSP, depend on the parameters appearing in Eq. (2.1) and on the interactions responsible for the soft breaking of SUSY. From a theoretical point of view, it is preferable to have a model that can explain the origin of the latter set of interactions. This can be done by assuming that SUSY is an exact symmetry of the theory that is broken spontaneously in the vacuum state, thereby generating the necessary soft SUSY breaking parameters. Mass sum rules [127] relating the masses of all particles within a supermultiplet imply [91] that spontaneous breaking of SUSY cannot be achieved solely with the superfields of the MSSM without contravening experimental limits. Therefore models of spontaneous SUSY breaking (SSB) introduce additional superfields that are singlets under the SM gauge group and so form a hidden sector. The spontaneous breaking of SUSY in this sector at some scale is then transmitted to the visible sector, consisting of the MSSM superfields, via shared interactions or an additional messenger sector. The form of the resulting soft SUSY breaking Lagrangian is dependent on the particular model of SSB that is constructed in this way. Apart from this, the interactions of the hidden sector with the visible sector are assumed to be suppressed so that the low-energy phenomenology, below the SSB scale, does not depend on the hidden sector states. Many models of SSB have been proposed in the literature, which differ in the nature of the hidden sector and messenger interactions.

Common examples include gravity mediated [128–134], gauge mediated [135–140], and anomaly mediated [141–146] SUSY breaking.

However, for the purposes of studying the low-energy phenomenology of the MSSM, it is often more convenient to simply introduce a generic set of interactions that break SUSY explicitly rather than choose a particular SUSY breaking mechanism at high energies. The couplings associated with these interactions must have positive mass dimension so as to break SUSY softly. Including only the standard set [96] of possible soft terms allowed by gauge invariance, the soft SUSY breaking Lagrangian for the MSSM in this approach is given by

$$\begin{aligned}
-\mathcal{L}^{\text{soft}}_{\text{MSSM}} = {} & m^2_{Q_{ij}}\tilde{Q}^\dagger_i\tilde{Q}_j + m^2_{u^c_{ij}}(\tilde{u}^c_i)^\dagger\tilde{u}^c_j + m^2_{d^c_{ij}}(\tilde{d}^c_i)^\dagger\tilde{d}^c_j + m^2_{L_{ij}}\tilde{L}^\dagger_i\tilde{L}_j + m^2_{e^c_{ij}}(\tilde{e}^c_i)^\dagger\tilde{e}^c_j \\
& + m^2_{H_u}|H_u|^2 + m^2_{H_d}|H_d|^2 + (B\mu H_d\cdot H_u + h.c.) \\
& + \left(T^U_{ij}\tilde{u}^c_i H_u\cdot\tilde{Q}_j + T^D_{ij}\tilde{d}^c_i\tilde{Q}_j\cdot H_d + T^E_{ij}\tilde{e}^c_i\tilde{L}\cdot H_d + h.c.\right) \\
& + \frac{1}{2}\left(M_1\tilde{B}\tilde{B} + M_2\tilde{W}\tilde{W} + M_3\tilde{G}\tilde{G} + h.c.\right). \qquad (2.5)
\end{aligned}$$

In this expression, the last line contains soft breaking masses for the superpartners of the gauge fields, the gauginos, and the second-to-last line contains trilinear scalar interactions corresponding to the allowed trilinear superpotential interactions in Eq. (2.1). Similarly, $B\mu$ is a soft SUSY breaking bilinear corresponding to the supersymmetric μ term. The remaining parameters in Eq. (2.5) are soft squared-masses for the Higgs scalars and the scalar partners of the SM fermions, the sfermions.

2.2 The Phenomenological MSSM

With appropriate choices for the parameters appearing in Eq. (2.5), the masses of the superpartners can be raised as required by experimental bounds, allowing, in principle, for phenomenologically viable MSSM scenarios to be constructed. Unfortunately, the MSSM with the general soft SUSY breaking interactions in Eq. (2.5) is described by 124 independent parameters [147]. This obviously makes detailed studies of the full parameter space infeasible. The number of free parameters can be substantially reduced, while still remaining agnostic about the mechanism of SSB, by assuming certain restrictions on the parameters that follow from experimental constraints. For example, one set of possible assumptions may be that

- There should be no new sources of CP-violation. Additional sources of CP-violation, beyond that in the SM quark sector, are tightly constrained by mea-

surements of electric dipole moments [148–151] and quark flavour changing processes [152]. The simplest way to be consistent with these limits is to require that all new phases in the MSSM vanish.

- There should be no flavour-changing neutral currents (FCNCs). FCNCs are expected to be highly suppressed in the SM through the GIM mechanism [153], and this is borne out by the current experimental bounds [95, 154]. Flavour off-diagonal elements appearing in the soft breaking Lagrangian of the MSSM would be expected to produce FCNCs in violation of these limits. To prevent this, the model can be required to satisfy the principle of minimal flavour violation (MFV) [155], in which flavour violation is determined only by the structure of the SM Yukawa couplings. This can be achieved by taking all soft scalar masses and trilinears to be flavour diagonal.

- The first and second generation sfermions should be degenerate. The mass splittings of the first and second generation squarks are similarly constrained by limits from flavour physics [156]. These limits can be satisfied by taking the scalar masses for the first and second generation sfermions to be the same. A similar assumption can be made for the soft breaking trilinears.

Taken together, the above assumptions lead to the framework that has become known as the phenomenological MSSM (pMSSM) [157, 158]. The pMSSM is characterised by $O(20)$ free parameters in addition to those of the SM, and therefore is significantly easier to study than the general MSSM.

The exact final number of parameters depends on how the assumptions are imposed. Typically, the first and second generation trilinears are taken to be proportional to the corresponding Yukawa couplings. As a result of the smallness of these couplings, the first and second generation trilinears are usually unimportant for phenomenological calculations, so that they may be set to zero. This leaves only the third generation trilinears T^U_{33}, T^D_{33} and T^E_{33} non-zero, which read

$$T^U_{33} = y^U_{33} A^U_{33} \equiv y_t A_t \,, \quad T^D_{33} = y^D_{33} A^D_{33} \equiv y_b A_b \,, \quad T^E_{33} = y^E_{33} A^E_{33} \equiv y_\tau A_\tau \,, \tag{2.6}$$

where we have introduced the parameters $A^f_{ij} = T^f_{ij}/y^f_{ij}$ for $f = U, D, E$. For convenience when discussing only the third generation, we use the shorter notation $y_t = y^U_{33}$, $y_b = y^D_{33}$ and $y_\tau = y^E_{33}$ to denote the top, bottom and tau Yukawa couplings. Requiring that the soft scalar squared-masses are flavour diagonal with degenerate first and

second generation entries leads to real squark soft breaking squared-masses of the form

$$m_Q^2 = \begin{pmatrix} M_{\tilde{q}_L}^2 & 0 & 0 \\ 0 & M_{\tilde{q}_L}^2 & 0 \\ 0 & 0 & m_{Q_3}^2 \end{pmatrix}, \quad m_{u^c}^2 = \begin{pmatrix} M_{\tilde{u}_R}^2 & 0 & 0 \\ 0 & M_{\tilde{u}_R}^2 & 0 \\ 0 & 0 & m_{u_3^c}^2 \end{pmatrix}, \\ m_{d^c}^2 = \begin{pmatrix} M_{\tilde{d}_R}^2 & 0 & 0 \\ 0 & M_{\tilde{d}_R}^2 & 0 \\ 0 & 0 & m_{d_3^c}^2 \end{pmatrix}, \tag{2.7}$$

and similarly for the slepton soft squared-masses,

$$m_L^2 = \begin{pmatrix} M_{\tilde{L}_L}^2 & 0 & 0 \\ 0 & M_{\tilde{L}_L}^2 & 0 \\ 0 & 0 & m_{L_3}^2 \end{pmatrix}, \quad m_{e^c}^2 = \begin{pmatrix} M_{\tilde{e}_R}^2 & 0 & 0 \\ 0 & M_{\tilde{e}_R}^2 & 0 \\ 0 & 0 & m_{e_3^c}^2 \end{pmatrix}. \tag{2.8}$$

The gaugino masses M_1, M_2 and M_3 remain unconstrained. Of the parameters μ, $m_{H_d}^2$, $m_{H_u}^2$ and $B\mu$, two can be fixed in terms of the other parameters by requiring that correct EWSB occurs, as will be discussed in Section 2.4. Taking these to be $m_{H_d}^2$ and $m_{H_u}^2$, μ and $B\mu$ remain free. Note that, in addition to the Lagrangian parameters, it is also necessary to specify the two VEVs of the neutral Higgs scalar fields. Since the magnitude of these VEVs may be fixed in terms of the known gauge boson masses, only the ratio $\tan\beta$ of the two VEVs need be specified. Thus, for our purposes the pMSSM is characterised by 19 real parameters beyond the SM parameters, namely the gaugino masses M_1, M_2, M_3, the trilinears A_f, $f = t, b, \tau$, the soft squared-masses $M_{\tilde{q}_L}^2$, $m_{Q_3}^2$, $M_{\tilde{u}_R}^2$, $m_{u_3^c}^2$, $M_{\tilde{d}_R}^2$, $m_{d_3^c}^2$, $M_{\tilde{L}_L}^2$, $m_{L_3}^2$, $M_{\tilde{e}_R}^2$, $m_{e_3^c}^2$, and the Higgs sector parameters μ, $B\mu$ and $\tan\beta$. The significantly reduced size of the pMSSM parameter space is certainly much more amenable to detailed studies, though complete explorations of it are still non-trivial exercises and require numerical methods with various levels of sophistication (see, e.g., Refs. [159–161]). When only particular sectors of the MSSM are of interest, more parameters can be eliminated or ignored on the basis that they have only minor impacts on the relevant observables. An example of such a case is the so-called "pMSSM-7" [162], in which only those parameters relevant to the Higgs sector are varied while the remaining parameters take fixed values.

2.3 The Constrained MSSM

The pMSSM is undoubtedly successful in reducing the number of free parameters that must be considered in the MSSM Lagrangian. However, from a theoretical perspective it would be preferable to explain the origin of the soft SUSY breaking parameters, rather than simply fixing them to phenomenologically acceptable values. In "top-down" models, a particular mechanism for SSB is assumed and the large number of soft parameters are expressed in terms of a much smaller number of underlying, fundamental parameters at high energies. From a practical perspective these models have far fewer free parameters than the pMSSM, making thorough explorations of the parameter space feasible. This necessarily comes at the cost of losing some of the range of possible physical scenarios, since the assumed relationships between the model parameters cannot realise all of the parameter configurations in the general model. This means that constrained models are more predictive than "bottom-up" models such as the pMSSM or general MSSM. The reduced size of the parameter space also lends itself to interpreting experimental searches, and allows for more robust exclusions bounds to be applied in constrained models[5].

As was noted in Section 2.1, in viable models of SSB a hidden sector is constructed that breaks SUSY spontaneously in the vacuum state. A necessary and sufficient condition for SUSY to be spontaneously broken [90, 164] can be obtained from the super-Poincaré algebra; see in particular Eq. (A.8e) in Appendix A. By solving the expression given there for P_μ and considering the $\mu = 0$ component, it follows that the Hamiltonian $H = P_0$ can be expressed in terms of the supersymmetric generators Q_α, $\overline{Q}_{\dot{\alpha}}$,

$$H = \frac{1}{4}\left(\{Q_1, \overline{Q}_{\dot{1}}\} + \{Q_2, \overline{Q}_{\dot{2}}\}\right) . \tag{2.9}$$

The condition that SUSY be unbroken in the vacuum state $|\Omega\rangle$ is equivalent to the fact that Q_α, $\overline{Q}_{\dot{\alpha}}$ annihilate $|\Omega\rangle$, i.e., $Q_\alpha|\Omega\rangle = 0$ and $\overline{Q}_{\dot{\alpha}}|\Omega\rangle = 0$, and hence $H|\Omega\rangle = 0$. In other words, the vacuum state necessarily has zero energy if SUSY is unbroken. If the vacuum state is not SUSY invariant so that $Q_\alpha|\Omega\rangle \neq 0$, $\overline{Q}_{\dot{\alpha}}|\Omega\rangle \neq 0$, then the vacuum state must have positive energy, i.e., $\langle\Omega|H|\Omega\rangle > 0$, since $\overline{Q} = Q^\dagger$. When this non-zero VEV does not develop via the formation of condensates or spacetime effects, for example when SUSY is not broken dynamically [90, 165, 166, 166–168], it

[5]For general soft SUSY breaking terms, the alternative is to produce limits in the context of simplified models [163], in which restrictions are placed on the masses and branching ratios in the model. Experimental analyses can then be optimised to target the resulting signal, so that the reported limits are strongest when the assumptions of the simplified model are approximately met, and (often significantly) weaker when this is not the case.

follows that the potential energy in the spontaneous SUSY breaking vacuum is non-vanishing, $\langle\Omega|V|\Omega\rangle > 0$. The scalar potential in models with unbroken SUSY is a sum of squares of F- and D-terms associated with the chiral and vector superfields, as can be seen from Eq. (A.42). SUSY will therefore be spontaneously broken if it can be arranged that at least one of these contributions has a non-zero VEV for all possible field configurations. To achieve this, models of SSB are constructed in such a way that at least one hidden sector superfield develops a non-zero VEV for its F-term or D-term. In the latter case, a non-zero VEV, $\langle D\rangle$, for the D-term of an Abelian vector superfield may be introduced through a Fayet-Iliopoulos term [169, 170] in the Lagrangian, $\mathcal{L} \supset -2\kappa[\hat{V}]_D = -\kappa D$. Alternatively, the F-terms of one or more chiral superfields can be arranged to develop non-zero VEVs $\langle F_i\rangle$. Models in this category are known as O'Raifeartaigh models [171], and have the benefit of avoiding some of the difficulties associated with successfully implementing SSB with the Fayet-Iliopoulos mechanism [103].

Once SUSY has been broken in the hidden sector, this breaking must be transmitted to the visible sector. The choice of a mediation method that does this sets the pattern of the resulting soft SUSY breaking parameters, but otherwise does not impact the visible sector phenomenology. Gravity mediated SUSY breaking models are one of the simplest ways to transmit SUSY breaking to the visible sector. This is because the role of the required messenger interactions is played by gravitational strength interactions between the hidden and visible sectors. These are automatically included in the theory once global SUSY is promoted to local SUSY, usually referred to as supergravity (SUGRA) [103, 172–178]. The connection to gravity can be seen from the super-Poincaré algebra; from Eq. (A.8e) it follows that invariance under local SUSY transformations also implies diffeomorphism invariance[6]. Generalising the globally SUSY invariant action to one that also respects local SUSY requires the introduction of a spin-3/2 gravitino that forms a supermultiplet with the massless spin-2 graviton. The breakdown of local SUSY by the VEV of a hidden sector F-term leads to the former becoming massive through the super-Higgs mechanism [179]. At the same time, soft SUSY breaking interactions for the visible sector fields are generated via non-renormalisable interactions with the hidden sector fields. These interactions are Planck scale suppressed, so that for sufficiently large F-term VEVs the soft masses may be at the weak or TeV scale.

[6]More explicitly, Eq. (A.8e) indicates that the effect of successive local SUSY transformations is equivalent to a local coordinate transformation generated by $P_\mu \propto \partial_\mu$, and thus a theory that is invariant under the action of local SUSY transformations must also be invariant under local coordinate transformations.

To illustrate this point [104], it is possible to consider a simple model in which the chiral superfields $\hat{\Phi}$ are divided into a set of visible sector fields $\hat{Z}$ and hidden sector fields $\hat{X}$. In SUGRA models, the Lagrangian depends[7] on the so-called Kähler potential,

$$\mathcal{G} = M_{Pl}^2 \left[K\left(\frac{\phi_I}{M_{Pl}}, \frac{\phi^{\dagger I}}{M_{Pl}} \right) - \ln \frac{|W(\phi_I)|^2}{M_{Pl}^6} \right] , \tag{2.10}$$

where the ϕ_I are the scalar components of the superfields, W is the superpotential with $\Phi_I \to \phi_I$, and K is a real function of the scalar fields. The F-term contribution to the scalar potential can be shown to be given by

$$V_F = -\exp\left(-\frac{\mathcal{G}}{M_{Pl}^2} \right) \left[M_{Pl}^2 \mathcal{G}^I (\mathcal{G}^{-1})_I{}^J \mathcal{G}_J + 3M_{Pl}^4 \right] , \tag{2.11}$$

where the shorthand notation

$$\mathcal{G}^I = \frac{\partial \mathcal{G}}{\partial \phi_I} , \quad \mathcal{G}_J = \frac{\partial \mathcal{G}}{\partial \phi^{\dagger J}} , \quad \mathcal{G}_J{}^I = \frac{\partial^2 \mathcal{G}}{\partial \phi_I \partial \phi^{\dagger J}} ,$$

has been used. The Kähler potential can then be taken to be of the form

$$\mathcal{G} = -z_I z^{\dagger I} - H(x_I, x^{\dagger I}) - M_{Pl}^2 \ln \frac{|W(z_I, x_I)|^2}{M_{Pl}^6} , \tag{2.12}$$

where z_I, x_I are the scalar components of the visible and hidden sector superfields, respectively. The choice of the simple form $-z_I z^{\dagger I}$ for the contribution of the visible sector fields to the non-superpotential part of the Kähler potential is made so that the soft SUSY breaking terms that will eventually result are flavour universal [131], to avoid violating constraints on FCNCs. The superpotential, on the other hand, is only assumed to be decomposable into a sum of terms each involving only fields in the visible or hidden sectors,

$$W(z_I, x_I) = W_o(z_I) + W_h(x_I) . \tag{2.13}$$

The hidden sector superpotential is then constructed so that one or more of the hidden sector fields have F-terms that develop VEVs, $\langle F_{X_I} \rangle \neq 0$, to spontaneously break SUSY. The corresponding gravitino mass that results from the super-Higgs mechanism

[7] A detailed discussion of the rather involved process of constructing a SUGRA model is not necessary for the work described in this thesis, and so will be omitted; further details can be found in, e.g., Refs. [103, 180].

is [177, 179, 181]

$$m_{3/2} = M_{Pl} \exp\left(-\frac{\langle \mathcal{G} \rangle}{M_{Pl}^2}\right) . \tag{2.14}$$

By substituting Eq. (2.12) into Eq. (2.11) and taking the "flat limit", $M_{Pl} \to \infty$, keeping $m_{3/2}$ fixed, one finds for this simple example that the surviving terms contain both the ordinary F-term contribution to the scalar potential in global SUSY, as well as soft SUSY breaking terms of the types given in Eq. (2.5) that are universal: all soft scalar masses $m_{ij}^2 = m_{3/2}^2$, all soft trilinears $A_{ijk} = A_0$, all soft bilinears $B_{ij} = B_0 = A_0 - m_{3/2}$, and the soft gaugino masses[8] $M_i = M_{1/2}$ at some high-scale $M_X \lesssim M_{Pl}$. As an approximation, this is often taken to be the GUT scale M_{GUT}. The sizes of the so-generated soft terms are controlled by the value of the gravitino mass, which can be chosen so that the soft SUSY breaking couplings are at the TeV scale. Allowing for slightly more general forms [182–186] of the Kähler potential than that in Eq. (2.12), it is possible to slightly relax the universality conditions to be of the form

$$m_{ij}^2(M_X) = m_0^2 \delta_{ij} , \quad A_{ijk}(M_X) = A_0 , \quad B_{ij} = B_0(M_X) , \quad M_i(M_X) = M_{1/2} . \tag{2.15}$$

Note that the flavour universality of the soft terms is, however, not maintained for arbitrary Kähler potentials; additional assumptions must still be imposed to achieve this. Applied to a model with a visible sector corresponding to the MSSM field content, one arrives at the soft term boundary conditions defining the constrained MSSM (CMSSM),

$$m_Q^2(M_X) = m_{u^c}^2(M_X) = m_{d^c}^2(M_X) = m_L^2(M_X) = m_{e^c}^2(M_X) = m_0^2 \mathbf{1} , \tag{2.16a}$$

$$m_{H_d}^2(M_X) = m_{H_u}^2(M_X) = m_0^2 , \tag{2.16b}$$

$$M_1(M_X) = M_2(M_X) = M_3(M_X) = M_{1/2} , \tag{2.16c}$$

$$T^f(M_X) = y^f(M_X) A_0 , \quad (f = U, D, E) , \tag{2.16d}$$

$$B\mu(M_X) = B_0 \mu(M_X) . \tag{2.16e}$$

In Eq. (2.16a) note that $\mathbf{1}$ indicates a 3×3 identity matrix. The CMSSM is thus characterised by only seven soft parameters, if A_0, B_0 and $M_{1/2}$ are allowed to be complex. If in addition it is required that there are no new sources of CP-violation, the soft SUSY breaking sector of the CMSSM is determined in terms of the four

[8] Strictly speaking, knowledge of the resulting soft gaugino masses also requires that an additional function, the gauge kinetic function $f_{ab}(\hat{\Phi}_I)$, is specified. Universal gaugino masses follow, for example, if $\langle f_{ab} \rangle \propto \delta_{ab}$ [104].

soft parameters m_0^2, A_0, B_0 and $M_{1/2}$. This is of course a drastic reduction in the number of soft parameters compared to the general MSSM, and is also substantially more constrained than the pMSSM. The CMSSM is accordingly much more predictive, with a parameter space that is more easily covered in numerical scans. With flavour universal, real soft terms at M_X, the model is also able to evade the most stringent constraints on FCNCs [187] and CP-violation [188–190].

In passing, it should be noted that this strategy can be used to generate not only the soft SUSY breaking parameters but also the bilinear visible sector superpotential couplings, $\mu^{IJ}\hat{Z}_I\hat{Z}_J$. For example, the Kähler potential may be assumed to contain non-renormalisable couplings between the visible and hidden sector fields of the form

$$\mathcal{G} = -z_I z^{\dagger I} - \left[\Gamma(x_I, x^{\dagger I}, z_I) + h.c.\right] - M_{Pl}^2 \ln \frac{|W(z_I, x_I)|^2}{M_{Pl}^6} \,. \tag{2.17}$$

with the additional couplings taking the form

$$\Gamma(x_I, x^{\dagger I}, z_I) = c^{MN}(x_I, x^{\dagger I}) z_M z_N \,. \tag{2.18}$$

One finds that, once the hidden sector fields develop VEVs, SUSY preserving bilinear terms $\mu^{IJ}(M_X)$ are generated with a scale that is naturally of the same order as the soft breaking terms; that is, this scale is set by the gravitino mass as well. Explicit bilinear couplings can then be forbidden in the visible sector superpotential by imposing, for example, a $U(1)$ Peccei-Quinn (PQ) symmetry, so that the visible sector superpotential contains only trilinear couplings,

$$W(z_I, x_I) = Y^{IJK} z_I z_J z_K + W_h(x_I) \,. \tag{2.19}$$

Generating the SUSY bilinear couplings in this way is known as the Giudice-Masiero mechanism [191]. It provides a natural way to arrange for a non-zero μ term in the MSSM that is of a similar size to the soft breaking masses, to which it otherwise might appear to be unrelated and might naturally be expected to be of order M_{Pl}, for example.

2.4 Electroweak Symmetry Breaking

Once the set of MSSM soft parameters has been determined, for example by choosing a particular high-energy boundary condition and evolving the model to low energies using the renormalisation group equations (RGEs), or by working in the pMSSM

framework, the particle mass spectrum can be determined and the properties of the model at low energies studied. Like in the SM, the physical mass eigenstates arise once the EW symmetry $SU(2)_L \times U(1)_Y$ is broken down to $U(1)_{\rm em}$. In the MSSM, the spontaneous breaking of EW symmetry involves both Higgs scalar fields H_u and H_d acquiring (in general) non-zero VEVs at the physical minimum of the scalar potential.

The relevant Higgs potential for EWSB in the MSSM contains F- and D-term contributions, per Eq. (A.42), as well as a subset of the soft SUSY breaking terms involving H_u and H_d,

$$V_{\rm MSSM} = V^F_{\rm MSSM} + V^D_{\rm MSSM} + V^{\rm soft}_{\rm MSSM} + \Delta V_{\rm MSSM}\,. \tag{2.20}$$

These three pieces are given by

$$V^F_{\rm MSSM} = |\mu|^2(|H_u|^2 + |H_d|^2)\,, \tag{2.21}$$

$$V^D_{\rm MSSM} = \frac{\bar{g}^2}{8}\left(|H_u|^2 - |H_d|^2\right)^2 + \frac{g_2^2}{2}|H_d^\dagger H_u|^2\,, \tag{2.22}$$

$$V^{\rm soft}_{\rm MSSM} = m^2_{H_d}|H_d|^2 + m^2_{H_u}|H_u|^2 + (B\mu H_d \cdot H_u + h.c.)\,. \tag{2.23}$$

In these expressions, g_2 and g_1 are the $SU(2)_L$ and GUT-normalised $U(1)_Y$ gauge couplings, $\bar{g}^2 = g_2^2 + \frac{3}{5}g_1^2$, and $\Delta V_{\rm MSSM}$ contains the higher-order corrections to the effective potential, $\Delta V_{\rm MSSM} = \Delta V^{(1)}_{\rm MSSM} + \Delta V^{(2)}_{\rm MSSM} + \ldots$, $\Delta V^{(n)}_{\rm MSSM}$ being the n-loop contribution. Near the physical minimum of the potential, the Higgs fields can be written

$$H_d = \begin{pmatrix} |H_d^0|e^{i\theta_d^0} \\ |H_d^-|e^{i\theta_d^-} \end{pmatrix}\,, \quad H_u = \begin{pmatrix} |H_u^+|e^{i\theta_u^+} \\ |H_u^0|e^{i\theta_u^0} \end{pmatrix}\,. \tag{2.24}$$

By making a local $SU(2)_L$ gauge transformation of the form [192]

$$U_1 = \begin{pmatrix} u_{11} & u_{12} \\ -u_{12}^* & u_{11}^* \end{pmatrix}\,, \tag{2.25}$$

with

$$\begin{aligned} u_{11} &= \frac{|H_u^0|}{\sqrt{|H_u^0|^2 + |H_u^+|^2}}\,, \\ u_{12} &= -\frac{|H_u^+|}{\sqrt{|H_u^0|^2 + |H_u^+|^2}} e^{i(\theta_u^+ - \theta_u^0)}\,, \end{aligned} \tag{2.26}$$

it is possible to set $\langle H_u^+ \rangle = 0$ at the physical minimum. After doing so, the Higgs fields have the form

$$H_d = \begin{pmatrix} |H_d^0| e^{i\theta_d^0} \\ |H_d^-| e^{i\theta_d^-} \end{pmatrix} , \quad H_u = \begin{pmatrix} 0 \\ |H_u^0| e^{i\theta_u^0} \end{pmatrix} ,$$

where for simplicity the same symbols as in Eq. (2.24) have been used, but it should be noted that they do not refer to the same quantities following the gauge transformation U_1. A second $SU(2)_L \times U(1)_Y$ transformation, of the form

$$U_2 = \begin{pmatrix} e^{-i\theta_d^0} & 0 \\ 0 & e^{-i\theta_d^-} \end{pmatrix} , \tag{2.27}$$

allows the phases of the components of H_d to be removed,

$$H_d = \begin{pmatrix} |H_d^0| \\ |H_d^-| \end{pmatrix} , \quad H_u = \begin{pmatrix} 0 \\ |H_u^0| e^{i\theta_u^0} \end{pmatrix} ,$$

and then a trivial rephasing $H_u \to e^{-i\theta_u^0} H_u$ can eliminate the phase of H_u^0. Therefore at the physical minimum, the VEVs $\langle H_d^0 \rangle$ and $\langle H_u^0 \rangle$ can be taken to be real and positive,

$$\langle H_d^0 \rangle = \frac{v_1}{\sqrt{2}} , \quad \langle H_u^0 \rangle = \frac{v_2}{\sqrt{2}} , \tag{2.28}$$

where $v_1, v_2 > 0$. The freedom to make these field redefinitions also allows any phase in the parameter $B\mu$ to be absorbed to make $B\mu \geq 0$, in which case all of the parameters in the Higgs scalar potential are real. In particular, this means that the MSSM Higgs potential does not contain any new sources of CP-violation at tree-level [193].

With $\langle H_u^+ \rangle = 0$ at the minimum of the potential, $U(1)_{\rm em}$ remains unbroken, that is,

$$Q\langle H_d \rangle = Q\langle H_u \rangle = 0 , \tag{2.29}$$

where $Q = T_3 + Y$ is the electric charge operator, provided that $\langle H_d^- \rangle = 0$ as well[9]. It is easily checked that $\langle H_d^- \rangle = 0$ leads to a stationary point of the potential when $\langle H_u^+ \rangle = 0$, for arbitrary values of v_1 and v_2. The condition for the $U(1)_{\rm em}$ symmetric vacuum to not be unstable reduces to the condition that the physical, charged Higgs state has positive mass.

[9]It is also necessary to ensure that at the minimum of the full scalar potential other scalar fields do not develop VEVs that break electromagnetism [194].

The conditions that must be satisfied to have a minimum of the potential at finite values of the neutral Higgs VEVs can then be worked out with $\langle H_u^+ \rangle = \langle H_d^- \rangle = 0$. Firstly, it should be required that the scalar potential be bounded from below so that such a minimum exists. In particular, along the D-flat direction $|H_u^0| = |H_d^0|$, $H_u^+ = H_d^- = 0$, the quartic terms in Eq. (2.22) vanish. Requiring that $V_{\text{MSSM}} > 0$ for large field values along this direction imposes the restriction

$$2|\mu|^2 + m_{H_d}^2 + m_{H_u}^2 > 2B\mu \,, \tag{2.30}$$

assuming $B\mu$ is real and positive. Using the shorthand $\partial V/\partial\langle\Phi\rangle = \partial V/\partial\Phi|_{\Phi=\langle\Phi\rangle}$, the EWSB conditions for a stationary point of the potential read

$$\frac{\partial V_{\text{MSSM}}}{\partial v_1} = \left(|\mu|^2 + m_{H_d}^2\right) v_1 + \frac{\bar{g}^2}{8}\left(v_1^2 - v_2^2\right) v_1 - B\mu v_2 + \frac{\partial \Delta V_{\text{MSSM}}}{\partial v_1} = 0 \,, \tag{2.31a}$$

$$\frac{\partial V_{\text{MSSM}}}{\partial v_2} = \left(|\mu|^2 + m_{H_u}^2\right) v_2 - \frac{\bar{g}^2}{8}\left(v_1^2 - v_2^2\right) v_2 - B\mu v_1 + \frac{\partial \Delta V_{\text{MSSM}}}{\partial v_2} = 0 \,. \tag{2.31b}$$

The corresponding conditions for the VEVs of the imaginary parts of the neutral Higgs fields are satisfied for $\langle \text{Im}\, H_d^0 \rangle = \langle \text{Im}\, H_u^0 \rangle = 0$, consistent with the observation that v_1, v_2 can be chosen real and positive. Eqs. (2.31a) and (2.31b) are also satisfied, at least at tree-level, for $v_1 = v_2 = 0$. Taking second derivatives of the scalar potential leads to the condition for the origin in field space to be an unstable point,

$$(|\mu|^2 + m_{H_u}^2)(|\mu|^2 + m_{H_d}^2) < (B\mu)^2 \,. \tag{2.32}$$

Provided this is the case, the stable EWSB minimum is expected to occur with $v_1, v_2 \neq 0$ given by the solutions of the above EWSB conditions.

The four complex scalar fields in the Higgs sector correspond to 8 real degrees of freedom, three of which are absorbed to produce the longitudinal polarisations of the $W^\pm$ and Z gauge bosons, as in the SM. For $v_1, v_2 > 0$, it is convenient to define the combinations

$$v^2 = v_1^2 + v_2^2 \,, \quad \tan\beta = \frac{v_2}{v_1} \,. \tag{2.33}$$

The running gauge boson masses[10] $m_W^{\overline{\text{DR}}}$ and $m_Z^{\overline{\text{DR}}}$ are then given by the expressions

$$m_W^{\overline{\text{DR}}} = \frac{g_2 v}{2} \,, \quad m_Z^{\overline{\text{DR}}} = \frac{\bar{g} v}{2} \,, \tag{2.34}$$

[10] In this thesis, we use a superscript $\overline{\text{DR}}$ to explicitly denote running tree-level masses, which is left off for physical masses. In some cases, a different symbol is used for the physical masses, e.g., M_Z, M_W, $M_{Z'}$ and M_t.

which are the same as in the SM with the replacement of the single SM Higgs VEV $v_{SM} \to v$. The $\overline{\text{DR}}$ masses are related to the known pole masses [95] M_Z and M_W by

$$M_Z^2 = (m_Z^{\overline{\text{DR}}})^2 - \text{Re}\,\Pi_{ZZ,T}^{\text{MSSM}}(M_Z^2)\,, \tag{2.35}$$

and similarly for M_W, where $\Pi_{ZZ,T}^{\text{MSSM}}(p^2)$ and $\Pi_{WW,T}^{\text{MSSM}}(p^2)$ are the transverse self-energies evaluated with external momentum p^2. An important feature of EWSB in the MSSM is that the EWSB conditions lead to a prediction for the EW scale, characterised by the Higgs VEV v or the Z boson mass, in terms of the superpotential and soft SUSY breaking parameters. This can be seen by taking linear combinations of Eq. (2.31a) and Eq. (2.31b), with the result that

$$\frac{(m_Z^{\overline{\text{DR}}})^2}{2} = -|\mu|^2 + \frac{\bar{m}_{H_d}^2 - \bar{m}_{H_u}^2 \tan^2\beta}{\tan^2\beta - 1}\,, \tag{2.36}$$

$$\sin 2\beta = \frac{2B\mu}{\bar{m}_{H_d}^2 + \bar{m}_{H_u}^2 + 2|\mu|^2}\,. \tag{2.37}$$

Traditionally when scanning the parameter space of the MSSM, the EWSB conditions written in this form are used to trade the parameters μ and $B\mu$ for M_Z and $\tan\beta$; that is, Eq. (2.36) and Eq. (2.37) are solved to obtain μ and $B\mu$ as functions of M_Z and $\tan\beta$. This allows the experimentally measured value of M_Z to be used as an input parameter, thus automatically excluding the many (phenomenologically uninteresting) parts of the parameter space that do not reproduce the observed gauge boson masses. For brevity, the corrections to the effective potential have here been absorbed by writing

$$\bar{m}_{H_d}^2 = m_{H_d}^2 + \frac{1}{v_1}\frac{\partial \Delta V_{\text{MSSM}}}{\partial v_1}\,, \quad \bar{m}_{H_u}^2 = m_{H_u}^2 + \frac{1}{v_2}\frac{\partial \Delta V_{\text{MSSM}}}{\partial v_2}\,. \tag{2.38}$$

The inclusion of ΔV_{MSSM} is extremely important for studying EWSB in the MSSM. The tree-level potential in the MSSM is known to be extremely sensitive to radiative corrections [195], which means that the one- and two-loop corrections to the effective potential are required to draw robust conclusions. At one-loop, the corrections can be expressed concisely as [195, 196]

$$\begin{aligned}\Delta V_{\text{MSSM}}^{(1)} &= \frac{1}{64\pi^2}\,\text{STr}\left[\mathcal{M}^4\left(\ln\frac{\mathcal{M}^2}{Q^2} - \frac{3}{2}\right)\right] \\ &\equiv \frac{1}{64\pi^2}\sum_{\Phi}(-1)^{2s_\Phi}(2s_\Phi+1)m_\Phi^4\left(\ln\frac{m_\Phi^2}{Q^2} - \frac{3}{2}\right)\,.\end{aligned} \tag{2.39}$$

Here $\mathcal{M}$ is a field-dependent mass matrix encompassing all those states with masses that depend on the Higgs VEVs, and $\mathrm{STr}(A)$ denotes the supertrace. The eigenvalues of $\mathcal{M}$, m_Φ, are the field-dependent running masses of the component fields Φ, with s_Φ being the spin of the state, and Q is the renormalisation scale. The supertrace in the first line and the sum in the second line are thus carried out over all states Φ whose masses depend on the Higgs VEVs. The two-loop contributions to ΔV_{MSSM} are somewhat more involved. Nevertheless, they have been computed for general renormalisable theories [196] and have been specialised to the MSSM [195], where their impact was found to be significant.

2.5 The Particle Spectrum of the MSSM

In addition to generating mass terms for the gauge bosons, following the breakdown of EW symmetry the other states in the spectrum also receive contributions to their masses from the Higgs VEVs. For example, the masses for the remaining SM states, namely the SM fermions, arise in a very similar fashion to that which occurs in the SM. The mass terms come from the superpotential Yukawa couplings, leading to $\overline{\mathrm{DR}}$ mass matrices with elements

$$(\mathcal{M}_u)_{ij} = \frac{y^U_{ji} v_2}{\sqrt{2}}\,, \quad (\mathcal{M}_d)_{ij} = \frac{y^D_{ji} v_1}{\sqrt{2}}\,, \quad (\mathcal{M}_e)_{ij} = \frac{y^E_{ji} v_1}{\sqrt{2}}\,, \tag{2.40}$$

which are basically identical to those in the SM with the obvious difference that the masses of the down-type quarks and leptons are generated by the VEV v_1, while those of the up-type quarks involve v_2. Diagonalising these mass matrices in the usual way, i.e., by diagonalising the Yukawa coupling matrices via

$$y^U_{\mathrm{diag}} = U_u^\dagger (y^U)^T V_u\,, \quad y^D_{\mathrm{diag}} = U_d^\dagger (y^D)^T V_d\,, \quad y^E_{\mathrm{diag}} = U_e^\dagger (y^E)^T V_e\,, \tag{2.41}$$

leads to the tree-level masses for the SM fermions, with $V_{CKM} = V_u^\dagger V_d$ and $U_{PMNS} = V_e^\dagger V_\nu$ being the ordinary CKM [197, 198] and PMNS [52–54, 199] matrices, and where V_ν would diagonalise the 3×3 matrix of Majorana neutrino masses if such a term were present in the Lagrangian[11]. In some instances it is sufficient to neglect flavour violating effects, in which case the off-diagonal Yukawa couplings will be neglected

[11] As will be discussed in Section 2.6, in the MSSM neutrinos are massless and V_ν is undefined; the convention we follow here for its definition is that of the SUSY Les Houches Accord [200, 201], in which unspecified high-scale physics is assumed to generate a set of effective Majorana neutrino masses.

and the diagonal elements of Eq. (2.40) yield the tree-level masses. The physical pole masses must be obtained by including the self-energy corrections to the mass matrices, which can be significant for some states. The use of tree-level expressions, neglecting flavour violation, is nevertheless helpful for deriving analytic insights into the spectrum. For numerical calculations, the inclusion of the self-energies is facilitated by the use of the precision spectrum generators to be discussed in Chapter 4. This also holds true for those masses that are either significantly modified compared to their values in the SM, or are entirely new.

2.5.1 The MSSM Higgs Sector

The presence of an extra Higgs doublet in the MSSM means that the Higgs sector is extended compared to the SM. Assuming the absence of CP-violating couplings at tree-level, the remaining five degrees of freedom in this sector after EWSB lead to two physical charged states $H^\pm$, a physical CP-odd pseudoscalar state A, and two CP-even states h, H.

The charged states arise from linear combinations of the fields H_u^+ and H_d^-, which do not mix with the other Higgs states due to the unbroken $U(1)_{\rm em}$. The squared mass matrix is obtained by taking second derivatives of $V_{\rm MSSM}$ with respect to H_u^+ and H_d^-, and reads

$$\mathcal{M}^2_{H^\pm} = \left(\frac{B\mu}{v_1 v_2} + \frac{g_2^2}{4}\right)\begin{pmatrix} v_2^2 & v_1 v_2 \\ v_1 v_2 & v_2^2 \end{pmatrix} \tag{2.42}$$

in the basis (H_d^-, H_u^{+*}), after eliminating the soft Higgs masses using the EWSB conditions. The requirement that $\langle H_u^+\rangle = \langle H_d^-\rangle = 0$ is not a local maximum of the potential implies that the eigenvalues of this matrix should be non-negative; in this case, $\det \mathcal{M}^2_{H^\pm} = 0$, indicating the existence of the massless Goldstone bosons $G^\pm$ that are absorbed as the longitudinal degrees of freedom of the $W^\pm$ bosons, while the charged Higgs mass is given by

$$(m^{\overline{\rm DR}}_{H^\pm})^2 = (m^{\overline{\rm DR}}_W)^2 + \frac{2B\mu}{\sin 2\beta} \geq (m^{\overline{\rm DR}}_W)^2\,, \tag{2.43}$$

when $B\mu \geq 0$, since $0 \leq \beta \leq \pi/2$. The corresponding mass eigenstate is given by the linear combinations

$$H^+ = H_d^{-*}\sin\beta + H_u^+\cos\beta\,, \tag{2.44}$$

while the orthogonal combination makes up $G^\pm$.

Similarly, if CP is not violated in the Higgs sector at tree-level, the real and imaginary parts of H_u^0 and H_d^0 do not mix with each other. The imaginary parts $\mathrm{Im}\, H_d^0 = \sigma_d/\sqrt{2}$ and $\mathrm{Im}\, H_u^0 = \sigma_u/\sqrt{2}$ mix to form the Goldstone boson G^0, absorbed as the longitudinal degree of freedom of the Z boson, and the CP-odd scalar A,

$$\begin{aligned} G^0 &= (-\sigma_d \cos\beta + \sigma_u \sin\beta)\ , \\ A &= (\sigma_d \sin\beta + \sigma_u \cos\beta)\ . \end{aligned} \tag{2.45}$$

In the basis (σ_d, σ_u) the tree-level squared mass matrix reads

$$\mathcal{M}_A^2 = B\mu \begin{pmatrix} \tan\beta & 1 \\ 1 & \frac{1}{\tan\beta} \end{pmatrix}\ , \tag{2.46}$$

from which it follows that $m_{G^0}^2 = 0$, and

$$(m_A^{\overline{\mathrm{DR}}})^2 = \frac{2B\mu}{\sin 2\beta}\,. \tag{2.47}$$

On the other hand, the real parts $\mathrm{Re}\, H_d^0 = (v_1 + \phi_d)/\sqrt{2}$ and $\mathrm{Re}\, H_u^0 = (v_2 + \phi_u)/\sqrt{2}$ mix with each other to produce two massive, CP-even scalars h and H. These are related by an orthogonal transformation,

$$\begin{pmatrix} h \\ H \end{pmatrix} = U_h \begin{pmatrix} \phi_d \\ \phi_u \end{pmatrix} = \begin{pmatrix} -\sin\alpha & \cos\alpha \\ \cos\alpha & \sin\alpha \end{pmatrix} \begin{pmatrix} \phi_d \\ \phi_u \end{pmatrix}\ , \tag{2.48}$$

where the matrix U_h diagonalises the tree level squared mass matrix for the CP-even Higgs states. In the basis (S_1, S_2), where

$$\begin{pmatrix} \phi_d \\ \phi_u \end{pmatrix} = \begin{pmatrix} \cos\beta & -\sin\beta \\ \sin\beta & \cos\beta \end{pmatrix} \begin{pmatrix} S_1 \\ S_2 \end{pmatrix}\ , \tag{2.49}$$

this is found to have elements

$$(\mathcal{M}_h^2)_{11} = (m_Z^{\overline{\mathrm{DR}}})^2 \cos^2 2\beta\,, \tag{2.50a}$$

$$(\mathcal{M}_h^2)_{12} = (\mathcal{M}_h^2)_{21} = -\frac{(m_Z^{\overline{\mathrm{DR}}})^2}{2} \sin 4\beta\,, \tag{2.50b}$$

$$(\mathcal{M}_h^2)_{22} = (m_A^{\overline{\mathrm{DR}}})^2 + (m_Z^{\overline{\mathrm{DR}}})^2 \sin^2 2\beta\,. \tag{2.50c}$$

The diagonalisation in this case can be done analytically; the tree-level masses are found to be

$$(m_{h,H}^{\overline{\rm DR}})^2 = \frac{1}{2}\Big\{(m_A^{\overline{\rm DR}})^2 + (m_Z^{\overline{\rm DR}})^2 \mp \sqrt{\Big[(m_A^{\overline{\rm DR}})^2 + (m_Z^{\overline{\rm DR}})^2\Big]^2 - 4(m_Z^{\overline{\rm DR}})^2(m_A^{\overline{\rm DR}})^2\cos^2 2\beta}\Big\}, \tag{2.51}$$

where by convention $m_h^2 < m_H^2$, and the tree-level mixing angle α satisfies [104]

$$\sin 2\alpha = -\left[\frac{(m_H^{\overline{\rm DR}})^2 + (m_h^{\overline{\rm DR}})^2}{(m_H^{\overline{\rm DR}})^2 - (m_h^{\overline{\rm DR}})^2}\right]\sin 2\beta\,, \tag{2.52a}$$

$$\cos 2\alpha = -\left[\frac{(m_A^{\overline{\rm DR}})^2 - (m_Z^{\overline{\rm DR}})^2}{(m_H^{\overline{\rm DR}})^2 - (m_h^{\overline{\rm DR}})^2}\right]\cos 2\beta\,, \tag{2.52b}$$

$$\tan 2\alpha = \frac{(m_A^{\overline{\rm DR}})^2 + (m_Z^{\overline{\rm DR}})^2}{(m_A^{\overline{\rm DR}})^2 - (m_Z^{\overline{\rm DR}})^2}\tan 2\beta\,, \tag{2.52c}$$

from which it follows that $-\pi/2 \leq \alpha \leq 0$.

The mass of the lightest CP-even Higgs, m_h^2, is always bounded from above by the smallest diagonal element in the squared mass matrix. From Eq. (2.50) it is clear that

$$m_h^{\overline{\rm DR}} \leq m_Z^{\overline{\rm DR}}|\cos 2\beta|\,. \tag{2.53}$$

The fact that $m_h^{\overline{\rm DR}} < m_Z^{\overline{\rm DR}}$ indicates that, in the MSSM, an acceptable Higgs mass can only be achieved with the help of large radiative corrections [202–204]. The size of these corrections has potentially significant consequences for the theory, as shall be discussed in Section 2.6. Additionally, because the loop corrections to m_h are sizeable, obtaining a precise estimate for the Higgs mass requires calculations to be done at as high a loop order as possible, which is theoretically challenging. Even when computed to two-loop order, the theory uncertainty on m_h is expected to be several GeV (see, for example, Ref. [205]), substantially larger than the current experimental uncertainty [28]. The heavy CP-even state, on the other hand, has its mass bounded from below by $m_A^{\overline{\rm DR}}$, and so in phenomenologically viable scenarios is expected to be somewhat heavier, $m_A^{\overline{\rm DR}}, m_H^{\overline{\rm DR}} > m_Z^{\overline{\rm DR}}$.

2.5.2 The Neutralino and Chargino Sectors

The fermion partners of the extended Higgs sector, the Higgsinos, mix with the EW gauginos after the breaking of $SU(2)_L \times U(1)_Y \to U(1)_{\rm em}$. The superpartners of the

charged Higgs states, $\tilde{H}_u^+$ and $\tilde{H}_d^-$, mix with the charged winos $\tilde{W}^\pm$ to form a set of chargino mass eigenstates $\tilde{\chi}_{1,2}^\pm$. The contributions to the chargino mass matrix consist of contributions from the superpotential couplings, cf. Eq. (A.41), and from the soft SUSY breaking Lagrangian. The resulting 2×2 mass matrix can be diagonalised analytically, with the result that

$$(m_{\tilde{\chi}_{1,2}^\pm}^{\overline{\rm DR}})^2 = \frac{1}{2}\Big\{|M_2|^2 + |\mu|^2 + 2(m_W^{\overline{\rm DR}})^2 \mp \sqrt{\Big[|M_2|^2 + |\mu|^2 + 2(m_W^{\overline{\rm DR}})^2\Big]^2 - 4\left|\mu M_2 - (m_W^{\overline{\rm DR}})^2 \sin 2\beta\right|^2}\Big\}. \tag{2.54}$$

The remaining neutral Higgsinos $\tilde{H}_d^0$ and $\tilde{H}_u^0$ mix with the neutral wino, $\tilde{W}_3$, and bino $\tilde{B}$, to produce four physical neutralinos. The 4×4 mass matrix in the basis $(\tilde{H}_d^0, \tilde{H}_u^0, \tilde{W}_3, \tilde{B})$,

$$\mathcal{M}_{\tilde{\chi}^0} = \begin{pmatrix} 0 & -\mu & \frac{g_2 v_1}{2} & -\frac{g_1 v_1}{2}\sqrt{\frac{3}{5}} \\ -\mu & 0 & -\frac{g_2 v_2}{2} & \frac{g_1 v_2}{2}\sqrt{\frac{3}{5}} \\ \frac{g_2 v_1}{2} & -\frac{g_2 v_2}{2} & M_2 & 0 \\ -\frac{g_1 v_1}{2}\sqrt{\frac{3}{5}} & \frac{g_1 v_2}{2}\sqrt{\frac{3}{5}} & 0 & M_1 \end{pmatrix}, \tag{2.55}$$

is diagonalised by the mixing matrix N to obtain the $\overline{\rm DR}$ masses,

$$\mathrm{diag}(m_{\tilde{\chi}_1^0}^{\overline{\rm DR}}, \ldots, m_{\tilde{\chi}_4^0}^{\overline{\rm DR}}) = N^* \mathcal{M}_{\tilde{\chi}^0} N^\dagger . \tag{2.56}$$

In this convention, the physical neutralinos are given by the linear combinations of the gauge eigenstates,

$$\tilde{\chi}_i^0 = N_{i1}\tilde{H}_d^0 + N_{i2}\tilde{H}_u^0 + N_{i3}\tilde{W}_3 + N_{i4}\tilde{B} . \tag{2.57}$$

The mixings N_{ij} play an important role in determining the couplings of the neutralinos to other states, and various aspects of the phenomenology associated with a parameter point depend strongly on the relative sizes of the mixing elements. This is particularly important in the context of studying the implications of the MSSM for DM. Since the neutralinos are R–parity odd, if $\tilde{\chi}_1^0$ is the LSP then it is a potential DM candidate. The behaviour of this DM candidate, from the present day relic density to its scattering cross section in direct detection experiments, is then heavily influenced by the sizes of the quantities N_{1j}, i.e., the composition of $\tilde{\chi}_1^0$. It is convenient to characterise this by the bino, wino and Higgsino fractions, $|N_{i4}|^2$, $|N_{i3}|^2$ and $|N_{i1}|^2 + |N_{i2}|^2$, respectively. When $|N_{i4}|^2 \gg |N_{i3}|^2, |N_{i1}|^2 + |N_{i2}|^2$, for example, $\tilde{\chi}_i^0$ is predominantly $\tilde{B}$ and is

said to be bino-like. Similar statements hold for the case of a wino- or Higgsino-like neutralino candidate; otherwise, when one or more fractions are comparable then the state is highly mixed. In general, the mass and mixing matrix elements are governed only by the parameters M_1, M_2, μ and $\tan\beta$. In models such as the CMSSM, where M_1 and M_2 are not independent, the neutralino sector is characterised by only the three[12] parameters $M_{1/2}$, μ and $\tan\beta$. While analytic expressions are known for the diagonalised masses [206–208], approximate expressions for the masses and mixings can be obtained using perturbation theory when the LSP is an almost pure state [209–211]. For example, if $|M_1| \ll |\mu|, |M_2|$, it is found that $\tilde{\chi}_1^0$ is approximately pure $\tilde{B}$, with $|N_{14}| \to 1$, while if $|\mu| \ll |M_1|, |M_2|$, then $\tilde{\chi}_1^0$ is a pure Higgsino state.

Unlike the EW gauginos, the gluino does not mix with any other states in the model, being the only colour octet fermion. The expression for the tree-level gluino mass is accordingly rather simple,

$$m_{\tilde{g}}^{\overline{\mathrm{DR}}} = M_3 \,. \tag{2.58}$$

The quantity M_3 runs quickly with scale, since the gluino is strongly interacting, and the radiative corrections must be included to obtain the scale-independent, physical gluino mass,

$$m_{\tilde{g}} = M_3(Q) + \Delta^{\tilde{g}}(Q) \,. \tag{2.59}$$

The corrections $\Delta^{\tilde{g}}$ are also large, yielding a contribution of up to 30% of the total mass [212] in parts of the parameter space, and thus are essential for accurately estimating the expected gluino mass.

2.5.3 The Sfermions

The remaining mass eigenstates in the MSSM, the scalar partners of the SM fermions, receive contributions to their masses from the soft SUSY breaking Lagrangian and from EWSB. In the most general case, the masses of the up-type squarks, down-type squarks and sleptons are obtained by diagonalising the three corresponding 6×6 matrices, as well as a 3×3 matrix for the sneutrinos, since the pairs of states coming from each generation share the same colour representation, electric charge, and R–parity and are able to mix. However, if flavour violating effects can be taken to be negligible, as occurs when it is assumed that the soft scalar squared masses $m_{Q_{ij}}^2$, $m_{L_{ij}}^2$, ... are flavour diagonal and the trilinears T_{ij}^f are proportional to the corresponding Yukawa

[12] The gauge couplings and v being fixed by low-energy data.

couplings, then the mass matrices substantially simplify. In this case, diagonalising each 6×6 matrix reduces to instead diagonalising three 2×2 matrices. Moreover, the small size of the first and second generation Yukawa couplings implies that the mixing within these generations is also small, and can reasonably be neglected. The resulting states are thus approximately the left- and right-handed gauge eigenstates, and the $\overline{\text{DR}}$ masses can then be read off from the diagonal mass matrix elements. This leads to the approximate sneutrino and first and second generation sfermion masses (where we note again that $i = 1, 2, 3$, $\alpha = 1, 2$, and below no sum over repeated indices is implied)

$$\left(m_{\tilde{d}_{L\alpha}}^{\overline{\text{DR}}}\right)^2 \approx m_{Q_{\alpha\alpha}}^2 + \left(-\frac{1}{2} + \frac{1}{3}\sin^2\theta_W\right)(m_Z^{\overline{\text{DR}}})^2 \cos 2\beta\,, \tag{2.60}$$

$$\left(m_{\tilde{d}_{R\alpha}}^{\overline{\text{DR}}}\right)^2 \approx m_{d^c_{\alpha\alpha}}^2 - \frac{1}{3}(m_Z^{\overline{\text{DR}}})^2 \sin^2\theta_W \cos 2\beta\,, \tag{2.61}$$

$$\left(m_{\tilde{u}_{L\alpha}}^{\overline{\text{DR}}}\right)^2 \approx m_{Q_{\alpha\alpha}}^2 + \left(\frac{1}{2} - \frac{2}{3}\sin^2\theta_W\right)(m_Z^{\overline{\text{DR}}})^2 \cos 2\beta\,, \tag{2.62}$$

$$\left(m_{\tilde{u}_{R\alpha}}^{\overline{\text{DR}}}\right)^2 \approx m_{u^c_{\alpha\alpha}}^2 + \frac{2}{3}(m_Z^{\overline{\text{DR}}})^2 \sin^2\theta_W \cos 2\beta\,, \tag{2.63}$$

$$\left(m_{\tilde{e}_{L\alpha}}^{\overline{\text{DR}}}\right)^2 \approx m_{L_{\alpha\alpha}}^2 + \left(-\frac{1}{2} + \sin^2\theta_W\right)(m_Z^{\overline{\text{DR}}})^2 \cos 2\beta\,, \tag{2.64}$$

$$\left(m_{\tilde{e}_{R\alpha}}^{\overline{\text{DR}}}\right)^2 \approx m_{e^c_{\alpha\alpha}}^2 - (m_Z^{\overline{\text{DR}}})^2 \sin^2\theta_W \cos 2\beta\,, \tag{2.65}$$

$$\left(m_{\tilde{\nu}_i}^{\overline{\text{DR}}}\right)^2 \approx m_{L_{ii}}^2 + \frac{1}{2}(m_Z^{\overline{\text{DR}}})^2 \cos 2\beta\,. \tag{2.66}$$

Compared to the first and second generations, the sizeable third generation Yukawa couplings are usually expected to lead to large mixings between the third generation states. The masses must be found by diagonalising the appropriate 2×2 mass matrices, leading to the $\overline{\text{DR}}$ masses for the stops, sbottoms and staus,

$$\begin{aligned}\left(m_{\tilde{t}_{1,2}}^{\overline{\text{DR}}}\right)^2 = \frac{1}{2}\Bigg\{ & m_{Q_{33}}^2 + m_{u^c_{33}}^2 + \frac{1}{2}(m_Z^{\overline{\text{DR}}})^2 \cos 2\beta + 2\left(m_t^{\overline{\text{DR}}}\right)^2 \\ & \mp \sqrt{\left[m_{Q_{33}}^2 - m_{u^c_{33}}^2 + \left(\frac{1}{2} - \frac{4}{3}\sin^2\theta_W\right)(m_Z^{\overline{\text{DR}}})^2 \cos 2\beta\right]^2 + 4X_t^2}\Bigg\}\,,\end{aligned} \tag{2.67}$$

$$\begin{aligned}\left(m_{\tilde{b}_{1,2}}^{\overline{\text{DR}}}\right)^2 = \frac{1}{2}\Bigg\{ & m_{Q_{33}}^2 + m_{d^c_{33}}^2 - \frac{1}{2}(m_Z^{\overline{\text{DR}}})^2 \cos 2\beta + 2\left(m_b^{\overline{\text{DR}}}\right)^2 \\ & \mp \sqrt{\left[m_{Q_{33}}^2 - m_{d^c_{33}}^2 + \left(-\frac{1}{2} + \frac{2}{3}\sin^2\theta_W\right)(m_Z^{\overline{\text{DR}}})^2 \cos 2\beta\right]^2 + 4X_b^2}\Bigg\}\,,\end{aligned} \tag{2.68}$$

$$\left(m_{\tilde{\tau}_{1,2}}^{\overline{\rm DR}}\right)^2 = \frac{1}{2}\Bigg\{ m_{L_{33}}^2 + m_{e_{33}^c}^2 - \frac{1}{2}(m_Z^{\overline{\rm DR}})^2 \cos 2\beta + 2\left(m_\tau^{\overline{\rm DR}}\right)^2 \mp \sqrt{\left[m_{L_{33}}^2 - m_{e_{33}^c}^2 + \left(-\frac{1}{2} + 2\sin^2\theta_W\right)(m_Z^{\overline{\rm DR}})^2 \cos 2\beta\right]^2 + 4X_\tau^2}\Bigg\}. \quad (2.69)$$

In these expressions, the mixing parameters X_t, X_b and X_τ are defined by

$$X_t = \frac{T_{33}^U v_2}{\sqrt{2}} - \frac{y_{33}^U \mu v_1}{\sqrt{2}}, \quad (2.70)$$

$$X_b = \frac{T_{33}^D v_1}{\sqrt{2}} - \frac{y_{33}^D \mu v_2}{\sqrt{2}}, \quad (2.71)$$

$$X_\tau = \frac{T_{33}^E v_1}{\sqrt{2}} - \frac{y_{33}^E \mu v_2}{\sqrt{2}}, \quad (2.72)$$

and the corresponding third generation fermion masses are taken to be those that result when flavour mixing is neglected, i.e., the $(3,3)$ components of Eq. (2.40). The potentially large mixings, together with the impact of the large Yukawa couplings on the evolution of the soft masses from high energies, mean that it is often the case that the third generation sfermions are found to be considerably lighter than their first and second generation counterparts. They have been the subjects of many searches at colliders, see, e.g., Refs. [213–216].

2.6 Why Might the MSSM not be Enough?

By virtue of their large couplings to the Higgs, the stops in particular also play an important role in the radiative corrections mentioned above that are necessary to reproduce the observed Higgs mass. For example, one method[13] to compute the Higgs mass makes use of the higher-order corrections to the MSSM effective potential, Eq. (2.39). In scenarios where $m_{Q_{33}}^2 = m_{u_{33}^c}^2 = M^2$, the result for the lightest Higgs mass at two-loop, leading-log order can then be written [218]

$$m_h^2 = (m_Z^{\overline{\rm DR}})^2 \cos^2 2\beta \left(1 - \frac{3}{8\pi^2}\frac{\bar{m}_t^2}{v^2}\ln\frac{M_S^2}{\bar{m}_t^2}\right) + \frac{3}{4\pi^2}\frac{\bar{m}_t^4}{v^2}\left[\frac{\tilde{X}_t}{2} + \ln\frac{M_S^2}{\bar{m}_t^2} + \frac{1}{16\pi^2}\left(\frac{3\bar{m}_t^2}{2v^2} - 8g_3^2\right)\left(\tilde{X}_t \ln\frac{M_S^2}{\bar{m}_t^2} + \ln^2\frac{M_S^2}{\bar{m}_t^2}\right)\right], \quad (2.73)$$

[13] Other approaches include direct diagrammatic calculations and the use of the renormalisation group techniques [217].

where g_3 is the $SU(3)_C$ gauge coupling and $\bar{m}_t = m_t^{\overline{\rm DR}}(m_t^{\overline{\rm DR}})$ is the scale at which the running parameters are evaluated at. In this expression, the SUSY scale is defined by $M_S^2 \equiv M^2 + \bar{m}_t^2$, characterising the size of the stop masses, while the size of the stop mixing is captured by the parameter

$$\tilde{X}_t = \frac{4X_t^2}{y_t^2 v_2^2 M_S^2}\left(1 - \frac{X_t^2}{6y_t^2 v_2^2 M_S^2}\right) . \tag{2.74}$$

In the limit of large $\tan\beta$, Eq. (2.73) provides an approximate upper bound on the lightest CP-even Higgs mass. It is evident from this expression that, in order to reproduce the observed 125 GeV Higgs mass, either the stops should be heavy[14], corresponding to large M_S, or the stop mixing X_t should be large.

However, large radiative corrections associated with the heavy third generation sfermions do not only impact the Higgs masses. From Eq. (2.36), it follows that heavy stops will also generate potentially large corrections through $\Delta V_{\rm MSSM}$, as can be seen by evaluating the relevant terms from the one-loop contribution,

$$\begin{aligned}\frac{(m_Z^{\overline{\rm DR}})^2}{2} = -|\mu|^2 + \frac{m_{H_d}^2 - m_{H_u}^2\tan^2\beta}{\tan^2\beta - 1} + \frac{3}{8\pi}^2 \frac{(m_t^{\overline{\rm DR}})^2}{v^2\cos 2\beta}\Bigg\{(m_{\tilde{t}_1}^{\overline{\rm DR}})^2\left[\ln\frac{(m_{\tilde{t}_1}^{\overline{\rm DR}})^2}{Q^2} - 1\right] \\ + (m_{\tilde{t}_2}^{\overline{\rm DR}})^2\left[\ln\frac{(m_{\tilde{t}_2}^{\overline{\rm DR}})^2}{Q^2} - 1\right]\Bigg\} + \dots ,\end{aligned} \tag{2.75}$$

where Q is the renormalisation scale at which the EWSB conditions are imposed. For large values of $m_{\tilde{t}_{1,2}}^{\overline{\rm DR}} \gg m_Z^{\overline{\rm DR}}$, as required to obtain $m_h \sim 125$ GeV, these corrections threaten to raise the predicted EW scale above its experimental value of ~ 91 GeV.

Heavy stop masses appearing in the higher-order corrections to the MSSM effective potential are not the only source of these problematic large corrections to the EW scale. Large stop masses imply that the running parameters, notably $m_{H_u}^2$ and $m_{H_d}^2$, also receive large corrections generated by the RG evolution down from the scale M_X at which the model's parameters are defined to the EWSB scale. In Eq. (2.75), the running soft parameters $m_{H_d}^2(Q)$, $m_{H_u}^2(Q)$ can then be written in terms of the more "fundamental" parameters $m_{H_d}^2(M_X)$, $m_{H_u}^2(M_X)$ by replacing

$$m_{H_d}^2(Q) = m_{H_d}^2(M_X) + \delta m_{H_d}^2 , \quad m_{H_u}^2(Q) = m_{H_u}^2(M_X) + \delta m_{H_u}^2 . \tag{2.76}$$

[14]For sufficiently high M_S, the calculation of the MSSM Higgs mass should instead be carried out using an effective field theory approach [218–224] (a review of the different approaches may be found in Ref. [205]). This ensures that large logarithmic contributions are resummed; we will briefly revisit this issue in Chapter 6.

Approximate expressions for the size of the radiative corrections $\delta m_{H_d}^2$, $\delta m_{H_u}^2$ can be obtained from the one- and two-loop RGEs for the soft masses, for example, the latter can be estimated at leading-log order by [225]

$$\delta m_{H_u}^2 \sim -\frac{3y_t^2}{8\pi^2}\left[m_{Q_{33}}^2(M_X) + m_{u_{33}^c}^2(M_X) + A_t(M_X)^2\right]\ln\frac{M_X}{Q}\,. \tag{2.77}$$

Complete expressions for the radiative corrections to the other running parameters in this approximation are given in Appendix B. Of course, Eq. (2.77) cannot be expected to be quantitatively accurate for large differences between the scale M_X and Q, such as occurs in the CMSSM where $M_X \sim 10^{16}$ GeV, but it does provide a reasonable estimate for the size of the radiative corrections in low-energy models such as the pMSSM. In either case, it nevertheless highlights the essential point that large stop masses, i.e., large values of $m_{Q_{33}}^2$ and $m_{u_{33}^c}^2$ corresponding to large M_S in Eq. (2.73), will also generate large radiative corrections on the right-hand side of Eq. (2.75). Moreover, it is not just heavy stop masses that have this effect. Unsuccessful searches for the MSSM superpartners, themselves a concrete problem for the model, place increasingly high lower bounds on the other soft parameters [226]. As shown in Appendix B, these parameters also enter into the corrections Eq. (2.76) at one- and two-loop order, and will lead to further large corrections to $m_Z^{\overline{\rm DR}}$ if they are sufficiently large. For the current set of experimental bounds, most of these corrections are subdominant compared to those from the soft masses, but this is not universally the case. In particular, the contribution from the gluino mass, which enters at two-loop order, can be significant [227].

The overall picture that emerges is one in which the apparently large SUSY scale M_S, implied by the observed Higgs mass and lack of observation of superpartners, leads to large radiative corrections that would push up the value of the EW scale characterised by $m_Z^{\overline{\rm DR}}$ [228]. The observed small value of $m_Z^{\overline{\rm DR}}$ then requires a degree of fine tuning between the parameters to explain this little hierarchy between M_Z and M_S [229–232]. Thus, while the MSSM is highly motivated by and solves the "big" hierarchy problem of the SM, it apparently suffers from another naturalness problem, known as the little hierarchy problem. Resolving this tension between the values of M_Z, m_h and M_S is one of the major motivations for considering non-minimal SUSY models. For example, in models with additional matter content, the Higgs mass already receives new contributions at tree-level, from extra F-terms in the scalar potential, that allow the tree-level upper bound to be increased and the need for heavy superpartners to be relaxed. This is exemplified by the model known as the next-to-

MSSM (NMSSM) [233, 234], in which an additional singlet superfield $\hat{S}$ couples to the Higgs doublets according to

$$\hat{W}_{\text{NMSSM}} \supset \lambda \hat{S} \hat{H}_d \cdot \hat{H}_u \,, \tag{2.78}$$

leading to a tree-level upper bound of the form [235, 236]

$$(m_{h_1}^{\overline{\text{DR}}})^2 \lesssim (m_Z^{\overline{\text{DR}}})^2 \cos^2 2\beta + \frac{\lambda^2 v^2}{2} \sin^2 2\beta \,. \tag{2.79}$$

With an increased tree-level upper bound in the NMSSM and similar models with extra matter content or new gauge symmetries, the radiative corrections can be smaller and the amount of fine tuning can potentially be reduced.

The need for the parameters on the right-hand side of Eq. (2.75) to very nearly cancel leads another puzzle in the MSSM, alluded to above in Section 2.3. This cancellation suggests that the μ parameter, a superpotential parameter, should be of a similar size to the soft SUSY breaking parameters $m_{H_d}^2$ and $m_{H_u}^2$. The mass scales in these two sectors are, *a priori*, unrelated. The need to provide a natural explanation for why these two scales should be similar is known as the μ problem in the MSSM [237]. One possible solution is for the μ parameter to share with the soft breaking parameters a hidden sector origin, as is achieved by the Giudice-Masiero mechanism discussed above. However, hidden sector mechanisms are, by construction, difficult to test experimentally. A popular alternative is therefore to extend the MSSM to instead generate an effective μ parameter dynamically. Returning to the NMSSM as an example, if the new singlet scalar field, S, acquires a VEV $\langle S \rangle = s/\sqrt{2}$, then the coupling in Eq. (2.78) will lead to an effective μ parameter, $\mu_{\text{eff}} = \lambda s/\sqrt{2}$. The value of the singlet VEV s will be set by the sizes of the soft parameters, through an additional EWSB condition, and thus the effective μ term is naturally of the same order of magnitude as the soft terms [237]. This possible solution to the μ problem is thus another reason to consider non-minimal SUSY models.

Beyond the above naturalness issues, which are the focus of this thesis, other shortcomings of the MSSM may also find possible solutions by considering non-minimal extensions. To give just a few examples,

- In the ordinary MSSM, neutrinos are massless like in the SM. Thus neutrino oscillations are currently one of the strongest pieces of evidence for the need to extend the model to accommodate massive neutrinos. Some mechanism should also account for the minuscule size of the neutrino masses, such as through radia-

tive mass generation [238–240] or a see-saw mechanism, which can be achieved in non-minimal models [241, 242].

- Acceptable baryogenesis, i.e., reproducing the observed baryon-antibaryon asymmetry, is difficult to achieve in the MSSM, as its ability to generate the required first order phase transition is restricted [243]. Non-minimal models, on the other hand, provide various ways of meeting the necessary conditions for successful baryogenesis [244], and so are more promising than the MSSM in this respect [245, 246].

- Gauge coupling unification at high energies is significantly improved in the MSSM compared to the SM [247–250], though it is still not exact (absent the effects of unknown threshold corrections at least). This suggests the possibility of embedding the MSSM particle content into a GUT model [83], such as those based on $SO(10)$ or E_6 [251]. In this case, the MSSM states are embedded in larger GUT multiplets, which may or may not lead to additional exotic states at the TeV scale.

- Constrained models such as the CMSSM are based on the possible inclusion of gravitational interactions through supergravity. However, minimal SUGRA (mSUGRA) is non-renormalisable, and should be regarded as an effective field theory description of an underlying theory that includes gravity [104]. Candidates for this theory, such as ten-dimensional heterotic $E_8 \times E_8'$ superstring theory [252, 253], can naturally lead to non-minimal SUSY models at low energies.

Taken together, the above issues provide good reasons to think that the minimal extension of the SM to be compatible with SUSY might not be enough, and motivate the study of non-minimal SUSY models instead. As an added bonus, many non-minimal models also lead to exotic collider phenomenology and possible new signals through which the model can be discovered. Motivated by the above arguments, we explore one such class of models that, at low energies, contain extra matter content beyond the MSSM and possess an extra $U(1)$ gauge symmetry.

Chapter 3

E_6 Inspired Supersymmetric Models

3.1 $U(1)$ Extensions of the MSSM

The MSSM is almost fully determined from the requirement that it be the minimal extension of the SM consistent with SUSY, but it is by no means the unique possible realisation of low-energy SUSY. Once the requirement for minimality is dropped, many different types of non-minimal models can be constructed. Most of these are in varying degrees motivated by the goal of addressing issues such as those discussed in Section 2.6, and all have their own advantages and disadvantages, which can be used to assess their relative merits.

The NMSSM, mentioned previously, is the simplest example of a non-minimal SUSY model. It extends the MSSM by the addition of a SM singlet superfield $\hat{S}$ while leaving all other aspects of the model unchanged. In the common case that a Z_3 symmetry is imposed to forbid new dimensionful superpotential parameters, the superpotential of the scale invariant NMSSM reads [235, 236, 254–257]

$$\hat{W}_{\text{NMSSM}} = \hat{W}_{\text{MSSM}}(\mu = 0) + \lambda \hat{S} \hat{H}_d \cdot \hat{H}_u + \frac{1}{3}\kappa \hat{S}^3 \,, \tag{3.1}$$

where $\hat{W}_{\text{MSSM}}(\mu = 0)$ is the MSSM superpotential, Eq. (2.1), with $\mu = 0$. The second term on the right-hand side leads to an effective μ term once S develops a VEV, allowing the NMSSM to solve the μ problem. The last term is necessary to break the global PQ symmetry that would be present otherwise and would lead to a physically unacceptable axion in the spectrum once it is spontaneously broken by the VEV of

S [233]. As noted above, with this simple expansion of the MSSM matter content, the μ problem can be solved and the Higgs mass increased at tree-level. Indeed, the NMSSM may also fare better than the MSSM when it comes to some of the other problems listed in Section 2.6; for example, in the NMSSM successful baryogenesis may be more easily achieved given the current experimental limits [258–260].

On the other hand, being such a simple extension the usual NMSSM still leaves some questions unanswered, such as the origin of neutrino masses. Furthermore, new problems arise in the NMSSM that are absent in the MSSM. The Z_3 symmetry implies that domain walls should have formed between parts of the early Universe that were causally disconnected during the EW phase transition [261]. Domain walls like this would be in conflict with observations of the CMB, however [261]. The most straightforward methods of solving this problem, by breaking the Z_3 symmetry, encounter another problem [262]. Since the new field is a singlet, it may couple to heavy degrees of freedom that might be expected to be present in an underlying GUT model, for instance. Such a coupling would in general induce large tadpole terms, linear in $\hat{S}$, in the superpotential and soft SUSY breaking Lagrangian at lower energies. These terms, which would generically be expected to be of order $\sim M_S M_X$ for the superpotential tadpole and $\sim M_S^2 M_X$ for the soft breaking tadpole, would in turn lead to a singlet VEV far larger than the EW or SUSY scale. As a result, the EW scale is once again destabilised, a naturalness problem known as the "tadpole problem" in the NMSSM [234, 263].

In the context of GUT models, the problematic couplings of the singlet to heavy degrees of freedom can be prevented if $\hat{S}$ is not a singlet under the full, unified gauge group. This suggests the possibility that a further, relatively straightforward extension of the model could be used to cure these problems. That is, by extending the gauge symmetry group as well as the matter content of the MSSM, the positive aspects of the NMSSM can be retained while also avoiding some of its problems. One of the simplest options is to consider models in which the SM gauge group is augmented with an additional $U(1)'$ symmetry. In addition to being arguably less complicated than additional non-Abelian gauge symmetries, $U(1)$ extensions of the SM are also very well motivated [264]. Models with one or more additional $U(1)$'s appear frequently when the SM gauge group emerges as the unbroken subgroup of a larger gauge group, and can emerge naturally in string inspired theories [264–277].

An acceptable $U(1)$ extension of the MSSM (USSM) that also solves the μ problem, with the gauge group

$$G = SU(3)_C \times SU(2)_L \times U(1)_Y \times U(1)' \,, \tag{3.2}$$

should at least incorporate the interactions of the MSSM and an effective μ term,

$$\hat{W}_{\text{USSM}} \supset \hat{W}_{\text{MSSM}}(\mu = 0) + \lambda \hat{S} \hat{H}_d \cdot \hat{H}_u \,, \tag{3.3}$$

where it is now assumed that $\hat{S}$, $\hat{H}_d$ and $\hat{H}_u$ are charged under $U(1)'$, while $\hat{S}$ is still a singlet under the SM gauge group. An elementary μ term can be forbidden by appropriate choice of the $U(1)'$ charges, as can the $\hat{S}^3$ term present in the NMSSM. This latter term is rendered unnecessary when the previous global PQ symmetry can be absorbed by the gauged $U(1)'$ [278], and the absence of the discrete Z_3 symmetry means that the formation of domain walls is avoided. In place of an unacceptable axion, the breakdown of $U(1)'$ when S develops a VEV leads to a massive Z' boson. The prospect of exciting phenomenology associated with the new Z' has generated significant interest in $U(1)$ extensions in the literature [229, 265, 267, 268, 270–275]. Since the Higgs doublets and $\hat{S}$ are charged under $U(1)'$, in addition to new F-terms in the scalar potential, extra $U(1)'$ D-terms can also persist in the scalar potential at the scale of gauge symmetry breaking [279, 280]. These extra contributions allow for the upper bound on the tree-level Higgs mass to be further increased [281–283] compared to the NMSSM. $U(1)$ extensions therefore have the potential to reduce even more the fine tuning associated with a 125 GeV Higgs mass.

While $U(1)$ extensions of the MSSM offer attractive solutions to some of its problems, they are also subject to restrictions that make their construction more involved than a simple singlet extension of the MSSM. Prominent among these is the requirement that the $U(1)'$ symmetry be non-anomalous. The need to avoid introducing gauge anomalies leads in general to non-trivial model building complications; for example, ensuring an anomaly free theory is one of the hurdles in successfully implementing SSB via the Fayet-Iliopoulos mechanism [103]. For an arbitrary $U(1)'$, anomaly cancellation requires that either the $U(1)'$ charges are family non-universal, or additional exotic fermions must be included in the model [264]. Thus if the $U(1)'$ charges are to be family universal, $U(1)$ extensions must necessarily extend the matter content of the MSSM as well, which may lead to interesting experimental signatures [278, 284–292]. An elegant approach to ensure anomaly cancellation is to have the $U(1)'$ arise as part of an unbroken subgroup of a larger, anomaly free group, rather than assigning $U(1)'$

charges in an ad hoc manner. In this scenario, anomalies are avoided provided that the matter content fills complete representations of the larger gauge group, or at least provided that any incomplete multiplets are present only in vector-like pairs so that their contributions to gauge anomalies cancel.

Viable models that take this approach can, for instance, be constructed from underlying $SO(10)$ or E_6 GUTs [269]. Models based on E_6 or one of its subgroups near the GUT scale can in particular be motivated by the fact that they arise naturally from the description of gravity provided by ten-dimensional $E_8 \times E_8'$ heterotic string theory [293–299]. Compactification of the additional six dimensions results in the breaking of E_8 to E_6 or one of its subgroups in the visible sector [299]. The remaining unbroken E_8' constitutes a hidden sector within which the spontaneous breakdown of SUGRA takes place. The visible and hidden sectors are only coupled through gravitational strength interactions, allowing the breaking of SUSY to be communicated from the hidden to the visible sector and generating a set of soft SUSY breaking parameters [182, 183], as discussed in Section 2.3.

The subsequent breakdown of E_6 may lead to low-energy models based on rank-5 or rank-6 gauge groups [300], since E_6 is itself a rank-6 group [301]. For instance, at the string scale[1] E_6 may be broken via the Hosotani mechanism [307] directly to

$$E_6 \to SU(3)_C \times SU(2)_L \times U(1)_Y \times U(1)_\chi \times U(1)_\psi \,, \tag{3.4}$$

where the two new $U(1)$ factors are those associated with the subgroups $E_6 \supset SO(10) \times U(1)_\psi \supset SU(5) \times U(1)_\chi \times U(1)_\psi$ [264, 269]. Further symmetry breaking can then reduce this rank-6 group to a rank-5 group with a single additional $U(1)'$, as given in Eq. (3.2), where the remaining $U(1)'$ is a linear combination of $U(1)_\chi$ and $U(1)_\psi$,

$$U(1)' = U(1)_\chi \cos\theta_{E_6} + U(1)_\psi \sin\theta_{E_6} \,. \tag{3.5}$$

The mixing angle θ_{E_6} characterises the resulting $U(1)'$ at low energies and depends on the choice of symmetry breaking pattern (for reviews of the various cases considered in the literature, see for example Refs. [264, 269, 308]). As noted above, the resulting model will be free of gauge anomalies provided that the low-energy matter content fills in complete representations of E_6. Since the fundamental representation of E_6 is 27-dimensional, this implies that the matter content of the SM and MSSM must be augmented with additional exotic states. The three generations of SM states can

[1] In the strong coupling regime of the ten-dimensional $E_8 \times E_8'$ string theory [302, 303], this scale can be comparable with the GUT scale [304–306].

be successfully accommodated in three **27**-plets of E_6. Each **27**-plet, $\mathbf{27}_i$, can be decomposed in terms of $SU(5)\times U(1)_\chi \times U(1)_\psi$ representations according to [264, 300]

$$\begin{aligned}\mathbf{27}_i \to &\left(\mathbf{10}, \frac{1}{\sqrt{24}}, -\frac{1}{\sqrt{40}}\right)_i + \left(\bar{\mathbf{5}}, \frac{1}{\sqrt{24}}, \frac{3}{\sqrt{40}}\right)_i + \left(\mathbf{1}, \frac{1}{\sqrt{24}}, -\frac{5}{\sqrt{40}}\right)_i \\ &+ \left(\bar{\mathbf{5}}, -\frac{2}{\sqrt{24}}, -\frac{2}{\sqrt{40}}\right)_i + \left(\mathbf{5}, -\frac{2}{\sqrt{24}}, \frac{2}{\sqrt{40}}\right)_i + \left(\mathbf{1}, \frac{4}{\sqrt{24}}, 0\right)_i . \end{aligned} \tag{3.6}$$

The SM states can be assigned to the first two factors, with $\hat{Q}_i$, $\hat{u}^c_i$, $\hat{e}^c_i$ being assigned to the first term and $\hat{L}_i$ and $\hat{d}^c_i$ to the second. The state assigned to the third term on the first line, $\hat{N}^c_i$, is a singlet under the SM gauge group, and can be identified with a right-handed neutrino. The multiplets in the second line contain new exotic states in each generation. The last term contains another SM singlet, $\hat{S}_i$. The components of the first term can be identified with a down-type Higgs doublet $\hat{H}_{di}$ and an $SU(2)_L$ singlet, colour triplet $\hat{\overline{D}}_i$, while the second contains an up-type Higgs $\hat{H}_{ui}$ and a colour triplet $\hat{D}_i$. The $U(1)_\psi$ and $U(1)_\chi$ charge assignments for the components of a single **27**-plet are summarised in Table 3.1. The doublets $\hat{H}_{ui}$ and $\hat{H}_{di}$ may be identified

	$\hat{Q}_i$	$\hat{u}^c_i$	$\hat{e}^c_i$	$\hat{L}_i$	$\hat{d}^c_i$	$\hat{N}^c_i$	$\hat{H}_{di}$	$\hat{\overline{D}}_i$	$\hat{H}_{ui}$	$\hat{D}_i$	$\hat{S}_i$
$\sqrt{\frac{5}{3}}Q^Y_i$	$\frac{1}{6}$	$-\frac{2}{3}$	1	$-\frac{1}{2}$	$\frac{1}{3}$	0	$-\frac{1}{2}$	$\frac{1}{3}$	$\frac{1}{2}$	$-\frac{1}{3}$	0
$2\sqrt{6}Q^\psi_i$	1	1	1	1	1	1	-2	-2	-2	-2	4
$2\sqrt{10}Q^\chi_i$	-1	-1	-1	3	3	-5	-2	-2	2	2	0

Table 3.1: The $U(1)_Y$, $U(1)_\psi$ and $U(1)_\chi$ charges of the chiral superfields contained within each **27**-plet of E_6.

as Higgs or inert Higgs doublets, the distinction being that the latter do not develop VEVs. The states $\hat{\overline{D}}_i$ and $\hat{D}_i$ have electric charge $\pm 1/3$ and carry $B-L$ charge twice that of ordinary quarks, and therefore may either be diquarks or leptoquarks.

The compelling theoretical motivation for these E_6 inspired models and the potential for interesting phenomenology associated with the above exotic states, along with at least one Z' boson associated with the breakdown of $U(1)'$, has garnered this class of models a great deal of attention in the past [229, 265, 267, 268, 270–275]. Possible signatures of the exotic states at colliders have been studied [309], as well as limits on the Z' mass [310]. In addition to observing these exotic states, an underlying E_6 GUT might leave identifiable fingerprints on the ordinary MSSM mass spectrum, such as in the pattern of first and second generation sfermion masses [311]. As these models

contain additional singlets, which may get VEVs, and have an extended gauge sector, they are able to solve the μ problem and raise the tree-level upper bound on the lightest Higgs mass above that in the NMSSM [286, 312–314], without the accompanying domain wall and tadpole problems. The accompanying enlarged Higgs [278, 313, 314] and neutralino [314–325] sectors have been extensively studied. Among the other possible avenues to be explored in models based on E_6, it has been proposed that the extra D-terms could solve the tachyon problems encountered in anomaly mediated SUSY breaking scenarios [326], while the inclusion of appropriate family symmetries could provide an explanation for the hierarchy of fermion masses and mixings [327–330]. Indeed, many further implications of these models have been considered, including for EWSB [276, 277, 312, 315, 331–333], neutrino physics [241, 242], leptogenesis [245, 246] and EW baryogenesis [334, 335], the muon anomalous magnetic moment [336, 337], electric dipole moments [316, 317], lepton flavour violating processes [318] and the possibility of CP-violation in the extended Higgs sector [338].

3.2 The Exceptional Supersymmetric Standard Model

A given low-energy, E_6 inspired model is characterised by a choice of symmetry breaking pattern, and hence the value of θ_{E_6}, as well as the matter multiplets that it contains. In the rank-5 model described by Eq. (3.5) both the singlets $\hat{S}_i$ and the right-handed neutrinos $\hat{N}_i^c$ are charged under the additional $U(1)'$, in general. For example, of the choices for $U(1)'$ shown in Table 3.2, the right-handed neutrinos carry charge in the $U(1)_\chi$, $U(1)_\psi$, $U(1)_\eta$ [298], and inert $U(1)_I$ [339] models. However, for

$U(1)'$	$\theta_{E_6} \in [-\pi, \pi)$
$U(1)_\chi$	0
$U(1)_\psi$	$\frac{\pi}{2}$
$U(1)_N$	$\arctan\sqrt{15}$
$U(1)_\eta$	$-\arctan\sqrt{\frac{5}{3}}$
$U(1)_I$	$\arctan\sqrt{\frac{3}{5}} - \pi$

Table 3.2: Values of θ_{E_6} for several commonly studied E_6 inspired models. The E$_6$SSM corresponds to the choice $U(1)' = U(1)_N$.

the choice of $\theta_{E_6} = \arctan\sqrt{15}$, the right-handed neutrinos are uncharged under the resulting $U(1)'$, denoted $U(1)_N$ [241, 242, 278, 340]. In this case, the right-handed

neutrinos N_i^c are total gauge singlets and are allowed to have superheavy Majorana masses. The see-saw mechanism can then be used to explain the observed neutrino masses and oscillations. Additionally, because the right-handed neutrinos are very heavy, they may generate a lepton asymmetry in the early Universe through their decays into states with $L = \pm 1$. This lepton asymmetry may subsequently be converted into the observed baryon asymmetry through the action of EW sphalerons [341, 342]. E_6 inspired SUSY models based on $U(1)_N$ are thus able to explain both the origin of neutrino masses and the baryon asymmetry through leptogenesis [245, 246], both of which are problems for the MSSM.

In this thesis, we focus on the particular E_6 inspired SUSY model with an additional $U(1)_N$ gauge symmetry known as the E$_6$SSM [278, 284]. Several different variants of the E$_6$SSM have been proposed and studied in the past [278, 284, 288, 289, 300, 328, 329, 343–348]. More generally, E_6 inspired SUSY models with $U(1)' = U(1)_N$ have been thoroughly investigated. For example, the possibility of mixing between doublet and singlet neutrinos [241], the effects of $Z - Z'$ mixing [319], the neutralino sector [315, 319, 320], the implications of the exotic states for dark matter [349], the renormalisation group flow [315, 350–353] and EWSB in the models [312, 315, 331] have all been considered. In the specific case of the E$_6$SSM, progress has also been made in calculating important radiative and higher-order corrections; the renormalisation of the VEVs that lead to EWSB has been calculated [354, 355], as have the effects of threshold corrections from heavy exotic states [356] necessary for matching the model to the MSSM below the mass scale of the exotics.

At low energies, the matter content of the E$_6$SSM is assumed to consist of the MSSM chiral superfields as well as exotic superfields, all contained within three complete **27**-plets of E_6. The assignment of the states is carried out as described following Eq. (3.6). With only these multiplets in the model, the unification of gauge couplings would not occur [264]. Gauge unification can be restored by adding additional states from additional incomplete multiplets in vector-like pairs, so as not to introduce gauge anomalies [333]. In the usual formulation of the E$_6$SSM, an $SU(2)$ doublet and anti-doublet, $\hat{L}_4$ and $\overline{\hat{L}}_4$, from incomplete $\mathbf{27}'$ and $\bar{\mathbf{27}}'$ multiplets are included for this purpose[2]. With these additional incomplete multiplets in the model, the gauge coupling running in the E$_6$SSM at the two-loop level in fact leads to unification more precisely than in the MSSM [350]. The chiral and vector superfields of the model are summarised in Table 3.3 and Table 3.4.

[2]Alternatively, if $\hat{L}_4$ and $\overline{\hat{L}}_4$ are not introduced it is possible to construct the model in such a way that two-step unification takes place instead [288, 343].

Supermultiplet	Spin-0	Spin-1/2	$SU(3)_C$	$SU(2)_L$	$\sqrt{\frac{5}{3}}Q_Y$	$\sqrt{40}Q_N$
$\hat{Q}_i$	$\begin{pmatrix}\tilde{u}_L\\ \tilde{d}_L\end{pmatrix}_i$	$\begin{pmatrix}u_L\\ d_L\end{pmatrix}_i$	**3**	**2**	$\frac{1}{6}$	1
$\hat{u}_i^c$	$\tilde{u}_{iR}^*$	u_{iR}^c	**3**	**1**	$-\frac{2}{3}$	1
$\hat{e}_i^c$	$\tilde{e}_{iR}^*$	e_{iR}^c	**1**	**1**	1	1
$\hat{L}_i$	$\begin{pmatrix}\tilde{\nu}_L\\ \tilde{e}_L\end{pmatrix}_i$	$\begin{pmatrix}\nu_L\\ e_L\end{pmatrix}_i$	**1**	**2**	$-\frac{1}{2}$	2
$\hat{d}_i^c$	$\tilde{d}_{iR}^*$	d_{iR}^c	**3**	**1**	$\frac{1}{3}$	2
$\hat{H}_{di}$	$\begin{pmatrix}H_{di}^0\\ H_{di}^-\end{pmatrix}$	$\begin{pmatrix}\tilde{H}_{di}^0\\ \tilde{H}_{di}^-\end{pmatrix}$	**1**	**2**	$-\frac{1}{2}$	-3
$\hat{\overline{D}}_i$	$\tilde{\overline{D}}_i$	$\overline{D}_i$	**3**	**1**	$\frac{1}{3}$	-3
$\hat{H}_{ui}$	$\begin{pmatrix}H_{ui}^+\\ H_{ui}^0\end{pmatrix}$	$\begin{pmatrix}\tilde{H}_{ui}^+\\ \tilde{H}_{ui}^0\end{pmatrix}$	**1**	**2**	$\frac{1}{2}$	-2
$\hat{D}_i$	$\tilde{D}_i$	D_i	**3**	**1**	$-\frac{1}{3}$	-2
$\hat{S}_i$	S_i	$\tilde{S}_i$	**1**	**1**	0	5
$\hat{N}_i^c$	$\tilde{N}_{iR}^*$	N_{iR}^c	**1**	**1**	0	0
$\hat{L}_4$	$\begin{pmatrix}L_4^0\\ L_4^-\end{pmatrix}$	$\begin{pmatrix}\tilde{L}_4^0\\ \tilde{L}_4^-\end{pmatrix}$	**1**	**2**	$-\frac{1}{2}$	2
$\hat{\overline{L}}_4$	$\begin{pmatrix}\overline{L}_4^+\\ \overline{L}_4^0\end{pmatrix}$	$\begin{pmatrix}\tilde{\overline{L}}_4^+\\ \tilde{\overline{L}}_4^0\end{pmatrix}$	**1**	**2**	$\frac{1}{2}$	-2

Table 3.3: Summary of the chiral superfields of the E$_6$SSM, showing their representations under $SU(3)_C$ and $SU(2)_L$, and their $U(1)_Y$ and $U(1)_N$ charges.

In principle, the most general low-energy superpotential of the E$_6$SSM would contain all those couplings that respect the E_6 gauge symmetry, as well as a set of E_6 violating interactions[3] that nonetheless are allowed by the remaining $SU(3)_C \times SU(2)_L \times U(1)_Y \times U(1)_N$ gauge symmetry. The most general low-energy superpotential [278] can thus be written

$$\hat{W}_{\mathrm{E_6SSM}} = \hat{W}_0 + \hat{W}_1 + \hat{W}_2 + \frac{1}{2}M_{ij}\hat{N}_i^c\hat{N}_j^c + \hat{W}_0' + \hat{W}_1' + \hat{W}_2', \tag{3.7}$$

[3]Either because they are not invariant under E_6 or only involve incomplete E_6 multiplets [278].

Supermultiplet	Spin-1/2	Spin-1	$SU(3)_C$	$SU(2)_L$	$\sqrt{\frac{5}{3}}Q_Y$	$\sqrt{40}Q_N$
$\hat{G}$	$\tilde{g}$	g	**8**	**1**	0	0
$\hat{W}$	$\tilde{W}^{\pm}$, $\tilde{W}^0$	$W^{\pm}$, W^0	**1**	**3**	0	0
$\hat{B}$	$\tilde{B}$	B	**1**	**1**	0	0
$\hat{B}'$	$\tilde{B}'$	B'	**1**	**1**	0	0

Table 3.4: Summary of the vector superfields of the E$_6$SSM and their transformation properties under the gauge symmetries.

where $\hat{W}_0$, $\hat{W}_1$ and $\hat{W}_2$ contain the E_6 invariant interactions and the remaining terms, including the Majorana masses for the right-handed neutrinos M_{ij}, break E_6. The contributions to Eq. (3.7) that are consistent with the E_6 gauge symmetry read

$$\begin{aligned}\hat{W}_0 &= \lambda_{ijk}\hat{S}_i\hat{H}_{dj}\cdot\hat{H}_{uk} + \kappa_{ijk}\hat{S}_i\hat{D}_j\hat{\overline{D}}_k + h^N_{ijk}\hat{N}^c_i\hat{H}_{uj}\cdot\hat{L}_k \\ &\quad + y^U_{ijk}\hat{u}^c_i\hat{H}_{uj}\cdot\hat{Q}_k + y^D_{ijk}\hat{d}^c_i\hat{Q}_j\cdot\hat{H}_{dk} + y^E_{ijk}\hat{e}^c_i\hat{L}_j\cdot\hat{H}_{dk}\,, \qquad (3.8a)\\ \hat{W}_1 &= g^Q_{ijk}\hat{D}_i\hat{Q}_j\cdot\hat{Q}_k + g^q_{ijk}\hat{\overline{D}}_i\hat{d}^c_j\hat{u}^c_k\,, \qquad (3.8b)\\ \hat{W}_2 &= \tilde{g}^N_{ijk}\hat{N}^c_i\hat{D}_j\hat{d}^c_k + \tilde{g}^E_{ijk}\hat{e}^c_i\hat{D}_j\hat{u}^c_k + \tilde{g}^D_{ijk}\hat{Q}_i\cdot\hat{L}_j\hat{\overline{D}}_k\,, \qquad (3.8c)\end{aligned}$$

while the E_6 violating contributions are

$$\begin{aligned}\hat{W}'_0 &= \mu_L\hat{L}_4\cdot\hat{\overline{L}}_4 + \mu'_i\hat{\overline{L}}_4\cdot\hat{L}_i + h_{ij}\hat{N}^c_i\hat{H}_{uj}\cdot\hat{L}_4 - h^E_{ij}\hat{e}^c_i\hat{H}_{dj}\cdot\hat{L}_4\,, \qquad (3.9a)\\ \hat{W}'_1 &= \frac{1}{3}\sigma_{ijk}\hat{N}^c_i\hat{N}^c_j\hat{N}^c_k + \Lambda_k\hat{N}^c_k + \lambda_{ij}\hat{S}_i\hat{H}_{dj}\cdot\hat{\overline{L}}_4 + g^N_{ij}\hat{N}^c_i\hat{\overline{L}}_4\cdot\hat{L}_j \\ &\quad + g^N_i\hat{N}^c_i\hat{\overline{L}}_4\cdot\hat{L}_4 + g^U_{ij}\hat{u}^c_i\hat{\overline{L}}_4\cdot\hat{Q}_j + \mu_{ij}\hat{H}_{ui}\cdot\hat{L}_j + \mu_i\hat{H}_{ui}\cdot\hat{L}_4 + \mu'_{ij}\hat{D}_i\hat{d}^c_j\,, \qquad (3.9b)\\ \hat{W}'_2 &= -g^D_{ij}\hat{Q}_i\cdot\hat{L}_4\hat{\overline{D}}_j\,. \qquad (3.9c)\end{aligned}$$

However, a model based on this superpotential would suffer from severe phenomenological problems. Although the difference $B-L$ is conserved in the E_6 preserving part of the superpotential[4], there is no consistent choice for the baryon and lepton numbers of $\hat{D}_i$ and $\hat{\overline{D}}_i$ that does not lead to B or L violation, if all terms in $\hat{W}_1$ and $\hat{W}_2$ are simultaneously present [300]. The general Yukawa couplings also allow flavour mixing and would imply the existence of FCNCs well above experimental limits.

Following the approach adopted in the MSSM, the model can be rescued by imposing a set of discrete symmetries to forbid the potentially dangerous operators. In the E$_6$SSM, this is made more complicated by the fact that there are multiple possible

[4]This is the case since $U(1)_{B-L}$ symmetry is a linear combination of $U(1)_Y$ and $U(1)_\chi$ [300].

choices that generalise R-parity in the MSSM [357]; of these, only two are compatible with successful leptogenesis [245]. It is also the case that, in the simplest variants of the E$_6$SSM, imposing a single discrete symmetry is not enough to prevent violations of experimental limits. In these models, agreement with experimental data can only be achieved by the imposition of at least

- One of the two acceptable exact Z_2 symmetries to forbid dangerous B and L violating operators. The two possible choices remove different subsets of terms from the general superpotential, and imply differing properties for the exotic $\hat{D}_i$, $\hat{\overline{D}}_i$ states. The first possibility is an exact Z_2^B symmetry, under which the lepton superfields and the exotic $\hat{D}_i$, $\hat{\overline{D}}_i$, $\hat{L}_4$ and $\hat{\overline{L}}_4$ superfields are odd and all others are even. The only other possibility is an exact Z_2^L under which only the lepton superfields and $\hat{L}_4$, $\hat{\overline{L}}_4$ are odd and all others are even. In the former case, all of the terms in $\hat{W}_1$ as well as $\hat{W}_1'$ are forbidden, and the exotic $\hat{D}_i$, $\hat{\overline{D}}_i$ superfields can be assigned non-zero B and L numbers simultaneously, identifying them as leptoquarks. In the case of invariance under Z_2^L, they may be assigned baryon number twice that of the ordinary quarks and so are diquarks, and all terms in $\hat{W}_2$, $\hat{W}_1'$ and $\hat{W}_2'$ are excluded.

- An approximate Z_2^H symmetry to suppress unacceptable FCNCs. To do so, it is first assumed that by appropriate field rotations only one generation of the Higgs and singlet superfields have scalar components that develop VEVs, with the Yukawa couplings chosen appropriately to ensure this. This is conventionally identified with the third generation, i.e., $\hat{H}_d \equiv \hat{H}_{d3}$, $\hat{H}_u \equiv \hat{H}_{u3}$ and $\hat{S} \equiv \hat{S}_3$ where $\langle H_d \rangle$, $\langle H_u \rangle$ and $\langle S \rangle$ are non-zero. This set of superfields is then assumed to be even under Z_2^H, while all others are odd, which has the effect of forbidding the couplings of the additional, inert Higgs doublets to the SM fermions, for instance. However, Z_2^H cannot be exact as otherwise all interactions allowing decays of the exotic quarks would be forbidden. Stringent limits [358–360] on the concentration of these states after their production in the early Universe [361, 362] rule this possibility out; thus, Z_2^H must be violated by small but non-zero Yukawa couplings of order $\sim 10^{-4} - 10^{-3}$ that respect the exact Z_2^B or Z_2^L symmetry [278, 363].

In the E$_6$SSM, it is also expected that the LSP and next-to-LSP (NLSP) would in general no longer be MSSM–like neutralinos[5], and would have masses that are roughly

[5]That is, neutralinos that are predominantly a mixture of the third generation Higgsinos $\tilde{H}_d$ and $\tilde{H}_u$ and the usual gauginos $\tilde{W}_3$ and $\tilde{B}$.

$60 - 65$ GeV [364–369]. These light states previously were investigated as viable DM candidates [349], but are now known to be ruled out by direct detection searches for DM [370–374] and limits on the exotic decays of the SM Higgs [367]. A viable modification of the E$_6$SSM [375] is to introduce a further Z_2^S [344] symmetry to suppress such exotic Higgs decays and to prevent the decays of the lightest MSSM–like neutralino into the LSP and NLSP. All of the above discrete symmetries do not commute with E_6, since different components within the same **27**-plet transform differently under their action. The need to introduce multiple exact and approximate Z_2 symmetries is an unattractive aspect of the simplest versions of the E$_6$SSM. It can be avoided in more complicated constructions [100, 101, 300, 347, 352], as shall be discussed in Chapter 6.

Once the necessary set of discrete symmetries has been imposed, the general superpotential Eq. (3.7) simplifies substantially. For concreteness, in the case that an exact Z_2^B symmetry is imposed the approximate superpotential at low energies can be written [363, 376]

$$\begin{aligned}\hat{W}_{\rm E_6SSM} \approx \hat{W}_{\rm MSSM}(\mu=0) + \lambda\hat{S}\hat{H}_d\cdot\hat{H}_u + \tilde{\lambda}_{\alpha\beta}\hat{S}\hat{H}_{d\alpha}\cdot\hat{H}_{u\beta} + \tilde{f}_{\alpha\beta}\hat{S}_\alpha\hat{H}_u\cdot\hat{H}_{d\beta} \\ + f_{\alpha\beta}\hat{S}_\alpha\hat{H}_{u\beta}\cdot\hat{H}_d + \kappa_{ij}\hat{S}\hat{D}_i\hat{\overline{D}}_j + \mu_L\hat{L}_4\cdot\hat{\overline{L}}_4\,,\end{aligned} \tag{3.10}$$

after integrating out the heavy right-handed neutrinos $\hat{N}_i^c$ and retaining only those Yukawa couplings that can be non-negligible. By making appropriate rotations of the superfields $(\hat{H}_{d\alpha}, \hat{H}_{u\alpha})$ and $(\hat{D}_i, \hat{\overline{D}}_i)$, the trilinear couplings $\tilde{\lambda}_{\alpha\beta}$ and κ_{ij} are chosen to be flavour diagonal, while the other new couplings $\tilde{f}_{i\alpha}$, $f_{i\alpha}$ are not, in general. Similarly, the inert Higgs doublets and $\hat{L}_4$, $\hat{\overline{L}}_4$ superfields are redefined to take $\mu_i' = 0$ [278]. The Higgs and singlet Yukawa couplings are expected to satisfy $\kappa_{ij}, \lambda \equiv \lambda_3 \gtrsim \tilde{\lambda}_{\alpha\beta} \gg f_{\alpha\beta}, \tilde{f}_{\alpha\beta}$ [363, 376] so that only H_d, H_u and S develop VEVs. An elementary μ term is forbidden by the $U(1)_N$ symmetry[6], but the superpotential still contains a bilinear term for the $\hat{L}_4$ and $\hat{\overline{L}}_4$ superfields. In principle, one might be concerned that this reintroduces a version of the μ problem in the model [264]. However, μ_L does not play a role in EWSB and so is not constrained to be of the order of the EWSB or soft mass scales. The principal restriction on μ_L in this model is that it be chosen so that approximate gauge unification is preserved, which can be achieved when μ_L is of the order of several TeV, depending on the values of the additional dimensionless couplings [350, 356]. The $\hat{L}_4\cdot\hat{\overline{L}}_4$ bilinear can then be induced following the breakdown of local

[6]This is not the case in general for other choices of $U(1)'$, e.g., a μ term for $\hat{H}_d$ and $\hat{H}_u$ is allowed under $U(1)_\chi$.

SUSY if the Kähler potential contains an extra term of the form $(\hat{X}_L\hat{L}_4\cdot\hat{\overline{L}}_4 + h.c.)$ [377] through the Giudice-Masiero mechanism.

Like in the MSSM, the superpotential interactions must be supplemented by a set of soft SUSY breaking interactions. The standard set of soft terms consistent with gauge invariance in the E$_6$SSM are

$$\begin{aligned}
-\mathcal{L}^{\rm soft}_{\rm E_6SSM} = {} & m^2_{H_u}|H_u|^2 + m^2_{H_d}|H_d|^2 + m^2_S|S|^2 + m^2_{H_{2,\alpha\beta}}(H_{u\alpha})^\dagger H_{u\beta} + m^2_{H_{1,\alpha\beta}}(H_{d\alpha})^\dagger H_{d\beta} \\
& + m^2_{\Sigma_{\alpha\beta}}S^\dagger_\alpha S_\beta + m^2_{D_{ij}}D^\dagger_i D_j + m^2_{\overline{D}_{ij}}\overline{D}^\dagger_i\overline{D}_j + m^2_{L_4}|L_4|^2 + m^2_{\overline{L}_4}|\overline{L}_4|^2 \\
& + m^2_{Q_{ij}}\tilde{Q}^\dagger_i\tilde{Q}_j + m^2_{u^c_{ij}}(\tilde{u}^c_i)^\dagger\tilde{u}^c_j + m^2_{d^c_{ij}}(\tilde{d}^c_i)^\dagger\tilde{d}^c_j + m^2_{L_{ij}}\tilde{L}^\dagger_i\tilde{L}_j \\
& + m^2_{e^c_{ij}}(\tilde{e}^c_i)^\dagger\tilde{e}^c_j + \left(\mu_L B_L L_4\cdot\overline{L}_4 + h.c.\right) \\
& + \Big(T_\lambda S H_d\cdot H_u + T^\kappa_{ij}S D_i\overline{D}_j + T^U_{ij}\tilde{u}^c_i H_u\cdot\tilde{Q}_j + T^D_{ij}\tilde{d}^c_i\tilde{Q}_j\cdot H_d \\
& + T^E_{ij}\tilde{e}^c_i\tilde{L}_j\cdot H_d + T^{\tilde{\lambda}}_{\alpha\beta}S H_{d\alpha}\cdot H_{u\beta} + T^{\tilde{f}}_{\alpha\beta}S_\alpha H_u\cdot H^d_\beta + T^f_{\alpha\beta}S_\alpha H^u_\beta\cdot H_d\Big) \\
& + \frac{1}{2}\Big(M_1\tilde{B}\tilde{B} + M_2\tilde{W}\tilde{W} + M_3\tilde{G}\tilde{G} + M_1'\tilde{B}'\tilde{B}' + 2M_{11}\tilde{B}\tilde{B}' + h.c.\Big). \quad (3.11)
\end{aligned}$$

The general soft SUSY breaking Lagrangian, in which all of the soft parameters are treated as independent, introduces a large number of additional free parameters on top of the extra couplings already present in the superpotential. The number of free parameters can be greatly reduced by considering a constrained model in which certain relations are assumed to hold between the soft parameters at some high scale. This is the case when the soft parameters are assumed to satisfy constraints inspired by gravity mediated SUSY breaking, leading to the constrained E$_6$SSM (CE$_6$SSM) [363, 376, 378]. Alternatively, for the purposes of studying the model at low energies, restrictions on the soft parameters analogous to those imposed in the pMSSM can also be enforced while remaining agnostic about a particular high-scale model of SSB.

A novel feature of the E$_6$SSM, and $U(1)$ extensions of the MSSM more generally, is the possibility of gauge kinetic mixing between $U(1)_Y$ and $U(1)_N$ in which a term proportional to $F^N_{\mu\nu}F^{Y\mu\nu}$, involving the $U(1)_N$ and $U(1)_Y$ field strengths $F^N_{\mu\nu}$ and $F^Y_{\mu\nu}$, is generated [379, 380]. Even if such a term is absent initially at high energies, for

instance at the GUT scale where[7]

$$g_1(M_X) \approx g_1'(M_X) \approx g_2(M_X) \approx g_3(M_X)\,, \tag{3.12}$$

g_1' being the GUT-normalised $U(1)_N$ gauge coupling, it will be generated by radiative corrections at scales below M_X through the RG flow [381, 382]. In practice, this mixing can be handled by working in a rotated basis for the $U(1)$ gauge fields where the mixing leads instead to non-zero off-diagonal gauge couplings [278, 383], i.e., in covariant derivatives one finds terms of the form $Q_{\hat{\Phi}}^T G A_\mu$ with

$$Q_{\hat{\Phi}} = \begin{pmatrix} Q_{\hat{\Phi}}^Y \\ Q_{\hat{\Phi}}^N \end{pmatrix}, \quad G = \begin{pmatrix} g_1 & g_{11} \\ 0 & g_1' \end{pmatrix}, \quad A_\mu = \begin{pmatrix} B_\mu \\ B_\mu' \end{pmatrix}. \tag{3.13}$$

This field redefinition is also responsible for the appearance of the mixed gaugino soft mass, M_{11}, in the last bracketed term of Eq. (3.11). In general in $U(1)$ extended models, gauge kinetic mixing can have a significant impact on the phenomenology [384–386]; it can, for instance, reduce the size of the limits on the Z' mass. It is natural to assume, however, that the mixing g_{11} vanishes at the GUT scale. It has then been found [278, 350, 363, 384] that, provided this is the case, in this particular model the kinetic mixing remains very small at all scales below M_X as well, $g_{11} \sim 0.02 \ll g_1, g_1'$, since the only non-vanishing contribution to the mixing comes from the $(\hat{L}_4, \hat{\overline{L}}_4)$ multiplet pair. Therefore, in all of the following work presented here the effects of gauge kinetic mixing have been neglected by setting $g_{11}(M_X) = 0$, $M_{11}(M_X) = 0$ and taking them to vanish at scales below this as well.

3.3 Gauge Symmetry Breaking in the E_6SSM

The breakdown of EWSB in the E_6SSM is made more complicated compared to the MSSM by the presence of (at least one) SM singlet that acquires a VEV. With the model building assumptions made above, the spontaneous breaking of $SU(2)_L \times U(1)_Y \times U(1)_N$ occurs as a result of H_d, H_u and S developing non-zero VEVs at the physical minimum of the Higgs potential. The relevant part of the scalar potential

[7] Since all of the low-energy matter content can be placed in complete $SU(5)$ multiplets with the exception of the doublets $\hat{L}_4$ and $\hat{\overline{L}}_4$, gauge coupling unification still occurs at the two-loop level for any value of $\alpha_3(M_Z)$, the strong coupling evaluated at the scale M_Z, consistent with the measured value [300, 350]

reads

$$V_{\rm E_6SSM} = V^F_{\rm E_6SSM} + V^D_{\rm E_6SSM} + V^{\rm soft}_{\rm E_6SSM} + \Delta V_{\rm E_6SSM}\,, \tag{3.14}$$

where the F-term, D-term and soft SUSY breaking contributions are

$$V^F_{\rm E_6SSM} = \lambda^2|S|^2(|H_d|^2 + |H_u|^2) + \lambda^2|H_d \cdot H_u|^2\,, \tag{3.15a}$$

$$V^D_{\rm E_6SSM} = \frac{\bar{g}^2}{8}\left(|H_u|^2 - |H_d|^2\right)^2 + \frac{g_2^2}{2}|H_d^\dagger H_u|^2 + \frac{g_1'^2}{2}(Q_1|H_d|^2 + Q_2|H_u|^2 + Q_S|S|^2)^2\,, \tag{3.15b}$$

$$V^{\rm soft}_{\rm E_6SSM} = m_S^2|S|^2 + m_{H_d}^2|H_d|^2 + m_{H_u}^2|H_u|^2 + (T_\lambda S H_d \cdot H_u + h.c.)\,, \tag{3.15c}$$

and $\Delta V_{\rm E_6SSM}$ contains the loop corrections to the effective potential, given at one-loop by the generalisation of Eq. (2.39) to also include contributions from the exotic states. The quantities Q_1, Q_2 and Q_S are the $U(1)_N$ charges of $\hat{H}_d$, $\hat{H}_u$ and $\hat{S}$, respectively[8]. There are several differences in $V_{\rm E_6SSM}$ compared to the analogous potential in the MSSM. In addition to the extra terms involving the singlet scalar, the potential also contains the expected additional F- and D-terms, corresponding to the last terms in Eq. (3.15a) and Eq. (3.15b). The first of these is also present in the NMSSM, see for example Ref. [234].

The analysis of gauge symmetry breaking in the E$_6$SSM proceeds in a very similar manner to that carried out in the MSSM in Section 2.4. Demanding that the Higgs fields H_d, H_u and the singlet S have real VEVs of the form

$$\langle H_d\rangle = \frac{1}{\sqrt{2}}\begin{pmatrix} v_1 \\ 0 \end{pmatrix}\,, \quad \langle H_u\rangle = \frac{1}{\sqrt{2}}\begin{pmatrix} 0 \\ v_2 \end{pmatrix}\,, \quad \langle S\rangle = \frac{s}{\sqrt{2}}\,, \tag{3.16}$$

at the physical minimum leads to the EWSB conditions

$$\frac{\partial V_{\rm E_6SSM}}{\partial v_1} = m_{H_d}^2 v_1 + \frac{\lambda^2}{2}(v_2^2 + s^2)v_1 - \frac{T_\lambda}{\sqrt{2}}s v_2 + \frac{\bar{g}^2}{8}(v_1^2 - v_2^2)v_1 + \Delta_{H_d} v_1 + \frac{\partial \Delta V_{\rm E_6SSM}}{\partial v_1} = 0\,, \tag{3.17a}$$

$$\frac{\partial V_{\rm E_6SSM}}{\partial v_2} = m_{H_u}^2 v_2 + \frac{\lambda^2}{2}(v_1^2 + s^2)v_2 - \frac{T_\lambda}{\sqrt{2}}s v_1 - \frac{\bar{g}^2}{8}(v_1^2 - v_2^2)v_2 + \Delta_{H_u} v_2 + \frac{\partial \Delta V_{\rm E_6SSM}}{\partial v_2} = 0\,, \tag{3.17b}$$

[8] If gauge kinetic mixing is not neglected, these should be replaced by the effective charges $\tilde{Q}_\Phi = Q^N_\Phi + g_{11}Q^Y_\Phi/g_1'$, where Q^N_Φ and Q^Y_Φ are the $U(1)_N$ and $U(1)_Y$ charges for the field Φ, respectively [278].

$$\frac{\partial V_{\rm E_6SSM}}{\partial s} = m_S^2 s + \frac{\lambda^2}{2}(v_2^2 + v_1^2)s - \frac{T_\lambda}{\sqrt{2}} v_2 v_1 + \Delta_S s + \frac{\partial \Delta V_{\rm E_6SSM}}{\partial s} = 0\,. \tag{3.17c}$$

The quantities Δ_Φ, with $\Phi = H_d, H_u, S$, appearing above are $U(1)_N$ D-term contributions that are absent in the MSSM and NMSSM, and are given by

$$\Delta_\Phi \equiv \frac{g_1'^2}{2}\left(Q_1 v_1^2 + Q_2 v_2^2 + Q_S s^2\right) Q_\Phi\,, \tag{3.18}$$

where Q_Φ is the $U(1)_N$ charge of the field Φ.

The breakdown of $SU(2)_L \times U(1)_Y \times U(1)_N \to U(1)_{\rm em}$ sees four massless Goldstone modes used to generate masses for the physical $W^\pm$, Z and Z' bosons, leaving 6 physical degrees of freedom in the scalar Higgs sector. The masses of the charged gauge bosons remain the same as in the MSSM, since S is a singlet under $SU(2)_L$. The neutral gauge boson masses, on the other hand, are rather different because the fields H_u^0 and H_d^0 are charged under both $U(1)$ groups and therefore the Z and Z' bosons mix even when gauge kinetic mixing is neglected. The tree-level masses $m_{Z_1}^{\overline{\rm DR}}$, $m_{Z_2}^{\overline{\rm DR}}$ of the physical Z and Z' bosons are then found by diagonalising the squared mass matrix

$$\mathcal{M}_{ZZ'}^2 = \begin{pmatrix} (m_Z^{\overline{\rm DR}})^2 & \Delta^2 \\ \Delta^2 & (m_{Z'}^{\overline{\rm DR}})^2 \end{pmatrix}, \tag{3.19}$$

where $(m_Z^{\overline{\rm DR}})^2 = \bar{g}^2 v^2/4$ and

$$(m_{Z'}^{\overline{\rm DR}})^2 = g_1'^2 v^2 \left(Q_1^2 \cos^2\beta + Q_2^2 \sin^2\beta\right) + g_1'^2 Q_S^2 s^2\,, \tag{3.20}$$

$$\Delta^2 = \frac{\bar{g} g_1'}{2} v^2 \left(Q_1 \cos^2\beta - Q_2 \sin^2\beta\right)\,. \tag{3.21}$$

The definitions of v and $\tan\beta$ are the same as in the MSSM, Eq. (2.33). The mixing between the two gauge bosons is strongly constrained by EW precision measurements [387], while LHC searches currently place lower bounds on the mass of the extra Z' in $U(1)_N$ models of $M_{Z_2} \gtrsim 3.4$ TeV [388]. Bounds on the mass of the Z' associated with other choices of $U(1)'$ are similarly large; for the models listed in Table 3.2, the limit varies from $M_{Z_2} \gtrsim 3.36$ TeV for $U(1)_\psi$ up to $M_{Z_2} \gtrsim 3.66$ TeV for $U(1)_\chi$, with the exclusion limit for other choices of θ_{E_6} falling between these two values. The physical Z' mass can be made acceptably large provided that the SM singlet VEV is large, $s \gtrsim 9$ TeV. This leads to negligible mixing between the physical states Z_1 and Z_2, with a mixing angle $\lesssim 10^{-4}$, so that the light state Z_1 is approximately the SM Z boson with $m_{Z_1}^{\overline{\rm DR}} \approx m_Z^{\overline{\rm DR}} = \bar{g} v/2$ and $v \approx 246$ GeV, while the heavier gauge boson

has its mass set by the singlet VEV with $m_{Z_2}^{\overline{\rm DR}} \approx m_{Z'}^{\overline{\rm DR}} \approx g_1' Q_S s$. The corresponding physical mass, $M_{Z'}$, is required to be above the experimental lower bound.

By taking linear combinations of Eqs. (3.17a) and (3.17b), it is possible to put the EWSB conditions into a form similar to that used in the MSSM to express the EW scale as a prediction of the model parameters, Eq. (2.36). One finds [389, 390] the result

$$\frac{(m_Z^{\overline{\rm DR}})^2}{2} = -\mu_{\rm eff}^2 + \frac{\bar{m}_{H_d}^2 - \bar{m}_{H_u}^2 \tan^2\beta}{\tan^2\beta - 1} + \frac{\Delta_{H_d} - \Delta_{H_u}\tan^2\beta}{\tan^2\beta - 1}\,, \tag{3.22}$$

$$\sin 2\beta = \frac{\sqrt{2} T_\lambda s}{\bar{m}_{H_d}^2 + \bar{m}_{H_u}^2 + 2\mu_{\rm eff}^2 + \Delta_{H_d} + \Delta_{H_u}}\,, \tag{3.23}$$

where Δ_{H_d}, Δ_{H_u} are the D-term contributions defined in Eq. (3.18) and the effective μ parameter is

$$\mu_{\rm eff} = \frac{\lambda s}{\sqrt{2}}\,. \tag{3.24}$$

The higher-order corrections have again been absorbed into the soft masses in the manner of Eq. (2.38). The first of these expressions, Eq. (3.22), exhibits an obvious difference compared to its MSSM equivalent, Eq. (2.36), in the form of the third term on the right-hand side. This term, involving the $U(1)'$ D-term contributions, can potentially be large, though its exact size depends somewhat on the $U(1)'$ charges. When it is, it constitutes yet another large contribution to the Z boson mass that must be cancelled against the other two terms. The impact of these new D-terms in the EWSB conditions introduces a new factor that must be assessed when discussing fine tuning in these models; their naturalness "cost" is investigated in Chapter 5.

3.4 The Particle Spectrum of the E_6SSM

The new $U(1)_N$ D-terms also influence many of the tree-level masses in the model, and in some cases amount to the most significant modification compared to the MSSM. This is the case for the sfermion partners of the SM fermions, for which the expressions for the masses are otherwise rather similar to those in the MSSM. In the absence of flavour mixing, and neglecting the usually small left- and right-handed mixing, the first and second generation sfermion masses and the three sneutrino masses in the E_6SSM are given by [363]

$$\left(m_{\tilde{d}_{L\alpha}}^{\overline{\rm DR}}\right)^2 \approx m_{Q_{\alpha\alpha}}^2 + \left(-\frac{1}{2} + \frac{1}{3}\sin^2\theta_W\right)(m_Z^{\overline{\rm DR}})^2 \cos 2\beta + \Delta_Q\,, \tag{3.25}$$

$$\left(m^{\overline{\rm DR}}_{\tilde{d}_{R\alpha}}\right)^2 \approx m^2_{d^c_{\alpha\alpha}} - \frac{1}{3}(m^{\overline{\rm DR}}_Z)^2 \sin^2\theta_W \cos 2\beta + \Delta_{d^c}\,, \tag{3.26}$$

$$\left(m^{\overline{\rm DR}}_{\tilde{u}_{L\alpha}}\right)^2 \approx m^2_{Q_{\alpha\alpha}} + \left(\frac{1}{2} - \frac{2}{3}\sin^2\theta_W\right)(m^{\overline{\rm DR}}_Z)^2 \cos 2\beta + \Delta_Q\,, \tag{3.27}$$

$$\left(m^{\overline{\rm DR}}_{\tilde{u}_{R\alpha}}\right)^2 \approx m^2_{u^c_{\alpha\alpha}} + \frac{2}{3}(m^{\overline{\rm DR}}_Z)^2 \sin^2\theta_W \cos 2\beta + \Delta_{u^c}\,, \tag{3.28}$$

$$\left(m^{\overline{\rm DR}}_{\tilde{e}_{L\alpha}}\right)^2 \approx m^2_{L_{\alpha\alpha}} + \left(-\frac{1}{2} + \sin^2\theta_W\right)(m^{\overline{\rm DR}}_Z)^2 \cos 2\beta + \Delta_L\,, \tag{3.29}$$

$$\left(m^{\overline{\rm DR}}_{\tilde{e}_{R\alpha}}\right)^2 \approx m^2_{e^c_{\alpha\alpha}} - (m^{\overline{\rm DR}}_Z)^2 \sin^2\theta_W \cos 2\beta + \Delta_{e^c}\,, \tag{3.30}$$

$$\left(m^{\overline{\rm DR}}_{\tilde{\nu}_i}\right)^2 \approx m^2_{L_{ii}} + \frac{1}{2}(m^{\overline{\rm DR}}_Z)^2 \cos 2\beta + \Delta_L\,, \tag{3.31}$$

where the Δ_Φ are the D-term contributions defined in Eq. (3.18). For the values of s required by limits on the Z' mass in $U(1)_N$ models, these are much larger than the $SU(2)_L$ and $U(1)_Y$ D-terms. Similarly, including the effects of mixing between the gauge eigenstates, the third generation sfermion masses are

$$\left(m^{\overline{\rm DR}}_{\tilde{t}_{1,2}}\right)^2 = \frac{1}{2}\Bigg\{m^2_{Q_{33}} + m^2_{u^c_{33}} + \frac{1}{2}(m^{\overline{\rm DR}}_Z)^2\cos 2\beta + \Delta_Q + \Delta_{u^c} + 2\left(m^{\overline{\rm DR}}_t\right)^2 \mp \sqrt{\left[m^2_{Q_{33}} - m^2_{u^c_{33}} + \left(\frac{1}{2} - \frac{4}{3}\sin^2\theta_W\right)(m^{\overline{\rm DR}}_Z)^2\cos 2\beta + \Delta_Q - \Delta_{u^c}\right]^2 + 4X_t^2}\Bigg\}, \tag{3.32}$$

$$\left(m^{\overline{\rm DR}}_{\tilde{b}_{1,2}}\right)^2 = \frac{1}{2}\Bigg\{m^2_{Q_{33}} + m^2_{d^c_{33}} - \frac{1}{2}(m^{\overline{\rm DR}}_Z)^2\cos 2\beta + \Delta_Q + \Delta_{d^c} + 2\left(m^{\overline{\rm DR}}_b\right)^2 \mp \sqrt{\left[m^2_{Q_{33}} - m^2_{d^c_{33}} + \left(-\frac{1}{2} + \frac{2}{3}\sin^2\theta_W\right)(m^{\overline{\rm DR}}_Z)^2\cos 2\beta + \Delta_Q - \Delta_{d^c}\right]^2 + 4X_b^2}\Bigg\}, \tag{3.33}$$

$$\left(m^{\overline{\rm DR}}_{\tilde{\tau}_{1,2}}\right)^2 = \frac{1}{2}\Bigg\{m^2_{L_{33}} + m^2_{e^c_{33}} - \frac{1}{2}(m^{\overline{\rm DR}}_Z)^2\cos 2\beta + \Delta_L + \Delta_{e^c} + 2\left(m^{\overline{\rm DR}}_\tau\right)^2 \mp \sqrt{\left[m^2_{L_{33}} - m^2_{e^c_{33}} + \left(-\frac{1}{2} + 2\sin^2\theta_W\right)(m^{\overline{\rm DR}}_Z)^2\cos 2\beta + \Delta_L - \Delta_{e^c}\right]^2 + 4X_\tau^2}\Bigg\}. \tag{3.34}$$

In addition to the appearance of the $U(1)_N$ D-term contributions, the mixing parameters X_t, X_b and X_τ are now also dependent on the singlet VEV as the MSSM μ

parameter is replaced by $\mu_{\rm eff}$,

$$X_t = \frac{T^U_{33} v}{\sqrt{2}} \sin\beta - \frac{\lambda y^U_{33} v s}{2} \cos\beta \,, \tag{3.35}$$

$$X_b = \frac{T^D_{33} v}{\sqrt{2}} \cos\beta - \frac{\lambda y^D_{33} v s}{2} \sin\beta \,, \tag{3.36}$$

$$X_\tau = \frac{T^E_{33} v}{\sqrt{2}} \cos\beta - \frac{\lambda y^E_{33} v s}{2} \sin\beta \,. \tag{3.37}$$

The substitution $\mu \to \mu_{\rm eff}$ in Eq. (2.54) is also sufficient to obtain the chargino masses in the E$_6$SSM. The number and composition of the charginos in the E$_6$SSM is unchanged from the MSSM, as the $U(1)_N$ gaugino $\tilde{B}'$ and the singlino $\tilde{S}$ are uncharged under $U(1)_{\rm em}$. This is also the case for the SM fermion masses, which continue to be given by Eq. (2.40). The tree-level gluino mass is also the same as in the MSSM, i.e., $m^{\overline{\rm DR}}_{\tilde{g}} = M_3$, and the physical pole mass is given by an expression similar to that in Eq. (2.59). The precise form [363] of the radiative correction $\Delta^{\tilde{g}}(Q)$ is on the other hand modified due to the presence of the additional coloured exotic states associated with the $\hat{D}_i$ and $\hat{\overline{D}}_i$ superfields.

3.4.1 Exotic States

The exotic states in the E$_6$SSM obviously have no counterparts in the MSSM, which makes them a potential distinguishing feature of the model. The possible mass spectrum of these states is thus very important for phenomenological studies. The spin-1/2 components of the $\hat{D}_i$ and $\hat{\overline{D}}_i$ superfields receive tree-level masses from the singlet VEV s. Under the assumption that the κ_{ij} couplings have been made flavour diagonal, these are

$$m^{\overline{\rm DR}}_{D_i} = \frac{\kappa_{ii} s}{\sqrt{2}} \,, \tag{3.38}$$

where no sum over i is implied. With this assumption there is also no substantial generation mixing between the spin-0 components, which form a set of 6 scalar leptoquark[9] mass eigenstates, $\tilde{D}_i$. However, since in general all of the diagonal couplings κ_{ii} can be non-negligible, it is still necessary to account for mixing within generations, and hence the masses are obtained by diagonalising three 2×2 mass matrices, leading

[9]Or diquarks, in the case that Z_2^L is imposed.

to the squared $\overline{\rm DR}$ masses

$$\left(m^{\overline{\rm DR}}_{\tilde{D}_{i1,2}}\right)^2 = \frac{1}{2}\Bigg[m^2_{D_{ii}} + m^2_{\overline{D}_{ii}} + \Delta_D + \Delta_{\overline{D}} + 2(m^{\overline{\rm DR}}_{D_i})^2 \mp \sqrt{\left[m^2_{D_{ii}} - m^2_{\overline{D}_{ii}} + \frac{2}{3}(m^{\overline{\rm DR}}_Z)^2 \sin^2\theta_W \cos 2\beta + \Delta_D - \Delta_{\overline{D}}\right]^2 + 4X^2_{D_i}}\Bigg], \tag{3.39}$$

where the mixing parameter X_{D_i} is given by

$$X_{D_i} = \frac{T^\kappa_{ii} s}{\sqrt{2}} - \frac{\kappa_{ii}\lambda v^2}{4}\sin 2\beta\,. \tag{3.40}$$

The exotic sector in the E$_6$SSM also involves the component fields of the two generations of inert Higgs and singlet superfields, $\hat{H}_{d\alpha}$, $\hat{H}_{u\alpha}$, and $\hat{S}_\alpha$, and the $\hat{L}_4$ and $\hat{\overline{L}}_4$ superfields. The spin-1/2 components of the former set lead to a set of inert charginos and neutralinos. The inert charginos $\tilde{H}^\pm_{I_\alpha}$, which are a mixture of the inert charged Higgs states $\tilde{H}^-_{d\alpha}$ and $\tilde{H}^+_{u\alpha}$, have tree-level masses given by

$$m_{\tilde{H}_{I_\alpha}} = \frac{\tilde{\lambda}_{\alpha\alpha} s}{\sqrt{2}}\,, \tag{3.41}$$

assuming the couplings $\tilde{\lambda}_{\alpha\beta}$ to be flavour diagonal. When the couplings $f_{\alpha\beta}$, $\tilde{f}_{\alpha\beta}$ are negligible compared to $\tilde{\lambda}_{\alpha\beta}$, Eq. (3.41) also gives the $\overline{\rm DR}$ masses of the inert Higgsinos, formed by linear combinations of the states $\tilde{H}^0_{d\alpha}$ and $\tilde{H}^0_{u\alpha}$. In this approximation, the masses of the inert scalar singlets are given solely by the soft mass and D-term contributions,

$$(m^{\overline{\rm DR}}_{S_{I_\alpha}})^2 = m^2_{\Sigma_{\alpha\alpha}} + \Delta_S\,, \tag{3.42}$$

leading to large masses for these states, while the neutral inert scalar Higgs masses follow from diagonalising a pair of 2×2 mass matrices,

$$\left(m^{\overline{\rm DR}}_{H^0_{\alpha_{1,2}}}\right)^2 = \frac{1}{2}\Bigg\{m^2_{H_{1,\alpha\alpha}} + m^2_{H_{2,\alpha\alpha}} + \Delta_{H_d} + \Delta_{H_u} + 2(m^{\overline{\rm DR}}_{\tilde{H}_{I\alpha}})^2 \mp \sqrt{\left[m^2_{H_{1,\alpha\alpha}} - m^2_{H_{2,\alpha\alpha}} + (m^{\overline{\rm DR}}_Z)^2\cos 2\beta + \Delta_{H_d} - \Delta_{H_u}\right]^2 + 4X^2_{H_\alpha}}\Bigg\}. \tag{3.43}$$

The mixing parameter X_{H_α} that appears here is defined to be

$$X_{H_\alpha} = \frac{T^{\tilde{\lambda}}_{\alpha\alpha} s}{\sqrt{2}} - \frac{\tilde{\lambda}_{\alpha\alpha}\lambda v^2}{4}\sin 2\beta\,, \tag{3.44}$$

and the same also enters into the tree-level masses for the charged inert Higgs states,

$$\begin{aligned}\left(m^{\overline{\rm DR}}_{H^\pm_{\alpha_{1,2}}}\right)^2 = \frac{1}{2}\Bigg\{ & m^2_{H_{1,\alpha\alpha}} + m^2_{H_{2,\alpha\alpha}} + \Delta_{H_d} + \Delta_{H_u} + 2(m^{\overline{\rm DR}}_{\tilde{H}_{I\alpha}})^2 \\ & \mp \sqrt{\left[m^2_{H_{1,\alpha\alpha}} - m^2_{H_{2,\alpha\alpha}} - (m^{\overline{\rm DR}}_Z)^2\cos 2\theta_W \cos 2\beta + \Delta_{H_d} - \Delta_{H_u}\right]^2 + 4X^2_{H_\alpha}}\Bigg\}.\end{aligned} \tag{3.45}$$

The remaining exotics, associated with the $\hat{L}_4$ and $\hat{\overline{L}}_4$ superfields, constitute a set of additional exotic neutral and charged exotic fermions and scalars. The masses of the spin-1/2 components, $\tilde{L}^\pm_4$ and $\tilde{L}^0_{4,1}$, $\tilde{L}^0_{4,2}$, are all set by the μ_L parameter,

$$m^{\overline{\rm DR}}_{\tilde{L}^\pm_4} = m^{\overline{\rm DR}}_{\tilde{L}^0_4} = \mu_L\,. \tag{3.46}$$

This parameter, as noted above, can be large, $\mu_L \sim 10$ TeV, and therefore these states tend to be very heavy in the E$_6$SSM and are not usually relevant for collider phenomenology. The masses of the spin-0 superpartners also receive soft SUSY breaking contributions; the neutral and charged scalar masses are given by

$$\begin{aligned}\left(m^{\overline{\rm DR}}_{L^0_{4_{1,2}}}\right)^2 = \frac{1}{2}\Bigg\{ & m^2_{L_4} + m^2_{\overline{L}_4} + \Delta_{L_4} + \Delta_{\overline{L}_4} + 2(m^{\overline{\rm DR}}_{\tilde{L}^0_4})^2 \\ & \mp \sqrt{\left[m^2_{L_4} - m^2_{\overline{L}_4} + (m^{\overline{\rm DR}}_Z)^2\cos 2\beta + \Delta_{L_4} - \Delta_{\overline{L}_4}\right]^2 + 4X^2_{L_4}}\Bigg\},\end{aligned} \tag{3.47}$$

$$\begin{aligned}\left(m^{\overline{\rm DR}}_{L^\pm_{4_{1,2}}}\right)^2 = \frac{1}{2}\Bigg\{ & m^2_{L_4} + m^2_{\overline{L}_4} + \Delta_{L_4} + \Delta_{\overline{L}_4} + 2(m^{\overline{\rm DR}}_{\tilde{L}^\pm_4})^2 \\ & \mp \sqrt{\left[m^2_{L_4} - m^2_{\overline{L}_4} - (m^{\overline{\rm DR}}_Z)^2\cos 2\theta_W \cos 2\beta + \Delta_{L_4} - \Delta_{\overline{L}_4}\right]^2 + 4X^2_{L_4}}\Bigg\}.\end{aligned} \tag{3.48}$$

The mixing parameter is simply given by mixing induced by the soft SUSY breaking bilinear $\mu_L B_L$, i.e.,

$$X_{L_4} = \mu_L B_L\,. \tag{3.49}$$

3.4.2 The E$_6$SSM Higgs Sector

The extension of the "active" set of Higgs superfields to include the SM singlet $\hat{S}$ implies that there are also new states present in the Higgs and neutralino sectors in the E$_6$SSM. As noted above, since the components of $\hat{S}$ are electromagnetically neutral, the number of charged Higgs states and charginos remains the same as in the MSSM. Unlike in the case of the charginos, the masses of the charged Higgs scalars, formed by the linear combination

$$H^+ = H_d^{-*} \sin\beta + H_u^+ \cos\beta \,, \tag{3.50}$$

are however modified by extra F-terms compared to their values in the MSSM,

$$(m_{H^\pm}^{\overline{\rm DR}})^2 = (m_W^{\overline{\rm DR}})^2 + \frac{\sqrt{2} T_\lambda s}{\sin 2\beta} - \frac{\lambda^2 v^2}{2} \,. \tag{3.51}$$

As in the MSSM, the linear combination orthogonal to Eq. (3.50) corresponds to the massless Goldstone bosons $G^\pm$ that constitute the longitudinal degrees of freedom of $W^\pm$.

The presence of the additional massive Z' boson in the E$_6$SSM and other similar E_6 inspired models means that, at least in the absence of CP-violation in the Higgs potential, the pseudoscalar Higgs sector is not enlarged compared to the MSSM. This can be contrasted with the situation in the NMSSM, where an extra CP-odd state appears associated with the extra degree of freedom coming from the imaginary part of the scalar field S [234]. In the E$_6$SSM, this state G' is swallowed together with the G^0 Goldstone mode when the Z and Z' bosons become massive. The corresponding linear combinations of $\mathrm{Im}\, H_d^0$, $\mathrm{Im}\, H_u^0$ and $\mathrm{Im}\, S$ are given by

$$\frac{G'}{\sqrt{2}} = \mathrm{Im}\, S \cos\varphi - \mathrm{Im}\, H_d^0 \sin\beta \sin\varphi - \mathrm{Im}\, H_u^0 \cos\beta \sin\varphi \,, \tag{3.52}$$

$$\frac{G^0}{\sqrt{2}} = \mathrm{Im}\, H_d^0 \cos\beta - \mathrm{Im}\, H_u^0 \sin\beta \,, \tag{3.53}$$

where the mixing angle φ is defined by

$$\tan\varphi = \frac{v}{2s} \sin 2\beta \,. \tag{3.54}$$

The sole physical CP-odd Higgs,

$$\frac{A}{\sqrt{2}} = \mathrm{Im}\, S \sin\varphi + \mathrm{Im}\, H_d^0 \sin\beta\cos\varphi + \mathrm{Im}\, H_u^0 \cos\beta\cos\varphi\,, \tag{3.55}$$

is found to have mass given by

$$(m_A^{\overline{\mathrm{DR}}})^2 = \frac{\sqrt{2}T_\lambda v}{\sin 2\varphi} \tag{3.56}$$

after diagonalising the corresponding 3×3 mass matrix using the rotations above. In the E$_6$SSM, where s must be large to satisfy limits on the Z' mass, Eq. (3.55) implies that A is predominantly composed of the MSSM–like $\mathrm{Im}\, H_d^0$ and $\mathrm{Im}\, H_u^0$, with the singlet mixing $\sin\varphi \to 0$ since $s \gg v$.

The CP-even Higgs sector is, like in the NMSSM, extended by an additional physical CP-even Higgs state. The physical states in this sector are composed of linear combinations of the real parts $\mathrm{Re}\, H_d^0 = (v_1 + \phi_d)/\sqrt{2}$, $\mathrm{Re}\, H_u^0 = (v_2 + \phi_u)/\sqrt{2}$ and $\mathrm{Re}\, S = (s + \phi_S)/\sqrt{2}$. In the basis (S_1, S_2, S_3) obtained by the rotation

$$\begin{pmatrix}\phi_d\\ \phi_u\\ \phi_S\end{pmatrix} = \begin{pmatrix}\cos\beta & -\sin\beta & 0\\ \sin\beta & \cos\beta & 0\\ 0 & 0 & 1\end{pmatrix}\begin{pmatrix}S_1\\ S_2\\ S_3\end{pmatrix}\,, \tag{3.57}$$

the 3×3 CP-even Higgs mass matrix $\mathcal{M}_h^2$ has elements

$$(\mathcal{M}_h^2)_{11} = (m_Z^{\overline{\mathrm{DR}}})^2\cos^2 2\beta + \frac{\lambda^2 v^2}{2}\sin^2 2\beta + g_1'^2 v^2 (Q_1\cos^2\beta + Q_2\sin^2\beta)^2\,, \tag{3.58a}$$

$$(\mathcal{M}_h^2)_{12} = (\mathcal{M}_h^2)_{21} = \left[\frac{\lambda^2 v^2}{4} - \frac{(m_Z^{\overline{\mathrm{DR}}})^2}{2}\right]\sin 4\beta + \frac{g_1'^2 v^2}{2}(Q_2 - Q_1)(Q_1\cos^2\beta + Q_2\sin^2\beta)\sin 2\beta\,, \tag{3.58b}$$

$$(\mathcal{M}_h^2)_{13} = (\mathcal{M}_h^2)_{31} = -\frac{T_\lambda v}{\sqrt{2}}\sin 2\beta + \lambda^2 v s + g_1'^2(Q_1\cos^2\beta + Q_2\sin^2\beta)Q_s v s\,, \tag{3.58c}$$

$$(\mathcal{M}_h^2)_{22} = \frac{\sqrt{2}T_\lambda s}{\sin 2\beta} + \left[(m_Z^{\overline{\mathrm{DR}}})^2 - \frac{\lambda^2 v^2}{2} + \frac{g_1'^2}{4}v^2(Q_2 - Q_1)^2\right]\sin^2 2\beta\,, \tag{3.58d}$$

$$(\mathcal{M}_h^2)_{23} = (\mathcal{M}_h^2)_{32} = -\frac{T_\lambda v}{\sqrt{2}}\cos 2\beta + \frac{g_1'^2}{2}(Q_2 - Q_1)Q_S v s\sin 2\beta\,, \tag{3.58e}$$

$$(\mathcal{M}_h^2)_{33} = \frac{T_\lambda v^2}{2\sqrt{2}s}\sin 2\beta + g_1'^2 Q_S^2 s^2\,, \tag{3.58f}$$

after using the EWSB conditions Eq. (3.17) to eliminate the soft Higgs masses $m^2_{H_d}$, $m^2_{H_u}$ and m^2_S.

The behaviour of the CP-even Higgs mass spectrum has been extensively studied [278]. In phenomenologically viable scenarios, both the singlet VEV $s \sim m^{\overline{\rm DR}}_{Z'}$ and the SUSY scale M_S are large. As a result, the mixing $(\mathcal{M}^2_h)_{23}$ is much smaller than the diagonal entry $(\mathcal{M}^2_h)_{33}$. Therefore one CP-even Higgs state, which is predominantly composed of the SM singlet field, is always almost degenerate in mass with the Z' gauge boson. The qualitative pattern of the remaining CP-even masses depends on the size of the coupling λ. If $\lambda < g'_1$ the singlet dominated CP-even state is very heavy and decouples, making the rest of the Higgs spectrum indistinguishable from the one in the MSSM. Conversely, when $\lambda \gtrsim g'_1$ the spectrum of Higgs bosons has a very hierarchical structure, which is similar to the one that appears in the NMSSM with approximate PQ symmetry [391–395]. In this case, the above mass matrix can be diagonalised using perturbation theory [395–398]. The heaviest CP-even, CP-odd and charged states are found to be almost degenerate and lie beyond the multi-TeV range whereas the mass of the second lightest CP-even Higgs state is set by the Z' boson mass. In either case, the mass of the lightest CP-even Higgs mass is set by the EW scale rather than by M_S or $M_{Z'}$, as follows from the expression for $(\mathcal{M}^2_h)_{11}$. Since $m^{\overline{\rm DR}}_{h_1}$ is always bounded from above by this element, it follows that the tree-level upper bound on the lightest CP-even Higgs mass in the E$_6$SSM is

$$(m^{\overline{\rm DR}}_{h_1})^2 \leq (m^{\overline{\rm DR}}_{Z})^2 \cos^2 2\beta + \frac{\lambda^2 v^2}{2} \sin^2 2\beta + g'^2_1 v^2 (Q_1 \cos^2\beta + Q_2 \sin^2\beta)^2 \,. \tag{3.59}$$

As expected, this exceeds the bounds in the MSSM and NMSSM. The last term on the right-hand side contains the additional $U(1)_N$ D-term contributions, while the second term is similar to that which appears in the NMSSM.

3.4.3 The Neutralino Sector

The additional neutralinos in the E$_6$SSM, when small Z^H_2 violating couplings are neglected[10], arise due to the presence of the spin-1/2 component of the SM singlet, $\tilde{S}$, and the $U(1)_N$ gaugino $\tilde{B}'$. The neutralino mass matrix is therefore a 6×6 matrix, from which the tree-level masses follow after diagonalisation with the mixing matrix N,

$$\text{diag}(m^{\overline{\rm DR}}_{\tilde{\chi}^0_1}, \ldots, m^{\overline{\rm DR}}_{\tilde{\chi}^0_6}) = N^* \mathcal{M}_{\tilde{\chi}^0} N^\dagger \,. \tag{3.60}$$

[10]When this is not the case, the neutralinos considered here also mix with the first and second generation Higgsinos and singlinos [349].

In the basis $(\tilde{H}_d^0, \tilde{H}_u^0, \tilde{W}_3, \tilde{B}, \tilde{B}', \tilde{S})$, the neutralino mass matrix $\mathcal{M}_{\tilde{\chi}^0}$ can be written in the form

$$\mathcal{M}_{\tilde{\chi}^0} = \begin{pmatrix} A & C^T \\ C & B \end{pmatrix}, \tag{3.61}$$

where A, B and C are, respectively, 4×4, 2×2 and 2×4 sub-matrices. The first of these, A, has the same structure as in the MSSM but with $\mu \to \mu_{\text{eff}}$, that is,

$$A = \begin{pmatrix} 0 & -\mu_{\text{eff}} & \frac{g_2 v_1}{2} & -\frac{g_1 v_1}{2}\sqrt{\frac{3}{5}} \\ -\mu_{\text{eff}} & 0 & -\frac{g_2 v_2}{2} & \frac{g_1 v_2}{2}\sqrt{\frac{3}{5}} \\ \frac{g_2 v_1}{2} & -\frac{g_2 v_2}{2} & M_2 & 0 \\ -\frac{g_1 v_1}{2}\sqrt{\frac{3}{5}} & \frac{g_1 v_2}{2}\sqrt{\frac{3}{5}} & 0 & M_1 \end{pmatrix}. \tag{3.62}$$

The sub-matrix B contains the terms responsible for mixing the new states $\tilde{B}'$ and $\tilde{S}$,

$$B = \begin{pmatrix} M_1' & g_1' Q_S s \\ g_1' Q_s s & 0 \end{pmatrix}, \tag{3.63}$$

and the sub-matrix C contains those terms that mix the MSSM–like Higgsinos and gauginos with these states,

$$C = \begin{pmatrix} g_1' Q_1 v_1 & g_1' Q_2 v_2 & 0 & 0 \\ -\frac{\lambda v_2}{\sqrt{2}} & -\frac{\lambda v_1}{\sqrt{2}} & 0 & 0 \end{pmatrix}. \tag{3.64}$$

It should be noted that, as discussed above, gauge kinetic mixing is neglected, so that the mixed $U(1)$ gaugino mass M_{11} is not present. In the E$_6$SSM, the neutralino masses are governed at low energies by the parameters λ, s, $\tan\beta$, M_1, M_2 and M_1', there being two additional parameters compared to the MSSM. In the CE$_6$SSM and similar models, the dependence on the three separate gaugino masses can be reduced to a dependence on only $M_{1/2}$, in which case four parameter are required to determine the neutralino masses. The analysis of the E$_6$SSM neutralino masses is therefore slightly more complicated than in the MSSM. It is again possible to make use of the fact that, in scenarios consistent with current experimental limits, the structure of the mass matrix simplifies so that approximate expressions for some of the mass eigenvalues can be obtained. When $s \gg v$ and $\lambda \ll g_1'$, the mixing between the MSSM–like neutralinos and $\tilde{S}$, $\tilde{B}'$ is negligible compared to the elements of the sub-matrix B. In this limit, the mixing can be neglected, so that the two heaviest neutralinos are

predominantly mixtures of $\tilde{B}'$ and $\tilde{S}$ and have masses given by

$$m^{\overline{\rm DR}}_{\tilde{\chi}^0_{5,6}} \approx \frac{1}{2}\left(M_1' \mp \sqrt{M_1'^2 + 4g_1'^2 Q_S^2 s^2}\right) , \tag{3.65}$$

assuming $M_1' > 0$. The four lighter neutralinos are in this case MSSM–like, with masses given by the eigenvalues of the 4×4 sub-matrix A. In general, however, the neutralino mass matrix must be diagonalised numerically to obtain the masses and mixings of the physical neutralinos; the extended neutralino sector and its phenomenological implications have been thoroughly studied in this way [314–325].

Given the many new states and Yukawa couplings in the E_6SSM, it is not surprising that studying the mass spectrum is more challenging than in the MSSM. The extra difficulty is compensated for by the fact that the model also has many interesting phenomenological implications. Detailed studies have established that the additional exotic matter and the Z' in the model would lead to distinctive LHC signatures [278, 284–292], as well as result in non-standard Higgs decays for sufficiently light exotics [347, 353, 367–369, 399–401]. Numerical analyses [356, 363, 376, 378, 402] allow for the particle spectrum to be understood in all parts of the model parameter space, without relying only on the approximations described above. In these studies, existing programs for calculating the mass spectrum in the MSSM were modified, by hand, to incorporate the new couplings and mass eigenstates, including the one- and two-loop RGEs and the most important radiative corrections. However, to carry out precise studies of E_6 inspired models, we seek to take into account all available higher-order corrections. Even starting from the MSSM and making the necessary modifications, this is a difficult and error prone endeavour. To avoid having to do so, to obtain the numerical results presented in the following chapters we have made use of several of the increasing number of powerful numerical tools that automate the study of BSM models, after making several improvements to these generic tools to support entire new classes of models instead of a single model at a time.

Chapter 4

Extensions to Mass Spectrum Generators for BSM Models

4.1 Automated Tools for BSM Models: Benefits and Limitations

Studies of the phenomenological implications of a new physics model, such as its collider signatures or DM candidates, require as inputs the mass spectrum of states in the model, as well as other observables such as production cross sections and decay branching ratios. In general, models such as the MSSM or E_6SSM introduce many new fields and couplings, leading to complicated expressions at tree-level for the masses of the physical states that often cannot be solved analytically. Moreover, to draw reliable conclusions about a model and make meaningful comparisons with experimental results, it is usually necessary to include a multitude of higher-order effects. These include loop corrections to the tree-level mass spectrum and branching ratios, as well as the RG evolution of the parameters between disparate energy scales. The model of interest must also be matched to known low-energy data, which is interpreted in the framework of the SM. More generally, the specification of model parameters at multiple renormalisation scales, such as at the GUT scale and at M_Z where the model is matched to the SM, constitutes a boundary value problem (BVP) that must be solved even before a mass spectrum can be calculated. The consistent solution of this BVP and the incorporation of all of these effects poses a significant obstacle for studying BSM models, but it is one that must be overcome in order to precisely understand the predictions of a model.

One approach to handle this complexity is to resort to simplified analytical approximations that render the calculations tractable, such as neglecting mixings between new states or assuming that subsets of the particles in the model can be decoupled and ignored for the purposes of a particular calculation. However, these approximations often only have a limited range of validity or impose special conditions on the model parameters, which limits the extent to which they can be used to arrive at generic conclusions about the model. In the worst case, it is also possible for large differences to exist between simplified analytical approximations and more precise results obtained numerically.

Historically, obtaining numerical results against which approximations could be validated and that could be used throughout the parameter space of a model required hand-writing a computer code for each new model. For realistic models, this is a highly non-trivial and error prone process. Nevertheless, the need for precise numerical predictions to compare against data and to confirm analytical results make this a necessary task. For certain well-motivated, widely studied models, significant efforts have led to several publicly available codes for studying their mass spectra. For example, spectrum generators such as `SOFTSUSY` [403], `SPheno` [404], `ISASUGRA` [405], and `SuSpect` [406] allow for the calculation of the mass spectrum in the MSSM at various levels of precision, while similar calculations in the NMSSM can be made using Next-to-Minimal-`SOFTSUSY` [407], `SPheno` [408], `NMSSMTools` [409–411] and `NMSSMCalc` [412]. In some cases, the capabilities of these codes extend to the calculation of decay branching ratios and flavour observables, or they may be linked to additional dedicated codes such as `HDECAY` [413, 414], `SDECAY` [415], `NMSDECAY` [416], `SUSY-HIT` [417] or `SFOLD` [418] for this purpose. The sustained development of these dedicated codes has led to a set of tools for these models that incorporate the highest precision corrections available and that are able to run quickly, which is essential for carrying out large parameter space scans. The availability of multiple independent public codes eliminates the need to write, from scratch, private routines to study these models, and allows for errors to be detected through comparisons between the codes [419–422].

Until relatively recently, the possibilities for studying other models were much more limited, to the extent that detailed numerical calculations still required the time-consuming creation of a private code. This is the case, for example, when studying non-minimal models such as the E_6SSM and related models, for which no dedicated tools are available. Previous numerical studies of the E_6SSM have therefore relied on privately implemented spectrum generators [356, 363]. The existing model specific codes are of limited utility for studying these alternative BSM models; consequently,

if models such as the MSSM or NMSSM are unable to account for an observed signal, the timely and precise study of new models can be difficult and fraught with potential errors. Recent progress in developing numerical tools that are applicable to general models has now greatly improved this situation. Packages such as `SARAH` [423–427] apply known results for the loop corrections and RGEs in general QFTs to automatically calculate the appropriate expressions in specific models, which are defined via an input model file specifying the field content and interactions. Codes such as `SPheno` and `FlexibleSUSY` [428, 429] can then use these results to create bespoke numerical spectrum generators, written in Fortran and C++, respectively, that are competitive with dedicated codes in terms of speed and precision. In a similar fashion, there now exist numerous generic codes for the calculation of the Feynman rules, such as `FeynRules` [430, 431] and `LanHEP` [432–436], or various different observables in a model. Examples of codes in this second category include `CalcHEP` [437, 438], `micrOMEGAs` [439–445], `Vevacious` [446], `MadGraph` [447, 448], `HiggsBounds` [449, 450], `HiggsSignals` [451], and `WHIZARD/O'Mega` [452, 453]. Interfaces to some of these codes can also be automatically generated for a model by `SARAH`, permitting easy passing of data between different codes to form an integrated environment for analysing a model; this work flow is illustrated in Figure 4.1. The availability of these tools significantly reduces the barriers to studying new models with high precision and in full generality.

Even so, the above tools are still not applicable, or necessarily convenient to use, for all possible models. When studying an individual model, one option is of course to modify the codes as required to suit the situation at hand. Programs such as `FlexibleSUSY` are explicitly designed to support this approach, by ensuring that the generated spectrum generator code is organised with a highly modular and customisable structure. Obstacles that prevent the application of these automated tools to large classes of models are better handled by extending and improving the codes to address them. For example, the BVP that must be solved in the CE_6SSM, as well as in other constrained models such as the fully constrained NMSSM (CNMSSM) [454–456], cannot be handled in `SPheno` and `FlexibleSUSY` without significant modifications. In this case, the limitation arises from the availability of only a single algorithm for solving the BVP, the widely used two-scale algorithm [208], which is ill-suited to solving the BVP in these constrained models. To address this, alternative BVP solver algorithms may be implemented that are better suited to solving constrained models. The addition of new methods has the benefit of increasing the flexibility of the tools, for example by allowing for new boundary conditions (BCs) in existing models. Since the convergence properties of different algorithms in general differ, this also permits more

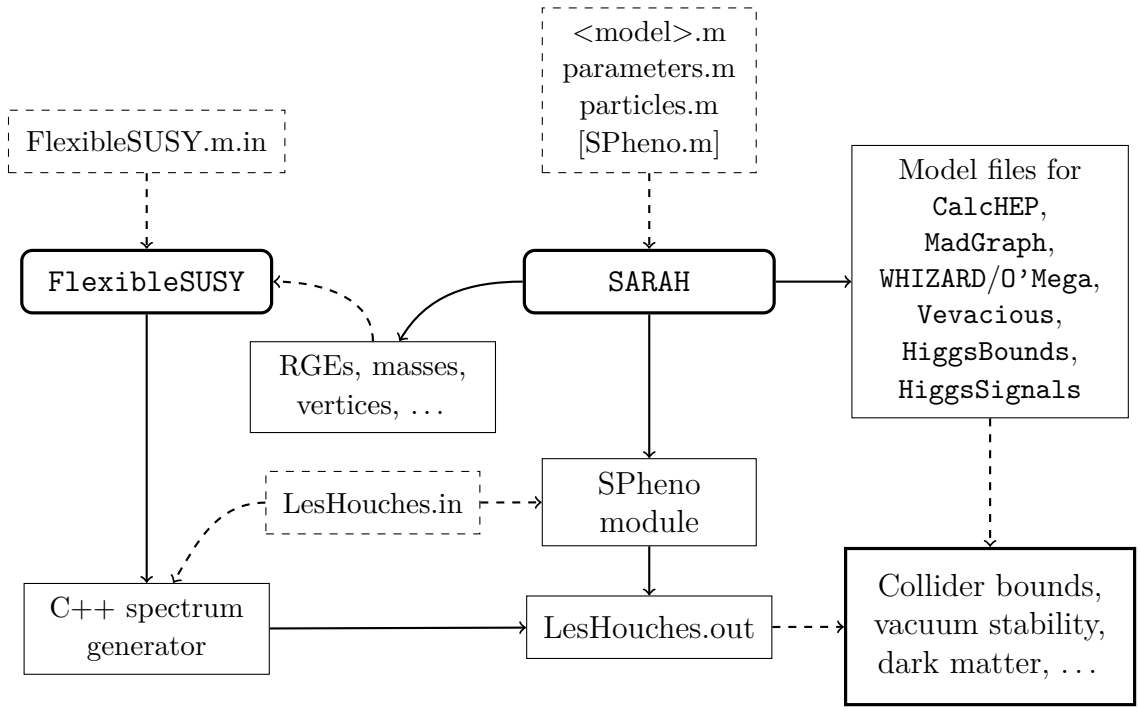

Figure 4.1: Relationships between the existing automated tools for the analysis of BSM models. A given model in `SARAH` and `FlexibleSUSY` is defined by a set of input model files, from which the required analytic expressions are derived. These in turn are used to produce numerical spectrum generators, either as a standalone program in the case of `FlexibleSUSY`, or as a module to be incorporated in `SPheno`. `SARAH` is also able to produce model files for the other automated tools shown, which together with the mass spectrum generated by `FlexibleSUSY/SPheno` allows for the study of a large number of different properties of the model.

complete explorations of model parameter spaces. In particular, if multiple solutions exist to the BVP, as occurs in the CMSSM [457, 458], then alternative BCs or BVP solvers may be used to find additional solutions that would otherwise be missed.

Any given tool will also be limited in the range of observables that it is able to calculate in the models it is applicable to. This may be either due to a lack of suitably general expressions for the quantity of interest, or such results may exist but not have been implemented into the code. The need to be able to compare a model against many different potential signals provides an impetus for ensuring a large number of observables can be calculated in any renormalisable model. Two complementary approaches exist to achieve this goal. In some instances, it is reasonable to implement the calculation of a missing observable directly into a given code. For example, the calculation of decay branching ratios can be conveniently added to spectrum generators such as `SPheno` and `FlexibleSUSY`, where direct access to the running model

parameters and RGEs allow for the correct handling of higher-order corrections to decay amplitudes. When this is not feasible, multiple codes may be combined into a tool chain in which information is passed between codes to calculate different observables. In this case, some care is necessary to ensure consistency between the conventions used in the codes, a source of error that is avoided when working within a single program and partially addressed by the use of the automatically generated interfaces illustrated in Figure 4.1. Irrespective of the approach taken, it is crucially important that the observables are calculated with sufficient precision to make a robust comparison against experimental data. This is best achieved with the use of numerical tools, which account for potential subtleties that can be easily missed when a simplified analytical approach is taken.

In this chapter, we describe several extensions to the code `FlexibleSUSY` that address some of these limitations. We first explain the implementation of an additional BVP solver in `FlexibleSUSY`. The resulting semi-analytic BVP solver generalises the numerical approach applied in previous studies of the CE_6SSM [356, 363] by using semi-analytic solutions to the RGEs of a model to express the low-energy model parameters in terms of their boundary values at high energies. In addition to being well suited for the study of constrained models, the new algorithm also opens up opportunities for the use of alternative BCs that may be more convenient for a given study, as shall be demonstrated in Chapter 7. The extension of `FlexibleSUSY` to calculate loop-induced digluon and diphoton decays of scalars is then described.

4.2 Semi-analytic RGE Solutions in General Models

The general BVP problem that must be solved in a model before calculating its mass spectrum consists of a set of BCs at several renormalisation scales, where various subsets of the model parameters are fixed, connected by a set of RGEs. The complete set of RGEs forms a coupled, non-linear system of ordinary differential equations (ODEs). In general, this BVP must be solved numerically, as closed form solutions to the RGEs are not known. For dimensionful parameters, however, at least the functional dependence on the boundary values of these parameters can be determined analytically. To do so, we take advantage of the relatively simple structure of the two-loop RGEs to derive semi-analytic solutions for the running parameters. These solutions fully express the dependence on the high-scale dimensionful parameters of the model, encoding the details of the running in a set of coefficients that are usually determined numerically.

This can in turn be used to construct a BVP solver that works directly in terms of the boundary values for the dimensionful parameters, rather than their running values obtained by numerical integration. This approach is applicable to both models with or without softly broken SUSY. However, the additional constraints on the renormalisation of the superpotential parameters in SUSY models lead to rather simple semi-analytic solutions for these parameters, which in turn simplifies the solutions for other parameters; hence we first present the form of the semi-analytic solutions in SUSY models before repeating the calculation in a general QFT.

4.2.1 SUSY Models

We consider a general model with softly broken SUSY, in which the chiral superfields $\hat{\Phi}_i$ transform under a gauge group G. The general superpotential is that given in Eq. (A.32), namely

$$W = \frac{1}{6}Y^{ijk}\hat{\Phi}_i\hat{\Phi}_j\hat{\Phi}_k + \frac{1}{2}\mu^{ij}\hat{\Phi}_i\hat{\Phi}_j + L^i\hat{\Phi}_i\,. \tag{4.1}$$

The superpotential interactions are accompanied by a standard set of soft interactions given by

$$-\mathcal{L}_{\text{soft}} = \left(\frac{1}{2}M_a\lambda^a\lambda^a + \frac{1}{6}T^{ijk}\phi_i\phi_j\phi_k + \frac{1}{2}b^{ij}\phi_i\phi_j + t^i\phi_i + h.c.\right) + \phi^{j*}(m^2)^i_j\phi_i\,, \tag{4.2}$$

where the index a ranges over each of the gauge groups, if G is a product group[1]. Note that the linear couplings L^i, t^i are only permitted for fields that are total singlets under G. No such fields are present in the MSSM or E_6SSM, but total singlets do arise in the NMSSM and in the extensions of the E_6SSM to be considered in later chapters.

General formulas for the two-loop RGEs in a model of this type have been known for quite some time [354, 355, 383, 459–462]. Importantly, the coupled system of differential equations divides into two sets, one containing the RGEs for the superpotential parameters and the other the soft SUSY breaking parameters. The RGEs in the former set do not depend on any parameters in the latter, and therefore the running of the superpotential parameters can be solved independently of the soft parameters. Moreover, the non-renormalisation theorem [86, 164, 463–465] ensures that the RGEs

[1]If G is a product group with multiple $U(1)$ factors, there will also be non-diagonal soft gaugino masses of the form $M_{ab}\lambda^a\lambda^b$, where a and b range over the different $U(1)$ factors. However, this does not alter the form of the resulting semi-analytic solutions.

for the dimensionful superpotential couplings μ^{ij} and L^i have the simple forms

$$\frac{d}{dt}\mu^{ij} = f^{ij}_{kp}(t)\mu^{kp} \quad \text{and} \quad \frac{d}{dt}L^i = g^i_p(t)L^p\,, \tag{4.3}$$

where $t = \ln\frac{Q}{Q_0}$ encodes the renormalisation scale, Q. The functions $f^{ij}_{kp}(t)$ and $g^i_p(t)$ depend only on the dimensionless superpotential couplings and the gauge couplings, which run independently of the dimensionful SUSY preserving couplings. The RGEs in Eq. (4.3) thus form a homogeneous system of linear ODEs with variable coefficients, with solutions given by

$$\mu^{ij}(t) = [c^\mu_\mu(t)]^{ij}_{kp}\mu^{kp}(0)\,, \tag{4.4}$$
$$L^i(t) = [c^L_L(t)]^i_p L^p(0)\,. \tag{4.5}$$

The coefficients satisfy the same differential equations, i.e.,

$$\frac{d}{dt}[c^\mu_\mu(t)]^{ij}_{kp} = f^{ij}_{mn}(t)[c^\mu_\mu(t)]^{mn}_{kp} \quad \text{and} \quad \frac{d}{dt}[c^L_L(t)]^i_p = g^i_k(t)[c^L_L(t)]^k_p\,,$$

subject to the initial conditions $[c^\mu_\mu(0)]^{ij}_{kp} = \delta^i_k\delta^j_p$, $[c^L_L(0)]^i_p = \delta^i_p$, and can be determined once the running gauge and Yukawa couplings Y^{ijk} are known. For example, in the simple case that the superpotential, Eq. (4.1), contains only a single, real bilinear coupling μ, Eq. (4.4) reduces to

$$\mu(t) = c^\mu_\mu(t)\mu(0) = \mu(0)\exp\left(\int_0^t f(t')dt'\right)\,, \tag{4.6}$$

where $f(t)$ is a function of the gauge and dimensionless superpotential couplings.

In a similar fashion, the two-loop RGEs for the soft breaking trilinear couplings T^{ijk} and gaugino masses M_a also form a homogeneous linear system, of the form

$$\begin{aligned}\frac{d}{dt}T^{ijk} &= A^{ijk}_{lmn}(t)T^{lmn} + B^{ijkb}(t)M_b\,,\\ \frac{d}{dt}M_a &= C_{almn}(t)T^{lmn} + D^b_a(t)M_b\,.\end{aligned} \tag{4.7}$$

Analogously to the case for the dimensionful superpotential parameters, the semi-analytic solutions read

$$T^{ijk}(t) = [c^T_T(t)]^{ijk}_{lmn}T^{lmn}(0) + [c^T_M(t)]^{ijkb}M_b(0)\,, \tag{4.8}$$
$$M_a(t) = [c^M_T(t)]_{almn}T^{lmn}(0) + [c^M_M(t)]^b_a M_b(0)\,. \tag{4.9}$$

With these in hand, the RGEs for the higher mass dimension soft parameters, namely, b^{ij}, $(m^2)^i_j$ and t^i can be expressed as a system of non-homogeneous, linear first order ODEs. The solution to the general two-loop RGEs for the soft bilinears b^{ij},

$$\frac{d}{dt}b^{ij} = I^{ij}_{kl}(t)b^{kl} + J^{ij}_{klmno}(t)\mu^{kl}T^{mno} + K^{ija}_{kl}\mu^{kl}M_a \equiv I^{ij}_{kl}(t)b^{kl} + F^{ij}(t)\,, \tag{4.10}$$

is given by

$$b^{ij}(t) = U^{ij}_{kl}(t)b^{kl}(0) + U^{ij}_{kl}(t)\int_0^t V^{kl}_{mn}(t')F^{mn}(t')dt'\,. \tag{4.11}$$

The functions $U^{ij}_{kl}(t)$, $V^{ij}_{kl}(t)$ follow from solving the corresponding homogeneous system, and satisfy

$$\frac{d}{dt}U^{ij}_{kl} = I^{ij}_{mn}(t)U^{mn}_{kl}\,, \quad U^{ij}_{mn}(t)V^{mn}_{kl}(t) = \delta^i_k\delta^j_l\,, \quad U^{ij}_{kl}(0) = \delta^i_k\delta^j_l\,. \tag{4.12}$$

After substituting the forms of the semi-analytic solutions Eqs. (4.4), (4.8) and (4.9) into the definition of the function $F^{ij}(t)$, the solution for the soft breaking bilinear b^{ij} becomes

$$b^{ij}(t) = [c^b_b(t)]^{ij}_{kl}b^{kl}(0) + [c^b_{\mu T}(t)]^{ij}_{abmno}\mu^{ab}(0)T^{mno}(0) + [c^b_{\mu M}(t)]^{ijc}_{ab}\mu^{ab}(0)M_c(0)\,. \tag{4.13}$$

The results for the soft scalar masses $(m^2)^i_j$ and the soft trilinears t^i are obtained in the same way. That is, given the two-loop RGEs for the soft scalar masses,

$$\begin{aligned}\frac{d}{dt}(m^2)^j_i &= W^{jl}_{ik}(t)(m^2)^k_l + X^j_{iklmnop}(t)T^{klm}(T^{nop})^* + Y^{jab}_i(t)M_aM^*_b \\ &\quad + Z^{ja}_{iklm}(t)(T^{klm})^*M_a + \bar{Z}^{ja}_{iklm}(t)T^{klm}M^*_a \\ &\equiv W^{jl}_{ik}(t)(m^2)^k_l + G^j_i(t)\,,\end{aligned} \tag{4.14}$$

the solution takes the same form as in Eq. (4.11). Expressed in terms of the initial values of the soft parameters, this reads

$$\begin{aligned}(m^2)^j_i(t) = {}& [c^{m^2}_{m^2}(t)]^{jl}_{ik}(m^2)^k_l(0) + [c^{m^2}_{MM^*}(t)]^{jab}_i M_a(0)M^*_b(0) + [c^{m^2}_{TM^*}(t)]^{ja}_{iklm}T^{klm}(0)M^*_a(0) \\ &+ [c^{m^2}_{T^*M}(t)]^{ja}_{iklm}T^{klm*}(0)M_a(0) + [c^{m^2}_{T^*T}(t)]^j_{iklmnop}T^{klm*}(0)T^{nop}(0)\,.\end{aligned} \tag{4.15}$$

Similarly, for the standard set of soft terms given in Eq. (4.2), the two-loop RGEs for the soft linear couplings can be written generically as

$$\frac{d}{dt}t^i = \alpha^i_j(t)t^j + \beta^{ia}_j(t)L^jM_a + \gamma^i_{jklm}(t)L^jT^{klm} + \rho^{ia}_{jklm}(t)\mu^{jk}\mu^{lm}M_a + \sigma^i_{jklm}(t)\mu^{jk}b^{lm}$$

$$
\begin{aligned}
&+ \tau^i_{jklmnop}(t)\mu^{jk}\mu^{lm}T^{nop} + \omega^{iab}_{jk}(t)\mu^{jk*}M_aM_b^* + \nu^{ia}_{jk}b^{jk*}M_a \\
&+ \xi^{ia}_{jklmn}(t)\mu^{jk*}T^{lmn}M_a^* + \zeta^i_{jklmn}(t)b^{jk*}T^{lmn} + \varphi^{ik}_{jlm}(t)\mu^{lm*}(m^2)^j_k \\
&+ \psi^i_{jklmnopq}\mu^{jk*}T^{lmn}T^{opq*} \\
&\equiv \alpha^i_j(t)t^j + H^i(t)\,. \qquad (4.16)
\end{aligned}
$$

Once the semi-analytic solutions for the lower mass dimension parameters are substituted in, the solution for t^i becomes

$$
\begin{aligned}
t^i(t) = {} & [c^t_t(t)]^i_j t^j(0) + [c^t_{LT}(t)]^i_{jklm}L^j(0)T^{klm}(0) + [c^t_{LM}(t)]^{ia}_j L^j(0)M_a(0) \\
&+ [c^t_{\mu\mu T}(t)]^i_{jklmnop}\mu^{jk}(0)\mu^{lm}(0)T^{nop}(0) + [c^t_{\mu\mu M}(t)]^{ia}_{jklm}\mu^{jk}(0)\mu^{lm}(0)M_a(0) \\
&+ [c^t_{\mu b}(t)]^i_{jklm}\mu^{jk}(0)b^{lm}(0) + [c^t_{\mu^* MM^*}(t)]^{iab}_{jk}\mu^{jk*}(0)M_a(0)M_b^*(0) \\
&+ [c^t_{\mu^* TT^*}(t)]^i_{jklmnopq}\mu^{jk*}(0)T^{lmn}(0)T^{opq*}(0) \\
&+ [c^t_{\mu^* TM^*}(t)]^{ia}_{jklmn}\mu^{jk*}(0)T^{lmn}(0)M_a^*(0) \\
&+ [c^t_{\mu^* T^* M}(t)]^{ia}_{jklmn}\mu^{jk*}T^{lmn*}(0)M_a(0) + [c^t_{b^* T}(t)]^i_{jklmn}b^{jk*}(0)T^{lmn}(0) \\
&+ [c^t_{b^* M}(t)]^{ia}_{jk}b^{jk*}(0)M_a(0) + [c^t_{\mu^* m^2}(t)]^{il}_{jkm}\mu^{jk*}(0)(m^2)^m_l(0)\,. \qquad (4.17)
\end{aligned}
$$

The presence of non-standard soft terms, beyond those present in Eq. (4.2), modifies the form of the two-loop RGEs and hence the semi-analytic solutions that follow from them. Of particular relevance for the purpose of implementing a BVP solver using these solutions is the case of Dirac gaugino masses. When the model under consideration contains chiral superfields that are singlets or transform in the adjoint representation of the gauge group, or a factor of it in the case of a product group, soft Dirac mass terms of the form [466–469]

$$
-\mathcal{L}_{\text{soft,non-standard}} \supset m^i_{Da}\psi_i\lambda^a + h.c.\,, \qquad (4.18)
$$

can be included, where the ψ_i are the additional singlet or adjoint representation fermions. As for SUSY models with standard soft terms, the general two-loop RGEs when Dirac gaugino masses are present are also known [462]. The RGEs for the Dirac masses m^i_{Da} themselves are rather simple, owing to their origin from "supersoft" operators [469] that receive only a wavefunction renormalisation, and can be written in the form

$$
\frac{d}{dt}m^i_{Da} = h^i_j(t)m^j_{Da}\,. \qquad (4.19)
$$

Consequently, the solutions for the masses m^i_{Da} read

$$m^i_{Da}(t) = [c^{m_{Da}}_{m_{Da}}(t)]^i_j m^j_{Da}(0)\,. \tag{4.20}$$

In addition to introducing new soft parameters, the inclusion of Dirac gaugino masses also generates extra contributions to the RGEs for the soft SUSY breaking linear couplings t^i. In particular, the function $H^i(t)$ defined in Eq. (4.16) is modified, $H^i(t) \to H^i(t) + \Delta H^i(t)$, where the new terms are of the form

$$\begin{aligned}\Delta H^i(t) = {} & \theta^{ika}_{jl}(t) m^j_{Da} (m^2)^l_k + \Sigma(t)^{iab}_{jklmn}(t) m^{j*}_{Da} m^{k*}_{Db} T^{lmn} \\ & + \Theta^{iabc}_{jk}(t) m^{j*}_{Da} m^{k*}_{Db} M_c(0) + \Phi^{iab}_{jklm}(t) \mu^{jk} m^l_{Da} m^m_{Db}\,.\end{aligned} \tag{4.21}$$

The corresponding modification to the solution, Eq. (4.17), is $t^i(t) \to t^i(t) + \Delta t^i(t)$, with the extra contribution

$$\begin{aligned}\Delta t^i(t) = {} & [c^t_{m_d m^2}(t)]^{iaj}_{kl} m^k_{Da}(0) (m^2)^l_j(0) + [c^t_{m_D M M^*}(t)]^{iabc}_j m^j_{Da}(0) M_b(0) M^*_c(0) \\ & + [c^t_{m_D T M^*}(t)]^{iab}_{jklm} m^j_{Da}(0) T^{klm}(0) M^*_b(0) \\ & + [c^t_{m_D T^* M}(t)]^{iab}_{jklm} m^j_{Da}(0) T^{klm*}(0) M_b(0) \\ & + [c^t_{m_D T T^*}(t)]^{ia}_{jklmnop} m^j_{Da}(0) T^{klm*}(0) T^{nop}(0) \\ & + [c^t_{m^*_D m^*_D T}(t)]^{iab}_{jklmn} m^{j*}_{Da}(0) m^{k*}_{Db}(0) T^{lmn}(0) \\ & + [c^t_{m^*_D m^*_D M}(t)]^{iabc}_{jk} m^{j*}_{Da}(0) m^{k*}_{Db}(0) M_c(0) \\ & + [c^t_{m_D m_D \mu}(t)]^{iab}_{jklm} m^j_{Da}(0) m^k_{Db}(0) \mu^{lm}(0)\,.\end{aligned} \tag{4.22}$$

4.2.2 Non-SUSY Models

The derivation of the semi-analytic solutions for the soft breaking parameters in SUSY models made use of the fact that the parameters in the model can be split into a sequence of sets, such that the evolution of the parameters in each set does not depend on any of the parameters in the subsequent sets. The system of RGEs for each set can then be integrated, one set at a time, substituting the solutions from previous sets where appropriate. This step-by-step approach is also applicable in non-SUSY models. In this case, the breakdown into separate sets is made solely on the basis of the mass dimension of the parameters. The process of obtaining the full set of semi-analytic solutions otherwise proceeds in much the same way as for SUSY models. The only significant difference is that, in general, all parameters of a given mass dimension will appear in the solutions, unlike for SUSY models, where the semi-analytic solutions

for the dimensionful superpotential parameters do not depend on any of the soft parameters.

To derive the semi-analytic solutions to the RGEs in a general gauge theory, we consider a model describing real scalars ϕ_i and two-component fermions ψ_i, transforming under a gauge group G. The parts of the Lagrangian containing the Yukawa interactions and scalar potential read

$$\begin{aligned} -\mathcal{L}_{\text{int}} = &\frac{1}{2!}(m^2)^{ij}\phi_i\phi_j + \frac{1}{3!}h^{ijk}\phi_i\phi_j\phi_k + \frac{1}{4!}\lambda^{ijkl}\phi_i\phi_j\phi_k\phi_l \\ &+ \frac{1}{2}\left(Y^{ijk}\phi_i\psi_j\psi_k + (M_f)^{ij}\psi_i\psi_j + h.c.\right) . \end{aligned} \tag{4.23}$$

The parameters $(m^2)^{ij}$, h^{ijk} and λ^{ijkl} are assumed to be real. The general two-loop RGEs for this model are well known [354, 355, 470–474], allowing the semi-analytic solutions to be derived in the same way as for SUSY models. In principle, linear terms for gauge singlets of the form $L^i\phi_i$ can also be written down, and the two-loop RGEs for the real couplings L^i have been calculated [462]. However, these terms can be removed by carrying out appropriate shifts on the fields. `SARAH`, and therefore `FlexibleSUSY`, currently does not calculate the RGEs for these parameters, rendering the semi-analytic expansion of L^i unnecessary. For this reason, we do not present the analytic form of the semi-analytic solution for L^i here alongside those expressions that are necessary for the semi-analytic BVP solver to be implemented in `FlexibleSUSY`; if required, it may be easily derived using the same methods applied to the generic expressions in Ref. [462].

The RGEs for the dimensionless couplings Y^{ijk} and λ^{ijkl}, together with those for the gauge couplings, can be integrated independently of the dimensionful parameters. Starting with the mass dimension one parameters, h^{ijk} and $(M_f)^{ij}$, the relevant RGEs take the generic form

$$\begin{aligned} \frac{d}{dt}h^{ijk} &= A^{ijk}_{lmn}(t)h^{lmn} + B^{ijk}_{lm}(t)(M_f)^{lm} + \bar{B}^{ijk}_{lm}(t)(M_f)^{lm*} , \\ \frac{d}{dt}(M_f)^{ij} &= C^{ij}_{lmn}(t)h^{lmn} + D^{ij}_{kl}(t)(M_f)^{kl} + \bar{D}^{ij}_{kl}(t)(M_f)^{kl*} . \end{aligned} \tag{4.24}$$

As for the mass dimension one soft parameters in SUSY models, Eq. (4.24) is a linear, homogeneous system, and the general solution can be written down immediately in terms of unknown coefficients, giving

$$h^{ijk}(t) = [c^h_h(t)]^{ijk}_{lmn}h^{lmn}(0) + [c^h_{M_f}(t)]^{ijk}_{lm}(M_f)^{lm}(0) + [c^h_{M^*_f}(t)]^{ijk}_{lm}(M_f)^{lm*}(0) , \tag{4.25}$$

$$(M_f)^{ij}(t) = [c_h^{M_f}(t)]^{ij}_{lmn} h^{lmn}(0) + [c_{M_f}^{M_f}(t)]^{ij}_{lm}(M_f)^{lm}(0) + [c_{M_f^*}^{M_f}(t)]^{ij}_{lm}(M_f)^{lm*}(0)\,. \quad (4.26)$$

The only significant difference, compared to the results Eq. (4.8) and Eq. (4.9) in SUSY models, is the additional term proportional to $(M_f)^{lm*}(0)$ that arises because of the complex conjugated terms that now appear in Eq. (4.24).

The semi-analytic solutions for the squared scalar masses $(m^2)^{ij}$ then follow from substituting these results into the two-loop RGEs for $(m^2)^{ij}$, which have the form

$$\begin{aligned}\frac{d}{dt}(m^2)^{ij} &= W^{ij}_{kl}(t)(m^2)^{kl} + X^{ij}_{klmnop}(t)h^{klm}h^{nop} + Y^{ij}_{klmn}(t)(M_f)^{kl}(M_f)^{mn} \\ &\quad + \tilde{Y}^{ij}_{klmn}(t)(M_f)^{kl*}(M_f)^{mn} + \bar{Y}^{ij}_{klmn}(t)(M_f)^{kl*}(M_f)^{mn*} \\ &\quad + Z^{ij}_{klmpq}(t)h^{klm}(M_f)^{pq} + \bar{Z}^{ij}_{klmpq}(t)h^{klm}(M_f)^{pq*} \\ &\equiv W^{ij}_{kl}(t)(m^2)^{kl} + G^{ij}(t)\,. \end{aligned} \quad (4.27)$$

The solution to the linear, non-homogeneous system that arises after substituting in the solutions for the dimension one parameters is arrived at in the same way as for the SUSY case. The general solution has the same form as that for the soft SUSY breaking bilinears b^{ij} in Eq. (4.11) and, since the source term $G^{ij}(t)$ is known, may be written as

$$\begin{aligned}(m^2)^{ij}(t) &= [c_{m^2}^{m^2}(t)]^{ij}_{kl}(m^2)^{kl}(0) + [c_{hh}^{m^2}(t)]^{ij}_{klmnop}h^{klm}(0)h^{nop}(0) \\ &\quad + [c_{hM_f}^{m^2}(t)]^{ij}_{klmpq}h^{klm}(0)(M_f)^{pq}(0) + [c_{hM_f^*}^{m^2}(t)]^{ij}_{klmpq}h^{klm}(0)(M_f)^{pq*}(0) \\ &\quad + [c_{M_fM_f}^{m^2}(t)]^{ij}_{klmn}(M_f)^{kl}(0)(M_f)^{mn}(0) \\ &\quad + [c_{M_fM_f^*}^{m^2}(t)]^{ij}_{klmn}(M_f)^{kl}(0)(M_f)^{mn*}(0) \\ &\quad + [c_{M_f^*M_f^*}^{m^2}(t)]^{ij}_{klmn}(M_f)^{kl*}(0)(M_f)^{mn*}(0)\,. \end{aligned} \quad (4.28)$$

Note that in general all of the scalar bilinear couplings must be considered together, and similarly all of the dimension one parameters are taken together. This can be contrasted with the case of a SUSY model, where the superpotential parameters could be treated separately to the soft breaking parameters.

4.3 The Semi-analytic BVP Solver Algorithm

The structure of the solutions derived above naturally suggests an iterative solution to the BVP that proceeds in two steps at each iteration. The solver algorithm implemented into `FlexibleSUSY` automatically determines the above semi-analytic solutions

in the model, given the set of BCs at some scale. Since the required coefficients may be determined knowing only the running of the dimensionless or SUSY preserving parameters, the first stage of each iteration step is for the BVP to solve iteratively for the SUSY preserving or dimensionless parameters. The semi-analytic coefficients at any scale can then be calculated. In a second step, the soft breaking or dimensionful parameters are expanded in terms of the semi-analytic solutions to the RGEs. The low-energy EWSB conditions and masses are thus expressed explicitly in terms of the parameter boundary values, allowing, for example, unknown quantities at one scale to be directly constrained at another. Upon using either the given boundary values, or fixing some of these values using, for example, the EWSB conditions, the soft or dimensionful parameters are determined. The whole process can then be iterated until a convergent solution is found. The semi-analytic solver algorithm thus requires two nested iterations: one, the outer iteration, determines the soft or dimensionful parameters, and a second, inner iteration carried out on each step of the outer iteration to determine the SUSY preserving or dimensionless parameters. The inner iteration uses the existing two-scale algorithm to solve for this set of parameters, which we now review.

4.3.1 Review of the Two-scale Algorithm

The two-scale BVP solver algorithm was initially developed for use in the MSSM [208], and is the standard approach implemented in most public spectrum generators for the MSSM and NMSSM. In general terms, the algorithm is formulated as a fixed point iteration (FPI), that is, it seeks a converged solution $\boldsymbol{p}_*$ for the set of running model parameters at a given input scale, $\boldsymbol{p}$, that satisfies

$$\boldsymbol{p}_* = \boldsymbol{f}(\boldsymbol{p}_*)\,, \tag{4.29}$$

where the function $\boldsymbol{f}$ is constructed such that a fixed point of $\boldsymbol{f}$ corresponds to a solution of the BVP.

As usually implemented in spectrum generators such as `SOFTSUSY`, `SPheno`, and `FlexibleSUSY`, boundary values for the model parameters are specified at either two or three different renormalisation scales. These are

1. A low-scale BC, at which the model is matched to the SM. Ordinarily, the scale of this matching is taken to occur at the scale $Q = M_Z$.

2. A SUSY-scale BC, applied at an intermediate scale $Q = M_S$. The definition of M_S is often chosen so as to minimise the scale dependence of the EWSB conditions [475] or the size of the dominant logarithmic corrections to the pole mass spectrum.

3. A high-scale BC applied at $Q = M_X$. For example, M_X may be defined as the GUT scale $M_X = M_{GUT}$ at which $g_1(M_{GUT}) = g_2(M_{GUT})$. For low-energy models in which the parameters are not assumed to be defined at some high scale, this BC can be omitted, and all parameters fixed at the low- and SUSY-scales instead.

At each scale, some number of the model parameters may be directly set to a set of given boundary values, or determined implicitly in terms of other model parameters. For instance, for a CMSSM parameter point characterised by values of the universal soft parameters m_0, $M_{1/2}$ and A_0, as well as $\operatorname{sign}\mu$ and $\tan\beta$, this may correspond to the high-scale BCs given in Eq. (2.16), where the high-scale M_X is not fixed, but must be determined so that the GUT scale condition[2]

$$g_1(M_X) = g_2(M_X) \tag{4.30}$$

holds.

The remaining running Lagrangian parameters, which in the MSSM include the gauge and Yukawa couplings, μ and $B\mu$, are fixed to reproduce known low-energy data and to ensure correct EWSB. In the MSSM, the latter is usually achieved by solving the two EWSB conditions, Eq. (2.31), for μ and $B\mu$ at the SUSY-scale M_S, defined by

$$M_S^2 = \prod_{i=1}^{6} (m_{\tilde{u}_i}^{\overline{\text{DR}}})^{|(Z_u)_{i3}|^2 + |(Z_u)_{i6})|^2} . \tag{4.31}$$

In the absence of flavour mixing, this condition reduces to the more conventional definition in terms of the geometric mean of the $\overline{\text{DR}}$ stop masses, $M_S = \sqrt{m_{\tilde{t}_1}^{\overline{\text{DR}}} m_{\tilde{t}_2}^{\overline{\text{DR}}}}$, which must be calculated by solving the BVP. More generally, in a given BSM model some subset of the model parameters will be fixed by solving the EWSB conditions at an appropriately defined scale. In general, this requires solving a non-linear system of equations, which was previously achieved in `FlexibleSUSY` using the variants of the multidimensional Newton's method provided by the GNU Scientific Library [476]. In some cases, the EWSB conditions can be written in a form that is efficiently solved

[2] In models such as the MSSM and E$_6$SSM, $g_3(M_X)$ is also approximately unified with $g_1(M_X)$ and $g_2(M_X)$, though this condition is not imposed directly.

using a FPI. This is the standard approach used by `SOFTSUSY` in the MSSM, for instance, where Eq. (2.36) can be rearranged to write

$$|\mu|^2 = \frac{\bar{m}_{H_d}^2 - \bar{m}_{H_u}^2 \tan^2\beta}{\tan^2\beta - 1} - \frac{1}{2}(m_Z^{\overline{\rm DR}})^2 \equiv g(|\mu|^2)\,, \tag{4.32}$$

which can be solved iteratively by taking successive guesses $|\mu_{n+1}|^2 = g(|\mu_n|^2)$ until the iterates μ_n converge to a fixed point. The resulting solution for μ can then be used in Eq. (2.37) to determine $B\mu$. When applicable, this FPI approach to solving the EWSB conditions can obtain a solution more quickly than the other numerical solvers available in `FlexibleSUSY`. During the course of the work done for this thesis, we therefore developed a FPI EWSB algorithm, generalising the method used in the MSSM, and implemented it into `FlexibleSUSY`. This EWSB solver is now currently the default method[3] used to solve the EWSB conditions. When a rearrangement that puts this system into the form of Eq. (4.29) cannot be found, or the FPI solution does not converge, the previously used numerical solvers are employed instead.

The gauge and Yukawa couplings can be fixed at the low-scale $Q = M_Z$ from low-energy observables. The particular observables chosen may depend on the spectrum generator being used; a standard choice, mandated by the SUSY Les Houches Accord (SLHA) [200, 201], is to use the electromagnetic and strong $\overline{\rm MS}$ couplings in the SM with 5 flavours at M_Z, $\alpha_{\rm e.m,SM}^{(5)\overline{\rm MS}}(M_Z)$ and $\alpha_{s,\rm SM}^{(5)\overline{\rm MS}}(M_Z)$, M_Z, the Fermi constant[4] G_F, and the top and tau pole masses M_t and M_τ and the running $\overline{\rm MS}$ bottom mass $m_b^{\overline{\rm MS}}(m_b)$. A complication arises here from the fact that the values of these quantities [95] are extracted from experimental data in the framework of the SM, with no BSM contributions. The presence of additional states in BSM models means that the experimental results would be reproduced for different values of parameters such as the gauge and Yukawa couplings in the model. To account for this, an appropriate set of threshold corrections [477] must be used to relate the various input parameters to the Lagrangian parameters in the full BSM model[5]. These threshold corrections also depend implicitly on the other parameters in the model through running masses appearing in the corrections, and are another component that must be determined iteratively as well in the course of solving the BVP.

[3] Starting from `FlexibleSUSY`-1.0.4.

[4] In `FlexibleSUSY`, the W pole mass M_W can be used instead, but this choice is not SLHA compliant.

[5] In general there are also corrections that must be applied to account for the various different ways in which the input parameters are defined. For example, in SUSY models where the running couplings are usually defined in the $\overline{\rm DR}$ renormalisation scheme, corrections must also be included for the conversion from $\overline{\rm MS}$ to $\overline{\rm DR}$ parameters [478].

The method employed in the two-scale algorithm to solve the BVP, given BCs such as the above, is in principle rather simple. The process is illustrated in Figure 4.2. After making an initial guess for the model parameters to obtain initial values for all

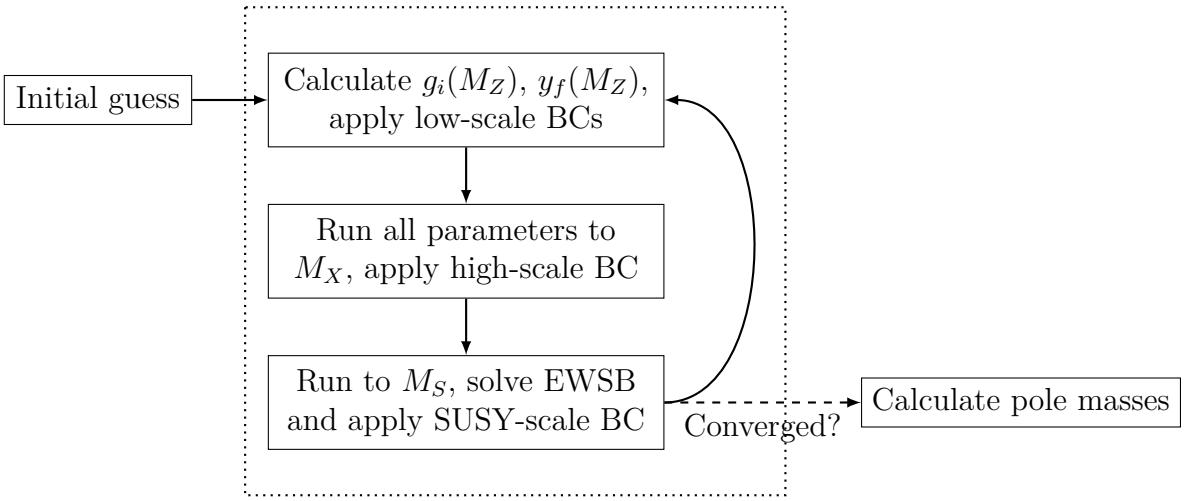

Figure 4.2: Diagram showing the steps of the two-scale fixed point algorithm to determine the pole mass spectrum. The steps within the dotted box define the iterated function $\boldsymbol{f}$ in Eq. (4.29).

model parameters, $\boldsymbol{p}_0$, at (say) the high-scale, the algorithm repeatedly runs between the three different boundary scales using the RGEs in the model, applying the relevant BCs at each scale. Each such iteration, corresponding to a single evaluation of the function $\boldsymbol{f}$ in Eq. (4.29), yields a new estimate for the parameters $\boldsymbol{p}^{(i)}$ that satisfy the BCs. A fixed point $\boldsymbol{p}_*$ of this process corresponds to a set of parameter values that satisfy all of the BCs at each scale, and is therefore a solution of the BVP. At this stage, the iteration stops and the pole mass spectrum and other observables can be calculated.

The exact steps that occur at each scale depend somewhat on the model under consideration and the code used; for example, one might choose to impose the EWSB conditions at the low-scale M_Z rather than the SUSY-scale. As a more detailed example, in a high-scale model such as the CMSSM the rough steps outlined in Figure 4.2 may be applied in the package `FlexibleSUSY` as follows [428]: starting from an initial guess for the model parameters and the $\overline{\text{DR}}/\overline{\text{MS}}$ mass spectrum,

1. All model parameters are run to the low-scale, where

   (a) The $\overline{\text{DR}}/\overline{\text{MS}}$ mass spectrum is calculated.

(b) The low-scale is recalculated, if it is not fixed to an input value such as the experimental value of M_Z.

(c) The gauge couplings $g_i(M_Z)$, $i = 1, 2, 3$, are calculated in the model, including the appropriate threshold corrections.

(d) Any additional constraints for the model parameters at this scale are applied[6].

2. All model parameters are run to the high-scale, where

(a) The high-scale is recalculated, if necessary. For example, in the case that M_X is defined by the unification condition Eq. (4.30), a new estimate for M_X is computed according to

$$M_X' = M_X \exp\left(\frac{g_2(M_X) - g_1(M_X)}{\beta_{g_1} - \beta_{g_2}}\right), \tag{4.33}$$

where β_{g_1} and β_{g_2} are the β functions for the gauge couplings g_1 and g_2.

(b) The BCs at this scale are applied. In the CMSSM, this corresponds to setting the soft parameters to their values given in Eq. (2.16).

3. All model parameters are run to the SUSY-scale, where

(a) The $\overline{\text{DR}}/\overline{\text{MS}}$ mass spectrum is recalculated.

(b) If necessary, the SUSY-scale is updated. For example, this may be done in the CMSSM using Eq. (4.31).

(c) The BCs, such as solving the EWSB conditions for μ and $B\mu$ in the CMSSM, are imposed.

4. Test if the iteration has converged, for instance by inspecting the relative changes in the $\overline{\text{DR}}/\overline{\text{MS}}$ masses compared to the previous iteration. If the iteration has not converged, return to 1.

If this iteration converges, a consistent solution to the BVP has been found and the running parameters are known at all scales between the low-scale and the high-scale. The pole mass spectrum can then be calculated after running the model parameters to the scale at which the pole masses are to be calculated. Conversely, it might be the case that the chosen boundary values yield an unphysical point, or the iteration

[6] In `FlexibleSUSY`, these are defined by the user of the package in a model file. The model file interface for `FlexibleSUSY` is described in detail in Refs. [97, 428].

may not converge. In the former case, problems such as tachyonic physical masses or a failure of EWSB can be used to conclude that the point is invalid, and should not be considered further in any analysis.

The package `FlexibleSUSY` implements the above algorithm in a very generic fashion, in which model specific physics details are hidden by abstract representations of a model and a set of BCs. This allows the code to be extremely general, and applicable to a wide range of models, while also being fast. The algorithm can also be easily generalised to include additional BCs, as well as matching conditions to treat towers of effective field theories. Further details of the implementation may be found in Refs. [428, 429].

4.3.2 Implementation of the Semi-analytic BVP Solver Algorithm

The two-scale algorithm, as implemented above, works in terms of the running parameters at each scale, obtained by numerically integrating the full system of RGEs for the model parameters. This becomes a limitation when the BCs cannot be easily expressed or solved in terms of the parameters at a single scale. For example, in the CMSSM the EWSB conditions are used to fix μ and $B\mu$, which allows the observed value of the VEV v, as well as $\tan\beta$, to be given as an input, thus ensuring that the correct gauge boson masses are reproduced. On the other hand, in a model such as the (Z_3-symmetric) CNMSSM or the CE$_6$SSM the analogous bilinear parameters are absent, and a different set of parameters must be selected to be fixed in order to be guaranteed correct EWSB. In these models, the soft scalar masses, including $m_{H_d}^2$, $m_{H_u}^2$, and at least one singlet mass m_S^2, are assumed to be universal at the GUT scale, as in Eq. (2.16b) with the additional constraint $m_S^2(M_X) = m_0^2$. However, in general if one or more of these soft parameters are fixed from the solution of the EWSB conditions, then after running to the high-scale the universality condition will be violated. Therefore in most cases a solution consistent with the BCs will not be found using the two-scale solver, and so the two-scale solver cannot (easily) be applied to solve the BVP.

In cases such as this, using the semi-analytic solutions to express low-energy parameters directly in terms of their boundary values becomes helpful. Rather than choosing a subset of the soft parameters to be fixed by the EWSB conditions, instead one of the boundary values, such as m_0, may be fixed instead. In this way, correct EWSB can be ensured while also remaining consistent with the constraints at the

high-scale. This may also be a more convenient choice in models such as the CMSSM, where it can be preferable for certain purposes to directly control parameters such as μ and treat m_0 as an EWSB output. This approach is used, for example, to study neutralino DM in the CMSSM in Chapter 7. The addition of the semi-analytic solver algorithm, which uses exactly this strategy, thus expands the types of models and BCs that can be handled in a code such as `FlexibleSUSY`.

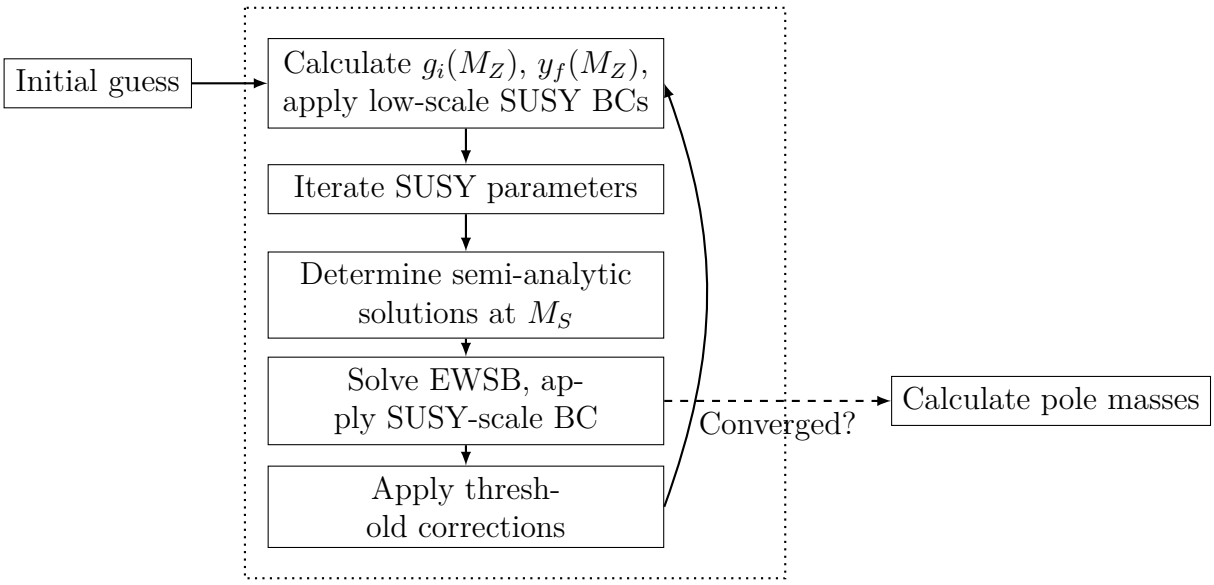

Figure 4.3: Diagram showing the steps of the semi-analytic algorithm. The set of steps in the dotted box make up the iterated function for which a fixed point is sought.

The semi-analytic algorithm that has been implemented in `FlexibleSUSY` is outlined in Figure 4.3. In the inner two-scale iteration, carried out at each step, consistent values for the SUSY preserving (in SUSY models) or dimensionless parameters (in non-SUSY models) at the low- and high-scale boundaries are determined. As for the two-scale solver, the locations of these boundaries need not be fixed; if necessary, updated estimates for the scales are calculated simultaneously during this iteration. Once this has converged, the resulting estimate for these parameters is used to compute the semi-analytic solutions for the soft SUSY breaking or dimensionful parameters, at which point the EWSB conditions may be solved and the $\overline{\text{DR}}/\overline{\text{MS}}$ mass spectrum calculated. The new values of the soft parameters are then used in the inner iteration for computing the required threshold corrections. The whole process is iterated until a fixed point is obtained, at which point the pole mass spectrum can be computed.

To illustrate the details of the semi-analytic algorithm, it is again useful to consider a single high-scale model such as the CMSSM [97]. Obtaining the initial guess in this

case is slightly more involved than in the two-scale solver, and corresponds to a first run of the inner iteration in which threshold corrections are ignored in every step. In a model such as the CMSSM, the initial guess consists of the following steps:

1. The known values of the SM gauge couplings at the scale M_Z are used to estimate the values of g_1, g_2 and g_3 at the scale M_t, ignoring threshold corrections.

2. An initial guess[7] at the low-scale is imposed at the scale M_t for some of the model parameters.

3. The SUSY preserving or dimensionless parameters are run to the initial guess for M_X and the high-scale BC for these parameters is imposed. An appropriate initial guess at the high-scale is then applied.

4. The model is run to the guess for the low-scale, and the low-scale BCs for the SUSY preserving or dimensionless parameters are applied.

5. The model is run to the current guess for M_X, where

   (a) If necessary, the guess for M_X is updated, for example by using Eq. (4.33).

   (b) The high-scale BCs for the SUSY preserving or dimensionless parameters are applied.

6. If the values of the SUSY preserving or dimensionless parameters have not converged, the process is repeated by returning to 4.

7. Once these parameters have converged, the model is run to the current guess for the low-scale. The semi-analytic solutions are calculated at this scale using the current guess for the scale at which the BCs for the soft or dimensionful parameters are applied. For example, in models such as the CMSSM this would typically be the current value of M_X.

8. The EWSB equations are solved at tree-level.

9. The $\overline{\text{DR}}/\overline{\text{MS}}$ mass spectrum is calculated.

At this stage, initial guesses for all of the model parameters, BC scales and the $\overline{\text{DR}}/\overline{\text{MS}}$ mass spectrum are available. The full iteration can now start. The steps are quite similar to those taken during the initial guess, except that the full set of threshold corrections are now applied:

[7] When applied in `FlexibleSUSY`, all initial guesses are again defined by the user in the model file, along with the definitions of the various scales and BCs.

1. The SUSY preserving or dimensionless parameters are determined in the inner two-scale iteration analogous to that in the initial guess, namely:

   (a) All model parameters are run to the low-scale and the $\overline{\text{DR}}/\overline{\text{MS}}$ mass spectrum is calculated.

   (b) The low-scale is recalculated, if it is not fixed.

   (c) The SM gauge couplings are calculated in the model, including the appropriate threshold corrections.

   (d) The low-scale constraints for the SUSY preserving or dimensionless parameters are applied.

   (e) All model parameters are run to the high-scale.

   (f) The high-scale is recalculated if necessary.

   (g) The high-scale BCs at this scale for the SUSY preserving or dimensionless parameters are applied.

   (h) The model parameters are run to the SUSY-scale and the SUSY-scale is updated if necessary, for example via Eq. (4.31).

   (i) The BCs for the SUSY preserving or dimensionless parameters are applied.

   (j) If the values of the SUSY preserving or dimensionless parameters have not converged, the iteration returns to 1a.

2. All model parameters are run to the scale at which the EWSB equations are to be solved, where

   (a) The coefficients in the semi-analytic solutions are determined at this scale, using the current estimate for the scale at which the relevant BCs are imposed. For example, in the CMSSM, the semi-analytic solutions given above for the soft gaugino masses, trilinears, scalar masses and bilinear reduce to

$$M_i(Q) = p_i(Q)A_0 + q_i(Q)M_{1/2}\,, \tag{4.34}$$
$$T_i(Q) = e_i(Q)A_0 + f_i(Q)M_{1/2}\,, \tag{4.35}$$
$$m_i^2(Q) = a_i(Q)m_0^2 + b_i(Q)M_{1/2}^2 + c_i(Q)M_{1/2}A_0 + d_i(Q)A_0^2\,, \tag{4.36}$$
$$B\mu(Q) = u(Q)B\mu(M_X) + v(Q)\mu(M_X)M_{1/2} + w(Q)\mu(M_X)A_0\,. \tag{4.37}$$

The coefficients are determined numerically by varying the values of $M_{1/2}$, A_0, m_0 and $B\mu(M_X)$ and integrating the RGEs from M_X to Q. For example, the coefficients $p_i(Q)$, $e_i(Q)$, $d_i(Q)$ and $w(Q)$ are obtained by keeping only $A_0 \neq 0$. A similar approach is followed to successively obtain all of the remaining coefficients.

(b) The calculated semi-analytic solutions are used to set the values of the soft SUSY breaking or dimensionful parameters at this scale.

(c) The $\overline{\text{DR}}/\overline{\text{MS}}$ mass spectrum is calculated and the scale at which EWSB occurs is updated.

(d) The EWSB conditions are solved at the loop-level.

3. Convergence of the iteration is tested for, ordinarily by evaluating the relative differences in the $\overline{\text{DR}}/\overline{\text{MS}}$ masses between consecutive iterations. If these have not converged, the outer iteration is repeated, returning to 1. Otherwise the iteration finishes.

If the iteration converges, all running parameters in the model are determined between the low- and high-scales. The remainder of the calculation, that is, the calculation of the pole mass spectrum and observables, or checking for physical problems, can then proceed in the same way as in the two-scale algorithm.

4.3.3 Tests and Comparisons of the BVP Solvers

The two-scale solver algorithm is widely used in public spectrum generators and therefore has been extensively tested for correctness and reliability. Thus, to test the new implementation of the semi-analytic algorithm into `FlexibleSUSY`, the results obtained with the new solver have been compared to those obtained using the two-scale solver in the CMSSM, the CNMSSM and the CE$_6$SSM. A hand-written prototype of the solver in the CMSSM and CSE$_6$SSM has also been tested; the results produced using this earlier version of the code are described in Chapter 7. Consistency checks between the two have been carried out by confirming that the same solution can be found in both solvers, provided it is a stable fixed point in both. In each of the models tested, the existing formulation of the model solved using the two-scale algorithm has been compared with versions of the model using alternative boundary conditions. For example, in the CMSSM, instead of the traditional approach of fixing $|\mu|^2$ and $B\mu$ using the EWSB conditions, the value of μ is provided as an input and m_0^2 and $B\mu(M_X)$ are determined from EWSB. The benchmark points used as inputs for the

semi-analytic solver in each model are displayed in Table 4.1. In all three models, the running parameters and pole mass spectra are found to differ at or below the level of 0.1%. `FlexibleSUSY` also runs an extensive suite of tests on a nightly basis; additional unit tests that perform these comparisons have been added to this suite.

Model	Unit test benchmark points for the semi-analytic solver
CMSSM	$M_{1/2} = 500$ GeV, $\tan\beta = 10$, $A_0 = 0$ GeV, $\mu(M_{SUSY}) = 623.36$ GeV
CNMSSM	$M_{1/2} = 133.33$ GeV, $\tan\beta = 10$, $\operatorname{sign}\mu_{\text{eff}} = -1$, $A_0 = -300$ GeV, $\lambda(M_X) = -0.05$
CE_6SSM	$\tan\beta = 10$, $\lambda(M_X) = 0.12$, $\kappa_{ii}(M_X) = 0.2$, $\mu_L(M_X) = 10$ TeV, $\mu_L B_L(M_X) = 0$ GeV^2, $s(M_{SUSY}) = 4$ TeV, $\tilde{\lambda}_{\alpha\alpha}(M_X) = 0.1$

Table 4.1: Input parameter values used for the unit tests comparing the results of the two-scale and semi-analytic algorithms in the CMSSM, CNMSSM and CE_6SSM. The notation for the CNMSSM follows that in Refs. [234, 407].

In carrying out these tests, important exceptions occur where non-negligible differences are found to be present between the two solvers. In some of these cases, one solver may fail to converge to a stable solution, whereas in others multiple solutions to the BVP are possible [457], with different stability properties in the two solvers. Nevertheless, such points still satisfy the BCs imposed at each scale and are indeed valid solutions. More generally, the solutions found using one algorithm have been checked to confirm that they are also fixed point solutions of the other; that is, they satisfy all of the BCs so that the parameter values remain unchanged after applying a single step of the iteration.

In some cases in these tests, the agreement between the two solvers can depend quite sensitively on small differences between them. To illustrate this, in Figure 4.4 the percentage changes in the $\overline{\text{DR}}$ mass spectrum in the CMSSM after running points obtained using the two-scale solver through a single step of the semi-analytic solver are shown; if the point is also a fixed point of the latter this change should be negligible. For a small number of points in this scan, the change after a single iteration can be on the level of several percent for a small number of points, reaching between 20% and 30% for some exceptional points. That these points initially appear not to be fixed points of the semi-analytic solver arises primarily from the sensitivity of the semi-analytic coefficients and the EWSB solution to the estimate for the high-scale M_X, as well as numerical errors in the integration of the RGEs. In particular, for the default convergence criteria imposed by `FlexibleSUSY`, the two-scale estimate for M_X is not close enough to convergence, leading to significant differences in the calculated low-

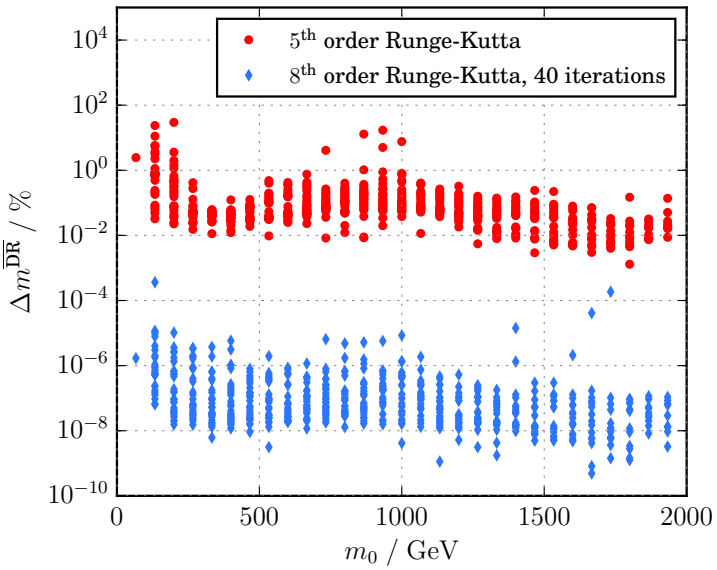

Figure 4.4: Percentage changes in the CMSSM $\overline{\text{DR}}$ mass spectrum after applying a single step of the semi-analytic solver to points obtained using the two-scale solver in a linear scan over $M_{1/2} \in [0, 300]$ GeV, $m_0 \in [0, 2]$ TeV, $A_0 = 0$ GeV, $\tan\beta = 40$ and $\mu > 0$. When run using the default Runge-Kutta algorithm provided by `FlexibleSUSY` and allowing the iteration to stop as soon as the precision goal of 10^{-4} is reached (red circles), changes between 1% and 30% are found for a small number of points. By using an 8^{th} order Runge-Kutta integrator, and ensuring convergence is reached in the estimate for M_X by forcing 40 iterations in the two-scale algorithm, these differences are reduced below the level of 0.001% (blue diamonds).

energy soft parameters. By requiring convergence in the estimate for M_X, together with the use of a higher-order Runge-Kutta integration[8] and requiring higher tolerance on the EWSB solution, the change after one iteration is reduced below the per mille level. This highlights the important fact that differences in the convergence properties of the two solvers can have an impact on the solutions found, even if a given point would be a fixed point of both solvers.

The typical runtimes for the two solvers in the CMSSM are compared in Figure 4.5. The distributions are obtained by randomly sampling from the parameter ranges $m_0 \in [0.2, 1]\,\text{TeV}$, $M_{1/2} \in [0.2, 1]\,\text{TeV}$, $\tan\beta \in [2, 30]$, $\text{sign}\,\mu \in \{-1, +1\}$ and $A_0 \in [-1, 1]\,\text{TeV}$. Compared to the two-scale solver, the semi-analytic solver is, unfortunately, significantly slower. For most points, the runtime is increased by a factor

[8]By default, `FlexibleSUSY` uses an adaptive 5^{th} order algorithm; this was replaced for these tests by the 8^{th} order Runge-Kutta-Fehlberg method provided by the Boost [479] library `odeint`.

of ~ 5. This increase in cost is mostly due to the increased number of iterations performed by the semi-analytic solver. For each outer iteration of the semi-analytic solver, the inner iteration typically runs through a similar number of iterations to the two-scale solver, with this number decreasing as convergence is approached on each outer iteration. Consequently, the total number of iterations for the semi-analytic solver tends to be larger than that for the two-scale solver by a similar factor. There is also an additional cost associated with running between scales to compute the semi-analytic coefficients.

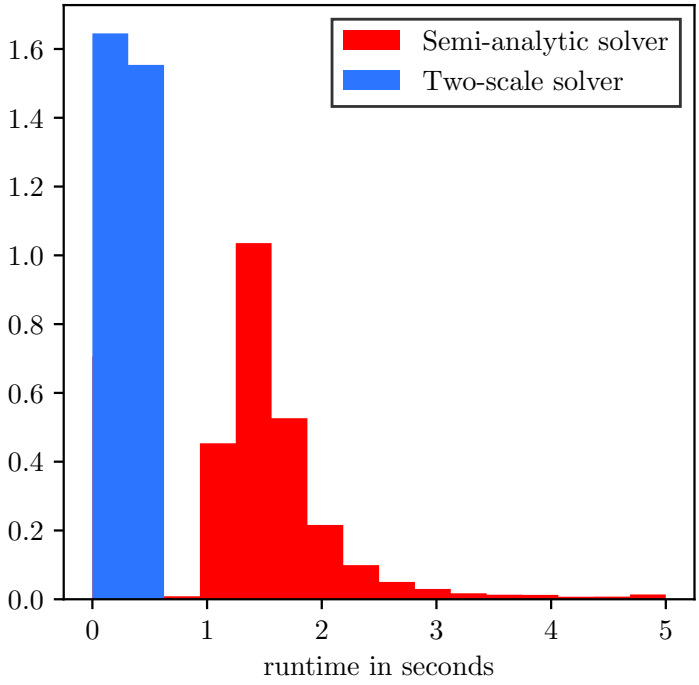

Figure 4.5: Runtime distributions of the CMSSM spectrum generators created with `FlexibleSUSY` using the two-scale and semi-analytic BVP solvers, obtained on an Intel i7-4702MQ CPU. The distributions are normalised to have an integral of unity.

While the semi-analytic solver suffers from an increased runtime compared to the two-scale solver, it is also able to provide complementary coverage of the parameter space to that of the two-scale solver. This is demonstrated in the left panel of Figure 4.6 in the CMSSM, where the solutions found by each solver are plotted in the $m_0 - \mu$ plane. In this case, the use of the semi-analytic solver allows for a large number of solutions to be found at small values of $\mu \ll m_0$; in this region, the two-scale solver

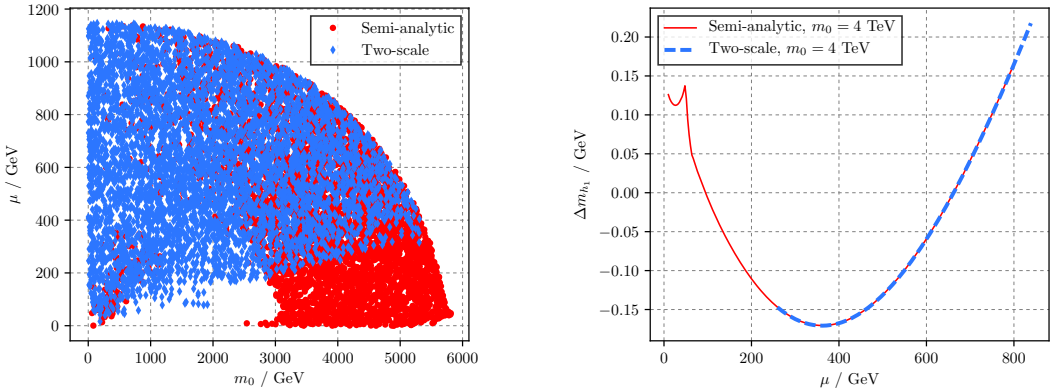

Figure 4.6: Left panel: Solutions found by the two-scale solver (blue diamonds) and the semi-analytic solver (red circles) in the $m_0 - \mu$ plane. For both solvers, $M_{1/2} \in [0, 1]$ TeV is randomly sampled, while $\tan\beta = 10$ and $A_0 = 0$ GeV. The solutions obtained using the two-scale solver are found by randomly sampling $m_0 \in [0, 6]$ TeV with sign $\mu = 1$, and those for the semi-analytic solver are found by randomly sampling $\mu \in [0, 1150]$ GeV. Right panel: Change in the calculated lightest CP-even Higgs mass Δm_{h_1} from a reference value of 121 GeV as a function of μ at fixed $m_0 = 4$ TeV for the two solvers. The solutions shown correspond to a vertical slice at fixed m_0 in the left-hand plot; $M_{1/2}$ is again varied in $[0, 1]$ TeV, $\tan\beta = 10$ and $A_0 = 0$ GeV.

is unable to find convergent solutions. These solutions lie in the well-known "focus point" region of the MSSM [480–482], and have interesting properties such as allowing for a relatively light Higgsino DM candidate while still predicting all of the sfermions to be heavy. In the context of the little hierarchy problem, focus point solutions may also be less fine tuned than solutions in other parts of the MSSM parameter space; this is discussed further in Section 5.1. The use of the semi-analytic solver allows this part of parameter space to be more thoroughly explored. Conversely, the two-scale solver is more effective for finding solutions with small m_0. In general terms, the regions of parameter space in which the two solvers are effective need not overlap, and the use of both in tandem allows for a more complete picture of the parameter space to be obtained.

In the regions in which both solvers do find solutions, there is excellent agreement between the two algorithms[9]. This is illustrated in the right panel of Figure 4.6, where the lightest CP-even Higgs mass, expressed as the difference from a baseline value of 121 GeV, is plotted for fixed $m_0 = 4$ TeV. When both solvers find a solution for this value of m_0, the two values of the Higgs mass agree very well. Note that,

[9]Provided the same solution is found, when multiple solutions exist.

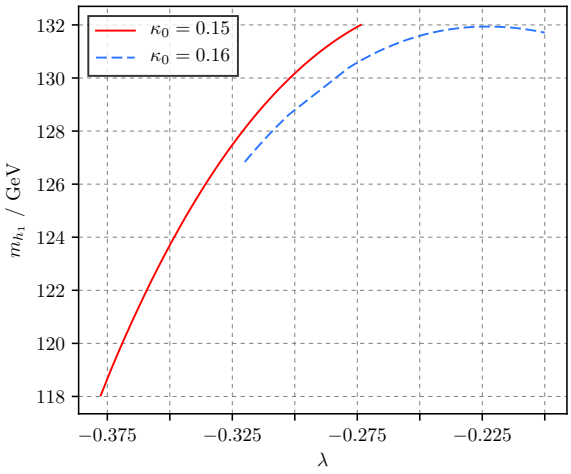

Figure 4.7: Lightest CP-even Higgs mass in the CE$_6$SSM as a function of the coupling $\lambda(M_X)$ defined at the GUT scale. The exotic couplings κ_{ij} are assumed to be diagonal and universal at the GUT scale, $\kappa_{ij}(M_X) = \kappa_0\delta_{ij}$, with $\kappa_0 = 0.15$ and $\kappa_0 = 0.16$ shown. Similarly, $\tilde{\lambda}_{\alpha\beta}(M_X) = \tilde{\lambda}_0\delta_{\alpha\beta}$ with $\tilde{\lambda}_0 = 0.1$. The remaining free parameters of the CE$_6$SSM, as defined in Ref. [363], are fixed to $\mu_L(M_X) = 10$ TeV, $\mu_L B_L(M_X) = 0$ GeV, $s(M_S) = 10$ TeV, and $\tan\beta = 10$. The universal soft parameters m_0, $M_{1/2}$ and A_0 are fixed by the EWSB conditions.

while the two-scale solver only finds a single solution for each value of μ, the semi-analytic solver finds multiple solutions in some cases, with the same value of $M_{1/2}$ and different values of μ. This leads to the sharp feature at low values of μ in Figure 4.6. Thus, importantly, both solvers can be used to explore the parameter space of the model, potentially picking up features that would be missed by either on its own, and consistent solutions are found in the regions where both succeed.

The longer runtime of the semi-analytic solver compared to the two-scale solver is also an acceptable trade-off when the model to be investigated cannot be handled easily using the two-scale solver. As a simple demonstration, in Figure 4.7 the lightest CP-even Higgs mass as a function of the coupling $\lambda(M_X)$ is plotted in the CE$_6$SSM, for two values of a single, universal exotic coupling $\kappa_{ij}(M_X) = \kappa_0\delta_{ij}$. Using the two-scale solver, ordinarily the soft Higgs masses $m^2_{H_u}$, $m^2_{H_d}$ and m^2_S would be fixed by EWSB in the E$_6$SSM, breaking the universality constraint in general. Solutions consistent with the CE$_6$SSM BCs must be found by means of a complex and slow scan, tuning other input parameters in order to find solutions to the EWSB conditions at the SUSY scale that run to universal values at M_X. The semi-analytic solver, on the other hand,

allows these solutions to be found directly, greatly simplifying the process of studying this constrained model. The addition of an additional BVP solver thus also extends the range of models that `FlexibleSUSY` can handle; we take advantage of this fact in Chapter 7 to study an alternative constrained E_6 inspired model.

4.4 Loop Induced Decays

The addition to `FlexibleSUSY` of the semi-analytic BVP solver provides greater flexibility in the kinds of BCs that can be handled, and allows a wider range of BSM models to be investigated. Computing the predicted pole mass spectrum of a model is a key requirement for testing that model against experiment, since the phenomenology associated with a particular parameter point is obviously strongly dependent on the mass spectrum for that point. Knowledge of the mass spectrum is a necessary ingredient for evaluating a model against experimental mass limits, but in general this is not sufficient on its own. Other observables such as production cross sections and decay branching ratios must also be calculated before such a comparison can be properly made. These quantities (or appropriate combinations thereof) are also important observables in themselves that can be used to constrain a model against an observed signal[10] or exclusion, which demands that they are also calculated as precisely as possible.

Extending spectrum generators for general models, such as those produced by `FlexibleSUSY`, to include the calculation of decays is therefore an important step as far as studying new models goes. Automation of the process of determining all possible decay channels, and enabling their calculation within the resulting spectrum generator, also has several advantages. Firstly, the use of a tool such as `FlexibleSUSY` or `SPheno` will ensure that possible decay channels are not missed, which would lead to a misleading calculation of the branching ratios or make checking constraints in the missed channels impossible. The corresponding couplings are also calculated in full generality, without neglecting mixing between states, for example. Higher-order corrections and loop induced decays must also, in general, be accounted for. Since the spectrum generator has full access to the calculated masses and running param-

[10]The work [98] reported in this section was originally prompted by the need, in the face of many oversimplified or even outright wrong calculations, to make available a correct, generic calculation of the diphoton and digluon decay rates of hypothetical states explaining the somewhat notorious 750 GeV excess observed by ATLAS [483] and CMS [484] in the diphoton channel. In this case the "signal" was simply a statistical fluctuation [485]. Despite this, the potential for incorrect conclusions to be made on the basis of an incomplete treatment of a model reinforces the importance of the precision tools described here.

eters, including their RG evolution, the corrections can be consistently handled with respect to the definitions of the parameters entering the calculation and the choice of renormalisation scale. From a practical perspective, this also reduces the amount of duplicated effort if the mass spectrum does not need to be recalculated.

Currently, a complete calculation of all decay channels in a model is not implemented in `FlexibleSUSY`. As a first step in this direction, during the work on this thesis the calculation of the loop induced decays of a neutral scalar or pseudoscalar state into two photons or two gluons was implemented into `FlexibleSUSY` [98]. From an experimental point of view, the diphoton decays of BSM states are particularly interesting to search for. In this channel, the background is expected to be a monotonically falling function of the diphoton invariant mass, dominated at lowest order by $q\bar{q} \to \gamma\gamma$ annihilation processes [486, 487] that do not produce resonances. Searches for new physics can therefore proceed simply, at least at face value, by identifying a resonant peak at a given diphoton invariant mass, for which a good experimental resolution can be achieved [483, 484]. Similarly, knowledge of the partial width for the digluon decays of a BSM state allows the production cross section via gluon fusion to be determined [488, 489]. Thus, a precise calculation of the loop induced effective couplings for these decays is highly desirable.

The calculation of the loop induced decays of a neutral scalar Φ implemented into `FlexibleSUSY` in a given model is done by constructing the appropriate generalisations of the known leading and higher-order expressions from the SM and MSSM [488]. At leading order (LO), the partial widths are calculated from

$$\Gamma_{LO}(\Phi \to \gamma\gamma) = \frac{G_F \alpha^2(0) m_\Phi^3}{128\sqrt{2}\pi^3} \left| \sum_f N_c^f Q_f^2 r_f^\Phi A_f(\tau_f) + \sum_s N_c^s Q_s^2 r_s^\Phi A_s(\tau_s) + \sum_V N_c^V Q_V^2 r_V^\Phi A_V(\tau_V) \right|^2 , \tag{4.38}$$

$$\Gamma_{LO}(\Phi \to gg) = \frac{G_F \alpha_s^2(m_\Phi) m_\Phi^3}{36\sqrt{2}\pi^3} \left| \frac{3}{2} \sum_f D_2^f r_f^\Phi A_f(\tau_f) + \frac{3}{2} \sum_s D_2^s r_s^\Phi A_s(\tau_s) + \frac{3}{2} \sum_V D_2^V r_V^\Phi A_V(\tau_V) \right|^2 , \tag{4.39}$$

where the sums are carried out over all charged or coloured fermions f, scalars s and vectors V for the diphoton and digluon widths, respectively. The couplings of these states to the scalar of interest, Φ, are written in terms of the reduced couplings r_f^Φ, r_s^Φ

and r_V^Φ, which are defined by

$$r_f^\Phi = \frac{v}{2m_f}\left(C^L_{\bar{f}f\Phi} + C^R_{\bar{f}f\Phi}\right) , \tag{4.40}$$

$$r_s^\Phi = \frac{v}{2m_s^2} C_{ss^\dagger\Phi} , \tag{4.41}$$

$$r_V^\Phi = \frac{v}{2m_V^2} C_{VV^\dagger\Phi} , \tag{4.42}$$

where v is the EW VEV, and the C_i are the couplings of the relevant states, with C^L/C^R denoting the left- and right-handed couplings for chiral interactions. The quantities N_c and Q correspond to the required colour factors and electromagnetic charges of the state, and D_2 is the quadratic Dynkin index of the $SU(3)_C$ representation of the state, assumed to be normalised to 1/2 in the fundamental representation. The form factors A_f, A_s and A_V are defined by

$$A_f(\tau) = \frac{2}{\tau^2}\left[\tau + (\tau-1)f(\tau)\right] , \tag{4.43}$$

$$A_s(\tau) = \frac{f(\tau)-\tau}{\tau^2} , \tag{4.44}$$

$$A_V(\tau) = -\frac{1}{\tau^2}\left[2\tau^2 + 3\tau + 3(2\tau-1)f(\tau)\right] , \tag{4.45}$$

with the function $f(\tau)$ given by

$$f(\tau) = \begin{cases} \arcsin^2\sqrt{\tau} & \text{for } \tau \le 1 , \\ -\frac{1}{4}\left(\ln\frac{1+\sqrt{1-\tau^{-1}}}{1-\sqrt{1-\tau^{-1}}} - i\pi\right)^2 & \text{for } \tau > 1 . \end{cases} \tag{4.46}$$

The loop functions are evaluated at $\tau_x = m_\Phi^2/(4m_x^2)$, for $x = f, s, V$. The decays of a pure pseudoscalar state A into diphotons and digluons have also been implemented into `FlexibleSUSY`; in this case, there are only contributions from fermions that couple to A, and the LO expressions read

$$\Gamma_{LO}(A \to \gamma\gamma) = \frac{G_F\alpha^2(0)m_A^3}{32\sqrt{2}\pi^3}\left|\sum_f N_c^f Q_f^2 r_f^A A_f^A(\tau_f)\right|^2 , \tag{4.47}$$

$$\Gamma_{LO}(A \to gg) = \frac{G_F\alpha_s^2(m_A)m_A^3}{36\sqrt{2}\pi^3}\left|3\sum_f D_2^f r_f^A A_f^A(\tau_f)\right|^2 . \tag{4.48}$$

The reduced couplings r_f^A are defined in the same way as in Eq. (4.40), with $C_{\bar{f}f\Phi}^{L/R} \to C_{\bar{f}fA}^{L/R}$, and the form factor is given by

$$A_f^A(\tau) = \frac{f(\tau)}{\tau} \,. \tag{4.49}$$

Even at LO, the use of a package such as `FlexibleSUSY` to evaluate the above partial widths has several important advantages. Somewhat obviously, the calculation of the above decay widths involves summing over all of the contributing diagrams, and by using `SARAH` or `FlexibleSUSY` it is guaranteed that no contributions will be missed. Similarly, the required couplings are automatically determined without neglecting potentially significant mixings. A more subtle issue arises from the choice of scale at which the couplings appearing in the above expressions are evaluated. In particular, in the LO formulas `FlexibleSUSY` makes use of the electromagnetic fine structure constant α evaluated in the Thompson limit with $Q \to 0$, since the decay is into real photons [489], while the strong coupling is evaluated at $Q = m_\Phi$ or $Q = m_A$, as appropriate. The use of these quantities at the incorrect scale can lead to quite substantial errors in the estimates for the partial widths, preventing a reliable comparison with limits on these quantities; for example, for $m_\Phi \approx 750$ GeV, the use of $\alpha_{\text{e.m.}}(m_\Phi)$ leads to a change of $\sim 10\%$ in the resulting partial width. The implementation of the LO decays into `FlexibleSUSY` automatically uses the correct scales, with the necessary RG evolution being easily handled as `FlexibleSUSY` has access to (at least) the complete 2-loop β functions in both the SM and the BSM model being considered.

Higher-order corrections to the diphoton and digluon effective couplings are also known to be important, and must be taken into account to the greatest extent possible for a precise calculation. In implementing these decays into `FlexibleSUSY`, the known next-to-LO (NLO), next-to-NLO (NNLO) and next-to-NNLO (N^3LO) corrections from the SM and MSSM are generalised, where possible, to the model under consideration. For the diphoton partial width, NLO QCD corrections from the SM and MSSM are applied for colour triplets in the loop. The corrections can be incorporated by means of modified reduced couplings [488],

$$r_f^{\Phi/A,NLO} = r_f^{\Phi/A,LO} \left(1 + C_{\Phi/A}^f(\tau_f)\frac{\alpha_s}{\pi}\right) , \tag{4.50}$$

and similarly for the scalar reduced coupling $r_s^{\Phi/A,NLO}$. The coefficients $C_{\Phi/A}^{f/s}$ can be written in the form

$$C_{\Phi}^{f/s}(\tau_{f/s}) = c_{\Phi_1}^{f/s}(Q_{NLO}) + c_{\Phi_2}^{f/s}(Q_{NLO}) \ln \frac{Q_{NLO}^2}{m_{f/s}^2}\,, \tag{4.51}$$

$$C_{A}^{f}(\tau_{f}) = c_{A_1}^{f}(Q_{NLO}) + c_{A_2}^{f}(Q_{NLO}) \ln \frac{Q_{NLO}^2}{m_{f}^2}\,. \tag{4.52}$$

A closed form expression for $C_{\Phi/A}^{f/s}$ valid over all mass ranges is not known. However, the limits when m_Φ is much lighter or heavier than the virtual states can be evaluated analytically. When $m_\Phi < m_{f/s}$, corresponding to the $\tau \to 0$ limit, the coefficients $c_{\Phi_2}^{f/s} \to 0$, while $c_{\Phi_1}^{f} \to -1$ and $c_{\Phi_1}^{s} \to 8/3$, and the NLO corrections applied by `FlexibleSUSY` reduce to

$$r_f^\Phi \to r_f^\Phi \left(1 - \frac{\alpha_s}{\pi}\right), \quad m_\Phi < m_f\,, \tag{4.53}$$

$$r_s^\Phi \to r_s^\Phi \left(1 + \frac{8\alpha_s}{3\pi}\right), \quad m_\Phi < m_s\,. \tag{4.54}$$

Both coefficients $c_{A_1}^f, c_{A_2}^f \to 0$ in this limit, and so no substitution is necessary. Analytic NLO corrections to the fermionic reduced couplings $r_f^{\Phi/A}$ are also applied in the limit of a heavy decaying state, when $m_{\Phi/A}^2 \geq 300 m_f^2$. In this limit, the leading and sub-leading logarithmic contributions to the coefficients $C_{\Phi/A}^f$ read

$$C_{\Phi/A}^f \to -\frac{1}{18}\left(\ln^2 4\tau - \pi^2\right) - \frac{2}{3}\ln 4\tau + 2\ln\frac{Q_{NLO}^2}{m_f^2} + \frac{i\pi}{3}\left(\frac{1}{3}\ln 4\tau + 2\right). \tag{4.55}$$

In these corrections, the renormalisation scale is chosen to be $Q_{NLO} = m_\Phi/2$, and it is at this scale that α_s is also evaluated in `FlexibleSUSY`. This choice of scale is made to absorb large logarithmic corrections and hence yield well-behaved couplings for large values of $m_{\Phi/A}$ compared to the masses of the states in the loop [488], which is now the phenomenologically preferred scenario. For intermediate values of $m_{\Phi/A}$, for which an analytic expression for the NLO corrections is not known, the table of values of the coefficients $C_{\Phi/A}^f$ obtained via numerical integration and made available in the code `HDECAY` has been extracted and used to interpolate the values of NLO corrections to the diphoton widths.

For the higher-order corrections to the partial width $\Gamma(\Phi \to gg)$, the known QCD corrections up to N^{3}LO have been implemented in `FlexibleSUSY`, and take the form

$$\Gamma(\Phi \to gg) = \Gamma_{LO}(\Phi \to gg) \left(1 + C_\Phi^{NLO} + C_\Phi^{NNLO} + C_\Phi^{N^3LO}\right) . \tag{4.56}$$

The corrections for a decaying pseudoscalar are only known to NNLO, and hence `FlexibleSUSY` incorporates these corrections as

$$\Gamma(A \to gg) = \Gamma_{LO}(\Phi \to gg) \left(1 + C_A^{NLO} + C_A^{NNLO}\right) . \tag{4.57}$$

The NLO, NNLO, and N^{3}LO contributions appearing here are given by [412, 488, 490–494]

$$C_\Phi^{NLO} = \left(\frac{95}{4} - \frac{7}{6} N_f\right) \frac{\alpha_s}{\pi} , \tag{4.58}$$

$$\begin{aligned} C_\Phi^{NNLO} = \Bigg[& \frac{149533}{288} - \frac{363\zeta(2)}{8} - \frac{495\zeta(3)}{8} + \frac{19}{8} \ln \frac{m_\Phi^2}{M_t^2} \\ & + N_f \left(-\frac{4157}{72} + \frac{11\zeta(2)}{2} + \frac{5\zeta(3)}{4} + \frac{2}{3} \ln \frac{m_\Phi^2}{M_t^2} \right) \\ & + N_f^2 \left(\frac{127}{108} - \frac{\zeta(2)}{6} \right) \Bigg] \frac{\alpha_s^2}{\pi^2} , \end{aligned} \tag{4.59}$$

$$\begin{aligned} C_\Phi^{N^3LO} \approx \Bigg(& 467.683620788 + 122.440972222 \ln \frac{m_\Phi^2}{M_t^2} \\ & + 10.9409722222 \ln^2 \frac{m_\Phi^2}{M_t^2} \Bigg) \frac{\alpha_s^3}{\pi^3} , \end{aligned} \tag{4.60}$$

$$C_A^{NLO} = \left(\frac{97}{4} - \frac{7}{6} N_f\right) \frac{\alpha_s}{\pi} , \tag{4.61}$$

$$C_A^{NNLO} = \left(\frac{237311}{864} - \frac{529\zeta(2)}{24} - \frac{445\zeta(3)}{8} + 5 \ln \frac{m_A^2}{M_t^2} \right) \frac{\alpha_s^2}{\pi^2} . \tag{4.62}$$

Here N_f is the number of active flavours at the scale of the decaying state, $m_{\Phi/A}$. For the implementation of these expressions into `FlexibleSUSY`, the strong coupling constant α_s is evaluated at $Q = m_{\Phi/A}$, using SM running. It is important to note that the above QCD corrections are calculated assuming only fermionic colour triplets and gluons contribute, and that additional BSM contributions are missing. For example, in SUSY models one would also expect additional contributions from the gluino and squarks. This introduces, in general, a potentially large uncertainty in the size of the higher-order corrections; for example, the contribution of a ~ 2 TeV gluino may yield a correction of order 10% of the total partial width [98]. An additional uncer-

tainty is introduced by using either $\overline{\text{DR}}/\overline{\text{MS}}$ or loop-corrected pole masses in these expressions; in `FlexibleSUSY`, by default the tree-level masses are used. While the difference between the two approaches is formally of two-loop order, in the presence of large mass hierarchies or large Yukawa couplings the differences in the amplitudes computed with either choice may still become large. Thus even with the use of these precision tools, there remain large uncertainties associated with the size of the higher-order corrections. Nevertheless, in some instances it is reasonable to expect that the contributions included into `FlexibleSUSY` will be the dominant ones. As an example, the contribution from squarks in the MSSM has been found to be well approximated by the corrections in the SM [495]. Motivated by this observation, we consider the SM corrections to usually be dominant compared to the as yet unknown BSM corrections. In the event that they are not appropriate for a given model, the higher-order corrections may also be switched off in `FlexibleSUSY` to work only in terms of the LO contributions.

With these caveats in mind, the accuracy of the effective couplings calculation in `FlexibleSUSY` has been tested by comparing the results in the SM with the state-of-the-art reference values provided by the Higgs cross section working group (HXSWG) [496]. The calculation of the loop induced diphoton and digluon decays was also implemented into `SPheno` simultaneously, allowing for a comparison between the two codes. The calculated partial widths are shown in Figure 4.8, and the corresponding relative errors compared to the HXSWG values are shown in Figure 4.9.

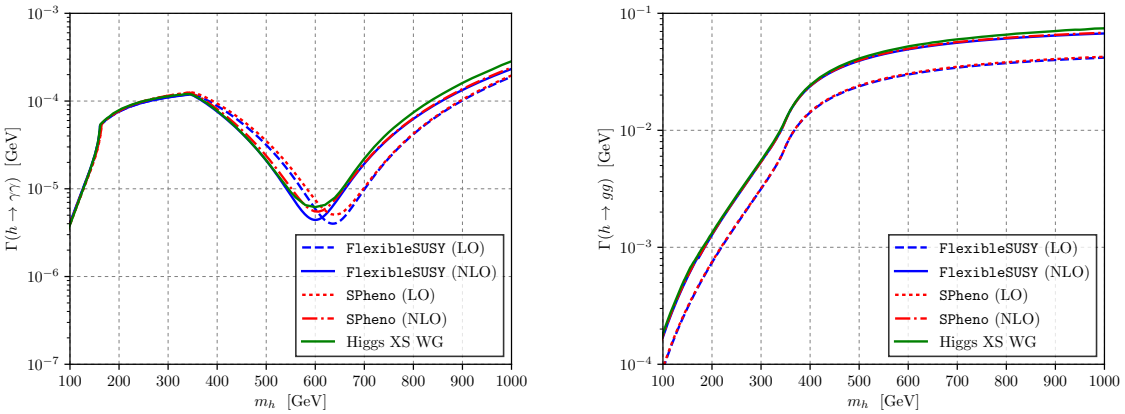

Figure 4.8: Plots of the partial widths calculated in the SM for the loop induced decays $h \to \gamma\gamma$ (left panel) and $h \to gg$ (right panel), calculated using `FlexibleSUSY` and `SPheno` at LO and NLO. In both plots, the reference values provided by the HXSWG are also shown for comparison.

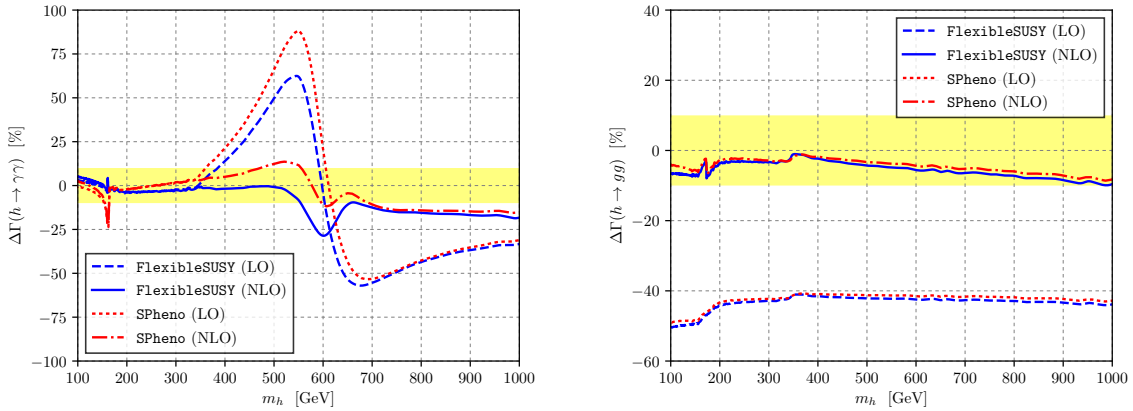

Figure 4.9: Plots of the relative errors compared to the reference values given in Ref. [496] for the partial widths of the processes $h \to \gamma\gamma$ (left panel) and $h \to gg$ (right panel) in the SM, calculated using `FlexibleSUSY` and `SPheno` at LO and NLO. The shaded region indicates $\pm 10\%$ errors compared to the HXSWG values.

In general, once higher-order corrections are included, there is good agreement between the partial widths calculated using `FlexibleSUSY` and `SPheno` and the HXSWG reference values. There is also good agreement between the two codes, though the results are not identical. This arises from differences in the calculated pole mass spectrum, which is partially due to differences in the higher-order corrections that enter into calculating the pole masses, as well as slightly different treatments of the running couplings appearing at leading and higher-orders. Over a large range of the SM Higgs mass, the results provided by `FlexibleSUSY` and `SPheno` are within 10% of the HXSWG values, provided that the higher-order corrections are included. These significantly modify the calculated partial widths; in particular, higher-order corrections increase the digluon partial width by a factor of $\sim 1.6 - 2$. This highlights the crucial importance of including these corrections to obtain a reasonable estimate for the partial decay widths in the model.

The implementation of these decays into `FlexibleSUSY` is an important improvement to the functionality of the code. The ability to calculate the effective couplings for diphoton and digluon decays allows to test general models against limits on these couplings from collider searches, and may be used as inputs to other Monte Carlo tools via the interfaces generated by `SARAH`. The usefulness of this capability was demonstrated in the wider context of the work for which this implementation of diphoton and digluon decays was done, described in further detail in Ref. [98]. In addition to extending `FlexibleSUSY` and `SPheno`, these packages were applied to the study of a selection

of some 40 different BSM models, both supersymmetric and non-supersymmetric, that were proposed as being able to yield a resonance in the diphoton channel that could be observed at the LHC[11]. Although many of these models involved complicated extensions of the SM, by implementing them in `SARAH` model files and producing spectrum generators using `SPheno` and `FlexibleSUSY`, numerical results for the mass spectra and the effective diphoton and digluon couplings could be obtained without the need to resort to making simplifying assumptions to make the models analytically tractable. Since these tools also include important higher-order corrections, our results in many cases represent significant improvements in precision compared to those available in the literature, obtained with no more effort than would be required to get a LO result. The use of a large number of models also validated the implementation of the diphoton and digluon decay widths in a wide range of exotic models, in addition to the tests in the SM described above. As a further demonstration of these tools, a new $U(1)'$ extension of the MSSM was proposed and studied. A key advantage coming from the use of the automated tool chain is the ability to easily test, in full generality, a large number of different constraints in the model. In this instance, model specific constraints on the Z' mass, the DM relic density, Higgs couplings, flavour violation and the stability of the vacuum were all used in combination with the diphoton and digluon decay widths to restrict the parameter space of the model.

Taken together with the addition of the new BVP solver, which is one of a large number of subsequent enhancements to `FlexibleSUSY` that are to be released as `FlexibleSUSY`-2.0 [97], the outcome of the work in this chapter has been to extend the scope and capabilities of `FlexibleSUSY` for the study of general BSM models. In the following chapters, we apply these generic tools, or prototype versions of them, to the study of a variety of E_6 inspired models, for which dedicated numerical tools are almost non-existent.

[11]For reasons of space, and since ultimately the candidate signal disappeared with more data, we do not report the full discussion on the model database here, preferring to focus on the extensions produced for `FlexibleSUSY`. The interested reader is encouraged to refer to Ref. [98] for a description of the models and the results found by applying these generic tools.

Chapter 5

Fine Tuning in the E_6SSM

5.1 A New Source of Fine Tuning

One of the key motivations for considering non-minimal models with all of their complications, such as the E_6SSM, is the need to address the little hierarchy problem in the MSSM. This arises because the tree-level lightest CP-even Higgs mass in the MSSM is bounded from above by $m_Z^{\overline{\rm DR}}$, as given in Eq. (2.53). Consistency with the observed 125 GeV Higgs mass therefore requires that the radiative corrections, e.g., those in Eq. (2.73), to m_{h_1} be very large. However, large loop corrections associated in particular with heavy stop masses or large stop mixing also imply large corrections to the MSSM prediction for the EW scale, Eq. (2.36), and these must be cancelled by fine tuning the parameters of the MSSM to maintain $M_Z \sim 91$ GeV. Given that one of the main benefits of SUSY is its ability to naturally stabilise the EW scale, the reintroduction of a delicate fine tuning[1] is undesirable.

In the E_6SSM, the tree-level upper bound on m_{h_1} is increased above $m_Z^{\overline{\rm DR}}$, Eq. (3.59), and the size of the required radiative corrections is correspondingly reduced. The analogous corrections to Eq. (3.22) can therefore be smaller while still being consistent with the Higgs mass measurement. This reduces the tension between simultaneously reproducing both $m_{h_1} \approx 125$ GeV and $M_Z \approx 91$ GeV. In particular, in high-scale models where there are large corrections due to the RG evolution from M_X to M_S the necessary fine tuning can be greatly reduced. This has been demonstrated in the CE_6SSM [389], which was found to be less fine tuned, in a sense to be defined in

[1] Albeit at a level not yet nearly as severe as is called for in the case of the GUT or Planck scale corrections that are of concern in the SM hierarchy problem and that might be encountered in non-SUSY GUTs.

the next section, than the CMSSM. However, as alluded to in Section 3.3, the $U(1)_N$ D-terms are not free of adverse effects. The prediction for $m_Z^{\overline{\rm DR}}$ gains an additional tree-level contribution, the last term in Eq. (3.22), from these D-terms. For values of the singlet VEV s required to satisfy LHC limits on $M_{Z'}$, $s \gtrsim 9$ TeV, the contributions proportional to v_1, v_2 in Eq. (3.18) are negligible so that

$$\Delta_\Phi \approx \frac{1}{2} g_1'^2 Q_\Phi Q_S s^2 \approx \frac{Q_\Phi}{2Q_S} (m_{Z'}^{\overline{\rm DR}})^2 \,, \tag{5.1}$$

by using Eq. (3.20). This implies that, in models where $Q_S \neq 0$, the D-term contributions are very large, $\Delta_{H_d}, \Delta_{H_u} \sim (m_{Z'}^{\overline{\rm DR}})^2 \gg (m_Z^{\overline{\rm DR}})^2$. Writing Eq. (3.22) in the form [389]

$$c(\tan\beta;\theta_{E_6}) \frac{(m_Z^{\overline{\rm DR}})^2}{2} \approx -\mu_{\rm eff}^2 + \frac{\bar{m}_{H_d}^2 - \bar{m}_{H_u}^2 \tan^2\beta}{\tan^2\beta - 1} + d(\tan\beta;\theta_{E_6}) \frac{(m_{Z'}^{\overline{\rm DR}})^2}{2} \,, \tag{5.2}$$

where the $O(1)$ prefactors c and d are given by

$$c(\tan\beta;\theta_{E_6}) = 1 - \frac{4}{(\tan^2\beta - 1)} \frac{g_1'^2}{\bar{g}^2} \left(Q_1 - Q_2 \tan^2\beta\right) \left(Q_1 \cos^2\beta + Q_2 \sin^2\beta\right) \,, \tag{5.3}$$

$$d(\tan\beta;\theta_{E_6}) = \frac{Q_1 - Q_2 \tan^2\beta}{Q_S \left(\tan^2\beta - 1\right)} \,, \tag{5.4}$$

the potential for a new tree-level fine tuning, due to limits on $M_{Z'}$ forcing the last term to be large, is made manifest [389, 497].

An important qualitative feature of this new source of fine tuning is that it does not depend on the assumptions made about the model parameters at high-scales. While the radiative corrections arising from RG running from M_X to M_S can be large, their size is strongly dependent on the unknown pattern of soft breaking masses at high energies. For example, it is known that in the CMSSM the sensitivity of $m_Z^{\overline{\rm DR}}$ to variations in the soft parameters is reduced in the focus point region [480, 498–503] where the RG evolution of the soft Higgs mass $m_{H_u}^2$ tends towards $m_Z^{\overline{\rm DR}}$ at low energies. As a result, the amount of fine tuning in a constrained model can vary significantly based on the assumed SSB mechanism. The size of the radiative effects also depends on the range of scales over which the parameters are run; they are smaller in models that are defined at a lower UV scale before running to the EW scale. If the couplings in the E_6SSM are only required to be perturbative up to this UV scale, the F-term contributions can be made larger, and further reductions in the size of the higher order corrections can be achieved. This is taken advantage of in "λSUSY" models [504, 505],

for example, where the singlet coupling λ is allowed to become non-perturbative at scales below the GUT scale. The amount of fine tuning can thus be adjusted by simply modifying the assumptions made about the model at the UV scale.

In contrast, the contribution from $M_{Z'}$ in the E$_6$SSM is always large whenever $M_{Z'}$ is large, irrespective of the value of the UV scale or the assumed UV boundary conditions. It therefore sets a lower bound on the size of the cancellations necessary in the model, which cannot be easily avoided without changing the choice of $U(1)'$ charges or modifying the matter content of the model. In this sense, the D-term fine tuning contribution is analogous to the contribution from the μ parameter in the MSSM, which has its magnitude bounded from below by collider searches for charginos [506]. By considering the model defined at low energies, where the radiative corrections are small, it is possible to derive conservative estimates for the minimal amount of fine tuning required to accommodate all experimental data and to make more robust comparisons between two models. With the aim of performing such a comparison to the MSSM, in this chapter we compute the fine tuning due to Z' limits in the E$_6$SSM and other E_6 inspired models defined at low energies.

5.2 Measures of Fine Tuning

In order to be able to make claims as to whether one model is more fine tuned than another, it is obviously necessary to have a quantitative measure of fine tuning to hand. A wide variety of candidate measures have been proposed [225, 229, 230, 480, 507–523], reflecting the fact that precisely what counts as fine tuning is not always clear. Different fine tuning measures choose a particular, quantifiable detail of a model's behaviour, and then identify it in some way with fine tuning. Each therefore captures a different aspect of the much more ambiguous concept of fine tuning. For instance, some measures emphasise the size of the cancellations that must be achieved, while others are based on the sensitivity of a model to variations in its parameters. Depending on the situation, one of these may be better than the other at characterising what is meant by fine tuning, or neither may be particularly useful. Even once a particular measure has been settled on, exactly how to apply it is not uniquely specified. The results for any given measure will depend on what is classed as a model parameter, what is to be calculated in terms of those parameters, and so on. In quantitative discussions of naturalness these various subtleties cannot easily be avoided, and must be kept in mind when comparing the results of a fine tuning calculation in two models or between two measures.

A particularly simple way to measure the fine tuning, Δ, is to evaluate the size of the cancellations that take place in the prediction for an observable quantity $\mathcal{O}$. Assuming that the value of $\mathcal{O}$ can be decomposed appropriately into a set of quantities C_i, e.g.,

$$\mathcal{O} = \sum_i C_i \,, \tag{5.5}$$

where the C_i might be model parameters or functions thereof, a measure of the size of any cancellations is given by

$$\Delta_C = \max_i \left| \frac{C_i}{\mathcal{O}} \right| . \tag{5.6}$$

The degree of fine tuning is then identified as $\Delta = \Delta_C$. The reasoning behind this definition is very simple. If any one of the C_i is much larger than $\mathcal{O}$, there must be a very precise cancellation occurring between two or more of the C_i, and the larger this cancellation is, the more fine tuned the model is. In the context of SUSY models, there are two widely used measures that adopt this picture of fine tuning. The two measures, denoted Δ_{HS} and Δ_{EW}, are defined in terms of the same observable, $(m_Z^{\overline{\rm DR}})^2$, but differ in the choice of the quantities C_i. Taking the MSSM as an example, the relevant breakdown into individual terms is obtained from Eq. (2.36),

$$\frac{(m_Z^{\overline{\rm DR}})^2}{2} = -|\mu|^2 + \frac{m_{H_d}^2 - \frac{t_1}{v_1} - m_{H_u}^2 \tan^2\beta + \frac{t_2}{v_2}\tan^2\beta}{\tan^2\beta - 1} \,, \tag{5.7}$$

where $t_i \equiv -\partial \Delta V_{\rm MSSM}/\partial v_i$. The measure Δ_{EW} is defined [225, 521–523] by taking each of the above terms at the scale of EWSB, say M_S, so that

$$\begin{gathered} C_1 = -|\mu(M_S)|^2 \,, \quad C_2 = \frac{m_{H_d}^2(M_S)}{\tan^2\beta - 1} \,, \quad C_3 = \frac{-m_{H_u}^2(M_S)\tan^2\beta}{\tan^2\beta - 1} \,, \\ C_4(\Phi) = \frac{-t_1(\Phi)}{v_1(\tan^2\beta - 1)} \,, \quad C_5(\Phi) = \frac{t_2(\Phi)\tan^2\beta}{v_2(\tan^2\beta - 1)} \,, \end{gathered} \tag{5.8}$$

where the notation $t_i(\Phi)$ indicates the contribution of the state Φ to the effective potential, and

$$\Delta_{EW} = \max_i \left| \frac{2C_i}{(m_Z^{\overline{\rm DR}})^2} \right| . \tag{5.9}$$

The definition of Δ_{HS} [523] differs in that the low energy parameters are written in terms of their values at the UV scale M_X according to Eq. (2.76), along with

$$|\mu(M_S)|^2 = |\mu(M_X)|^2 + \delta|\mu|^2 \,, \tag{5.10}$$

and the individual terms are taken to be

$$\begin{aligned} B_1 &= -|\mu(M_X)|^2\,, & B_2 &= -\delta|\mu|^2\,, \\ B_3 &= \frac{m_{H_d}^2(M_X)}{\tan^2\beta - 1}\,, & B_4 &= \frac{\delta m_{H_d}^2}{\tan^2\beta - 1}\,, \\ B_5 &= -\frac{m_{H_u}^2(M_X)\tan^2\beta}{\tan^2\beta - 1}\,, & B_6 &= -\frac{\delta m_{H_u}^2\tan^2\beta}{\tan^2\beta - 1}\,, \\ B_7(\Phi) &= \frac{-t_1(\Phi)}{v_1(\tan^2\beta - 1)}\,, & B_8(\Phi) &= \frac{t_2(\Phi)\tan^2\beta}{v_2(\tan^2\beta - 1)}\,. \end{aligned} \tag{5.11}$$

The measure Δ_{HS} is then defined with respect to the high-scale contributions instead,

$$\Delta_{HS} = \max_i \left| \frac{2B_i}{(m_Z^{\overline{\rm DR}})^2} \right| . \tag{5.12}$$

Both Δ_{EW} and Δ_{HS} have the virtue that they are easily applied to the MSSM or another SUSY model. The value of Δ_{EW} is also independent of assumptions about the underlying parameters at M_X, since it depends only on the values of the model parameters at M_S, and so is independent of the chosen model of SSB [521]. On the other hand, both measures give reasonable measures of fine tuning only when cancellations between the C_i or B_i are genuinely fine tuned. This is not always true, for example, in constrained models some or all of the various terms might be correlated by their dependence on some set of fundamental parameters, in which case some amount of cancellation is entirely natural [225]. A somewhat related problem is that it is not clear how the grouping of contributions into the various C_i, B_i should be done in general. To illustrate these issues in the MSSM, note that $\delta m_{H_d}^2$ and $\delta m_{H_u}^2$ both depend on $m_{H_u}^2(M_X)$, so that the contribution from the latter, single parameter actually appears in multiple (non-independent) B_i, each of which is potentially large and would lead to a high value of Δ_{HS}. Arguably, one could extract the contribution of $m_{H_u}^2(M_X)$ from each and combine these parts into a single factor in Δ_{HS}. The same large cancellation between the correlated terms $m_{H_u}^2(M_X)$ and $\delta m_{H_u}^2(M_X)$, if it leads to a small $m_{H_u}^2(M_S)$, would be regarded as natural by Δ_{EW}. However, Δ_{EW} misses the effects of correlations among the low-scale parameters that might emerge naturally from an underlying high-scale theory.

A method of accounting for natural cancellations among the C_i of Eq. (5.5) considers the dependence of $\mathcal{O}$ on the hypothesised, fundamental model parameters, $\{p_i\}$. One might expect that, if cancellations among the C_i can be explained in terms of some genuine underlying relationships, then the value of $\mathcal{O}$ should not change much as the

$\{p_i\}$ are varied, and this should be largely independent of the scale of the parameters p_i. In this case, the C_i will change in a correlated fashion to maintain the cancellation yielding the observed $\mathcal{O}$. If the C_i are independent in this model, and the large cancellation comes about from fine tuning the values of some of the p_i, then by varying the fundamental parameters this cancellation would be spoilt, and $\mathcal{O}$ should change by a large amount. That is, $\mathcal{O}$ would be observed to be highly sensitive to variations in the model parameters $\{p_i\}$. Thus the sensitivity of $\mathcal{O}$ can also be used to characterise fine tuning. This is the motivation behind the traditional Ellis-Barbieri-Giudice measure [229, 230], defined by

$$\Delta_{BG} = \max_i \Delta_{p_i}\,, \quad \Delta_{p_i} \equiv \left| \frac{\partial \ln (m_Z^{\overline{\rm DR}})^2}{\partial \ln p_i} \right|\,, \tag{5.13}$$

corresponding to the choice $\mathcal{O} = (m_Z^{\overline{\rm DR}})^2$, though one might also consider choosing the measured pole mass $\mathcal{O} = M_Z^2$ instead. Intuitively, each Δ_{p_i} corresponds to the percentage variation in the observable for a 1% change in the parameter p_i, and is independent of the scale of p_i and $\mathcal{O}$ [507]. The measure Δ_{BG}, or a modified version in which the sensitivities Δ_{p_i} are combined in quadrature,

$$\Delta_{BG} = \sqrt{\sum_i \Delta_{p_i}^2}\,, \tag{5.14}$$

has been extremely widely applied in fine tuning studies; see, for example, Refs. [389, 498, 524–549]. Once a model has been specified in terms of a set of parameters $\{p_i\}$, it is also relatively straightforward to compute the individual sensitivities Δ_{p_i}. For this reason, and to facilitate comparisons with previous work, we employ $\Delta = \Delta_{BG}$ as defined in Eq. (5.13) to quantify the fine tuning in the E_6SSM here.

Nevertheless, it should be kept in mind that the measure Δ_{BG} is not without its shortcomings. Just as large cancellations may not be indicative of fine tuning, a high sensitivity of the observable $\mathcal{O}$ to the model parameters may also be naturally explained in some cases. A classic example [507] is the size of the proton mass, which is naturally a sensitive function of α_3 due to the RG evolution of the strong coupling. The value of Δ_{BG} is also sensitive to the definitions of the parameters to which it is applied, with the choice of calculating the sensitivity with respect to p_i or p_i^2, for example, introducing a factor of two difference in the result. The same is true concerning the definition of the observable $\mathcal{O}$. In general, whether or not the parameters $\{p_i\}$ are genuinely fundamental is unknown, and relationships between the

chosen set in some underlying theory may drastically alter the calculated fine tuning [225]. Several alternative measures have been proposed, for example in Refs. [507–510, 519, 520] that are able to rectify some of these problems.

The measures Δ_{EW}, Δ_{HS} and Δ_{BG} also share several deficiencies that make their interpretation unclear. In their simplest forms, each considers only a single observable at a single point in parameter space. Fine tuning in a BSM model may be required in several observables though, either individually or to simultaneously reproduce their experimental values [519]. At individual parameter points, the corresponding cancellations might be large or sensitivities high, but the above three measures do not capture whether this is a generic feature of the whole model; that is, the measures do not adequately address whether a model that has a low $\Delta_{EW/HS/BG}$ for an arbitrarily small neighbourhood of a given point, but large tunings everywhere else, is natural. This so-called "second order" fine tuning [550] is a property of the entire model that is not directly captured by local tuning measures without resorting to extensive parameter space scans. Compounding all of these issues is the fact that, in the end, the interpretation of the final number produced by any one of the above measures is extremely subjective. The acceptable size of Δ is a matter of individual taste, which often changes over time. The computed fine tuning does not, for instance, admit a well-defined translation into a degree of belief in a given model [550], nor does it answer how much more natural one model is compared to another in light of data.

The latter question invites the possibility of quantifying fine tuning using Bayesian methods. In these approaches, one considers the posterior probability of a model M given observed data D,

$$P(M|D) = \frac{\mathcal{Z}(D,M)}{P(D)} P(M)\,, \tag{5.15}$$

where $P(M)$ and $P(D)$ are the prior probability of the model and the (unknown) total probability to observe the data D, respectively. The Bayesian evidence $\mathcal{Z}(D,M)$ is given by

$$\mathcal{Z}(D,M) = \int_\Omega \mathcal{L}_D(p_i;M)\pi(p_i|M)d^n p_i\,, \tag{5.16}$$

where $\mathcal{L}_D(p_i;M) \equiv P(D|p_i,M)$ is the likelihood of the data for a given set of values of the n model parameters p_i, $\pi(p_i|M)$ is the prior probability for that set of values, and the integration is carried out over the entire n-dimensional parameter space Ω. The concept of naturalness is automatically incorporated into this calculation since if in the model M one must fine tune the parameters to fit measured values of the observables, the region with high likelihood will occupy a tiny prior volume [232, 550–556], thus suppressing the posterior. In practice, when computing the evidence for a model one

trades a subset of the model parameters $\{p_i\}$ for a set of k observables $\{\mathcal{O}_j\}$ to avoid unnecessarily considering regions in Ω where incorrect values of $\mathcal{O}_j$ are obtained in the model. This change of variables modifies the priors by the appearance of the Jacobian $|J|$ for the transformation from the model parameters to the observables. Moreover, the inverse of this Jacobian matrix contains the derivatives that appear in the traditional measure, Eq. (5.13), if M_Z is chosen among the set of observables [551, 552, 554], albeit combined with others in a more complicated way when $k > 1$.

More generally, a model that is free of fine tuning can be considered to be one where the parametrisation is such that all of the parameters are in fact observables [550, 554]. This implies that a useful measure of fine tuning is $\Delta_J = 1/|J|$ [554], so that the tuning is the ratio of the infinitesimal observable space volume element to the infinitesimal parameter space element[2]. Points for which Δ_J is large, that is fine tuned, are thus automatically assigned a low effective likelihood in the evidence calculation. The Bayesian approach provides an elegant means of describing fine tuning in a model, but it is also more complicated to apply, and it has not yet been as widely used. In particular, the full evidence calculation in a general model is extremely computationally intensive, and in practice only makes sense in the context of a full model comparison [555]. For the purposes of understanding how the amount of fine tuning varies with $M_{Z'}$, it is sufficient to adopt the simpler method of calculating Δ_J or Δ_{BG} at each point, this being faster while also giving at least some sense of how changing Z' mass limits will penalise E_6 inspired models compared to the MSSM. As noted above, we make use of Δ_{BG} as it has already been widely used in other studies. Fortunately, given that the derivatives appearing in Δ_{BG} and Δ_J are quite similar, there are not expected to be too large discrepancies between the results obtained using one or the other.

5.3 Calculating Fine Tuning in the E_6SSM

To determine Δ_{BG}, the required sensitivities Δ_{p_i} may be calculated directly from the expression for $(m_Z^{\overline{\rm DR}})^2$ in terms of the parameters p_i for a particular model. This leads to a so-called master formula for calculating the fine tuning. A master formula for the E_6SSM, obtained from the tree-level scalar potential, was presented in Ref. [389]. In order to derive the expression presented there, the fact that $s \gg v$ was made use of to neglect certain $O(v^2)$ terms in the EWSB conditions, greatly simplifying the

[2]This coincides with the measure proposed in Ref. [519] when the interval of variation is taken to zero.

final result. For the purposes of exploring a wider class of E_6 inspired models, here we present the master formula without neglecting any terms. The complete tree-level master formula is somewhat complicated. This is because, unlike in the MSSM, even at tree-level it is not possible to solve explicitly for the VEVs v_1, v_2 in terms of the Lagrangian parameters. It may be written in the form

$$\Delta_{p_i} = |C|^{-1} \times \frac{|p_i|}{m_Z^{\overline{\rm DR}}} \left| \sum_q \tilde{\Delta}_q \frac{\partial q}{\partial p_i} \right|, \tag{5.17}$$

where the sum is over all low-energy running parameters appearing in the tree-level EWSB conditions. By analogy with the pMSSM, in the E$_6$SSM we take these to be $q \in \{\lambda, A_\lambda, m_{H_d}^2, m_{H_u}^2, m_S^2, g_1, g_2, g_1'\}$, where A_λ is defined by writing $T_\lambda = \lambda A_\lambda$.

To write down the various parts of the tree-level master formula, it is convenient to define the quantities

$$z_i = \epsilon_{ijk} \frac{\partial f_j}{\partial s} \frac{\partial f_k}{\partial \tan\beta}, \tag{5.18}$$

where

$$f_1 = \frac{\partial V_{\rm E_6SSM}}{\partial v_1}, \quad f_2 = \frac{\partial V_{\rm E_6SSM}}{\partial v_2}, \quad f_3 = \frac{\partial V_{\rm E_6SSM}}{\partial s}, \tag{5.19}$$

are the EWSB conditions, Eq. (3.17), taken at tree-level. The relevant partial derivatives are

$$\begin{aligned}
\frac{\partial f_1}{\partial \tan\beta} &= -\frac{2m_Z^{\overline{\rm DR}}}{\bar{g}} \cos^2\beta \Bigg\{ \frac{\lambda A_\lambda s}{\sqrt{2}} \cos\beta + \sin\beta \Bigg[m_{H_d}^2 + \frac{s^2}{2}\left(\lambda^2 + g_1'^2 Q_1 Q_S\right) \\
&\quad + (m_Z^{\overline{\rm DR}})^2 \left(\frac{5}{2} - \frac{4\lambda^2}{\bar{g}^2} - \frac{4g_1'^2}{\bar{g}^2} Q_1 Q_2 + \frac{6g_1'^2}{\bar{g}^2} Q_1^2 \right) \Bigg] \\
&\quad + 3(m_Z^{\overline{\rm DR}})^2 \sin^3\beta \left[\frac{2\lambda^2}{\bar{g}^2} - 1 + \frac{2g_1'^2}{\bar{g}^2}\left(Q_1 Q_2 - Q_1^2\right) \right] \Bigg\}, \\
\frac{\partial f_1}{\partial s} &= \frac{2m_Z^{\overline{\rm DR}}}{\bar{g}} \left[s\left(\lambda^2 + g_1'^2 Q_1 Q_S\right)\cos\beta - \frac{\lambda A_\lambda}{\sqrt{2}} \sin\beta \right], \\
\frac{\partial f_2}{\partial \tan\beta} &= \frac{2m_Z^{\overline{\rm DR}}}{\bar{g}} \cos^2\beta \Bigg\{ \frac{\lambda A_\lambda s}{\sqrt{2}} \sin\beta + \cos\beta \Bigg[m_{H_u}^2 + \frac{s^2}{2}\left(\lambda^2 + g_1'^2 Q_2 Q_S\right) \\
&\quad + (m_Z^{\overline{\rm DR}})^2 \left(\frac{5}{2} - \frac{4\lambda^2}{\bar{g}^2} - \frac{4g_1'^2}{\bar{g}^2} Q_1 Q_2 + \frac{6g_1'^2}{\bar{g}^2} Q_2^2 \right) \Bigg] \\
&\quad + 3(m_Z^{\overline{\rm DR}})^2 \cos^3\beta \left[\frac{2\lambda^2}{\bar{g}^2} - 1 + \frac{2g_1'^2}{\bar{g}^2}\left(Q_1 Q_2 - Q_2^2\right) \right] \Bigg\},
\end{aligned}$$

$$\frac{\partial f_2}{\partial s} = \frac{2m_Z^{\overline{\rm DR}}}{\bar{g}}\left[s\left(\lambda^2 + g_1'^2 Q_2 Q_S\right)\sin\beta - \frac{\lambda A_\lambda}{\sqrt{2}}\cos\beta\right],$$
$$\frac{\partial f_3}{\partial \tan\beta} = \frac{2(m_Z^{\overline{\rm DR}})^2}{\bar{g}^2}\cos^2\beta\left[g_1'^2 Q_S s\left(Q_2 - Q_1\right)\sin 2\beta - \sqrt{2}\lambda A_\lambda \cos 2\beta\right],$$
$$\frac{\partial f_3}{\partial s} = m_S^2 + \frac{2\lambda^2 (m_Z^{\overline{\rm DR}})^2}{\bar{g}^2} + \frac{g_1'^2}{2} Q_S\left[\frac{4(m_Z^{\overline{\rm DR}})^2}{\bar{g}^2}\left(Q_1\cos^2\beta + Q_2\sin^2\beta\right) + 3Q_S s^2\right].$$

For a running parameter q appearing in the tree-level EWSB conditions, the corresponding contribution to the sensitivity Δ_{p_i} is given by

$$\tilde{\Delta}_q = z_1\frac{\partial f_1}{\partial q} + z_2\frac{\partial f_2}{\partial q} + z_3\frac{\partial f_3}{\partial q}. \tag{5.20}$$

It is straightforward to compute the appropriate derivatives directly from the EWSB conditions, Eq. (3.17). Similarly, the quantity C appearing in Eq. (5.17) is given by

$$C = \frac{1}{2}\left(z_1\frac{\partial f_1}{\partial m_Z^{\overline{\rm DR}}} + z_2\frac{\partial f_2}{\partial m_Z^{\overline{\rm DR}}} + z_3\frac{\partial f_3}{\partial m_Z^{\overline{\rm DR}}}\right), \tag{5.21}$$

with

$$\frac{\partial f_1}{\partial m_Z^{\overline{\rm DR}}} = \frac{2}{\bar{g}}\cos\beta\left[m_{H_d}^2 + \frac{\lambda^2 s^2}{2} + \frac{g_1'^2}{2}Q_1 Q_S s^2 + \frac{6g_1'^2}{\bar{g}^2}Q_1^2 (m_Z^{\overline{\rm DR}})^2\right] - \sqrt{2}\frac{\lambda A_\lambda s}{\bar{g}}\sin\beta$$
$$+ \frac{3(m_Z^{\overline{\rm DR}})^2}{\bar{g}}\cos\beta\cos 2\beta + \frac{6}{\bar{g}^3}(m_Z^{\overline{\rm DR}})^2\sin\beta\sin 2\beta\left[\lambda^2 + g_1'^2\left(Q_1 Q_2 - Q_1^2\right)\right],$$
$$\frac{\partial f_2}{\partial m_Z^{\overline{\rm DR}}} = \frac{2}{\bar{g}}\sin\beta\left[m_{H_u}^2 + \frac{\lambda^2 s^2}{2} + \frac{g_1'^2}{2}Q_2 Q_S s^2 + \frac{6g_1'^2}{\bar{g}^2}Q_2^2 (m_Z^{\overline{\rm DR}})^2\right] - \sqrt{2}\frac{\lambda A_\lambda s}{\bar{g}}\cos\beta$$
$$- \frac{3(m_Z^{\overline{\rm DR}})^2}{\bar{g}}\sin\beta\cos 2\beta + \frac{6}{\bar{g}^3}(m_Z^{\overline{\rm DR}})^2\cos\beta\sin 2\beta\left[\lambda^2 + g_1'^2\left(Q_1 Q_2 - \tilde{Q}_2{}^2\right)\right],$$
$$\frac{\partial f_3}{\partial m_Z^{\overline{\rm DR}}} = \frac{4m_Z^{\overline{\rm DR}}}{\bar{g}^2}\left[\lambda^2 s - \frac{\lambda A_\lambda}{\sqrt{2}}\sin 2\beta + g_1'^2 Q_S s\left(Q_1\cos^2\beta + Q_2\sin^2\beta\right)\right].$$

While the tree-level master formula is a useful start, it is well known in the MSSM that radiative corrections can significantly change, and in fact reduce the fine tuning [557]. It is therefore essential when studying the fine tuning to account for the loop corrections to the effective potential. To do so it is more convenient to work with the EWSB conditions in the form of Eq. (3.17) rather than Eq. (3.22). The general procedure is as follows[3]. For a model in which m fields develop real VEVs, we require

[3]This method has also previously been applied in the NMSSM; see, for example, Ref. [558].

that the m minimisation conditions,

$$f_1 = f_2 = \cdots = f_m = 0\,, \tag{5.22}$$

continue to hold under an arbitrary variation in a model parameter $p \to p + \delta p$, so that the variations δf_i satisfy

$$\delta f_1 = \delta f_2 = \cdots = \delta f_m = 0\,. \tag{5.23}$$

Each f_i is a function of the VEVs v_j as well as l running parameters q_k evaluated at the scale of EWSB, $f_i = f_i(v_j, q_k)$. It follows that for each f_i,

$$\sum_{j=1}^{m} \frac{\partial f_i}{\partial v_j}\frac{\partial v_j}{\partial p} + \sum_{k=1}^{l} \frac{\partial f_i}{\partial q_k}\frac{\partial q_k}{\partial p} = 0\,. \tag{5.24}$$

The quantities $\frac{\partial f_i}{\partial v_j}$ are simply the elements of the CP-even Higgs squared mass matrix $\mathcal{M}_h^2$ of the model before carrying out any field rotations. For example, in the E_6SSM this corresponds to the mass matrix in the basis (ϕ_d, ϕ_u, ϕ_S), where the ϕ_i are as defined before Eq. (3.57). When evaluated for all n model parameters, the above system of equations can be concisely expressed as

$$\mathcal{M}_h^2 \begin{pmatrix} \frac{\partial v_1}{\partial p_1} & \cdots & \frac{\partial v_1}{\partial p_n} \\ \vdots & \ddots & \vdots \\ \frac{\partial v_m}{\partial p_1} & \cdots & \frac{\partial v_m}{\partial p_n} \end{pmatrix} = - \begin{pmatrix} \frac{\partial f_1}{\partial q_1} & \cdots & \frac{\partial f_1}{\partial q_l} \\ \vdots & \ddots & \vdots \\ \frac{\partial f_m}{\partial q_1} & \cdots & \frac{\partial f_m}{\partial q_l} \end{pmatrix} \begin{pmatrix} \frac{\partial q_1}{\partial p_1} & \cdots & \frac{\partial q_1}{\partial p_n} \\ \vdots & \ddots & \vdots \\ \frac{\partial q_l}{\partial p_1} & \cdots & \frac{\partial q_l}{\partial p_n} \end{pmatrix}. \tag{5.25}$$

The quantities forming the first matrix on the right-hand side, along with $\mathcal{M}_h^2$, are easily calculated by differentiating the conditions in Eq. (3.17) with respect to the VEVs and the running parameters. The remaining derivatives $\partial q_k/\partial p$ must be determined using the RGEs. Once these have been obtained, it is straightforward to solve for the $\partial v_i/\partial p$. The sensitivities Δ_{p_i} are then obtained as linear combinations of the $\partial v_i/\partial p$ and $\partial q_k/\partial p$. By including the contributions coming from $\Delta V_{\mathrm{E_6SSM}}$, the higher order corrections are easily, if tediously, incorporated. In the MSSM, the dominant corrections come from the stops, with the contributions from other states being much smaller, and so it is reasonable to include only the contributions from the stops and the top quark appearing in Eq. (2.39). In the E_6SSM, we similarly include only the dominant corrections involving the stops and top, so that for the numerical results

presented below we have taken

$$\Delta V_{\rm E_6SSM} \approx \frac{3}{32\pi^2}\Bigg\{(m_{\tilde{t}_1}^{\overline{\rm DR}})^4\left[\ln\frac{(m_{\tilde{t}_1}^{\overline{\rm DR}})^2}{Q^2}-\frac{3}{2}\right]+(m_{\tilde{t}_2}^{\overline{\rm DR}})^4\left[\ln\frac{(m_{\tilde{t}_2}^{\overline{\rm DR}})^2}{Q^2}-\frac{3}{2}\right]$$
$$-2(m_t^{\overline{\rm DR}})^4\left[\ln\frac{(m_t^{\overline{\rm DR}})^2}{Q^2}-\frac{3}{2}\right]\Bigg\}, \tag{5.26}$$

where the stop masses are as given in Eq. (3.32), and the renormalisation scale in all of the fine tuning calculations presented here is taken to be $Q = M_S = \sqrt{m_{\tilde{t}_1}^{\overline{\rm DR}}(M_S)m_{\tilde{t}_2}^{\overline{\rm DR}}(M_S)}$.

Evaluating the derivatives $\partial q_k/\partial p$ must, in general, be done by numerically integrating the two-loop RGEs. Simple forms for the derivatives can be obtained by constructing the semi-analytic solutions discussed in Section 4.2.1 that express the each low-energy parameter q in terms of the model parameters $\{p_i\}$. The semi-analytic coefficients must still be numerically determined, though, which is time consuming and therefore is an obstacle to doing large scans of the parameter space. When the model parameters are defined at scales M_X not too far above M_S, as we do here, it is possible to derive approximate analytic expressions for the various coefficients that exhibit good accuracy over the range of scales considered. Although a low-energy parameter can then be expressed analytically in terms of the approximate coefficients, it is more convenient to rearrange the result into a power series in the parameter $t \equiv \ln(M_S/M_X)$ to identify the leading and sub-leading logarithmic contributions coming from RG running. The approximate formulas are easily derived by solving the two-loop RGE for the parameter q,

$$\frac{dq}{dt} \equiv \beta_q = \frac{1}{16\pi^2}\beta_q^{(1)} + \frac{1}{(16\pi^2)^2}\beta_q^{(2)}\,, \tag{5.27}$$

using a Picard iteration, with the result that

$$q(M_S) = q(M_X) + \int_0^t \beta_q(t')dt'$$
$$\approx q(M_X) + \frac{t}{16\pi^2}\left(\beta_q^{(1)} + \frac{\beta_q^{(2)}}{16\pi^2}\right) + \frac{t^2}{32\pi^2}\frac{d\beta_q^{(1)}}{dt} + O(t^2)\,. \tag{5.28}$$

Expanded to this order, we obtain the leading-log (LL) and next-to-LL (NLL) contributions at two-loop order. The $O(t^2)$ terms not displayed above are formally of three-loop order and thus are neglected. The derivative of the one-loop β function is

given by

$$\frac{d\beta_q^{(1)}}{dt} = \frac{1}{16\pi^2}\sum_{q_k}\beta_{q_k}^{(1)}\frac{\partial\beta_q^{(1)}}{\partial q_k}, \tag{5.29}$$

where the sum is over all of the running parameters appearing in $\beta_q^{(1)}$. The β functions appearing on the right-hand side of Eqs. (5.28) and (5.29) are evaluated at the scale M_X, allowing the derivatives of the parameters at M_S with respect to the high-scale parameters at M_X to be evaluated analytically. Explicit results for the relevant series expansions in the MSSM and E_6 models are presented in Appendix B and Appendix C.

5.4 Naturalness Impact of Z' Limits in the E$_6$SSM

Using the approach outlined above, we are able to scan the low-energy parameter space of the MSSM and E$_6$SSM and calculate the fine tuning in each. To do so, we implemented the above expressions for computing the fine tuning in a modified version of the E$_6$SSM spectrum generator that was used in previous fine tuning studies of the E$_6$SSM [389]. This code implemented two-loop RGEs for all parameters except the soft scalar masses. To properly include the fine tuning impact of M_3, which enters only at two-loop order in the RG running of the soft masses, the original code was extended to make use of the two-loop RGEs generated by `SARAH` and `FlexibleSUSY`. The CP-even Higgs masses are calculated including the leading one-loop effective potential contributions given in Ref. [363] and for the light Higgs we use the leading two-loop[4] contributions from Ref. [278], which are a generalisation of the corrections in the MSSM and NMSSM calculated using effective field theory techniques [218, 561]. To scan over the MSSM parameter space, the equivalent MSSM fine tuning expressions were implemented into a modified version of `SOFTSUSY`-3.3.10. For consistency with the results produced in the E_6 models, and for computational speed, for our main scans only the dominant one- and two-loop corrections to the CP-even Higgs masses were included.

5.4.1 Stop Mass Fine Tuning

As discussed in Section 2.6, heavy stops are expected to lead to substantial fine tuning, and hence many works on natural SUSY have focused on light stops, with much theoretical effort being applied to find models in which it is easier to get a 125 GeV

[4]While full two-loop corrections to the Higgs masses, in the gaugeless limit, can now be calculated for a general model in `SARAH` [559, 560], this capability was not available at the time our numerical study was done, and such corrections go beyond the required precision for studying fine tuning here.

Higgs boson and light stops simultaneously and much experimental effort to search for light stops. This is entirely appropriate since there are many good reasons to expect the soft masses to be set at high energies by some mechanism for SSB. However, this is not the only possibility and, as noted above, the fine tuning problem depends strongly on the RG evolution from the high-scale, as the soft Higgs masses that appear in the EWSB conditions pick up contributions from the soft squark masses.

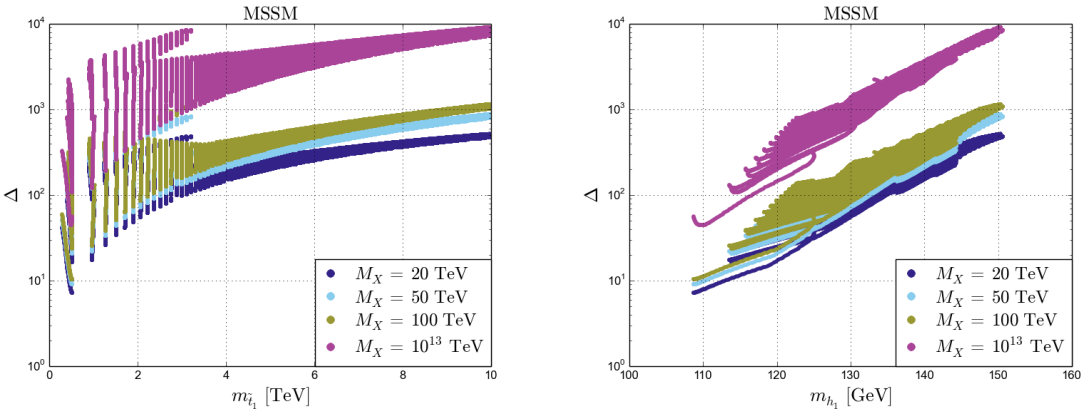

Figure 5.1: Left panel: Scatter plot of fine tuning in the MSSM as a function of the lightest stop mass, $m_{\tilde{t}_1}$, for the cutoff scales (from bottom to top) $M_X = 20$ TeV, $M_X = 50$ TeV, $M_X = 100$ TeV and $M_X = 10^{16}$ GeV. Right panel: Scatter plot of fine tuning in the MSSM as a function of the lightest Higgs mass, m_{h_1}, for the cutoff scales (from bottom to top) $M_X = 20$ TeV, $M_X = 50$ TeV, $M_X = 100$ TeV and $M_X = 10^{16}$ GeV.

To illustrate this, in the left panel of Figure 5.1 we show the variation in fine tuning for $M_X = 20$ TeV, 50 TeV, 100 TeV and 10^{16} GeV when we scan over the stop masses and mixing, with 500 GeV $\leq m_{Q_3}, m_{u_3^c} \leq 10$ TeV and -3810 GeV $\leq A_t \leq -20$ GeV. We adopt the pMSSM boundary conditions defined in Section 2.2, and fix the remaining parameters such that at M_S they have the values $\mu = -97.5$, $B \equiv B\mu/\mu = -84.8$, $M_1 = 92.1$, $M_2 = 95.9$, $M_3 = 352$, $A_b = -117.9$, $A_\tau = -7.8$, $M_{\tilde{L}_L} = m_{L_3} = 400$, $M_{\tilde{e}_R} = m_{e_i} = 204$, $M_{\tilde{q}_L} = 438$, $M_{\tilde{u}_R} = 436$ and $M_{\tilde{d}_R} = m_{d_3^c} = 438$ GeV. Although we should stress that making these parameter values will lead to a spectrum that is in conflict with the LHC limits, doing so ensures that fine tuning due to the other parameters is small, so that we avoid washing out the fine tuning impact of the stops when the tuning is small[5] as can be the case when the stop masses are less than 1 TeV. Note that the Higgs mass is also allowed to vary in this scan, as shown

[5]For models in which the spectrum is heavier, when the stop masses are small the fine tuning reaches a lower bound imposed by other heavier parameters.

in the right panel of Figure 5.1. This illustrates the tuning problem that has become prominent since the discovery of the 125 GeV Higgs boson. It can be seen that raising the stop masses is also pushing up the Higgs mass, meaning that heavier Higgs masses require more fine tuning. However, for a low value of the UV scale M_X this tuning is not so severe unless the stops are very heavy, and a 125 GeV Higgs can be obtained without much tuning in this unrealistic case where the other sources of tuning have been minimised. On the other hand, the tuning becomes more severe as we increase the cutoff such that for $M_X = 10^{16}$ GeV a lightest stop mass of $1-3$ TeV can result in a fine tuning of $\approx 100 - 1000$ and the minimum tuning we find[6] for a 125 GeV Higgs is ≈ 200, as shown in Figure 5.1.

5.4.2 Fine Tuning at Low Energies

Since the stop mass does not have such a large impact on the fine tuning when the scale M_X is very low we can use this to see more clearly the impact of the Z' mass on fine tuning. To do so we select a fixed low $M_X = 20$ TeV and compare the fine tuning in the MSSM and E_6SSM for two different values of the Z' mass. We choose to look at $M_{Z'} = 2.5$ TeV, corresponding to the ATLAS limits at the time the numerical work presented here was done [562], and $M_{Z'} = 4.5$ TeV, which is expected to be in reach in run II at the LHC [563]. We then compare the fine tuning calculated in each case to the tuning in the MSSM. For this comparison, we have performed a six-dimensional parameter space scan in both the MSSM and E_6SSM, varying those parameters most relevant for the fine tuning and the Higgs mass. Therefore, the set of parameters which we vary includes μ, B and $\tan\beta$ for the MSSM, and λ, A_λ and $\tan\beta$, for the E_6SSM, which appear at tree-level in the EWSB conditions of the models. While the RGE contribution from large stop masses to the fine tuning is small for such a low M_X, the stop contributions to the effective potential can potentially play a significant role in reducing the fine tuning. For this reason it is still important to properly treat the tuning associated with stop contributions to the one-loop effective potential, and so we also scan over the soft masses $m^2_{Q_3}$, $m^2_{u^c_3}$ and the trilinear coupling A_t. The relevant parameters and ranges that were scanned over are summarised in Table 5.1. We also repeat each scan for three different values of M_2 to allow more variation in the chargino masses.

[6]Note that in this calculation of the Higgs mass there is a significant theoretical error, even with leading two-loop corrections, which must be borne in mind when thinking about what the results imply for the minimum fine tuning in the model consistent with a 125 GeV Higgs.

In this case, we now consider realistic scenarios, where the parameters that are not scanned over are set to values which keep the associated states comfortably above their experimental limits. Therefore in both the MSSM and E$_6$SSM all other soft scalar masses are set to 5 TeV. We require a valid spectrum with no tachyonic states to exclude points which would have an unrealistic minimum, for example due to the appearance of charge or colour breaking (CCB) minima. In the E$_6$SSM, we adopt "pMSSM-like" boundary conditions. That is, we work in the third family approximation, taking the first and second generation Yukawa couplings to be zero, and we also assume that their associated soft trilinears vanish. Similarly, we take $A_b = A_\tau = 0$ GeV. The $U(1)$ gaugino soft mass M_1 was fixed to $M_1 = 300$ GeV, and we fix $M_3 = 2000$ GeV. Additionally, in the E$_6$SSM the $U(1)_N$ gaugino soft mass M_1' is held fixed with $M_1' = M_1 = 300$ GeV, and $\mu_L = 5$ TeV.

MSSM	E$_6$SSM
$2 \leq \tan\beta \leq 50$	$2 \leq \tan\beta \leq 50$
-1 TeV $\leq \mu \leq 1$ TeV	$-3 \leq \lambda \leq 3$
-1 TeV $\leq B \leq 1$ TeV	-10 TeV $\leq A_\lambda \leq 10$ TeV
200 GeV $\leq m_{Q_3} \leq 2000$ GeV	200 GeV $\leq m_{Q_3} \leq 2000$ GeV
200 GeV $\leq m_{u_3^c} \leq 2000$ GeV	200 GeV $\leq m_{u_3^c} \leq 2000$ GeV
-10 TeV $\leq A_t \leq 10$ TeV	-10 TeV $\leq A_t \leq 10$ TeV
$M_2 = 100$, 1050, 2000 GeV	$M_2 = 100$, 1050, 2000 GeV

Table 5.1: The parameters scanned over and the ranges of values used in the MSSM and the E$_6$SSM models.

In Figure 5.2, results from these scans are plotted showing the tuning for each case against the lightest Higgs mass. As expected, the dependence on the Higgs mass is now quite weak, while the minimum tuning in the model for the E$_6$SSM is increased by the mass of the Z' boson. In the case of a very low cutoff the tuning required to get a 125 GeV Higgs is not so large. However, the tuning from the Z' mass appears already at tree-level and is, therefore, not suppressed when the cutoff scale is low. In our scan we find that, for the points with the lower value of $M_{Z'}$, which is already ruled out by the most recent limits, and having an approximately 125 GeV Higgs, the minimum fine tuning that can be achieved is $\Delta_{\text{min}} \approx 121$. If run II of the LHC further pushes up the limit on the Z' mass to be above 4.5 TeV then the fine tuning in the model will be greater than at least $\Delta_{\text{min}} \approx 394$ for Higgs masses between 124.5 and 125.5 GeV.

This demonstrates the two important points about these $U(1)$ extensions anticipated in the discussion at the start of this chapter – first, that limits on the Z' mass

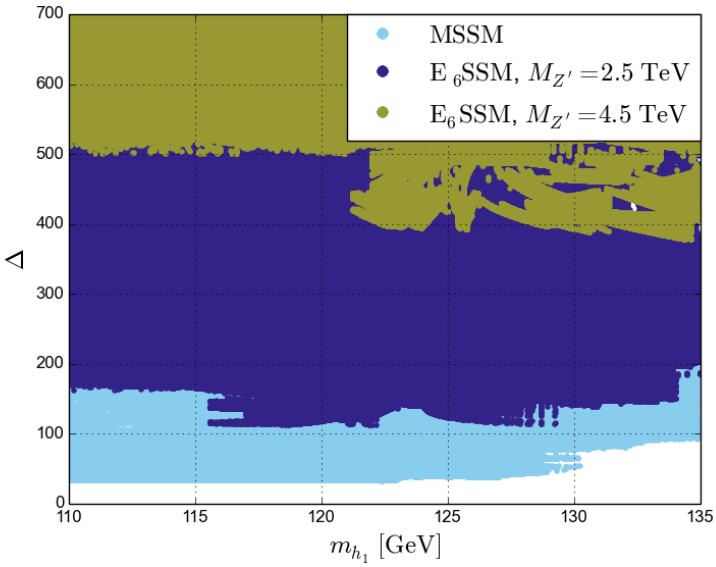

Figure 5.2: Scatter plot of fine tuning against the lightest Higgs mass for the MSSM (light blue, bottom band), the E$_6$SSM with $M_{Z'} = 2.5$ TeV (dark blue, middle band) and the E$_6$SSM with $M_{Z'} = 4.5$ TeV (dark yellow, top band). Note that there are points for which the fine tuning in the MSSM and the E$_6$SSM with $M_{Z'} = 2.5$ TeV is larger than is visible on this plot and those below; however, these points are obscured by the overlaid data for the E$_6$SSM with $M_{Z'} = 4.5$ TeV, and it is the lower bound on the achievable tuning that is of interest here.

play an incredibly important role in constraining natural scenarios in such models and, second, that the tuning from the Z' limits in these models depends less on assumptions about SUSY breaking than the tuning required by the 125 GeV Higgs measurement that is believed to be a problem in the MSSM.

Because of the tree-level nature of the Z' fine tuning, as discussed in Section 5.1 the effect of the Z' limits can usefully be compared to the impact of chargino limits in the MSSM, which place a bound on the magnitude of $|\mu|$, or $|\mu_{\rm eff}|$ in $U(1)$ extensions. The LEP bound [506] on chargino masses, excluding $m_{\tilde{\chi}_1^\pm} \lesssim 104$ GeV, implies that $|\mu|$ should only be greater than ~ 100 GeV, which is not substantially larger than M_Z. Consequently the bound from LEP is not high enough to have an impact on the fine tuning obtained in the models and parameter space regions that we have studied, as we have checked explicitly. Significantly larger lower bounds on the μ parameter, and therefore on the fine tuning, may arise from chargino limits coming from LHC searches. However, the chargino limits from the LHC depend the mass difference between the lightest chargino and lightest neutralino and on whether there are light sleptons or sneutrinos. Current limits placed by CMS and ATLAS exclude lightest chargino masses between ~ 700 GeV and ~ 1150 GeV if there are light sleptons [564–566], with much weaker bounds if there are no light sleptons or sneutrinos.

Nonetheless, for the MSSM the impact of potential chargino mass limits is shown in Figure 5.3. There we see that if the full parameter space with $m_{\tilde{\chi}_1^\pm} < 700$ GeV could be excluded, the impact would be to make the tuning in the MSSM with a 20 TeV UV scale similar to that of the E_6SSM with the same high-scale and a Z' mass of ≈ 2.5 TeV. In the E_6SSM, while raising the chargino limit can have the same impact in principle, the current limits on the Z' mass are already the dominant source of tuning, and the bounds on chargino masses do not have a noticeable effect.

Finally, it should be emphasised that while in Figure 5.2 the E_6SSM appears more fine tuned than the MSSM, this result depends on the high-scale boundary, M_X, where the parameters are assumed to be set by some SUSY breaking mechanism. This can be compared with the results of Ref. [389] in which the CE_6SSM was found to be less tuned than the CMSSM. Since a 125 GeV Higgs can be achieved in the E_6SSM with lighter stops, then if M_X is large, the larger stop masses of the MSSM can make that model more fine tuned due to large RGE effects.

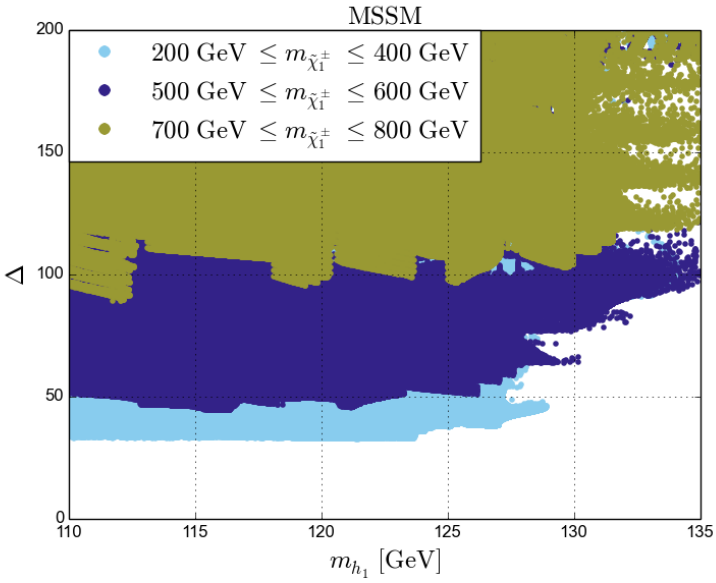

Figure 5.3: Scatter plot of fine tuning as a function of the lightest Higgs mass in the MSSM with 200 GeV $\leq m_{\tilde{\chi}_1^\pm} \leq$ 400 GeV shown in light blue (bottom band), 500 GeV $\leq m_{\tilde{\chi}_1^\pm} \leq$ 600 GeV in dark blue (middle band), and 700 GeV $\leq m_{\tilde{\chi}_1^\pm} \leq$ 800 GeV in dark yellow (top band).

5.5 Benchmark Scenarios

To further illustrate this point, we looked at how the tuning varies with M_X for several low tuning benchmarks in the MSSM and E$_6$SSM. These benchmarks are defined in Table 5.2 and the variation in the fine tuning with M_X for these points is shown in Figure 5.4. Since the behaviour is quite complicated we now discuss these in detail to gain some insight into the many differences in the tuning between the two models.

In the top panel of Figure 5.4 one can see that the MSSM BM1 tuning (dotted curve) steadily climbs as the cutoff scale is increased, as one would expect when the tuning originates from large soft masses entering from the RGEs. The panel on the middle left confirms this, showing that the largest tuning contributions come from Δ_{A_t} and $\Delta_{m^2_{H_u}}$ with the former being the larger sensitivity until $M_X \approx 10^8$ GeV at which point $\Delta_{m^2_{H_u}}$ takes over, leading to the small kink in overall tuning that can be seen in the dotted curve in the top panel. In this case we have chosen a point with large mixing, which is known to reduce the MSSM tuning. We found this does not eliminate the tuning as there is still a strong sensitivity to A_t, but we did find that large mixing lead to less fine tuning overall for the points we examined.

	MSSM BM1	MSSM BM2	E$_6$SSM BM1	E$_6$SSM BM2
$\tan\beta(M_Z)$	10	10	10	10
$s(M_S)$ [GeV]	$\cdots$	$\cdots$	6700	6700
$\kappa_{11,22,33}(M_S)$	$\cdots$	$\cdots$	0.6	0.52
$\tilde{\lambda}_{11,22}(M_S)$	$\cdots$	$\cdots$	0.2	0.13
$\mu_{(\text{eff})}(M_S)$ [GeV]	689.7	1013.5	1093.3	1313.0
$B_{(\text{eff})}(M_S)$ [GeV]	345.7	1032.5	3792.7	817.8
$A_\tau(M_S)$ [GeV]	0	-5057.9	0	-88.5
$A_b(M_S)$ [GeV]	0	-5707.2	0	-1720.7
$A_t(M_S)$ [GeV]	-3335.7	-2734.8	-1100	-1103.2
$M^2_{\tilde{L}_L}(M_S)$ [GeV^2]	2.5×10^7	6.35×10^6	2.5×10^7	4.94×10^6
$m^2_{L_3}(M_S)$ [GeV^2]	2.5×10^7	6.22×10^6	2.5×10^7	4.90×10^6
$M^2_{\tilde{e}_R}(M_S)$ [GeV^2]	2.5×10^7	6.27×10^6	2.5×10^7	5.21×10^6
$m^2_{e^c_3}(M_S)$ [GeV^2]	2.5×10^7	6.03×10^6	2.5×10^7	5.11×10^6
$M^2_{\tilde{q}_L}(M_S)$ [GeV^2]	2.5×10^7	7.37×10^6	2.5×10^7	5.76×10^6
$m^2_{Q_3}(M_S)$ [GeV^2]	4.45×10^6	3.97×10^6	4.50×10^5	3.61×10^6
$M^2_{\tilde{u}_R}(M_S)$ [GeV^2]	2.5×10^7	7.30×10^6	2.5×10^7	5.54×10^6
$m^2_{u^c_3}(M_S)$ [GeV^2]	4.0×10^6	6.60×10^5	5.86×10^5	2.04×10^6
$M^2_{\tilde{d}_R}(M_S)$ [GeV^2]	2.5×10^7	7.30×10^6	2.5×10^7	5.88×10^6
$m^2_{d^c_3}(M_S)$ [GeV^2]	2.5×10^7	7.03×10^6	2.5×10^7	5.78×10^6
$m^2_{H_d}(M_S)$ [GeV^2]	1.82×10^6	8.96×10^6	4.06×10^7	1.04×10^7
$m^2_{H_u}(M_S)$ [GeV^2]	-3.60×10^5	-9.35×10^5	5.0×10^5	-2.66×10^5
$m^2_S(M_S)$ [GeV^2]	$\cdots$	$\cdots$	-3.10×10^6	-3.17×10^6
$M_1(M_S)$ [GeV]	300	260.8	300	173.4
$M_2(M_S)$ [GeV]	2000	479.2	1050	281.4
$M_3(M_S)$ [GeV]	2000	1312.3	2000	1200
$M'_1(M_S)$ [GeV]	$\cdots$	$\cdots$	300	175.2
$m^{\overline{\text{DR}}}_{Z'}$ [GeV]	$\cdots$	$\cdots$	2473.2	2512.7
m_{h_1} [GeV]	124.3	124.4	125.0	126.2
$m_{\tilde{t}_1}$ [GeV]	1942.1	861.6	993.8	1665.0
$m_{\tilde{t}_2}$ [GeV]	2220.1	2023.9	1174.8	2094.4
$m_{\tilde{g}}$ [GeV]	2259.8	1472.9	2290.0	1407.4
$\Delta(M_X = 20$ TeV)	157.3	242.8	165.3	402.1
$\Delta(M_X = 10^{16}$ GeV)	1089.0	949.0	1722.3	546.7

Table 5.2: Parameters for the MSSM and E$_6$SSM benchmark points. In the E$_6$SSM, we define μ_{eff} as in Eq. (3.24) and $B_{\text{eff}} = A_\lambda$. The soft masses $m^2_{H_d}$, $m^2_{H_u}$ and m^2_S are those that satisfy the EWSB conditions including the one-loop corrections involving the top and stops. For E$_6$SSM BM1 (BM2) we also set $\mu_L = 5000.0$ (897.9) GeV, $B_L\mu_L = 5000.0$ (-4.21×10^5) GeV^2, $A_{\kappa_{11,22,33}} = 0$ (-1389.2) GeV, $A_{\tilde{\lambda}_{11,22}} = 0$ (-52.9) GeV, $m^2_{D_{11,22,33}} = 2.5\times10^7$ (4.81×10^6) GeV^2, $m^2_{\overline{D}_{11,22,33}} = 2.5\times10^7$ (4.90×10^6) GeV^2, $m^2_{H_1{}_{11,22}} = 2.5\times10^7$ (4.46×10^6) GeV^2, $m^2_{H_2{}_{11,22}} = 2.5\times10^7$ (4.81×10^6) GeV^2, $m^2_{\Sigma_{11,22}} = 2.5\times10^7$ (5.28×10^6) GeV^2, $m^2_{L_4} = 2.5\times10^7$ (4.94×10^6) GeV^2 and $m^2_{\overline{L}_4} = 2.5\times10^7$ (4.87×10^6) GeV^2.

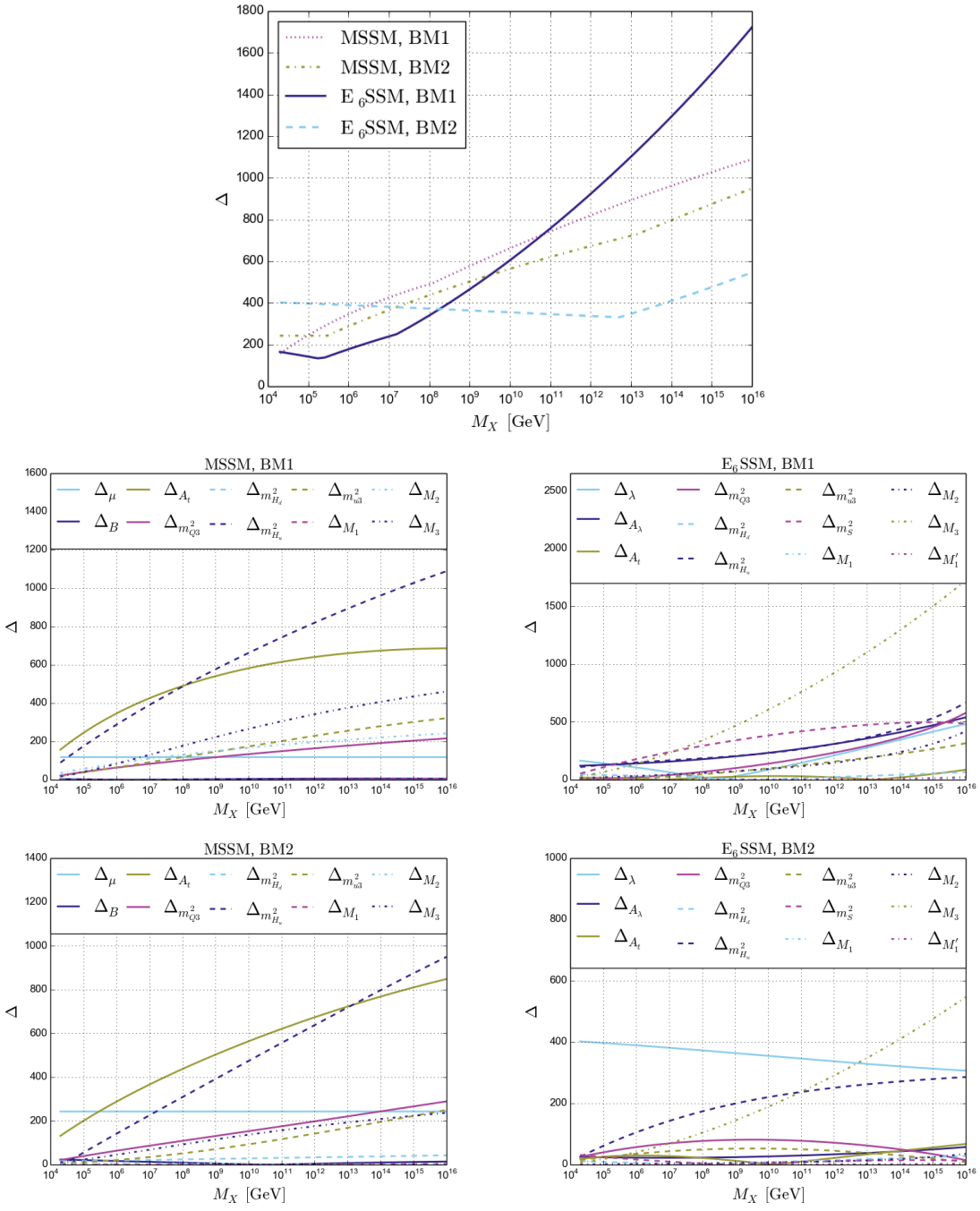

Figure 5.4: Top panel: Scatter plot of the fine tuning as a function of the cutoff scale M_X for the four benchmark points given in Table 5.2. Middle left panel: Individual sensitivities for MSSM BM1 plotted against the high-scale M_X which give the overall tuning shown by the dotted line in the top panel. Middle right panel: Individual sensitivities for E$_6$SSM BM1 plotted against the high-scale M_X which give the overall tuning shown by the solid line in the top panel. Bottom left panel: Individual sensitivities for MSSM BM2 plotted against the high-scale M_X which give the overall tuning shown by the dash-dotted line in the top panel. Bottom right panel: Individual sensitivities for E$_6$SSM BM2 plotted against the high-scale M_X which give the overall tuning shown by the dashed line in the top panel.

Comparing the MSSM tunings to the E$_6$SSM tunings one can see that which point is more fine tuned depends on the scale at which the parameters are defined. This illustrates that any statement about which model is more tuned depends on the high-scale boundary, M_X. For E$_6$SSM BM1 the fine tuning is shown by the solid curve in the top panel of Figure 5.4 and the individual sensitivities are given in the middle right panel. The tuning actually reduces initially as the cutoff is increased from 20 TeV. This occurs because the largest sensitivity is initially Δ_λ (shown in solid light blue in the middle right panel). This contains some terms proportional to $(m_{Z'}^{\overline{\rm DR}})^2$, which provide the dominant contribution to this sensitivity at very low M_X. However, as M_X is increased contributions from the soft masses become more important and these actually start to cancel the large contribution to Δ_λ coming from $m_{Z'}^{\overline{\rm DR}}$ until Δ_λ passes through zero. At the same time though these large soft masses also cause other sensitivities to grow, in particular Δ_{M_3}. The fine tuning rises with M_X once $M_X \gtrsim 10^5 - 10^6$ GeV, but remains lower than that of the other points, until $M_X \approx 10^8$ GeV. Eventually the Δ_{M_3} sensitivity leads to this point being the most fine-tuned of the four shown in Figure 5.4. Although the gluino mass and $M_3(M_S)$ have similar values to those in the MSSM BM1 point, in the E$_6$SSM $M_3(M_X)$ is larger due to the altered RGE running from exotic matter[7]. This is in turn why E$_6$SSM BM1 has a larger tuning at larger values of M_X, coming from Δ_{M_3}. Interestingly other sensitivities are suppressed by this effect since at the same time larger M_3 at higher scales reduces the soft squark masses at M_X. Therefore, the stop mass contributions are ameliorated, compared to the MSSM, both by allowing lighter stops at M_S and by the modified RGE running. Even so, the stops still do lead to $\Delta_{m_{H_u}^2}$ increasing with the cutoff through the usual mechanism[8].

By contrast the tuning for E$_6$SSM BM2 is very different, as is shown by the dashed line in the top panel of Figure 5.4, with the individual sensitivities given in the bottom right panel. This point was chosen as it had a much lighter gluino mass that was, at the time this study was done, just above the experimental limit of 1.4 TeV [567]. At 20 TeV this benchmark is not amongst the lowest tuned points, since at that scale the tree-level tuning from $m_{Z'}^{\overline{\rm DR}}$ dominates. However, the reduction in M_3 means that Δ_{M_3} is substantially lower and only becomes the dominant tuning at a much larger scale

[7]This altered RG running is a result of the exotic matter introduced to keep the extra $U(1)$ anomaly free.

[8]Wherein $m_{H_u}^2(M_S)$ receives a positive contribution from $m_{H_u}^2(M_X)$ and a negative contribution from $m_{Q_3}^2(M_X)$ and $m_{u_3^c}^2(M_X)$, allowing heavy stop masses to cause fine tuning. In this case $m_{H_u}^2(M_S)$ is held fixed so as the scale M_X increases the values of these soft masses at the high-scale will be larger and there will be a bigger cancellation between them, increasing the sensitivity of $m_Z^{\overline{\rm DR}}$ to both $m_{H_u}^2$ and the soft scalar masses for the stops.

of $M_X \gtrsim 10^{12} - 10^{13}$ GeV, giving a tuning at 10^{16} GeV of ≈ 546, which is far below that of the other three benchmark points.

In addition to this, the soft parameters in E$_6$SSM BM2 follow a pattern similar to that found in the constrained model. With the exception of the parameters $m^2_{Q_3}$, $m^2_{u^c_3}$, $m^2_{H_d}$, $m^2_{H_u}$, and M_3, the values of which are given in Table 5.2, the soft masses at the SUSY scale correspond to the values that result in the CE$_6$SSM with $m_0 = 2.2$ TeV, $M_{1/2} = 1003$ GeV, $A_0 = 500$ GeV, $\kappa_{11,22,33}(M_X) = 0.1923$, $\lambda(M_X) = 0.2646$ and $\tilde{\lambda}_{11,22}(M_X) = 0.1$. This leads to a significant reduction in the contributions to the RG running of $m^2_{H_u}$ and $m^2_{Q_3}$ coming from terms of the form $g_1^2\Sigma_1$ and, to a lesser extent, $g_1'^2\Sigma_1'$. Here we define for the E$_6$SSM (see also Eqs. (C.6) and (C.7) for general E_6 inspired models)

$$\begin{aligned}
\Sigma_1 &= \mathrm{Tr}(m^2_Q) - 2\,\mathrm{Tr}(m^2_{u^c}) + \mathrm{Tr}(m^2_{d^c}) + \mathrm{Tr}(m^2_{e^c}) - \mathrm{Tr}(m^2_L) + m^2_{H_u} + \mathrm{Tr}(m^2_{H_2}) \\
&\quad - m^2_{H_d} - \mathrm{Tr}(m^2_{H_1}) + \mathrm{Tr}(m^2_{\overline{D}}) - \mathrm{Tr}(m^2_D) - m^2_{L_4} + m^2_{\overline{L}_4}\,, \\
\Sigma_1' &= 6\,\mathrm{Tr}(m^2_Q) + 3\,\mathrm{Tr}(m^2_{u^c}) + 6\,\mathrm{Tr}(m^2_{d^c}) + \mathrm{Tr}(m^2_{e^c}) + 4\,\mathrm{Tr}(m^2_L) - 4m^2_{H_u} - 4\,\mathrm{Tr}(m^2_{H_2}) \\
&\quad - 6m^2_{H_d} - 6\,\mathrm{Tr}(m^2_{H_1}) + 5m^2_S + 5\,\mathrm{Tr}(m^2_\Sigma) - 9\,\mathrm{Tr}(m^2_{\overline{D}}) - 6\,\mathrm{Tr}(m^2_D) \\
&\quad + 4m^2_{L_4} - 4m^2_{\overline{L}_4}\,.
\end{aligned}$$

In the unconstrained case, this contribution acts to drive up the values of $m^2_{Q_3}$ and $m^2_{H_u}$, and thus the associated tuning sensitivities, at the cutoff scale M_X. In the case of E$_6$SSM BM2, on the other hand, the reduced splitting between the soft masses leads to a much smaller contribution from these terms. Together with the reduction in M_3 described above, this allows to maintain the observed low fine tuning at very large values of M_X. MSSM benchmark BM2, corresponding to the dash-dotted line in the top panel of Figure 5.4, with individual sensitivities shown in the bottom left panel, is designed to be similar to E$_6$SSM BM2, for a reasonable comparison. However, from the individual sensitivities one can see that the behaviour is quite similar to MSSM BM1, though in this case $\Delta_{m^2_{H_u}}$ becomes the largest tuning at a higher M_X and does not reach such large values, since more of the tuning is from the mixing in this case.

5.6 Alternative E_6 Inspired Models

The exact level of tuning from the Z' depends on the charges of the extra $U(1)$ gauge symmetry it is associated with. In Figure 5.5 we look at the fine tuning for other $U(1)$ extensions for the same Z' masses as we did for the E$_6$SSM. To simplify the analysis we fix $\tan\beta = 10$, but scan over the remaining parameters as in Table 5.1 and fix

the rest to the same values we used in the scan carried out for Figure 5.2. In order to more clearly identify the lower bound on the obtainable tuning in each model, the parameter values for points in these main grid scans with a low fine tuning were then used as the starting points for smaller scans about those values. In these smaller scans the parameters were more finely varied to populate the low fine tuning regions.

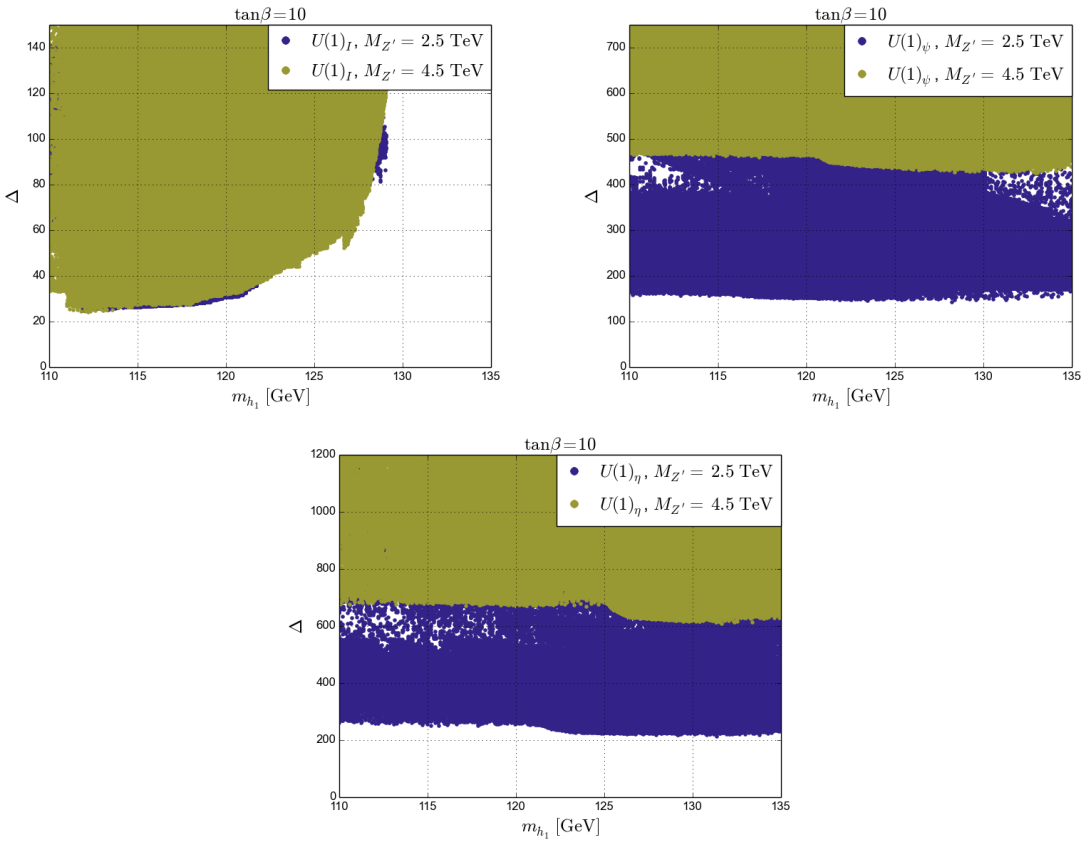

Figure 5.5: Top left panel: Scatter plot of the fine tuning against the lightest Higgs mass in the $U(1)_I$ model. Top right panel: Scatter plot of the fine tuning against the lightest Higgs mass in the $U(1)_\psi$ model. Bottom panel: Scatter plot of the fine tuning against the lightest Higgs mass in the $U(1)_\eta$ model. In each plot points with $M_{Z'} = 2.5$ TeV are shown in dark blue (bottom band), and points with $M_{Z'} = 4.5$ TeV are shown in dark yellow (top band).

As can be seen in Figure 5.5, the severity of the tunings varies quite a bit. This is because the charges appear as coefficients in front of the Z' mass in the EWSB conditions. These charges significantly change the value of the coefficient d in Eq. (5.2). The values of the coefficient d in each model, for $\tan\beta = 10$, are $\{-0.01, 0.40, 0.50, 0.81\}$

for $\{U(1)_I, U(1)_N, U(1)_\psi, U(1)_\eta\}$. The size of this coefficient thus determines which of the models is the most tuned.

Interestingly, the coefficient d is very small (and negative) in the case of the $U(1)_I$. This allows a dramatic reduction in the fine tuning from the $U(1)_I$ symmetry. This is a result of the $U(1)_I$ charge of H_u vanishing, which means that the D-term contribution to the lightest Higgs, which is predominantly H_u at large $\tan\beta$, is suppressed. This makes it difficult to raise the Higgs mass in the same way as happens in the other models and explains why heavier Higgs values in this model are not obtained in the scan. Therefore the fine tuning behaviour in this model is much closer to that of the MSSM, and in this case raising the Z' mass limit to 4.5 TeV will have little impact on naturalness. A naïve estimate of the tuning using the d coefficient suggests that Z' limits need to be around 15 TeV before they will significantly raise the tuning in the $U(1)_I$ model.

5.7 Conclusions

Prior to stringent experimental constraints on the mass of the lightest Higgs boson and squarks in supersymmetric models, a rather simple picture of natural SUSY emerged from theoretical reasoning. In this picture, it was expected that the soft masses associated with the stops should not be much bigger than 100 GeV, as at the EW scale they enter the EWSB condition for $m_Z^{\overline{\rm DR}}$ through RG running. While we have focused on the tension arising from the need to reconcile this scenario with the observation of a 125 GeV Higgs in the MSSM, this little hierarchy problem has in fact been evident since LEP first obtained the constraint $m_{h_1} \geq 114.4$ GeV [568, 569], which is already sufficiently far above the tree-level upper bound in the MSSM to introduce significant fine tuning in constrained models.

This observation has provided one important motivation, among others, for considering $U(1)$ extensions of the MSSM that are based at high energies on a unified E_6 gauge group, since the additional F- and D-term contributions raise the tree-level Higgs mass and reduce the need for large radiative corrections. However, as we have discussed in this chapter, such models come with their own potential fine tuning problem, since a large singlet VEV, proportional to the mass of the new Z' boson, appears in the EWSB condition for $m_Z^{\overline{\rm DR}}$ at tree-level. Though it has been found in a previous study that in one such E_6 inspired model, the CE$_6$SSM, the fine tuning is less severe than the CMSSM, it is nevertheless still significant.

In light of these difficulties it is important to consider whether the simple picture of natural SUSY is wrong in some way, or if there are other possibilities that allow naturalness to be preserved. For example, the conclusions drawn about fine tuning in the aforementioned constrained models depend strongly on the assumptions about the value of the scale of SSB, M_X, and the pattern of soft parameters at this scale. If this scale is lowered, or the SSB mechanism changed, the degree of fine tuning can be significantly changed. It is therefore useful to ask, are there are ways to constrain the naturalness of these models that do not rely upon assumptions about how SUSY is broken?

The goal of this chapter has been to investigate exactly this question in the MSSM and several E_6 inspired models. Since the RG evolution links the soft masses together and causes the fine tuning problems associated with the stop and gluino masses, the most conservative approach to placing naturalness limits is to choose a low value of M_X. In this case, the SSB model dependent fine tuning impact associated with the RG flow is minimised, while any fine tuning that arises at tree-level persists. In the MSSM, the most direct way to constrain naturalness in this way is through limits on the chargino masses. Unfortunately, the current LHC limits on charginos are not model independent and thereby leave many gaps where one can have light charginos.

Our results in this chapter have shown that in the E_6 models considered, there is an additional way to constrain naturalness, which also leads to a more robust bound on the attainable fine tuning. This comes about through the already high Z' mass limit. Even taking $M_X = 20$ TeV for setting the soft masses, the lowest tuning in the E$_6$SSM compatible with a Z' mass of 2.5 TeV is found to be $\Delta \approx 121$, while if the LHC run II can place a limit of 4.5 TeV on M'_Z then the tuning would be approximately 394. This is quite a bit larger than the current tuning required in the MSSM consistent with a 125 GeV Higgs mass, of around 38. We interpret this as meaning that, in the most conservative limits one can place on naturalness in these two models, the tuning in the E$_6$SSM is worse. The tuning bound imposed by the need for a Z' of mass at least 2.5 TeV is equivalent to that which would occur in the MSSM if there are no charginos below 700 GeV.

The role of assumptions about the high-scale model can be nicely illustrated by contrasting the results obtained in this conservative approach with those that are obtained as M_X is raised. The study of the benchmark points presented in Section 5.5 demonstrates that exactly which point within a model, or for that matter which model, is more fine tuned depends very strongly on M_X. The tuning in the E$_6$SSM is sufficiently complicated by the interplay of the different sources of tension in the EWSB

conditions that a small reduction in fine tuning can even occur for a moderate increase in M_X. However, as M_X increases towards the scale where the gauge couplings unify, the familiar tunings from the MSSM do dominate, though with tunings from the gluino mass appearing to be more significant relative to those from soft scalar masses.

The primary focus of this work has been on the E_6SSM, since it has the attractive features of being able to account for the observed neutrino masses and baryogenesis, and has been studied from a naturalness perspective previously. Alternative $U(1)$ extensions, following from a different symmetry breaking pattern, can also be constructed, and the impact from Z' limits can also be investigated to see whether the situation can be improved compared to the case of $U(1)_N$. For the cases considered, we have found that for fixed $\tan\beta$ there is still a lower bound on the fine tuning due to the Z' mass, and that this becomes worse for larger Z' masses. This highlights the importance of Z' searches for constraining naturalness in a variety of E_6 inspired, $U(1)$ extensions of the MSSM. The actual amount of fine tuning is found to be very dependent on the precise set of $U(1)'$ charges. The $U(1)_I$ model shows the least tuning due to the vanishing charge of the H_u state. This model is quite interesting in the sense that it provides a solution to the μ problem while avoiding the large tuning, at least for current experimental limits, from the Z' mass. However, these are conservative limits on naturalness that we have set, and in the $U(1)_I$ model the suppression of the additional D-term contributions means that there is no solution to the usual tuning coming from the large stops needed to get a 125 GeV Higgs mass, which becomes a problem as the UV scale is raised.

Additionally, while the fine tuning can in some cases be decreased by altering the $U(1)'$ charge assignments, this comes at the cost of some of the benefits associated with the choice of $U(1)_N$. It was pointed out in Section 3.2 that, of the models considered in this chapter, only those based on $U(1)_N$ such as the E_6SSM contain total singlet right-handed neutrinos, allowing for the observed neutrino masses to be explained using the see-saw mechanism and for successful leptogenesis to occur. It would be preferable if the fine tuning could be reduced while retaining these successful features of the model. In the next chapter, we consider an interesting modification of the E_6SSM that, it will be argued, can achieve precisely this goal, in addition to having a variety of other positive features.

Chapter 6

An E_6 Inspired Model with Exact Custodial Symmetry

6.1 An Alternative to the E$_6$SSM

The E$_6$SSM is a well motivated extension of the MSSM that solves many of the open problems discussed in Section 2.6. It is also one of the simplest formulations of an E_6 inspired model with a $U(1)_N$ gauge symmetry. It is not unique, however, and in this chapter we consider an alternative E_6 inspired model with many appealing features and several advantages over the simplest variants of the E$_6$SSM. This alternative model still leads to a $U(1)$ extension of the MSSM with an additional $U(1)_N$ gauge symmetry, ensuring that the origin of neutrino masses and baryogenesis can still be accounted for, as emphasised in Chapter 3. The starting point for its construction is the observation that the breakdown of E_6 into the SM gauge group with two additional $U(1)$ factors, as in Eq. (3.4), can be achieved in orbifold GUT models [297, 298, 570–579]. The elegant motivation for the model, coming as it does from an E_6 GUT, is thus retained. The model considered here [100, 101, 300, 347, 352] is constructed from an underlying five- or six-dimensional orbifold GUT. In this framework [300] E_6 can be broken directly to $SU(3)_C \times SU(2)_L \times U(1)_Y \times U(1)_\chi \times U(1)_\psi$ at or near the GUT scale M_X. The additional $U(1)_\chi \times U(1)_\psi$ is then broken near M_X to $U(1)_N \times Z_2^M$, where Z_2^M is the same matter parity as defined in Eq. (2.3).

The matter content now differs in an important way to the E$_6$SSM. Below M_X, the three complete **27**-plets of E_6 that are usually present in the E$_6$SSM are accompanied by a set of pairs of multiplets M_l, $\overline{M}_l$, coming from incomplete $\mathbf{27'}$ and $\overline{\mathbf{27'}}$ representations, respectively. The required splitting to leave only incomplete multiplets,

which can be problematic in ordinary four-dimensional GUTs, is neatly achieved in orbifold models like the one considered here [580–585]. As for the case of introducing the multiplets $\hat{L}_4$ and $\overline{\hat{L}}_4$ in the E$_6$SSM, gauge anomalies cancel since the fields from M_l and $\overline{M}_l$ carry opposite $U(1)$ charges. The exact set of M_l, $\overline{M}_l$ multiplets is not uniquely specified, and must be chosen to define the model. The SM matter content, as in the E$_6$SSM, is accommodated in the three complete **27**-plets, which also contain exotic states.

This extended set of matter multiplets permits an important change to be made to one of the model building assumptions of the ordinary E$_6$SSM. In the E$_6$SSM, while the exotic states have enticing implications for collider phenomenology, the many new couplings that accompany them would, in the most general case, lead to severe conflicts with current constraints. As was briefly discussed in Section 3.2, in the simplest versions of the E$_6$SSM multiple exact and approximate discrete Z_2 symmetries are imposed to suppress the most dangerous of these couplings. Currently, the phenomenologically viable variants of the E$_6$SSM impose at least three different Z_2 symmetries [344, 375]. None of these discrete symmetries commute with E_6, because not all of the fields within a given multiplet have the same Z_2 charges. Although the need to impose discrete symmetries to avoid phenomenological problems is not uncommon in BSM models, the situation in the E$_6$SSM is substantially more complicated than in the MSSM, for instance, where the single Z_2^M matter parity is sufficient [300]. The need to impose a comparatively large number of discrete symmetries to arrive at an acceptable model is an undesirable feature of the E$_6$SSM.

This is remedied in the alternative model now considered, in which a single, exact $\tilde{Z}_2^H$ symmetry, commuting with E_6, is imposed. Under this custodial symmetry, all components of the **27**-plets are odd, thereby forbidding both interactions that generate large FCNCs and those that would lead to rapid proton decay. Doing so precludes any of the components of the **27**-plets from getting VEVs to break EW symmetry. This means that all of the **27**-plet Higgs states H_{ui}, H_{di} are inert and cannot be identified with the usual MSSM Higgs doublets. But, at the same time the multiplets M_l and $\overline{M}_l$ may be either even or odd under $\tilde{Z}_2^H$, allowing some of them to get VEVs for spontaneous symmetry breaking. The particular set of M_l, $\overline{M}_l$ multiplets, and their transformation properties under $\tilde{Z}_2^H$, define the specific variant of the model to be considered.

6.2 The SE$_6$SSM and the CSE$_6$SSM

In this thesis, we consider the case in which the set of multiplets M_l and $\overline{M}_l$ includes two pairs of $SU(2)_L$ doublets, H_u and $\overline{H}_u$, H_d and $\overline{H}_d$, as well as a pair of singlets S and $\overline{S}$. The fields H_u, H_d, S and $\overline{S}$ are postulated to be even under $\tilde{Z}_2^H$ symmetry and are responsible for the breaking of $SU(2)_L \times U(1)_Y \times U(1)_N \to U(1)_{\rm em}$ at the TeV scale[1]. On the other hand, the doublets $\overline{H}_u$ and $\overline{H}_d$ are assumed to be odd under $\tilde{Z}_2^H$, so that they can mix with a combination of the **27**-plet states, defined to be the third generation H_3^u, H_3^d. In this case they may form vector-like states with masses of order M_X, and so may be integrated out of the low-energy spectrum.

With only this set of multiplets, the imposed $\tilde{Z}_2^H$ would forbid any renormalisable operators allowing the exotic quarks to decay. In Chapter 3 it was noted that the same problem occurs in the E$_6$SSM when Z_2^H symmetry is exact, leading to conflicts with limits on the relic concentration of exotic matter [358–360]. By allowing Z_2^H to be violated by small Yukawa couplings, the exotic states are able to decay. In the usual case where it is assumed that this breaking is mostly due to Yukawa couplings of $\hat{D}_i$, $\hat{\overline{D}}_i$ to the third generation MSSM chiral superfields, the exotic D-fermions mostly decay via the channels [278, 290, 309]

$$D \to t + \tilde{\tau}\,, \quad D \to \tau + \tilde{t}\,, \quad D \to b + \tilde{\nu}_\tau\,, \quad D \to \nu_\tau + \tilde{b}\,, \tag{6.1}$$

when Z_2^B symmetry is imposed. The subsequent decays of these states mean that if the exotics are produced at colliders they may lead to an enhancement in the cross sections for $pp \to t\bar{t}\tau^+\tau^- + X$ and $pp \to b\bar{b}\tau^+\tau^- + X$. However, in this alternative E_6 model the $\tilde{Z}_2^H$ is required to be exact, and the above Yukawa couplings are forbidden. Instead, a pair of $\tilde{Z}_2^H$ even $SU(2)_L$ doublets L_4 and $\overline{L}_4$ with the quantum numbers of leptons are once again included, this time as part of the set of M_l and $\overline{M}_l$ multiplets, at the TeV scale. These couple to the exotic D_i, $\overline{D}_i$ and so allow the exotic quarks to decay. This choice also implies that D_i and $\overline{D}_i$ are leptoquarks in this scenario, as for the case of Z_2^B symmetry in the E$_6$SSM.

In addition to the above sets of multiplets, a pure singlet superfield $\hat{\phi}$ is also included in the spectrum below the GUT scale, which is uncharged under all of the gauge symmetries [347]. This superfield is likewise taken to be even under $\tilde{Z}_2^H$ so

[1]The initial breaking of $U(1)_\psi \times U(1)_\chi \to U(1)_N \times Z_2^M$ can be achieved with the VEVs of a multiplet pair N_H^c and $\overline{N}_H^c$ with the quantum numbers of right-handed neutrinos. These VEVs may also be responsible for the generation of Majorana masses for the **27**-plet right-handed neutrinos; the full details of the construction can be found in Ref. [300].

that the superpotential may contain a term proportional to $\hat{\phi}\hat{S}\hat{\overline{S}}$. This is necessary to stabilise the scalar potential, as shall be demonstrated in Section 6.3, and the scalar component ϕ of $\hat{\phi}$ is allowed to develop a non-zero VEV. The component fields of $\hat{H}_u$, $\hat{H}_d$, $\hat{S}$, $\hat{\overline{S}}$ and $\hat{\phi}$ are all expected to get masses at or below the TeV scale. Thus after integrating out superheavy states the low-energy matter content in this model, here referred to as the SE$_6$SSM, consists of the superfields shown in Table 6.1. At low

	$\hat{Q}_i$	$\hat{u}^c_i$	$\hat{d}^c_i$	$\hat{L}_i$	$\hat{e}^c_i$	$\hat{D}_i$	$\hat{\overline{D}}_i$	$\hat{S}_i$	$\hat{H}_{u\alpha}$	$\hat{H}_{d\alpha}$	$\hat{H}_u$	$\hat{H}_d$	$\hat{S}$	$\hat{\overline{S}}$	$\hat{L}_4$	$\hat{\overline{L}}_4$
$SU(3)_C$	**3**	$\overline{\mathbf{3}}$	$\overline{\mathbf{3}}$	**1**	**1**	**3**	$\overline{\mathbf{3}}$	**1**	**1**	**1**	**1**	**1**	**1**	**1**	**1**	**1**
$SU(2)_L$	**2**	**1**	**1**	**2**	**1**	**1**	**1**	**1**	**2**	**2**	**2**	**2**	**1**	**1**	**2**	$\overline{\mathbf{2}}$
$\sqrt{\frac{5}{3}}Q^Y_i$	$\frac{1}{6}$	$-\frac{2}{3}$	$\frac{1}{3}$	$-\frac{1}{2}$	1	$-\frac{1}{3}$	$\frac{1}{3}$	0	$\frac{1}{2}$	$-\frac{1}{2}$	$\frac{1}{2}$	$-\frac{1}{2}$	0	0	$-\frac{1}{2}$	$\frac{1}{2}$
$\sqrt{40}Q^N_i$	1	1	2	2	1	-2	-3	5	-2	-3	-2	-3	5	-5	2	-2
$\tilde{Z}^H_2$	$-$	$-$	$-$	$-$	$-$	$-$	$-$	$-$	$-$	$-$	$+$	$+$	$+$	$+$	$+$	$+$
Z^M_2	$-$	$-$	$-$	$-$	$-$	$+$	$+$	$+$	$+$	$+$	$+$	$+$	$+$	$+$	$-$	$-$
Z^E_2	$+$	$+$	$+$	$+$	$+$	$-$	$-$	$-$	$-$	$-$	$+$	$+$	$+$	$+$	$-$	$-$

Table 6.1: Summary of the chiral superfields present at low energies, showing their representations and charges under the gauge symmetries as well as their transformation properties under the discrete symmetries $\tilde{Z}^H_2$, Z^M_2 and Z^E_2. Note that the pure singlet field $\hat{\phi}$ is omitted from the table, as it transforms trivially under all of the symmetries.

energies and neglecting suppressed non-renormalisable interactions, the most general superpotential, initially containing terms such as those in Eq. (3.7), reduces to the simpler form [347]

$$\begin{aligned}\hat{W}_{\rm SE_6SSM} = {} & \lambda\hat{S}\hat{H}_d\cdot\hat{H}_u - \sigma\hat{\phi}\hat{S}\hat{\overline{S}} + \frac{\kappa_\phi}{3}\hat{\phi}^3 + \frac{\mu_\phi}{2}\hat{\phi}^2 + \Lambda_F\hat{\phi} + \tilde{\lambda}_{\alpha\beta}\hat{S}\hat{H}_{d\alpha}\cdot\hat{H}_{u\beta} + \kappa_{ij}\hat{S}\hat{D}_i\hat{\overline{D}}_j \\ & + \tilde{f}_{i\alpha}\hat{S}_i\hat{H}_u\cdot\hat{H}_{d\alpha} + f_{i\alpha}\hat{S}_i\hat{H}_{u\alpha}\cdot\hat{H}_d - g^D_{ij}\hat{Q}_i\cdot\hat{L}_4\hat{\overline{D}}_j - h^E_{i\alpha}\hat{e}^c_i\hat{H}_{d\alpha}\cdot\hat{L}_4 + \mu_L\hat{L}_4\cdot\hat{\overline{L}}_4 \\ & + \tilde{\sigma}\hat{\phi}\hat{\overline{L}}_4\cdot\hat{L}_4 + y^U_{ij}\hat{u}^c_i\hat{H}_u\cdot\hat{Q}_j + y^D_{ij}\hat{d}^c_i\hat{Q}_j\cdot\hat{H}_d + y^E_{ij}\hat{e}^c_i\hat{L}_j\cdot\hat{H}_d\,. \end{aligned} \tag{6.2}$$

The exact $\tilde{Z}^H_2$ symmetry forbids all terms of the form $\mathbf{27}\times\mathbf{27}\times\mathbf{27}$, so that the allowed trilinear interactions involving non-singlet fields are of the form $\mathbf{27'}\times\mathbf{27'}\times\mathbf{27'}$ or $\mathbf{27'}\times\mathbf{27}\times\mathbf{27}$. Note that, while the notation used in this section matches that used in the E$_6$SSM, the meanings and origins of the various terms are subtly different. For instance, the $\lambda\hat{S}\hat{H}_d\cdot\hat{H}_u$ in the E$_6$SSM is an example of a $\mathbf{27}\times\mathbf{27}\times\mathbf{27}$ interaction, whereas in the SE$_6$SSM it involves only states from incomplete $\mathbf{27'}$ multiplets. Otherwise, the shared parts of the E$_6$SSM and SE$_6$SSM superpotentials are rather similar. In particular, by making rotations of the superfields $(\hat{H}_{d\alpha}, \hat{H}_{u\alpha})$ and $(\hat{D}_i, \hat{\overline{D}}_i)$, the trilinear couplings $\tilde{\lambda}_{\alpha\beta}$ and κ_{ij} are again chosen to be flavour diagonal. The same cannot be done for the other new couplings $\tilde{f}_{i\alpha}$, $f_{i\alpha}$, g^D_{ij} and $h^E_{i\alpha}$, in general.

As in the E$_6$SSM, the superpotential also contains several bilinear terms, such as those of the form $\mathbf{27}' \times \overline{\mathbf{27}'}$, that are consistent with all of the gauge and discrete symmetries. The corresponding couplings, for example μ_L, can be generated in the usual way, namely via the Giudice-Masiero mechanism.

As well as being invariant under the single imposed $\tilde{Z}_2^H$ symmetry, the superpotential is also invariant under the residual Z_2^M symmetry resulting from the breakdown of $U(1)_\psi \times U(1)_\chi \to U(1)_N \times Z_2^M$. The presence of multiple Z_2 symmetries suggests that it is not unreasonable to expect multiple stable states that may play the role of DM. To reveal the identity of the possible DM states, it is convenient to define [300] a combination of these two Z_2 symmetries by $\tilde{Z}_2^H = Z_2^M \times Z_2^E$. The transformation properties of each field under this Z_2^E symmetry are also shown in Table 6.1. While in previous chapters we used the term exotic states in the rather loose sense of those states that are not present in the MSSM, in the SE$_6$SSM we adopt a more precise terminology in which the exotic states are exactly the Z_2^E odd states. Since the Lagrangian is separately invariant under $\tilde{Z}_2^H$ and Z_2^M, it is also invariant under Z_2^E. In particular, this means that the lightest Z_2^E-odd, i.e., exotic state is absolutely stable and so can potentially be a DM candidate. The automatically conserved matter parity Z_2^M, meanwhile, also implies the existence of a stable state, and is equivalent to R–parity as defined in the MSSM. Examination of the possible cases shows that these two states are in fact distinct, so that the model has the rather interesting feature of containing two DM candidates. In the case that the stable, lightest Z_2^E odd state is not also the lightest R–parity odd state, then the lightest R–parity odd state must be stable, as usual. Conversely, if the lightest Z_2^E odd state is also the lightest R–parity odd state, then either the lightest R–parity even, Z_2^E odd state or the lightest R–parity odd, Z_2^E even state (depending on which is lighter) is absolutely stable.

In the E$_6$SSM, the phenomenological problems associated with the lightest inert neutralinos are avoided by introducing a Z_2^S symmetry. These states tend to be the lightest exotic states in the spectrum, and are predominantly combinations of the fermionic components of the inert singlet superfields $\hat{S}_i$. Just as in the E$_6$SSM, substantial masses for these inert singlinos, of more than ~ 1 eV, are ruled out by measurements of the SM-like Higgs branching ratios and the DM relic density. The solution adopted in the SE$_6$SSM is to require that the inert singlino masses are much lighter than 1 eV, which can be achieved provided that the couplings $\tilde{f}_{i\alpha}, f_{i\alpha} \lesssim 10^{-6}$.

This results in the inert singlinos forming hot DM, giving a negligible contribution to the observed relic density[2].

In this case, the second DM candidate should account fully or partially for the DM density, with the latter possibility requiring either additional DM candidates or a non-standard thermal history of the Universe to be consistent with measurements. The sub-eV inert singlinos are both the lightest exotic and lightest R–parity odd states in the spectrum. This implies that the lightest R–parity even exotic state or the lightest R–parity odd, Z_2^E even state is a possible second DM candidate. Table 6.1 indicates that the possible exotic candidates are the exotic squarks arising from the superfields $(\hat{D}_i, \hat{\overline{D}}_i)$, the inert Higgs scalars coming from the mixing of $(\hat{S}_i, \hat{H}_{u\alpha}, \hat{H}_{d\alpha})$, or the fermionic components of $(\hat{L}_4, \hat{\overline{L}}_4)$. The masses of these states are required to be sufficiently heavy to have evaded detection to date. In particular, for large values of the SUSY breaking scale M_S the scalars receive large soft SUSY breaking masses and can be of similar mass to the ordinary squarks. The fermionic components of $(\hat{L}_4, \hat{\overline{L}}_4)$, meanwhile, receive a supersymmetric mass contribution from the superpotential bilinear term $\mu_L \hat{L}_4 \cdot \hat{\overline{L}}_4$. Exactly as in the E$_6$SSM, this parameter is not constrained by the requirement of successful EWSB and therefore need not be small. The principal constraints on the value of μ_L come from requiring that gauge unification still occurs, as before, and that the states associated with $\hat{L}_4$ and $\hat{\overline{L}}_4$ are light enough so that the exotic leptoquarks D_i, $\overline{D}_i$ decay sufficiently quickly. This means that the lightest R–parity odd, Z_2^E even state tends to be the stable state corresponding to the lightest neutralino with $Z_2^E = +1$. Depending on the composition of this state, it may then account for some or all of the DM relic density, as in the MSSM.

As usual in low-energy SUSY models, quantities like the composition of the lightest neutralino are governed both by the superpotential interactions in Eq. (6.2) as well as (a subset of) the soft SUSY breaking interactions. Including the standard set of soft scalar masses, soft trilinears, and soft gaugino masses, the full set of soft SUSY breaking terms that we consider is [347]

$$
\begin{aligned}
-\mathcal{L}^{\text{soft}}_{\text{SE}_6\text{SSM}} = {} & m^2_{H_u}|H_u|^2 + m^2_{H_d}|H_d|^2 + m^2_S|S|^2 + m^2_{\overline{S}}|\overline{S}|^2 + m^2_{\Sigma_{ij}} S_i^\dagger S_j + m^2_\phi|\phi|^2 \\
& + m^2_{H_{2,\alpha\beta}}(H_{u\alpha})^\dagger H_{u\beta} + m^2_{H_{1,\alpha\beta}}(H_{d\alpha})^\dagger H_{d\beta} + m^2_{D_{ij}} D_i^\dagger D_j + m^2_{\overline{D}_{ij}} \overline{D}_i^\dagger \overline{D}_j \\
& + m^2_{L_4}|L_4|^2 + m^2_{\overline{L}_4}|\overline{L}_4|^2 + m^2_{Q_{ij}} \tilde{Q}_i^\dagger \tilde{Q}_j + m^2_{u^c_{ij}} (\tilde{u}^c_i)^\dagger \tilde{u}^c_j + m^2_{d^c_{ij}} (\tilde{d}^c_i)^\dagger \tilde{d}^c_j \\
& + m^2_{L_{ij}} \tilde{L}_i^\dagger \tilde{L}_j + m^2_{e^c_{ij}} (\tilde{e}^c_i)^\dagger \tilde{e}^c_j + \left(\mu_L B_L L_4 \cdot \overline{L}_4 + \frac{\mu_\phi B_\phi}{2}\phi^2 + \Lambda_S \phi + h.c. \right)
\end{aligned}
$$

[2]The presence of very light neutral fermions in the particle spectrum may also lead to some interesting implications for the neutrino physics (see, for example, Ref. [586]).

$$
\begin{aligned}
&+\Big(T_\lambda S H_d\cdot H_u - T_\sigma \phi S\overline{S} + T^\kappa_{ij} S D_i \overline{D}_j + T^U_{ij}\tilde{u}^c_i H_u\cdot \tilde{Q}_j + T^D_{ij}\tilde{d}^c_i \tilde{Q}_j\cdot H_d\\
&+ T^E_{ij}\tilde{e}^c_i \tilde{L}\cdot H_d + T^{\tilde{\lambda}}_{\alpha\beta} S H_{d\alpha}\cdot H_{u\beta} + T^{\tilde{f}}_{i\alpha} S_i H_u\cdot H_{d\alpha} + T^f_{i\alpha} S_i H_{u\alpha}\cdot H_d\\
&+ T_{\tilde{\sigma}}\phi\overline{L}_4\cdot L_4 + \frac{T_{\kappa_\phi}}{3}\phi^3 - T^{g^D}_{ij}\tilde{Q}_i\cdot L_4\overline{D}_j - T^{h^E}_{i\alpha}\tilde{e}^c_i H_{d\alpha}\cdot L_4 + h.c.\Big)\\
&+\frac{1}{2}\Big(M_1\tilde{B}\tilde{B} + M_2\tilde{W}\tilde{W} + M_3\tilde{G}\tilde{G} + M'_1\tilde{B}'\tilde{B}' + 2M_{11}\tilde{B}\tilde{B}' + h.c.\Big)\,. \qquad (6.3)
\end{aligned}
$$

To reduce the number of free parameters in the model, in the remainder of this thesis we consider a constrained version of the model, denoted the CSE$_6$SSM. The CSE$_6$SSM is defined by imposing boundary conditions inspired by gravity mediated SSB at the GUT scale M_X where all gauge couplings coincide, as defined in Eq. (3.12). Since at low energies the matter content of the SE$_6$SSM can be placed into complete $SU(5)$ multiplets, with the exceptions of the doublets $\hat{L}_4$ and $\hat{\overline{L}}_4$, gauge coupling unification still occurs at the two-loop level for any value of $\alpha_3(M_Z)$ consistent with the measured value [300, 350], like in the E$_6$SSM. The situation concerning gauge kinetic mixing is also essentially the same as it was in the simpler model; we assume that the off-diagonal gauge coupling g_{11} and the mixed gaugino mass M_{11} vanish at M_X and remain zero at all scales below this. For the same reasons noted when discussing gauge kinetic mixing in the E$_6$SSM, if these parameters vanish at the GUT scale they also remain small at all scales below this, so that their effects can be neglected.

The remaining soft masses satisfy high-scale relations analogous to those applied in the CMSSM, Eq. (2.16). The soft scalar masses squared are taken to be flavour diagonal with diagonal elements set to the common value m_0^2 at M_X, and similarly the gaugino masses (with the exception of M_{11}, as noted above) are assumed to unify to the value $M_{1/2}$ at this scale. The values of the soft breaking trilinears are related to a single common trilinear parameter A_0 by

$$
\begin{aligned}
T_\lambda(M_X) &= \lambda(M_X)A_0\,, & T_\sigma(M_X) &= \sigma(M_X)A_0\,,\\
T^\kappa_{ij}(M_X) &= \kappa_{ij}(M_X)A_0\,, & T^U_{ij}(M_X) &= y^U_{ij}(M_X)A_0\,,\\
T^D_{ij}(M_X) &= y^D_{ij}(M_X)A_0\,, & T^E_{ij}(M_X) &= y^E_{ij}(M_X)A_0\,,\\
T^{\tilde{\lambda}}_{\alpha\beta}(M_X) &= \tilde{\lambda}_{\alpha\beta}(M_X)A_0\,, & T^{\tilde{f}}_{i\alpha}(M_X) &= \tilde{f}_{i\alpha}(M_X)A_0\,,\\
T^f_{i\alpha}(M_X) &= f_{i\alpha}(M_X)A_0\,, & T_{\tilde{\sigma}}(M_X) &= \tilde{\sigma}(M_X)A_0\,,\\
T_{\kappa_\phi}(M_X) &= \kappa_\phi(M_X)A_0\,, & T^{g^D}_{ij}(M_X) &= g^D_{ij}(M_X)A_0\,,\\
T^{h^E}_{i\alpha}(M_X) &= h^E_{i\alpha}(M_X)A_0\,. & &
\end{aligned} \qquad (6.4)
$$

Similarly, the soft breaking bilinears are assumed to unify, $B_L(M_X) = B_\phi(M_X) = B_0$. The parameter B_0 is taken to be independent of A_0; this can be done assuming that these soft terms are also generated via a Giudice-Masiero term, as used to produce the superpotential bilinears. The soft breaking tadpole Λ_S is not required to be related to other soft parameters by the high-scale boundary condition.

With this choice of boundary conditions, the underlying parameters in the CSE$_6$SSM consist of the new superpotential couplings, namely $\lambda(M_X)$, $\sigma(M_X)$, $\kappa_\phi(M_X)$, $\mu_\phi(M_X)$, $\Lambda_F(M_X)$, $\tilde{\lambda}_{\alpha\beta}(M_X)$, $\kappa_{ij}(M_X)$, $\tilde{f}_{i\alpha}(M_X)$, $f_{i\alpha}(M_X)$, $g^D_{ij}(M_X)$, $h^E_{i\alpha}(M_X)$, $\mu_L(M_X)$ and $\tilde{\sigma}(M_X)$, and the soft breaking parameters m_0, $M_{1/2}$, A_0, B_0 and Λ_S. The analysis of the model is also simplified by assuming that all of these parameters are real, which also helps to avoid limits on CP-violation. Once these high-scale parameters, together with the MSSM gauge and Yukawa couplings are specified, the CSE$_6$SSM at low energies can be studied by integrating the RGEs, given in Appendix D, from M_X to the EWSB scale.

6.3 Gauge Symmetry Breaking in the SE$_6$SSM

At low energies, the Higgs fields H_u, H_d, S, $\overline{S}$ and ϕ develop non-zero VEVs breaking $SU(2)_L \times U(1)_Y \times U(1)_N \to U(1)_{\rm em}$. The relevant part of the SE$_6$SSM scalar potential can again be divided into parts,

$$V_{\rm SE_6SSM} = V^F_{\rm SE_6SSM} + V^D_{\rm SE_6SSM} + V^{\rm soft}_{\rm SE_6SSM} + \Delta V_{\rm SE_6SSM}\,. \tag{6.5}$$

The F-term, D-term and soft contributions are now

$$\begin{aligned} V^F_{\rm SE_6SSM} &= \lambda^2|S|^2(|H_d|^2+|H_u|^2) + \sigma^2|\phi|^2|S|^2 + |\lambda H_d\cdot H_u - \sigma\phi\overline{S}|^2 \\ &\quad + |\kappa_\phi\phi^2 + \mu_\phi\phi + \Lambda_F - \sigma S\overline{S}|^2\,, \qquad (6.6) \\ V^D_{\rm SE_6SSM} &= \frac{\bar{g}^2}{8}(|H_u|^2-|H_d|^2)^2 + \frac{g_2^2}{2}|H_d^\dagger H_u|^2 \\ &\quad + \frac{g_1'^2}{2}(Q_1|H_d|^2 + Q_2|H_u|^2 + Q_S|S|^2 - Q_S|\overline{S}|^2)^2\,, \qquad (6.7) \\ V^{\rm soft}_{\rm SE_6SSM} &= m^2_{H_d}|H_d|^2 + m^2_{H_u}|H_u|^2 + m^2_S|S|^2 + m^2_{\overline{S}}|\overline{S}|^2 + m^2_\phi|\phi|^2 \\ &\quad + \left(\frac{T_{\kappa_\phi}}{3}\phi^3 + \frac{\mu_\phi}{2}B_\phi\phi^2 + \Lambda_S\phi + T_\lambda S H_d\cdot H_u - T_\sigma\phi S\overline{S} + h.c.\right), \qquad (6.8) \end{aligned}$$

and $\Delta V_{\rm SE_6SSM}$ as usual contains the loop corrections to the effective potential. Because S and $\overline{S}$ have the same $U(1)_N$ charge, there is a D-flat direction in which the quartic

terms in $V^D_{\mathrm{SE_6SSM}}$ vanish for $|S| = |\overline{S}| \to \infty$ and with the remaining fields vanishing. If it were the case that $\sigma = 0$, then when $m_S^2 + m_{\overline{S}}^2 < 0$ the potential is unstable along this direction, i.e., it is not bounded below [347]. The superpotential term $\sigma\hat{\phi}\hat{S}\hat{\overline{S}}$ is included to counteract this, since it generates an F-term contribution $|\sigma|^2|S|^2|\overline{S}|^2$ that renders the potential stable in this direction.

The interactions of the multiple singlets S, $\overline{S}$ and ϕ are also responsible for the potential improvement in the fine tuning associated with the Z' mentioned at the end of the previous chapter. There it was demonstrated that, in the E$_6$SSM, increasingly high limits on the mass of an unobserved Z' boson imply large D-terms are present in the EWSB conditions and cause a substantial fine tuning. This came about because, for $m_{Z'}^{\overline{\mathrm{DR}}}$ to be large, the E$_6$SSM singlet VEV involved in breaking $SU(2)_L \times U(1)_Y \times U(1)_N \to U(1)_{\mathrm{em}}$ must also be large, $s \sim m_{Z'}^{\overline{\mathrm{DR}}}$. As a result, the EW scale, $m_Z^{\overline{\mathrm{DR}}} \sim v$, receives a large tree-level contribution proportional to $m_{Z'}^{\overline{\mathrm{DR}}}$ through the $U(1)_N$ D-terms,

$$\Delta_\Phi = \frac{g_1'^2}{2}\left(Q_1 v_1^2 + Q_2 v_2^2 + Q_S s^2\right) Q_\Phi \approx \frac{Q_\Phi}{2Q_S}(m_{Z'}^{\overline{\mathrm{DR}}})^2\,,$$

as follows from Eq. (5.2). The fine tuning required to keep $m_Z^{\overline{\mathrm{DR}}}$ small while at the same time having $m_{Z'}^{\overline{\mathrm{DR}}}$ large enough to avoid the current experimental limits is problematic for a model that is in part motivated by the possibility of solving the fine tuning in the MSSM implied by a 125 GeV Higgs mass.

In the SE$_6$SSM, on the other hand, close to the D-flat direction $|S| = |\overline{S}|$ in field space, the D-term contributions from S and $\overline{S}$ very nearly cancel. As a result, the D-term contribution can be suppressed even when the singlet VEVs, which again set the Z' mass, are large. Thus provided that the soft parameters can be chosen so that the physical minimum lies approximately along this D-flat direction, the unnatural D-term contributions to $m_Z^{\overline{\mathrm{DR}}}$ that are a problem for the E$_6$SSM can be made substantially smaller, reducing the associated fine tuning. In contrast to alternative $U(1)$ extensions such as $U(1)_I$, where the reduction in tuning comes from the alternative set of $U(1)'$ charges, in the SE$_6$SSM it arises from the additional multiplets present at low energies, while the benefits of choosing $U(1)' = U(1)_N$ are retained. Although the size of the Z' contribution to the EWSB conditions is reduced in the SE$_6$SSM, it should also be noted that this mechanism involving multiple singlets simultaneously prevents the Higgs mass from receiving substantial corrections from extra D-terms. In the parameter space where these D-terms are heavily suppressed the lightest tree-level Higgs mass is very similar to that found in the MSSM [347], and large radiative corrections are required to raise the physical mass to 125 GeV.

At the physical minimum of this potential, the VEVs of the Higgs fields are taken to be of the form

$$\begin{aligned}
&\langle H_d\rangle = \frac{1}{\sqrt{2}}\begin{pmatrix} v_1 \\ 0 \end{pmatrix}, \quad \langle H_u\rangle = \frac{1}{\sqrt{2}}\begin{pmatrix} 0 \\ v_2 \end{pmatrix}, \\
&\langle S\rangle = \frac{s_1}{\sqrt{2}}, \quad \langle \overline{S}\rangle = \frac{s_2}{\sqrt{2}}, \quad \langle \phi\rangle = \frac{\varphi}{\sqrt{2}}.
\end{aligned} \tag{6.9}$$

The corresponding conditions for these non-zero VEVs to be a stationary point of the potential are found to be,

$$\begin{aligned}
\frac{\partial V_{\rm SE_6SSM}}{\partial v_1} &= m^2_{H_d} v_1 - \frac{T_\lambda}{\sqrt{2}} s_1 v_2 + \frac{\lambda^2}{2}(v_2^2 + s_1^2) v_1 + \frac{\lambda\sigma}{2} v_2 s_2 \varphi + \frac{\bar{g}^2}{8}(v_1^2 - v_2^2) v_1 \\
&\quad + \frac{g_1'^2}{2}(Q_1 v_1^2 + Q_2 v_2^2 + Q_S s_1^2 - Q_S s_2^2) Q_1 v_1 + \frac{\partial \Delta V_{\rm SE_6SSM}}{\partial v_1} = 0, \qquad (6.10a) \\
\frac{\partial V_{\rm SE_6SSM}}{\partial v_2} &= m^2_{H_u} v_2 - \frac{T_\lambda}{\sqrt{2}} s_1 v_1 + \frac{\lambda^2}{2}(v_1^2 + s_1^2) v_2 + \frac{\lambda\sigma}{2} v_1 s_2 \varphi - \frac{\bar{g}^2}{8}(v_1^2 - v_2^2) v_2 \\
&\quad + \frac{g_1'^2}{2}(Q_1 v_1^2 + Q_2 v_2^2 + Q_S s_1^2 - Q_S s_2^2) Q_2 v_2 + \frac{\partial \Delta V_{\rm SE_6SSM}}{\partial v_2} = 0, \qquad (6.10b) \\
\frac{\partial V_{\rm SE_6SSM}}{\partial s_1} &= m^2_S s_1 - \frac{T_\lambda}{\sqrt{2}} v_1 v_2 - \frac{T_\sigma}{\sqrt{2}} \varphi s_2 + \frac{\sigma^2}{2} \varphi^2 s_1 \\
&\quad + \sigma s_2 \left(\frac{\sigma}{2} s_1 s_2 - \frac{\kappa_\phi}{2}\varphi^2 - \frac{\mu_\phi}{\sqrt{2}}\varphi - \Lambda_F \right) + \frac{\lambda^2}{2}(v_1^2 + v_2^2) s_1 \\
&\quad + \frac{g_1'^2}{2}(Q_1 v_1^2 + Q_2 v_2^2 + Q_S s_1^2 - Q_S s_2^2) Q_S s_1 + \frac{\partial \Delta V_{\rm SE_6SSM}}{\partial s_1} = 0, \qquad (6.10c) \\
\frac{\partial V_{\rm SE_6SSM}}{\partial s_2} &= m^2_S s_2 - \frac{T_\sigma}{\sqrt{2}} \varphi s_1 + \frac{\sigma^2}{2} \varphi^2 s_2 + \frac{\lambda\sigma}{2} \varphi v_1 v_2 \\
&\quad + \sigma s_1 \left(\frac{\sigma}{2} s_1 s_2 - \frac{\kappa_\phi}{2}\varphi^2 - \frac{\mu_\phi}{\sqrt{2}}\varphi - \Lambda_F \right) \\
&\quad - \frac{g_1'^2}{2}(Q_1 v_1^2 + Q_2 v_2^2 + Q_S s_1^2 - Q_S s_2^2) Q_S s_2 + \frac{\partial \Delta V_{\rm SE_6SSM}}{\partial s_2} = 0, \qquad (6.10d) \\
\frac{\partial V_{\rm SE_6SSM}}{\partial \varphi} &= m^2_\phi \varphi - \frac{T_\sigma}{\sqrt{2}} s_1 s_2 + \mu_\phi B_\phi \varphi + \sqrt{2}\Lambda_S + \frac{T_{\kappa_\phi}}{\sqrt{2}}\varphi^2 + \frac{\sigma^2}{2}(s_1^2 + s_2^2)\varphi + \frac{\lambda\sigma}{2} s_2 v_1 v_2 \\
&\quad - 2\left(\frac{\sigma}{2} s_1 s_2 - \frac{\kappa_\phi}{2}\varphi^2 - \frac{\mu_\phi}{\sqrt{2}}\varphi - \Lambda_F \right)\left(\kappa_\phi \varphi + \frac{\mu_\phi}{\sqrt{2}} \right) + \frac{\partial \Delta V_{\rm SE_6SSM}}{\partial \varphi} = 0. \qquad (6.10e)
\end{aligned}$$

Of the 14 degrees of freedom associated with this larger set of Higgs fields, after EWSB four massless Goldstone modes are swallowed to generate masses for the physical $W^\pm$, Z and Z' bosons. The masses of the charged gauge bosons remain the same as in the MSSM and the E$_6$SSM. The fields H_u^0 and H_d^0 are still charged under both $U(1)_Y$ and

$U(1)_N$, and so $Z - Z'$ mixing occurs as in the E$_6$SSM. It is convenient to supplement the usual definition of v and $\tan\beta$, Eq. (2.33), with the analogous quantities for the two SM singlet VEVs,

$$s^2 = s_1^2 + s_2^2\,, \quad \tan\theta = \frac{s_2}{s_1}\,. \tag{6.11}$$

The expression for the $Z - Z'$ mass matrix is then identical to that in the E$_6$SSM, with the single singlet VEV in the E$_6$SSM replaced by s as defined in Eq. (6.11). Moreover, the same constraints hold on the combined VEV s, so that current Z' limits require $s = \sqrt{s_1^2 + s_2^2} \gtrsim 9$ TeV. In this case, the mixing between the physical states is tiny, so that $Z_1 \approx Z$ and $Z_2 \approx Z'$, with expressions for the tree-level masses that are unchanged from those in the E$_6$SSM.

In the E$_6$SSM, the value of the tree-level Z' mass can be directly related to the size of the SUSY scale through EWSB. It can be seen from the EWSB conditions, Eq. (3.17), that the scale of the singlet VEV, and hence the Z' mass, is set by the scale of the soft SUSY breaking masses, taken to be of the order of the SUSY scale M_S. When v is much smaller than either M_S or $M_{Z'}$, as is required by experimental data, by keeping only those terms that are $O(M_S^2)$ or larger it follows from Eq. (3.17c) that, at tree-level,

$$s^2 \approx \frac{(m_{Z'}^{\overline{\rm DR}})^2}{g_1'^2 Q_S^2} \approx -\frac{2m_S^2}{g_1'^2 Q_S^2}\,, \tag{6.12}$$

where the first approximate equality follows from Eq. (3.20) with $s \gg v$ [389]. This makes it clear that in the E$_6$SSM the singlet VEV and $M_{Z'}$ are both set by the SUSY scale, with $M_{Z'} \sim M_S$. As a result, a fine tuning price is not the only consequence of large Z' mass limits in the E$_6$SSM. Turning Eq. (6.12) around, it is evident that a large $M_{Z'}$ implies that M_S is large as well. Therefore when the Z' mass is above experimental limits, $M_{Z'} \gtrsim 3.4$ TeV, the superpartners with SUSY scale masses also tend to be in the multi-TeV range and so are not likely to be observed at the LHC [347]. In fact, in the E$_6$SSM this implicit lower bound on the sparticle masses is as stringent, if not more so, than the current LHC limits. For example, in the CE$_6$SSM a Z' mass of ~ 3.8 TeV can correspond to first and second generation squark masses of $\sim 2.5 - 3$ TeV, when neglecting limits on the gluino mass that also push up the possible squark masses [378]. While dedicated limits have not been determined in the CE$_6$SSM, this can be compared with those in the CMSSM where 2 TeV squarks remain viable [226]. The discrepancy is even more dramatic for the third generation sfermions, for which the experimental limits are much weaker (depending on the interpretation model, in the sub-TeV range [214, 215, 587]) but the Z' limit leads to multi-TeV masses for these states. The prospect that the sfermions in the E$_6$SSM might be unobservable at the

LHC is, from the phenomenological point of view, a disappointing aspect of this model [347].

Very much unlike in the E_6SSM, in the SE_6SSM the relationship between the Z' mass and the SUSY breaking scale can be much less rigid. This comes about again as a result of the interplay between the terms involving the singlets S, $\overline{S}$ and ϕ. The simplest case occurs when the VEVs s_1, s_2 lie close to the aforementioned D-flat direction and $m_S^2 + m_{\overline{S}}^2 < 0$, which can occur when $|\sigma|$ is small [300]. In this scenario, the stable minimum occurs at large values of the singlet VEVs given approximately by [347]

$$|\varphi| \sim |s_1| \approx |s_2| \sim \frac{1}{\sigma}\sqrt{|m_S^2 + m_{\overline{S}}^2|}\,, \tag{6.13}$$

from which it follows that $M_{Z'} \sim M_S/\sigma \gg M_S$. This implies that in the SE_6SSM the Z' mass need not be set by the SUSY scale, allowing it to be much larger to satisfy the experimental limits on $M_{Z'}$ while still having observable superpartners. Thus the SE_6SSM has the attractive feature that the Z' can be very heavy while still predicting superpartners with masses within reach at the LHC, by breaking the tight coupling between $M_{Z'}$ and M_S. In this chapter and the next, we focus primarily on the parts of the parameter space where this is achieved.

Even when $m_S^2 + m_{\overline{S}}^2 \geq 0$, it remains possible to find acceptable solutions to the EWSB conditions that realise this pattern of masses. Mass spectra with $M_{Z'} \gg M_S$ correspond to s_1, s_2 and φ being much larger than M_S. The appropriate stationary points of the scalar potential in Eq. (6.5) arise instead if Λ_F, Λ_S are large, with $\Lambda_F \gg M_S^2$ and $\Lambda_S \gg M_S^3$. In this case the structure of the potential is further simplified if the dimensionless couplings κ_ϕ and σ are small. Then in the leading approximation the quartic part of the scalar potential in Eq. (6.5) is just given by

$$\frac{g_1'^2}{2}\tilde{Q}_S^2(|S|^2 - |\overline{S}|^2)^2\,, \tag{6.14}$$

so that in the limit $|s_1|, |s_2| \to \infty$ the SM singlet VEVs still tend to lie approximately along the D-flat direction $s_1 \approx s_2$. The magnitude of these VEVs is large due to the small value of σ,

$$|\varphi| \sim |s_1| \approx |s_2| \sim \sqrt{\frac{2\Lambda_F}{\sigma}}\,. \tag{6.15}$$

In general, the singlet VEVs do not lie exactly along the D-flat direction being considered, since $m_S^2 \neq m_{\overline{S}}^2$. The deviation from this direction is quantified by the value of $\tan\theta$, which can be estimated from the EWSB conditions. By combining Eq. (6.10c)

and Eq. (6.10d), it follows that

$$\tan^2\theta \approx \frac{m_S^2 + \frac{\sigma^2}{2}\varphi^2 + \frac{g_1'^2}{2}\tilde{Q}_S^2 s^2}{m_{\overline{S}}^2 + \frac{\sigma^2}{2}\varphi^2 + \frac{g_1'^2}{2}\tilde{Q}_S^2 s^2}\,. \tag{6.16}$$

If the VEVs of the SM singlets φ, s_1 and s_2 are rather large due to the large values of parameters Λ_F and Λ_S then $M_{Z'} \gg M_S$, in marked difference to the situation in the E$_6$SSM, and from Eq. (6.16) it follows that $\tan\theta \approx 1$. Moreover, if the Yukawa couplings λ, σ, $\tilde{\lambda}_{\alpha\beta}$, κ_{ij}, $\tilde{f}_{i\alpha}$ and $f_{i\alpha}$ are small, then for the high-scale BC $m_S^2(M_X) = m_{\overline{S}}^2(M_X) = m_0^2$ the running of m_S^2 and $m_{\overline{S}}^2$ is such that at the scale of EWSB $m_S^2 \approx m_{\overline{S}}^2$. As a result, the value of $\tan\theta$ is extremely close to unity in this scenario. This region of parameter space is of particular interest, since the small Yukawa couplings imply that the exotic fermions are relatively light and so might be discovered at the LHC, as can be seen by looking at the particle mass spectrum of the SE$_6$SSM.

6.4 Modifications to the Particle Spectrum

The predictions for the masses of these exotic states, along with the neutralino and Higgs sectors, are substantially different in the SE$_6$SSM compared to the E$_6$SSM because of the extended Higgs sector. Much of the rest of the mass spectrum is otherwise changed only slightly. This is true for the MSSM sfermion masses, which, under the previous assumptions of negligible flavour mixing and small mixings in the first and second generations, continue to be given by Eqs. (3.25) to (3.31) for the first and second generation sfermions and the sneutrinos, and by Eqs. (3.32), (3.33) and (3.34) for the third generation sfermions. The only difference in the case of the first and second generation masses is that the $U(1)_N$ D-term contributions now have a contribution from the extra singlet $\overline{S}$ and read

$$\Delta_\Phi = \frac{g_1'^2}{2} Q_\Phi v^2 \left(Q_1 \cos^2\beta + Q_2 \sin^2\beta\right) + \frac{g_1'^2}{2} Q_\Phi Q_S s^2 \cos 2\theta\,. \tag{6.17}$$

Compared to the E$_6$SSM, where $\Delta_\Phi \sim (m_{Z'}^{\overline{\rm DR}})^2$ for large s, this D-term contribution can be significantly smaller even when s is large, due to the suppression by $\cos 2\theta$, while the sign of the contribution to the masses remains the same. Consequently in the parts of the parameter space where $M_{Z'} \gg M_S$ it can still be the case that the sfermions masses remain $O(M_S)$, as expected. The modified D-terms also appear in the third generation masses. The mixing parameters are also slightly different, requiring the

substitution $s \to s_1$ so that in the SE$_6$SSM,

$$X_t = \frac{T^U_{33} v}{\sqrt{2}} \sin\beta - \frac{\lambda y^U_{33} v s}{2} \cos\beta \cos\theta \,, \tag{6.18}$$

$$X_b = \frac{T^D_{33} v}{\sqrt{2}} \cos\beta - \frac{\lambda y^D_{33} v s}{2} \sin\beta \cos\theta \,, \tag{6.19}$$

$$X_\tau = \frac{T^E_{33} v}{\sqrt{2}} \cos\beta - \frac{\lambda y^E_{33} v s}{2} \sin\beta \cos\theta \,. \tag{6.20}$$

Of course, while these states can be lighter than $M_{Z'}$, to be phenomenologically viable they cannot be too light; in this chapter and the next we require $M_S \gtrsim 1$ TeV, with $M_S \gg M_Z$ to avoid limits from collider searches. The substitution $s \to s_1$ must also be made in the chargino masses, which are identical to the ones in the MSSM with $\mu \to \mu_{\rm eff}$ and

$$\mu_{\rm eff} = \frac{\lambda s_1}{\sqrt{2}} = \frac{\lambda s}{\sqrt{2}} \cos\theta \,. \tag{6.21}$$

This is because the vector supermultiplet $\hat{B}'$ and the additional singlet fields are electrically neutral, and so the fermion components of these superfields do not mix with the charged Higgsino and gaugino states.

Where the expressions for the MSSM sfermion and the chargino masses are similar to those found in the E$_6$SSM, the masses for the SM fermions and the gluino are unchanged in going from the E$_6$SSM to the SE$_6$SSM. The SM fermion masses are obtained from Eq. (2.40), and the tree-level gluino mass remains $m^{\overline{\rm DR}}_{\tilde{g}} = M_3$. The radiative corrections to this quantity are again essential for accurately estimating the physical gluino mass, i.e.,

$$m_{\tilde{g}} = M_3(M_S) + \Delta^{\tilde{g}}(M_S) \,,$$

for which the one-loop corrections $\Delta^{\tilde{g}}$ can be quite large, of up to 20%–30%, as in the MSSM. Pair production of gluinos would lead to a significant enhancement in $p\,p \to q\bar{q}q\bar{q} + E_T^{miss} + X$, with X denoting any number of light quark or gluon jets [363]. This signature can be used to discover the model when $m_{\tilde{g}}$ is within the LHC reach, or exclude regions of SE$_6$SSM parameter space where this is the case, thus making a good estimate of $m_{\tilde{g}}$ important for constraining the model. As the SE$_6$SSM contains the same coloured states as in the E$_6$SSM, the form of these radiative corrections $\Delta^{\tilde{g}}$ is unchanged between the two models.

6.4.1 The Neutralino Sector

The neutralino sector of the SE_6SSM is extended compared to its equivalent in the E_6SSM because the neutral fermion components of $\hat{H}_u$, $\hat{H}_d$, $\hat{S}$, $\hat{\overline{S}}$ and $\hat{\phi}$ as well as the neutral gauginos may all mix. This leads to a $Z_2^E = +1$ neutralino sector that is twice as large as the MSSM neutralino sector. The neutralino mass eigenstates, $\tilde{\chi}_i^0$, $i = 1, \ldots, 8$, are now linear combinations of the neutral Higgsino and singlino fields $\tilde{H}_u^0$, $\tilde{H}_d^0$, $\tilde{S}$, $\tilde{\overline{S}}$, $\tilde{\phi}$, and the gauginos $\tilde{B}$, $\tilde{W}_3$, and $\tilde{B}'$. Their tree-level masses are obtained by diagonalising the mass matrix in the usual way,

$$\mathrm{diag}(m_{\tilde{\chi}_1^0}^{\overline{\mathrm{DR}}}, \ldots, m_{\tilde{\chi}_8^0}^{\overline{\mathrm{DR}}}) = N^* M_{\tilde{\chi}^0} N^\dagger \,. \tag{6.22}$$

The 8×8 tree-level mass matrix in the basis $(\tilde{H}_d^0, \tilde{H}_u^0, \tilde{W}_3, \tilde{B}, \tilde{B}', \tilde{S}\cos\theta - \tilde{\overline{S}}\sin\theta, \tilde{S}\sin\theta + \tilde{\overline{S}}\cos\theta, \tilde{\phi})$ in the SE_6SSM can be written in block matrix form similar to that in Eq. (3.61), i.e.,

$$\mathcal{M}_{\tilde{\chi}^0} = \begin{pmatrix} A & C^T \\ C & B \end{pmatrix} .$$

The sub-matrices A, B and C are now all 4×4 matrices. The upper left sub-matrix A has the same structure as the neutralino mass matrix in the MSSM with $\mu \to \mu_{\mathrm{eff}}$, and is given by Eq. (3.62) with the appropriate value of μ_{eff} for the SE_6SSM being that given in Eq. (6.21). The remaining two sub-matrices then contain the mass terms for the additional SM singlet neutralinos and their mixings with the MSSM-like neutralino sector,

$$B = \begin{pmatrix} M_1' & g_1' Q_S s & 0 & 0 \\ g_1' Q_S s & \frac{\sigma\varphi}{\sqrt{2}} \sin 2\theta & -\frac{\sigma\varphi}{\sqrt{2}} \cos 2\theta & 0 \\ 0 & -\frac{\sigma\varphi}{\sqrt{2}} \cos 2\theta & -\frac{\sigma\varphi}{\sqrt{2}} \sin 2\theta & -\frac{\sigma s}{\sqrt{2}} \\ 0 & 0 & -\frac{\sigma s}{\sqrt{2}} & \mu_\phi + \sqrt{2}\kappa_\phi \varphi \end{pmatrix} , \tag{6.23}$$

$$C = \begin{pmatrix} Q_1 g_1' v \cos\beta & Q_2 g_1' v \sin\beta & 0 & 0 \\ -\frac{\lambda v}{\sqrt{2}} \sin\beta \cos\theta & -\frac{\lambda v}{\sqrt{2}} \cos\beta \cos\theta & 0 & 0 \\ -\frac{\lambda v}{\sqrt{2}} \sin\beta \sin\theta & -\frac{\lambda v}{\sqrt{2}} \cos\beta \sin\theta & 0 & 0 \\ 0 & 0 & 0 & 0 \end{pmatrix} . \tag{6.24}$$

For general values of the parameters and VEVs, the neutralino mass matrix of the SE_6SSM is clearly more complicated than its counterparts in the MSSM and E_6SSM. In the regions of parameter space that are of interest, however, the mass matrix has a rather simple structure so that the MSSM-like neutralinos and the states beyond the

MSSM tend not to mix. Inspection of Eq. (6.23) shows that two of the neutralinos, those that are a mixture of $\tilde{B}'$ and $\tilde{S}\cos\theta - \tilde{\overline{S}}\sin\theta$, have their masses set by the large value of $m_{Z'}^{\overline{\rm DR}}$ required by experiment. For large values of the singlet VEV, the value of $\mu_{\rm eff}$ would be similarly large unless λ is taken to be sufficiently small. For large values of $\mu_{\rm eff} \gg 1$ TeV the states that are superpositions of $\tilde{H}_u^0$ and $\tilde{H}_d^0$ become very heavy, leading to two very heavy pure Higgsino neutralinos with masses much larger than 1 TeV. This is not so interesting from a phenomenological point of view, as such heavy Higgsinos would not be observable. Moreover, in large parts of the parameter space[3] these pure Higgsinos would not make acceptable DM candidates, as they would be present today with too high a relic abundance [588]. It is therefore preferable to restrict λ to small values so that $\mu_{\rm eff} \lesssim 1$ TeV. When $\lambda \ll \sigma$ while σ is rather small and $M_{Z'} \gg M_S$ as implied by Eq. (6.15), the states that are a mixture of $\tilde{B}'$ and $\tilde{S}\cos\theta - \tilde{\overline{S}}\sin\theta$ become very heavy and decouple from the rest of the spectrum. For very large s, Eq. (6.16) implies that $\tan\theta \approx 1$ to high precision, allowing the masses of the states to be expressed approximately as

$$m_{\tilde{\chi}_{7,8}^0}^{\overline{\rm DR}} \approx m_{Z'}^{\overline{\rm DR}} \left[\frac{\sqrt{2}M_1' + \sigma\varphi}{2\sqrt{2}m_{Z'}^{\overline{\rm DR}}} \pm \sqrt{1 + \frac{\left(\sqrt{2}M_1' - \sigma\varphi\right)^2}{8(m_{Z'}^{\overline{\rm DR}})^2}} \right] \sim m_{Z'}^{\overline{\rm DR}} . \tag{6.25}$$

When $M_S \gg M_Z$ and λ is small, the mixing of the remaining extra states, which are a mixture of $\tilde{S}\sin\theta + \tilde{\overline{S}}\cos\theta$ and $\tilde{\phi}$, and the MSSM-like neutralinos is also highly suppressed. The masses of physical states formed by the mixture of these two remaining singlet states are then approximately given by

$$m_{\tilde{\chi}_{5,6}^0}^{\overline{\rm DR}} \approx \frac{1}{2}\left[\mu_\phi + \frac{\varphi}{\sqrt{2}}(2\kappa_\phi - \sigma) \pm \sqrt{2\sigma^2 s^2 + \left(\mu_\phi + \frac{\varphi}{\sqrt{2}}(2\kappa_\phi + \sigma)\right)^2} \right] \sim M_S . \tag{6.26}$$

For large values of $M_S \gtrsim 1$ TeV, these states will be heavy. Due to the lack of significant mixing, this means that they can also be ignored in the first approximation as far as determining the mass of the second DM candidate goes.

Provided this is the case, the neutralino DM candidate discussed above is expected to be predominantly MSSM-like, that is, a mixture of $\tilde{H}_d$, $\tilde{H}_u$, $\tilde{W}_3$ and $\tilde{B}$, with mass given by the lightest eigenvalue of the 4×4 sub-matrix A. In particular, since this matrix is identical to the MSSM neutralino mass matrix (with $\mu \to \mu_{\rm eff}$), when $M_S \gg$

[3]The possible exceptions being scenarios in which the effective annihilation cross section is significantly modified due to, e.g., coannihilations or annihilations near a resonance.

M_Z the masses of the four lightest neutralinos are determined by $\tan\beta$, μ_{eff}, M_1 and M_2 as they are in the MSSM. In the CSE$_6$SSM, the condition of universal gaugino masses at M_X further implies that

$$M_1 \approx 1.1 M_1' \approx 0.5 M_2 \approx 0.3 M_3 \approx 0.2 M_{1/2} \tag{6.27}$$

at low energies, which can be obtained from the semi-analytic solutions for the gaugino masses in the model. Apart from $\tan\beta$, the MSSM-like neutralino sector then only depends on the two parameters μ_{eff} and $M_{1/2}$. The low-energy values of M_1, M_2 and M_3 can also be compared to the equivalent relations found in the CMSSM,

$$M_1 \approx 0.5 M_2 \approx 0.15 M_3 \approx 0.4 M_{1/2}\,, \tag{6.28}$$

which are quite different because of the modified RG flow, due to the exotic states, in the SE$_6$SSM.

6.4.2 The Exotic Sector

The states that are odd under Z_2^E do not mix with the ordinary MSSM states or the Higgs fields, forming a separate sector containing a DM candidate as well as additional exotic states, some of which may generate spectacular collider signals. As mentioned above, the DM candidate in this sector is expected to be an almost massless inert singlino, which is the lightest of the inert neutralinos. The inert neutralino sector is formed by the fermion components ($\tilde{S}_i$, $\tilde{H}_{u\alpha}$ and $\tilde{H}_{d\alpha}$) of the superfields $\hat{S}_i$, $\hat{H}_{u\alpha}$ and $\hat{H}_{d\alpha}$. The scalar components of the corresponding superfields also mix to form a set of inert charged and neutral Higgs scalars. The general inert neutralino and neutral inert Higgs mass matrices are 7×7 matrices. In the basis $((\tilde{H}_{d1}^0 + \tilde{H}_{u1}^0)/\sqrt{2}, (\tilde{H}_{u1}^0 - \tilde{H}_{d1}^0)/\sqrt{2}, (\tilde{H}_{d2}^0 + \tilde{H}_{u2}^0)/\sqrt{2}, (\tilde{H}_{u2}^0 - \tilde{H}_{d2}^0)/\sqrt{2}, \tilde{S}_1, \tilde{S}_2, \tilde{S}_3)$, the inert neutralino mass matrix is of the form

$$M_{\tilde{\chi}_I^0} = \begin{pmatrix} A_I & C_I^T \\ C_I & 0 \end{pmatrix}, \tag{6.29}$$

where

$$A_I = \text{diag}\left(-m_{\tilde{H}_{I1}^0}^{\overline{\text{DR}}}, m_{\tilde{H}_{I1}^0}^{\overline{\text{DR}}}, -m_{\tilde{H}_{I2}^0}^{\overline{\text{DR}}}, m_{\tilde{H}_{I2}^0}^{\overline{\text{DR}}}\right) \tag{6.30}$$

contains the tree-level masses of the inert Higgsinos, $m_{\tilde{H}_{I\alpha}^0}^{\overline{\text{DR}}} = \tilde{\lambda}_{\alpha\alpha} s \cos\theta/\sqrt{2}$, in the absence of mixing with the inert singlinos, while the mixing is given by the 3×4

sub-matrix C_I with elements

$$\begin{aligned}(C_I)_{i1} &= \frac{v}{2}\left(f_{i1}\cos\beta + \tilde{f}_{i1}\sin\beta\right), \quad (C_I)_{i2} = \frac{v}{2}\left(f_{i1}\cos\beta - \tilde{f}_{i1}\sin\beta\right), \\ (C_I)_{i3} &= \frac{v}{2}\left(f_{i2}\cos\beta + \tilde{f}_{i2}\sin\beta\right), \quad (C_I)_{i4} = \frac{v}{2}\left(f_{i2}\cos\beta - \tilde{f}_{i2}\sin\beta\right).\end{aligned} \tag{6.31}$$

To yield almost massless hot DM candidates, the couplings of the inert singlinos are required to satisfy $f_{i\alpha}, \tilde{f}_{i\alpha} \lesssim 10^{-6}$. Then, provided that $\tilde{\lambda}_{\alpha\beta} \gtrsim 10^{-6}$, the mixing between the inert Higgsinos and the inert singlinos is entirely negligible, and the inert neutralinos correspond to two degenerate pairs of inert Higgsinos with tree-level masses given by Eq. (6.30) and three almost massless inert singlinos. This is rather similar to the situation in the E_6SSM considered in Section 3.4.1. The inert charginos similarly have tree-level masses given by $m^{\overline{\rm DR}}_{\tilde{H}^{\pm}_{I\alpha}} = |m^{\overline{\rm DR}}_{\tilde{H}^{0}_{I\alpha}}|$.

When the couplings $f_{i\alpha}$, $\tilde{f}_{i\alpha}$ are negligibly small, the mass matrix associated with the scalar components of the superfields $\hat{S}_i$, $\hat{H}_{u\alpha}$ and $\hat{H}_{d\alpha}$ also simplifies in a similar fashion. In this case, the mixing between the neutral inert Higgs scalars ($H_{u\alpha}$ and $H_{d\alpha}$) and the inert singlets S_i can be ignored and the corresponding mass matrix decomposes into a 3×3 singlet mass matrix and a 4×4 mass matrix for the inert Higgs scalars[4]. The family-diagonal structure of the couplings $\tilde{\lambda}_{\alpha\beta}$, as well as the fact that the off-diagonal soft scalar masses vanish at the GUT scale, ensures that the mixing between generations is very small. Thus the mass matrix for the inert singlets is approximately diagonal, with the tree-level masses for the inert singlet scalars given by

$$\left(m^{\overline{\rm DR}}_{S_{Ii}}\right)^2 = m^2_{\Sigma_{ii}} + \Delta_{S_i}. \tag{6.32}$$

For $\tan\theta \approx 1$, the inert singlet masses are therefore $\sim M_S$, and so are somewhat lighter than $M_{Z'}$. This can be contrasted with the situation in the E_6SSM, where the D-terms appearing in Eq. (3.42) are $\sim M_{Z'}$. In the absence of generation mixing, the inert Higgs mass matrix again decomposes into two 2×2 matrices. The resulting tree-level masses can be written in the same way as in Eq. (3.43). In addition to now involving the modified D-terms, the mixing parameter X_{H_α} is significantly modified, reading in the SE$_6$SSM,

$$X_{H_\alpha} = \frac{T^{\tilde{\lambda}}_{\alpha\alpha} s}{\sqrt{2}}\cos\theta - \frac{\tilde{\lambda}_{\alpha\alpha}}{4}\left(\lambda v^2 \sin 2\beta + 2\sigma\varphi s \sin\theta\right). \tag{6.33}$$

[4]Strictly speaking, for non-zero f and $\tilde{f}$ couplings, the inert neutral Higgs sector should actually be decomposed into CP-eigenstates. This leads to 7 CP-even scalars and 7 CP-odd scalars. When the couplings $f_{i\alpha}$ and $\tilde{f}_{i\alpha}$ are neglected, these states instead form 7 complex scalar mass eigenstates described by the mentioned 3×3 and 4×4 mass matrices.

The same comments hold for the inert charged Higgs states, which continue to be given by an expression of the form Eq. (3.45) with the modified D-terms and the mixing in Eq. (6.33) used instead.

The contribution to the mixing proportional to $\sigma\varphi s \sim M_S M_{Z'}$ can be of the order of the soft mass contributions to the masses. This means that it can be large enough to drive one of the squared masses negative, indicating that the physical vacuum is unstable. To prevent this potentially dangerous term from causing these tachyonic states, the inert Higgs couplings $\tilde{\lambda}_{\alpha\beta}$ should not be too large. In practice, we take these couplings to be not much larger than λ, e.g., $\tilde{\lambda}_{\alpha\beta} \sim 10^{-3}$, to satisfy this requirement. Doing so implies that the mixing is rather small so that the inert scalars tend to have masses of order M_S. At the same time, small values of the Yukawas $\tilde{\lambda}_{\alpha\beta}$ imply that the inert Higgsinos and charginos can be light, with masses not much heavier than the lightest $Z_2^E = +1$ neutralino, in which case they may be observable in LHC searches. The exact $\tilde{Z}_2^H$ symmetry forbids the Yukawa couplings of the inert Higgs and singlet superfields to ordinary quark and lepton superfields. In the E$_6$SSM where the Z_2 symmetry suppressing FCNCs is only approximate, such couplings in general are permitted along with those for the ordinary Higgs fields, leading to the inert Higgsinos and charginos decaying predominantly into third generation fermion-sfermion pairs [278]. The absence of these couplings in the SE$_6$SSM due to $\tilde{Z}_2^H$ symmetry means that the decay channels of the inert Higgsinos are rather different in this model. Pair production of the Z_2^E and R–parity odd inert Higgsinos and charginos can occur through off-shell W and Z bosons. They then decay into an inert singlino and an on-shell W or Z boson, or a Z_2^E even Higgs boson, through the mixing induced by the $f_{i\alpha}$ and $\tilde{f}_{i\alpha}$ superpotential couplings. When both of the produced states decay into gauge bosons it is expected that they should lead to enhancements in the rates of $p\,p \to Z\,Z + E_T^{miss} + X$, $p\,p \to W\,Z + E_T^{miss} + X$ and $p\,p \to W\,W + E_T^{miss} + X$.

The choice of flavour diagonal couplings κ_{ij} also means that there is no substantial mixing between generations of the exotic leptoquarks, D_i and $\overline{D}_i$. The 6×6 mass matrix for the scalar leptoquarks reduces to three 2×2 matrices, with tree-level masses given by similar expressions to those in the E$_6$SSM, Eq. (3.39). The only difference again is in the form of the D-terms and the mixing parameter,

$$X_{D_i} = \frac{T^{\kappa}_{ii} s}{\sqrt{2}} \cos\theta - \frac{\kappa_{ii}}{4}\left(\lambda v^2 \sin 2\beta + 2\sigma\varphi s \sin\theta\right) . \tag{6.34}$$

The corresponding spin-1/2 leptoquark masses are $m_{D_i}^{\overline{\rm DR}} = \kappa_{ii} s \cos\theta/\sqrt{2}$. The same potentially dangerous contribution to the mixing that occurs in the inert Higgs mass

matrices is also present here. To ensure that this does not lead to an instability of the physical vacuum, the couplings κ_{ij} can be required to be small as well, $\kappa_{ij} \sim 10^{-3}$. As is the case for the inert Higgs states, this leads to the scalar leptoquarks $\tilde{D}_i$ being heavier, with masses of the order of M_S, while the exotic fermions D_i can be light. These exotic fermion states are coloured and, once past threshold, can be pair produced at the 13 TeV LHC. They subsequently decay with missing energy via a decay chain involving an initial decay into an ordinary squark (quark) and an exotic L_4 fermion (scalar) component, through the couplings g^D_{ij}. This is followed by a decay involving the couplings $h^E_{i\alpha}$ of the exotic L_4 state into a lepton and inert Higgs or singlet (inert neutralino). If a hierarchy exists in the sizes of the couplings g^D_{ij} and $h^E_{i\alpha}$ as is present in the SM Yukawas, then such a process leads to an enhancement in signals with third generation final states, namely in $p\,p \to t\,\bar{t}\,\tau^+\,\tau^- + E_t^{miss} + X$ and $p\,p \to b\,\bar{b}\,\tau^+\,\tau^- + E_T^{miss} + X$.

For the branching ratio of these leptoquark decays to be significant, and also for the lifetimes of the exotic leptoquarks to be sufficiently short, the states associated with $\hat{L}_4$ and $\hat{\overline{L}}_4$ should not be too heavy. The set of states associated with $\hat{L}_4$ and $\hat{\overline{L}}_4$ contains the same physical states as in the E$_6$SSM. The fermion and scalar components of $\hat{L}_4$ and $\hat{\overline{L}}_4$ form a set of exotic lepton and slepton states that do not mix with the other exotic fields. The fermion components lead to a pair of charged and neutral states $\tilde{L}_4^{\pm}$ and $\tilde{L}^0_{4,1}$, $\tilde{L}^0_{4,2}$ with degenerate tree-level masses now given by

$$m^{\overline{\rm DR}}_{\tilde{L}_4^{\pm}} = m^{\overline{\rm DR}}_{\tilde{L}_4^{0}} = \mu_L - \frac{\tilde{\sigma}\varphi}{\sqrt{2}}\,. \tag{6.35}$$

Note that this differs from the corresponding expressions in the E$_6$SSM, where the tree-level masses depend only on μ_L. The expressions for the neutral and charged exotic sleptons, on the other hand, take the same form as in the E$_6$SSM, Eq. (3.47) and Eq. (3.48), with the $\overline{\rm DR}$ fermion masses now given by Eq. (6.35) and the mixing given by

$$X_{L_4} = \mu_L B_L - \frac{T_{\tilde{\sigma}}\varphi}{\sqrt{2}} + \tilde{\sigma}\left(\frac{\sigma}{4}s^2\sin 2\theta - \frac{\kappa_\phi}{2}\varphi^2 - \frac{\mu_\phi}{\sqrt{2}}\varphi - \Lambda_F\right). \tag{6.36}$$

By tuning the above mixing parameter, the exotic sleptons could be made light enough so that the exotic D fermions decay rapidly enough. Alternatively, these states are allowed to be heavier than the spin-1/2 leptoquarks provided that the couplings g^D and h^E are taken to be sufficiently large. Taking values for these couplings of $\sim 10^{-2}$ lead to lifetimes of the exotic fermions short enough to be consistent with constraints

from Big Bang nucleosynthesis. At the same time, the impact of the couplings g^D and h^E on the mass spectrum and DM predictions is negligible for these small values of the couplings. Consequently they may be safely varied in this range without having any substantial impact on the other sectors.

6.4.3 The Higgs Sector

The Higgs sector of the SE$_6$SSM is substantially different from the simplest version of the E$_6$SSM. In the SE$_6$SSM the sector responsible for the breakdown of gauge symmetry involves five multiplets of scalar fields H_u, H_d, S, $\overline{S}$ and ϕ that give rise to ten physical degrees of freedom in the Higgs sector. These form a set of charged and neutral Higgs bosons. The unbroken $U(1)_{\rm em}$ symmetry ensures that the charged components of H_u and H_d do not mix with the other Higgs and singlet fields. The two massive charged Higgs states are still formed by the linear combination

$$H^+ = H_d^{-*} \sin\beta + H_u^+ \cos\beta \,, \tag{6.37}$$

since the additional singlets are all electromagnetically neutral, but the charged Higgs mass is now given by

$$\left(m_{H^\pm}^{\overline{\rm DR}}\right)^2 = \frac{\sqrt{2}s}{\sin 2\beta}\left(T_\lambda \cos\theta - \frac{\lambda\sigma\varphi}{\sqrt{2}}\sin\theta\right) - \frac{\lambda^2}{2}v^2 + \frac{g_2^2}{4}v^2 \,. \tag{6.38}$$

The linear combination orthogonal to Eq. (6.37) constitutes the longitudinal degrees of freedom of the $W^\pm$ bosons, as expected.

In the absence of CP-violation in the Higgs sector, the real and imaginary parts of the neutral components of the Higgs and singlets fields do not mix, which now leads to three physical CP-odd Higgs bosons and five CP-even states. The Goldstone states that are absorbed by the Z and Z' bosons are mixtures of the imaginary parts of H_d^0, H_u^0, S and $\overline{S}$,

$$\begin{aligned} G &= \sqrt{2}(\mathrm{Im}\, H_d^0 \cos\beta - \mathrm{Im}\, H_u^0 \sin\beta) \,, \\ G' &= \sqrt{2}(\mathrm{Im}\, S \cos\theta - \mathrm{Im}\, \overline{S} \sin\theta)\cos\gamma - \sqrt{2}(\mathrm{Im}\, H_u^0 \cos\beta + \mathrm{Im}\, H_d^0 \sin\beta)\sin\gamma \,, \end{aligned} \tag{6.39}$$

where $\tan\gamma$ is defined analogously to $\tan\varphi$ in the E$_6$SSM,

$$\tan\gamma = \frac{v}{2s}\sin 2\beta \,. \tag{6.40}$$

For phenomenologically viable scenarios with $s \gg v$, $\tan\gamma$ goes to zero. Expressed in terms of the field basis (P_1, P_2, P_3), where

$$\begin{aligned} P_1 &= \sqrt{2}(\mathrm{Im}\, H_u^0 \cos\beta + \mathrm{Im}\, H_d^0 \sin\beta)\cos\gamma + \sqrt{2}(\mathrm{Im}\, S\cos\theta - \mathrm{Im}\,\overline{S}\sin\theta)\sin\gamma\,, \\ P_2 &= \sqrt{2}(\mathrm{Im}\, S\sin\theta + \mathrm{Im}\,\overline{S}\cos\theta)\,, \\ P_3 &= \sqrt{2}\,\mathrm{Im}\,\phi\,, \end{aligned} \tag{6.41}$$

the pseudoscalar mass matrix $\mathcal{M}_A^2$ has elements

$$\begin{aligned} (\mathcal{M}_A^2)_{11} &= \frac{\sqrt{2}s}{\sin 2\beta\cos^2\gamma}\left(T_\lambda\cos\theta - \frac{\lambda\sigma\varphi}{\sqrt{2}}\sin\theta\right)\,, \\ (\mathcal{M}_A^2)_{12} &= (\mathcal{M}_A^2)_{21} = \frac{v}{\sqrt{2}\cos\gamma}\left(T_\lambda\sin\theta + \frac{\lambda\sigma\varphi}{\sqrt{2}}\cos\theta\right)\,, \\ (\mathcal{M}_A^2)_{13} &= (\mathcal{M}_A^2)_{31} = \frac{\lambda\sigma v s}{2\cos\gamma}\sin\theta\,, \\ (\mathcal{M}_A^2)_{22} &= \frac{2\sigma\varphi}{\sin 2\theta}\left(\frac{\kappa_\phi}{2}\varphi + \frac{\mu_\phi}{\sqrt{2}} + \frac{\Lambda_F}{\varphi}\right) + \frac{v^2\sin 2\beta}{\sqrt{2}s\sin 2\theta}\left(T_\lambda\sin^3\theta - \frac{\lambda\sigma\varphi}{\sqrt{2}}\cos^3\theta\right) \\ &\quad + \frac{\sqrt{2}T_\sigma\varphi}{\sin 2\theta}\,, \\ (\mathcal{M}_A^2)_{23} &= (\mathcal{M}_A^2)_{32} = \frac{T_\sigma s}{\sqrt{2}} - \sigma s\left(\kappa_\phi\varphi + \frac{\mu_\phi}{\sqrt{2}}\right) - \frac{\lambda\sigma}{4}v^2\sin 2\beta\cos\theta\,, \\ (\mathcal{M}_A^2)_{33} &= \frac{T_\sigma s^2}{2\sqrt{2}\varphi}\sin 2\theta - 2\mu_\phi B_\phi - \frac{3T_{\kappa_\phi}}{\sqrt{2}}\varphi - \frac{\sqrt{2}}{\varphi}(\mu_\phi\Lambda_F + \Lambda_S) + \sigma\kappa_\phi s^2\sin 2\theta \\ &\quad - \frac{\kappa_\phi\mu_\phi}{\sqrt{2}}\varphi - 4\kappa_\phi\Lambda_F + \frac{\sigma\mu_\phi s^2}{2\sqrt{2}\varphi}\sin 2\theta - \frac{\lambda\sigma s}{4\varphi}v^2\sin\theta\sin 2\beta\,. \end{aligned} \tag{6.42}$$

In the parameter space of interest, the structure of the full 3×3 matrix is such that it can be approximately diagonalised analytically. Because $M_{Z'}, M_S \gg M_Z$ and we restrict our attention to small values of λ, the mixings between P_1 and P_2, P_3 are rather small and may be safely neglected. In this approximation, the mass of one CP-odd state is set by $(\mathcal{M}_A^2)_{11}$. Thus it has almost the same mass as the charged Higgs states. The masses of two other CP-odd states are set by $\tilde{m}_\pm^{\overline{\mathrm{DR}}}$, given by

$$\left(\tilde{m}_\pm^{\overline{\mathrm{DR}}}\right)^2 \approx \frac{1}{2}\left\{(\mathcal{M}_A^2)_{22} + (\mathcal{M}_A^2)_{33} \pm \sqrt{[(\mathcal{M}_A^2)_{22} - (\mathcal{M}_A^2)_{33}]^2 + 4(\mathcal{M}_A^2)_{23}^2}\right\}\,. \tag{6.43}$$

It follows from Eq. (6.43) that in some cases $\tilde{m}_-^{\overline{\mathrm{DR}}}$ can be rather small so that the lightest CP-odd state A_1 becomes the lightest particle in the spectrum. This happens, for example, in the limit $\kappa_\phi, \mu_\phi, \Lambda_F, \Lambda_S \to 0$, when $m_{A_1}^{\overline{\mathrm{DR}}}$ vanishes and the superpotential

possesses a global $U(1)_{PQ}$ PQ symmetry which is spontaneously broken by the VEVs s_1, s_2 and φ. For small but non-vanishing $U(1)_{PQ}$ violating couplings, the state A_1 is a light pseudo-Goldstone boson of the approximate PQ symmetry and can be lighter than the SM-like Higgs. In this case, the decay $h_1 \to A_1\, A_1$ is kinematically allowed and can in principle lead to non-negligible branching fractions for non-standard decays of the SM Higgs [347]. Even for larger values of the couplings κ_ϕ, μ_ϕ, Λ_F and Λ_S, m_{A_1} may be small provided that the remaining parameters in Eq. (6.43) are tuned so that $\tilde{m}_-^{\overline{\rm DR}} \to 0$. It is important to note that in either case, the vanishing of $m_{A_1}^{\overline{\rm DR}} \approx \tilde{m}_-^{\overline{\rm DR}}$ does not also require that the lightest neutralino mass becomes small, as occurs for example in the PQ-symmetric NMSSM. Indeed, from Eq. (6.25) and Eq. (6.26) it is clear that the singlino dominated states should remain heavy, while $m_{\tilde{\chi}_1^0}$ is governed by the values of the gaugino masses and $\mu_{\rm eff}$. This means that by varying the other Lagrangian parameters for fixed $M_{1/2}$ and $\mu_{\rm eff}$, the value of m_{A_1} can be chosen independently of $m_{\tilde{\chi}_1^0}$. In particular, for a given $m_{\tilde{\chi}_1^0}$ this allows for the possibility of resonant annihilations $\tilde{\chi}_1^0\, \tilde{\chi}_1^0 \to A_1 \to$ *SM particles* with $m_{A_1} \approx 2m_{\tilde{\chi}_1^0}$, leading to regions of parameter space in which the well-known A-funnel mechanism is responsible for setting the DM relic density [589–591].

The real parts of H_d^0, H_u^0, S, $\overline{S}$ and ϕ form five physical CP-even Higgs states, h_i, related by the unitary transformation

$$\begin{pmatrix} h_1 \\ h_2 \\ h_3 \\ h_4 \\ h_5 \end{pmatrix} = U_h \begin{pmatrix} \Phi_d \\ \Phi_u \\ \Phi_S \\ \Phi_{\overline{S}} \\ \Phi_\phi \end{pmatrix}, \tag{6.44}$$

where U_h diagonalises the CP-even Higgs mass matrix, $\mathcal{M}_h^2$, and

$$\begin{aligned} \mathrm{Re}\, H_d^0 &= \frac{1}{\sqrt{2}}\left(v_1 + \Phi_d\right), \quad \mathrm{Re}\, H_u^0 = \frac{1}{\sqrt{2}}\left(v_2 + \Phi_u\right), \\ \mathrm{Re}\, S &= \frac{1}{\sqrt{2}}\left(s_1 + \Phi_S\right), \quad \mathrm{Re}\, \overline{S} = \frac{1}{\sqrt{2}}\left(s_2 + \Phi_{\overline{S}}\right), \\ \mathrm{Re}\, \phi &= \frac{1}{\sqrt{2}}\left(\varphi + \Phi_\phi\right). \end{aligned}$$

In the basis $(S_1, S_2, S_3, S_4, S_5)$, where

$$\begin{aligned}
\Phi_S &= S_1 \cos\theta + S_2 \sin\theta\,, \\
\Phi_{\overline{S}} &= -S_1 \sin\theta + S_2 \cos\theta\,, \\
\Phi_\phi &= S_3\,, \\
\Phi_d &= S_5 \cos\beta - S_4 \sin\beta\,, \\
\Phi_u &= S_5 \sin\beta + S_4 \cos\beta\,,
\end{aligned} \tag{6.45}$$

and using the EWSB conditions Eq. (6.10) to eliminate the soft Higgs masses, this has elements

$$\begin{aligned}
(\mathcal{M}_h^2)_{11} &= g_1'^2 Q_S^2 s^2 - \frac{\sigma^2 s^2}{2}\sin^2 2\theta + \sqrt{2}T_\sigma \varphi \sin 2\theta + \left(\kappa_\phi \sigma \varphi^2 + \sqrt{2}\sigma\mu_\phi\varphi + 2\sigma\Lambda_F\right)\sin 2\theta \\
&\quad + \frac{T_\lambda}{2\sqrt{2}s} v^2 \cos\theta \sin 2\beta - \frac{\lambda\sigma\varphi}{4s} v^2 \sin\theta \sin 2\beta\,, \\
(\mathcal{M}_h^2)_{12} &= (\mathcal{M}_h^2)_{21} = \frac{\sigma^2 s^2}{4}\sin 4\theta - \sqrt{2}T_\sigma\varphi\cos 2\theta - \left(\kappa_\phi\sigma\varphi^2 + \sqrt{2}\sigma\mu_\phi\varphi + 2\sigma\Lambda_F\right)\cos 2\theta \\
&\quad + \frac{T_\lambda}{2\sqrt{2}s} v^2 \sin\theta \sin 2\beta + \frac{\lambda\sigma\varphi}{4s} v^2 \cos\theta \sin 2\beta\,, \\
(\mathcal{M}_h^2)_{13} &= (\mathcal{M}_h^2)_{31} = \sigma^2 \varphi s \cos 2\theta - \frac{\lambda\sigma}{4} v^2 \sin\theta \sin 2\beta\,, \\
(\mathcal{M}_h^2)_{14} &= (\mathcal{M}_h^2)_{41} = \frac{g_1'^2}{2} Q_S (Q_2 - Q_1) s v \sin 2\beta - \frac{T_\lambda}{\sqrt{2}} v \cos\theta \cos 2\beta \\
&\quad - \frac{\lambda\sigma}{2}\varphi v \sin\theta \cos 2\beta\,, \\
(\mathcal{M}_h^2)_{15} &= (\mathcal{M}_h^2)_{51} = g_1'^2 Q_S (Q_1 \cos^2\beta + Q_2 \sin^2\beta) s v - \frac{T_\lambda}{\sqrt{2}} v \cos\theta \sin 2\beta + \lambda^2 v s \cos^2\theta \\
&\quad - \frac{\lambda\sigma}{2}\varphi v \sin\theta \sin 2\beta\,, \\
(\mathcal{M}_h^2)_{22} &= \frac{\sigma^2 s^2}{2}\sin^2 2\theta + \frac{\sqrt{2}T_\sigma\varphi}{\sin 2\theta}\cos^2 2\theta + \left(\kappa_\phi\sigma\varphi^2 + \sqrt{2}\sigma\mu_\phi\varphi + 2\sigma\Lambda_F\right)\frac{\cos^2 2\theta}{\sin 2\theta} \\
&\quad + \frac{T_\lambda v^2}{2\sqrt{2}s\cos\theta}\sin^2\theta \sin 2\beta - \frac{\lambda\sigma\varphi v^2}{4s\sin\theta}\cos^2\theta \sin 2\beta\,, \\
(\mathcal{M}_h^2)_{23} &= (\mathcal{M}_h^2)_{32} = -\frac{T_\sigma}{\sqrt{2}} s + \sigma^2 \varphi s \sin 2\theta - \sigma s\left(\kappa_\phi\varphi + \frac{\mu_\phi}{\sqrt{2}}\right) \\
&\quad + \frac{\lambda\sigma}{4} v^2 \cos\theta \sin 2\beta\,, \\
(\mathcal{M}_h^2)_{24} &= (\mathcal{M}_h^2)_{42} = \left(-\frac{T_\lambda}{\sqrt{2}} v \sin\theta + \frac{\lambda\sigma}{2}\varphi v \cos\theta\right)\cos 2\beta\,,
\end{aligned} \tag{6.46}$$

$$
\begin{aligned}
(\mathcal{M}_h^2)_{25} &= (\mathcal{M}_h^2)_{52} = \frac{\lambda^2}{2} sv \sin 2\theta + \left(-\frac{T_\lambda}{\sqrt{2}} v \sin\theta + \frac{\lambda\sigma}{2}\varphi v \cos\theta \right) \sin 2\beta \,, \\
(\mathcal{M}_h^2)_{33} &= \frac{T_\sigma s^2}{2\sqrt{2}\varphi} \sin 2\theta - \sqrt{2}\frac{\Lambda_S}{\varphi} + \frac{T_{\kappa_\phi}}{\sqrt{2}}\varphi + \mu_\phi \left(\frac{\sigma s^2}{2\sqrt{2}\varphi} \sin 2\theta + 3\frac{\kappa_\phi \varphi}{\sqrt{2}} - \frac{\sqrt{2}\Lambda_F}{\varphi} \right) \\
&\quad + 2\kappa_\phi^2 \varphi^2 - \frac{\lambda\sigma s}{4\varphi} v^2 \sin\theta \sin 2\beta \,, \\
(\mathcal{M}_h^2)_{34} &= (\mathcal{M}_h^2)_{43} = \frac{\lambda\sigma}{2} sv \sin\theta \cos 2\beta \,, \\
(\mathcal{M}_h^2)_{35} &= (\mathcal{M}_h^2)_{53} = \frac{\lambda\sigma}{2} sv \sin\theta \sin 2\beta \,, \\
(\mathcal{M}_h^2)_{44} &= \left[(m_Z^{\overline{\rm DR}})^2 - \frac{\lambda^2 v^2}{2} + \frac{g_1'^2}{4}(Q_2 - Q_1)^2 v^2 \right) \sin^2 2\beta \\
&\quad + \frac{\sqrt{2}s}{\sin 2\beta} \left(T_\lambda \cos\theta - \frac{\lambda\sigma\varphi}{\sqrt{2}} \sin\theta \right) \,, \\
(\mathcal{M}_h^2)_{45} &= (\mathcal{M}_h^2)_{54} = \left[\frac{\lambda^2 v^2}{4} - \frac{(m_Z^{\overline{\rm DR}})^2}{2} \right] \sin 4\beta + \frac{g_1'^2}{2} v^2 (Q_2 - Q_1) \\
&\quad \times (Q_1 \cos^2\beta + Q_2 \sin^2\beta) \sin 2\beta \,, \\
(\mathcal{M}_h^2)_{55} &= (m_Z^{\overline{\rm DR}})^2 \cos^2 2\beta + \frac{\lambda^2}{2} v^2 \sin^2 2\beta + g_1'^2 v^2 (Q_1 \cos^2\beta + Q_2 \sin^2\beta)^2 \,.
\end{aligned}
$$

With the exceptions of $(\mathcal{M}_h^2)_{45}$, $(\mathcal{M}_h^2)_{54}$ and $(\mathcal{M}_h^2)_{55}$, the size of the mass matrix elements is determined by the singlet VEVs s and φ. For small values of λ such that $\lambda s \sim \sigma s \sim \sigma\varphi \sim M_S$, it is therefore expected that all but the lightest state have masses of the order of the SUSY scale or heavier. In particular, for $\lambda \sim \sigma \to 0$ the element $(\mathcal{M}_h^2)_{11} \sim (m_{Z'}^{\overline{\rm DR}})^2 \gg M_S^2$, while all other matrix elements are substantially smaller. Thus the mass of the heaviest CP-even state is approximately degenerate with the Z' mass. After neglecting all terms which are proportional to λv in Eqs. (6.46) it is easy to see that in the limit $M_S \gg M_Z$ the mass of another CP-even state is set by $(\mathcal{M}_h^2)_{44}$, i.e., this state is almost degenerate with the charged Higgs states, while the masses of two other CP-even states are determined by $m_\pm^{\overline{\rm DR}}$,

$$
\left(m_\pm^{\overline{\rm DR}} \right)^2 \approx \frac{1}{2} \left\{ (\mathcal{M}_h^2)_{22} + (\mathcal{M}_h^2)_{33} \pm \sqrt{\left[(\mathcal{M}_h^2)_{22} - (\mathcal{M}_h^2)_{33} \right]^2 + 4(\mathcal{M}_h^2)_{23}^2} \right\} . \tag{6.47}
$$

The mass of the lightest state, on the other hand, is bounded from above by the smallest element $(\mathcal{M}_h^2)_{55}$, i.e., the tree-level lightest CP-even Higgs mass satisfies a

tree-level upper bound similar to that found in the E_6SSM,

$$\left(m_{h_1}^{\overline{\rm DR}}\right)^2 \leq (m_Z^{\overline{\rm DR}})^2 \cos^2 2\beta + \frac{\lambda^2}{2} v^2 \sin^2 2\beta + g_1'^2 v^2 (Q_1 \cos^2\beta + Q_2 \sin^2\beta)^2 \,. \quad (6.48)$$

Consequently $h_1 \approx S_5$ is always light, and for $M_S \gg M_Z$ is SM-like in its interactions. The upper bound on the tree-level Higgs mass is as expected larger than that in the MSSM. However, radiative corrections remain very important for obtaining a physical Higgs mass of 125 GeV.

The above considerations on the particle spectrum, taken together with the rest of the discussion in this chapter, suggest that in addition to being theoretically well motivated, the SE_6SSM also has interesting implications for collider searches and cosmology. The single exact $\tilde{Z}_2^H$ symmetry supersedes the multiple discrete symmetries imposed in the simplest variants of the E_6SSM. When combined with the automatically conserved Z_2^M, this has the interesting consequence that there are two DM candidates in the spectrum. In the EWSB conditions, the presence of additional singlets allows the large $U(1)_N$ D-terms to be cancelled in allowed parts of the parameter space, potentially reducing the associated fine tuning of the EW scale. There is also now a mechanism for the Z' mass to be much heavier than the SUSY scale, implying that the sfermions can be substantially lighter than the Z'. The SE_6SSM therefore addresses several shortcomings of the E_6SSM, while still being an anomaly free, $U(1)_N$ extension of the MSSM as desired.

The tree-level discussion so far also implies that in the regions of the CSE_6SSM parameter space of interest, the mass spectrum is split, with heavy scalars such as the MSSM sfermions having masses that are $O(M_S)$, and light neutralinos and exotic fermions, which can have distinctive collider signatures. The situation concerning DM appears to be rather different to that in the E_6SSM. In the simplest E_6SSM variant, the light inert singlinos that tend to form DM are now ruled out. In the E_6SSM with a Z_2^S symmetry, the possible DM phenomenology is richer [344, 375]; observations can be reproduced with an MSSM-like neutralino that is predominantly bino or Higgsino, a predominantly inert Higgsino, or a state with substantial admixtures of all three, the inert singlinos now being exactly massless. In the SE_6SSM, on the other hand, the latter states are only very light, forming a subdominant hot DM component, while the lightest $Z_2^E = +1$ neutralino is a candidate for cold DM. Therefore in the SE_6SSM, the possible DM scenarios can be similar to those in the MSSM, but with the possibility of discovering additional exotics at the LHC. Even so, the above conclusions have all been arrived at based on simple tree-level arguments. As highlighted in Chapter 4,

it is imperative that radiative corrections be incorporated to properly understand the phenomenology of the model. In particular, the need to reproduce $m_{h_1} = 125.09$ GeV is a tough constraint on parameter space that is only satisfiable when these are included. With this in mind, in the next chapter we study the mass spectrum and DM scenarios in the model when these essential higher order corrections are included, and determine some of the current constraints on, and future prospects for, the CSE$_6$SSM.

Chapter 7

Dark Matter Scenarios in the CSE_6SSM

7.1 Dark Matter in BSM Models

The nature of DM is currently one of the most important and exciting open questions in particle physics. Assuming it to be composed of one or more new particles, it is clear that DM cannot be accounted for by SM particles. It is therefore one of the strongest pieces of evidence for the existence of BSM physics; successfully explaining it is a key test of a BSM theory. In models that attempt to do so, the plethora of experimental observations related to DM can be used to generate additional constraints on the model's parameter space. In addition to its attractive theoretical features, the CSE_6SSM, due to the presence of two discrete symmetries $\tilde{Z}_2^H$ and Z_2^M, contains two stable candidates for DM. The considerations of the previous chapter indicate that one of these, a Z_2^E even neutralino, should be MSSM-like and could potentially account for the observed relic density of DM particles. In this chapter, we examine this interesting possibility and assess the viability of the scenarios found in light of constraints coming from collider searches, cosmological observations, and terrestrial DM direct detection searches. Given that the DM candidates we investigate are MSSM-like, we simultaneously consider the analogous situations in the CMSSM as well, highlighting where the models are similar and which features of the CSE_6SSM would distinguish it from the CMSSM.

Our strategy for doing so is to compute the mass spectrum in the CSE_6SSM and CMSSM, including important radiative corrections, using our extensions to the code `FlexibleSUSY`. The higher order corrections calculated using `FlexibleSUSY` are es-

sential for comparing to results from collider searches. At the same time, the physical masses are also inputs into the calculation of the DM relic density and interaction cross sections. These properties of the DM candidate must then be reliably computed to judge a model's compatibility with the inferred limits from CMB measurements [68–70] and direct detection searches [370–374]. Before explaining our methodology for doing so and presenting the results, it is helpful to first review the basic steps that go into extracting the DM predictions of a BSM model.

7.1.1 Calculation of the Relic Density

In the models considered here, the WIMP DM candidate, χ, is a cold thermal relic, so that it is initially in local thermodynamic equilibrium with other states in the early Universe. As the Universe expands, it is assumed that at a given time the DM candidate goes out of equilibrium as the expansion rate of the Universe exceeds the WIMP interaction rate. After this so-called freeze-out point, the WIMP is decoupled, so that its number density n_χ changes only with the expansion of the Universe [592–596]. The present day abundance is computed by solving a Boltzmann equation that can be written in the form [597–601]

$$\frac{dn_\chi}{dt} + 3Hn_\chi = -\langle\sigma_{\text{eff}}v\rangle\left(n_\chi^2 - n_{\chi,\text{eq.}}^2\right) . \tag{7.1}$$

Here H is the Hubble parameter and $n_{\chi,\text{eq.}}$ is the equilibrium number density. The number density n_χ appearing in Eq. (7.1) is the sum of the number densities [600] of each species i that eventually annihilates into the WIMP DM candidate,

$$n_\chi = \sum_{i=1}^{N} n_i \, , \tag{7.2}$$

with N being the total number of such species. The second term on the left-hand side of Eq. (7.1) corresponds to the dilution of n_χ with the expansion of the Universe, while the right-hand side describes changes in the number density as a result of particle interactions. The thermally averaged effective cross section, $\langle\sigma_{\text{eff}}v\rangle$, contains the essential particle physics inputs that are required to compute the WIMP number density, and must be computed in the context of a given BSM model. In particular, a reliable calculation of $\langle\sigma_{\text{eff}}v\rangle$ must account for cases such as coannihilations involving additional states or resonant annihilations, which can significantly change the predicted cross section [600]. Eq. (7.1) is more conveniently solved by introducing the abundance $Y \equiv n_\chi/s$, where s is the entropy density, and the parameter $x = m_\chi/T$,

where m_χ is the WIMP mass and T the temperature. By using the fact that the entropy per unit comoving volume, sa^3, is constant[1] and that $T \propto a^{-1}$, Eq. (7.1) can then be rewritten in the form (for more detailed reviews of this derivation and the following discussion see, e.g., Refs. [72, 125, 594])

$$\frac{dY}{dx} = -\frac{\langle \sigma_{\text{eff}} v \rangle s}{Hx} \left(Y^2 - Y_{\text{eq.}}^2 \right) . \tag{7.3}$$

The relic density $\Omega = \rho_\chi / \rho_c = n_\chi m_\chi / \rho_c$ of the WIMP is defined as the ratio of the WIMP mass density ρ_χ to the critical density

$$\rho_c = \frac{3H^2}{8\pi G_N} . \tag{7.4}$$

Since $n_\chi = Y(x)s(x)$, the present day relic density, i.e., at $T \to 0$, is given by

$$\Omega h^2 = \frac{m_\chi s_0 h^2}{\rho_c} Y(x \to \infty) , \tag{7.5}$$

where $h = H_0/(100\text{km}\cdot\text{s}^{-1}\cdot\text{Mpc}^{-1}) \approx 0.678$ [70] is the Hubble constant and $s_0 \approx 2.9 \times 10^3$ cm^{-3} is the present day entropy density [594]. The essential step in determining Ωh^2 is therefore obtaining the value of $Y_\infty \equiv Y(x \to \infty)$ for the effective cross section $\langle \sigma_{\text{eff}} v \rangle$ in a given BSM model. In general, Eq. (7.3) must be integrated numerically from $x = 0$ to the present photon temperature, although simple estimates for Ωh^2 can be obtained in the so-called freeze-out approximation [597]. The task of numerically integrating Eq. (7.3) to obtain the predicted relic density in a general BSM model, without using the freeze-out approximation[2] [440], can be carried out using a software tool such as `micrOMEGAs`, when linked to `CalcHEP`. The obtained value $(\Omega h^2)_{\text{th.}}$ can then be compared to the observed value [70],

$$(\Omega h^2)_{\text{exp.}} = 0.1188 \pm 0.0010 , \tag{7.6}$$

to determine if a model parameter point is ruled out; a point leading to a predicted $(\Omega h^2)_{\text{th.}} > (\Omega h^2)_{\text{exp.}}$ would overclose the Universe, assuming the standard cosmological history, and thus is ruled out. Points for which the predicted relic density does not

[1] Here $a \equiv a(t)$ is the scale factor appearing in the Friedmann-Lemaître-Robertson-Walker metric; the Hubble parameter is given by $H(t) = \dot{a}/a$, where an overdot indicates differentiation with respect to universal time t.

[2] Actually, `micrOMEGAs` also provides a version of the calculation that uses this approximation as well, so it can be used if desired, but this is not the default method.

exceed the value in Eq. (7.6) are not ruled out in the same way, though in this case additional contributions to DM are required.

7.1.2 Direct Detection of Dark Matter

In addition to the relic density constraint, terrestrial direct detection searches for DM also place significant restrictions on possible DM candidates. Direct detection searches, which are based on detecting the recoil of nuclei after interacting with an incident WIMP [602], place limits on the interaction cross section of a WIMP with nuclei. The reported limits arise from comparing the observed number of signal events to the average number expected for a given WIMP candidate. This can be calculated by integrating the differential recoil rate per unit detector mass, which for a neutralino DM candidate can be written (this is reviewed in Refs. [125, 603, 604])

$$\frac{dR}{dE} = \frac{1}{2m_\chi m_r^2}\sigma(q)\rho_{\chi,\text{local}}\eta\left(v_{\min}(E), t\right) , \tag{7.7}$$

where E is the nuclear recoil energy, m_r is the reduced mass of the WIMP and nucleus, and the function η describes the (time-dependent) WIMP velocity distribution, with $v_{\min}$ being the minimum WIMP velocity yielding a recoil energy of E. The differential rate also depends on the local DM density $\rho_{\chi,\text{local}}$ and an effective scattering cross section,

$$\sigma(q) = \sigma_{SI/SD}F^2_{SI/SD}(q) , \tag{7.8}$$

where q is the momentum transfer, $\sigma_{SI/SD}$ is the scattering cross section in the limit of zero momentum transfer, and $F^2_{SI/SD}(q)$ is a form factor accounting for the spatial structure of the nucleus [605]. The subscripts SI and SD indicate that the corresponding WIMP-nucleus interaction is spin-independent or spin-dependent, respectively; in direct detection experiments the former is usually more relevant [604], for which reason we focus on it in the remainder of this chapter. Nevertheless, it should be noted that limits, e.g., those in Refs. [606, 607], can also be put on SD interactions as well and can be an additional constraint on models of DM.

The SI cross section σ_{SI} can be written in the form [604]

$$\sigma_{SI} = \frac{4}{\pi}m_r^2\left[Zf_p + (A-Z)f_n\right]^2 , \tag{7.9}$$

where Z is the atomic number and A is the mass number of the nucleus, and the coefficients f_p and f_n describe the effective WIMP-nucleon couplings for the proton

and neutron, respectively. It is commonly assumed that the effective couplings are not isospin violating, $f_p \approx f_n$, so that the WIMP-nucleon cross sections σ^p_{SI}, σ^n_{SI}, are approximately equal [608]. This is usually a reasonable assumption for neutralino DM candidates, though in some scenarios isospin violating effects can be relevant [609]. Assuming this to be the case, the WIMP-nucleus scattering cross section can be written

$$\sigma_{SI} \approx \frac{m_r^2 (m_p + m_\chi)^2}{m_p^2 m_\chi^2} A^2 \sigma^p_{SI} \,, \tag{7.10}$$

where the SI scattering cross section for a single proton reads

$$\sigma^p_{SI} = \frac{4 m_p^2 m_\chi^2}{\pi (m_p + m_\chi)^2} f_p^2 \,. \tag{7.11}$$

Here m_p is the proton mass, and the effective coupling f_p is given by [610]

$$\frac{f_p}{m_p} = \sum_{q=u,d,s} f^p_{Tq} C_q + \frac{2}{27} f^p_{TQ} \sum_{q=c,b,t} C_q \,, \tag{7.12}$$

where for a nucleon $N = p$ or n,

$$m_N f^N_{Tq} = \langle N | m_q(Q) \bar{q} q | N \rangle \,, \quad f^N_{TQ} = 1 - \sum_{q=u,d,s} f^N_{Tq} \,, \tag{7.13}$$

and C_q is the Wilson coefficient for the operator $m_q(Q) \bar{\chi} \chi \bar{q} q$ with running quark mass $m_q(Q)$ [609]. In the following we take the nucleon scalar couplings to have the values[3] $f^N_{Tu} \approx 0.0153$, $f^N_{Td} \approx 0.0191$ and $f^N_{Ts} \approx 0.0447$.

The calculation of the effective SI scattering cross section for a particular model therefore requires deriving the effective coupling of χ to quarks. Given a BSM model, nowadays this can be done efficiently by codes such as `micrOMEGAs`. To convert a limit on the number of signal events in a detector into one on the SI WIMP-nucleon cross section, it is also necessary to assume values for the other factors contributing to Eq. (7.7). Limits such as those presented by the LUX collaboration [374] are based on a local DM density

$$\rho_{\chi,\text{local}} = 0.3 \text{ GeV} \cdot \text{cm}^{-3} \,, \tag{7.14}$$

[3]The values of these hadronic matrix elements are the default values used in `micrOMEGAs`-4.1.8, as determined in Ref. [444] from lattice results. A review of some recent determinations of the required sigma terms $\sigma_{\pi N}$ and σ_s has been given in Ref. [611], while an extraction of these quantities from phenomenological inputs using chiral effective field theory has been presented in Refs. [612, 613].

and a Maxwellian velocity distribution for DM, which allows the calculation of $\eta(v_{\min}(E), t)$. The values of these quantities are variously inferred from astrophysical measurements, such as stellar kinematics in the Milky Way, and numerical simulations of galaxy evolution. However, there are often substantial uncertainties in these astrophysical inputs (for reviews of their determination and the associated uncertainties, see, e.g., Ref. [614]). Modifying any of these assumptions can have a non-trivial impact on direct detection limits [615, 616].

A particularly simple example is when the proposed DM candidate only accounts for a small fraction of the total DM density, that is, when $(\Omega h^2)_{\text{th.}} < (\Omega h^2)_{\text{exp.}}$. In this case, it would be expected that the local density of the WIMP will be lower than that in Eq. (7.14), implying a reduced signal event rate. This in turn means that larger scattering cross sections can be consistent with the experimental data, weakening the obtained limit on σ^p_{SI}. A simple estimate of how much weaker the limit is can be made by rescaling the experimental limit by the fraction of the total DM density accounted for by the particular WIMP candidate. That is, as a rough guide a point can be considered to be consistent with direct detection limits provided that the predicted scattering cross section σ^p_{SI} satisfies

$$(\Omega h^2)_{\text{th.}} \sigma^p_{SI} \leq (\Omega h^2)_{\text{exp.}} \sigma^{p,\text{LUX}}_{SI}(m_\chi)\,, \tag{7.15}$$

where $\sigma^{p,\text{LUX}}_{SI}(m_\chi)$ is the experimental limit, here taken to be that from LUX, at the WIMP mass m_χ. The use of the scaled limit, Eq. (7.15), can dramatically alter the allowed parameter space regions in a model, as we find below, and should therefore be kept in mind when interpreting direct detection limits.

7.2 Scanning the CSE$_6$SSM Parameter Space

We now proceed to investigate the mass spectra and possible DM candidates in the CSE$_6$SSM suggested by the tree-level considerations presented in Chapter 6, calculating the DM observables described above and comparing to limits from the LHC. To study scenarios that are able to account for the observed relic DM density with a MSSM-like DM candidate, a dedicated CSE$_6$SSM spectrum generator was created[4] using `FlexibleSUSY`-1.1.0 and `SARAH`-4.5.6. As explained in Chapter 4, this approach provides a precise determination of the mass spectrum by making use of the full two-loop RGEs and one-loop self-energies for all of the masses. The accurate inclusion

[4]All of the code used for the analysis presented in this chapter is available at `https://doi.org/10.5281/zenodo.215628`.

of the most significant radiative corrections is particularly important for the determination of the Higgs mass, given the strong constraints arising from the precise experimental measurement [28]. For a set of fields that mix after EWSB to form mass eigenstates, the tree-level mass matrix is corrected by a matrix of self-energies. Thus, in principle the five physical Higgs masses can be determined from the poles in the propagator after including these self-energies by solving

$$\det\left[p_i^2\mathbf{1} - \mathcal{M}_h^2(M_S) + \Sigma_h(p_i^2)\right] = 0 \tag{7.16}$$

with $m_{h_i}^2 = \mathrm{Re}(p_i^2)$ and where $\mathcal{M}_h^2(M_S)$ is the tree-level Higgs mass matrix, Eq. (6.46), evaluated here at M_S, and $\Sigma_h(p^2)$ denotes the self-energies. The general one-loop contributions to the self-energies for the CP-even Higgs states, as well as all other states in the spectrum, are automatically included in the mass spectrum calculated using `FlexibleSUSY`. For the calculation of the CP-odd and CP-even Higgs mass, the leading two-loop contributions from the known NMSSM [617] and MSSM [618–622] expressions were initially also included[5], since the additional contributions from new states are expected to be small by virtue of the small exotic Yukawa couplings considered, as discussed in Section 6.4.2.

However, for large values of $M_S \gg M_Z$ this strategy leads to large logarithmic contributions to the Higgs masses due to heavy states, which should be resummed to get an accurate estimate for the Higgs mass. The discussion in Section 6.4 indicates that the SUSY spectrum in the CSE$_6$SSM is split, containing many heavy scalars, notably the MSSM sfermions and the exotic scalars, as well as light neutralinos and exotic fermions. Such a situation is well handled by an effective field theory (EFT) approach to calculate the lightest Higgs mass, in which the large logarithms are resummed. In the MSSM, the largest of these contributions is usually associated with the third generation sfermions, and in particular the stops. In the SE$_6$SSM, there are also contributions from the heavy exotic scalars that should be accounted for. Because the exotic Yukawa couplings $\tilde{\lambda}_{\alpha\beta}$ and κ_{ij} are very small in the models we consider, these logarithmic corrections to the Higgs mass are very small and can be neglected compared to the contributions from the stops and other MSSM sfermions[6]. In our study of the CSE$_6$SSM parameter space, to obtain the light CP-even Higgs mass we therefore make use of the known EFT calculation in the MSSM, which includes the

[5] At the time that this work was done, `FlexibleSUSY` did not have the capability to automatically include the general two-loop corrections calculated by `SARAH`.

[6] The contributions from the exotic states to Eq. (7.16) were explicitly confirmed to be numerically negligible compared to those from the stops and sbottoms.

dominant contributions to the Higgs mass. While a complete EFT calculation including the exotic states would be more accurate[7], in this case the accuracy of our calculation is not expected to be significantly reduced, due to the small size of the exotic contributions.

To apply this MSSM EFT calculation to the CSE$_6$SSM, at the SUSY scale defined by $M_S = \sqrt{m^{\overline{\rm DR}}_{\tilde{t}_1} m^{\overline{\rm DR}}_{\tilde{t}_2}}$, a simple tree-level matching to the MSSM is performed. In this simple matching procedure, the $\overline{\rm DR}$ MSSM soft scalar masses $m^2_{Q_{ii}}$, $m^2_{u^c_{ii}}$, $m^2_{d^c_{ii}}$, $m^2_{L_{ii}}$, $m^2_{e^c_{ii}}$, gaugino masses M_1, M_2, M_3 and soft trilinear $A_t \equiv T^U_{33}/y^U_{33}$ are set at M_S to their values obtained in the CSE$_6$SSM after running from M_X. The MSSM μ parameter is set to its effective value at M_S, Eq. (6.21), while an effective MSSM pseudoscalar mass, $(m_A)_{\rm eff}$, is obtained from the effective soft bilinear

$$(B\mu)_{\rm eff} = \frac{T_\lambda s}{\sqrt{2}} \cos\theta - \frac{\lambda\sigma}{2} s\varphi \sin\theta \,. \tag{7.17}$$

The physical lightest CP-even Higgs mass is then calculated using `SUSYHD`-1.0.2 [624] to obtain a more accurate estimate for the SM-like Higgs mass. The remaining heavy CP-even Higgs masses are computed using the ordinary fixed order approach, Eq. (7.16).

The nature of the DM candidate in the CSE$_6$SSM varies throughout the parameter space, which we scan to examine some of the possible scenarios. The parameters determining the masses and compositions of the MSSM-like DM candidates are $\tan\beta$, $M_{1/2}$ and $\mu_{\rm eff}$. To study this state, it is most convenient to vary the parameters $M_{1/2}$ and $\mu_{\rm eff}$, as the latter controls the Higgsino masses and therefore choosing $M_{1/2}$ and $\mu_{\rm eff}$ permits the composition of the lightest neutralino to be directly chosen. To avoid considering parts of the parameter space that lead to incorrect EWSB, a subset of the other free parameters are fixed using the EWSB conditions, Eq. (6.10). Since the CSE$_6$SSM is a constrained model, it is well suited for applying the semi-analytic algorithm described in Chapter 4. In this case, the semi-analytic solutions allow the parameters at the SUSY scale to be expanded directly in terms of the fundamental parameters at the GUT scale M_X. This allows the EWSB conditions to fix high-scale parameters directly. In this case, upon substituting the semi-analytic solutions for the soft Higgs mass $m^2_{H_d}$, $m^2_{H_u}$, m^2_S, $m^2_{S'}$ and m^2_ϕ, the universal scalar mass m_0 can be fixed using Eq. (6.10). The `FlexibleSUSY`-generated CSE$_6$SSM spectrum generator was modified to make use of a prototype version of the semi-analytic BVP solver to achieve this. Four additional parameters can be fixed using the remaining EWSB

[7]Such a calculation was indeed made available [623] shortly after the numerical work presented here was completed.

conditions. To maintain consistency with the Z' limits, it is desirable to control $m_{Z'}^{\overline{\rm DR}}$ directly by using s as a free parameter. The VEVs s_1, s_2 are then fixed by using an EWSB condition to determine $\tan\theta$. The remaining three EWSB conditions allow to fix φ, as well as the values of $\Lambda_F(M_X)$ and $\Lambda_S(M_X)$. To take advantage of the mechanism Eq. (6.15) to obtain $M_{Z'} \gg M_S$, the coupling σ is kept as a free input parameter. For sufficiently small values of σ, it is expected that the solutions for Λ_F, Λ_S will be large, and the physical minimum will lie close to the D-flat direction discussed in Section 6.3. The EWSB conditions are solved including the full one-loop corrections to the effective potential, Eq. (2.39) with exotic contributions, and the leading two-loop corrections from the NMSSM and MSSM mentioned previously.

After fixing the parameters m_0, $\tan\theta$, φ, $\Lambda_F(M_X)$ and $\Lambda_S(M_X)$, the remaining parameters listed after Eq. (6.4) are still free, up to the constraint of requiring a viable mass spectrum. To satisfy the limits on the Z' mass, we choose $M_{Z'}$ well above the current limits, putting $M_{Z'} \approx 240$ TeV. This requires a very large value of $s = 650$ TeV at the SUSY scale. Acceptably small values of $\mu_{\rm eff} \lesssim 1$ TeV, yielding an MSSM-like Higgsino that could reproduce the DM relic density, are then achieved for very small $|\lambda|$, though $\mu_{\rm eff}$ is still large enough to evade limits from LEP. In this study of the CSE$_6$SSM we focus on scenarios in which the LSP is either a mixed bino-Higgsino or pure Higgsino DM candidate. To do so, we considered $|\lambda(M_X)| = 9.15181 \times 10^{-4}$ and $|\lambda(M_X)| = 2.4 \times 10^{-3}$, for both $\lambda < 0$ and $\lambda > 0$. Because $\tan\theta \approx 1$ for such large values of s, this corresponds to $|\mu_{\rm eff}(M_X)| \approx 347$ GeV and $|\mu_{\rm eff}(M_X)| \approx 898$ GeV, giving values at the SUSY scale of $|\mu_{\rm eff}(M_S)| \approx 417$ GeV and $|\mu_{\rm eff}(M_S)| \approx 1046$ GeV, respectively[8].

Per the discussion in Section 6.4.2, to prevent tachyonic states in the exotic sector, the exotic couplings cannot be too large; for our scans we chose fixed values satisfying $\tilde{\lambda}_{\alpha\beta}(M_X)$, $\kappa_{ij}(M_X) \leq 3 \times 10^{-3}$. Additionally, to simplify our analysis we took these couplings to be family universal with $\tilde{\lambda}_{\alpha\beta}(M_X) = \tilde{\lambda}_0\delta_{\alpha\beta}$ and $\kappa_{ij}(M_X) = \kappa_0\delta_{ij}$. A SUSY scale somewhat below $M_{Z'}$ was obtained by choosing small $\sigma(M_X) = 2 \times 10^{-2}$. Light inert singlinos in the spectrum were ensured by choosing extremely small values for the couplings $\tilde{f}_{i\alpha}$ and $f_{i\alpha}$, while for simplicity we set the couplings $\tilde{\sigma}(M_X)$, $\mu_\phi(M_X)$, $g_{ij}^D(M_X)$ and $h_{i\alpha}^E(M_X)$ to zero. It should be stressed that the impact of the latter

[8] The values of $|\mu_{\rm eff}|$ given are the mean values over all of the obtained valid solutions presented in the following sections. The exact values of $|\mu_{\rm eff}(M_S)|$ and $|\mu_{\rm eff}(M_X)|$ vary over the parameter space scanned, since $\tan\theta$ varies slightly over the scanned region, as it is an EWSB output parameter, and the RG evolution also changes slightly due to sparticle threshold corrections. For the smaller value of $|\lambda(M_X)|$, the solutions we present have 409 GeV $\leq |\mu_{\rm eff}(M_S)| \leq$ 425 GeV, and 344 GeV $\leq |\mu_{\rm eff}(M_X)| \leq$ 349 GeV. For the larger $|\lambda(M_X)|$ value we obtain solutions with 1032 GeV $\leq |\mu_{\rm eff}(M_S)| \leq$ 1063 GeV, and 892 GeV $\leq |\mu_{\rm eff}(M_X)| \leq$ 903 GeV.

two sets of couplings on the quantities we investigate is numerically negligible. We have checked that their values could also be increased to satisfy constraints on the exotic lifetimes without altering our results. We also chose $\kappa_\phi(M_X) = 10^{-2}$, and $\mu_L(M_X) = 10$ TeV. While the above fixed couplings impact the mass spectrum, they do not play a significant role in the predictions for DM, for the scenarios considered here in which the DM candidate is the lightest MSSM-like neutralino, and hence we do not scan over them. The high-scale boundary condition for the CSE$_6$SSM, at which these parameter settings hold, is applied at the GUT scale, which is defined by the condition $g_1(M_X) = g_2(M_X)$. This condition is solved iteratively, as described in Ref. [428]. Since gauge coupling unification still occurs in the SE$_6$SSM, Eq. (3.12) is also found to hold at the solution for M_X.

For $\lambda \ll \bar{g}$, the tree-level upper bound on the SM-like Higgs mass is maximised for large $\tan\beta$. We take here $\tan\beta(M_Z) = 10$ to saturate this limit. In both the CMSSM and the CSE$_6$SSM, the transformation $M_{1/2} \to -M_{1/2}$, $A_0 \to -A_0$, $B_0 \to -B_0$ and $\mu_{\text{eff}} \to -\mu_{\text{eff}}$ leaves our results invariant. We use this symmetry to fix $M_{1/2} \geq 0$. Setting $B_0 = 0$, we scanned over $M_{1/2}$ and A_0 by uniformly sampling in the intervals [0 TeV, 20 TeV] and [−20 TeV, 20 TeV], respectively, to find solutions with the correct Higgs mass and an allowed DM relic density. The relic density and direct detection cross section were calculated numerically with `micrOMEGAs`-4.1.8, using `CalcHEP` model files automatically generated with `SARAH`. The values of the CSE$_6$SSM parameters used are summarised in Table 7.1.

For this choice of parameters the lightest neutralino is expected to be MSSM-like in its composition and couplings. At the same time, the spectrum and the RG flow of couplings in the CSE$_6$SSM is very different to that in the CMSSM. While the two models may in this limit make very similar predictions concerning DM, the ranges of parameter space in which this occurs and their collider signatures can therefore be quite distinct. This makes it interesting to compare the CSE$_6$SSM and CMSSM directly. To do this comparison, we also generated a CMSSM spectrum generator using `FlexibleSUSY` and `SARAH` as described above, and modified it to make use of the semi-analytic BVP algorithm. Conventionally in the CMSSM, the EWSB conditions, Eq. (2.31), are used to fix μ and $B\mu$, but this is inconvenient for studying the neutralino sector. Using the freedom provided by the use of the semi-analytic RGE solutions, here the MSSM EWSB conditions are used to fix m_0 and B_0 at the GUT scale, and $M_{1/2}$ and A_0 were scanned over the same ranges as in the CSE$_6$SSM. This was done for values of $\mu(M_S)$ fixed to the mean values obtained in the CSE$_6$SSM, that is, $|\mu(M_S)| = 417$ GeV and $|\mu(M_S)| = 1046$ GeV, respectively. The same fixed value of $\tan\beta(M_Z) = 10$

	$\lambda(M_X) = \pm 9.15181 \times 10^{-4}$	$\lambda(M_X) = \pm 2.4 \times 10^{-3}$
$\sigma(M_X)$	2×10^{-2}	2×10^{-2}
$\kappa_\phi(M_X)$	10^{-2}	10^{-2}
$\tilde{\lambda}_{\alpha\beta}(M_X) = \tilde{\lambda}_0 \delta_{\alpha\beta}$	10^{-3}	3×10^{-3}
$\kappa_{ij}(M_X) = \kappa_0 \delta_{ij}$	10^{-3}	1.4×10^{-3}, 3×10^{-3}
$\tilde{f}_{11}(M_X)$, $\tilde{f}_{22}(M_X)$, $\tilde{f}_{31}(M_X)$	10^{-7}	10^{-7}
$f_{11}(M_X)$, $f_{22}(M_X)$, $f_{32}(M_X)$	10^{-7}	10^{-7}
$\mu_L(M_X)$ [TeV]	10	10
$s(M_S)$ [TeV]	650	650
$M_{1/2}$ [TeV]	$[0, 20]$	$[0, 20]$
A_0 [TeV]	$[-20, 20]$	$[-20, 20]$
$\tan\beta(M_Z)$	10	10

Table 7.1: Summary of the fixed parameter values and allowed ranges used in the CSE$_6$SSM for the two values of $|\lambda(M_X)|$ considered. The free parameters $\tilde{\sigma}(M_X)$, $\mu_\phi(M_X)$, B_0, $g^D_{ij}(M_X)$, $h^E_{i\alpha}(M_X)$ and the $\tilde{f}_{i\alpha}(M_X)$, $f_{i\alpha}(M_X)$ not shown are set to zero in both cases. The parameters m_0, $\tan\theta$, φ, Λ_F and Λ_S are fixed by the requirement of correct EWSB. In the CMSSM, the same ranges are taken for $M_{1/2}$ and A_0 for the comparison scans with $\mu(M_S) = \pm 417$ GeV and $\mu(M_S) = \pm 1046$ GeV, and we set $\tan\beta(M_Z) = 10$ as well. The EWSB conditions are used to fix m_0 and B_0 in the CMSSM.

was used. In this way we are able to present a more direct comparison of the two models, in which analogous parameters are approximately matched between the two[9]. The CMSSM solutions that we obtained have a heavy SUSY scale as well, so that we again used `SUSYHD` to compute the lightest Higgs mass. The predicted DM relic density and direct detection cross section were calculated in `micrOMEGAs` using model files generated by `SARAH`[10].

In both models, valid points were selected by imposing the theoretical constraints that the point should have a valid spectrum with correct EWSB and no tachyonic states. We required that all couplings remain perturbative up to the GUT scale. Since we perform only a naïve matching to the MSSM in the EFT calculation, we allowed for an uncertainty of ± 3 GeV in the result for m_{h_1}, which is somewhat larger than is reported by `SUSYHD`. For the CSE$_6$SSM we accepted points with calculated light Higgs masses satisfying 122 GeV $\leq m_{h_1} \leq$ 128 GeV, and for comparison we

[9]We emphasise that our approach in the CMSSM differs from the conventional approach in the literature, in which μ would be determined by the EWSB conditions and m_0 is an input parameter.

[10]The results obtained this way are in very good agreement with those found from using the MSSM implementation already available in `micrOMEGAs`, provided some care is taken to define the quark mass parameters that implicitly enter into Eq. (7.12) consistently.

allowed the same range of Higgs masses in the CMSSM. As noted following Eq. (7.6), points with $(\Omega h^2)_{\text{th.}} > (\Omega h^2)_{\text{exp.}}$ are ruled out, and we exclude them from the valid points presented below. On the other hand, if the relic density bound is not saturated the point is still considered to be valid.

To make a clear comparison of the impact of collider bounds on the CSE$_6$SSM and CMSSM, model specific limits should be applied to each. However in the CSE$_6$SSM the RGEs drive the sfermions to masses which are substantially larger than the gaugino masses, creating a hierarchical spectrum that persists even with the decoupling of the Z' mass from the rest of the spectrum. This means that typically LHC collider limits come from the gaugino sector, especially the gluino which is produced through strong interactions. The gluino decays in an MSSM-like manner and as a result the gluino mass limit set in the CMSSM in the heavy sfermion limit should, to a reasonable approximation, apply to the gluino in the CSE$_6$SSM also[11]. To show where current and future collider limits constrain the models, we prefer to show explicit gluino mass contours in each model, along with contours for the physical first generation squark mass, $m_{\tilde{u}_6}$. Note that this is approximately degenerate with the other first and second generation squark masses as well, i.e., $m_{\tilde{q}_{1,2}} \approx m_{\tilde{u}_6}$.

7.3 Mixed Bino-Higgsino Dark Matter

Using the above framework for scanning the CMSSM and CSE$_6$SSM, we explore parts of the parameter space in both models containing a viable neutralino DM candidate at or below the TeV scale. We first consider cases with a light Higgsino mass term of $|\mu_{(\text{eff})}(M_S)| \approx 417$ GeV. The results obtained in the two models for this value of $|\mu_{(\text{eff})}|$ are compared in Figure 7.1 and Figure 7.2.

In the top row of Figure 7.1 we compare the mass of the SM-like Higgs in the two models. In both we find solutions consistent with $m_{h_1} \approx 125$ GeV, but the allowed regions in the $M_{1/2} - m_0$ plane clearly differ quite substantially. For such large values of s and small values of λ the tree-level mass of the lightest CP-even Higgs in the SE$_6$SSM is approximately the same as it is in the MSSM, $(m_{h_1}^{\overline{\text{DR}}})^2 \approx (m_Z^{\overline{\text{DR}}})^2 \cos^2 2\beta$, as follows from approximately diagonalising the mass matrix in Eq. (6.46). Without substantial tree-level contributions from the additional F- and D-terms, a 125 GeV Higgs is achieved with large radiative corrections in the CSE$_6$SSM as well as in the

[11] A more thorough treatment involves reinterpreting existing searches, for which a variety of tools, such as `CheckMATE` [625], `MadAnalysis` [626], `SModelS` [627] or `Fastlim` [628] are available. Since the situation is fairly simple in this case, with very heavy sfermions, we consider this unnecessary here and beyond the scope of the current analysis.

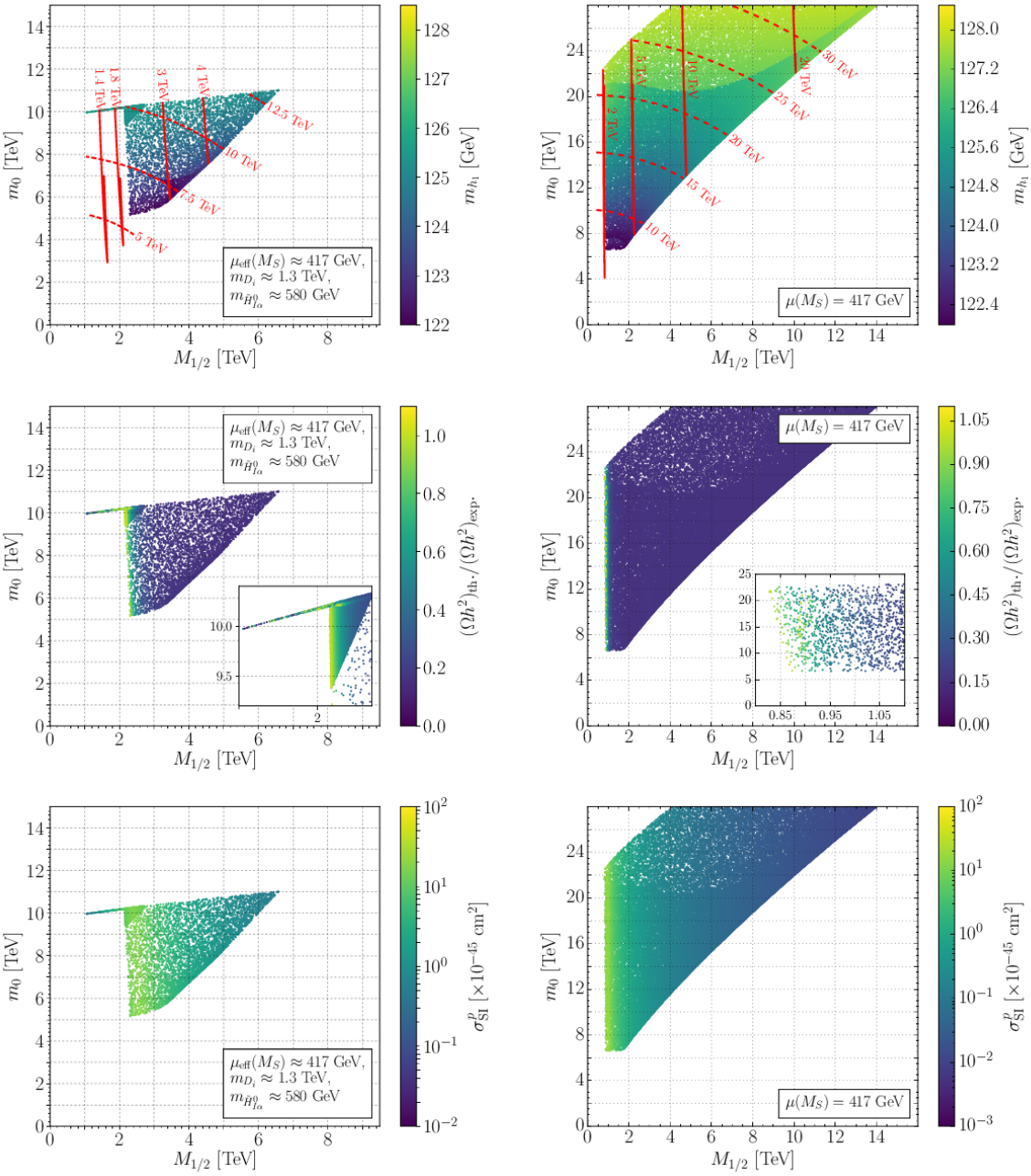

Figure 7.1: Contour plots in the $M_{1/2} - m_0$ plane of the lightest CP-even Higgs mass (top row), DM relic density (middle row) and proton SI cross section (bottom row) in the CSE$_6$SSM with $\mu_{\text{eff}}(M_X) \approx 347$ GeV (left column) and CMSSM with $\mu(M_S) = 417$ GeV (right column). In the top row, we also show contours of the gluino (solid lines) and squark (dashed lines) masses. At large values of $M_{1/2}$, where $\tilde{\chi}^0_1$ is a light Higgsino, the relic density saturates with $(\Omega h^2)_{\text{th.}}/(\Omega h^2)_{\text{exp.}} \approx 0.15$.

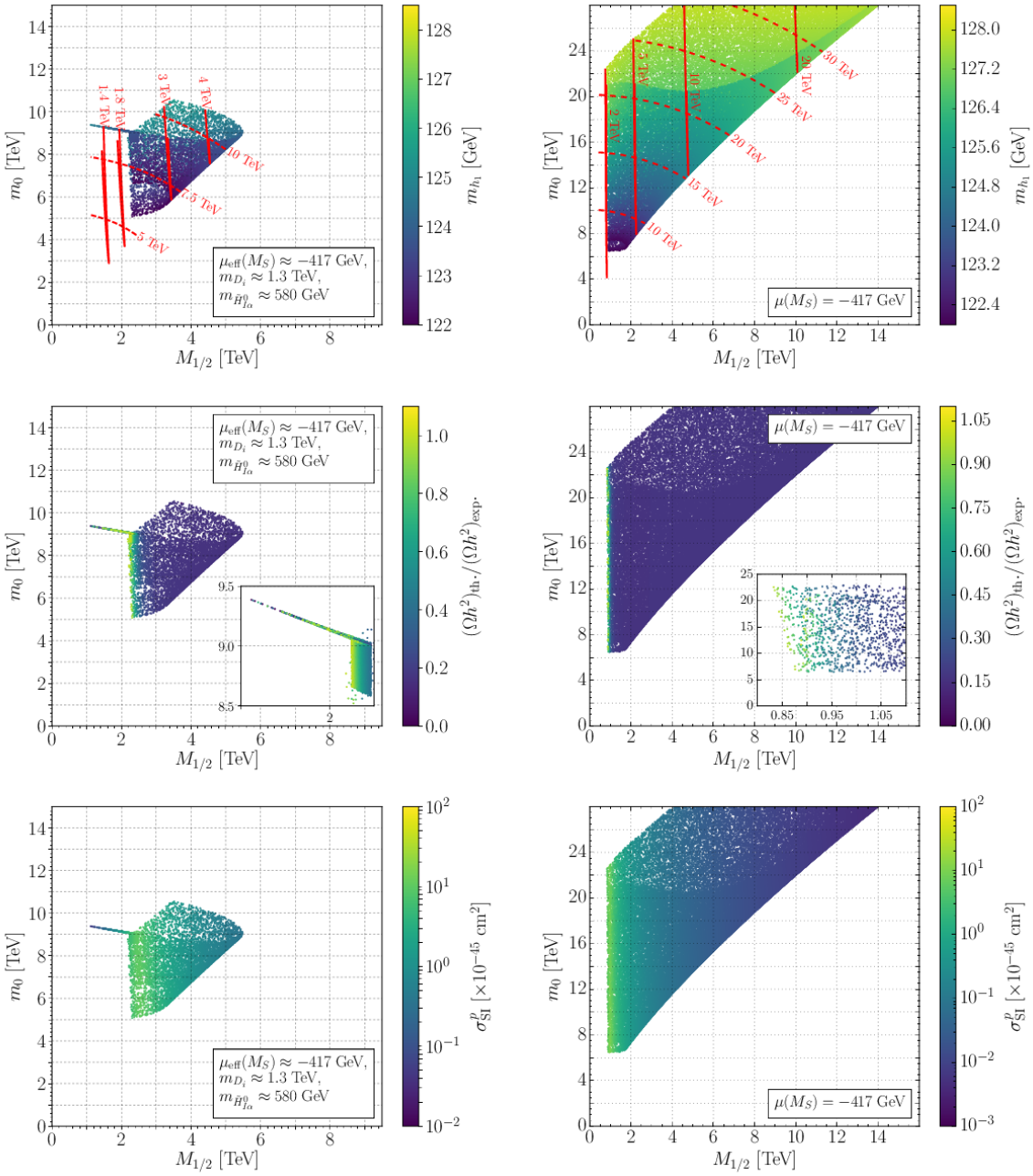

Figure 7.2: Contour plots in the $M_{1/2} - m_0$ plane of the lightest CP-even Higgs mass (top row), DM relic density (middle row) and proton SI cross section (bottom row) in the CSE$_6$SSM with $\mu_{\text{eff}}(M_X) \approx -347$ GeV (left column) and CMSSM with $\mu(M_S) = -417$ GeV (right column). In the top row, we show contours of the gluino (solid lines) and squark (dashed lines) masses. As for the positive μ_{eff} case, at large $M_{1/2}$ the relic density reaches a limiting value of $(\Omega h^2)_{\text{th.}}/(\Omega h^2)_{\text{exp.}} \approx 0.15$.

CMSSM. In principle, these would result from either large sparticle masses, particularly stop masses, or large stop mixing. However, increasing A_0 or $M_{1/2}$ to generate large mixings for fixed $\mu_{(\text{eff})}$ leads to the value of m_0 increasing as needed to satisfy the EWSB conditions. As a result in the solutions we obtain $m_0 > A_0, M_{1/2}$ and large enough radiative corrections must arise from sufficiently heavy sparticle masses instead. The effect of the Higgs mass constraint can be clearly seen in the top row of Figure 7.1 and Figure 7.2, where the requirement $m_{h_1} \geq 122$ GeV imposes the lower bound on m_0 for small values of $M_{1/2}$.

The right-most boundary of the solution region is a consequence of determining m_0^2 from the EWSB conditions. When the soft masses and SUSY scale are large and $|\mu_{(\text{eff})}| \ll M_{1/2}$, as is the case here, the resulting function for $m_0^2(M_{1/2}, A_0)$, defined implicitly by the EWSB conditions, has a minimum at each $M_{1/2}$ with $m^2_{0,\text{min}}(M_{1/2}) > 0$. For example, at tree-level and neglecting small D-term contributions the EWSB conditions lead to an expression of the form $m_0^2 = \xi_1 M_{1/2}^2 + \xi_2 M_{1/2} A_0 + \xi_3 A_0^2 + \xi_0 |\mu_{(\text{eff})}|^2$ where the coefficients $\xi_1, \xi_3 > 0$ and $\xi_0, \xi_2 < 0$ for $\tan\beta = 10$ are set by the RG flow. Because it is found that $\xi_1 - \xi_2^2/(4\xi_3) > 0$, for fixed $|\mu_{(\text{eff})}| \ll M_{1/2}$ there is a non-trivial lower bound on the value of m_0^2. Hence when $\mu_{(\text{eff})}$ is fixed, we do not find points with values of m_0 below this boundary for each given value of $M_{1/2}$. This can be contrasted with the usual procedure in the CMSSM, where lower values of m_0^2 can be found by varying $|\mu|$ and $B\mu$ to compensate.

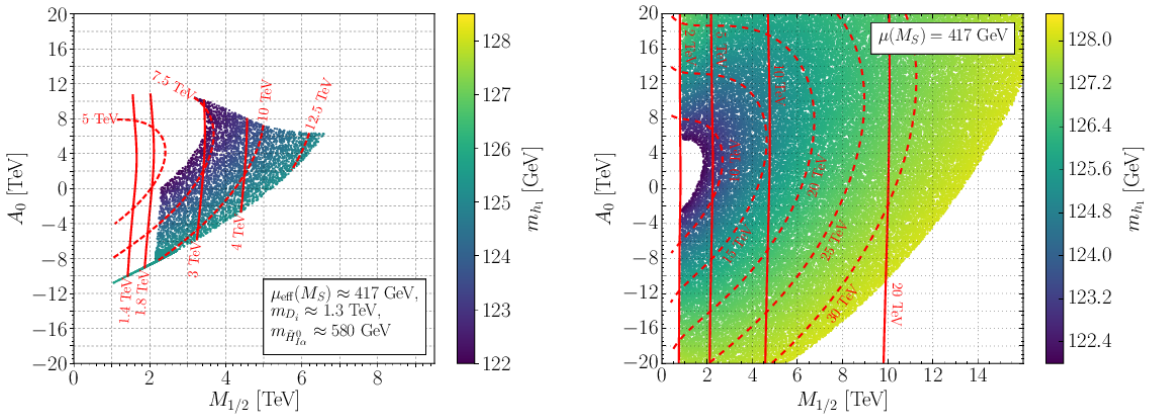

Figure 7.3: Contour plots of the lightest CP-even Higgs mass in the $M_{1/2} - A_0$ plane in the CSE$_6$SSM with $\mu_{\text{eff}}(M_X) \approx 347$ GeV (left) and the CMSSM with $\mu(M_S) = 417$ GeV (right). Also shown are contours of the gluino (solid lines) and squark (dashed lines) masses for both models.

In the CMSSM, the Higgs mass constraint $m_{h_1} \leq 128$ GeV also puts an upper bound on the possible values of $M_{1/2}$. This is shown in Figure 7.3, where we plot

m_{h_1} in the $M_{1/2} - A_0$ plane in both models for $\mu_{(\text{eff})} > 0$. The upper bound on m_{h_1} cuts off the solution region at large values of $M_{1/2}$ in Figure 7.3 in the CMSSM. In comparison, in the CSE$_6$SSM the region at large $M_{1/2}$ is ruled out by the presence of tachyonic states. The lower right region of the CSE$_6$SSM $M_{1/2} - A_0$ plane in Figure 7.3 is excluded by tachyonic pseudoscalars A_i, while the uppermost boundary is due to tachyonic CP-even Higgs states. This corresponds to the much more restrictive upper bound on m_0 in the CSE$_6$SSM in Figure 7.1 compared to the CMSSM. The same is true for $\mu_{(\text{eff})} < 0$ in Figure 7.2, though the position of the boundary is modified, leading to the much smaller range of acceptable m_0 values in the CSE$_6$SSM for this value of $|\mu_{\text{eff}}|$. It should be noted, however, that these results are obtained for a single value of s. It is expected that if s and λ are allowed to vary while maintaining fixed μ_{eff}, additional solutions would be obtained, as is found in the CE$_6$SSM [363, 378]. It is important to emphasise that in the CSE$_6$SSM there is still additional parameter space available, and that the constraints shown here apply only for a single value of $M_{Z'}$ in the model.

The large values of m_0 required result in a large SUSY scale and all scalars except the SM-like Higgs h_1, and the lightest pseudoscalar A_1 in the CSE$_6$SSM, are very heavy. In the top row of Figure 7.1 and Figure 7.2 we show contours of the gluino and first and second generation squark masses. The viable solutions that we find in the CSE$_6$SSM all have squark masses $m_{\tilde{q}_{1,2}} \geq 5.4$ TeV, while in our CMSSM solutions $m_{\tilde{q}_{1,2}} \geq 6.5$ TeV. While much lighter than $M_{Z'}$, these states are not observable at the LHC. On the other hand, the small exotic couplings lead to light exotic fermions. For $|\mu_{\text{eff}}(M_X)| \approx 347$ GeV, the choice of $\kappa_0 = 10^{-3}$ leads to exotic D fermion masses of ≈ 1.3 TeV. Similarly, setting $\tilde{\lambda}_0 = 10^{-3}$ leads to inert Higgsinos with masses ≈ 580 GeV. Both sets of states are therefore light enough to be produced at the LHC and would be detectable via the signatures discussed in Section 6.4.2. Given the increasingly large SUSY scale required by LHC searches in constrained models, this makes searches targeting the exotic spin-1/2 leptoquark and inert Higgsino states attractive for still being able to probe the CSE$_6$SSM parameter space. Because the exotic couplings cannot be too large in the scenarios considered here, improved limits on these states would strongly constrain the solutions we have found with very small values of $|\mu_{\text{eff}}|$.

In addition to the restriction on the allowed values of m_0, there is also a lower bound on $M_{1/2}$ in both models, which is determined by the relic density constraint. The behaviour in the CMSSM in this case is well understood. When M_1 is sufficiently large, $\tilde{\chi}_1^0$ is a nearly pure, light Higgsino that is underabundant [629]. The opposite limit, with small $M_{1/2}$ and $M_1 \lesssim \mu$, leads to an almost pure bino LSP that is overabundant,

due to its small annihilation cross section. Therefore requiring $\Omega h^2 \leq 0.1188$ amounts to placing a lower bound on $M_{1/2}$ for fixed μ.

Since $\mu_{(\text{eff})}$ is small in this case, an acceptable relic density is achieved with relatively low values of $M_{1/2}$. The minimal allowed value of $M_{1/2}$ in the CMSSM, $M_{1/2} \approx 0.85$ TeV, leads to $M_1 \approx \mu$ and the LSP is a so-called "well-tempered" highly mixed bino-Higgsino state [588] that saturates the relic density. This region is evident in the middle rows of Figure 7.1 and Figure 7.2 as an extremely narrow strip at the minimum value of $M_{1/2}$ (shown in greater detail in the insets) where $(\Omega h^2)_{\text{th.}} \approx 0.1188$, while for larger $M_{1/2}$ the Higgsino DM candidate leads to $(\Omega h^2)_{\text{th.}} \ll 0.1188$. From comparing the left and right panels in the middle rows of Figure 7.1 and Figure 7.2 it is clear that similar behaviour occurs for the $Z_2^E = +1$ DM candidate in the CSE$_6$SSM. From Eq. (6.27) and Eq. (6.28) it follows that the necessary value of M_1 occurs for smaller values of $M_{1/2}$ in the CMSSM.

The low allowed values of $M_{1/2}$ imply that in the light $\mu_{(\text{eff})}$ scenario the gluino as well as the ordinary neutralino and chargino states can be light. Though the location of the well-tempered strip in the $M_{1/2} - m_0$ plane differs in the two models, the masses of the gluino, neutralino and charginos are still rather similar. For example, in both models in this strip $m_{\tilde{\chi}_1^0} \approx 370$ GeV. In the CMSSM, we find that $m_{\tilde{g}} \gtrsim 2.1$ TeV, the minimum value occurring in the well-tempered region. A very similar result can be seen in the CSE$_6$SSM, with $m_{\tilde{g}} \gtrsim 2$ TeV except for a narrow line of solutions where the gluino can be as light as $m_{\tilde{g}} \approx 1$ TeV.

For these solutions, the bino DM candidate is viable due to the A-funnel mechanism. In the CMSSM, m_A is only light enough so that $m_A \approx 2m_{\tilde{\chi}_1^0}$ at large $\tan\beta \gtrsim 50$ [590]. Because we only considered $\tan\beta(M_Z) = 10$ in our scans, $m_A > 6$ TeV is always very heavy in our CMSSM results and the A-funnel region is not accessible. In the CSE$_6$SSM, for a given value of $\tan\beta$ and $M_{1/2}$ one can make $m_{A_1} \approx 2m_{\tilde{\chi}_1^0}$ light by fine tuning A_0 appropriately. This corresponds to the lower boundary of the solution region in Figure 7.3. Therefore even for $\tan\beta(M_Z) = 10$ light bino DM can satisfy the relic density constraint in the CSE$_6$SSM. This does, however, imply a substantial fine tuning; in our scans, additional points were sampled from this region to overcome this.

In either the bulk or A-funnel regions, the gluino is thus observable at run II or at the high luminosity LHC (HL-LHC); indeed, gluino masses under 2 TeV are already rather close to the limits based on the most recent $\sqrt{s} = 13$ TeV data [630–633] and so LHC searches will soon be probing this part of the parameter space. Similarly, both models also predict light neutralinos and charginos with masses of a

few hundred GeV. To be precise, our CMSSM solutions satisfy 366 GeV $\leq m_{\tilde{\chi}_1^0} \leq$ 452 GeV, 428 GeV $\leq m_{\tilde{\chi}_2^0} \leq$ 453 GeV and 419 GeV $\leq m_{\tilde{\chi}_1^\pm} \leq$ 453 GeV, while in the CSE$_6$SSM the ranges are 182 GeV $\leq m_{\tilde{\chi}_1^0} \leq$ 426 GeV, 335 GeV $\leq m_{\tilde{\chi}_2^0} \leq$ 438 GeV, and 335 GeV $\leq m_{\tilde{\chi}_1^\pm} \leq$ 431 GeV. This suggests the neutralinos and charginos could also be discoverable at the HL-LHC [634] in the small $\mu_{(\text{eff})}$ case. The overall picture for the solutions presented with $|\mu(M_S)| \approx 417$ GeV is of a split spectrum, with unobservably heavy scalars but light exotic fermions and electroweak-inos, as well as a sufficiently light gluino. This scenario would therefore predict interesting collider phenomenology in tandem with accounting for the observed DM relic density.

However, while small values of $\mu_{(\text{eff})}$ permit the neutralinos and gluino to be observable at the LHC, models with a highly mixed bino-Higgsino DM candidate are strongly constrained by null results from direct detection experiments. In the bottom rows of Figure 7.1 and Figure 7.2 we show the $\tilde{\chi}_1^0$-proton SI cross section, given by Eq. (7.11), for each sign of $\mu_{(\text{eff})}$. In the region where $(\Omega h^2)_{\text{th.}}$ matches the observed value, the direct detection cross section peaks at $\sim 10^{-45} - 10^{-44}$ cm^2 and is above the 90% exclusion limits set by LUX [373, 374]. In both the CSE$_6$SSM and CMSSM, the SI cross section in this part of the parameter space is dominated by t-channel exchange of the lightest CP-even Higgs h_1. Keeping only the leading contribution to the Wilson coefficients C_q in Eq. (7.12), the SI part of the $\tilde{\chi}_1^0$-nucleon cross section takes the form [367]

$$\sigma_{SI}^p = \frac{4 m_{\tilde{\chi}_1^0}^2 m_p^4}{\pi v^2 m_{h_1}^4 (m_{\tilde{\chi}_1^0} + m_p)^2} |g_{h_1 \chi_1 \chi_1} F^p|^2 \,, \tag{7.18}$$

where

$$F^p = \sum_{q=u,d,s} f_{Tq}^p + \frac{2}{27} \sum_{Q=c,b,t} f_{TQ}^p \,, \tag{7.19}$$

with f_{Tq}^p, f_{TQ}^p defined as in Eq. (7.13). The size of the cross section in Eq. (7.18) is set by the $h_1\, \tilde{\chi}_1^0\, \tilde{\chi}_1^0$ coupling $g_{h_1 \chi_1 \chi_1}$, which is given by

$$g_{h_1 \chi_1 \chi_1} = \frac{1}{2} \left(\sqrt{\frac{3}{5}} g_1 N_{14} - g_2 N_{13} \right) \left[N_{11} (U_h)_{11} - N_{12} (U_h)_{12} \right] \,, \tag{7.20}$$

where the neutralino mixing matrix elements N_{ij} are defined in Eq. (6.22) and the Higgs mixing matrix U_h is defined by Eq. (6.44). In the CSE$_6$SSM, the contributions to this coupling involving the singlet mixing components N_{1j}, $j = 5, 6, 7, 8$, are negligible in our case and have been ignored in Eq. (7.20). In the highly mixed case with

$|\mu| \approx M_1$ and $N_{13} \lesssim N_{14}$, the products $N_{11}N_{14}$ and $N_{12}N_{14}$ that appear above are large and the SI cross section is enhanced [609]. Therefore points with a mixed bino-Higgsino DM candidate that saturates the relic abundance are excluded, for both[12] signs of $\mu_{(\text{eff})}$. As $M_{1/2}$ is increased (decreased) so that $\tilde{\chi}_1^0$ has a smaller (larger) bino component, the SI cross section decreases as $N_{14} \to 0$ ($N_{11}, N_{12} \to 0$). Additionally, the reduction in Ωh^2 for larger values of $M_{1/2}$ implies a reduction in the local number density of WIMPs and thereby weakens the limits from direct detection, as estimated from Eq. (7.15). Thus points away from the well-tempered strip may still avoid the direct detection limits. In the CSE$_6$SSM, the presence of the A-funnel region also allows for solutions with $(\Omega h^2)_{\text{th.}} \approx (\Omega h^2)_{\text{exp.}}$ and a predicted SI cross section below current limits for $\lambda < 0$. Nevertheless, as discussed below future limits are expected to probe a substantial portion of the remaining parameter space. Therefore scenarios with small $\mu_{(\text{eff})}$ and a mixed bino-Higgsino $\tilde{\chi}_1^0$ are very tightly constrained.

7.4 Pure Higgsino Dark Matter

This situation can be compared with the case when the DM candidate is a heavy, almost pure Higgsino. These scenarios are less constrained by direct detection limits due to both the weaker limits at high WIMP masses and the suppression of the SI scattering cross section for a pure Higgsino LSP [635]. Analyses of the CMSSM parameter space that also account for limits from collider searches suggest that this part of the parameter space is favoured by experimental constraints [636], though scenarios with a relatively light LSP can still fit the data [637]. To see that this is also true in the CSE$_6$SSM, in Figure 7.4 and Figure 7.5 we compare the CSE$_6$SSM with $|\mu_{\text{eff}}(M_S)| \approx 1046$ GeV to the CMSSM with $|\mu(M_S)| = 1046$ GeV.

As in the previous case with small $\mu_{(\text{eff})}$, the region in which we find solutions in the CSE$_6$SSM is much smaller than in the CMSSM. The upper bound on m_0 again arises from tachyonic CP-even and CP-odd Higgs states that occur as $|A_0|$ is increased. At the same time, the minimum value of $M_{1/2}$ that satisfies the relic density constraint is much larger. This is because a relic density consistent with Eq. (7.6) requires $\tilde{\chi}_1^0$ to be nearly purely Higgsino with $m_{\tilde{\chi}_1^0} \approx 1$ TeV, which is achieved for $|M_1| \gtrsim |\mu_{(\text{eff})}| \approx 1$ TeV. The condition of universal gaugino masses at M_X then means that the gluino is now very heavy along with the sfermions. In the CSE$_6$SSM we find solutions with

[12]For $\mu_{(\text{eff})} < 0$ the SI cross section is slightly smaller, due to a cancellation between the contributions from the up- and down-type Higgsinos, but this is not significant enough to evade the current limits.

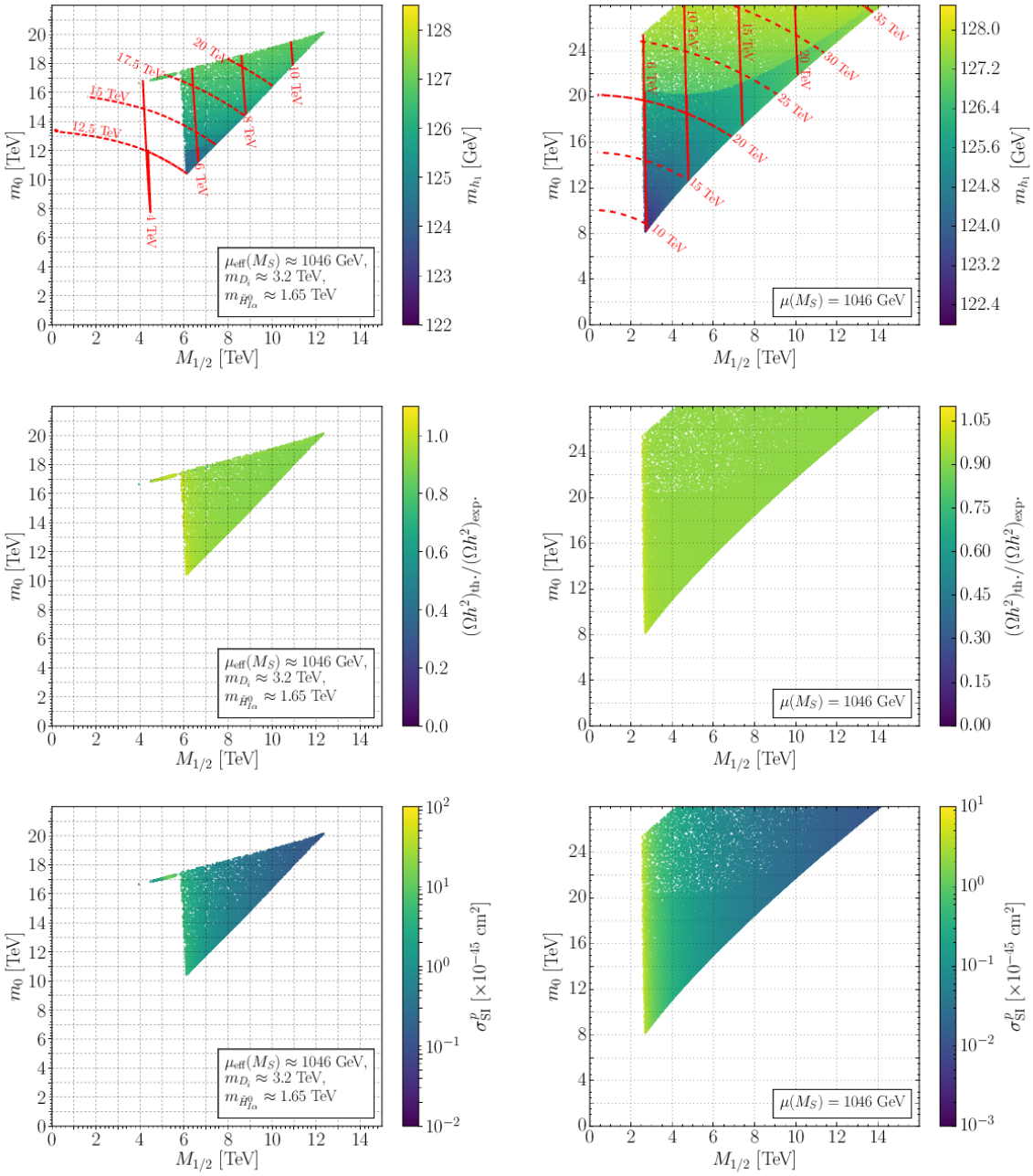

Figure 7.4: Contour plots in the $M_{1/2} - m_0$ plane of the lightest CP-even Higgs mass (top row), DM relic density (middle row) and proton SI cross section (bottom row) in the CSE$_6$SSM with $\mu_{\text{eff}}(M_X) \approx 898$ GeV (left column) and CMSSM with $\mu(M_S) = 1046$ GeV (right column). In the top row, we show contours of the gluino (solid lines) and squark (dashed lines) masses.

$m_{\tilde{g}} \geq 3.8$ TeV, compared to the minimum value of $m_{\tilde{g}} \geq 5.7$ TeV in the CMSSM scan.

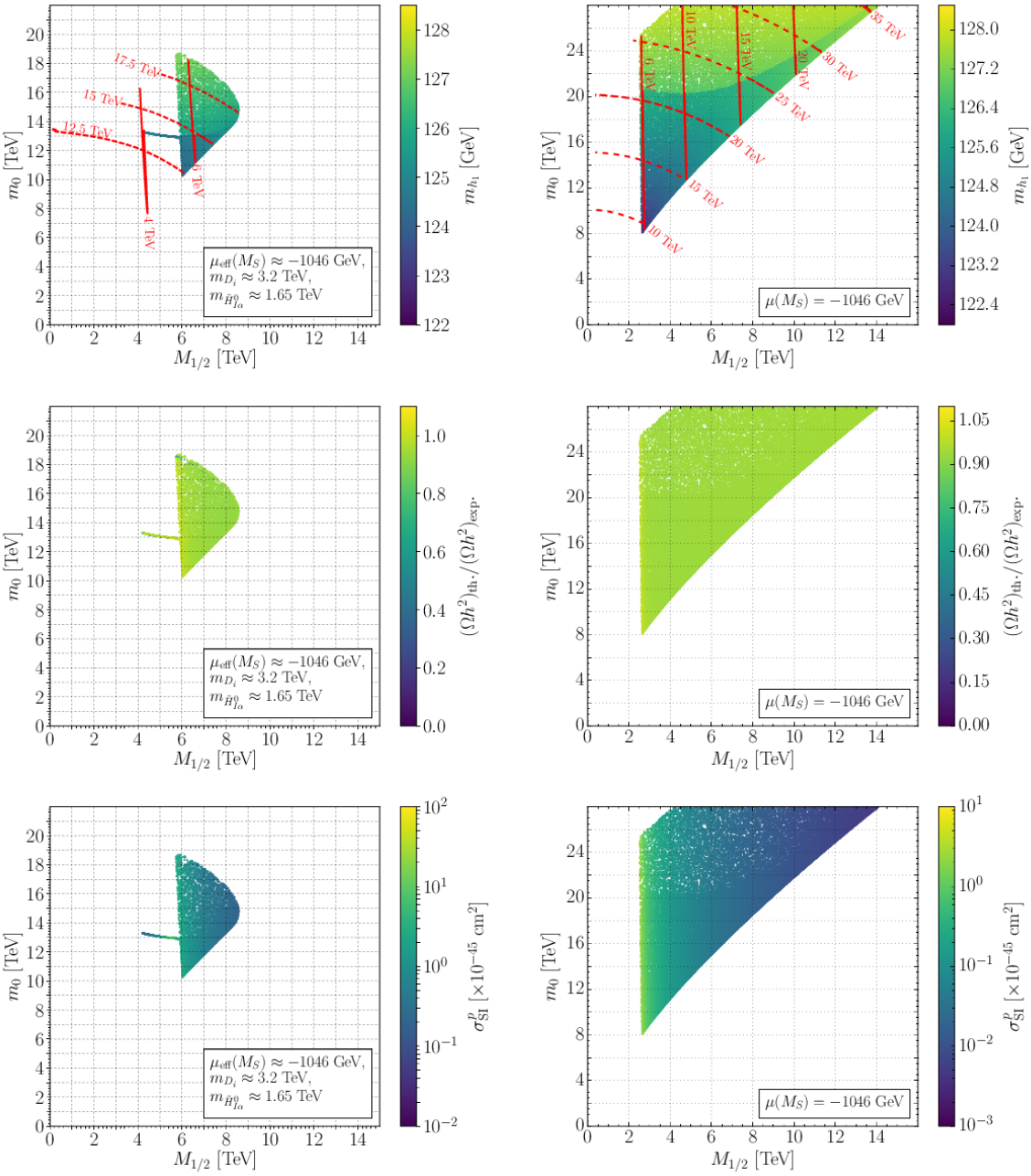

Figure 7.5: Contour plots in the $M_{1/2} - m_0$ plane of the lightest CP-even Higgs mass (top row), DM relic density (middle row) and proton SI cross section (bottom row) in the CSE$_6$SSM with $\mu_{\text{eff}}(M_X) \approx -898$ GeV (left column) and CMSSM with $\mu(M_S) = -1046$ GeV (right column). In the top row, we show contours of the gluino (solid lines) and squark (dashed lines) masses.

The prospects for an LHC discovery in this scenario are fairly poor in the CMSSM, as the gluino and all sfermions would be out of reach at run II.

For the CSE$_6$SSM points shown in Figure 7.4 and Figure 7.5 we considered slightly larger exotic couplings with $\kappa_0 = \tilde{\lambda}_0 = 3 \times 10^{-3}$. The couplings are required to be large enough to ensure that $\tilde{\chi}_1^0$ is still the stable second DM candidate, rather than one of the exotic sector possibilities. The exotic fermions are correspondingly heavier, with masses satisfying 3 TeV $\leq m_{D_i} \leq$ 3.3 TeV and 1.63 TeV $\leq m_{\tilde{H}^0_{I\alpha}} \leq$ 1.67 TeV, which also makes them unlikely to be observable at run II or at the HL-LHC. Note however that, in addition to being able to vary $M_{Z'}$, there is also some freedom to vary the exotic couplings to obtain lighter exotic states. We illustrate this in Figure 7.6, where we plot the valid solutions with $\kappa_0 = 1.4 \times 10^{-3}$, giving D fermion masses of $m_{D_i} \in [1.5 \text{ TeV}, 1.6 \text{ TeV}]$, comparable with the potential exclusion reach for third generation squarks at the HL-LHC [638]. For fixed $|\lambda(M_X)| = 2.4 \times 10^{-3}$ the effect of this is to slightly increase the minimum allowed value of $M_{1/2}$ outside of the A-funnel region. This is due to an increase in the calculated $(\Omega h^2)_{\text{th.}}$, which was already rather close to the value from Planck observations. The larger value of the relic density in turn arises because of the increase in $\mu_{\text{eff}}(M_S)$ that results for smaller values of κ_0 in the RG running; this can be seen, for example, from Eq. (D.17). A compensating small reduction in $\lambda(M_X)$ can be used to maintain the low-energy value of μ_{eff} and therefore $(\Omega h^2)_{\text{th.}}$, in which case the smaller values of $M_{1/2}$ shown in Figure 7.4 and Figure 7.5 continue to be allowed. The presence of light exotics is an important possible signature that allows the model to be discovered when the SUSY breaking scale is very heavy, as well as distinguishing the E_6 inspired model from the CMSSM.

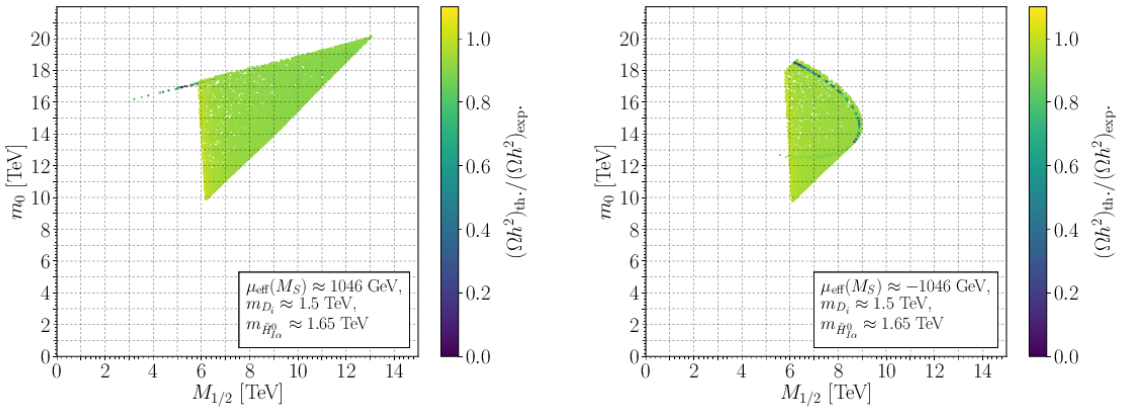

Figure 7.6: Contour plots in the $M_{1/2} - m_0$ plane of the DM relic density in the CSE$_6$SSM with $\mu_{\text{eff}}(M_S) \approx 1046$ GeV (left) and $\mu_{\text{eff}}(M_S) \approx -1046$ GeV (right), with reduced values of the exotic Yukawa couplings $\kappa_{ij}(M_X)$ such that $m_{D_i} \approx 1.5$ TeV.

As can be seen in the middle rows of Figure 7.4 and Figure 7.5, and in Figure 7.6, the prediction for the relic density in the CSE$_6$SSM remains similar to that in the CMSSM. In both models a Higgsino with a mass of approximately 1 TeV saturates the observed value in Eq. (7.6). The narrow A-funnel region at lower $M_{1/2}$ is again accessible in the CSE$_6$SSM by tuning A_0 to reduce m_{A_1}. As large mixings are no longer required to reproduce the relic density for $|\mu_{(\text{eff})}| \approx 1$ TeV, a large fraction of the solutions found have a predicted SI cross section below the current LUX limits. Points in both models with $M_{1/2}$ where the LSP transitions from being pure bino to pure Higgsino, i.e., where $M_1 \approx \mu_{(\text{eff})}$ near the lower bound on $M_{1/2}$, present a larger cross section that is in excess of the LUX limits. Therefore even for heavy $\mu_{(\text{eff})}$ in the CMSSM and CSE$_6$SSM constraints can be put on the parameter space by direct detection searches. At larger $M_{1/2}$ (that is, where M_1 is significantly larger than $\mu_{(\text{eff})}$) the models currently evade the SI direct detection limits, and are very unlikely to be probed by direct collider searches in the near future if the exotic fermions in the CSE$_6$SSM are not light. However, this part of the CSE$_6$SSM, and CMSSM, parameter space will be constrained by results from XENON1T.

7.5 Benchmark Scenarios

Before considering the impact on the CSE$_6$SSM parameter space coming from the current set of constraints and the projected impacts of limits from XENON1T, we present a set of benchmark points as specific examples illustrating the above scenarios. In Table 7.2 we show the model parameters defining six benchmark points along with the predicted mass spectra. The points labelled BM1, BM2, and BM3 have a $Z_2^E = +1$ DM candidate that is a mixed bino-Higgsino state, while the remaining benchmarks have a pure Higgsino DM candidate. All of the benchmarks reproduce the observed SM-like Higgs mass, within theoretical errors.

In all of the benchmarks, the sfermions are rather heavy due to the large values of m_0 required to reproduce the 125 GeV Higgs mass. The prospects for observing any of these states at the LHC are therefore poor. Small values of the exotic Yukawa couplings permit the exotic fermions to be light, making these states much more promising as discovery channels for all of the benchmarks. For example, BM1 has exotic leptoquarks with masses well below current limits on the gluino and should be easily discoverable at run II of the LHC. For BM2, BM3, BM4 and BM6, the exotic quarks are slightly heavier but should still be quite comfortably within the reach of the LHC run II. The fact that the exotic couplings are not tightly constrained by DM

	BM 1	**BM 2**	**BM 3**	**BM 4**	**BM 5**	**BM 6**
$\lambda(M_X)$	0.0009152	0.0009886	0.0007052	0.002295	0.00047	0.0005
$\tilde{\lambda}_{11,22}(M_X)$	0.001	0.0013	0.0012	0.003	0.0016	0.0012
$\kappa_{11,22,33}(M_X)$	0.001	0.0013	0.0012	0.00135	0.0016	0.0012
$M_{1/2}$ [GeV]	2227.79	2407.79	1617.79	5800.98	1900.00	2017.79
m_0 [GeV]	9586.46	9494.22	8800.16	$1.084 \cdot 10^4$	7396.89	7410.12
A_0 [GeV]	−7281.96	−6481.96	−7541.96	2129.63	−4600.00	−4441.96
$1 - \tan\theta$	$1.5 \cdot 10^{-6}$	$1.9 \cdot 10^{-6}$	$2.4 \cdot 10^{-6}$	$9.4 \cdot 10^{-7}$	$5.3 \cdot 10^{-6}$	$2.7 \cdot 10^{-6}$
φ [TeV]	−1633	−1493	−1737	−708	−1713	−1621
$\Lambda_F^{1/2}$ [TeV]	127	120	131	108	139	133
$\Lambda_S^{1/3}$ [TeV]	98	91	102	61	101	96
$m_{\tilde{q}_{1,2}}$ [GeV]	9400	9400	8500	12500	7300	7350
$m_{\tilde{l}}$ [GeV]	9500	9400	8700	11000	7330	7350
$m_{\tilde{b}_1}$ [GeV]	7577	7616	6759	10801	5927	5992
$m_{\tilde{b}_2}$ [GeV]	9361	9364	8438	12411	7287	7345
$m_{\tilde{t}_1}$ [GeV]	5476	5550	4802	8582	4326	4396
$m_{\tilde{t}_2}$ [GeV]	7580	7619	6762	10803	5931	5995
$m_{H^\pm} \approx m_{A_2} \approx m_{h_3}$ [GeV]	9381	9312	8576	11056	7245	7266
m_{A_1} [GeV]	5193	6605	2723	9978	931	3650
m_{A_3} [GeV]	42896	39797	44939	25797	43985	41946
m_{h_1} [GeV]	125.22	125.04	124.96	125.04	124.04	124.10
m_{h_2} [GeV]	8208	8289	7985	8048	7072	7195
m_{h_4} [GeV]	38770	36136	40469	24529	39664	37913
$M_{Z'} \approx m_{h_5}$ [GeV]	$2.4 \cdot 10^5$	$2.4 \cdot 10^5$	$2.4 \cdot 10^5$	$2.4 \cdot 10^5$	$2.4 \cdot 10^5$	$2.4 \cdot 10^5$
$m_{\tilde{D}_{i1}}$ [GeV]	8523	8430	7016	12308	4520	5562
$m_{\tilde{D}_{i2}}$ [GeV]	10376	10516	9966	12662	9698	9062
m_{D_i} [GeV]	1243	1575	1499	1540	1943	1489
$m_{H^\pm_{I\alpha_1}}$ [GeV]	8938	8762	7862	10433	5799	6309
$m_{H^\pm_{I\alpha_2}}$ [GeV]	10056	10091	9490	11986	8696	8328
$m_{H_{I\alpha_1}}$ [GeV]	13406	13332	12935	14251	12123	12189
$m_{H_{I\alpha_2}}$ [GeV]	17161	17113	16944	17584	16560	16494
$m_{\tilde{H}^\pm_{I\alpha}} \approx m_{\tilde{H}^0_{I\alpha_{1,2}}}$ [GeV]	580	750	700	1663	929	699
$m_{S_{Ii}}$ [GeV]	25593	25516	25663	24875	25583	25567
$m_{L^\pm_{4_1}}$ [GeV]	17580	17468	17355	17512	16663	16657
$m_{L^\pm_{4_2}}$ [GeV]	18465	18422	18021	19611	17470	17513
$m_{L^0_{4_1}}$ [GeV]	19994	19886	19870	19671	19345	19336
$m_{L^0_{4_2}}$ [GeV]	20771	20724	20449	21557	20039	20072
$m_{\tilde{L}^\pm_4} \approx m_{\tilde{L}^0_{4_{1,2}}}$ [GeV]	15358	15314	15439	14955	15436	15447

Table 7.2: Parameters for the benchmark points BM1–BM6 and the resulting sparticle masses. Those parameters not shown here are set equal to the values used in the scans of the CSE$_6$SSM parameter space. For brevity, we show an approximate mass $m_{\tilde{q}_{1,2}}$ for the first and second generation up- and down-type squarks. The exact masses of all four states are within ±100 GeV of this value. Similarly, $m_{\tilde{l}}$ represents an approximate mass for all sleptons, with the exact masses all lying within ±150 GeV of the given value.

limits does, however, mean that the exotic states can also be heavier, and potentially more difficult to observe at the LHC. BM5 is an example of this scenario, having leptoquarks that are heavier than in the other benchmarks that may be challenging to find with 300 fb^{-1} of integrated luminosity. Even so, they are still light enough for a discovery to be possible at the LHC. As noted in Section 6.4.2, the pair production of these states would be expected to lead to an enhancement in $p\,p \to t\,\bar{t}\,\tau^+\,\tau^- + E_t^{miss} + X$ and $p\,p \to b\,\bar{b}\,\tau^+\,\tau^- + E_T^{miss} + X$. The potential for discovering the model through the decays of these states means that dedicated studies on these exotic states would be extremely valuable.

Although the sfermions are rather heavy, in all benchmark points other than BM4 the MSSM-like neutralinos and charginos are also light in addition to the exotic states. The neutralino and chargino masses are shown in Table 7.3. While these are weakly interacting states, they are very light, so it is reasonable to expect some discovery potential, in particular from the production of a neutralino-chargino pair, which leads to an enhancement of $pp \to lll + E_T^{miss} + X$. The branching ratios for the processes $\tilde{\chi}_2^0 \to \tilde{\chi}_1^0 l\bar{l}$ and $\tilde{\chi}_1^\pm \to \tilde{\chi}_1^0 l\nu_l$, obtained using the generated `CalcHEP` model files, are shown in Table 7.3. For the scenarios considered here, the process $\tilde{\chi}_2^0 \to \tilde{\chi}_1^0 l\bar{l}$ proceeds almost entirely through diagrams involving a virtual Z, with diagrams involving a virtual Higgs being a negligible contribution due to the small mass splitting between $m_{\tilde{\chi}_2^0}$ and $m_{\tilde{\chi}_1^0}$ and the small Higgs couplings to leptons and quarks[13]. Therefore the discovery prospects are expected to be rather similar to those in the WZ-mediated scenario of Ref. [634].

The relic density and direct detection limits allow much stronger constraints to be placed on the gaugino sector more generally. The composition of the lightest neutralino, the relic density along with a breakdown of the various contributions to the annihilation cross section and the SI and SD cross sections are also given in Table 7.3. Since the inert singlinos are almost massless and their contribution to the total relic density is negligible, the total relic density shown is that due to the lightest neutralino.

Benchmarks with a light, mixed bino-Higgsino candidate, lying in the low $M_{1/2}$ regions of Figure 7.1 and Figure 7.2, have the largest SI cross sections due to the large mixings. These points, namely BM1, BM2, and BM3, are already experiencing significant tension with the current set of LUX limits, and would be discovered almost immediately at XENON1T. An advantage of achieving the relic density with a light DM candidate is that $M_{1/2}$ can be much smaller, so that the gluino may be within reach of the LHC as well. If this is the case, gluino pair production would lead to

[13]Note that the decay of $\tilde{\chi}_2^0$ into $\tilde{\chi}_1^0 + t\bar{t}$ is not kinematically allowed.

	BM 1	**BM 2**	**BM 3**	**BM 4**	**BM 5**	**BM 6**
$m_{\tilde{g}}$ [GeV]	2099	2256	1541	5230	1716	1839
$m_{\tilde{\chi}_1^\pm}$ [GeV]	422	454	320	1034	216	231
$m_{\tilde{\chi}_2^\pm} \approx m_{\tilde{\chi}_4^0}$ [GeV]	780	845	570	2129	645	682
$m_{\tilde{\chi}_1^0}$ [GeV]	375	409	264	1024	204	219
$m_{\tilde{\chi}_2^0}$ [GeV]	433	464	338	1038	226	241
$m_{\tilde{\chi}_3^0}$ [GeV]	445	479	338	1159	336	358
$m_{\tilde{\chi}_5^0}$ [GeV]	25394	23602	26745	14546	26437	25249
$m_{\tilde{\chi}_6^0}$ [GeV]	29853	27651	31546	16364	31173	29737
$m_{\tilde{\chi}_7^0}$ [GeV]	231028	232102	230097	238639	230406	231254
$m_{\tilde{\chi}_8^0}$ [GeV]	258656	257259	259681	249541	259532	258784
$\lvert(Z_N)_{14}\rvert^2$	0.6318	0.6075	0.7210	0.0691	0.0679	0.0624
$\lvert(Z_N)_{13}\rvert^2$	0.0081	0.0075	0.0106	0.0028	0.0180	0.0165
$\lvert(Z_N)_{11}\rvert^2 + \lvert(Z_N)_{12}\rvert^2$	0.3601	0.3850	0.2685	0.9281	0.9141	0.9211
BR($\tilde{\chi}_1^- \to \tilde{\chi}_1^0 l \bar{\nu}_l$)	0.2220	0.2220	0.2220	0.2280	0.2260	0.2260
BR($\tilde{\chi}_2^0 \to \tilde{\chi}_1^0 l \bar{l}$)	0.0689	0.0689	0.0684	0.0733	0.0670	0.0674
Ωh^2	0.1188	0.1185	0.1187	0.1184	0.01055	0.009626
σ_{SI}^p [$\times 10^{-45}$ cm^2]	5.88	6.14	4.84	2.35	4.67	4.32
σ_{SD}^p [$\times 10^{-41}$ cm^2]	6.4	5.58	10.0	0.3529	15.8	12.8
σ_{SI}^n [$\times 10^{-45}$ cm^2]	5.97	6.24	4.91	2.39	4.75	4.39
σ_{SD}^n [$\times 10^{-41}$ cm^2]	4.9	4.27	7.66	0.2699	12.1	9.78
$\tilde{\chi}_1^0\tilde{\chi}_1^0 \to t\bar{t}$ (%)	44.9	39.0	60.0	0.6	0.5	3.3
$\tilde{\chi}_1^0\tilde{\chi}_1^0 \to W^+W^-$ (%)	20.6	19.4	21.6	5.0	27.9	22.0
$\tilde{\chi}_1^0\tilde{\chi}_1^0 \to ZZ$ (%)	13.2	12.8	11.4	3.9	18.4	14.1
$\tilde{\chi}_1^0\tilde{\chi}_1^0 \to Zh_1$ (%)	2.9	2.7	2.9	0.7	0.0	1.7
$\tilde{\chi}_1^0\tilde{\chi}_1^0 \to h_1h_1$ (%)	0.5	0.4	0.9	0.02	0.1	0.1
$\tilde{\chi}_1^0\tilde{\chi}_1^- \to W^-Z$ (%)	0.8	1.1	0.2	1.4	0.2	1.4
$\tilde{\chi}_1^0\tilde{\chi}_1^- \to W^-h_1$ (%)	1.3	1.6	0.3	1.5	2.7	2.6
$\tilde{\chi}_1^+\tilde{\chi}_1^- \to W^+W^-$ (%)	0.1	0.1	$2 \cdot 10^{-3}$	1.9	0.5	0.7
$\tilde{\chi}_1^0\tilde{\chi}_1^- \to \gamma W^-$ (%)	0.6	0.8	0.1	1.4	1.5	1.5
$\tilde{\chi}_1^0\tilde{\chi}_1^- \to d_i\bar{u}_i$ (%)	8.8	12.0	1.6	25.7	29.4	30.0
$\tilde{\chi}_1^0\tilde{\chi}_1^- \to l_i^-\bar{\nu}_{l_i}$ (%)	2.7	3.8	0.5	8.8	10.7	10.8
$\tilde{\chi}_2^0\tilde{\chi}_1^- \to d_i\bar{u}_i$ (%)	0.2	0.4	$3 \cdot 10^{-3}$	12.0	0.7	1.2
$\tilde{\chi}_1^0\tilde{\chi}_2^0 \to d_i\bar{d}_i$ (%)	0.9	1.4	0.07	6.4	1.5	2.0
$\tilde{\chi}_1^0\tilde{\chi}_2^0 \to u_i\bar{u}_i$ (%)	0.8	1.3	0.06	4.7	0.9	1.3
$\tilde{\chi}_1^+\tilde{\chi}_1^- \to d_i\bar{d}_i$ (%)	0.1	0.2	$4 \cdot 10^{-3}$	3.0	0.9	1.2
$\tilde{\chi}_1^+\tilde{\chi}_1^- \to u_i\bar{u}_i$ (%)	0.2	0.3	$6 \cdot 10^{-3}$	4.9	1.1	1.6
$\tilde{\chi}_2^0\tilde{\chi}_1^- \to l_i^-\bar{\nu}_{l_i}$ (%)	0.1	0.1	$9 \cdot 10^{-4}$	4.1	0.2	0.4

Table 7.3: Masses of the charginos and neutralinos, the bino, wino and Higgsino components of the lightest neutralino, the branching ratios for the decays $\tilde{\chi}_1^- \to \tilde{\chi}_1^0 l \bar{\nu}_l$, $\tilde{\chi}_2^0 \to \tilde{\chi}_1^0 l \bar{l}$ (with $l = e, \mu$) and the predicted relic density and WIMP-nucleon scattering cross sections for the benchmark points BM1–6. Also shown are the approximate percentage contributions to the annihilation cross section from the indicated channels for each benchmark. Note that these contributions have been computed using the freeze-out approximation.

a considerable enhancement of $pp \to q\bar{q}q\bar{q} + E_T^{miss} + X$. In both BM1 and BM2 the gluino mass is fairly large, though the LHC should still be able to discover them, at least with the high luminosity upgrade [639]. In BM3 the gluino, along with the leptoquarks, is very light and discovery of both should be possible with 300 fb^{-1} of integrated luminosity at the LHC.

The remaining benchmarks correspond to scenarios in which the lightest MSSM-like neutralino is an almost pure Higgsino state. As can be seen from Figure 7.4 and Figure 7.5, outside of the A-funnel regions the observed relic density is reproduced when $m_{\tilde{\chi}_1^0} \approx 1$ TeV. The need for the bino to be heavier in this case means that the gluino is above the reach of LHC run II. BM4 is an example of such a scenario. The suppressed mixing also ensures that the SI cross section is much lower, reducing the tension with the LUX direct detection limits. It is expected that XENON1T will still be in a position to either discover or rule out points such as BM4, as will be shown explicitly in the next section.

Alternatively, viable points that evade limits on the SI cross section can be found by allowing the Higgsino LSP to be light. This corresponds to points in the large $M_{1/2}$ parts of the CSE$_6$SSM parameter space in Figure 7.1 and Figure 7.2. The points BM5 and BM6 are examples of these scenarios, having a Higgsino DM candidate that is too light to account for all of the observed DM relic density. Although for these points the SI cross section is larger than in BM4, the direct detection event rate is substantially decreased since $(\Omega h^2)_{\text{th.}} < (\Omega h^2)_{\text{exp.}}$. This allows both to evade the LUX limits and also reduces the sensitivity of XENON1T to these points. While $M_{1/2}$ is not small, the gluino is still light enough to be accessible at run II. In contrast to BMs 1–3, these points could therefore be discovered at run II of the LHC, without being in tension with the current LUX limits or being observed in the early XENON1T data. However, this comes at the cost of requiring an additional source of DM in this scenario in order to explain the observed relic density. It follows from these benchmarks that limits on the parameter space of the CSE$_6$SSM can be placed by both collider searches and DM direct detection searches, with one or the other being more effective in different parts of the parameter space.

7.6 Impact of Current and Future Searches

In Figure 7.7 we show the current and future regions probed by LUX and XENON1T for $|\mu_{(\text{eff})}(M_S)| \approx 417$ GeV in the CSE$_6$SSM and the CMSSM. LUX limits from 2015 already essentially exclude the well-tempered bino-Higgsino solution region at low $m_{\tilde{g}}$,

i.e., low $M_{1/2}$, where the SI cross section is enhanced by large mixings. The effect of the more recent 2016 limit is to extend this exclusion to larger gluino masses, despite the reduction in the predicted relic density and SI cross section. This is as expected from the results of dedicated MSSM studies [640, 641]. XENON1T [642] is projected to exclude (or perhaps indirectly discover) even larger values of $m_{\tilde{g}}$. In this CMSSM scenario, XENON1T can potentially exclude $\tilde{g}$ masses up to $4-5$ TeV.

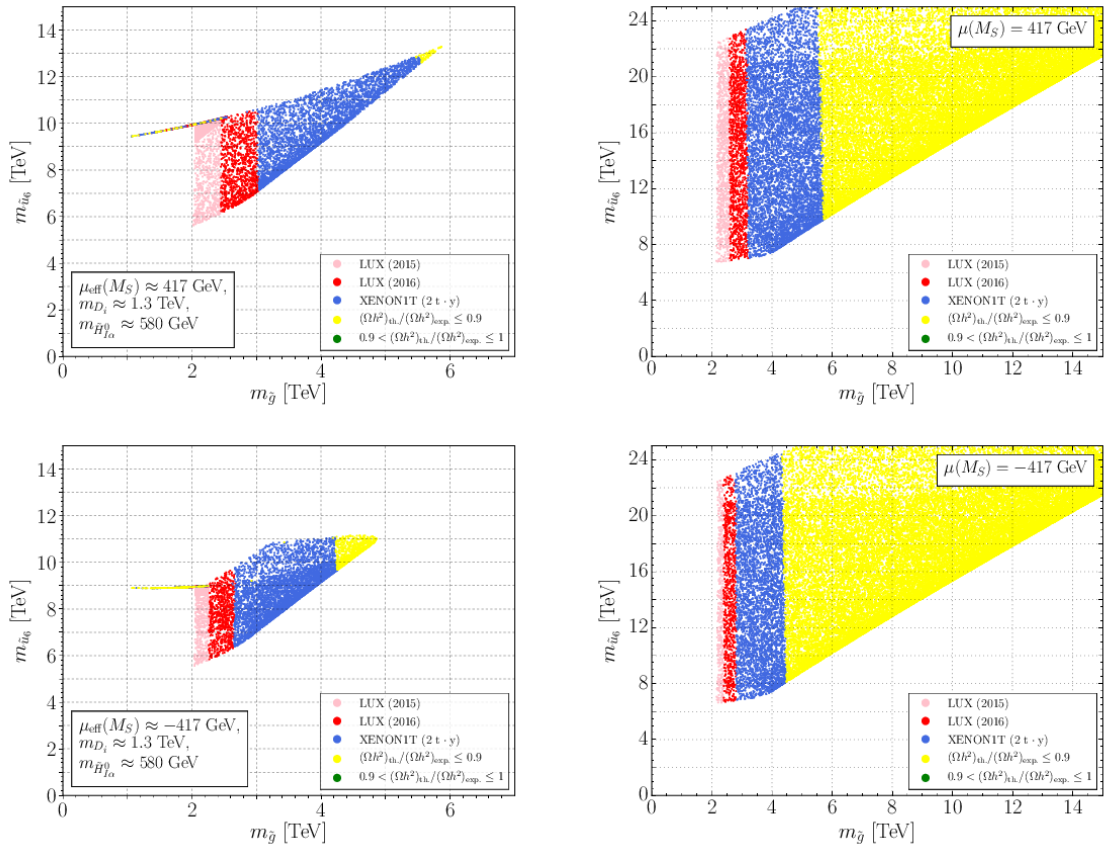

Figure 7.7: Plots of direct detection and collider constraints in the $m_{\tilde{g}} - m_{\tilde{u}_6}$ plane in the CSE$_6$SSM with $|\mu_{\rm eff}(M_X)| \approx 347$ GeV (left column) and the CMSSM with $|\mu(M_S)| = 417$ GeV (right column). In the top row, $\mu_{\rm (eff)}(M_X) > 0$, and in the bottom row $\mu_{\rm (eff)}(M_X) < 0$. In each plot, we show points that have a SI cross section in excess of the 2015 [373] and 2016 [374] LUX limits (pink and red, respectively) and points that are not currently excluded but are within the projected reach [642] of XENON1T (blue). In each case, the exclusion limit is determined according to Eq. (7.15). Finally, points that are not excluded by any limits but that predict a relic density that is less than 90% of the measured value are shown in yellow, while those points with $0.9 < (\Omega h^2)_{\rm th.}/(\Omega h^2)_{\rm exp.} \leq 1$ are shown in green.

The exclusions set by direct detection searches in the CSE$_6$SSM are to some extent similar to those in the CMSSM. In particular, outside of the A–funnel region in the CSE$_6$SSM, the LUX limits exclude gluino masses $m_{\tilde{g}} \lesssim 3$ TeV for $\mu_{(\text{eff})} > 0$ and $m_{\tilde{g}} \lesssim 2.5$ TeV for $\mu_{(\text{eff})} < 0$ in both models. Similarly, XENON1T will be able to probe gluino masses up to $4 - 5$ TeV in the CSE$_6$SSM as well. This accounts for a large fraction of as yet unexcluded solutions in the CSE$_6$SSM.

However, as can be seen from the left column of Figure 7.7, some points in the A-funnel region will still not be excluded by LUX or XENON1T. These points have a suppressed SI cross section or do not saturate the relic density bound, or both. This is also true in both models for those points not excluded at large $m_{\tilde{g}}$. Points close to the well-tempered region, where the amount of mixing is still relatively large, only escape being excluded if they lead to an extremely small relic density. If it is required that the LSP explains a substantial fraction of the observed relic abundance, for example $(\Omega h^2)_{\text{th.}}/(\Omega h^2)_{\text{exp.}} > 0.1$, then these points are removed. This is illustrated in Figure 7.8, where we show the variation in the bino fraction for points satisfying this criterion. The effect of the direct detection limits is to heavily restrict the amount of mixing allowed. The surviving points are forced to either be almost pure bino, at small $M_{1/2}$, or almost pure Higgsino at large $M_{1/2}$ and hence having a heavy SUSY spectrum.

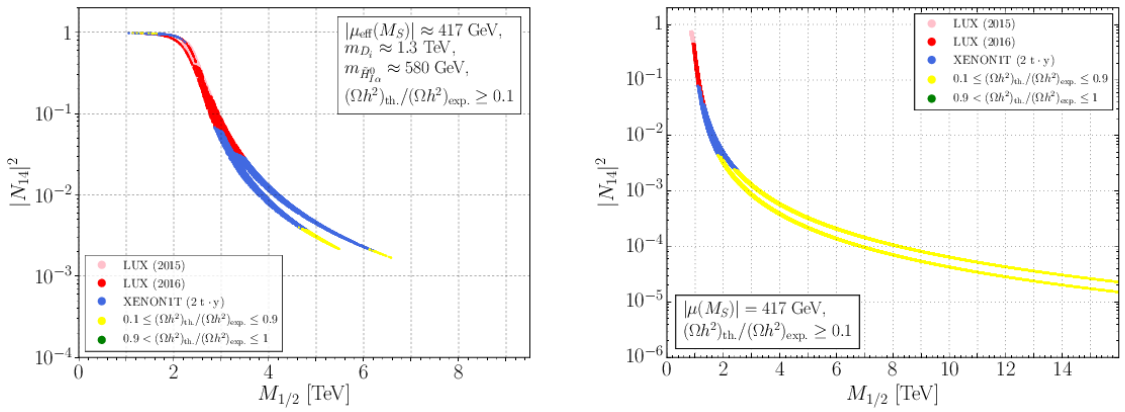

Figure 7.8: Plots showing points excluded by direct detection constraints in the $M_{1/2} - |N_{14}|^2$ plane in the CSE$_6$SSM (left) and CMSSM (right) for $|\mu_{(\text{eff})}(M_S)| \approx 417$ GeV, after also requiring that the LSP accounts for at least 10% of the observed relic density. The scaling of the limits and the colour coding is otherwise the same as in Figure 7.7.

While the A-funnel points will not be observable at XENON1T, the fact that $m_{\tilde{g}} \lesssim 2$ TeV for these solutions means that most are in reach of LHC searches targeting gluinos. This highlights the complementary nature of collider and direct detection

searches; similar observations have been made for the CMSSM (see, for example, Ref. [643]). Given the similarity of the lightest $Z_2^E = +1$ neutralinos in the CSE$_6$SSM to the ordinary MSSM neutralino sector, it is not so surprising that this continues to hold. In particular, results from XENON1T will be able to constrain the CSE$_6$SSM (and CMSSM) at much higher SUSY scales than are expected to be reached at the LHC. We conclude from this that direct detection searches, if no WIMPs are observed, will be able to place indirect limits on the sparticle masses much higher than can be achieved at run II, when the neutralino does not annihilate via special mechanisms such as the A-funnel. Thus direct detection limits are a particularly strong constraint on the CSE$_6$SSM parameter space.

The solutions that we find with a heavy Higgsino DM candidate lead to gluino and MSSM sfermion masses beyond the exclusion reach at run II. This is shown in Figure 7.9. Consequently there are effectively no constraints on this part of parameter space coming from collider limits, at least in the CMSSM. In the CSE$_6$SSM, the possibility of light exotic fermions, as in Figure 7.6, would allow for the model to be discovered even if all MSSM-like states and exotic scalars are heavy. However, if these states are also heavy then limits from direct detection searches are much more effective at constraining the parameter space.

Prior to the most recent LUX limits, all of our solutions with heavy $|\mu_{(\text{eff})}|$ were consistent with direct detection limits. This is no longer true for the 2016 LUX limits, which now exclude points with $M_1 \approx \mu_{(\text{eff})}$. Therefore the current direct detection limits are already probing the heavy $|\mu_{(\text{eff})}|$ parameter space. Scenarios with a highly mixed bino-Higgsino $\tilde{\chi}_1^0$ accounting for at least 10% of the relic abundance are again all excluded by the current limits. This is shown in Figure 7.10. Thus in the case that the LSP is relevant for addressing the DM problem, direct detection limits place stringent constraints on the allowable bino-Higgsino admixture. More extensive coverage of the valid, low mixing regions will require results from XENON1T, however.

It is clear that in the CSE$_6$SSM, results from XENON1T will place very strong constraints on the parameter space, as it should be possible to cover almost all of the allowed region. As for the previous small $|\mu_{(\text{eff})}|$ case, the surviving regions are the A-funnel region and at very large $m_{\tilde{g}}$. In this scenario the A-funnel region cannot be searched for directly at the LHC; from the left column of Figure 7.9 it can be seen that the gluino mass is always greater than ≈ 4 TeV. An interesting question is to what extent indirect DM detection experiments or results from flavour physics can constrain the CSE$_6$SSM here; we leave this for a future study. On the other hand, for very heavy spectra without light exotic fermions neither collider searches

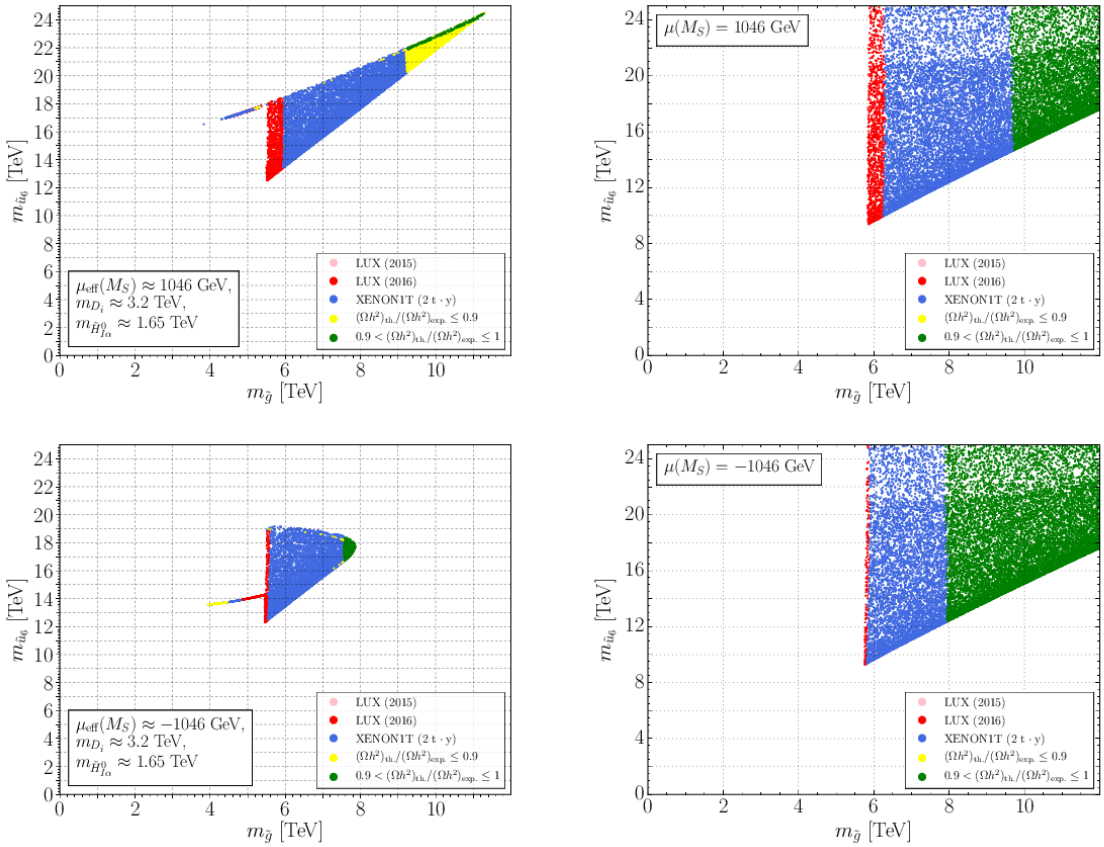

Figure 7.9: Plots of constraints in the $m_{\tilde{g}} - m_{\tilde{u}_6}$ plane in the CSE$_6$SSM with $|\mu_{\rm eff}(M_X)| \approx 898$ GeV (left column) and the CMSSM with $|\mu(M_S)| = 1046$ GeV (right column). In the top row, $\mu_{\rm (eff)}(M_X) > 0$, and in the bottom row $\mu_{\rm (eff)}(M_X) < 0$. The colour coding is the same as in Figure 7.7.

nor results from XENON1T will constrain the CSE$_6$SSM or the CMSSM. Even more sensitive direct detection experiments, such as results from LZ [644], will be required to directly search for these scenarios.

It should be noted that the large number of solutions for which $(\Omega h^2)_{\rm th.}$ is indicated as being less than 90% of the Planck value in Figure 7.9 still account for a very large fraction of the observed relic abundance. Small changes in $\lambda(M_X)$, or $\mu(M_X)$ in the CMSSM, are enough to closely reproduce the value in Eq. (7.6) without significantly changing any other results, unlike in the light Higgsino case where the DM candidate is severely underabundant assuming a standard freeze-out scenario. At large $M_{1/2}$ the relic density is still fully accounted for by the Higgsino DM candidate. Unfortunately, while these scenarios can explain the observed DM density entirely, the

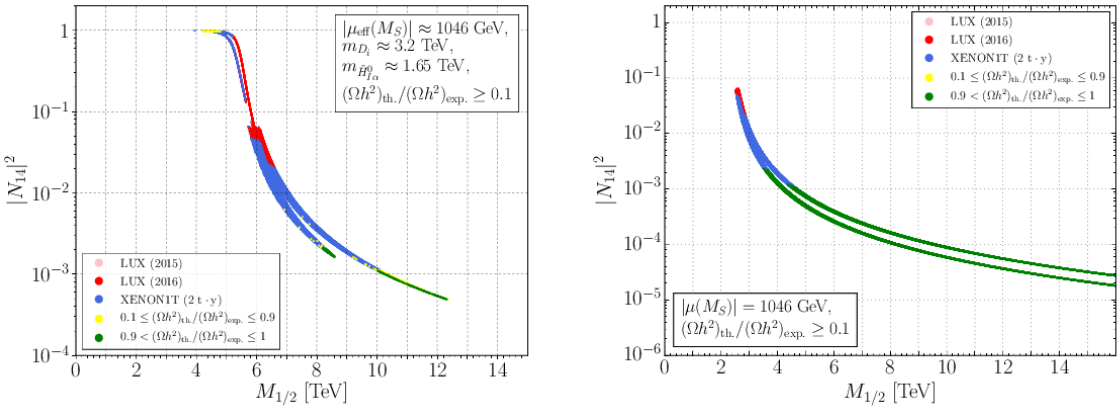

Figure 7.10: Plots showing points excluded by direct detection constraints in the $M_{1/2} - |N_{14}|^2$ plane in the CSE$_6$SSM (left) and CMSSM (right) for $|\mu_{(\rm eff)}(M_S)| \approx 1046$ GeV, after also requiring that the LSP accounts for at least 10% of the observed relic density. The scaling of the limits and the colour coding is the same as in Figure 7.7.

expected collider phenomenology is rather uninteresting as all states are too heavy to be observable.

7.7 Conclusions

In Chapter 6, we introduced the SE$_6$SSM as an alternative to the simplest variants of the E$_6$SSM, and showed how it has the attractive feature of improving some of the shortcomings of the simpler models. As the SE$_6$SSM is a $U(1)_N$ extension of the MSSM, the model allows the standard see-saw mechanism for neutrino masses and a leptogenesis explanation of the matter-anti-matter asymmetry. The single $\tilde{Z}_2^H$ symmetry, meanwhile, replaces the multiple discrete symmetries imposed in the E$_6$SSM, and together with R–parity leads to multiple DM candidates. The discussion of the mass spectrum at tree-level suggested that the exotic states in the model could be light, leading to potentially spectacular collider signals, and that DM could be accounted for by an MSSM-like, $Z_2^E = +1$ neutralino. The extremely light singlino, which would be the second DM candidate, yields a hot DM component that contributes negligibly to the observed relic density.

The numerical work in this chapter is aimed at validating this picture in the CSE$_6$SSM, incorporating important higher order corrections to the mass spectrum, and allows for the constraints on the model to be determined. We have performed a detailed exploration of the parameter space of both the CMSSM and CSE$_6$SSM and

compared the results found in each. In general, both models contain viable DM candidates, but direct detection limits are placing increasingly stringent constraints on the allowed parameter space. In both models the observed relic density can be fitted with a pure Higgsino neutralino that has a mass around 1 TeV. Alternatively the same can be achieved with a mixed bino-Higgsino DM candidate, requiring a fine tuning of M_1 and $\mu_{(\text{eff})}$ so that $\tilde{\chi}_1^0$ is well-tempered. This allows for lighter neutralino masses to be viable DM candidates; in the examples presented above, $m_{\tilde{\chi}_1^0} \approx 400$ GeV. However, recent direct detection results have placed strong limits on this mixing, leading to a serious tension between fitting the observed relic density and evading direct detection limits. Indeed, the recent LUX 2016 direct detection limits constrain Higgsino-bino mixing to such a great extent that the well-tempered strip is ruled out in both models, for both light and heavy neutralinos.

Unlike in the CMSSM, in the CSE$_6$SSM the extended CP-odd Higgs sector allows for the correct relic density to be achieved for lighter $M_{1/2}$ due to the A-funnel mechanism. This scenario is only possible in the CMSSM for much larger values of $\tan\beta$ than considered in the results presented here. Scenarios in which the A-funnel is active in the CSE$_6$SSM exist for both the heavier and lighter Higgsino masses considered. For lighter Higgsino masses this A-funnel region, which can escape even the projected future direct detection limits from XENON1T, will on the other hand be probed by the LHC during run II. This demonstrates an important complementarity between collider searches and experiments for the direct detection of DM.

These special regions aside, however, it is now rather difficult to explain DM in the lighter Higgsino mass scenarios. If one gives up the requirement that the lightest neutralino account for the complete DM relic density, then many scenarios are still viable and have phenomenology that will be probed with run II of the LHC. Since the sfermions will still be very heavy the main signatures arise from the production of gluinos, charginos and neutralinos, with MSSM-like signatures. The potentially light exotic states in the E_6 inspired model are an exciting possibility for discovering the model even when the other sparticles are very heavy via the signatures discussed in Section 6.4.2, which is an advantage that the CSE$_6$SSM has over the CMSSM.

Heavier scenarios with a Higgsino DM candidate of around 1 TeV are also not currently constrained so much by direct detection and it is possible to fit the relic density in both the CMSSM and CSE$_6$SSM for a wide range of the parameter space. Unfortunately, these scenarios have a rather heavy spectrum which is not accessible to the LHC. They will, however, be probed by future direct detection experiments, such as XENON1T, which will be able to probe most of the viable solutions we have

found in the CSE$_6$SSM. Therefore the future impact of XENON1T, as well as even more sensitive experiments such as LZ, on the CSE$_6$SSM will be very significant.

Chapter 8

Summary

E_6 inspired models are well-motivated extensions of the MSSM that have the potential to address some of the outstanding problems of minimal SUSY. Arising naturally from superstring inspired constructions, models like the E_6SSM extend the gauge group of the MSSM with at least one additional $U(1)'$ symmetry. This gauge symmetry can be used to forbid an elementary μ term, while the VEV of a singlet field can be used to dynamically generate an effective μ parameter, solving the μ problem. Anomaly cancellation requires that the matter content of these models also contains exotic matter fields, as well as a heavy Z' boson. These features allow the tree-level light Higgs mass to be raised compared to the MSSM, in turn reducing the need for large radiative corrections to reproduce the observed mass of 125 GeV. As a result, E_6 inspired models have the potential to solve both the big and little hierarchy problems.

The low-energy $U(1)'$ charge assignments depend on the choice of gauge symmetry breaking pattern in the construction of the model. The E_6SSM corresponds to the case in which the $U(1)'$ is defined such that the right-handed neutrinos are total singlets, and thus do not participate in gauge interactions. In this unique case, small non-zero neutrino masses can be generated through a see-saw mechanism, and successful baryogenesis achieved via leptogenesis. E_6 inspired models with a $U(1)_N$ gauge symmetry are therefore able to solve both of these key problems in the SM and the MSSM. The presence of exotic states and a Z' boson might lead to distinctive collider signatures; the interesting phenomenology associated with these states has contributed to these models receiving a substantial amount of attention in the literature. Detailed studies of complicated BSM models like the E_6SSM are very difficult, however. In Chapter 4, we outlined work we undertook to facilitate precision numerical studies of models such as the CE_6SSM and CSE_6SSM. This included the implementation of a new BVP solver

and the calculation of the loop-induced diphoton and digluon decay widths of scalars and pseudoscalars in general models, which are important for collider studies.

In this thesis, we have shown that the appearance of the new Z' boson also has important consequences for the naturalness of the simplest variant of the E$_6$SSM and other similar E_6 inspired models. The same $U(1)'$ D-terms that help to raise the Higgs mass at tree-level also provide a tree-level contribution to the EW scale. If the D-terms are large, then this implies that fine tuning is necessary to maintain an acceptably light Z boson mass. In the E$_6$SSM, the size of the D-terms can be related to the Z' mass, which is required to satisfy $M_{Z'} \gtrsim 3.4$ TeV by LHC searches. The D-term contributions are as a result already quite sizeable, suggesting the possible existence of a substantial fine tuning. As argued in Chapter 5, the tuning associated with the Z' mass limits is not dependent on assumptions about the high-scale boundary conditions imposed on the model. This is in stark contrast to the usual radiative corrections that lead to the little hierarchy problem, which are highly dependent on these assumptions. By considering both the E$_6$SSM and the MSSM at low energies, we effectively eliminated the fine tuning effects of these model dependent contributions, revealing the residual fine tuning associated with the size of $M_{Z'}$.

The results of doing so showed that the limits on $M_{Z'}$ can be used to set conservative lower bounds on the fine tuning in the E_6 inspired models considered. In the E$_6$SSM, previous run I limits of $M_{Z'} \gtrsim 2.5$ TeV already impose a fine tuning equivalent to that which would occur in the MSSM if charginos were required to have masses above 700 GeV. This exclusion of the Z' mass has already been strengthened at run II, so that these limits already significantly challenge the naturalness of the E$_6$SSM at low energies. Despite this, when radiative corrections are not minimised, it is still possible for the E$_6$SSM to be less fine tuned than the MSSM, emphasising the model dependence of these contributions. At low energies, the Z' fine tuning can be reduced by considering alternative E_6 inspired models, such as those with a $U(1)_I$ symmetry, but the positive aspects of the $U(1)_N$ symmetry are then sacrificed.

One way to avoid this fine tuning in $U(1)_N$ models is to consider extensions of the E$_6$SSM in which the matter content suppresses the problematic D-terms. In Chapter 6, we reviewed an E_6 inspired model with an exact custodial $\tilde{Z}_2^H$ symmetry that does exactly this. Moreover, the single $\tilde{Z}_2^H$ in the SE$_6$SSM suffices to forbid all dangerous operators leading to FCNCs and rapid proton decay. This is a significant improvement over the simplest variants of the E$_6$SSM, which have the undesirable feature that multiple exact and approximate discrete symmetries have to be imposed to be viable. The inclusion of a pure singlet state, required to stabilise the scalar

potential, also provides a mechanism through which the SUSY scale can be well below $M_{Z'}$. This breaks the tight relationship in the E$_6$SSM that results in $M_S \sim M_{Z'}$ and forces the superpartners to be much heavier than is otherwise required by collider searches and the Higgs mass constraint. We introduced a constrained version of the model, the CSE$_6$SSM, with boundary conditions inspired by gravity mediated SUSY breaking, and discussed the expected structure of the mass spectrum. The automatic conservation of a Z_2^M matter parity together with the imposed $\tilde{Z}_2^M$ implies the existence of two DM candidates in the CSE$_6$SSM, one of which we showed can be MSSM-like and so may fully account for the observed DM relic density.

To demonstrate this, in Chapter 7 we carried out a detailed numerical study of the parameter space of the CSE$_6$SSM. The model was directly compared to analogous scenarios in the CMSSM, and the impact of collider and DM constraints was assessed. Both the CSE$_6$SSM and CMSSM contain regions of parameter space consistent with a 125 GeV Higgs and that lead to a DM candidate that saturates the Planck measurement of the relic density. However, direct detection searches put very strict limits on the identity of the DM candidate; an LSP with a significant bino-Higgsino mixing is now largely ruled out due to its enhanced SI scattering cross section. The DM relic density can still viably be accounted for in both models by a pure Higgsino with a mass of ~ 1 TeV, for $\tan\beta = 10$. In constrained scenarios, this implies that the rest of the MSSM superpartners are very heavy and unobservable at the LHC. In the CSE$_6$SSM, the extended pseudoscalar sector means that at $\tan\beta = 10$ it is possible for the lightest CP-odd Higgs to be light, opening up the opportunity to also explain the relic density with a light LSP that undergoes resonant annihilations in an A-funnel region. While these scenarios would have evaded direct detection searches, they are eminently testable at run II of the LHC due to the light predicted gluino masses.

In general, we found that direct detection searches are able to probe much heavier SUSY scales than will be accessible at the LHC. The next generation of searches, such as XENON1T and LZ, will have a significant impact on the parameter space of the CSE$_6$SSM, improving on what are already very strong constraints on the parameter space. A distinctive feature of the E_6 inspired models studied is that it remains possible for the exotic fermions to be light. These would have distinctive collider signatures, and allow for the model to be discovered at the LHC and distinguished from the MSSM, even if the rest of the SUSY spectrum is required to be heavy by DM direct detection constraints. The complementary limits coming from collider and DM searches continue to place impressive limits on the parameter space of the E_6 inspired models considered in this thesis.

Nevertheless, there still remain phenomenologically viable scenarios in the parameter spaces of the E_6SSM and SE_6SSM to be explored, some of which will be probed in the coming years. The exciting possibility of observing the exotic states from E_6 suggests one important future direction to explore. The role that these states could play in discovering the model emphasises the importance of dedicated theoretical studies and experimental searches for them; as yet, precise limits obtained in the context of these models are not available. Other less well studied aspects of these E_6 inspired models, such as their predictions for flavour physics and, in the case of the SE_6SSM, the consequences of the extended dark sector, also provide interesting possibilities for future research. With improved numerical tools available, the barriers to performing these studies have been substantially reduced. Our theoretical understanding of these complicated models can therefore be expected to keep pace with the rapid experimental progress expected in coming years. With their connections to naturalness and string-inspired origin, the resulting discovery or exclusion of the E_6 inspired models considered here can be hoped to shed light on the nature of fundamental physics at high energies.

Appendix A

Review of SUSY Model Building

In this appendix we summarise the required formalism and generic results used in constructing models of softly broken SUSY. The general results presented here may be applied directly to the MSSM and the E_6 inspired models considered in the main body of the text to obtain, in particular, the scalar potential relevant to EWSB and the mass matrices and interaction vertices in each model. More detailed treatments and derivations of the results given here may be found, for example, in Refs. [103, 104].

A.1 The Super-Poincaré Algebra

The continuous symmetries of the SM can be categorised into spacetime and internal symmetries. The full spacetime symmetry obeyed by the interactions of the SM is described by the Poincaré group, corresponding to invariance under Lorentz transformations and spacetime translations. The Poincaré group is a 10 parameter group, parametrised in the vicinity of the identity transformation by a constant 4-vector a^μ and a second-rank antisymmetric tensor $\omega_{\mu\nu} = -\omega_{\nu\mu}$ such that an infinitesimal Poincaré transformation acting on the spacetime coordinate x^μ can be written

$$x^{\mu\prime} = \left(\delta^{\mu'}_{\nu} + \omega^{\mu'}_{\nu}\right) x^\nu + a^{\mu'} \,. \tag{A.1}$$

The corresponding generators are P^μ, the generators of spacetime translations, and $M^{\mu\nu}$, which generate Lorentz boosts and rotations. Group elements corresponding to translations a^μ and Lorentz transformations Λ can then be written as

$$U(a) = \exp\left(i a^\mu P_\mu\right) \,, \quad U(\Lambda) = \exp\left(-\frac{i}{2}\omega^{\mu\nu} M_{\mu\nu}\right) \,. \tag{A.2}$$

The Lie algebra of the group, that is, the Poincaré algebra, may be deduced by constructing representations of the group in terms of differential operators, identified by considering the actions of the generators on test functions $f(x^\mu)$. For example, the requirement that $f'(x') = f(x - \delta x) = U(\delta x) f(x)$ for infinitesimal δx allows one to deduce that[1]

$$P_\mu = i\partial_\mu \,, \tag{A.3}$$

while similar considerations for the generators $M_{\mu\nu}$ lead to[2] [82]

$$M_{\mu\nu} = -i\left(x_\mu \partial_\nu - x_\nu \partial_\mu\right) . \tag{A.4}$$

One can then directly evaluate all of the possible commutators to arrive at the Poincaré algebra,

$$[P_\mu, P_\nu] = 0 \,, \tag{A.5a}$$

$$[M_{\mu\nu}, P_\rho] = i\left(\eta_{\nu\rho} P_\mu - \eta_{\mu\rho} P_\nu\right) , \tag{A.5b}$$

$$[M_{\mu\nu}, M_{\rho\sigma}] = -i\left(\eta_{\mu\rho} M_{\nu\sigma} - \eta_{\mu\sigma} M_{\nu\rho} - \eta_{\nu\rho} M_{\mu\sigma} + \eta_{\nu\sigma} M_{\mu\rho}\right) . \tag{A.5c}$$

The continuous internal symmetries of the SM correspond to the gauge symmetry group $SU(3)_C \times SU(2)_L \times U(1)_Y$. More generally, one can consider a field theory invariant under Poincaré transformations and some set of internal symmetries, such that the Lie algebra corresponding to the full symmetry group contains as subalgebras the Poincaré algebras and an algebra defined by a set of generators T^a. The classic CM theorem [89] puts a very strong constraint on the structure of the full symmetry group, provided several assumptions, such as the S-matrix being non-trivial and analytic, are satisfied. When these hold, the theorem states that the full symmetry group of the S-matrix is locally isomorphic to the direct product of the Poincaré group and the group generated by the T^a, that is,

$$[T^a, P_\mu] = [T^a, M_{\mu\nu}] = 0 \,. \tag{A.6}$$

Thus the spacetime symmetries of the model cannot be extended in a non-trivial fashion when the assumptions of the CM theorem are met. The SM is such a case; the group of continuous symmetries is a direct product of the Poincaré group and $SU(3)_C \times SU(2)_L \times U(1)_Y$.

[1] Our conventions for 4-vectors are $x^\mu = (t, \boldsymbol{x})$, $\partial_\mu = (\partial/\partial t, \boldsymbol{\nabla})$, with the metric $\eta^{\mu\nu} = \mathrm{diag}(+1, -1, -1, -1)$ and working in natural units with $\hbar = c = 1$.

[2] Note that, in general, a term corresponding to the spin could also be included.

Theories in which the set of spacetime symmetries is enlarged must violate the assumptions of the CM theorem. One way to do so is to allow the generators of the symmetry group to satisfy a Lie superalgebra[3] rather than an ordinary Lie algebra. In this case, to each generator T^a there is associated a degree $|T^a| \in \{0, 1\}$, where generators for which $|T^a| = 0$ are said to be even, and those for which $|T^a| = 1$ are odd. The Lie bracket of the algebra is generalised to a superbracket that satisfies

$$\left[T^a, T^b\right] = -(-1)^{|T^a||T^b|}\left[T^b, T^a\right], \tag{A.7}$$

so that the even and odd generators in the theory will be found to obey commutation and anticommutation relations.

The appropriate generalisation of the CM theorem to this scenario is the HLS theorem [88]. It states that, under the previous assumptions of the CM theorem, the most general such superalgebra is generated by a set of even and odd generators, where the odd generators are spinorial and belong to the $(\frac{1}{2}, 0)$ and $(0, \frac{1}{2})$ representations of the Lorentz group, while the even generators are a direct sum of the generators of the Poincaré group and other, internal symmetry generators. While the internal symmetries continue to trivially commute with the generators of the Poincaré group, the odd generators $\{Q^i_\alpha, \overline{Q}^i_{\dot\alpha}\}$, where $i = 1, \ldots, N$ and α, $\dot\alpha$ are two-component spinor indices, satisfy non-trivial commutation and anticommutation relations with P_μ and $M_{\mu\nu}$. The odd generators Q^i_α and $\overline{Q}^i_{\dot\alpha} = (Q^i_\alpha)^\dagger$ are the generators of SUSY transformations, and constitute the most general extension of the Poincaré group consistent with the assumptions of the CM and HLS theorems, yielding the super-Poincaré group. The number of distinct odd generators N is not restricted by the HLS theorem. However, theories having extended SUSY with $N > 1$ are not regarded as being relevant from the phenomenological point of view, despite their interesting theoretical properties. This is because, for example, they do not admit chiral fermions [645]. Models of low-energy SUSY therefore usually have $N = 1$ and contain only a single copy of the generators $\{Q_\alpha, \overline{Q}_{\dot\alpha}\}$. Taking into account the expected form of the commutation relations for the different types of generators, Eq. (A.7), the various commutators and anticommutators may be evaluated [104]. In addition to the commutation relations of the Poincaré algebra, one finds also that the SUSY generators satisfy

$$[Q_\alpha, M_{\mu\nu}] = (\sigma_{\mu\nu})_\alpha{}^\beta Q_\beta\,, \tag{A.8a}$$

$$\left[\overline{Q}^{\dot\alpha}, M_{\mu\nu}\right] = (\bar\sigma_{\mu\nu})^{\dot\alpha}{}_{\dot\beta}\overline{Q}^{\dot\beta}\,, \tag{A.8b}$$

[3] i.e., a Z_2-graded Lie algebra

$$[Q_\alpha, P_\mu] = \left[\overline{Q}^{\dot{\alpha}}, P_\mu\right] = 0\,, \tag{A.8c}$$

$$\{Q_\alpha, Q_\beta\} = \left\{\overline{Q}^{\dot{\alpha}}, \overline{Q}^{\dot{\beta}}\right\} = 0\,, \tag{A.8d}$$

$$\left\{Q_\alpha, \overline{Q}_{\dot{\beta}}\right\} = 2\,(\sigma^\mu)_{\alpha\dot{\beta}}\,P_\mu\,, \tag{A.8e}$$

$$\left\{\overline{Q}^{\dot{\alpha}}, Q^\beta\right\} = 2\,(\bar{\sigma}^\mu)^{\dot{\alpha}\beta}\,P_\mu\,, \tag{A.8f}$$

where $\sigma^{\mu\nu} \equiv \frac{i}{4}\,(\sigma^\mu\bar{\sigma}^\nu - \sigma^\nu\bar{\sigma}^\mu)$ and the 4-vectors of Pauli matrices are defined by $\sigma^\mu \equiv (\mathbf{1}_{2\times2}, \boldsymbol{\sigma})$ and $\bar{\sigma}^\mu \equiv (\mathbf{1}_{2\times2}, -\boldsymbol{\sigma})$. Eq. (A.5) and Eq. (A.8) together constitute the super-Poincaré algebra. From it, one may immediately deduce a number of consequences of unbroken SUSY. For example, it follows immediately from Eq. (A.8c) that $[Q_\alpha, P^2] = 0$, and thus states that are transformed into one another under the action of a SUSY transformation, i.e., the members of a SUSY multiplet, would be mass degenerate if SUSY were not broken. A slightly more subtle consequence of the SUSY algebra is that within a supermultiplet the number of fermionic and bosonic degrees of freedom must be equal, which can be seen by considering the trace of the operator $(-1)^{2S}\{Q_\alpha, \overline{Q}_{\dot{\beta}}\}$ where S is the spin operator (see, e.g., Refs. [84, 104] for a derivation of this result). Therefore in a SUSY model each fermion is necessarily accompanied by an appropriate number of bosonic partners, and vice versa. Some of the further consequences of this algebra are applied in Chapter 2.

A.2 Superspace and Superfields

Models possessing $N = 1$ SUSY are most efficiently expressed using the superfield formalism. In this approach, the ordinary spacetime coordinates x^μ are supplemented by a set of four, anticommuting spinorial coordinates θ^α and $\bar{\theta}_{\dot{\alpha}}$ with mass dimension $-1/2$. The set $z = (x^\mu, \theta^\alpha, \bar{\theta}_{\dot{\alpha}})$ defines a point in superspace, and functions $\hat{F}(z)$ on superspace are known as superfields [87]. By virtue of the anticommuting nature of θ and $\bar{\theta}$, power series expansions in θ and $\bar{\theta}$ of arbitrary superfields always contain a finite number of terms. Therefore, for example, a general commuting superfield $\hat{S}$ carrying no Lorentz or spinor indices can be written

$$\begin{aligned}\hat{S}(z) = {} & a(x) + \theta\xi(x) + \bar{\theta}\bar{\chi}(x) + \theta\theta b(x) + \bar{\theta}\bar{\theta}c(x) + \bar{\theta}\bar{\sigma}^\mu\theta v_\mu(x) \\ & + \bar{\theta}\bar{\theta}\theta\zeta(x) + \theta\theta\bar{\theta}\bar{\lambda}(x) + \frac{1}{2}\theta\theta\bar{\theta}\bar{\theta}d(x)\,,\end{aligned} \tag{A.9}$$

where spinor indices are contracted as $\theta\theta \equiv \theta^\alpha\theta_\alpha$, $\bar\theta\bar\theta \equiv \bar\theta_{\dot\alpha}\bar\theta^{\dot\alpha}$ and so on[4]. In this case, a, b, c, and d are complex scalar fields, v_μ is a complex vector field, and ξ, $\bar\chi$, ζ, and $\bar\lambda$ are two-component spinors.

Superfields provide an intuitive way of realising the effect of global SUSY transformations. In superspace, SUSY transformations generated by Q_α and $\overline{Q}_{\dot\alpha}$ correspond to rigid translations on superspace [87, 647]. An infinitesimal transformation parametrised by the two-component spinors ϵ, $\bar\epsilon$ can be written

$$z \to (x^\mu - i\theta\sigma^\mu\bar\epsilon + i\epsilon\sigma^\mu\bar\theta, \theta + \epsilon, \bar\theta + \bar\epsilon)\,. \tag{A.10}$$

As for the generators P_μ, $M_{\mu\nu}$, the SUSY generators Q and $\overline{Q}$ can be represented in terms of differential operators by requiring that they induce the above transformation on superfields, with the result that one can write

$$Q_\alpha = -i\left[\frac{\partial}{\partial\theta^\alpha} + i(\sigma^\mu\bar\theta)_\alpha\partial_\mu\right], \quad \overline{Q}^{\dot\alpha} = -i\left[\frac{\partial}{\partial\bar\theta_{\dot\alpha}} + i(\bar\sigma^\mu\theta)^{\dot\alpha}\partial_\mu\right]. \tag{A.11}$$

Note that partial derivatives with respect to the anticommuting variables θ, $\bar\theta$ are themselves anticommuting and satisfy identities such as

$$\begin{aligned}
\frac{\partial\theta^\alpha}{\partial\theta^\beta} &= \delta^\alpha_\beta\,, & \frac{\partial\bar\theta^{\dot\alpha}}{\partial\bar\theta^{\dot\beta}} &= \delta^{\dot\alpha}_{\dot\beta}\,,\\
\frac{\partial\theta_\alpha}{\partial\theta^\beta} &= -\epsilon_{\beta\alpha}\,, & \frac{\partial\bar\theta_{\dot\alpha}}{\partial\bar\theta^{\dot\beta}} &= -\epsilon_{\dot\beta\dot\alpha}\,,\\
\frac{\partial\theta^\alpha}{\partial\bar\theta_{\dot\beta}} &= 0\,, & \frac{\partial\bar\theta_{\dot\alpha}}{\partial\theta^\beta} &= 0\,,
\end{aligned}$$

with the Leibniz rule for arbitrary anticommuting quantities ψ, ξ reading

$$\partial(\psi\xi) = (\partial\psi)\xi - \psi(\partial\xi)$$

for $\partial = \partial/\partial\theta^\alpha$ or $\partial = \partial/\partial\bar\theta_{\dot\alpha}$. By demanding that the result of acting with Q and $\overline{Q}$ on a superfield $\hat S$ is itself a superfield, i.e., that the SUSY algebra closes [648], the transformation properties for the various component fields a, b, ... can be deduced [87, 649, 650]. Of particular note is the fact that the component field d is unchanged up to a total derivative, and therefore the $\theta\theta\bar\theta\bar\theta$ component of an arbitrary superfield can be an acceptable contribution to a SUSY invariant action. This contribution,

[4]For a review of two-component spinor formalism, see Ref. [646].

referred to as a D-term, can be picked out by integrating,

$$[\hat{S}]_D \equiv \int d^4\theta\, \hat{S} = \frac{d}{2}\,. \tag{A.12}$$

The Berezin integral [651] introduced here is defined by writing

$$d^2\theta = -\frac{1}{4} d\theta^\alpha d\theta_\alpha\,, \quad d^2\bar{\theta} = -\frac{1}{4} d\bar{\theta}_{\dot{\alpha}} d\bar{\theta}^{\dot{\alpha}}\,, \quad d^4\theta = d^2\bar{\theta} d^2\theta\,. \tag{A.13}$$

It has the properties

$$\int d^2\theta\, \theta\theta = \int d^2\bar{\theta}\, \bar{\theta}\bar{\theta} = \int d^4\theta\, \theta\theta\bar{\theta}\bar{\theta} = 1\,,$$
$$\int d^2\theta\, \theta^\alpha\theta^\beta = -\frac{1}{2}\epsilon^{\alpha\beta}\,, \quad \int d^2\bar{\theta}\, \bar{\theta}_{\dot{\alpha}}\bar{\theta}_{\dot{\beta}} = -\frac{1}{2}\epsilon_{\dot{\alpha}\dot{\beta}}\,.$$

One may also define the anticommuting equivalents of Dirac delta functions by

$$\delta^{(2)}(\theta) = \theta\theta\,, \quad \delta^{(2)}(\bar{\theta}) = \bar{\theta}\bar{\theta}\,,$$

as well as the integration by parts identities

$$\int d^2\theta\, \frac{\partial}{\partial\theta^\alpha}\hat{S} = \int d^2\bar{\theta}\, \frac{\partial}{\partial\bar{\theta}_{\dot{\alpha}}}\hat{S} = 0\,.$$

The former can be used to define the F-term associated with a superfield $\hat{S}$,

$$[\hat{S}]_F = \int d^4\theta\, \delta^{(2)}(\bar{\theta})\hat{S} = b\,, \tag{A.14}$$

which is also relevant for the purpose of constructing SUSY invariant actions.

Arbitrary superfields furnish reducible representations of the SUSY algebra in general [87, 649]. Irreducible representations are obtained by imposing constraints on general superfields. The two irreducible representations that are usually considered relevant for model building are the chiral superfields and the vector superfields. To define a chiral superfield, chiral covariant derivatives given by

$$\mathcal{D}_\alpha = \frac{\partial}{\partial\theta^\alpha} - i(\sigma^\mu\bar{\theta})_\alpha\partial_\mu \quad \text{and} \quad \overline{\mathcal{D}}^{\dot{\alpha}} = \frac{\partial}{\partial\bar{\theta}_{\dot{\alpha}}} - i(\bar{\sigma}^\mu\theta)^{\dot{\alpha}}\partial_\mu \tag{A.15}$$

are introduced [649]. A left-chiral superfield $\hat{\Phi}$ is then defined by the constraint

$$\overline{\mathcal{D}}_{\dot{\alpha}}\hat{\Phi} = 0\,. \tag{A.16}$$

Similarly, a right-chiral superfield is defined by the constraint $\mathcal{D}_\alpha \hat{\Phi}^\dagger = 0$. Explicit component field expressions for the left- and right-chiral superfields may be obtained by making a change of variables to $y^\mu = x^\mu - i\theta\sigma^\mu\bar{\theta}$ [652] and solving the constraint, Eq. (A.16). The results are found to be [85]

$$\begin{aligned}
\hat{\Phi}(z) &= \phi(x) - i\theta\sigma^\mu\bar{\theta}\partial_\mu\phi(x) - \frac{1}{4}\theta\theta\bar{\theta}\bar{\theta}\partial^\mu\partial_\mu\phi(x) + \sqrt{2}\theta\psi(x) \\
&\quad + \frac{i}{\sqrt{2}}\theta\theta\partial_\mu\psi(x)\sigma^\mu\bar{\theta} + \theta\theta F(x)\,, \\
\hat{\Phi}^\dagger(z) &= \phi^*(x) + i\theta\sigma^\mu\bar{\theta}\partial_\mu\phi^*(x) - \frac{1}{4}\theta\theta\bar{\theta}\bar{\theta}\partial^\mu\partial_\mu\phi^*(x) + \sqrt{2}\bar{\theta}\bar{\psi}(x) \\
&\quad - \frac{i}{\sqrt{2}}\bar{\theta}\bar{\theta}\theta\sigma^\mu\partial_\mu\bar{\psi}(x) + \bar{\theta}\bar{\theta}F^*(x)\,.
\end{aligned} \tag{A.17}$$

The components of a chiral superfield consist of two complex scalar fields ϕ and F and a Weyl fermion ψ; note that the number of bosonic and fermionic degrees of freedom are equal, as expected from the super-Poincaré algebra [104]. The field F is an auxiliary field, and can be eliminated by making use of the equations of motion. By evaluating the transformation laws of the components ϕ, ψ and F under SUSY translations it is found that F transforms as a total derivative. Therefore the F-term associated with a chiral superfield, $[\hat{\Phi}]_F$, can give a contribution to a SUSY invariant action [87].

A vector superfield, $\hat{V}$, is defined by imposing the reality constraint [85, 87]

$$\hat{V} = \hat{V}^\dagger\,. \tag{A.18}$$

Retaining only those terms that are real in Eq. (A.9) gives the component fields,

$$\begin{aligned}
\hat{V}(z) &= C(x) + \sqrt{2}\theta\xi(x) + \bar{\theta}\bar{\xi}(x) + \theta\theta M(x) + \bar{\theta}\bar{\theta}M^*(x) + \theta\sigma^\mu\bar{\theta}A_\mu(x) \\
&\quad + \theta\theta\bar{\theta}\left[\bar{\lambda}(x) - \frac{i}{\sqrt{2}}\bar{\sigma}^\mu\partial_\mu\xi(x)\right] + \bar{\theta}\bar{\theta}\theta\left[\lambda(x) - \frac{i}{\sqrt{2}}\sigma^\mu\partial_\mu\bar{\xi}(x)\right] \\
&\quad + \theta\theta\bar{\theta}\bar{\theta}\left[\frac{1}{2}D(x) - \frac{1}{4}\partial^\mu\partial_\mu C(x)\right]\,.
\end{aligned} \tag{A.19}$$

The components of the general vector superfield consist of a real vector field A_μ, a real auxiliary field D, and a complex Weyl spinor λ, as well as the real auxiliary field C, the complex auxiliary field M, and the auxiliary Weyl spinor ξ. The latter three fields can be eliminated by means of a supergauge transformation [104]; for example,

by appropriate choice of a chiral superfield $i\hat{\Lambda}$, the transformation

$$\hat{V} \to \hat{V} + i\left(\hat{\Lambda} - \hat{\Lambda}^\dagger\right) \tag{A.20}$$

can be used to eliminate the additional auxiliary fields. This leads to the Wess-Zumino gauge expression for $\hat{V}$ [650],

$$\hat{V}_{WZ}(z) = \theta\sigma^\mu\bar{\theta}A_\mu(x) + \theta\theta\bar{\theta}\bar{\lambda}(x) + \bar{\theta}\bar{\theta}\theta\lambda(x) + \frac{1}{2}\theta\theta\bar{\theta}\bar{\theta}D(x)\,. \tag{A.21}$$

As for a general superfield, the D-term coming from a vector superfield gives a possible (real) contribution to a SUSY invariant action.

A.3 Supersymmetric Lagrangians

The Lagrangian for a given SUSY model is constructed from F- and D-terms obtained from a set of chiral and vector superfields, and functions thereof, in such a way as to generalise the structures familiar from non-SUSY gauge theory. The model is assumed to be invariant under local gauge transformations belonging to a compact Lie group G, which may be a direct product of multiple group factors. For each such group factor there is associated a vector superfield $\hat{V}_i^a$, where the indices i, j, ..., label the corresponding group and a, b, ..., the group generator. The matter content of the theory consists of a set of left-chiral superfields $\hat{\Phi}_I$ that transform in a representation R of G. The generalisation to the superfield formalism of local gauge transformations on the chiral and vector superfields is [653, 654]

$$\hat{\Phi}_I \to (e^{-i\hat{\Lambda}})_I{}^J\hat{\Phi}_J\,, \tag{A.22}$$

$$\hat{\Phi}^{\dagger I} \to \hat{\Phi}^{\dagger J}(e^{i\hat{\Lambda}})_J{}^I\,, \tag{A.23}$$

$$e^{\hat{V}} \to e^{-i\hat{\Lambda}^\dagger}e^{\hat{V}}e^{i\hat{\Lambda}}\,, \tag{A.24}$$

$$e^{-\hat{V}} \to e^{-i\hat{\Lambda}}e^{-\hat{V}}e^{i\hat{\Lambda}^\dagger}\,, \tag{A.25}$$

where the gauge transformation is parametrised by a set of chiral superfields $\hat{\Lambda}_i^a$, here absorbed into the quantities

$$\hat{\Lambda}_I{}^J \equiv 2g_i\hat{\Lambda}_i^a(T_i^a)_I{}^J\,, \quad \hat{V}_I{}^J \equiv 2g_i\hat{V}_i^a(T_i^a)_I{}^J\,, \tag{A.26}$$

where the T_i^a are the generators corresponding to the product group G_i.

The full (classical) Lagrangian $\mathcal{L}$ is decomposed into the pieces

$$\mathcal{L} = \mathcal{L}_{\hat{\Phi}} + \mathcal{L}_{\text{int}} + \mathcal{L}_{\mathcal{W}} \,, \tag{A.27}$$

corresponding to kinetic terms for the chiral superfields, $\mathcal{L}_{\hat{\Phi}}$, interactions between the chiral superfields, $\mathcal{L}_{\text{int}}$, and kinetic terms for the vector superfields, $\mathcal{L}_{\mathcal{W}}$. A set of kinetic terms for the chiral superfields consistent with the requirements of SUSY and gauge invariance can be obtained from the D-term of the vector superfield [654],

$$\begin{aligned} \mathcal{L}_{\hat{\Phi}} &= \left[\hat{\Phi}^{\dagger I}(e^{\hat{V}})_I{}^J\hat{\Phi}_J\right]_D & \text{(A.28)} \\ &= (\nabla^\mu\phi)^{\dagger I}(\nabla_\mu\phi)_I + i\bar{\psi}^I\bar{\sigma}^\mu(\nabla_\mu\psi)_I - \sqrt{2}g_i\left[\bar{\lambda}_i^a\bar{\psi}^I(T_i^a)_I{}^J\phi_J + h.c.\right] \\ &\quad + F^{\dagger I}F_I + g_iD_i^a\phi^{\dagger I}(T_i^a)_I{}^J\phi_J \,, & \text{(A.29)} \end{aligned}$$

where ∇^μ is the usual gauge covariant derivative,

$$(\nabla^\mu)_I{}^J = \partial^\mu\delta_I^J + ig_iA_i^{\mu a}(T_i^a)_I{}^J \,. \tag{A.30}$$

The second expression, Eq. (A.29), is obtained by specialising to Wess-Zumino gauge and explicitly calculating the result in terms of component fields; nevertheless, the result is supergauge invariant and therefore holds more generally. Kinetic terms for the fields F_I and D_i^a are absent, so that they play the role of auxiliary fields as expected and may be integrated out.

Since the chiral covariant derivatives, Eq. (A.15), are linear differential operators and satisfy a product rule, products of left-chiral superfields are themselves left-chiral superfields, and similarly products of right-chiral superfields are also right-chiral superfields. Thus the F-term of any such product will be SUSY invariant. SUSY analogues of the ordinary Yukawa couplings and mass terms are incorporated into the model by taking [104]

$$\mathcal{L}_{\text{int}} = \left[\hat{W}(\hat{\Phi}_I) + h.c.\right]_F \,, \tag{A.31}$$

where the function $\hat{W}(\hat{\Phi}_I)$ has mass dimension 3 and is known as the superpotential. The requirement that $\hat{W}$ be a left-chiral superfield implies that it is a function only of the left-chiral superfields $\hat{\Phi}_I$, i.e., it is holomorphic in the $\hat{\Phi}_I$. Up to this restriction, $\hat{W}$ may contain any terms consistent with gauge invariance. A general, renormalisable superpotential takes the form [645]

$$\hat{W}(\hat{\Phi}_I) = \frac{1}{6}Y^{IJK}\hat{\Phi}_I\hat{\Phi}_J\hat{\Phi}_K + \frac{1}{2}\mu^{IJ}\hat{\Phi}_I\hat{\Phi}_J + L^I\hat{\Phi}_I \,, \tag{A.32}$$

where invariance under SUSY requires that the couplings Y^{IJK} and μ^{IJ} be totally symmetric in their indices. Similarly, the linear couplings L^I are allowed only for those superfields that are gauge singlets.

The remaining part of the Lagrangian, $\mathcal{L}_{\mathcal{W}}$, contains the gauge kinetic terms as well as additional contributions dictated by invariance under SUSY. The appropriate terms are obtained [654] by introducing the left- and right-chiral superfields

$$\mathcal{W}_\alpha = -\frac{1}{4}\overline{\mathcal{D}\mathcal{D}}\left(e^{-\hat{V}}\mathcal{D}_\alpha e^{\hat{V}}\right), \quad \overline{\mathcal{W}}^{\dot{\alpha}} = -\frac{1}{4}\mathcal{D}\mathcal{D}\left(e^{\hat{V}}\overline{\mathcal{D}}^{\dot{\alpha}} e^{-\hat{V}}\right). \tag{A.33}$$

These field strengths transform covariantly under supergauge transformations,

$$\mathcal{W}_\alpha \to e^{-i\hat{\Lambda}}\mathcal{W}_\alpha e^{i\hat{\Lambda}}, \quad \overline{\mathcal{W}}^{\dot{\alpha}} \to e^{i\hat{\Lambda}}\overline{\mathcal{W}}^{\dot{\alpha}} e^{-i\hat{\Lambda}}, \tag{A.34}$$

and consequently a gauge invariant contribution to the action can be produced by taking the F-term

$$\mathcal{L}_{\mathcal{W}} = \frac{1}{16k_i^2 g_i^2}\,\mathrm{Tr}\left[\mathcal{W}\mathcal{W} + \overline{\mathcal{W}\mathcal{W}}\right]_F \tag{A.35}$$

$$= i\bar{\lambda}_i^a \bar{\sigma}^\mu (\nabla_\mu \lambda_i)^a - \frac{1}{4}F^a_{i\mu\nu}F_i^{a\mu\nu} + \frac{1}{2}D_i^a D_i^a, \tag{A.36}$$

where k_i is the Dynkin index of the representation and $F^a_{i\mu\nu}$ is the ordinary field strength tensor for the product group G_i,

$$F^a_{i\mu\nu} = \partial_\mu A^a_{i\nu} - \partial_\nu A^a_{i\mu} - g_i f_i^{abc} A^b_{i\mu} A^c_{i\nu}. \tag{A.37}$$

The expression in terms of component fields follows by making the definition

$$\mathcal{W}_\alpha = 2g_i \mathcal{W}^a_{i\alpha} T_i^a \tag{A.38}$$

and evaluating the above F-term in Wess-Zumino gauge. Note that, in general one could also include a generalisation of the CP-violating θ-term [84], of the form

$$\mathcal{L}_{\mathcal{W},\Theta} = -i\frac{g_i^2\Theta_i}{32\pi^2}\left[\mathcal{W}_i^{a\alpha}\mathcal{W}^a_{i\alpha}\right]_F + h.c., \tag{A.39}$$

which may have non-trivial effects for non-Abelian gauge groups. Additionally, for vector superfields $\hat{V}_i$ associated with $U(1)$ factors, a Fayet-Iliopoulos term [169],

$$\mathcal{L}_{FI} = -2\kappa[\hat{V}_i]_D, \tag{A.40}$$

can be present. Such terms are not gauge invariant, and therefore are forbidden, for non-Abelian vector superfields.

The full Lagrangian, expressed in terms of component fields, is thus

$$\begin{aligned}\mathcal{L} = &(\nabla^\mu\phi)^{\dagger I}(\nabla_\mu\phi)_I + i\bar{\psi}^I\bar{\sigma}^\mu(\nabla_\mu\psi)_I + i\bar{\lambda}_i^a\bar{\sigma}^\mu(\nabla_\mu\lambda_i)^a - \frac{1}{4}F^a_{i\mu\nu}F_i^{a\mu\nu} \\ &- \sqrt{2}g_i\left[\bar{\lambda}_i^a\bar{\psi}^I(T_i^a)_I{}^J\phi_J + h.c.\right] - V(\phi_I,\phi^{\dagger J}) \\ &- \left[\frac{1}{2}\psi_I\psi_J\left.\frac{\partial^2\hat{W}}{\partial\hat{\Phi}_I\partial\hat{\Phi}_J}\right|_{\theta=\bar{\theta}=0} + h.c.\right], \end{aligned} \tag{A.41}$$

where the scalar potential is given by

$$V(\phi_I,\phi^{\dagger J}) = F^{\dagger I}F_I + \frac{1}{2}D_i^aD_i^a\,. \tag{A.42}$$

Note in particular that this is a sum of squares, so that $V \geq 0$. As mentioned above, the fields F_I and D_i^a lack kinetic terms, and can be eliminated by making use of the equations of motion to write

$$F_I = -\left.\frac{\partial\hat{W}^\dagger}{\partial\hat{\Phi}^{\dagger I}}\right|_{\theta=\bar{\theta}=0}, \quad D_i^a = -g_i\phi^{\dagger I}(T_i^a)_I{}^J\phi_J \quad \text{(no sum over } i)\,, \tag{A.43}$$

leading to the scalar potential being expressed in terms of the physical scalar fields ϕ_I. For phenomenologically viable models of SUSY, the resulting SUSY invariant interactions must be supplemented by a set of soft SUSY breaking interactions as well. These may be added explicitly or SUSY may be spontaneously broken, as discussed in Section 2.1 and Section 2.3.

Appendix B

Approximate RGE Solutions in the MSSM

In this appendix we present the approximate solutions to the two-loop RGEs in the MSSM required for the fine tuning calculation of Chapter 5. The solution for a parameter p is found by expanding the exact solution for p obtained from the RGEs and keeping the two-loop leading- and next-to-leading log contributions. This yields the approximation

$$p(M_S) \approx p(M_X) + \frac{t}{16\pi^2}\left(\beta_p^{(1)} + \frac{\beta_p^{(2)}}{16\pi^2}\right) + \frac{t^2}{(16\pi^2)^2} b_p^{(2)}(M_X)\,, \tag{B.1}$$

where $\beta_p^{(n)}$ is the n-loop contribution to the β function for p and $t = \ln(M_S/M_X)$. For brevity, we have defined

$$b_p^{(2)}(M_X) = \frac{1}{2}\sum_{q_k} \beta_{q_k}^{(1)} \frac{\partial \beta_p^{(1)}}{\partial q_k}\,, \tag{B.2}$$

where the sum over all running parameters q_k that appear in $\beta_p^{(1)}$ is evaluated at M_X. Provided that M_S and M_X are not too widely separated, Eq. (B.1) is a reasonable approximation to the exact solution to the RGE for p. For the analytical fine tuning calculation, these solutions must be constructed for all of the parameters appearing in the EWSB conditions. In the MSSM, to simplify the calculations we apply pMSSM-like boundary conditions. That is, the first and second generation Yukawa couplings and soft SUSY breaking trilinears are neglected, since they are small. The soft scalar masses are also taken to be diagonal, and the soft gaugino masses are assumed to be real. We also use the less cumbersome notation $y_t \equiv y_{33}^U$, $y_b \equiv y_{33}^D$, $y_\tau \equiv y_{33}^E$ and define $A_t \equiv T_{33}^U/y_{33}^U$, $A_b \equiv T_{33}^D/y_{33}^D$ and $A_\tau \equiv T_{33}^E/y_{33}^E$.

At tree-level, the parameters relevant for computing the fine tuning in the MSSM are μ, $B \equiv B\mu/\mu$, $m_{H_u}^2$ and $m_{H_d}^2$. The one- and two-loop MSSM β functions are well known [208, 459], so we do not reproduce them here. The corresponding $O(t^2)$ contributions for each of these parameters are

$$\begin{aligned}
b_\mu^{(2)} &= \frac{\mu}{2}\Bigg[45y_t^4 + 45y_b^4 + 9y_\tau^4 + 30y_t^2y_b^2 + 6y_t^2y_\tau^2 + 18y_b^2y_\tau^2 - 32g_3^2(y_t^2+y_b^2) \\
&\quad - 12g_2^2(3y_t^2+3y_b^2+y_\tau^2) - \frac{4}{5}g_1^2(11y_t^2+8y_b^2+6y_\tau^2) + 3g_2^4 \\
&\quad - \frac{189}{25}g_1^4 + \frac{18}{5}g_1^2g_2^2\Bigg], \qquad \text{(B.3a)} \\
b_B^{(2)} &= 72y_t^4A_t + 72y_b^4A_b + 16y_\tau^4A_\tau + 12y_t^2y_b^2(A_t+A_b) + 12y_\tau^2y_b^2(A_b+A_\tau) \\
&\quad - 32g_3^2y_t^2(A_t-M_3) - 32g_3^2y_b^2(A_b-M_3) \\
&\quad - 18g_2^2y_t^2(A_t-M_2) - 18g_2^2y_b^2(A_b-M_2) - 6g_2^2y_\tau^2(A_\tau-M_2) \\
&\quad - \frac{26}{5}g_1^2y_t^2(A_t-M_1) - \frac{14}{5}g_1^2y_b^2(A_b-M_1) - \frac{18}{5}g_1^2y_\tau^2(A_\tau-M_1) \\
&\quad + 12g_2^4M_2 + \frac{396}{25}g_1^4M_1\,, \qquad \text{(B.3b)} \\
b_{m_{H_d}^2}^{(2)} &= 72y_b^4\left(m_{H_d}^2 + m_{Q_{33}}^2 + m_{d_{33}^c}^2 + 2A_b^2\right) \\
&\quad + 6y_t^2y_b^2\left[m_{H_u}^2 + m_{H_d}^2 + 2m_{Q_{33}}^2 + m_{u_{33}^c}^2 + m_{d_{33}^c}^2 + (A_t+A_b)^2\right] \\
&\quad + 12y_\tau^2y_b^2\left[2m_{H_d}^2 + m_{Q_{33}}^2 + m_{d_{33}^c}^2 + m_{L_{33}}^2 + m_{e_{33}^c}^2 + (A_\tau+A_b)^2\right] \\
&\quad + 16y_\tau^4\left(m_{H_d}^2 + m_{L_{33}}^2 + m_{e_{33}^c}^2 + 2A_\tau^2\right) \\
&\quad - 32g_3^2y_b^2\left(m_{H_d}^2 + m_{Q_{33}}^2 + m_{d_{33}^c}^2 + A_b^2 - 2M_3A_b + 2M_3^2\right) \\
&\quad - 18g_2^2y_b^2\left(m_{H_d}^2 + m_{Q_{33}}^2 + m_{d_{33}^c}^2 + A_b^2 - 2M_2A_b + 2M_2^2\right) \\
&\quad - 6g_2^2y_\tau^2\left(m_{H_d}^2 + m_{L_{33}}^2 + m_{e_{33}^c}^2 + A_\tau^2 - 2M_2A_\tau + 2M_2^2\right) \\
&\quad - \frac{14}{5}g_1^2y_b^2\left(m_{H_d}^2 + m_{Q_{33}}^2 + m_{d_{33}^c}^2 + A_b^2 - 2M_1A_b + 2M_1^2\right) \\
&\quad - \frac{18}{5}g_1^2y_\tau^2\left(m_{H_d}^2 + m_{L_{33}}^2 + m_{e_{33}^c}^2 + A_\tau^2 - 2M_1A_\tau + 2M_1^2\right) \\
&\quad - 18g_2^4M_2^2 - \frac{198}{25}g_1^4\left(\mathcal{S} + 3M_1^2\right)\,, \qquad \text{(B.3c)} \\
b_{m_{H_u}^2}^{(2)} &= 72y_t^4\left(m_{H_u}^2 + m_{Q_{33}}^2 + m_{u_{33}^c}^2 + 2A_t^2\right) \\
&\quad + 6y_t^2y_b^2\left[m_{H_u}^2 + m_{H_d}^2 + 2m_{Q_{33}}^2 + m_{u_{33}^c}^2 + m_{d_{33}^c}^2 + (A_t+A_b)^2\right] \\
&\quad - 32g_3^2y_t^2\left(m_{H_u}^2 + m_{Q_{33}}^2 + m_{u_{33}^c}^2 + A_t^2 - 2A_tM_3 + 2M_3^2\right) \\
&\quad - 18g_2^2y_t^2\left(m_{H_u}^2 + m_{Q_{33}}^2 + m_{u_{33}^c}^2 + A_t^2 - 2A_tM_2 + 2M_2^2\right)
\end{aligned}$$

$$
\begin{aligned}
&- \frac{26}{5} g_1^2 y_t^2 \left(m_{H_u}^2 + m_{Q_{33}}^2 + m_{u_{33}^c}^2 + A_t^2 - 2 A_t M_1 + 2 M_1^2 \right) \\
&- 18 g_2^4 M_2^2 + \frac{198}{25} g_1^4 \left(\mathcal{S} - 3 M_1^2 \right) . \qquad \text{(B.3d)}
\end{aligned}
$$

In these expressions the quantity $\mathcal{S}$ is defined by

$$
\mathcal{S} = m_{H_u}^2 - m_{H_d}^2 + \mathrm{Tr}(m_Q^2) - \mathrm{Tr}(m_L^2) - 2\,\mathrm{Tr}(m_{u^c}^2) + \mathrm{Tr}(m_{d^c}^2) + \mathrm{Tr}(m_{e^c}^2) . \qquad \text{(B.4)}
$$

If, in addition, the one-loop contributions to the effective potential from top and stop loops are included, it is also necessary to construct the expansions for $m_{Q_{33}}^2$, $m_{u_{33}^c}^2$ and A_t. The $O(t^2)$ contributions read

$$
\begin{aligned}
b^{(2)}_{m_{Q_{33}}^2} &= 24 y_t^4 \left(m_{H_u}^2 + m_{Q_{33}}^2 + m_{u_{33}^c}^2 + 2 A_t^2 \right) + 24 y_b^4 \left(m_{H_d}^2 + m_{Q_{33}}^2 + m_{d_{33}^c}^2 + 2 A_b^2 \right) \\
&\quad + 4 y_t^2 y_b^2 \left[m_{H_u}^2 + m_{H_d}^2 + 2 m_{Q_{33}}^2 + m_{u_{33}^c}^2 + m_{d_{33}^c}^2 + (A_t + A_b)^2 \right] \\
&\quad + 2 y_b^2 y_\tau^2 \left[2 m_{H_d}^2 + m_{Q_{33}}^2 + m_{L_{33}}^2 + m_{d_{33}^c}^2 + m_{e_{33}^c}^2 + (A_b + A_\tau)^2 \right] \\
&\quad - \frac{32}{3} g_3^2 y_t^2 \left(m_{H_u}^2 + m_{Q_{33}}^2 + m_{u_{33}^c}^2 + A_t^2 - 2 M_3 A_t + 2 M_3^2 \right) \\
&\quad - \frac{32}{3} g_3^2 y_b^2 \left(m_{H_d}^2 + m_{Q_{33}}^2 + m_{d_{33}^c}^2 + A_b^2 - 2 M_3 A_b + 2 M_3^2 \right) \\
&\quad - 6 g_2^2 y_t^2 \left(m_{H_u}^2 + m_{Q_{33}}^2 + m_{u_{33}^c}^2 + A_t^2 - 2 M_2 A_t + 2 M_2^2 \right) \\
&\quad - 6 g_2^2 y_b^2 \left(m_{H_d}^2 + m_{Q_{33}}^2 + m_{d_{33}^c}^2 + A_b^2 - 2 M_2 A_b + 2 M_2^2 \right) \\
&\quad - \frac{26}{15} g_1^2 y_t^2 \left(m_{H_u}^2 + m_{Q_{33}}^2 + m_{u_{33}^c}^2 + A_t^2 - 2 M_1 A_t + 2 M_1^2 \right) \\
&\quad - \frac{14}{15} g_1^2 y_b^2 \left(m_{H_d}^2 + m_{Q_{33}}^2 + m_{d_{33}^c}^2 + A_b^2 - 2 M_1 A_b + 2 M_1^2 \right) \\
&\quad + 96 g_3^4 M_3^2 - 18 g_2^4 M_2^2 + \frac{66}{25} g_1^4 (\mathcal{S} - M_1^2) , \qquad \text{(B.5a)} \\
b^{(2)}_{m_{u_{33}^c}^2} &= 48 y_t^4 \left(m_{H_u}^2 + m_{Q_{33}}^2 + m_{u_{33}^c}^2 + 2 A_t^2 \right) \\
&\quad + 4 y_t^2 y_b^2 \left[m_{H_u}^2 + m_{H_d}^2 + 2 m_{Q_{33}}^2 + m_{u_{33}^c}^2 + m_{d_{33}^c}^2 + (A_t + A_b)^2 \right] \\
&\quad - \frac{64}{3} g_3^2 y_t^2 \left(m_{H_u}^2 + m_{Q_{33}}^2 + m_{u_{33}^c}^2 + A_t^2 - 2 M_3 A_t + 2 M_3^2 \right) \\
&\quad - 12 g_2^2 y_t^2 \left(m_{H_u}^2 + m_{Q_{33}}^2 + m_{u_{33}^c}^2 + A_t^2 - 2 M_2 A_t + 2 M_2^2 \right) \\
&\quad - \frac{52}{15} g_1^2 y_t^2 \left(m_{H_u}^2 + m_{Q_{33}}^2 + m_{u_{33}^c}^2 + A_t^2 - 2 M_1 A_t + 2 M_1^2 \right) \\
&\quad + 96 g_3^4 M_3^2 - \frac{264}{25} g_1^4 \left(\mathcal{S} + 4 M_1^2 \right) , \qquad \text{(B.5b)} \\
b^{(2)}_{A_t} &= 144 y_t^4 A_t + 24 y_b^4 A_b + 14 y_t^2 y_b^2 (A_t + A_b) + 2 y_b^2 y_\tau^2 (A_b + A_\tau)
\end{aligned}
$$

$$
\begin{aligned}
&- 64 g_3^2 y_t^2 (A_t - M_3) - 36 g_2^2 y_t^2 (A_t - M_2) - \frac{52}{5} g_1^2 y_t^2 (A_t - M_1) \\
&- \frac{32}{3} g_3^2 y_b^2 (A_b - M_3) - 6 g_2^2 y_b^2 (A_b - M_2) - \frac{14}{15} g_1^2 y_b^2 (A_b - M_1) \\
&- 64 g_3^4 M_3 + 12 g_2^4 M_2 + \frac{572}{25} g_1^4 M_1 \,. \qquad \text{(B.5c)}
\end{aligned}
$$

Appendix C

Approximate RGE Solutions in the E_6SSM

Approximate analytic solutions to the two-loop RGEs of the E_6SSM can be obtained in a similar way to as in the MSSM. In this appendix, we present the results for a general set of $U(1)'$ charges, assuming the superpotential and soft terms are otherwise the same as for the E_6SSM, Eq. (3.10) and Eq. (3.11). Two-loop RGEs for the gauge and Yukawa couplings, gaugino masses and soft trilinears, along with the one-loop RGEs for the soft scalar masses, were originally obtained in Ref. [363]. The results presented in Chapter 5 are obtained using the full[1] two-loop RGEs calculated by `SARAH`, which, for the E_6 inspired models considered here, are based on the general results presented in Refs. [383, 459]. This allows the RGEs to be calculated in models with multiple non-orthogonal $U(1)$ gauge symmetries, where the trace of matrix formed from the $U(1)_Y$ charges and the additional $U(1)'$ does not vanish, that is,

$$\sum_{\Phi} Q_{\Phi}^{Y} Q'_{\Phi} \neq 0\,, \tag{C.1}$$

where Q_{Φ}^{Y} and Q'_{Φ} are the $U(1)_Y$ and $U(1)'$ charges of the field Φ, respectively.

When the trace in Eq. (C.1) is non-zero, gauge kinetic mixing will be generated during the RG evolution. In the E_6 inspired models considered in this thesis, this is the case due to the presence of the incomplete multiplets such as $\hat{L}_4$ and $\hat{\overline{L}}_4$; if the

[1]The version of `SARAH` used to generate the expressions presented here is missing extra terms associated with the multiple, non-orthogonal $U(1)$ symmetries that appear in the RGEs for the trilinear and bilinear soft masses. For consistency we present the expressions required to reproduce the results of Chapter 5, but the reader should be aware that there are in general small, additional contributions to the β functions for the soft trilinears and bilinears that are not included here.

models contained only complete **27**-plets then this trace would vanish. As discussed in Section 3.2, if the off-diagonal gauge coupling vanishes at the GUT scale, then a small value of g_{11} results at the EW scale. For example, $g_{11} \approx 0.02$ in the E$_6$SSM [278], and so it does not play a large role. Since the induced kinetic mixing is small, and the general RGEs including its effects are very large and unwieldy, in the expressions shown here gauge kinetic mixing is neglected[2].

At tree-level in the EWSB conditions the parameters that must be considered are λ, T_λ, $m^2_{H_u}$, $m^2_{H_d}$, m^2_S and g_1, g_2 and g'_1. When kinetic mixing is neglected, the one- and two-loop contributions to the β functions for the relevant gauge couplings read

$$\beta^{(1)}_{g_1} = \frac{48}{5} g_1^3 \,, \tag{C.2a}$$

$$\beta^{(2)}_{g_1} = \frac{2}{25} g_1^3 \Big(30 g_1'^2 \Pi^Y_Q + 117 g_1^2 + 135 g_2^2 + 300 g_3^2 - 10\Sigma_\kappa - 15\Sigma_\lambda - 65 y_t^2 - 35 y_b^2 - 45 y_\tau^2 \Big) \,, \tag{C.2b}$$

$$\beta^{(1)}_{g_2} = 4 g_2^3 \,, \tag{C.2c}$$

$$\beta^{(2)}_{g_2} = \frac{2}{5} g_2^3 \Big(5 g_1'^2 \Pi^L_Q + 9 g_1^2 + 115 g_2^2 + 60 g_3^2 - 5\Sigma_\lambda - 15 y_t^2 - 15 y_b^2 - 5 y_\tau^2 \Big) \,, \tag{C.2d}$$

$$\beta^{(1)}_{g'_1} = g_1'^3 \Sigma_Q \,, \tag{C.2e}$$

$$\beta^{(2)}_{g'_1} = \frac{2}{5} g_1'^3 \Big[-15\Sigma_\kappa \Big(Q^2_{\bar{D}} + Q^2_D + Q^2_S \Big) - 30 y_b^2 \Big(Q^2_{d^c} + Q^2_1 + Q^2_Q \Big) + 120 g_3^2 \Pi^C_Q - 10 y_\tau^2 \Big(Q^2_{e^c} + Q^2_L + Q^2_1 \Big) + 15 g_2^2 \Pi^L_Q + 10 g_1'^2 \Pi_Q + 6 g_1^2 \Pi^Y_Q - 10\Sigma_\lambda \Big(Q^2_S + Q^2_1 + Q^2_2 \Big) - 30 y_t^2 \Big(Q^2_{u^c} + Q^2_2 + Q^2_Q \Big) \Big] \,, \tag{C.2f}$$

where the full β functions are as given in Eq. (5.27) and Q_Φ is the $U(1)'$ charge for the field Φ. As in the MSSM, the first and second generation Yukawa couplings are neglected, along with their associated soft trilinears in the RGEs for the soft masses below. In order to keep these expressions compact, we use the notation

$$\Sigma_Q = \sum_\Phi Q^2_\Phi = \frac{321}{40} \cos^2\theta_{E_6} + \frac{217}{24} \sin^2\theta_{E_6} + \frac{27}{8\sqrt{15}} \sin 2\theta_{E_6}$$

[2] In `SARAH`, this is achieved by means of a Boolean flag, `NoU1Mixing`, which fixes the β functions for the off-diagonal gauge couplings and $U(1)$ gaugino masses to be zero at all scales.

to denote the trace over the $U(1)'$ charges, along with[3]

$$\begin{aligned}
\Sigma_Q^Y &= \sum_\Phi \sqrt{\frac{5}{3}} Q_\Phi^Y Q_\Phi = -\frac{3}{\sqrt{10}} \cos\theta_{E_6} - \frac{1}{\sqrt{6}} \sin\theta_{E_6} \,, \\
\Pi_Q &= \sum_\Phi Q_\Phi^4 = \frac{2049}{1600} \cos^4\theta_{E_6} + \frac{483}{80\sqrt{15}} \cos^3\theta_{E_6} \sin\theta_{E_6} + \frac{681}{160} \cos^2\theta_{E_6} \sin^2\theta_{E_6} \\
&\qquad + \frac{9}{16\sqrt{15}} \cos\theta_{E_6} \sin^3\theta_{E_6} + \frac{1297}{576} \sin^4\theta_{E_6} \,, \\
\Pi_Q^Y &= \sum_\Phi \left(\sqrt{\frac{5}{3}} Q_\Phi^Y \right)^2 Q_\Phi^2 = \frac{59}{40} \cos^2\theta_{E_6} + \frac{31}{24} \sin^2\theta_{E_6} + \frac{3}{8\sqrt{15}} \sin 2\theta_{E_6} \,, \\
\Pi_Q^L &= 3Q_1^2 + 3Q_2^2 + Q_{L_4}^2 + Q_{\overline{L}_4}^2 + 3Q_L^2 + 9Q_Q^2 \\
&= \frac{39}{20} \cos^2\theta_{E_6} + \frac{19}{12} \sin^2\theta_{E_6} + \frac{3}{4\sqrt{15}} \sin 2\theta_{E_6} \,, \\
\Pi_Q^C &= Q_{d^c}^2 + Q_D^2 + Q_{\overline{D}}^2 + 2Q_Q^2 + Q_{u^c}^2 \,.
\end{aligned}$$

In these expressions the $U(1)_Y$ and $U(1)'$ charges are assumed to be GUT-normalised. The expressions in terms of the E_6 mixing angle θ_{E_6} follow from the definition, Eq. (3.5), of the additional $U(1)'$, with the charge assignments as given in Table 3.1. They hold provided that $U(1)$ mixing is neglected. Similarly, we write

$$\begin{aligned}
\Sigma_\lambda &= \tilde{\lambda}_{11}^2 + \tilde{\lambda}_{22}^2 + \lambda^2 \,, \qquad & \Sigma_\kappa &= \kappa_{11}^2 + \kappa_{22}^2 + \kappa_{33}^2 \,, \\
\Pi_\lambda &= \tilde{\lambda}_{11}^4 + \tilde{\lambda}_{22}^4 + \lambda^4 \,, \qquad & \Pi_\kappa &= \kappa_{11}^4 + \kappa_{22}^4 + \kappa_{33}^4 \,.
\end{aligned}$$

The corresponding $O(t^2)$ coefficients for the gauge couplings are simply

$$b_{g_1}^{(2)} = \frac{3456}{25} g_1^5 \,, \tag{C.3a}$$

$$b_{g_2}^{(2)} = 24 g_2^5 \,, \tag{C.3b}$$

$$b_{g_1'}^{(2)} = \frac{3}{2} g_1'^5 \Sigma_Q^2 \,. \tag{C.3c}$$

[3]The first of these is the trace in Eq. (C.1), which is assumed to vanish in Ref. [459]. In `SARAH`, $U(1)$ mixing is neglected by removing the RGEs for the off-diagonal gauge couplings and settings these couplings to zero in all of the remaining RGEs. This still leaves some terms involving this trace, and so the RGEs shown here do not reduce to those which would be obtained from Refs. [363, 459] unless $\Sigma_Q^Y = 0$. Note also that these contributions in the soft trilinear and bilinear RGEs have been missed in the version of `SARAH` used to generate them.

The one- and two-loop contributions to the β function for λ and the $O(t^2)$ coefficient in the series expansion are

$$\begin{aligned}
\beta_\lambda^{(1)} &= \lambda\Big[2\lambda^2 + 2\Sigma_\lambda + 3\Sigma_\kappa + 3y_t^2 + 3y_b^2 + y_\tau^2 - 3g_2^2 - \frac{3}{5}g_1^2 \\
&\quad - 2\left(Q_1^2 + Q_2^2 + Q_S^2\right)g_1'^2\Big], \qquad \text{(C.4a)} \\
\beta_\lambda^{(2)} &= \lambda\Big\{ - 2\lambda^2\left(\lambda^2 + 2\Sigma_\lambda + 3\Sigma_\kappa\right) - 4\Pi_\lambda - 6\Pi_\kappa - 3\lambda^2\left(3y_t^2 + 3y_b^2 + y_\tau^2\right) \\
&\quad - 3\left(3y_t^4 + 3y_b^4 + 2y_t^2y_b^2 + y_\tau^4\right) + 6g_2^2\Sigma_\lambda + \frac{2}{5}g_1^2\left(2y_t^2 - y_b^2 + 3y_\tau^2 + 2\Sigma_\kappa + 3\Sigma_\lambda\right) \\
&\quad + g_1'^2\Big[4Q_S^2\lambda^2 - 6\left(Q_2^2 - Q_Q^2 - Q_{u^c}^2\right)y_t^2 - 6\left(Q_1^2 - Q_Q^2 - Q_{d^c}^2\right)y_b^2 \\
&\quad - 2\left(Q_1^2 - Q_L^2 - Q_{e^c}^2\right)y_\tau^2 - 6\left(Q_S^2 - Q_D^2 - Q_{\overline{D}}^2\right)\Sigma_\kappa - 4\left(Q_S^2 - Q_1^2 - Q_2^2\right)\Sigma_\lambda\Big] \\
&\quad + 16g_3^2\left(y_t^2 + y_b^2 + \Sigma_\kappa\right) + \frac{33}{2}g_2^4 + \frac{297}{50}g_1^4 + 2g_1'^4\Big[2Q_1^4 + 2Q_2^4 + 2Q_S^4 \\
&\quad + \left(Q_1^2 + Q_2^2 + Q_S^2\right)\Sigma_Q\Big] + \frac{9}{5}g_1^2g_2^2 + 6g_1'^2g_2^2\left(Q_1^2 + Q_2^2\right) \\
&\quad + \frac{6}{5}g_1^2g_1'^2\left[Q_1^2 + Q_2^2 + (Q_2 - Q_1)\,\Sigma_Q^Y\right]\Big\}, \qquad \text{(C.4b)} \\
b_\lambda^{(2)} &= \lambda\Big\{2\lambda^2\left(3\lambda^2 + 4\Sigma_\lambda + 6\Sigma_\kappa\right) + 4\Pi_\lambda + 6\Pi_\kappa + 6\left(\Sigma_\lambda + \frac{3}{2}\Sigma_\kappa\right)^2 \\
&\quad + 7\lambda^2\left(3y_t^2 + 3y_b^2 + y_\tau^2\right) + \left(3y_t^2 + 3y_b^2 + y_\tau^2\right)(2\Sigma_\lambda + 3\Sigma_\kappa) \\
&\quad + 3\left(\frac{15}{2}y_t^4 + \frac{15}{2}y_b^4 + \frac{3}{2}y_\tau^4 + 5y_b^2y_t^2 + 3y_b^2y_\tau^2 + y_t^2y_\tau^2\right) \\
&\quad - \frac{1}{5}g_1^2\left(12\lambda^2 + 16y_b^2 + 22y_t^2 + 12y_\tau^2 + 12\Sigma_\lambda + 13\Sigma_\kappa\right) \\
&\quad - 3g_2^2\left(4\lambda^2 + 6y_t^2 + 6y_b^2 + 2y_\tau^2 + 4\Sigma_\lambda + 3\Sigma_\kappa\right) - 16g_3^2\left(y_t^2 + y_b^2 + \Sigma_\kappa\right) \\
&\quad - 2g_1'^2\Big[4\left(Q_1^2 + Q_2^2 + Q_S^2\right)\left(\lambda^2 + \Sigma_\lambda\right) + 3\Sigma_\kappa\left(Q_1^2 + Q_2^2 + Q_S^2 + Q_D^2 + Q_{\overline{D}}^2\right) \\
&\quad + 3y_b^2\left(2Q_1^2 + Q_2^2 + Q_{d^c}^2 + Q_Q^2 + Q_S^2\right) + 3y_t^2\left(Q_1^2 + 2Q_2^2 + Q_Q^2 + Q_S^2 + Q_{u^c}^2\right) \\
&\quad + y_\tau^2\left(2Q_1^2 + Q_2^2 + Q_{e^c}^2 + Q_L^2 + Q_S^2\right)\Big] - \frac{15}{2}g_2^4 - \frac{279}{50}g_1^4 \\
&\quad + 2g_1'^4\left(Q_1^2 + Q_2^2 + Q_S^2\right)\left(Q_1^2 + Q_2^2 + Q_S^2 - \Sigma_Q\right) + \frac{9}{5}g_1^2g_2^2 \\
&\quad + 6g_1'^2g_2^2\left(Q_1^2 + Q_2^2 + Q_S^2\right) + \frac{6}{5}g_1^2g_1'^2\left(Q_1^2 + Q_2^2 + Q_S^2\right)\Big\}. \qquad \text{(C.4c)}
\end{aligned}$$

Using the shorthand notation $T_t \equiv T^U_{33}$, $T_b \equiv T^D_{33}$ and $T_\tau \equiv T^E_{33}$, the expressions for the corresponding soft trilinear T_λ read

$$\begin{aligned}
\beta^{(1)}_{T_\lambda} &= T_\lambda\Big[2\lambda^2 + 2\Sigma_\lambda + 3\Sigma_\kappa + 3y_t^2 + 3y_b^2 + y_\tau^2 - 3g_2^2 - \frac{3}{5}g_1^2 - 2\left(Q_1^2 + Q_2^2 + Q_S^2\right)g_1'^2\Big] \\
&\quad + \lambda\Big[4\lambda T_\lambda + 4\Sigma_{T_\lambda} + 6\Sigma_{T_\kappa} + 6y_tT_t + 6y_bT_b + 2y_\tau T_\tau + 6g_2^2M_2 + \frac{6}{5}g_1^2M_1 \\
&\quad + 4g_1'^2M_1'\left(Q_1^2 + Q_2^2 + Q_S^2\right)\Big], \qquad \text{(C.5a)} \\
\beta^{(2)}_{T_\lambda} &= T_\lambda\Big\{ - 2\lambda^2\left(\lambda^2 + 2\Sigma_\lambda + 3\Sigma_\kappa\right) - 4\Pi_\lambda - 6\Pi_\kappa - 3\lambda^2\left(3y_t^2 + 3y_b^2 + y_\tau^2\right) \\
&\quad - 3\left(3y_t^4 + 3y_b^4 + 2y_t^2y_b^2 + y_\tau^4\right) + 6g_2^2\Sigma_\lambda + \frac{2}{5}g_1^2\left(2y_t^2 - y_b^2 + 3y_\tau^2 + 2\Sigma_\kappa + 3\Sigma_\lambda\right) \\
&\quad + g_1'^2\Big[4Q_S^2\lambda^2 - 6\left(Q_2^2 - Q_Q^2 - Q_{u^c}^2\right)y_t^2 - 6\left(Q_1^2 - Q_Q^2 - Q_{d^c}^2\right)y_b^2 \\
&\quad - 2\left(Q_1^2 - Q_L^2 - Q_{e^c}^2\right)y_\tau^2 - 6\left(Q_S^2 - Q_D^2 - Q_{\overline{D}}^2\right)\Sigma_\kappa - 4\left(Q_S^2 - Q_1^2 - Q_2^2\right)\Sigma_\lambda\Big] \\
&\quad + 16g_3^2\left(y_t^2 + y_b^2 + \Sigma_\kappa\right) + \frac{33}{2}g_2^4 + \frac{297}{50}g_1^4 + 2g_1'^4\Big[2Q_1^4 + 2Q_2^4 + 2Q_S^4 \\
&\quad + \left(Q_1^2 + Q_2^2 + Q_S^2\right)\Sigma_Q\Big] + \frac{9}{5}g_1^2g_2^2 + 6g_1'^2g_2^2\left(Q_1^2 + Q_2^2\right) + \frac{6}{5}g_1^2g_1'^2\left(Q_1^2 + Q_2^2\right)\Big\} \\
&\quad + \lambda\Big\{ - 4\lambda T_\lambda\left(\lambda^2 + 2\Sigma_\lambda + 3\Sigma_\kappa\right) - 4\lambda^2\left(\lambda T_\lambda + 2\Sigma_{T_\lambda} + 3\Sigma_{T_\kappa}\right) - 16\Pi_{T_\lambda} \\
&\quad - 24\Pi_{T_\kappa} - 6\lambda T_\lambda\left(3y_t^2 + 3y_b^2 + y_\tau^2\right) - 6\lambda^2\left(3y_tT_t + 3y_bT_b + y_\tau T_\tau\right) \\
&\quad - 12\Big[3y_t^3T_t + 3y_b^3T_b + y_ty_b\left(y_tT_b + y_bT_t\right) + y_\tau^3T_\tau\Big] \\
&\quad + 32g_3^2\Big[y_tT_t + y_bT_b + \Sigma_{T_\kappa} - \left(y_t^2 + y_b^2 + \Sigma_\kappa\right)M_3\Big] + 12g_2^2\left(\Sigma_{T_\lambda} - \Sigma_\lambda M_2\right) \\
&\quad + \frac{2}{5}g_1^2\Big[4y_tT_t - 2y_bT_b + 6y_\tau T_\tau + 4\Sigma_{T_\kappa} + 6\Sigma_{T_\lambda} \\
&\quad - 2\left(2y_t^2 - y_b^2 + 3y_\tau^2 + 2\Sigma_\kappa + 3\Sigma_\lambda\right)M_1\Big] \\
&\quad + 4g_1'^2\Big[3y_t\left(Q_Q^2 - Q_2^2 + Q_{u^c}^2\right)\left(T_t - y_tM_1'\right) + 3y_b\left(Q_Q^2 - Q_1^2 + Q_{d^c}^2\right)\left(T_b - y_bM_1'\right) \\
&\quad + y_\tau\left(Q_L^2 - Q_1^2 + Q_{e^c}^2\right)\left(T_\tau - y_\tau M_1'\right) + 2Q_S^2\lambda\left(T_\lambda - \lambda M_1'\right) \\
&\quad + 2\left(Q_1^2 + Q_2^2 - Q_S^2\right)\left(\Sigma_{T_\lambda} - \Sigma_\lambda M_1'\right) + 3\left(Q_D^2 + Q_{\overline{D}}^2 - Q_S^2\right)\left(\Sigma_{T_\kappa} - \Sigma_\kappa M_1'\right)\Big] \\
&\quad - 66g_2^4M_2 - \frac{594}{25}g_1^4M_1 - 8g_1'^4M_1'\Big[2\left(Q_1^4 + Q_2^4 + Q_S^4\right) + \left(Q_1^2 + Q_2^2 + Q_S^2\right)\Sigma_Q\Big] \\
&\quad - \frac{18}{5}g_2^2g_1^2\left(M_2 + M_1\right) - 12g_2^2g_1'^2\left(Q_1^2 + Q_2^2\right)\left(M_2 + M_1'\right)
\end{aligned}$$

$$- \frac{12}{5} g_1^2 g_1'^2 \left(Q_1^2 + Q_2^2\right) \left(M_1 + M_1'\right) \Bigg\}, \tag{C.5b}$$

$$\begin{aligned}
b_{T_\lambda}^{(2)} = \lambda \Bigg[& 4\lambda T_\lambda + 4\Sigma_{T_\lambda} + 6\Sigma_{T_\kappa} + 6 y_t T_t + 6 y_b T_b + 2 y_\tau T_\tau + 6 g_2^2 M_2 + \frac{6}{5} g_1^2 M_1 \\
& + 4 g_1'^2 M_1' \left(Q_1^2 + Q_2^2 + Q_S^2\right) \Bigg] \times \Bigg[2\lambda^2 + 2\Sigma_\lambda + 3\Sigma_\kappa + 3 y_t^2 + 3 y_b^2 + y_\tau^2 - 3 g_2^2 \\
& - \frac{3}{5} g_1^2 - 2 \left(Q_1^2 + Q_2^2 + Q_S^2\right) g_1'^2 \Bigg] + T_\lambda \Bigg\{ 2\lambda^2 \left(3\lambda^2 + 4\Sigma_\lambda + 6\Sigma_\kappa\right) + 4\Pi_\lambda + 6\Pi_\kappa \\
& + 6 \left(\Sigma_\lambda + \frac{3}{2}\Sigma_\kappa\right)^2 + 7\lambda^2 \left(3 y_t^2 + 3 y_b^2 + y_\tau^2\right) + \left(3 y_t^2 + 3 y_b^2 + y_\tau^2\right) \left(2\Sigma_\lambda + 3\Sigma_\kappa\right) \\
& + 3 \left(\frac{15}{2} y_t^4 + \frac{15}{2} y_b^4 + \frac{3}{2} y_\tau^4 + 5 y_b^2 y_t^2 + 3 y_b^2 y_\tau^2 + y_t^2 y_\tau^2\right) \\
& - \frac{1}{5} g_1^2 \left(12\lambda^2 + 16 y_b^2 + 22 y_t^2 + 12 y_\tau^2 + 12\Sigma_\lambda + 13\Sigma_\kappa\right) \\
& - 3 g_2^2 \left(4\lambda^2 + 6 y_t^2 + 6 y_b^2 + 2 y_\tau^2 + 4\Sigma_\lambda + 3\Sigma_\kappa\right) - 16 g_3^2 \left(y_t^2 + y_b^2 + \Sigma_\kappa\right) \\
& - 2 g_1'^2 \Bigg[4 \left(Q_1^2 + Q_2^2 + Q_S^2\right) \left(\lambda^2 + \Sigma_\lambda\right) + 3\Sigma_\kappa \left(Q_1^2 + Q_2^2 + Q_S^2 + Q_D^2 + Q_{\overline{D}}^2\right) \\
& + 3 y_b^2 \left(2 Q_1^2 + Q_2^2 + Q_{d^c}^2 + Q_Q^2 + Q_S^2\right) + 3 y_t^2 \left(Q_1^2 + 2 Q_2^2 + Q_Q^2 + Q_S^2 + Q_{u^c}^2\right) \\
& + y_\tau^2 \left(2 Q_1^2 + Q_2^2 + Q_{e^c}^2 + Q_L^2 + Q_S^2\right) \Bigg] - \frac{15}{2} g_2^4 - \frac{279}{50} g_1^4 \\
& + 2 g_1'^4 \left(Q_1^2 + Q_2^2 + Q_S^2\right) \left(Q_1^2 + Q_2^2 + Q_S^2 - \Sigma_Q\right) + \frac{9}{5} g_1^2 g_2^2 + 6 g_1'^2 g_2^2 \left(Q_1^2 + Q_2^2 + Q_S^2\right) \\
& + \frac{6}{5} g_1^2 g_1'^2 \left(Q_1^2 + Q_2^2 + Q_S^2\right) \Bigg\} + \lambda \Bigg[48\lambda^3 T_\lambda + 16\Pi_{T_\lambda} + 24\Pi_{T_\kappa} \\
& + 8\lambda \sum_{\alpha=1}^{2} \tilde{\lambda}_{\alpha\alpha} \left(\tilde{\lambda}_{\alpha\alpha} T_\lambda + T_{\alpha\alpha}^{\tilde{\lambda}} \lambda\right) + 36\lambda \sum_{i=1}^{3} \kappa_{ii} \left(\kappa_{ii} T_\lambda + T_{ii}^{\kappa} \lambda\right) \\
& + 16\lambda \sum_{\alpha=1}^{2} \tilde{\lambda}_{\alpha\alpha} \left(T_\lambda \tilde{\lambda}_{\alpha\alpha} + \lambda T_{\alpha\beta}^{\tilde{\lambda}}\right) + 8 \sum_{\alpha=1}^{2} \sum_{\beta=1}^{2} \tilde{\lambda}_{\alpha\alpha} \tilde{\lambda}_{\beta\beta} \left(T_{\alpha\alpha}^{\tilde{\lambda}} \tilde{\lambda}_{\beta\beta} + \tilde{\lambda}_{\alpha\alpha} T_{\beta\beta}^{\tilde{\lambda}}\right) \\
& + 18 \sum_{i=1}^{3} \sum_{j=1}^{3} \kappa_{ii} \kappa_{jj} \left(\kappa_{ii} T_{jj}^{\kappa} + T_{ii}^{\kappa} \kappa_{jj}\right) + 24 \sum_{\alpha=1}^{2} \sum_{j=1}^{3} \tilde{\lambda}_{\alpha\alpha} \kappa_{jj} \left(\tilde{\lambda}_{\alpha\alpha} T_{jj}^{\kappa} + T_{\alpha\alpha}^{\tilde{\lambda}} \kappa_{jj}\right) \\
& + 72 y_t^3 T_t + 72 y_b^3 T_b + 16 y_\tau^3 T_\tau + 12 y_t y_b \left(T_t y_b + y_t T_b\right) + 12 y_b y_\tau \left(T_b y_\tau + y_b T_\tau\right) \\
& + 30\lambda y_t \left(T_\lambda y_t + \lambda T_t\right) + 30\lambda y_b \left(T_\lambda y_b + \lambda T_b\right) + 10\lambda y_\tau \left(T_\lambda y_\tau + \lambda T_\tau\right) \\
& - 32 g_3^2 y_t \left(T_t - y_t M_3\right) - 32 g_3^2 y_b \left(T_b - y_b M_3\right) - 32 g_3^2 \left(\Sigma_{T_\kappa} - M_3 \Sigma_\kappa\right) \\
& - 12 g_2^2 \lambda \left(T_\lambda - \lambda M_2\right) - 18 g_2^2 y_t \left(T_t - y_t M_2\right) - 18 g_2^2 y_b \left(T_b - y_b M_2\right) \\
& - 6 g_2^2 y_\tau \left(T_\tau - y_\tau M_2\right) - 12 g_2^2 \left(\Sigma_{T_\lambda} - M_2 \Sigma_\lambda\right) - \frac{12}{5} g_1^2 \lambda \left(T_\lambda - \lambda M_1\right) \\
& - \frac{26}{5} g_1^2 y_t \left(T_t - y_t M_1\right) - \frac{14}{5} g_1^2 y_b \left(T_b - y_b M_1\right) - \frac{18}{5} g_1^2 y_\tau \left(T_\tau - y_\tau M_1\right)
\end{aligned}$$

$$
\begin{aligned}
&- \frac{12}{5} g_1^2 \left(\Sigma_{T_\lambda} - M_1 \Sigma_\lambda\right) - \frac{8}{5} g_1^2 \left(\Sigma_{T_\kappa} - M_1 \Sigma_\kappa\right) \\
&- 8 g_1'^2 \lambda \left(Q_1^2 + Q_2^2 + Q_S^2\right) \left(T_\lambda - \lambda M_1'\right) - 12 g_1'^2 y_t \left(Q_2^2 + Q_Q^2 + Q_{u^c}^2\right) \left(T_t - y_t M_1'\right) \\
&- 12 g_1'^2 y_b \left(Q_1^2 + Q_Q^2 + Q_{d^c}^2\right) \left(T_b - y_b M_1'\right) - 4 g_1'^2 y_\tau \left(Q_1^2 + Q_L^2 + Q_{e^c}^2\right) \left(T_\tau - y_\tau M_1'\right) \\
&- 8 g_1'^2 \left(Q_1^2 + Q_2^2 + Q_S^2\right) \left(\Sigma_{T_\lambda} - M_1' \Sigma_\lambda\right) - 12 g_1'^2 \left(Q_S^2 + Q_D^2 + Q_{\overline{D}}^2\right) \left(\Sigma_{T_\kappa} - M_1' \Sigma_\kappa\right) \\
&+ 48 g_2^4 M_2 + \frac{576}{25} g_1^4 M_1 + 8 g_1'^4 M_1' \Sigma_Q \left(Q_1^2 + Q_2^2 + Q_S^2\right) \Big] ,
\end{aligned} \tag{C.5c}
$$

where

$$
\begin{aligned}
\Sigma_{T_\lambda} &= \tilde{\lambda}_{11} T_{11}^{\tilde{\lambda}} + \tilde{\lambda}_{22} T_{22}^{\tilde{\lambda}} + \lambda T_\lambda , \qquad & \Sigma_{T_\kappa} &= \kappa_{11} T_{11}^{\kappa} + \kappa_{22} T_{22}^{\kappa} + \kappa_{33} T_{23}^{\kappa} , \\
\Pi_{T_\lambda} &= \tilde{\lambda}_{11}^3 T_{11}^{\tilde{\lambda}} + \tilde{\lambda}_{22}^3 T_{22}^{\tilde{\lambda}} + \lambda^3 T_\lambda , \qquad & \Pi_{T_\kappa} &= \kappa_{11}^3 T_{11}^{\kappa} + \kappa_{22}^3 T_{22}^{\kappa} + \kappa_{33}^3 T_{33}^{\kappa} ,
\end{aligned}
$$

with the couplings $\tilde{\lambda}_{\alpha\beta}$, κ_{ij}, $T_{\alpha\beta}^{\tilde{\lambda}}$ and T_{ij}^{κ} assumed to be flavour diagonal. Defining

$$
\begin{aligned}
\Sigma_1 = {} & \operatorname{Tr}(m_Q^2) - 2 \operatorname{Tr}(m_{u^c}^2) + \operatorname{Tr}(m_{d^c}^2) + \operatorname{Tr}(m_{e^c}^2) - \operatorname{Tr}(m_L^2) + m_{H_u}^2 + \operatorname{Tr}(m_{H_2}^2) \\
& - m_{H_d}^2 - \operatorname{Tr}(m_{H_1}^2) + \operatorname{Tr}(m_{\overline{D}}^2) - \operatorname{Tr}(m_D^2) - m_{L_4}^2 + m_{\overline{L}_4}^2 ,
\end{aligned} \tag{C.6}
$$

$$
\begin{aligned}
\Sigma_1' = {} & 6 Q_Q \operatorname{Tr}(m_Q^2) + 3 Q_{u^c} \operatorname{Tr}(m_{u^c}^2) + 3 Q_{d^c} \operatorname{Tr}(m_{d^c}^2) + Q_{e^c} \operatorname{Tr}(m_{e^c}^2) + 2 Q_L \operatorname{Tr}(m_L^2) \\
& + 2 Q_2 m_{H_u}^2 + 2 Q_2 \operatorname{Tr}(m_{H_2}^2) + 2 Q_1 m_{H_d}^2 + 2 Q_1 \operatorname{Tr}(m_{H_1}^2) + Q_S m_S^2 + Q_S \operatorname{Tr}(m_\Sigma^2) \\
& + 3 Q_{\overline{D}} \operatorname{Tr}(m_{\overline{D}}^2) + 3 Q_D \operatorname{Tr}(m_D^2) + 2 Q_{L_4} m_{L_4}^2 + 2 Q_{\overline{L}_4} m_{\overline{L}_4}^2 ,
\end{aligned} \tag{C.7}
$$

the one- and two-loop β functions and the $O(t^2)$ coefficients for $m_{H_d}^2$ are

$$
\begin{aligned}
\beta_{m_{H_d}^2}^{(1)} = {} & 2\lambda^2 \left(m_{H_d}^2 + m_{H_u}^2 + m_S^2\right) + 2 T_\lambda^2 + 6 y_b^2 \left(m_{H_d}^2 + m_{Q_{33}}^2 + m_{d_{33}^c}^2\right) + 6 T_b^2 \\
& + 2 y_\tau^2 \left(m_{H_d}^2 + m_{L_{33}}^2 + m_{e_{33}^c}^2\right) + 2 T_\tau^2 - 6 g_2^2 M_2^2 - \frac{6}{5} g_1^2 M_1^2 - 8 Q_1^2 g_1'^2 M_1'^2 \\
& - \frac{3}{5} g_1^2 \Sigma_1 + 2 Q_1 g_1'^2 \Sigma_1' ,
\end{aligned} \tag{C.8a}
$$

$$
\begin{aligned}
\beta_{m_{H_d}^2}^{(2)} = {} & -36 y_b^4 \left(m_{H_d}^2 + m_{Q_{33}}^2 + m_{d_{33}^c}^2\right) - 12 y_\tau^4 \left(m_{H_d}^2 + m_{L_{33}}^2 + m_{e_{33}^c}^2\right) - 72 y_b^2 T_b^2 - 24 y_\tau^2 T_\tau^2 \\
& - 6 y_t^2 y_b^2 \left(m_{H_d}^2 + m_{H_u}^2 + 2 m_{Q_{33}}^2 + m_{u_{33}^c}^2 + m_{d_{33}^c}^2\right) - 6 \left(y_t T_b + y_b T_t\right)^2 \\
& - 4\lambda^4 \left(m_{H_d}^2 + m_{H_u}^2 + m_S^2\right) - 24 \lambda^2 T_\lambda^2 - 4\lambda^4 \Big(2 m_{H_d}^2 + 2 m_{H_u}^2 + 2 m_S^2\Big) \\
& - \lambda^2 \sum_{\alpha=1}^{2} \Big[4 \tilde{\lambda}_{\alpha\alpha}^2 \left(m_{H_d}^2 + m_{H_u}^2 + 2 m_S^2 + m_{H_{1,\alpha\alpha}}^2 + m_{H_{2,\alpha\alpha}}^2\right) \Big] \\
& - \lambda^2 \sum_{i=1}^{3} \Big[6 \kappa_{ii}^2 \left(m_{H_d}^2 + m_{H_u}^2 + 2 m_S^2 + m_{D_{ii}}^2 + m_{\overline{D}_{ii}}^2\right) \Big] - 4 \sum_{\alpha=1}^{2} \left(\tilde{\lambda}_{\alpha\alpha} T_\lambda + \lambda T_{\alpha\alpha}^{\tilde{\lambda}}\right)^2
\end{aligned}
$$

$$
\begin{aligned}
&- 6\sum_{i=1}^{3}(\kappa_{ii}T_\lambda + \lambda T^{\kappa}_{ii})^2 - 6\lambda^2 y_t^2\left(m^2_{H_d} + 2m^2_{H_u} + m^2_S + m^2_{Q_{33}} + m^2_{u^c_{33}}\right)\\
&- 6\left(\lambda T_t + y_t T_\lambda\right)^2 + 32 g_3^2 y_b^2\left(m^2_{H_d} + m^2_{Q_{33}} + m^2_{d^c_{33}} + 2M_3^2\right) + 32 g_3^2\left(T_b^2 - 2y_b T_b M_3\right)\\
&+ \frac{6}{5}g_1^2 y_t^2\left(3m^2_{H_u} + m^2_{Q_{33}} - 4m^2_{u^c_{33}}\right) - \frac{2}{5}g_1^2 y_b^2\left(11m^2_{H_d} - m^2_{Q_{33}} - 4m^2_{d^c_{33}} + 4M_1^2\right)\\
&- \frac{4}{5}g_1^2\left(T_b^2 - 2y_b T_b M_1\right) + \frac{6}{5}g_1^2 y_\tau^2\left(m^2_{H_d} + m^2_{L_{33}} + 4m^2_{e^c_{33}} + 4M_1^2\right)\\
&+ \frac{12}{5}g_1^2\left(T_\tau^2 - 2y_\tau T_\tau M_1\right) + \frac{6}{5}g_1^2\lambda^2\left(m^2_{H_d} - m^2_{H_u}\right) + \frac{6}{5}g_1^2\sum_{\alpha=1}^{2}\tilde{\lambda}^2_{\alpha\alpha}\left(m^2_{H_{1,\alpha\alpha}} - m^2_{H_{2,\alpha\alpha}}\right)\\
&+ \frac{6}{5}g_1^2\sum_{i=1}^{3}\kappa_{ii}^2\left(m^2_{\overline{D}_{ii}} - m^2_{D_{ii}}\right) + 12 g_1'^2 y_b^2\left(Q_Q^2 + Q_{d^c}^2 - Q_1^2\right)\\
&\times\left(m^2_{H_d} + m^2_{Q_{33}} + m^2_{d^c_{33}} + 2M_1'^2\right) + 12 g_1'^2\left(Q_Q^2 + Q_{d^c}^2 - Q_1^2\right)\left(T_b^2 - 2y_b T_b M_1'\right)\\
&- 24 Q_1 g_1'^2 y_b^2\left(Q_1 m^2_{H_d} + Q_Q m^2_{Q_{33}} + Q_{d^c} m^2_{d^c_{33}}\right) + 4 g_1'^2 y_\tau^2\left(Q_L^2 + Q_{e^c}^2 - Q_1^2\right)\\
&\times\left(m^2_{H_d} + m^2_{L_{33}} + m^2_{e^c_{33}} + 2M_1'^2\right) + 4 g_1'^2\left(Q_L^2 + Q_{e^c}^2 - Q_1^2\right)\left(T_\tau^2 - 2y_\tau T_\tau M_1'\right)\\
&- 8 Q_1 g_1'^2 y_\tau^2\left(Q_1 m^2_{H_d} + Q_L m^2_{L_{33}} + Q_{e^c} m^2_{e^c_{33}}\right)\\
&- 24 Q_1 g_1'^2 y_t^2\left(Q_2 m^2_{H_u} + Q_Q m^2_{Q_{33}} + Q_{u^c} m^2_{u^c_{33}}\right) + 4 g_1'^2\lambda^2\left(Q_2^2 + Q_S^2 - Q_1^2\right)\\
&\times\left(m^2_{H_d} + m^2_{H_u} + m^2_S + 2M_1'^2\right) + 4 g_1'^2\left(Q_2^2 + Q_S^2 - Q_1^2\right)\left(T_\lambda^2 - 2\lambda T_\lambda M_1'\right)\\
&- 8 Q_1 g_1'^2\lambda^2\left(Q_1 m^2_{H_d} + Q_2 m^2_{H_u} + Q_S m^2_S\right)\\
&- 8 Q_1 g_1'^2\sum_{\alpha=1}^{2}\tilde{\lambda}^2_{\alpha\alpha}\left(Q_1 m^2_{H_{1,\alpha\alpha}} + Q_2 m^2_{H_{2,\alpha\alpha}} + Q_S m^2_S\right)\\
&- 12 Q_1 g_1'^2\sum_{i=1}^{3}\kappa_{ii}^2\left(m^2_S + m^2_{D_{ii}} + m^2_{\overline{D}_{ii}}\right)\\
&- \frac{16}{5}g_3^2 g_1^2\left[\mathrm{Tr}(m_Q^2) - 2\,\mathrm{Tr}(m_{u^c}^2) + \mathrm{Tr}(m_{d^c}^2) + \mathrm{Tr}(m_{\overline{D}}^2) - \mathrm{Tr}(m_D^2)\right]\\
&+ 32 Q_1 g_3^2 g_1'^2\Big[2Q_Q\,\mathrm{Tr}(m_Q^2) + Q_{u^c}\,\mathrm{Tr}(m_{u^c}^2) + Q_{d^c}\,\mathrm{Tr}(m_{d^c}^2)\\
&+ Q_{\overline{D}}\,\mathrm{Tr}(m_{\overline{D}}^2) + Q_D\,\mathrm{Tr}(m_D^2)\Big] + 3g_2^4\Big[29M_2^2 + m^2_{L_4} + m^2_{\overline{L}_4} + 3\,\mathrm{Tr}(m_Q^2) + \mathrm{Tr}(m_L^2)\\
&+ m^2_{H_d} + \mathrm{Tr}(m^2_{H_1}) + m^2_{H_u} + \mathrm{Tr}(m^2_{H_2})\Big] + \frac{9}{5}g_2^2 g_1^2\Big[2\left(M_1^2 + M_1M_2 + M_2^2\right) + m^2_{L_4}\\
&- m^2_{\overline{L}_4} - \mathrm{Tr}(m_Q^2) + \mathrm{Tr}(m_L^2) - m^2_{H_u} - \mathrm{Tr}(m^2_{H_2}) + m^2_{H_d} + \mathrm{Tr}(m^2_{H_1})\Big]\\
&+ 12 Q_1 g_2^2 g_1'^2\Big[2Q_1\left(M_1'^2 + M_1'M_2 + M_2^2\right) + Q_{L_4}m^2_{L_4} + Q_{\overline{L}_4}m^2_{\overline{L}_4}\\
&+ 3Q_Q\,\mathrm{Tr}(m_Q^2) + Q_L\,\mathrm{Tr}(m_L^2) + Q_1 m^2_{H_d} + Q_1\,\mathrm{Tr}(m^2_{H_1}) + Q_2 m^2_{H_u} + Q_2\,\mathrm{Tr}(m^2_{H_2})\Big]\\
&+ \frac{1}{25}g_1^4\Big[891M_1^2 + 18m^2_{L_4} + 2\,\mathrm{Tr}(m_{d^c}^2) + 10\,\mathrm{Tr}(m_D^2) + 2\,\mathrm{Tr}(m_{\overline{D}}^2) - 18\,\mathrm{Tr}(m_{e^c}^2)
\end{aligned}
$$

$$
\begin{aligned}
&+ 18m_{H_d}^2 + 18\,\mathrm{Tr}(m_{H_1}^2) + 18\,\mathrm{Tr}(m_L^2) + 2\,\mathrm{Tr}(m_Q^2) + 56\,\mathrm{Tr}(m_{u^c}^2)\Big] \\
&- \frac{4}{5}g_1^2 g_1'^2\Big[6Q_1\Big(3Q_{d^c} + 3Q_{\overline{D}} - 3Q_D + 3Q_{e^c} - 4Q_1 + 3Q_2 + Q_{\overline{L}_4} - Q_{L_4} \\
&- 3Q_L + 3Q_Q - 6Q_{u^c}\Big)\left(M_1^2 + M_1 M_1' + M_1'^2\right) + 3Q_{\overline{L}_4}^2 m_{\overline{L}_4}^2 - 3Q_{L_4}^2 m_{L_4}^2 \\
&+ 3Q_{d^c}^2\,\mathrm{Tr}(m_{d^c}^2) + 3Q_{\overline{D}}^2\,\mathrm{Tr}(m_{\overline{D}}^2) - 3Q_D^2\,\mathrm{Tr}(m_D^2) + 3Q_{e^c}^2\,\mathrm{Tr}(m_{e^c}^2) - 3Q_1^2 m_{H_d}^2 \\
&- 3Q_1^2\,\mathrm{Tr}(m_{H_1}^2) + 3Q_2^2 m_{H_u}^2 + 3Q_2^2\,\mathrm{Tr}(m_{H_2}^2) - 3Q_L^2\,\mathrm{Tr}(m_L^2) + 3Q_Q^2\,\mathrm{Tr}(m_Q^2) \\
&- 6Q_{u^c}^2\,\mathrm{Tr}(m_{u^c}^2) + 3Q_1 Q_{\overline{L}_4} m_{\overline{L}_4}^2 - 9Q_1 Q_{L_4} m_{L_4}^2 + 4Q_1 Q_{d^c}\,\mathrm{Tr}(m_{d^c}^2) \\
&+ 4Q_1 Q_{\overline{D}}\,\mathrm{Tr}(m_{\overline{D}}^2) - 8Q_1 Q_D\,\mathrm{Tr}(m_D^2) - 9Q_1^2 m_{H_d}^2 - 9Q_1^2\,\mathrm{Tr}(m_{H_1}^2) + 3Q_1 Q_2 m_{H_u}^2 \\
&+ 3Q_1 Q_2\,\mathrm{Tr}(m_{H_2}^2) - 9Q_1 Q_L\,\mathrm{Tr}(m_L^2) + 5Q_1 Q_Q\,\mathrm{Tr}(m_Q^2) - 20Q_1 Q_{u^c}\,\mathrm{Tr}(m_{u^c}^2)\Big] \\
&+ 8Q_1 g_1'^4\Big[3Q_1 M_1'^2\Big(9Q_{d^c}^2 + 9Q_{\overline{D}}^2 + 9Q_D^2 + 3Q_{e^c}^2 + 8Q_1^2 + 6Q_2^2 + 2Q_{\overline{L}_4}^2 + 2Q_{L_4}^2 \\
&+ 6Q_L^2 + 18Q_Q^2 + 3Q_S^2 + 9Q_{u^c}^2\Big) + 2Q_{\overline{L}_4}^3 m_{\overline{L}_4}^2 + 2Q_{L_4}^3 m_{L_4}^2 + 3Q_{d^c}^3\,\mathrm{Tr}(m_{d^c}^2) \\
&+ 3Q_{\overline{D}}^3\,\mathrm{Tr}(m_{\overline{D}}^2) + 3Q_D^3\,\mathrm{Tr}(m_D^2) + Q_{e^c}^3\,\mathrm{Tr}(m_{e^c}^2) + 2Q_1^3 m_{H_d}^2 + 2Q_1^3\,\mathrm{Tr}(m_{H_1}^2) \\
&+ 2Q_2^3 m_{H_u}^2 + 2Q_2^3\,\mathrm{Tr}(m_{H_2}^2) + 2Q_L^3\,\mathrm{Tr}(m_L^2) + 6Q_Q^3\,\mathrm{Tr}(m_Q^2) + Q_S^3 m_S^2 \\
&+ Q_S^3\,\mathrm{Tr}(m_\Sigma^2) + 3Q_{u^c}^3\,\mathrm{Tr}(m_{u^c}^2) + 2Q_1 Q_{\overline{L}_4}^2 m_{\overline{L}_4}^2 + 2Q_1 Q_{L_4}^2 m_{L_4}^2 \\
&+ 3Q_1 Q_{d^c}^2\,\mathrm{Tr}(m_{d^c}^2) + 3Q_1 Q_{\overline{D}}^2\,\mathrm{Tr}(m_{\overline{D}}^2) + 3Q_1 Q_D^2\,\mathrm{Tr}(m_D^2) + Q_1 Q_{e^c}^2\,\mathrm{Tr}(m_{e^c}^2) \\
&+ 2Q_1^3 m_{H_d}^2 + 2Q_1^3\,\mathrm{Tr}(m_{H_1}^2) + 2Q_1 Q_2^2 m_{H_u}^2 + 2Q_1 Q_2^2\,\mathrm{Tr}(m_{H_2}^2) + 2Q_1 Q_L^2\,\mathrm{Tr}(m_L^2) \\
&+ 6Q_1 Q_Q^2\,\mathrm{Tr}(m_Q^2) + Q_1 Q_S^2 m_S^2 + Q_1 Q_S^2\,\mathrm{Tr}(m_\Sigma^2) + 3Q_1 Q_{u^c}^2\,\mathrm{Tr}(m_{u^c}^2)\Big], \qquad \text{(C.8b)}
\end{aligned}
$$

$$
\begin{aligned}
b_{m_{H_d}^2}^{(2)} &= 72y_b^4\left(m_{H_d}^2 + m_{Q_{33}}^2 + m_{d_{33}^c}^2\right) + 144y_b^2 T_b^2 + 16y_\tau^4\left(m_{H_d}^2 + m_{L_{33}}^2 + m_{e_{33}^c}^2\right) \\
&+ 32y_\tau^2 T_\tau^2 + 16\lambda^4\left(m_{H_d}^2 + m_{H_u}^2 + m_S^2\right) + 32\lambda^2 T_\lambda^2 \\
&+ 6y_t^2 y_b^2\left(m_{H_d}^2 + m_{H_u}^2 + 2m_{Q_{33}}^2 + m_{u_{33}^c}^2 + m_{d_{33}^c}^2\right) + 6\left(y_t T_b + y_b T_t\right)^2 \\
&+ 12y_b^2 y_\tau^2\left(2m_{H_d}^2 + m_{Q_{33}}^2 + m_{d_{33}^c}^2 + m_{L_{33}}^2 + m_{e_{33}^c}^2\right) + 12\left(y_b T_\tau + y_\tau T_b\right)^2 \\
&+ 6\lambda^2 y_t^2\left(m_{H_d}^2 + 2m_{H_u}^2 + m_S^2 + m_{Q_{33}}^2 + m_{u_{33}^c}^2\right) + 6\left(\lambda T_t + y_t T_\lambda\right)^2 \\
&+ 12\lambda^2 y_b^2\left(2m_{H_d}^2 + m_{H_u}^2 + m_S^2 + m_{Q_{33}}^2 + m_{d_{33}^c}^2\right) + 12\left(\lambda T_b + y_b T_\lambda\right)^2 \\
&+ 4\lambda^2 y_\tau^2\left(2m_{H_d}^2 + m_{H_u}^2 + m_S^2 + m_{L_{33}}^2 + m_{e_{33}^c}^2\right) + 4\left(\lambda T_\tau + y_\tau T_\lambda\right)^2 \\
&+ 4\sum_{\alpha=1}^{2}\left[\lambda^2\tilde{\lambda}_{\alpha\alpha}^2\left(m_{H_{1,\alpha\alpha}}^2 + m_{H_{2,\alpha\alpha}}^2 + m_{H_d}^2 + m_{H_u}^2 + 2m_S^2\right) + \left(\lambda T_{\alpha\alpha}^{\tilde{\lambda}} + \tilde{\lambda}_{\alpha\alpha} T_\lambda\right)^2\right] \\
&+ 6\sum_{i=1}^{3}\left[\lambda^2\kappa_{ii}^2\left(m_{H_d}^2 + m_{H_u}^2 + 2m_S^2 + m_{D_{ii}}^2 + m_{\overline{D}_{ii}}^2\right) + \left(\lambda T_{ii}^{\kappa} + \kappa_{ii} T_\lambda\right)^2\right] \\
&- 32g_3^2 y_b^2\left(m_{H_d}^2 + m_{Q_{33}}^2 + m_{d_{33}^c}^2 + 2M_3^2\right) - 32g_3^2\left(T_b^2 - 2y_b T_b M_3\right)
\end{aligned}
$$

$$
\begin{aligned}
&- 18g_2^2y_b^2\left(m_{H_d}^2+m_{Q_{33}}^2+m_{d_{33}^c}^2+2M_2^2\right)-18g_2^2\left(T_b^2-2y_bT_bM_2\right)\\
&- 6g_2^2y_\tau^2\left(m_{H_d}^2+m_{L_{33}}^2+m_{e_{33}^c}^2+2M_2^2\right)-6g_2^2\left(T_\tau^2-2y_\tau T_\tau M_2\right)\\
&- 6g_2^2\lambda^2\left(m_{H_d}^2+m_{H_u}^2+m_S^2+2M_2^2\right)-6g_2^2\left(T_\lambda^2-2\lambda T_\lambda M_2\right)\\
&- \frac{14}{5}g_1^2y_b^2\left(m_{H_d}^2+m_{Q_{33}}^2+m_{d_{33}^c}^2+2M_1^2\right)-\frac{14}{5}g_1^2\left(T_b^2-2y_bT_bM_1\right)\\
&- \frac{18}{5}g_1^2y_\tau^2\left(m_{H_d}^2+m_{L_{33}}^2+m_{e_{33}^c}^2+2M_1^2\right)-\frac{18}{5}g_1^2\left(T_\tau^2-2y_\tau T_\tau M_1\right)\\
&- \frac{6}{5}g_1^2\lambda^2\left(m_{H_d}^2+m_{H_u}^2+m_S^2+2M_1^2\right)-\frac{6}{5}g_1^2\left(T_\lambda^2-2\lambda T_\lambda M_1\right)\\
&- 12g_1'^2y_b^2\left(Q_1^2+Q_Q^2+Q_{d^c}^2\right)\left(m_{H_d}^2+m_{Q_{33}}^2+m_{d_{33}^c}^2+2M_1'^2\right)\\
&- 12g_1'^2\left(Q_1^2+Q_Q^2+Q_{d^c}^2\right)\left(T_b^2-2y_bT_bM_1'\right)+12Q_1g_1'^2T_b^2\left(Q_1+Q_Q+Q_{d^c}\right)\\
&+ 6g_1'^2y_b^2\left(Q_1+Q_Q+Q_{d^c}\right)\left(2Q_1m_{H_d}^2+2Q_1m_{Q_{33}}^2+2Q_1m_{d_{33}^c}^2+\Sigma_1'\right)\\
&- 4g_1'^2y_\tau^2\left(Q_1^2+Q_L^2+Q_{e^c}^2\right)\left(m_{H_d}^2+m_{L_{33}}^2+m_{e_{33}^c}^2+2M_1'^2\right)\\
&- 4g_1'^2\left(Q_1^2+Q_L^2+Q_{e^c}^2\right)\left(T_\tau^2-2y_\tau T_\tau M_1'\right)+4Q_1g_1'^2T_\tau^2\left(Q_1+Q_L+Q_{e^c}\right)\\
&+ 2g_1'^2y_\tau^2\left(Q_1+Q_L+Q_{e^c}\right)\left(2Q_1m_{H_d}^2+2Q_1m_{L_{33}}^2+2Q_1m_{e_{33}^c}^2+\Sigma_1'\right)\\
&+ 12Q_1g_1'^2y_t^2\left(Q_2+Q_Q+Q_{u^c}\right)\left(m_{H_u}^2+m_{Q_{33}}^2+m_{u_{33}^c}^2\right)\\
&+ 12Q_1g_1'^2T_t^2\left(Q_2+Q_Q+Q_{u^c}\right)\\
&- 4g_1'^2\lambda^2\left(Q_1^2+Q_2^2+Q_S^2\right)\left(m_{H_d}^2+m_{H_u}^2+m_S^2+2M_1'^2\right)\\
&- 4g_1'^2\left(Q_1^2+Q_2^2+Q_S^2\right)\left(T_\lambda^2-2\lambda T_\lambda M_1'\right)+2g_1'^2\lambda^2\left(Q_1+Q_2+Q_S\right)\Sigma_1'\\
&+ 4Q_1g_1'^2\lambda^2\left(Q_1+Q_2+Q_S\right)\left(m_{H_d}^2+m_{H_u}^2+m_S^2\right)+4Q_1g_1'^2T_\lambda^2\left(Q_1+Q_2+Q_S\right)\\
&+ 4Q_1g_1'^2\left(Q_1+Q_2+Q_S\right)\sum_{\alpha=1}^{2}\left[\tilde{\lambda}_{\alpha\alpha}^2\left(m_{H_{1,\alpha\alpha}}^2+m_{H_{2,\alpha\alpha}}^2+m_S^2\right)+(T_{\alpha\alpha}^{\tilde{\lambda}})^2\right]\\
&+ 6Q_1g_1'^2\left(Q_S+Q_D+Q_{\overline{D}}\right)\sum_{i=1}^{3}\left[\kappa_{ii}^2\left(m_S^2+m_{D_{ii}}^2+m_{\overline{D}_{ii}}^2\right)+(T_{ii}^{\kappa})^2\right]\\
&- 96Q_1g_3^2g_1'^2M_3^2\left(2Q_Q+Q_{u^c}+Q_{d^c}+Q_D+Q_{\overline{D}}\right)-72g_2^4M_2^2\\
&- 12Q_1g_2^2g_1'^2M_2^2\left(9Q_Q+3Q_L+3Q_1+3Q_2+Q_{\overline{L}_4}+Q_{L_4}\right)-\frac{288}{25}g_1^4\left(\Sigma_1+3M_1^2\right)\\
&- \frac{3}{5}g_1^2g_1'^2\Big[4Q_1M_1^2\Big(2Q_{d^c}+2Q_{\overline{D}}+2Q_D+6Q_{e^c}+3Q_1+3Q_2+Q_{\overline{L}_4}+Q_{L_4}\\
&+ 3Q_L+Q_Q+8Q_{u^c}\Big)-4M_1'^2\Big(3Q_{d^c}^2+3Q_{\overline{D}}^2-3Q_D^2+3Q_{e^c}^2-3Q_1^2+3Q_2^2\\
&+ Q_{\overline{L}_4}^2-Q_{L_4}^2-3Q_L^2+3Q_Q^2-6Q_{u^c}^2\Big)+\left(\Sigma_1'-2Q_1\Sigma_1\right)\Sigma_Q^Y\Big]\\
&- 4Q_1g_1'^4\Big[2M_1'^2\Big(9Q_{d^c}^3+9Q_{\overline{D}}^3+9Q_D^3+3Q_{e^c}^3+6Q_1^3+6Q_2^3+2Q_{\overline{L}_4}^3+2Q_{L_4}^3
\end{aligned}
$$

$$+ 6Q_L^3 + 18Q_Q^3 + 3Q_S^3 + 9Q_{u^c}^3\Big) + \Big(6Q_1 M_1'^2 - \Sigma_1'\Big)\,\Sigma_Q\Big]\,. \tag{C.8c}$$

Similarly, those for $m_{H_u}^2$ read

$$\begin{aligned}
\beta_{m_{H_u}^2}^{(1)} &= 2\lambda^2\left(m_{H_d}^2 + m_{H_u}^2 + m_S^2\right) + 2T_\lambda^2 + 6y_t^2\left(m_{H_u}^2 + m_{Q_{33}}^2 + m_{u_{33}^c}^2\right) + 6T_t^2 \\
&\quad - 6g_2^2 M_2^2 - \frac{6}{5}g_1^2 M_1^2 - 8Q_2^2 g_1'^2 M_1'^2 + \frac{3}{5}g_1^2\Sigma_1 + 2Q_2 g_1'^2\Sigma_1'\,, \qquad \text{(C.9a)} \\
\beta_{m_{H_u}^2}^{(2)} &= -36y_t^4\left(m_{H_u}^2 + m_{Q_{33}}^2 + m_{u_{33}^c}^2\right) - 6y_t^2 y_b^2\left(m_{H_u}^2 + m_{H_d}^2 + 2m_{Q_{33}}^2 + m_{u_{33}^c}^2 + m_{d_{33}^c}^2\right) \\
&\quad - 72y_t^2 T_t^2 - 6\left(y_t T_b + y_b T_t\right)^2 - 12\lambda^4\left(m_{H_d}^2 + m_{H_u}^2 + m_S^2\right) - 24\lambda^2 T_\lambda^2 \\
&\quad - 4\lambda^2\sum_{\alpha=1}^{2}\tilde{\lambda}_{\alpha\alpha}^2\left(m_{H_d}^2 + m_{H_u}^2 + 2m_S^2 + m_{H_{1,\alpha\alpha}}^2 + m_{H_{2,\alpha\alpha}}^2\right) \\
&\quad - 6\lambda^2\sum_{i=1}^{3}\kappa_{ii}^2\left(m_{H_d}^2 + m_{H_u}^2 + 2m_S^2 + m_{D_{ii}}^2 + m_{\overline{D}_{ii}}^2\right) - 4\sum_{\alpha=1}^{2}\left(\tilde{\lambda}_{\alpha\alpha}T_\lambda + \lambda T_{\alpha\alpha}^{\tilde{\lambda}}\right)^2 \\
&\quad - 6\sum_{i=1}^{3}\left(\kappa_{ii}T_\lambda + \lambda T_{ii}^{\kappa}\right)^2 - 6\lambda^2 y_b^2\left(2m_{H_d}^2 + m_{H_u}^2 + m_S^2 + m_{Q_{33}}^2 + m_{d_{33}^c}^2\right) \\
&\quad - 2\lambda^2 y_\tau^2\left(2m_{H_d}^2 + m_{H_u}^2 + m_S^2 + m_{L_{33}}^2 + m_{e_{33}^c}^2\right) - 6\left(\lambda T_b + y_b T_\lambda\right)^2 \\
&\quad - 2\left(\lambda T_\tau + y_\tau T_\lambda\right)^2 + 32g_3^2 y_t^2\left(m_{H_u}^2 + m_{Q_{33}}^2 + m_{u_{33}^c}^2 + 2M_3^2\right) \\
&\quad + 32g_3^2\left(T_t^2 - 2y_t T_t M_3\right) + \frac{2}{5}g_1^2 y_t^2\left(-5m_{H_u}^2 + m_{Q_{33}}^2 + 16m_{u_{33}^c}^2 + 8M_1^2\right) \\
&\quad + \frac{8}{5}g_1^2\left(T_t^2 - 2y_t T_t M_1\right) + \frac{6}{5}g_1^2 y_b^2\left(3m_{H_d}^2 - m_{Q_{33}}^2 - 2m_{d_{33}^c}^2\right) \\
&\quad + \frac{6}{5}g_1^2 y_\tau^2\left(m_{H_d}^2 + m_{L_{33}}^2 - 2m_{e_{33}^c}^2\right) + \frac{6}{5}g_1^2\lambda^2\left(m_{H_d}^2 - m_{H_u}^2\right) \\
&\quad + \frac{6}{5}g_1^2\sum_{\alpha=1}^{2}\tilde{\lambda}_{\alpha\alpha}^2\left(m_{H_{1,\alpha\alpha}}^2 - m_{H_{2,\alpha\alpha}}^2\right) + \frac{6}{5}g_1^2\sum_{i=1}^{3}\kappa_{ii}^2\left(m_{D_{ii}}^2 - m_{\overline{D}_{ii}}^2\right) \\
&\quad + 12g_1'^2 y_t^2\left(Q_Q^2 + Q_{u^c}^2 - Q_2^2\right)\left(m_{H_u}^2 + m_{Q_{33}}^2 + m_{u_{33}^c}^2 + 2M_1'^2\right) \\
&\quad + 12g_1'^2\left(Q_Q^2 + Q_{u^c}^2 - Q_2^2\right)\left(T_t^2 - 2y_t T_t M_1'\right) \\
&\quad - 24Q_2 g_1'^2 y_t^2\left(Q_2 m_{H_u}^2 + Q_Q m_{Q_{33}}^2 + Q_{u^c} m_{u_{33}^c}^2\right) \\
&\quad - 24Q_2 g_1'^2 y_b^2\left(Q_1 m_{H_d}^2 + Q_Q m_{Q_{33}}^2 + Q_{d^c} m_{d_{33}^c}^2\right) \\
&\quad - 8Q_2 g_1'^2 y_\tau^2\left(Q_1 m_{H_d}^2 + Q_L m_{L_{33}}^2 + Q_{e^c} m_{e_{33}^c}^2\right) \\
&\quad + 4g_1'^2\lambda^2\left(Q_1^2 - Q_2^2 + Q_S^2\right)\left(m_{H_d}^2 + m_{H_u}^2 + m_S^2 + 2M_1'^2\right) \\
&\quad + 4g_1'^2\left(Q_1^2 - Q_2^2 + Q_S^2\right)\left(T_\lambda^2 - 2\lambda T_\lambda M_1'\right) \\
&\quad - 8Q_2 g_1'^2\lambda^2\left(Q_1 m_{H_d}^2 + Q_2 m_{H_u}^2 + Q_S m_S^2\right)
\end{aligned}$$

$$
\begin{aligned}
&- 8Q_2 g_1'^2 \sum_{\alpha=1}^{2} \tilde{\lambda}_{\alpha\alpha}^2 \left(Q_1 m_{H_{1,\alpha\alpha}}^2 + Q_2 m_{H_{2,\alpha\alpha}}^2 + Q_S m_S^2\right) \\
&- 12Q_2 g_1'^2 \sum_{i=1}^{3} \kappa_{ii}^2 \left(Q_S m_S^2 + Q_D m_{D_{ii}}^2 + Q_{\overline{D}} m_{\overline{D}_{ii}}^2\right) \\
&+ \frac{16}{5} g_3^2 g_1^2 \left[\mathrm{Tr}(m_Q^2) - 2\,\mathrm{Tr}(m_{u^c}^2) + \mathrm{Tr}(m_{d^c}^2) + \mathrm{Tr}(m_{\overline{D}}^2) - \mathrm{Tr}(m_D^2)\right] \\
&+ 32Q_2 g_3^2 g_1'^2 \Big[2Q_Q\,\mathrm{Tr}(m_Q^2) + Q_{u^c}\,\mathrm{Tr}(m_{u^c}^2) + Q_{d^c}\,\mathrm{Tr}(m_{d^c}^2) + Q_{\overline{D}}\,\mathrm{Tr}(m_{\overline{D}}^2) \\
&+ Q_D\,\mathrm{Tr}(m_D^2)\Big] + 3g_2^4 \Big[29M_2^2 + m_{L_4}^2 + m_{\overline{L}_4}^2 + 3\,\mathrm{Tr}(m_Q^2) + \mathrm{Tr}(m_L^2) + m_{H_d}^2 \\
&+ \mathrm{Tr}(m_{H_1}^2) + m_{H_u}^2 + \mathrm{Tr}(m_{H_2}^2)\Big] + \frac{9}{5} g_2^2 g_1^2 \Big[2\left(M_1^2 + M_1 M_2 + M_2^2\right) + m_{\overline{L}_4}^2 \\
&- m_{L_4}^2 + \mathrm{Tr}(m_Q^2) - \mathrm{Tr}(m_L^2) + m_{H_u}^2 + \mathrm{Tr}(m_{H_2}^2) - m_{H_d}^2 - \mathrm{Tr}(m_{H_1}^2)\Big] \\
&+ 12Q_2 g_2^2 g_1'^2 \Big[2Q_2\left(M_1'^2 + M_1' M_2 + M_2^2\right) + Q_{L_4} m_{L_4}^2 + Q_{\overline{L}_4} m_{\overline{L}_4}^2 \\
&+ 3Q_Q\,\mathrm{Tr}(m_Q^2) + Q_L\,\mathrm{Tr}(m_L^2) + Q_1 m_{H_d}^2 + Q_1\,\mathrm{Tr}(m_{H_1}^2) + Q_2 m_{H_u}^2 + Q_2\,\mathrm{Tr}(m_{H_2}^2)\Big] \\
&+ \frac{1}{25} g_1^4 \Big[891M_1^2 + 18m_{\overline{L}_4}^2 + 10\,\mathrm{Tr}(m_{d^c}^2) + 2\,\mathrm{Tr}(m_D^2) + 10\,\mathrm{Tr}(m_{\overline{D}}^2) + 54\,\mathrm{Tr}(m_{e^c}^2) \\
&+ 18m_{H_u}^2 + 18\,\mathrm{Tr}(m_{H_2}^2) + 4\,\mathrm{Tr}(m_Q^2) - 8\,\mathrm{Tr}(m_{u^c}^2)\Big] \\
&+ \frac{4}{5} g_1^2 g_1'^2 \Big[6Q_2\Big(3Q_{d^c} + Q_{\overline{D}} - 3Q_D + 3Q_{e^c} - 3Q_1 + 4Q_2 + Q_{\overline{L}_4} - Q_{L_4} - 3Q_L \\
&+ 3Q_Q - 6Q_{u^c}\Big)\left(M_1^2 + M_1 M_1' + M_1'^2\right) + 3Q_{\overline{L}_4}^2 m_{\overline{L}_4}^2 - 3Q_{L_4}^2 m_{L_4}^2 \\
&+ 3Q_{d^c}^2\,\mathrm{Tr}(m_{d^c}^2) + 3Q_{\overline{D}}^2\,\mathrm{Tr}(m_{\overline{D}}^2) - 3Q_D^2\,\mathrm{Tr}(m_D^2) + 3Q_{e^c}^2\,\mathrm{Tr}(m_{e^c}^2) - 3Q_1^2 m_{H_d}^2 \\
&- 3Q_1^2\,\mathrm{Tr}(m_{H_1}^2) + 3Q_2^2 m_{H_u}^2 + 3Q_2^2\,\mathrm{Tr}(m_{H_2}^2) - 3Q_L^2\,\mathrm{Tr}(m_L^2) + 3Q_Q^2\,\mathrm{Tr}(m_Q^2) \\
&- 6Q_{u^c}^2\,\mathrm{Tr}(m_{u^c}^2) + 9Q_2 Q_{\overline{L}_4} m_{\overline{L}_4}^2 - 3Q_2 Q_{L_4} m_{L_4}^2 + 8Q_2 Q_{d^c}\,\mathrm{Tr}(m_{d^c}^2) \\
&+ 8Q_2 Q_{\overline{D}}\,\mathrm{Tr}(m_{\overline{D}}^2) - 4Q_2 Q_D\,\mathrm{Tr}(m_D^2) + 12Q_2 Q_{e^c}\,\mathrm{Tr}(m_{e^c}^2) - 3Q_2 Q_1 m_{H_d}^2 \\
&- 3Q_2 Q_1\,\mathrm{Tr}(m_{H_1}^2) + 9Q_2^2 m_{H_u}^2 + 9Q_2^2\,\mathrm{Tr}(m_{H_2}^2) - 3Q_2 Q_L\,\mathrm{Tr}(m_L^2) \\
&+ 7Q_2 Q_Q\,\mathrm{Tr}(m_Q^2) - 4Q_2 Q_{u^c}\,\mathrm{Tr}(m_{u^c}^2)\Big] \\
&+ 8Q_2 g_1'^4 \Big[3Q_2 M_1'^2\Big(9Q_{d^c}^2 + 9Q_{\overline{D}}^2 + 9Q_D^2 + 3Q_{e^c}^2 + 6Q_1^2 + 8Q_2^2 + 2Q_{\overline{L}_4}^2 + 2Q_{L_4}^2 \\
&+ 6Q_L^2 + 18Q_Q^2 + 3Q_S^2 + 9Q_{u^c}^2\Big) + 2Q_{\overline{L}_4}^3 m_{\overline{L}_4}^2 + 2Q_{L_4}^3 m_{L_4}^2 + 3Q_{d^c}^3\,\mathrm{Tr}(m_{d^c}^2) \\
&+ 3Q_{\overline{D}}^3\,\mathrm{Tr}(m_{\overline{D}}^2) + 3Q_D^3\,\mathrm{Tr}(m_D^2) + Q_{e^c}^3\,\mathrm{Tr}(m_{e^c}^2) + 2Q_1^3 m_{H_d}^2 + 2Q_1^3\,\mathrm{Tr}(m_{H_1}^2) \\
&+ 2Q_2^3 m_{H_u}^2 + 2Q_2^3\,\mathrm{Tr}(m_{H_2}^2) + 2Q_L^3\,\mathrm{Tr}(m_L^2) + 6Q_Q^3\,\mathrm{Tr}(m_Q^2) + Q_S^3 m_S^2 \\
&+ Q_S^3\,\mathrm{Tr}(m_\Sigma^2) + 3Q_{u^c}^3\,\mathrm{Tr}(m_{u^c}^2) + 2Q_2 Q_{\overline{L}_4}^2 m_{\overline{L}_4}^2 + 2Q_2 Q_{L_4}^2 m_{L_4}^2 \\
&+ 3Q_2 Q_{d^c}^2\,\mathrm{Tr}(m_{d^c}^2) + 3Q_2 Q_{\overline{D}}^2\,\mathrm{Tr}(m_{\overline{D}}^2) + 3Q_2 Q_D^2\,\mathrm{Tr}(m_D^2) + Q_2 Q_{e^c}^2\,\mathrm{Tr}(m_{e^c}^2)
\end{aligned}
$$

$$
\begin{aligned}
&+ 2Q_2Q_1^2 m_{H_d}^2 + 2Q_2Q_1^2\,\mathrm{Tr}(m_{H_1}^2) + 2Q_2^3 m_{H_u}^2 + 2Q_2^3\,\mathrm{Tr}(m_{H_2}^2) + 2Q_2Q_L^2\,\mathrm{Tr}(m_L^2)\\
&+ 6Q_2Q_Q^2\,\mathrm{Tr}(m_Q^2) + Q_2Q_S^2 m_S^2 + Q_2Q_S^2\,\mathrm{Tr}(m_\Sigma^2) + 3Q_2Q_{u^c}^2\,\mathrm{Tr}(m_{u^c}^2)\Big], \qquad \text{(C.9b)}\\
b^{(2)}_{m_{H_u}^2} &= 72y_t^4\left(m_{H_u}^2 + m_{Q_{33}}^2 + m_{u_{33}^c}^2\right) + 144y_t^2T_t^2 + 16\lambda^4\left(m_{H_d}^2 + m_{H_u}^2 + m_S^2\right) + 32\lambda^2T_\lambda^2\\
&+ 6y_t^2y_b^2\left(m_{H_d}^2 + m_{H_u}^2 + 2m_{Q_{33}}^2 + m_{u_{33}^c}^2 + m_{d_{33}^c}^2\right) + 6\left(y_tT_b + y_bT_t\right)^2\\
&+ 12\lambda^2y_t^2\left(m_{H_d}^2 + 2m_{H_u}^2 + m_S^2 + m_{Q_{33}}^2 + m_{u_{33}^c}^2\right) + 12\left(\lambda T_t + y_tT_\lambda\right)^2\\
&+ 6\lambda^2y_b^2\left(2m_{H_d}^2 + m_{H_u}^2 + m_S^2 + m_{Q_{33}}^2 + m_{d_{33}^c}^2\right) + 6\left(\lambda T_b + y_bT_\lambda\right)^2\\
&+ 2\lambda^2y_\tau^2\left(2m_{H_d}^2 + m_{H_u}^2 + m_S^2 + m_{L_{33}}^2 + m_{e_{33}^c}^2\right) + 2\left(\lambda T_\tau + y_\tau T_\lambda\right)^2\\
&+ 4\sum_{\alpha=1}^{2}\left[\lambda^2\tilde{\lambda}_{\alpha\alpha}^2\left(m_{H_{1,\alpha\alpha}}^2 + m_{H_{2,\alpha\alpha}}^2 + m_{H_d}^2 + m_{H_u}^2 + 2m_S^2\right) + \left(\lambda T_{\alpha\alpha}^{\tilde{\lambda}} + \tilde{\lambda}_{\alpha\alpha}T_\lambda\right)^2\right]\\
&+ 6\sum_{i=1}^{3}\left[\lambda^2\kappa_{ii}^2\left(m_{H_d}^2 + m_{H_u}^2 + 2m_S^2 + m_{D_{ii}}^2 + m_{\overline{D}_{ii}}^2\right) + \left(\lambda T_{ii}^{\kappa} + \kappa_{ii}T_\lambda\right)^2\right]\\
&- 32g_3^2y_t^2\left(m_{H_u}^2 + m_{Q_{33}}^2 + m_{u_{33}^c}^2 + 2M_3^2\right) - 32g_3^2\left(T_t^2 - 2y_tT_tM_3\right)\\
&- 18g_2^2y_t^2\left(m_{H_u}^2 + m_{Q_{33}}^2 + m_{u_{33}^c}^2 + 2M_2^2\right) - 18g_2^2\left(T_t^2 - 2y_tT_tM_2\right)\\
&- 6g_2^2\lambda^2\left(m_{H_d}^2 + m_{H_u}^2 + m_S^2 + 2M_2^2\right) - 6g_2^2\left(T_\lambda^2 - 2\lambda T_\lambda M_2\right)\\
&- \frac{26}{5}g_1^2y_t^2\left(m_{H_u}^2 + m_{Q_{33}}^2 + m_{u_{33}^c}^2 + 2M_1^2\right) - \frac{26}{5}g_1^2\left(T_t^2 - 2y_tT_tM_1\right)\\
&- \frac{6}{5}g_1^2\lambda^2\left(m_{H_d}^2 + m_{H_u}^2 + m_S^2 + 2M_1^2\right) - \frac{6}{5}g_1^2\left(T_\lambda^2 - 2\lambda T_\lambda M_1\right)\\
&- 12g_1'^2y_t^2\left(Q_2^2 + Q_Q^2 + Q_{u^c}^2\right)\left(m_{H_u}^2 + m_{Q_{33}}^2 + m_{u_{33}^c}^2 + 2M_1'^2\right)\\
&- 12g_1'^2\left(Q_2^2 + Q_Q^2 + Q_{u^c}^2\right)\left(T_t^2 - 2y_tT_tM_1'\right) + 12Q_2g_1'^2T_t^2\left(Q_2 + Q_Q + Q_{u^c}\right)\\
&+ 6g_1'^2y_t^2\left(Q_2 + Q_Q + Q_{u^c}\right)\left(2Q_2m_{H_u}^2 + 2Q_2m_{Q_{33}}^2 + 2Q_2m_{u_{33}^c}^2 + \Sigma_1'\right)\\
&+ 12Q_2g_1'^2y_b^2\left(Q_1 + Q_Q + Q_{d^c}\right)\left(m_{H_d}^2 + m_{Q_{33}}^2 + m_{d_{33}^c}^2\right)\\
&+ 12Q_2g_1'^2T_b^2\left(Q_1 + Q_Q + Q_{d^c}\right) + 4Q_2g_1'^2T_\tau^2\left(Q_1 + Q_L + Q_{e^c}\right)\\
&+ 4Q_2g_1'^2y_\tau^2\left(Q_1 + Q_L + Q_{e^c}\right)\left(m_{H_d}^2 + m_{L_{33}}^2 + m_{e_{33}^c}^2\right)\\
&- 4g_1'^2\lambda^2\left(Q_1^2 + Q_2^2 + Q_S^2\right)\left(m_{H_d}^2 + m_{H_u}^2 + m_S^2 + 2M_1'^2\right)\\
&- 4g_1'^2\left(Q_1^2 + Q_2^2 + Q_S^2\right)\left(T_\lambda^2 - 2\lambda T_\lambda M_1'\right) + 2g_1'^2\lambda^2\left(Q_1 + Q_2 + Q_S\right)\Sigma_1'\\
&+ 4Q_2g_1'^2\lambda^2\left(Q_1 + Q_2 + Q_S\right)\left(m_{H_d}^2 + m_{H_u}^2 + m_S^2\right) + 4Q_2g_1'^2T_\lambda^2\left(Q_1 + Q_2 + Q_S\right)\\
&+ 4Q_2g_1'^2\left(Q_1 + Q_2 + Q_S\right)\sum_{\alpha=1}^{2}\left[\tilde{\lambda}_{\alpha\alpha}^2\left(m_{H_{1,\alpha\alpha}}^2 + m_{H_{2,\alpha\alpha}}^2 + m_S^2\right) + (T_{\alpha\alpha}^{\tilde{\lambda}})^2\right]\\
&+ 6Q_2g_1'^2\left(Q_S + Q_D + Q_{\overline{D}}\right)\sum_{i=1}^{3}\left[\kappa_{ii}^2\left(m_S^2 + m_{D_{ii}}^2 + m_{\overline{D}_{ii}}^2\right) + (T_{ii}^{\kappa})^2\right]
\end{aligned}
$$

$$
\begin{aligned}
&- 96Q_2 g_3^2 g_1'^2 M_3^2 \left(2Q_Q + Q_{u^c} + Q_{d^c} + Q_D + Q_{\overline{D}}\right) - 72 g_2^4 M_2^2 \\
&- 12Q_2 g_2^2 g_1'^2 M_2^2 \left(9Q_Q + 3Q_L + 3Q_1 + 3Q_2 + Q_{\overline{L}_4} + Q_{L_4}\right) \\
&+ \frac{288}{25} g_1^4 \left(\Sigma_1 - 3M_1^2\right) - \frac{3}{5} g_1^2 g_1'^2 \Big[4Q_2 M_1^2 \Big(2Q_{d^c} + 2Q_{\overline{D}} + 2Q_D + 6Q_{e^c} + 3Q_1 \\
&+ 3Q_2 + Q_{\overline{L}_4} + Q_{L_4} + 3Q_L + Q_Q + 8Q_{u^c}\Big) + 4M_1'^2 \Big(3Q_{d^c}^2 + 3Q_{\overline{D}}^2 - 3Q_D^2 \\
&+ 3Q_{e^c}^2 - 3Q_1^2 + 3Q_2^2 + Q_{\overline{L}_4}^2 - Q_{L_4}^2 - 3Q_L^2 + 3Q_Q^2 - 6Q_{u^c}^2\Big) \\
&- \left(2Q_2\Sigma_1 + \Sigma_1'\right)\Sigma_Q^Y\Big] - 4Q_2 g_1'^4 \Big[2M_1'^2 \Big(9Q_{d^c}^3 + 9Q_{\overline{D}}^3 + 9Q_D^3 + 3Q_{e^c}^3 + 6Q_1^3 \\
&+ 6Q_2^3 + 2Q_{\overline{L}_4}^3 + 2Q_{L_4}^3 + 6Q_L^3 + 18Q_Q^3 + 3Q_S^3 + 9Q_{u^c}^3\Big) \\
&+ \left(6Q_2 M_1'^2 - \Sigma_1'\right)\Sigma_Q\Big], \qquad \text{(C.9c)}
\end{aligned}
$$

while those for m_S^2 are

$$
\begin{aligned}
\beta_{m_S^2}^{(1)} &= 4\lambda^2 \left(m_{H_d}^2 + m_{H_u}^2 + m_S^2\right) + 4T_\lambda^2 \\
&+ \sum_{\alpha=1}^{2} \left[4\tilde{\lambda}_{\alpha\alpha}^2 \left(m_{H_{1,\alpha\alpha}}^2 + m_{H_{2,\alpha\alpha}}^2 + m_S^2\right) + 4(T_{\alpha\alpha}^{\tilde{\lambda}})^2\right] \\
&+ \sum_{i=1}^{3} \left[6\kappa_{ii}^2 \left(m_S^2 + m_{D_{ii}}^2 + m_{\overline{D}_{ii}}^2\right) + 6(T_{ii}^{\kappa})^2\right] - 8Q_S^2 g_1'^2 M_1'^2 + 2Q_S g_1'^2 \Sigma_1', \qquad \text{(C.10a)} \\
\beta_{m_S^2}^{(2)} &= -16\lambda^4 \left(m_{H_d}^2 + m_{H_u}^2 + m_S^2\right) - 32\lambda^2 T_\lambda^2 \\
&- \sum_{\alpha=1}^{2} \left[16\tilde{\lambda}_{\alpha\alpha}^4 \left(m_{H_{1,\alpha\alpha}}^2 + m_{H_{2,\alpha\alpha}}^2 + m_S^2\right) + 32\tilde{\lambda}_{\alpha\alpha}^2 (T_{\alpha\alpha}^{\tilde{\lambda}})^2\right] \\
&- \sum_{i=1}^{3} \left[24\kappa_{ii}^4 \left(m_{D_{ii}}^2 + m_{\overline{D}_{ii}}^2 + m_S^2\right) + 48\kappa_{ii}^2 (T_{ii}^{\kappa})^2\right] \\
&- 12\lambda^2 y_t^2 \left(2m_{H_u}^2 + m_{H_d}^2 + m_S^2 + m_{Q_{33}}^2 + m_{u_{33}^c}^2\right) - 12\left(\lambda T_t + y_t T_\lambda\right)^2 \\
&- 12\lambda^2 y_b^2 \left(m_{H_u}^2 + 2m_{H_d}^2 + m_S^2 + m_{Q_{33}}^2 + m_{d_{33}^c}^2\right) - 12\left(\lambda T_b + y_b T_\lambda\right)^2 \\
&- 4\lambda^2 y_\tau^2 \left(m_{H_u}^2 + 2m_{H_d}^2 + m_S^2 + m_{L_{33}}^2 + m_{e_{33}^c}^2\right) - 4\left(\lambda T_\tau + y_\tau T_\lambda\right)^2 \\
&+ 32 g_3^2 \sum_{i=1}^{3} \left[\kappa_{ii}^2 \left(m_S^2 + m_{D_{ii}}^2 + m_{\overline{D}_{ii}}^2 + 2M_3^2\right) + (T_{ii}^{\kappa})^2 - 2\kappa_{ii} T_{ii}^{\kappa} M_3\right] \\
&+ 12 g_2^2 \lambda^2 \left(m_{H_d}^2 + m_{H_u}^2 + m_S^2 + 2M_2^2\right) + 12 g_2^2 \left(T_\lambda^2 - 2\lambda T_\lambda M_2\right) \\
&+ 12 g_2^2 \sum_{\alpha=1}^{2} \left[\tilde{\lambda}_{\alpha\alpha}^2 \left(m_{H_{1,\alpha\alpha}}^2 + m_{H_{2,\alpha\alpha}}^2 + m_S^2 + 2M_2^2\right) + (T_{\alpha\alpha}^{\tilde{\lambda}})^2 - 2\tilde{\lambda}_{\alpha\alpha} T_{\alpha\alpha}^{\tilde{\lambda}} M_2\right] \\
&+ \frac{12}{5} g_1^2 \lambda^2 \left(m_{H_d}^2 + m_{H_u}^2 + m_S^2 + 2M_1^2\right) + \frac{12}{5} g_1^2 \left(T_\lambda^2 - 2\lambda T_\lambda M_1\right)
\end{aligned}
$$

$$
\begin{aligned}
&+\frac{12}{5}g_1^2\sum_{\alpha=1}^{2}\Big[\tilde{\lambda}_{\alpha\alpha}^2\left(m_{H_{1,\alpha\alpha}}^2+m_{H_{2,\alpha\alpha}}^2+m_S^2+2M_1^2\right)+(T_{\alpha\alpha}^{\tilde{\lambda}})^2-2\tilde{\lambda}_{\alpha\alpha}T_{\alpha\alpha}^{\tilde{\lambda}}M_1\Big]\\
&+\frac{8}{5}g_1^2\sum_{i=1}^{3}\Big[\kappa_{ii}^2\left(m_S^2+m_{D_{ii}}^2+m_{\overline{D}_{ii}}^2+2M_1^2\right)+(T_{ii}^{\kappa})^2-2\kappa_{ii}T_{ii}^{\kappa}M_1\Big]\\
&+8g_1'^2\lambda^2\left(Q_1^2+Q_2^2-Q_S^2\right)\left(m_{H_d}^2+m_{H_u}^2+m_S^2+2M_1'^2\right)\\
&-8Q_Sg_1'^2\lambda^2\left(Q_1m_{H_d}^2+Q_2m_{H_u}^2+Q_Sm_S^2\right)+8g_1'^2\left(Q_1^2+Q_2^2-Q_S^2\right)\left(T_\lambda^2-2\lambda T_\lambda M_1'\right)\\
&+4g_1'^2\sum_{\alpha=1}^{2}\Big\{2\tilde{\lambda}_{\alpha\alpha}^2\left(Q_1^2+Q_2^2-Q_S^2\right)\left(m_{H_{1,\alpha\alpha}}^2+m_{H_{2,\alpha\alpha}}^2+m_S^2+2M_1'^2\right)\\
&-2Q_S\tilde{\lambda}_{\alpha\alpha}^2\left(Q_1m_{H_{1,\alpha\alpha}}^2+Q_2m_{H_{2,\alpha\alpha}}^2+Q_Sm_S^2\right)+2\left[(T_{\alpha\alpha}^{\tilde{\lambda}})^2-2\tilde{\lambda}_{\alpha\alpha}T_{\alpha\alpha}^{\tilde{\lambda}}M_1'\right]\\
&\times\left(Q_1^2+Q_2^2-Q_S^2\right)\Big\}+4g_1'^2\sum_{i=1}^{3}\Big\{3\kappa_{ii}^2\left(Q_D^2+Q_{\overline{D}}^2-Q_S^2\right)\\
&\times\left(m_S^2+m_{D_{ii}}^2+m_{\overline{D}_{ii}}^2+2M_1'^2\right)-3Q_S\kappa_{ii}^2\left(Q_Sm_S^2+Q_Dm_{D_{ii}}^2+Q_{\overline{D}}m_{\overline{D}_{ii}}^2\right)\\
&+3\left[(T_{ii}^{\kappa})^2-2\kappa_{ii}T_{ii}^{\kappa}M_1'\right]\left(Q_D^2+Q_{\overline{D}}^2-Q_S^2\right)\Big\}\\
&-24Q_Sg_1'^2y_t^2\left(Q_2m_{H_u}^2+Q_Qm_{Q_{33}}^2+Q_{u^c}m_{u_{33}^c}^2\right)\\
&-24Q_Sg_1'^2y_b^2\left(Q_1m_{H_d}^2+Q_Qm_{Q_{33}}^2+Q_{d^c}m_{d_{33}^c}^2\right)\\
&-8Q_Sg_1'^2y_\tau^2\left(Q_1m_{H_d}^2+Q_Lm_{L_{33}}^2+Q_{e^c}m_{e_{33}^c}^2\right)\\
&+32Q_Sg_3^2g_1'^2\Big[2Q_Q\,\mathrm{Tr}(m_Q^2)+Q_{u^c}\,\mathrm{Tr}(m_{u^c}^2)+Q_{d^c}\,\mathrm{Tr}(m_{d^c}^2)+Q_D\,\mathrm{Tr}(m_D^2)\\
&+Q_{\overline{D}}\,\mathrm{Tr}(m_{\overline{D}}^2)\Big]+12Q_Sg_2^2g_1'^2\Big[Q_{\overline{L}_4}m_{\overline{L}_4}^2+Q_{L_4}m_{L_4}^2+3Q_Q\,\mathrm{Tr}(m_Q^2)+Q_L\,\mathrm{Tr}(m_L^2)\\
&+Q_1m_{H_d}^2+Q_1\,\mathrm{Tr}(m_{H_1}^2)+Q_2m_{H_u}^2+Q_2\,\mathrm{Tr}(m_{H_2}^2)\Big]\\
&+\frac{4}{5}Q_Sg_1^2g_1'^2\Big[3Q_{\overline{L}_4}m_{\overline{L}_4}^2+3Q_{L_4}m_{L_4}^2+2Q_{d^c}\,\mathrm{Tr}(m_{d^c}^2)+2Q_{\overline{D}}\,\mathrm{Tr}(m_{\overline{D}}^2)\\
&+2Q_D\,\mathrm{Tr}(m_D^2)+6Q_{e^c}\,\mathrm{Tr}(m_{e^c}^2)+3Q_1m_{H_d}^2+3Q_1\,\mathrm{Tr}(m_{H_1}^2)+3Q_2m_{H_u}^2\\
&+3Q_2\,\mathrm{Tr}(m_{H_2}^2)+3Q_L\,\mathrm{Tr}(m_L^2)+Q_Q\,\mathrm{Tr}(m_Q^2)+8Q_{u^c}\,\mathrm{Tr}(m_{u^c}^2)\Big]\\
&+8Q_Sg_1'^4\Big[3Q_SM_1'^2\big(9Q_{d^c}^2+9Q_{\overline{D}}^2+9Q_D^2+3Q_{e^c}^2+6Q_1^2+6Q_2^2+2Q_{\overline{L}_4}^2\\
&+2Q_{L_4}^2+6Q_L^2+18Q_Q^2+5Q_S^2+9Q_{u^c}^2\big)+2Q_{\overline{L}_4}^3m_{\overline{L}_4}^2+2Q_{L_4}^3m_{L_4}^2\\
&+3Q_{d^c}^3\,\mathrm{Tr}(m_{d^c}^2)+3Q_{\overline{D}}^3\,\mathrm{Tr}(m_{\overline{D}}^2)+3Q_D^3\,\mathrm{Tr}(m_D^2)+Q_{e^c}^3\,\mathrm{Tr}(m_{e^c}^2)+2Q_1^3m_{H_d}^2\\
&+2Q_1^3\,\mathrm{Tr}(m_{H_1}^2)+2Q_2^3m_{H_u}^2+2Q_2^3\,\mathrm{Tr}(m_{H_2}^2)+2Q_L^3\,\mathrm{Tr}(m_L^2)+6Q_Q^3\,\mathrm{Tr}(m_Q^2)\\
&+Q_S^3m_S^2+Q_S^3\,\mathrm{Tr}(m_\Sigma^2)+3Q_{u^c}^3\,\mathrm{Tr}(m_{u^c}^2)+2Q_SQ_{\overline{L}_4}^2m_{\overline{L}_4}^2+2Q_SQ_{L_4}^2m_{L_4}^2\\
&+3Q_SQ_{d^c}^2\,\mathrm{Tr}(m_{d^c}^2)+3Q_SQ_{\overline{D}}^2\,\mathrm{Tr}(m_{\overline{D}}^2)+3Q_SQ_D^2\,\mathrm{Tr}(m_D^2)+Q_SQ_{e^c}^2\,\mathrm{Tr}(m_{e^c}^2)
\end{aligned}
$$

$$
\begin{aligned}
&+ 2Q_S Q_1^2 m_{H_d}^2 + 2Q_S Q_1^2 \,\mathrm{Tr}(m_{H_1}^2) + 2Q_S Q_2^2 m_{H_u}^2 + 2Q_S Q_2^2 \,\mathrm{Tr}(m_{H_2}^2) \\
&+ 2Q_S Q_L^2 \,\mathrm{Tr}(m_L^2) + 6Q_S Q_Q^2 \,\mathrm{Tr}(m_Q^2) + Q_S^3 m_S^2 + Q_S^3 \,\mathrm{Tr}(m_\Sigma^2) \\
&+ 3Q_S Q_{u^c}^2 \,\mathrm{Tr}(m_{u^c}^2)\Big], \qquad \text{(C.10b)} \\
b_{m_S^2}^{(2)} &= 32\lambda^4 \left(m_{H_d}^2 + m_{H_u}^2 + m_S^2\right) + 64\lambda^2 T_\lambda^2 \\
&+ 16 \sum_{\alpha=1}^{2} \left[\tilde{\lambda}_{\alpha\alpha}^4 \left(m_{H_{1,\alpha\alpha}}^2 + m_{H_{2,\alpha\alpha}}^2 + m_S^2\right) + 2\tilde{\lambda}_{\alpha\alpha}^2 (T_{\alpha\alpha}^{\tilde{\lambda}})^2\right] \\
&+ 24 \sum_{i=1}^{3} \left[\kappa_{ii}^4 \left(m_S^2 + m_{D_{ii}}^2 + m_{\overline{D}_{ii}}^2\right) + 2\kappa_{ii}^2 (T_{ii}^{\kappa})^2\right] \\
&+ 16 \sum_{\alpha=1}^{2} \left[\lambda^2 \tilde{\lambda}_{\alpha\alpha}^2 \left(m_{H_d}^2 + m_{H_u}^2 + m_{H_{1,\alpha\alpha}}^2 + m_{H_{2,\alpha\alpha}}^2 + 2m_S^2\right) + \left(\lambda T_{\alpha\alpha}^{\tilde{\lambda}} + \tilde{\lambda}_{\alpha\alpha} T_\lambda\right)^2\right] \\
&+ 8 \sum_{\alpha=1}^{2} \sum_{\beta=1}^{2} \left[\tilde{\lambda}_{\alpha\alpha}^2 \tilde{\lambda}_{\beta\beta}^2 \left(m_{H_{1,\alpha\alpha}}^2 + m_{H_{2,\alpha\alpha}}^2 + m_{H_{1,\beta\beta}}^2 + m_{H_{2,\beta\beta}}^2 + 2m_S^2\right)\right. \\
&\left. + \left(\tilde{\lambda}_{\alpha\alpha} T_{\beta\beta}^{\tilde{\lambda}} + \tilde{\lambda}_{\beta\beta} T_{\alpha\alpha}^{\tilde{\lambda}}\right)^2\right] + 24 \sum_{i=1}^{3} \left[\lambda^2 \kappa_{ii}^2 \left(m_{H_d}^2 + m_{H_u}^2 + 2m_S^2 + m_{D_{ii}}^2 + m_{\overline{D}_{ii}}^2\right)\right. \\
&\left. + \left(\lambda T_{ii}^{\kappa} + \kappa_{ii} T_\lambda\right)^2\right] + 24 \sum_{\alpha=1}^{2} \sum_{i=1}^{3} \left[\tilde{\lambda}_{\alpha\alpha}^2 \kappa_{ii}^2 \left(m_{H_{1,\alpha\alpha}}^2 + m_{H_{2,\alpha\alpha}}^2 + 2m_S^2 + m_{D_{ii}}^2 + m_{\overline{D}_{ii}}^2\right)\right. \\
&\left. + \left(\tilde{\lambda}_{\alpha\alpha} T_{ii}^{\kappa} + \kappa_{ii} T_{\alpha\alpha}^{\tilde{\lambda}}\right)^2\right] + 18 \sum_{i=1}^{3} \sum_{j=1}^{3} \left[\kappa_{ii}^2 \kappa_{jj}^2 \left(2m_S^2 + m_{D_{ii}}^2 + m_{\overline{D}_{ii}}^2 + m_{D_{jj}}^2 + m_{\overline{D}_{jj}}^2\right)\right. \\
&\left. + \left(\kappa_{ii} T_{jj}^{\kappa} + \kappa_{jj} T_{ii}^{\kappa}\right)^2\right] + 12\lambda^2 y_t^2 \left(2m_{H_u}^2 + m_{H_d}^2 + m_S^2 + m_{Q_{33}}^2 + m_{u_{33}^c}^2\right) \\
&+ 12\lambda^2 y_b^2 \left(m_{H_u}^2 + 2m_{H_d}^2 + m_S^2 + m_{Q_{33}}^2 + m_{d_{33}^c}^2\right) \\
&+ 4\lambda^2 y_\tau^2 \left(2m_{H_d}^2 + m_{H_u}^2 + m_S^2 + m_{L_{33}}^2 + m_{e_{33}^c}^2\right) + 12\left(\lambda T_t + y_t T_\lambda\right)^2 \\
&+ 12\left(\lambda T_b + y_b T_\lambda\right)^2 + 4\left(\lambda T_\tau + y_\tau T_\lambda\right)^2 \\
&- 32 g_3^2 \sum_{i=1}^{3} \left[\kappa_{ii}^2 \left(m_S^2 + m_{D_{ii}}^2 + m_{\overline{D}_{ii}}^2 + 2M_3^2\right) + (T_{ii}^{\kappa})^2 - 2\kappa_{ii} T_{ii}^{\kappa} M_3\right] \\
&- 12 g_2^2 \lambda^2 \left(m_{H_d}^2 + m_{H_u}^2 + m_S^2 + 2M_2^2\right) - 12 g_2^2 \left(T_\lambda^2 - 2\lambda T_\lambda M_2\right) \\
&- 12 g_2^2 \sum_{\alpha=1}^{2} \left[\tilde{\lambda}_{\alpha\alpha}^2 \left(m_{H_{1,\alpha\alpha}}^2 + m_{H_{2,\alpha\alpha}}^2 + m_S^2 + 2M_2^2\right) + (T_{\alpha\alpha}^{\tilde{\lambda}})^2 - 2\tilde{\lambda}_{\alpha\alpha} T_{\alpha\alpha}^{\tilde{\lambda}} M_2\right] \\
&- \frac{12}{5} g_1^2 \lambda^2 \left(m_{H_d}^2 + m_{H_u}^2 + m_S^2 + 2M_1^2\right) - \frac{12}{5} g_1^2 \left(T_\lambda^2 - 2\lambda T_\lambda M_1\right) \\
&- \frac{12}{5} g_1^2 \sum_{\alpha=1}^{2} \left[\tilde{\lambda}_{\alpha\alpha}^2 \left(m_{H_{1,\alpha\alpha}}^2 + m_{H_{2,\alpha\alpha}}^2 + m_S^2 + 2M_1^2\right) + (T_{\alpha\alpha}^{\tilde{\lambda}})^2 - 2\tilde{\lambda}_{\alpha\alpha} T_{\alpha\alpha}^{\tilde{\lambda}} M_1\right] \\
&- \frac{8}{5} g_1^2 \sum_{i=1}^{3} \left[\kappa_{ii}^2 \left(m_S^2 + m_{D_{ii}}^2 + m_{\overline{D}_{ii}}^2 + 2M_1^2\right) + (T_{ii}^{\kappa})^2 - 2\kappa_{ii} T_{ii}^{\kappa} M_1\right]
\end{aligned}
$$

$$
\begin{aligned}
&- 8g_1'^2\lambda^2\left(Q_1^2+Q_2^2+Q_S^2\right)\left(m_{H_d}^2+m_{H_u}^2+m_S^2+2M_1'^2\right)\\
&+ 4g_1'^2\lambda^2\left(Q_1+Q_2+Q_S\right)\left(Q_S m_{H_d}^2+Q_S m_{H_u}^2+Q_S m_S^2+\Sigma_1'\right)\\
&- 8g_1'^2\left(Q_1^2+Q_2^2+Q_S^2\right)\left(T_\lambda^2-2\lambda T_\lambda M_1'\right)+4Q_S g_1'^2 T_\lambda^2\left(Q_1+Q_2+Q_S\right)\\
&+ 2g_1'^2\sum_{\alpha=1}^{2}\Big\{-4\tilde{\lambda}_{\alpha\alpha}^2\left(Q_1^2+Q_2^2+Q_S^2\right)\left(m_{H_{1,\alpha\alpha}}^2+m_{H_{2,\alpha\alpha}}^2+m_S^2+2M_1'^2\right)\\
&+ 2\tilde{\lambda}_{\alpha\alpha}^2\left(Q_1+Q_2+Q_S\right)\left(Q_S m_{H_{1,\alpha\alpha}}^2+Q_S m_{H_{2,\alpha\alpha}}^2+Q_S m_S^2+\Sigma_1'\right)\\
&- 4\left(Q_1^2+Q_2^2+Q_S^2\right)\left[(T_{\alpha\alpha}^{\tilde{\lambda}})^2-2\tilde{\lambda}_{\alpha\alpha}T_{\alpha\alpha}^{\tilde{\lambda}}M_1'\right]+2Q_S(T_{\alpha\alpha}^{\tilde{\lambda}})^2\left(Q_1+Q_2+Q_S\right)\Big\}\\
&+ 2g_1'^2\sum_{i=1}^{3}\Big\{-6\kappa_{ii}^2\left(Q_S^2+Q_D^2+Q_{\overline{D}}^2\right)\left(m_S^2+m_{D_{ii}}^2+m_{\overline{D}_{ii}}^2+2M_1'^2\right)\\
&+ 3\kappa_{ii}^2\left(Q_S+Q_D+Q_{\overline{D}}\right)\left(Q_S m_S^2+Q_S m_{D_i}^2+Q_S m_{\overline{D}_i}^2+\Sigma_1'\right)\\
&- 6\left(Q_S^2+Q_D^2+Q_{\overline{D}}^2\right)\left[(T_{ii}^{\kappa})^2-2\kappa_{ii}T_{ii}^{\kappa}M_1'\right]+3Q_S(T_{ii}^{\kappa})^2\left(Q_S+Q_D+Q_{\overline{D}}\right)\Big\}\\
&+ 12Q_S g_1'^2 y_t^2\left(Q_2+Q_Q+Q_{u^c}\right)\left(m_{H_u}^2+m_{Q_{33}}^2+m_{u_{33}^c}^2\right)\\
&+ 12Q_S g_1'^2 y_b^2\left(Q_1+Q_Q+Q_{d^c}\right)\left(m_{H_d}^2+m_{Q_{33}}^2+m_{d_{33}^c}^2\right)\\
&+ 4Q_S g_1'^2 y_\tau^2\left(Q_1+Q_L+Q_{e^c}\right)\left(m_{H_d}^2+m_{L_{33}}^2+m_{e_{33}^c}^2\right)\\
&+ 12Q_S g_1'^2 T_t^2\left(Q_2+Q_Q+Q_{u^c}\right)+12Q_S g_1'^2 T_b^2\left(Q_1+Q_Q+Q_{d^c}\right)\\
&+ 4Q_S g_1'^2 T_\tau^2\left(Q_1+Q_L+Q_{e^c}\right)-96Q_S g_3^2 g_1'^2 M_3^2\left(2Q_Q+Q_{u^c}+Q_{d^c}+Q_D+Q_{\overline{D}}\right)\\
&- 12Q_S g_2^2 g_1'^2 M_2^2\Big(9Q_Q+3Q_L+3Q_1+3Q_2+Q_{\overline{L}_4}+Q_{L_4}\Big)\\
&- \frac{6}{5}Q_S g_1^2 g_1'^2\Big[2M_1^2\Big(2Q_{d^c}+2Q_{\overline{D}}+2Q_D+6Q_{e^c}+3Q_1+3Q_2+Q_{\overline{L}_4}\\
&+ Q_{L_4}+3Q_L+Q_Q+8Q_{u^c}\Big)-\Sigma_1\Sigma_Q^Y\Big]-4Q_S g_1'^4\Big[2M_1'^2\Big(9Q_{d^c}^3+9Q_{\overline{D}}^3+9Q_D^3\\
&+ 3Q_{e^c}^3+6Q_1^3+6Q_2^3+2Q_{\overline{L}_4}^3+2Q_{L_4}^3+6Q_L^3+18Q_Q^3+3Q_S^3+9Q_{u^c}^3\Big)\\
&+ \left(6Q_S M_1'^2-\Sigma_1'\right)\Sigma_Q\Big]. \qquad \text{(C.10c)}
\end{aligned}
$$

If the one-loop contributions to the effective potential from top and stop loops are also included, it is necessary to consider the expansions for y_t, T_t, $m_{Q_{33}}^2$ and $m_{u_{33}^c}^2$. The required expressions for y_t read

$$
\begin{aligned}
\beta_{y_t}^{(1)} &= y_t\left[\lambda^2+6y_t^2+y_b^2-\frac{16}{3}g_3^2-3g_2^2-\frac{13}{15}g_1^2-2g_1'^2\left(Q_2^2+Q_Q^2+Q_{u^c}^2\right)\right], \qquad \text{(C.11a)}\\
\beta_{y_t}^{(2)} &= y_t\Big\{-22y_t^4-5y_b^4-5y_t^2y_b^2-y_b^2y_\tau^2-\lambda^2\left(\lambda^2+3y_t^2+4y_b^2+y_\tau^2+2\Sigma_\lambda+3\Sigma_\kappa\right)\\
&\quad+2g_1'^2\left[\lambda^2\left(Q_1^2-Q_2^2+Q_S^2\right)+2y_t^2\left(2Q_Q^2+Q_{u^c}^2\right)+y_b^2\left(Q_1^2-Q_Q^2+Q_{d^c}^2\right)\right]
\end{aligned}
$$

$$
\begin{aligned}
&+ 16g_3^2y_t^2 + 6g_2^2y_t^2 + g_1^2\left(\frac{6}{5}y_t^2 + \frac{2}{5}y_b^2\right) + \frac{128}{9}g_3^4 + \frac{33}{2}g_2^4 + \frac{3913}{450}g_1^4 \\
&+ 2g_1'^4\left[2\left(Q_2^4 + Q_Q^4 + Q_{u^c}^4\right) + \left(Q_2^2 + Q_Q^2 + Q_{u^c}^2\right)\Sigma_Q\right] + 8g_3^2g_2^2 + \frac{136}{45}g_3^2g_1^2 \\
&+ \frac{32}{3}g_3^2g_1'^2\left(Q_Q^2 + Q_{u^c}^2\right) + g_2^2g_1^2 + 6g_2^2g_1'^2\left(Q_2^2 + Q_Q^2\right) \\
&+ \frac{2}{5}g_1^2g_1'^2\left[3Q_2^2 + \frac{1}{3}Q_Q^2 + \frac{16}{3}Q_{u^c}^2 + \left(3Q_2 + Q_Q - 4Q_{u^c}\right)\Sigma_Q^Y\right]\Bigg\}, \qquad \text{(C.11b)}
\end{aligned}
$$

$$
\begin{aligned}
b_{y_t}^{(2)} = y_t\Bigg\{&54y_t^4 + \frac{13}{2}y_b^4 + 13y_t^2y_b^2 + y_b^2y_\tau^2 + \lambda^2\left(\frac{5}{2}\lambda^2 + 15y_t^2 + 5y_b^2 + y_\tau^2 + 2\Sigma_\lambda + 3\Sigma_\kappa\right) \\
&- \frac{16}{3}g_3^2\left(\lambda^2 + 2y_b^2 + 12y_t^2\right) - 6g_2^2\left(\lambda^2 + y_b^2 + 6y_t^2\right) - g_1^2\left(\frac{22}{15}\lambda^2 + \frac{4}{3}y_b^2 + \frac{52}{5}y_t^2\right) \\
&- 2g_1'^2\Big[\lambda^2\left(Q_1^2 + 2Q_2^2 + Q_S^2 + Q_Q^2 + Q_{u^c}^2\right) + y_b^2\left(Q_1^2 + Q_2^2 + 2Q_Q^2 + Q_{u^c}^2 + Q_{d^c}^2\right) \\
&+ 12y_t^2\left(Q_2^2 + Q_Q^2 + Q_{u^c}^2\right)\Big] + \frac{128}{9}g_3^4 - \frac{15}{2}g_2^4 - \frac{143}{18}g_1^4 \\
&+ 2g_1'^4\left(Q_2^2 + Q_Q^2 + Q_{u^c}^2\right)\left(Q_2^2 + Q_Q^2 + Q_{u^c}^2 - \Sigma_Q\right) + 16g_3^2g_2^2 + \frac{208}{45}g_3^2g_1^2 \\
&+ \frac{32}{3}g_3^2g_1'^2\left(Q_2^2 + Q_Q^2 + Q_{u^c}^2\right) + \frac{13}{5}g_2^2g_1^2 + 6g_2^2g_1'^2\left(Q_2^2 + Q_Q^2 + Q_{u^c}^2\right) \\
&+ \frac{26}{15}g_1^2g_1'^2\left(Q_2^2 + Q_Q^2 + Q_{u^c}^2\right)\Bigg\}, \qquad \text{(C.11c)}
\end{aligned}
$$

and those for T_t read

$$
\begin{aligned}
\beta_{T_t}^{(1)} = {}& T_t\left[\lambda^2 + 6y_t^2 + y_b^2 - \frac{16}{3}g_3^2 - 3g_2^2 - \frac{13}{15}g_1^2 - 2g_1'^2\left(Q_2^2 + Q_Q^2 + Q_{u^c}^2\right)\right] \\
&+ y_t\Big[2\lambda T_\lambda + 12y_tT_t + 2y_bT_b + \frac{32}{3}g_3^2M_3 + 6g_2^2M_2 + \frac{26}{15}g_1^2M_1 \\
&+ 4g_1'^2M_1'\left(Q_2^2 + Q_Q^2 + Q_{u^c}^2\right)\Big], \qquad \text{(C.12a)}
\end{aligned}
$$

$$
\begin{aligned}
\beta_{T_t}^{(2)} = T_t\Bigg\{&-22y_t^4 - 5y_b^4 - 5y_t^2y_b^2 - y_b^2y_\tau^2 - \lambda^2\left(\lambda^2 + 3y_t^2 + 4y_b^2 + y_\tau^2 + 2\Sigma_\lambda + 3\Sigma_\kappa\right) \\
&+ 2g_1'^2\left[\lambda^2\left(Q_1^2 - Q_2^2 + Q_S^2\right) + 2y_t^2\left(2Q_Q^2 + Q_{u^c}^2\right) + y_b^2\left(Q_1^2 - Q_Q^2 + Q_{d^c}^2\right)\right] \\
&+ 16g_3^2y_t^2 + 6g_2^2y_t^2 + g_1^2\left(\frac{6}{5}y_t^2 + \frac{2}{5}y_b^2\right) + \frac{128}{9}g_3^4 + \frac{33}{2}g_2^4 + \frac{3913}{450}g_1^4 \\
&+ 2g_1'^4\left[2\left(Q_2^4 + Q_Q^4 + Q_{u^c}^4\right) + \left(Q_2^2 + Q_Q^2 + Q_{u^c}^2\right)\Sigma_Q\right] + 8g_3^2g_2^2 + \frac{136}{45}g_3^2g_1^2 \\
&+ \frac{32}{3}g_3^2g_1'^2\left(Q_Q^2 + Q_{u^c}^2\right) + g_2^2g_1^2 + 6g_2^2g_1'^2\left(Q_2^2 + Q_Q^2\right) \\
&+ \frac{2}{5}g_1^2g_1'^2\left[3Q_2^2 + \frac{1}{3}Q_Q^2 + \frac{16}{3}Q_{u^c}^2\right]\Bigg\} + y_t\Bigg\{-88y_t^3T_t - 20y_b^3T_b \\
&- 10y_ty_b\left(y_bT_t + y_tT_b\right) - 2y_by_\tau\left(y_bT_\tau + y_\tau T_b\right)
\end{aligned}
$$

$$
\begin{aligned}
&- 2\lambda T_\lambda \left(2\lambda^2 + 3y_t^2 + 4y_b^2 + y_\tau^2 + 2\Sigma_\lambda + 3\Sigma_\kappa\right) \\
&- 2\lambda^2 \left(3y_t T_t + 4y_b T_b + y_\tau T_\tau + 2\Sigma_{T_\lambda} + 3\Sigma_{T_\kappa}\right) + 32 g_3^2 y_t \left(T_t - y_t M_3\right) \\
&+ 12 g_2^2 y_t \left(T_t - y_t M_2\right) + \frac{2}{5} g_1^2 \Big[6y_t T_t + 2y_b T_b - \left(6y_t^2 + 2y_b^2\right) M_1\Big] \\
&+ 4 g_1'^2 \Big[\lambda \left(Q_1^2 - Q_2^2 + Q_S^2\right)\left(T_\lambda - \lambda M_1'\right) + 2y_t \left(2Q_Q^2 + Q_{u^c}^2\right)\left(T_t - y_t M_1'\right) \\
&+ y_b \left(Q_1^2 - Q_Q^2 + Q_{d^c}^2\right)\left(T_b - y_b M_1'\right)\Big] - \frac{512}{9} g_3^4 M_3 - 66 g_2^4 M_2 - \frac{7826}{225} g_1^4 M_1 \\
&- 8 g_1'^4 M_1' \Big[2\left(Q_2^4 + Q_Q^4 + Q_{u^c}^4\right) + \left(Q_2^2 + Q_Q^2 + Q_{u^c}^2\right)\Sigma_Q\Big] - 16 g_3^2 g_2^2 \left(M_3 + M_2\right) \\
&- \frac{272}{45} g_3^2 g_1^2 \left(M_3 + M_1\right) - \frac{64}{3} g_3^2 g_1'^2 \left(Q_Q^2 + Q_{u^c}^2\right)\left(M_3 + M_1'\right) - 2 g_2^2 g_1^2 \left(M_2 + M_1\right) \\
&- \frac{4}{15} g_1^2 g_1'^2 \left(9Q_2^2 + Q_Q^2 + 16 Q_{u^c}^2\right)\left(M_1 + M_1'\right) \\
&- 12 g_2^2 g_1'^2 \left(Q_2^2 + Q_Q^2\right)\left(M_2 + M_1'\right)\Big\}, \qquad \text{(C.12b)}
\end{aligned}
$$

$$
\begin{aligned}
b_{T_t}^{(2)} = y_t \Big[&2\lambda T_\lambda + 12 y_t T_t + 2 y_b T_b + \frac{32}{3} g_3^2 M_3 + 6 g_2^2 M_2 + \frac{26}{15} g_1^2 M_1 \\
&+ 4 g_1'^2 M_1' \left(Q_2^2 + Q_Q^2 + Q_{u^c}^2\right)\Big] \times \Big[\lambda^2 + 6y_t^2 + y_b^2 - \frac{16}{3} g_3^2 - 3 g_2^2 - \frac{13}{15} g_1^2 \\
&- 2 g_1'^2 \left(Q_2^2 + Q_Q^2 + Q_{u^c}^2\right)\Big] + T_t \Big\{54 y_t^4 + \frac{13}{2} y_b^4 + 13 y_t^2 y_b^2 + y_b^2 y_\tau^2 \\
&+ \lambda^2 \left(\frac{5}{2}\lambda^2 + 15 y_t^2 + 5 y_b^2 + y_\tau^2 + 2\Sigma_\lambda + 3\Sigma_\kappa\right) - \frac{16}{3} g_3^2 \left(\lambda^2 + 2y_b^2 + 12 y_t^2\right) \\
&- 6 g_2^2 \left(\lambda^2 + y_b^2 + 6 y_t^2\right) - g_1^2 \left(\frac{22}{15}\lambda^2 + \frac{4}{3} y_b^2 + \frac{52}{5} y_t^2\right) \\
&- 2 g_1'^2 \Big[\lambda^2 \left(Q_1^2 + 2Q_2^2 + Q_S^2 + Q_Q^2 + Q_{u^c}^2\right) + y_b^2 \left(Q_1^2 + Q_2^2 + 2Q_Q^2 + Q_{u^c}^2 + Q_{d^c}^2\right) \\
&+ 12 y_t^2 \left(Q_2^2 + Q_Q^2 + Q_{u^c}^2\right)\Big] + \frac{128}{9} g_3^4 - \frac{15}{2} g_2^4 - \frac{143}{18} g_1^4 \\
&+ 2 g_1'^4 \left(Q_2^2 + Q_Q^2 + Q_{u^c}^2\right)\left(Q_2^2 + Q_Q^2 + Q_{u^c}^2 - \Sigma_Q\right) + 16 g_3^2 g_2^2 + \frac{208}{45} g_3^2 g_1^2 \\
&+ \frac{32}{3} g_3^2 g_1'^2 \left(Q_2^2 + Q_Q^2 + Q_{u^c}^2\right) + \frac{13}{5} g_2^2 g_1^2 + 6 g_2^2 g_1'^2 \left(Q_2^2 + Q_Q^2 + Q_{u^c}^2\right) \\
&+ \frac{26}{15} g_1^2 g_1'^2 \left(Q_2^2 + Q_Q^2 + Q_{u^c}^2\right)\Big\} + y_t \Big[144 y_t^3 T_t + 24 y_b^3 T_b + 14 y_t y_b \left(y_t T_b + T_t y_b\right) \\
&+ 2 y_b y_\tau \left(y_b T_\tau + T_b y_\tau\right) + 18\lambda y_t \left(\lambda T_t + T_\lambda y_t\right) + 8\lambda y_b \left(\lambda T_b + T_\lambda y_b\right) \\
&+ 2\lambda y_\tau \left(\lambda T_\tau + T_\lambda y_\tau\right) + 16\lambda^3 T_\lambda + 4\lambda \sum_{\alpha=1}^{2} \tilde{\lambda}_{\alpha\alpha} \left(\lambda T_{\alpha\alpha}^{\tilde{\lambda}} + T_\lambda \tilde{\lambda}_{\alpha\alpha}\right) \\
&+ 6\lambda \sum_{i=1}^{3} \kappa_{ii} \left(\lambda T_{ii}^{\kappa} + T_\lambda \kappa_{ii}\right) - 64 g_3^2 y_t \left(T_t - y_t M_3\right) - \frac{32}{3} g_3^2 y_b \left(T_b - y_b M_3\right) \\
&- 36 g_2^2 y_t \left(T_t - y_t M_2\right) - 6 g_2^2 y_b \left(T_b - y_b M_2\right) - 6 g_2^2 \lambda \left(T_\lambda - \lambda M_2\right)
\end{aligned}
$$

$$
\begin{aligned}
&- \frac{52}{5} g_1^2 y_t \left(T_t - y_t M_1\right) - \frac{14}{15} g_1^2 y_b \left(T_b - y_b M_1\right) - \frac{18}{15} g_1^2 \lambda \left(T_\lambda - \lambda M_1\right) \\
&- 24 g_1'^2 y_t \left(Q_2^2 + Q_Q^2 + Q_{u^c}^2\right) \left(T_t - y_t M_1'\right) - 4 g_1'^2 y_b \left(Q_1^2 + Q_Q^2 + Q_{d^c}^2\right) \left(T_b - y_b M_1'\right) \\
&- 4 g_1'^2 \lambda \left(Q_1^2 + Q_2^2 + Q_S^2\right) \left(T_\lambda - \lambda M_1'\right) + 48 g_2^4 M_2 + \frac{832}{25} g_1^4 M_1 \\
&+ 8 g_1'^4 M_1' \Sigma_Q \left(Q_2^2 + Q_Q^2 + Q_{u^c}^2\right) \Big] . \qquad \text{(C.12c)}
\end{aligned}
$$

The one- and two-loop β functions and the resulting $O(t^2)$ coefficient for $m_{Q_{33}}^2$ are

$$
\begin{aligned}
\beta_{m_{Q_{33}}^2}^{(1)} &= 2 y_t^2 \left(m_{H_u}^2 + m_{Q_{33}}^2 + m_{u_{33}^c}^2\right) + 2 T_t^2 + 2 y_b^2 \left(m_{H_d}^2 + m_{Q_{33}}^2 + m_{d_{33}^c}^2\right) + 2 T_b^2 \\
&\quad - \frac{32}{3} g_3^2 M_3^2 - 6 g_2^2 M_2^2 - \frac{2}{15} g_1^2 M_1^2 - 8 Q_Q^2 g_1'^2 M_1'^2 + \frac{1}{5} g_1^2 \Sigma_1 + 2 Q_Q g_1'^2 \Sigma_1' , \qquad \text{(C.13a)} \\
\beta_{m_{Q_{33}}^2}^{(2)} &= -20 y_t^4 \left(m_{H_u}^2 + m_{Q_{33}}^2 + m_{u_{33}^c}^2\right) - 20 y_b^4 \left(m_{H_d}^2 + m_{Q_{33}}^2 + m_{d_{33}^c}^2\right) \\
&\quad - 2 y_\tau^2 y_b^2 \left(2 m_{H_d}^2 + m_{Q_{33}}^2 + m_{L_{33}}^2 + m_{d_{33}^c}^2 + m_{e_{33}^c}^2\right) - 40 y_t^2 T_t^2 - 40 y_b^2 T_b^2 \\
&\quad - 2 \left(y_b T_\tau + y_\tau T_b\right)^2 - 2 \lambda^2 y_t^2 \left(2 m_{H_u}^2 + m_{H_d}^2 + m_S^2 + m_{Q_{33}}^2 + m_{u_{33}^c}^2\right) \\
&\quad - 2 \lambda^2 y_b^2 \left(m_{H_u}^2 + 2 m_{H_d}^2 + m_S^2 + m_{Q_{33}}^2 + m_{d_{33}^c}^2\right) - 2 \left(\lambda T_t + y_t T_\lambda\right)^2 \\
&\quad - 2 \left(\lambda T_b + y_b T_\lambda\right)^2 + \frac{2}{5} g_1^2 y_t^2 \left(m_{H_u}^2 + 3 m_{Q_{33}}^2 + 8 m_{u_{33}^c}^2 + 8 M_1^2\right) \\
&\quad + \frac{8}{5} g_1^2 \left(T_t^2 - 2 y_t T_t M_1\right) + \frac{2}{5} g_1^2 y_b^2 \left(5 m_{H_d}^2 + m_{Q_{33}}^2 + 4 M_1^2\right) \\
&\quad + \frac{4}{5} g_1^2 \left(T_b^2 - 2 y_b T_b M_1\right) + \frac{2}{5} g_1^2 y_\tau^2 \left(m_{H_d}^2 + m_{L_{33}}^2 - 2 m_{e_{33}^c}^2\right) \\
&\quad + \frac{2}{5} g_1^2 \lambda^2 \left(m_{H_d}^2 - m_{H_u}^2\right) + \frac{2}{5} g_1^2 \sum_{\alpha=1}^{2} \tilde{\lambda}_{\alpha\alpha}^2 \left(m_{H_{1,\alpha\alpha}}^2 - m_{H_{2,\alpha\alpha}}^2\right) \\
&\quad + \frac{2}{5} g_1^2 \sum_{i=1}^{3} \kappa_{ii}^2 \left(m_{D_{ii}}^2 - m_{\overline{D}_{ii}}^2\right) \\
&\quad + 4 g_1'^2 y_t^2 \left(Q_2^2 - Q_Q^2 + Q_{u^c}^2\right) \left(m_{H_u}^2 + m_{Q_{33}}^2 + m_{u_{33}^c}^2 + 2 M_1'^2\right) \\
&\quad + 4 g_1'^2 \left(Q_2^2 - Q_Q^2 + Q_{u^c}^2\right) \left(T_t^2 - 2 y_t T_t M_1'\right) \\
&\quad - 24 Q_Q g_1'^2 y_t^2 \left(Q_2 m_{H_u}^2 + Q_Q m_{Q_{33}}^2 + Q_{u^c} m_{u_{33}^c}^2\right) \\
&\quad + 4 g_1'^2 y_b^2 \left(Q_1^2 - Q_Q^2 + Q_{d^c}^2\right) \left(m_{H_d}^2 + m_{Q_{33}}^2 + m_{d_{33}^c}^2 + 2 M_1'^2\right) \\
&\quad + 4 g_1'^2 \left(Q_1^2 - Q_Q^2 + Q_{d^c}^2\right) \left(T_b^2 - 2 y_b T_b M_1'\right) \\
&\quad - 24 Q_Q g_1'^2 y_b^2 \left(Q_1 m_{H_d}^2 + Q_Q m_{Q_{33}}^2 + Q_{d^c} m_{d_{33}^c}^2\right) \\
&\quad - 8 Q_Q g_1'^2 y_\tau^2 \left(Q_1 m_{H_d}^2 + Q_L m_{L_{33}}^2 + Q_{e^c} m_{e_{33}^c}^2\right) \\
&\quad - 8 Q_Q g_1'^2 \lambda^2 \left(Q_1 m_{H_d}^2 + Q_2 m_{H_u}^2 + Q_S m_S^2\right)
\end{aligned}
$$

$$
\begin{aligned}
&- 8Q_Q g_1'^2 \sum_{\alpha=1}^{2} \tilde{\lambda}_{\alpha\alpha}^2 \left(Q_1 m_{H_{1,\alpha\alpha}}^2 + Q_2 m_{H_{2,\alpha\alpha}}^2 + Q_S m_S^2\right) \\
&- 12Q_Q g_1'^2 \sum_{i=1}^{3} \kappa_{ii}^2 \left(Q_S m_S^2 + Q_D m_{D_{ii}}^2 + Q_{\overline{D}} m_{\overline{D}_{ii}}^2\right) \\
&+ \frac{16}{3} g_3^4 \left[10M_3^2 + 2\,\mathrm{Tr}(m_Q^2) + \mathrm{Tr}(m_{u^c}^2) + \mathrm{Tr}(m_{d^c}^2) + \mathrm{Tr}(m_D^2) + \mathrm{Tr}(m_{\overline{D}}^2)\right] \\
&+ 32 g_3^2 g_2^2 \left(M_2^2 + M_2 M_3 + M_3^2\right) + \frac{16}{45} g_3^2 g_1^2 \Big[2\left(M_1^2 + M_1 M_3 + M_3^2\right) + 3\,\mathrm{Tr}(m_Q^2) \\
&+ 3\,\mathrm{Tr}(m_{d^c}^2) - 6\,\mathrm{Tr}(m_{u^c}^2) - 3\,\mathrm{Tr}(m_D^2) + 3\,\mathrm{Tr}(m_{\overline{D}}^2)\Big] \\
&+ \frac{32}{3} Q_Q g_3^2 g_1'^2 \Big[4Q_Q \left(M_1'^2 + M_1' M_3 + M_3^2\right) + 6Q_Q\,\mathrm{Tr}(m_Q^2) + 3Q_{u^c}\,\mathrm{Tr}(m_{u^c}^2) \\
&+ 3Q_{d^c}\,\mathrm{Tr}(m_{d^c}^2) + 3Q_D\,\mathrm{Tr}(m_D^2) + 3Q_{\overline{D}}\,\mathrm{Tr}(m_{\overline{D}}^2)\Big] + 3g_2^4 \Big[29M_2^2 + m_{\overline{L}_4}^2 + m_{L_4}^2 \\
&+ 3\,\mathrm{Tr}(m_Q^2) + \mathrm{Tr}(m_L^2) + m_{H_d}^2 + \mathrm{Tr}(m_{H_1}^2) + m_{H_u}^2 + \mathrm{Tr}(m_{H_2}^2)\Big] \\
&+ \frac{1}{5} g_2^2 g_1^2 \Big[2\left(M_1^2 + M_1 M_2 + M_2^2\right) + 3m_{\overline{L}_4}^2 - 3m_{L_4}^2 + 3\,\mathrm{Tr}(m_Q^2) - 3\,\mathrm{Tr}(m_L^2) \\
&+ 3m_{H_u}^2 + 3\,\mathrm{Tr}(m_{H_2}^2) - 3m_{H_d}^2 - 3\,\mathrm{Tr}(m_{H_1}^2)\Big] \\
&+ 12 Q_Q g_2^2 g_1'^2 \Big[2Q_Q \left(M_1'^2 + M_1' M_2 + M_2^2\right) + Q_{\overline{L}_4} m_{\overline{L}_4}^2 + Q_{L_4} m_{L_4}^2 + 3Q_Q\,\mathrm{Tr}(m_Q^2) \\
&+ Q_L\,\mathrm{Tr}(m_L^2) + Q_1 m_{H_d}^2 + Q_1\,\mathrm{Tr}(m_{H_1}^2) + Q_2 m_{H_u}^2 + Q_2\,\mathrm{Tr}(m_{H_2}^2)\Big] \\
&+ \frac{1}{75} g_1^4 \Big[289M_1^2 + 12m_{\overline{L}_4}^2 - 6m_{L_4}^2 + 6\,\mathrm{Tr}(m_{d^c}^2) - 2\,\mathrm{Tr}(m_D^2) + 6\,\mathrm{Tr}(m_{\overline{D}}^2) \\
&+ 42\,\mathrm{Tr}(m_{e^c}^2) - 6m_{H_d}^2 - 6\,\mathrm{Tr}(m_{H_1}^2) + 12m_{H_u}^2 + 12\,\mathrm{Tr}(m_{H_2}^2) - 6\,\mathrm{Tr}(m_L^2) \\
&+ 2\,\mathrm{Tr}(m_Q^2) - 24\,\mathrm{Tr}(m_{u^c}^2)\Big] + \frac{4}{15} g_1^2 g_1'^2 \Big[2Q_Q \big(9Q_{d^c} + 9Q_{\overline{D}} - 9Q_D + 9Q_{e^c} \\
&- 9Q_1 + 9Q_2 + 3Q_{\overline{L}_4} - 3Q_{L_4} - 9Q_L + 10Q_Q - 18Q_{u^c}\big) \left(M_1^2 + M_1 M_1' + M_1'^2\right) \\
&+ 3Q_{\overline{L}_4}^2 m_{\overline{L}_4}^2 - 3Q_{L_4}^2 m_{L_4}^2 + 3Q_{d^c}^2\,\mathrm{Tr}(m_{d^c}^2) + 3Q_{\overline{D}}^2\,\mathrm{Tr}(m_{\overline{D}}^2) - 3Q_D^2\,\mathrm{Tr}(m_D^2) \\
&+ 3Q_{e^c}^2\,\mathrm{Tr}(m_{e^c}^2) - 3Q_1^2 m_{H_d}^2 - 3Q_1^2\,\mathrm{Tr}(m_{H_1}^2) + 3Q_2^2 m_{H_u}^2 + 3Q_2^2\,\mathrm{Tr}(m_{H_2}^2) \\
&- 3Q_L^2\,\mathrm{Tr}(m_L^2) - 3Q_Q^2\,\mathrm{Tr}(m_Q^2) - 6Q_{u^c}^2\,\mathrm{Tr}(m_{u^c}^2) + 15Q_Q Q_{\overline{L}_4} m_{\overline{L}_4}^2 + 3Q_Q Q_{L_4} m_{L_4}^2 \\
&+ 12Q_Q Q_{d^c}\,\mathrm{Tr}(m_{d^c}^2) + 12Q_Q Q_{\overline{D}}\,\mathrm{Tr}(m_{\overline{D}}^2) + 24Q_Q Q_{e^c}\,\mathrm{Tr}(m_{e^c}^2) + 3Q_Q Q_1 m_{H_d}^2 \\
&+ 3Q_Q Q_1\,\mathrm{Tr}(m_{H_1}^2) + 15Q_Q Q_2 m_{H_u}^2 + 15Q_2\,\mathrm{Tr}(m_{H_2}^2) + 3Q_Q Q_L\,\mathrm{Tr}(m_L^2) \\
&+ 15Q_Q^2\,\mathrm{Tr}(m_Q^2) + 12Q_Q Q_{u^c}\,\mathrm{Tr}(m_{u^c}^2)\Big] + 8Q_Q g_1'^4 \Big[3Q_Q M_1'^2 \big(9Q_{d^c}^2 + 9Q_{\overline{D}}^2 + 9Q_D^2 \\
&+ 3Q_{e^c}^2 + 6Q_1^2 + 6Q_2^2 + 2Q_{\overline{L}_4}^2 + 2Q_{L_4}^2 + 6Q_L^2 + 20Q_Q^2 + 3Q_S^2 + 9Q_{u^c}^2\big) \\
&+ 2Q_{\overline{L}_4}^3 m_{\overline{L}_4}^2 + 2Q_{L_4}^3 m_{L_4}^2 + 3Q_{d^c}^3\,\mathrm{Tr}(m_{d^c}^2) + 3Q_{\overline{D}}^3\,\mathrm{Tr}(m_{\overline{D}}^2) + 3Q_D^3\,\mathrm{Tr}(m_D^2)
\end{aligned}
$$

$$
\begin{aligned}
&+ Q_{e^c}^3 \operatorname{Tr}(m_{e^c}^2) + 2Q_1^3 m_{H_d}^2 + 2Q_1^3 \operatorname{Tr}(m_{H_1}^2) + 2Q_2^3 m_{H_u}^2 + 2Q_2^3 \operatorname{Tr}(m_{H_2}^2) \\
&+ 2Q_L^3 \operatorname{Tr}(m_L^2) + 6Q_Q^3 \operatorname{Tr}(m_Q^2) + Q_S^3 m_S^2 + Q_S^3 \operatorname{Tr}(m_\Sigma^2) + 3Q_{u^c}^3 \operatorname{Tr}(m_{u^c}^2) \\
&+ 2Q_Q Q_{\overline{L}_4}^2 m_{\overline{L}_4}^2 + 2Q_Q Q_{L_4}^2 m_{L_4}^2 + 3Q_Q Q_{d^c}^2 \operatorname{Tr}(m_{d^c}^2) + 3Q_Q Q_{\overline{D}}^2 \operatorname{Tr}(m_{\overline{D}}^2) \\
&+ 3Q_Q Q_D^2 \operatorname{Tr}(m_D^2) + Q_Q Q_{e^c}^2 \operatorname{Tr}(m_{e^c}^2) + 2Q_Q Q_1^2 m_{H_d}^2 + 2Q_Q Q_1^2 \operatorname{Tr}(m_{H_1}^2) \\
&+ 2Q_Q Q_2^2 m_{H_u}^2 + 2Q_Q Q_2^2 \operatorname{Tr}(m_{H_2}^2) + 2Q_Q Q_L^2 \operatorname{Tr}(m_L^2) + 6Q_Q^3 \operatorname{Tr}(m_Q^2) \\
&+ Q_Q Q_S^2 m_S^2 + Q_Q Q_S^2 \operatorname{Tr}(m_\Sigma^2) + 3Q_Q Q_{u^c}^2 \operatorname{Tr}(m_{u^c}^2) \Big], \qquad \text{(C.13b)}
\end{aligned}
$$

$$
\begin{aligned}
b_{m_{Q_{33}}^2}^{(2)} &= 24y_t^4 \left(m_{H_u^2} + m_{Q_{33}}^2 + m_{u_{33}^c}^2\right) + 24y_b^4 \left(m_{H_d}^2 + m_{Q_{33}}^2 + m_{d_{33}^c}^2\right) + 48y_t^2 T_t^2 + 48y_b^2 T_b^2 \\
&+ 4y_t^2 y_b^2 \left(m_{H_u}^2 + m_{H_d}^2 + 2m_{Q_{33}}^2 + m_{u_{33}^c}^2 + m_{d_{33}^c}^2\right) + 4\left(y_t T_b + y_b T_t\right)^2 \\
&+ 2y_b^2 y_\tau^2 \left(2m_{H_d}^2 + m_{Q_{33}}^2 + m_{d_{33}^c}^2 + m_{L_{33}}^2 + m_{e_{33}^c}^2\right) + 2\left(y_\tau T_b + y_b T_\tau\right)^2 \\
&+ 2\lambda^2 y_t^2 \left(m_{H_d}^2 + 2m_{H_u}^2 + m_S^2 + m_{Q_{33}}^2 + m_{u_{33}^c}^2\right) + 2\left(\lambda T_t + y_t T_\lambda\right)^2 \\
&+ 2\lambda^2 y_b^2 \left(2m_{H_d}^2 + m_{H_u}^2 + m_S^2 + m_{Q_{33}}^2 + m_{d_{33}^c}^2\right) + 2\left(\lambda T_b + y_b T_\lambda\right)^2 \\
&- \frac{32}{3} g_3^2 y_t^2 \left(m_{H_u}^2 + m_{Q_{33}}^2 + m_{u_{33}^c}^2 + 2M_3^2\right) - \frac{32}{3} g_3^2 \left(T_t^2 - 2y_t T_t M_3\right) \\
&- \frac{32}{3} g_3^2 y_b^2 \left(m_{H_d}^2 + m_{Q_{33}}^2 + m_{d_{33}^c}^2 + 2M_3^2\right) - \frac{32}{3} g_3^2 \left(T_b^2 - 2y_b T_b M_3\right) \\
&- 6g_2^2 y_t^2 \left(m_{H_u}^2 + m_{Q_{33}}^2 + m_{u_{33}^c}^2 + 2M_2^2\right) - 6g_2^2 \left(T_t^2 - 2y_t T_t M_2\right) \\
&- 6g_2^2 y_b^2 \left(m_{H_d}^2 + m_{Q_{33}}^2 + m_{d_{33}^c}^2 + 2M_2^2\right) - 6g_2^2 \left(T_b^2 - 2y_b T_b M_2\right) \\
&- \frac{26}{15} g_1^2 y_t^2 \left(m_{H_u}^2 + m_{Q_{33}}^2 + m_{u_{33}^c}^2 + 2M_1^2\right) - \frac{26}{15} g_1^2 \left(T_t^2 - 2y_t T_t M_1\right) \\
&- \frac{14}{15} g_1^2 y_b^2 \left(m_{H_d}^2 + m_{Q_{33}}^2 + m_{d_{33}^c}^2 + 2M_1^2\right) - \frac{14}{15} g_1^2 \left(T_b^2 - 2y_b T_b M_1\right) \\
&- 4g_1'^2 y_t^2 \left(Q_2^2 + Q_Q^2 + Q_{u^c}^2\right) \left(m_{H_u}^2 + m_{Q_{33}}^2 + m_{u_{33}^c}^2 + 2M_1'^2\right) \\
&- 4g_1'^2 \left(Q_2^2 + Q_Q^2 + Q_{u^c}^2\right) \left(T_t^2 - 2y_t T_t M_1'\right) + 12Q_Q g_1'^2 T_t^2 \left(Q_2 + Q_Q + Q_{u^c}\right) \\
&+ 2g_1'^2 y_t^2 \left(Q_2 + Q_Q + Q_{u^c}\right) \left(6Q_Q m_{H_u}^2 + 6Q_Q m_{Q_{33}}^2 + 6Q_Q m_{u_{33}^c}^2 + \Sigma_1'\right) \\
&- 4g_1'^2 y_b^2 \left(Q_1^2 + Q_Q^2 + Q_{d^c}^2\right) \left(m_{H_d}^2 + m_{Q_{33}}^2 + m_{d_{33}^c}^2 + 2M_1'^2\right) \\
&- 4g_1'^2 \left(Q_1^2 + Q_Q^2 + Q_{d^c}^2\right) \left(T_b^2 - 2y_b T_b M_1'\right) + 12Q_Q g_1'^2 T_b^2 \left(Q_1 + Q_Q + Q_{d^c}\right) \\
&+ 2g_1'^2 y_b^2 \left(Q_1 + Q_Q + Q_{d^c}\right) \left(6Q_Q m_{H_d}^2 + 6Q_Q m_{Q_{33}}^2 + 6Q_Q m_{d_{33}^c}^2 + \Sigma_1'\right) \\
&+ 4Q_Q g_1'^2 y_\tau^2 \left(Q_1 + Q_L + Q_{e^c}\right) \left(m_{H_d}^2 + m_{L_{33}}^2 + m_{e_{33}^c}^2\right) \\
&+ 4Q_Q g_1'^2 T_\tau^2 \left(Q_1 + Q_L + Q_{e^c}\right) + 4Q_Q g_1'^2 \lambda^2 \left(Q_1 + Q_2 + Q_S\right) \\
&\times \left(m_{H_d}^2 + m_{H_u}^2 + m_S^2\right) + 4Q_Q g_1'^2 T_\lambda^2 \left(Q_1 + Q_2 + Q_S\right) \\
&+ 4Q_Q g_1'^2 \left(Q_1 + Q_2 + Q_S\right) \sum_{\alpha=1}^{2} \left[\tilde{\lambda}_{\alpha\alpha}^2 \left(m_{H_{1,\alpha\alpha}}^2 + m_{H_{2,\alpha\alpha}}^2 + m_S^2\right) + (T_{\alpha\alpha}^{\tilde{\lambda}})^2\right]
\end{aligned}
$$

$$
\begin{aligned}
&+ 6Q_Q g_1'^2 \left(Q_S + Q_D + Q_{\overline{D}}\right) \sum_{i=1}^{3} \left[\kappa_{ii}^2 \left(m_S^2 + m_{D_{ii}}^2 + m_{\overline{D}_{ii}}^2\right) + (T_{ii}^{\kappa})^2\right] \\
&- 96 Q_Q g_3^2 g_1'^2 M_3^2 \left(2Q_Q + Q_{u^c} + Q_{d^c} + Q_D + Q_{\overline{D}}\right) - 72 g_2^4 M_2^2 \\
&- 12 Q_Q g_2^2 g_1'^2 M_2^2 \left(9Q_Q + 3Q_L + 3Q_1 + 3Q_2 + Q_{\overline{L}_4} + Q_{L_4}\right) + \frac{96}{25} g_1^4 \left(\Sigma_1 - M_1^2\right) \\
&- \frac{1}{5} g_1^2 g_1'^2 \Big[12 Q_Q M_1^2 \Big(2Q_{d^c} + 2Q_{\overline{D}} + 2Q_D + 6Q_{e^c} + 3Q_1 + 3Q_2 + Q_{\overline{L}_4} + Q_{L_4} \\
&+ 3Q_L + Q_Q + 8Q_{u^c}\Big) + 4M_1'^2 \Big(3Q_{d^c}^2 + 3Q_{\overline{D}}^2 - 3Q_D^2 + 3Q_{e^c}^2 - 3Q_1^2 + 3Q_2^2 \\
&+ Q_{\overline{L}_4}^2 - Q_{L_4}^2 - 3Q_L^2 + 3Q_Q^2 - 6Q_{u^c}^2\Big) - \left(6Q_Q \Sigma_1 + \Sigma_1'\right) \Sigma_Q^Y\Big] \\
&- 4 Q_Q g_1'^4 \Big[2M_1'^2 \Big(9Q_{d^c}^3 + 9Q_{\overline{D}}^3 + 9Q_D^3 + 3Q_{e^c}^3 + 6Q_1^3 + 6Q_2^3 + 2Q_{\overline{L}_4}^3 + 2Q_{L_4}^3 \\
&+ 6Q_L^3 + 18Q_Q^3 + 3Q_S^3 + 9Q_{u^c}^3\Big) + \left(6Q_Q M_1'^2 - \Sigma_1'\right) \Sigma_Q\Big] . \qquad \text{(C.13c)}
\end{aligned}
$$

Finally, the relevant expressions for the soft mass $m_{u_{33}^c}^2$ read

$$
\begin{aligned}
\beta_{m_{u_{33}^c}^2}^{(1)} &= 4y_t^2 \left(m_{H_u}^2 + m_{Q_{33}}^2 + m_{u_{33}^c}^2\right) + 4T_t^2 - \frac{32}{3} g_3^2 M_3^2 - \frac{32}{15} g_1^2 M_1^2 - 8 Q_{u^c}^2 g_1'^2 M_1'^2 \\
&\quad - \frac{4}{5} g_1^2 \Sigma_1 + 2 Q_{u^c} g_1'^2 \Sigma_1' , \qquad \text{(C.14a)} \\
\beta_{m_{u_{33}^c}^2}^{(2)} &= -32 y_t^4 \left(m_{H_u}^2 + m_{Q_{33}}^2 + m_{u_{33}^c}^2\right) - 4 y_t^2 y_b^2 \left(m_{H_u}^2 + m_{H_d}^2 + 2m_{Q_{33}}^2 + m_{u_{33}^c}^2 + m_{d_{33}^c}^2\right) \\
&\quad - 64 y_t^2 T_t^2 - 4 \left(y_t T_b + y_b T_t\right)^2 - 4\lambda^2 y_t^2 \left(2m_{H_u}^2 + m_{H_d}^2 + m_S^2 + m_{Q_{33}}^2 + m_{u_{33}^c}^2\right) \\
&\quad - 4 \left(\lambda T_t + y_t T_\lambda\right)^2 + 12 g_2^2 y_t^2 \left(m_{H_u}^2 + m_{Q_{33}}^2 + m_{u_{33}^c}^2 + 2M_2^2\right) \\
&\quad + 12 g_2^2 \left(T_t^2 - 2 y_t T_t M_2\right) - \frac{4}{5} g_1^2 y_t^2 \left(-5m_{H_u}^2 - m_{Q_{33}}^2 + 9m_{u_{33}^c}^2 + 2M_1^2\right) \\
&\quad - \frac{4}{5} g_1^2 \left(T_t^2 - 2 y_t T_t M_1\right) - \frac{8}{5} g_1^2 y_b^2 \left(3m_{H_d}^2 - m_{Q_{33}}^2 - 2m_{d_{33}^c}^2\right) \\
&\quad - \frac{8}{5} g_1^2 y_\tau^2 \left(m_{H_d}^2 + m_{L_{33}}^2 - 2m_{e_{33}^c}^2\right) - \frac{8}{5} g_1^2 \lambda^2 \left(m_{H_d}^2 - m_{H_u}^2\right) \\
&\quad - \frac{8}{5} g_1^2 \sum_{\alpha=1}^{2} \tilde{\lambda}_{\alpha\alpha}^2 \left(m_{H_{1,\alpha\alpha}}^2 - m_{H_{2,\alpha\alpha}}^2\right) - \frac{8}{5} g_1^2 \sum_{i=1}^{3} \kappa_{ii}^2 \left(m_{D_{ii}}^2 - m_{\overline{D}_{ii}}^2\right) \\
&\quad + 8 g_1'^2 y_t^2 \left(Q_2^2 + Q_Q^2 - Q_{u^c}^2\right) \left(m_{H_u}^2 + m_{Q_{33}}^2 + m_{u_{33}^c}^2 + 2M_1'^2\right) \\
&\quad + 8 g_1'^2 \left(Q_2^2 + Q_Q^2 - Q_{u^c}^2\right) \left(T_t^2 - 2 y_t T_t M_1'\right) \\
&\quad - 24 Q_{u^c} g_1'^2 y_t^2 \left(Q_2 m_{H_u}^2 + Q_Q m_{Q_{33}}^2 + Q_{u^c} m_{u_{33}^c}^2\right) \\
&\quad - 24 Q_{u^c} g_1'^2 y_b^2 \left(Q_1 m_{H_d}^2 + Q_Q m_{Q_{33}}^2 + Q_{d^c} m_{d_{33}^c}^2\right) \\
&\quad - 8 Q_{u^c} g_1'^2 y_\tau^2 \left(Q_1 m_{H_d}^2 + Q_L m_{L_{33}}^2 + Q_{e^c} m_{e_{33}^c}^2\right)
\end{aligned}
$$

$$
\begin{aligned}
&- 12Q_{u^c}g_1'^2\sum_{i=1}^{3}\kappa_{ii}^2\left(Q_S m_S^2 + Q_D m_{D_{ii}}^2 + Q_{\overline{D}} m_{\overline{D}_{ii}}^2\right)\\
&- 8Q_{u^c}g_1'^2\lambda^2\left(Q_1 m_{H_d}^2 + Q_2 m_{H_u}^2 + Q_S m_S^2\right)\\
&- 8Q_{u^c}g_1'^2\sum_{\alpha=1}^{2}\tilde{\lambda}_{\alpha\alpha}^2\left(Q_1 m_{H_d}^2 + Q_2 m_{H_u}^2 + Q_S m_S^2\right)\\
&+ \frac{16}{3}g_3^4\left[10M_3^2 + \mathrm{Tr}(m_{d^c}^2) + \mathrm{Tr}(m_D^2) + \mathrm{Tr}(m_{\overline{D}}^2) + 2\,\mathrm{Tr}(m_Q^2) + \mathrm{Tr}(m_{u^c}^2)\right]\\
&+ \frac{64}{45}g_3^2g_1^2\Big[8\left(M_1^2 + M_1M_3 + M_3^2\right) - 3\,\mathrm{Tr}(m_{d^c}^2) + 3\,\mathrm{Tr}(m_D^2) - 3\,\mathrm{Tr}(m_{\overline{D}}^2)\\
&- 3\,\mathrm{Tr}(m_Q^2) + 6\,\mathrm{Tr}(m_{u^c}^2)\Big] + \frac{8}{3}Q_{u^c}g_3^2g_1'^2\Big[16Q_{u^c}\left(M_1'^2 + M_1'M_3 + M_3^2\right)\\
&+ 12Q_{d^c}\,\mathrm{Tr}(m_{d^c}^2) + 12Q_D\,\mathrm{Tr}(m_D^2) + 12Q_{\overline{D}}\,\mathrm{Tr}(m_{\overline{D}}^2) + 24Q_Q\,\mathrm{Tr}(m_Q^2)\\
&+ 12Q_{u^c}\,\mathrm{Tr}(m_{u^c}^2)\Big] + \frac{12}{5}g_2^2g_1^2\Big[m_{L_4}^2 - m_{\overline{L}_4}^2 + m_{H_d}^2 + \mathrm{Tr}(m_{H_1}^2) - m_{H_u}^2\\
&- \mathrm{Tr}(m_{H_2}^2) + \mathrm{Tr}(m_L^2) - \mathrm{Tr}(m_Q^2)\Big] + 12Q_{u^c}g_2^2g_1'^2\Big[Q_{L_4}m_{L_4}^2 + Q_{\overline{L}_4}m_{\overline{L}_4}^2\\
&+ Q_1 m_{H_d}^2 + Q_1\,\mathrm{Tr}(m_{H_1}^2) + Q_2 m_{H_u}^2 + Q_2\,\mathrm{Tr}(m_{H_2}^2) + Q_L\,\mathrm{Tr}(m_L^2) + 3Q_Q\,\mathrm{Tr}(m_Q^2)\Big]\\
&+ \frac{4}{75}g_1^4\Big[1261M_1^2 + 21m_{L_4}^2 + 3m_{\overline{L}_4}^2 + 4\,\mathrm{Tr}(m_{d^c}^2) + 12\,\mathrm{Tr}(m_D^2) + 4\,\mathrm{Tr}(m_{\overline{D}}^2)\\
&- 12\,\mathrm{Tr}(m_{e^c}^2) + 21m_{H_d}^2 + 21\,\mathrm{Tr}(m_{H_1}^2) + 3m_{H_u}^2 + 3\,\mathrm{Tr}(m_{H_2}^2) + 21\,\mathrm{Tr}(m_L^2)\\
&+ 3\,\mathrm{Tr}(m_Q^2) + 64\,\mathrm{Tr}(m_{u^c}^2)\Big] + \frac{4}{15}g_1^2g_1'^2\Big[-8Q_{u^c}\Big(9Q_{d^c} + 9Q_{\overline{D}} - 9Q_D + 9Q_{e^c}\\
&- 9Q_1 + 9Q_2 + 3Q_{\overline{L}_4} - 3Q_{L_4} - 9Q_L + 9Q_Q - 22Q_{u^c}\Big)\left(M_1^2 + M_1M_1' + M_1'^2\right)\\
&+ 12Q_{L_4}^2m_{L_4}^2 - 12Q_{\overline{L}_4}^2m_{\overline{L}_4}^2 - 12Q_{d^c}^2\,\mathrm{Tr}(m_{d^c}^2) - 12Q_{\overline{D}}^2\,\mathrm{Tr}(m_{\overline{D}}^2) + 12Q_D^2\,\mathrm{Tr}(m_D^2)\\
&- 12Q_{e^c}^2\,\mathrm{Tr}(m_{e^c}^2) + 12Q_1^2m_{H_d}^2 + 12Q_1^2\,\mathrm{Tr}(m_{H_1}^2) - 12Q_2^2m_{H_u}^2 - 12Q_2^2\,\mathrm{Tr}(m_{H_2}^2)\\
&+ 12Q_L^2\,\mathrm{Tr}(m_L^2) - 12Q_Q^2\,\mathrm{Tr}(m_Q^2) + 12Q_{u^c}^2\,\mathrm{Tr}(m_{u^c}^2) - 15Q_{\overline{L}_4}Q_{u^c}m_{\overline{L}_4}^2\\
&+ 33Q_{L_4}Q_{u^c}m_{L_4}^2 - 18Q_{u^c}Q_{d^c}\,\mathrm{Tr}(m_{d^c}^2) - 18Q_{u^c}Q_{\overline{D}}\,\mathrm{Tr}(m_{\overline{D}}^2)\\
&+ 30Q_{u^c}Q_D\,\mathrm{Tr}(m_D^2) - 6Q_{u^c}Q_{e^c}\,\mathrm{Tr}(m_{e^c}^2) + 33Q_{u^c}Q_1m_{H_d}^2 + 33Q_{u^c}Q_1\,\mathrm{Tr}(m_{H_1}^2)\\
&- 15Q_{u^c}m_{H_u}^2 - 15Q_{u^c}Q_2\,\mathrm{Tr}(m_{H_2}^2) + 33Q_{u^c}Q_L\,\mathrm{Tr}(m_L^2) - 21Q_{u^c}Q_Q\,\mathrm{Tr}(m_Q^2)\\
&+ 84Q_{u^c}^2\,\mathrm{Tr}(m_{u^c}^2)\Big] + 8Q_{u^c}g_1'^4\Big[3Q_{u^c}M_1'^2\Big(9Q_{d^c}^2 + 9Q_{\overline{D}}^2 + 9Q_D^2 + 3Q_{e^c}^2 + 6Q_1^2\\
&+ 6Q_2^2 + 2Q_{\overline{L}_4}^2 + 2Q_{L_4}^2 + 6Q_L^2 + 18Q_Q^2 + 3Q_S^2 + 11Q_{u^c}^2\Big) + 2Q_{L_4}^3m_{L_4}^2\\
&+ 2Q_{\overline{L}_4}^3m_{\overline{L}_4}^2 + 3Q_{d^c}^3\,\mathrm{Tr}(m_{d^c}^2) + 3Q_{\overline{D}}^3\,\mathrm{Tr}(m_{\overline{D}}^2) + 3Q_D^3\,\mathrm{Tr}(m_D^2) + Q_{e^c}^3\,\mathrm{Tr}(m_{e^c}^2)\\
&+ 2Q_1^3m_{H_d}^2 + 2Q_1^3\,\mathrm{Tr}(m_{H_1}^2) + 2Q_2^3m_{H_u}^2 + 2Q_2^3\,\mathrm{Tr}(m_{H_2}^2) + 2Q_L^3\,\mathrm{Tr}(m_L^2)\\
&+ 6Q_Q^3\,\mathrm{Tr}(m_Q^2) + Q_S^3m_S^2 + Q_S^3\,\mathrm{Tr}(m_\Sigma^2) + 3Q_{u^c}^3\,\mathrm{Tr}(m_{u^c}^2) + 2Q_{u^c}Q_{L_4}^2m_{L_4}^2\\
&+ 2Q_{u^c}Q_{\overline{L}_4}^2m_{\overline{L}_4}^2 + 3Q_{u^c}Q_{d^c}^2\,\mathrm{Tr}(m_{d^c}^2) + 3Q_{u^c}Q_{\overline{D}}^2\,\mathrm{Tr}(m_{\overline{D}}^2) + 3Q_{u^c}Q_D^2\,\mathrm{Tr}(m_D^2)
\end{aligned}
$$

$$
\begin{aligned}
&+ Q_{u^c} Q_{e^c}^2 \operatorname{Tr}(m_{e^c}^2) + 2 Q_{u^c} Q_1^2 m_{H_d}^2 + 2 Q_{u^c} Q_1^2 \operatorname{Tr}(m_{H_1}^2) + 2 Q_{u^c} Q_2^2 m_{H_u}^2 \\
&+ 2 Q_{u^c} Q_2^2 \operatorname{Tr}(m_{H_2}^2) + 2 Q_{u^c} Q_L^2 \operatorname{Tr}(m_L^2) + 6 Q_{u^c} Q_Q^2 \operatorname{Tr}(m_Q^2) + Q_{u^c} Q_S^2 m_S^2 \\
&+ Q_{u^c} Q_S^2 \operatorname{Tr}(m_\Sigma^2) + 3 Q_{u^c}^3 \operatorname{Tr}(m_{u^c}^2) \Big] , \qquad \text{(C.14b)} \\
b^{(2)}_{m^2_{u^c_{33}}} &= 48 y_t^4 \left(m_{H_u}^2 + m_{Q_{33}}^2 + m_{u^c_{33}}^2 \right) + 4 y_t^2 y_b^2 \left(m_{H_u}^2 + m_{H_d}^2 + 2 m_{Q_{33}}^2 + m_{u^c_{33}}^2 + m_{d^c_{33}}^2 \right) \\
&+ 96 y_t^2 T_t^2 + 4 \left(y_t T_b + y_b T_t \right)^2 + 4 \lambda^2 y_t^2 \left(2 m_{H_u}^2 + m_{H_d}^2 + m_S^2 + m_{Q_{33}}^2 + m_{u^c_{33}}^2 \right) \\
&+ 4 \left(\lambda T_t + y_t T_\lambda \right)^2 - \frac{64}{3} g_3^2 y_t^2 \left(m_{H_u}^2 + m_{Q_{33}}^2 + m_{u^c_{33}}^2 + 2 M_3^2 \right) \\
&- \frac{64}{3} g_3^2 \left(T_t^2 - 2 y_t T_t M_3 \right) - 12 g_2^2 y_t^2 \left(m_{H_u}^2 + m_{Q_{33}}^2 + m_{u^c_{33}}^2 + 2 M_2^2 \right) \\
&- 12 g_2^2 \left(T_t^2 - 2 y_t T_t M_2 \right) - \frac{52}{15} g_1^2 y_t^2 \left(m_{H_u}^2 + m_{Q_{33}}^2 + m_{u^c_{33}}^2 + 2 M_1^2 \right) \\
&- \frac{52}{15} g_1^2 \left(T_t^2 - 2 y_t T_t M_1 \right) - 8 g_1'^2 \left(Q_2^2 + Q_Q^2 + Q_{u^c}^2 \right) \left(T_t^2 - 2 y_t T_t M_1' \right) \\
&- 8 g_1'^2 y_t^2 \left(Q_2^2 + Q_Q^2 + Q_{u^c}^2 \right) \left(m_{H_u}^2 + m_{Q_{33}}^2 + m_{u^c_{33}}^2 + 2 M_1'^2 \right) \\
&+ 4 g_1'^2 y_t^2 \left(Q_2 + Q_Q + Q_{u^c} \right) \left(3 Q_{u^c} m_{H_u}^2 + 3 Q_{u^c} m_{Q_{33}}^2 + 3 Q_{u^c} m_{u^c_{33}}^2 + \Sigma_1' \right) \\
&+ 12 Q_{u^c} g_1'^2 T_t^2 \left(Q_2 + Q_Q + Q_{u^c} \right) + 12 Q_{u^c} g_1'^2 T_b^2 \left(Q_1 + Q_Q + Q_{d^c} \right) \\
&+ 12 Q_{u^c} g_1'^2 y_b^2 \left(Q_1 + Q_Q + Q_{d^c} \right) \left(m_{H_d}^2 + m_{Q_{33}}^2 + m_{d^c_{33}}^2 \right) \\
&+ 4 Q_{u^c} g_1'^2 y_\tau^2 \left(Q_1 + Q_L + Q_{e^c} \right) \left(m_{H_d}^2 + m_{L_{33}}^2 + m_{e^c_{33}}^2 \right) \\
&+ 4 Q_{u^c} g_1'^2 T_\tau^2 \left(Q_1 + Q_L + Q_{e^c} \right) + 4 Q_{u^c} g_1'^2 T_\lambda^2 \left(Q_1 + Q_2 + Q_S \right) \\
&+ 4 Q_{u^c} g_1'^2 \lambda^2 \left(Q_1 + Q_2 + Q_S \right) \left(m_{H_d}^2 + m_{H_u}^2 + m_S^2 \right) \\
&+ 4 Q_{u^c} g_1'^2 \left(Q_1 + Q_2 + Q_S \right) \sum_{\alpha=1}^{2} \left[\tilde{\lambda}_{\alpha\alpha}^2 \left(m_{H_{1,\alpha\alpha}}^2 + m_{H_{2,\alpha\alpha}}^2 + m_S^2 \right) + (T_{\alpha\alpha}^{\tilde{\lambda}})^2 \right] \\
&+ 6 Q_{u^c} g_1'^2 \left(Q_S + Q_D + Q_{\overline{D}} \right) \sum_{i=1}^{3} \left[\kappa_{ii}^2 \left(m_S^2 + m_{D_{ii}}^2 + m_{\overline{D}_{ii}}^2 \right) + (T_{ii}^{\kappa})^2 \right] \\
&- 96 Q_{u^c} g_3^2 g_1'^2 M_3^2 \left(2 Q_Q + Q_{u^c} + Q_{d^c} + Q_D + Q_{\overline{D}} \right) \\
&- 12 Q_{u^c} g_2^2 g_1'^2 M_2^2 \left(9 Q_Q + 3 Q_L + 3 Q_1 + 3 Q_2 + Q_{L_4} + Q_{\overline{L}_4} \right) \\
&- \frac{384}{25} g_1^4 \left(\Sigma_1 + 4 M_1^2 \right) + \frac{2}{5} g_1^2 g_1'^2 \Big[8 M_1'^2 (3 Q_{d^c}^2 + 3 Q_{\overline{D}}^2 - 3 Q_D^2 + 3 Q_{e^c}^2 - 3 Q_1^2 \\
&+ 3 Q_2^2 + Q_{\overline{L}_4}^2 - Q_{L_4}^2 - 3 Q_L^2 + 3 Q_Q^2 - 6 Q_{u^c}^2) + 6 Q_{u^c} M_1^2 (2 Q_{d^c} + 2 Q_{\overline{D}} + 2 Q_D \\
&+ 6 Q_{e^c} + 3 Q_1 + 3 Q_2 + Q_{\overline{L}_4} + Q_{L_4} + 3 Q_L + Q_Q + 8 Q_{u^c}) + (3 Q_{u^c} \Sigma_1 - 2 \Sigma_1') \Sigma_Q^Y \Big] \\
&- 4 Q_{u^c} g_1'^4 \Big[2 M_1'^2 (9 Q_{d^c}^3 + 9 Q_D^3 + 9 Q_{\overline{D}}^3 + 3 Q_{e^c}^3 + 6 Q_1^3 + 6 Q_2^3 + 2 Q_{\overline{L}_4}^3 + 2 Q_{L_4}^3 \\
&+ 6 Q_L^3 + 18 Q_Q^3 + 3 Q_S^3 + 9 Q_{u^c}^3) + \left(6 Q_{u^c} M_1'^2 - \Sigma_1' \right) \Sigma_Q \Big] . \qquad \text{(C.14c)}
\end{aligned}
$$

Appendix D

SE_6SSM RGEs

In this appendix we present the complete set of two-loop RGEs for the SE_6SSM, required for the analysis presented in Chapter 7. These RGEs were automatically derived using `SARAH`-4.5.6. The β function for a parameter p is given by Eq. (5.27), i.e.,

$$\frac{dp}{dt} = \beta_p = \frac{\beta_p^{(1)}}{(4\pi)^2} + \frac{\beta_p^{(2)}}{(4\pi)^4}\,,$$

where $t = \ln(Q/M_X)$ contains the renormalisation scale Q at which p is evaluated. In the following we present the one- and two-loop contributions, $\beta_p^{(1)}$ and $\beta_p^{(2)}$, respectively, for the running parameters of the SE_6SSM.

D.1 Gauge Couplings

As discussed in Section 3.2, in general, kinetic mixing of $U(1)_Y$ and $U(1)_N$ leads to a set of RGEs for the Abelian gauge couplings that involve a set of off-diagonal gauge couplings. In the triangle basis of Eq. (3.13), these RGEs can be written

$$\frac{dG}{dt} = G \times B\,, \tag{D.1}$$

where the matrix of β functions is

$$B = \begin{pmatrix} \beta_{g_1} g_1^2 & 2g_1 g_1' \beta_{g_{11}} + 2g_1 g_{11} \beta_{g_1} \\ 0 & g_1'^2 \beta_{g_1'} + 2g_1' g_{11} \beta_{g_{11}} + g_{11}^2 \beta_{g_1} \end{pmatrix}. \tag{D.2}$$

In the E_6SSM and SE_6SSM, the off-diagonal β function $\beta_{g_{11}}$ is rather small; in particular, in the SE_6SSM $\beta_{g_{11}}^{(1)} = -\sqrt{6}/5$ at one-loop. As discussed in Section 3.2, the

effects of kinetic mixing are therefore small if g_{11} vanishes at the GUT scale, and so we neglect it. When this is done, the two-loop RGEs for the diagonal Abelian gauge couplings are

$$\beta_{g_1}^{(1)} = \frac{48}{5} g_1^3 \,, \tag{D.3}$$

$$\begin{aligned}\beta_{g_1}^{(2)} = g_1^3 \Big[& \frac{234}{25} g_1^2 + \frac{81}{25} g_1'^2 + \frac{54}{5} g_2^2 + 24 g_3^2 - \frac{6}{5}|\lambda|^2 - \frac{6}{5}|\tilde{\sigma}|^2 - \frac{26}{5}\operatorname{Tr}\Big(y^U y^{U\dagger}\Big) \\ & - \frac{14}{5}\operatorname{Tr}\Big(y^D y^{D\dagger}\Big) - \frac{18}{5}\operatorname{Tr}\Big(y^E y^{E\dagger}\Big) - \frac{4}{5}\operatorname{Tr}\Big(\kappa\kappa^\dagger\Big) - \frac{6}{5}\operatorname{Tr}\Big(\tilde{\lambda}\tilde{\lambda}^\dagger\Big) \\ & - \frac{6}{5}\operatorname{Tr}\Big(f f^\dagger\Big) - \frac{6}{5}\operatorname{Tr}\Big(\tilde{f}\tilde{f}^\dagger\Big) - \frac{14}{5}\operatorname{Tr}\Big(g^D g^{D\dagger}\Big) - \frac{18}{5}\operatorname{Tr}\Big(h^E h^{E\dagger}\Big)\Big] \,,\end{aligned} \tag{D.4}$$

$$\beta_{g_1'}^{(1)} = \frac{213}{20} g_1'^3 \,, \tag{D.5}$$

$$\begin{aligned}\beta_{g_1'}^{(2)} = g_1'^3 \Big[& \frac{81}{25} g_1^2 + \frac{2457}{200} g_1'^2 + \frac{51}{5} g_2^2 + 24 g_3^2 - \frac{19}{5}|\lambda|^2 - \frac{5}{2}|\sigma|^2 \\ & - \frac{4}{5}|\tilde{\sigma}|^2 - \frac{9}{5}\operatorname{Tr}\Big(y^U y^{U\dagger}\Big) - \frac{21}{5}\operatorname{Tr}\Big(y^D y^{D\dagger}\Big) - \frac{7}{5}\operatorname{Tr}\Big(y^E y^{E\dagger}\Big) \\ & - \frac{57}{10}\operatorname{Tr}\Big(\kappa\kappa^\dagger\Big) - \frac{19}{5}\operatorname{Tr}\Big(\tilde{\lambda}\tilde{\lambda}^\dagger\Big) - \frac{19}{5}\operatorname{Tr}\Big(f f^\dagger\Big) \\ & - \frac{19}{5}\operatorname{Tr}\Big(\tilde{f}\tilde{f}^\dagger\Big) - \frac{21}{5}\operatorname{Tr}\Big(g^D g^{D\dagger}\Big) - \frac{7}{5}\operatorname{Tr}\Big(h^E h^{E\dagger}\Big)\Big] \,.\end{aligned} \tag{D.6}$$

The β functions for the $SU(2)_L$ and $SU(3)_C$ gauge couplings are the same irrespective of whether or not the kinetic mixing is taken into account. They are

$$\beta_{g_2}^{(1)} = 4 g_2^3 \,, \tag{D.7}$$

$$\begin{aligned}\beta_{g_2}^{(2)} = g_2^3 \Big[& \frac{18}{5} g_1^2 + \frac{17}{5} g_1'^2 + 46 g_2^2 + 24 g_3^2 - 2|\lambda|^2 - 2|\tilde{\sigma}|^2 - 6\operatorname{Tr}\Big(y^U y^{U\dagger}\Big) \\ & - 6\operatorname{Tr}\Big(y^D y^{D\dagger}\Big) - 2\operatorname{Tr}\Big(y^E y^{E\dagger}\Big) - 2\operatorname{Tr}\Big(\tilde{\lambda}\tilde{\lambda}^\dagger\Big) - 2\operatorname{Tr}\Big(f f^\dagger\Big) \\ & - 2\operatorname{Tr}\Big(\tilde{f}\tilde{f}^\dagger\Big) - 6\operatorname{Tr}\Big(g^D g^{D\dagger}\Big) - 2\operatorname{Tr}\Big(h^E h^{E\dagger}\Big)\Big] \,,\end{aligned} \tag{D.8}$$

$$\beta_{g_3}^{(1)} = 0 \,, \tag{D.9}$$

$$\begin{aligned}\beta_{g_3}^{(2)} = g_3^3 \Big[& 3 g_1^2 + 3 g_1'^2 + 9 g_2^2 + 48 g_3^2 - 4\operatorname{Tr}\Big(y^U y^{U\dagger}\Big) - 4\operatorname{Tr}\Big(y^D y^{D\dagger}\Big) \\ & - 2\operatorname{Tr}\Big(\kappa\kappa^\dagger\Big) - 4\operatorname{Tr}\Big(g^D g^{D\dagger}\Big)\Big] \,.\end{aligned} \tag{D.10}$$

D.2 Superpotential Trilinear Couplings

When gauge kinetic mixing is neglected, the running of the dimensionless superpotential couplings is described by the following two-loop β functions:

$$\begin{aligned}
\beta_{y^D}^{(1)} &= y^D\Big(3y^{D\dagger}y^D + y^{U\dagger}y^U + g^{D*}g^{DT}\Big) + y^D\Big[-\frac{7}{15}g_1^2 - \frac{7}{10}g_1'^2 - 3g_2^2 - \frac{16}{3}g_3^2 \\
&\quad + |\lambda|^2 + 3\,\mathrm{Tr}\Big(y^D y^{D\dagger}\Big) + \mathrm{Tr}\Big(y^E y^{E\dagger}\Big) + \mathrm{Tr}\Big(ff^\dagger\Big)\Big]\,, \qquad \text{(D.11)} \\
\beta_{y^D}^{(2)} &= y^D\Big\{y^{U\dagger}y^U\Big[\frac{4}{5}g_1^2 + \frac{1}{5}g_1'^2 - |\lambda|^2 - 3\,\mathrm{Tr}\Big(y^U y^{U\dagger}\Big) - \mathrm{Tr}\Big(\tilde{f}\tilde{f}^\dagger\Big)\Big] \\
&\quad + y^{D\dagger}y^D\Big[\frac{4}{5}g_1^2 + \frac{6}{5}g_1'^2 + 6g_2^2 - 3|\lambda|^2 - 9\,\mathrm{Tr}\Big(y^D y^{D\dagger}\Big) - 3\,\mathrm{Tr}\Big(y^E y^{E\dagger}\Big) \\
&\quad - 3\,\mathrm{Tr}\Big(ff^\dagger\Big)\Big] + g^{D*}g^{DT}\Big[\frac{2}{5}g_1^2 + \frac{3}{5}g_1'^2 - |\tilde{\sigma}|^2 - 3\,\mathrm{Tr}\Big(g^D g^{D\dagger}\Big) - \mathrm{Tr}\Big(h^E h^{E\dagger}\Big)\Big] \\
&\quad - 4y^{D\dagger}y^D y^{D\dagger}y^D - 2y^{U\dagger}y^U y^{D\dagger}y^D - 2y^{U\dagger}y^U y^{U\dagger}y^U - 2g^{D*}g^{DT}y^{D\dagger}y^D \\
&\quad - 2g^{D*}g^{DT}g^{D*}g^{DT} - g^{D*}\kappa^T\kappa^* g^{DT}\Big\} + y^D\Big\{\frac{413}{90}g_1^4 + \frac{77}{10}g_1'^4 + \frac{33}{2}g_2^4 \\
&\quad + \frac{128}{9}g_3^4 - \frac{7}{30}g_1^2 g_1'^2 + g_1^2 g_2^2 + \frac{8}{9}g_1^2 g_3^2 + \frac{3}{2}g_1'^2 g_2^2 + \frac{4}{3}g_1'^2 g_3^2 + 8g_2^2 g_3^2 - 3|\lambda|^4 \\
&\quad - \frac{2}{5}g_1^2\Big[\mathrm{Tr}\Big(y^D y^{D\dagger}\Big) - 3\,\mathrm{Tr}\Big(y^E y^{E\dagger}\Big)\Big] + g_1'^2\Big[-\frac{3}{5}\,\mathrm{Tr}\Big(y^D y^{D\dagger}\Big) - \frac{1}{5}\,\mathrm{Tr}\Big(y^E y^{E\dagger}\Big) \\
&\quad + \mathrm{Tr}\Big(ff^\dagger\Big)\Big] + 16g_3^2\,\mathrm{Tr}\Big(y^D y^{D\dagger}\Big) + |\lambda|^2\Big[g_1'^2 - |\sigma|^2 - 2\,\mathrm{Tr}\Big(\tilde{\lambda}\tilde{\lambda}^\dagger\Big) \\
&\quad - 3\,\mathrm{Tr}\Big(\kappa\kappa^\dagger\Big) - 3\,\mathrm{Tr}\Big(y^U y^{U\dagger}\Big) - \mathrm{Tr}\Big(\tilde{f}\tilde{f}^\dagger\Big)\Big] - 3\,\mathrm{Tr}\Big(ff^\dagger ff^\dagger\Big) - 2\,\mathrm{Tr}\Big(ff^\dagger\tilde{f}\tilde{f}^\dagger\Big) \\
&\quad - 3\,\mathrm{Tr}\Big(g^D g^{D\dagger}y^{DT}y^{D*}\Big) - 2\,\mathrm{Tr}\Big(h^E h^{E\dagger}y^E y^{E\dagger}\Big) - 9\,\mathrm{Tr}\Big(y^D y^{D\dagger}y^D y^{D\dagger}\Big) \\
&\quad - 3\,\mathrm{Tr}\Big(y^D y^{U\dagger}y^U y^{D\dagger}\Big) - 3\,\mathrm{Tr}\Big(y^E y^{E\dagger}y^E y^{E\dagger}\Big) - \mathrm{Tr}\Big(\tilde{\lambda}\tilde{\lambda}^\dagger f^T f^*\Big)\Big\}\,, \qquad \text{(D.12)} \\
\beta_{y^U}^{(1)} &= y^U\Big(y^{D\dagger}y^D + 3y^{U\dagger}y^U + g^{D*}g^{DT}\Big) + y^U\Big[-\frac{13}{15}g_1^2 - \frac{3}{10}g_1'^2 - 3g_2^2 - \frac{16}{3}g_3^2 \\
&\quad + |\lambda|^2 + 3\,\mathrm{Tr}\Big(y^U y^{U\dagger}\Big) + \mathrm{Tr}\Big(\tilde{f}\tilde{f}^\dagger\Big)\Big]\,, \qquad \text{(D.13)} \\
\beta_{y^U}^{(2)} &= y^U\Big\{y^{U\dagger}y^U\Big[\frac{2}{5}g_1^2 + \frac{3}{5}g_1'^2 + 6g_2^2 - 3|\lambda|^2 - 9\,\mathrm{Tr}\Big(y^U y^{U\dagger}\Big) - 3\,\mathrm{Tr}\Big(\tilde{f}\tilde{f}^\dagger\Big)\Big] \\
&\quad + y^{D\dagger}y^D\Big[\frac{2}{5}g_1^2 + \frac{3}{5}g_1'^2 - |\lambda|^2 - 3\,\mathrm{Tr}\Big(y^D y^{D\dagger}\Big) - \mathrm{Tr}\Big(y^E y^{E\dagger}\Big) - \mathrm{Tr}\Big(ff^\dagger\Big)\Big] \\
&\quad + g^{D*}g^{DT}\Big[\frac{2}{5}g_1^2 + \frac{3}{5}g_1'^2 - |\tilde{\sigma}|^2 - 3\,\mathrm{Tr}\Big(g^D g^{D\dagger}\Big) - \mathrm{Tr}\Big(h^E h^{E\dagger}\Big)\Big] \\
&\quad - 2y^{D\dagger}y^D y^{D\dagger}y^D - 2y^{D\dagger}y^D y^{U\dagger}y^U - 4y^{U\dagger}y^U y^{U\dagger}y^U - 2g^{D*}g^{DT}y^{U\dagger}y^U \\
&\quad - 2g^{D*}g^{DT}g^{D*}g^{DT} - g^{D*}\kappa^T\kappa^* g^{DT}\Big\} + y^U\Big\{\frac{3913}{450}g_1^4 + \frac{81}{25}g_1'^4 + \frac{33}{2}g_2^4
\end{aligned}$$

$$
\begin{aligned}
&+\frac{128}{9}g_3^4+\frac{161}{300}g_1^2g_1'^2+g_1^2g_2^2+\frac{136}{45}g_1^2g_3^2+\frac{3}{4}g_1'^2g_2^2+\frac{8}{15}g_1'^2g_3^2+8g_2^2g_3^2\\
&-3|\lambda|^4+\frac{4}{5}g_1^2\,\mathrm{Tr}\Big(y^Uy^{U\dagger}\Big)+\frac{3}{2}g_1'^2\Big[-\frac{1}{5}\,\mathrm{Tr}\Big(y^Uy^{U\dagger}\Big)+\mathrm{Tr}\Big(\tilde{f}\tilde{f}^\dagger\Big)\Big]\\
&+16g_3^2\,\mathrm{Tr}\Big(y^Uy^{U\dagger}\Big)+|\lambda|^2\Big[\frac{3}{2}g_1'^2-|\sigma|^2-2\,\mathrm{Tr}\Big(\tilde{\lambda}\tilde{\lambda}^\dagger\Big)-3\,\mathrm{Tr}\Big(\kappa\kappa^\dagger\Big)\\
&-3\,\mathrm{Tr}\Big(y^Dy^{D\dagger}\Big)-\mathrm{Tr}\Big(y^Ey^{E\dagger}\Big)-\mathrm{Tr}\Big(ff^\dagger\Big)\Big]-2\,\mathrm{Tr}\Big(ff^\dagger\tilde{f}\tilde{f}^\dagger\Big)\\
&-3\,\mathrm{Tr}\Big(\tilde{f}\tilde{f}^\dagger\tilde{f}\tilde{f}^\dagger\Big)-\mathrm{Tr}\Big(\tilde{f}h^{E\dagger}h^E\tilde{f}^\dagger\Big)-\mathrm{Tr}\Big(\tilde{f}\tilde{\lambda}^\dagger\tilde{\lambda}\tilde{f}^\dagger\Big)-3\,\mathrm{Tr}\Big(g^Dg^{D\dagger}y^{UT}y^{U*}\Big)\\
&-3\,\mathrm{Tr}\Big(y^Dy^{U\dagger}y^Uy^{D\dagger}\Big)-9\,\mathrm{Tr}\Big(y^Uy^{U\dagger}y^Uy^{U\dagger}\Big)\Big\},
\end{aligned}
\tag{D.14}
$$

$$
\begin{aligned}
\beta_{y^E}^{(1)}=&\Big(2h^Eh^{E\dagger}+3y^Ey^{E\dagger}\Big)y^E+y^E\Big[-\frac{9}{5}g_1^2-\frac{7}{10}g_1'^2-3g_2^2+|\lambda|^2+3\,\mathrm{Tr}\Big(y^Dy^{D\dagger}\Big)\\
&+\mathrm{Tr}\Big(y^Ey^{E\dagger}\Big)+\mathrm{Tr}\Big(ff^\dagger\Big)\Big],
\end{aligned}
\tag{D.15}
$$

$$
\begin{aligned}
\beta_{y^E}^{(2)}=&\Big\{y^Ey^{E\dagger}\Big[\frac{3}{2}g_1'^2+6g_2^2-3|\lambda|^2-9\,\mathrm{Tr}\Big(y^Dy^{D\dagger}\Big)-3\,\mathrm{Tr}\Big(y^Ey^{E\dagger}\Big)-3\,\mathrm{Tr}\Big(ff^\dagger\Big)\Big]\\
&+h^Eh^{E\dagger}\Big[-\frac{6}{5}g_1^2+\frac{6}{5}g_1'^2+6g_2^2-2|\tilde{\sigma}|^2-6\,\mathrm{Tr}\Big(g^Dg^{D\dagger}\Big)-2\,\mathrm{Tr}\Big(h^Eh^{E\dagger}\Big)\Big]\\
&-2h^E\tilde{f}^\dagger\tilde{f}h^{E\dagger}-2h^Eh^{E\dagger}h^Eh^{E\dagger}-2h^E\tilde{\lambda}^\dagger\tilde{\lambda}h^{E\dagger}-2y^Ey^{E\dagger}h^Eh^{E\dagger}\\
&-4y^Ey^{E\dagger}y^Ey^{E\dagger}\Big\}y^E+y^E\Big\{\frac{189}{10}g_1^4+\frac{77}{10}g_1'^4+\frac{33}{2}g_2^4+\frac{3}{20}g_1^2g_1'^2+\frac{9}{5}g_1^2g_2^2\\
&+\frac{39}{20}g_1'^2g_2^2-3|\lambda|^4+\frac{2}{5}g_1^2\Big[-\mathrm{Tr}\Big(y^Dy^{D\dagger}\Big)+3\,\mathrm{Tr}\Big(y^Ey^{E\dagger}\Big)\Big]\\
&+g_1'^2\Big[-\frac{3}{5}\,\mathrm{Tr}\Big(y^Dy^{D\dagger}\Big)-\frac{1}{5}\,\mathrm{Tr}\Big(y^Ey^{E\dagger}\Big)+\mathrm{Tr}\Big(ff^\dagger\Big)\Big]+16g_3^2\,\mathrm{Tr}\Big(y^Dy^{D\dagger}\Big)\\
&+|\lambda|^2\Big[g_1'^2-|\sigma|^2-2\,\mathrm{Tr}\Big(\tilde{\lambda}\tilde{\lambda}^\dagger\Big)-3\,\mathrm{Tr}\Big(\kappa\kappa^\dagger\Big)-3\,\mathrm{Tr}\Big(y^Uy^{U\dagger}\Big)-\mathrm{Tr}\Big(\tilde{f}\tilde{f}^\dagger\Big)\Big]\\
&-3\,\mathrm{Tr}\Big(ff^\dagger ff^\dagger\Big)-2\,\mathrm{Tr}\Big(ff^\dagger\tilde{f}\tilde{f}^\dagger\Big)-3\,\mathrm{Tr}\Big(g^Dg^{D\dagger}y^{DT}y^{D*}\Big)\\
&-2\,\mathrm{Tr}\Big(h^Eh^{E\dagger}y^Ey^{E\dagger}\Big)-9\,\mathrm{Tr}\Big(y^Dy^{D\dagger}y^Dy^{D\dagger}\Big)-3\,\mathrm{Tr}\Big(y^Dy^{U\dagger}y^Uy^{D\dagger}\Big)\\
&-3\,\mathrm{Tr}\Big(y^Ey^{E\dagger}y^Ey^{E\dagger}\Big)-\mathrm{Tr}\Big(\tilde{\lambda}\tilde{\lambda}^\dagger f^Tf^*\Big)\Big\},
\end{aligned}
\tag{D.16}
$$

$$
\begin{aligned}
\beta_\lambda^{(1)}=&\lambda\Big[4|\lambda|^2+|\sigma|^2-\frac{3}{5}g_1^2-\frac{19}{10}g_1'^2-3g_2^2+3\,\mathrm{Tr}\Big(y^Uy^{U\dagger}\Big)+3\,\mathrm{Tr}\Big(y^Dy^{D\dagger}\Big)\\
&+\mathrm{Tr}\Big(y^Ey^{E\dagger}\Big)+2\,\mathrm{Tr}\Big(\tilde{\lambda}\tilde{\lambda}^\dagger\Big)+3\,\mathrm{Tr}\Big(\kappa\kappa^\dagger\Big)+\mathrm{Tr}\Big(ff^\dagger\Big)+\mathrm{Tr}\Big(\tilde{f}\tilde{f}^\dagger\Big)\Big],
\end{aligned}
\tag{D.17}
$$

$$
\begin{aligned}
\beta_\lambda^{(2)}=&\lambda\Big\{\frac{297}{50}g_1^4+\frac{551}{25}g_1'^4+\frac{33}{2}g_2^4+\frac{27}{100}g_1^2g_1'^2+\frac{9}{5}g_1^2g_2^2+\frac{39}{20}g_1'^2g_2^2-10|\lambda|^4\\
&-2|\sigma|^2\Big(|\kappa_\phi|^2+|\sigma|^2+|\tilde{\sigma}|^2\Big)+\frac{2}{5}g_1^2\Big[2\,\mathrm{Tr}\Big(y^Uy^{U\dagger}\Big)-\mathrm{Tr}\Big(y^Dy^{D\dagger}\Big)
\end{aligned}
$$

$$
\begin{aligned}
&+ 3\,\mathrm{Tr}\Big(y^E y^{E\dagger}\Big) + 2\,\mathrm{Tr}\Big(\kappa\kappa^\dagger\Big) + 3\,\mathrm{Tr}\Big(\tilde{\lambda}\tilde{\lambda}^\dagger\Big)\Big] - g_1'^2\Big[\frac{3}{10}\,\mathrm{Tr}\Big(y^U y^{U\dagger}\Big) \\
&+ \frac{3}{5}\,\mathrm{Tr}\Big(y^D y^{D\dagger}\Big) + \frac{1}{5}\,\mathrm{Tr}\Big(y^E y^{E\dagger}\Big) + \frac{6}{5}\,\mathrm{Tr}\Big(\tilde{\lambda}\tilde{\lambda}^\dagger\Big) + \frac{9}{5}\,\mathrm{Tr}\Big(\kappa\kappa^\dagger\Big) \\
&- \mathrm{Tr}\Big(ff^\dagger\Big) - \frac{3}{2}\,\mathrm{Tr}\Big(\tilde{f}\tilde{f}^\dagger\Big)\Big] + 6g_2^2\,\mathrm{Tr}\Big(\tilde{\lambda}\tilde{\lambda}^\dagger\Big) + 16g_3^2\Big[\mathrm{Tr}\Big(y^U y^{U\dagger}\Big) \\
&+ \mathrm{Tr}\Big(y^D y^{D\dagger}\Big) + \mathrm{Tr}\Big(\kappa\kappa^\dagger\Big)\Big] + |\lambda|^2\Big[\frac{6}{5}g_1^2 + \frac{13}{10}g_1'^2 + 6g_2^2 - 2|\sigma|^2 \\
&- 9\,\mathrm{Tr}\Big(y^U y^{U\dagger}\Big) - 9\,\mathrm{Tr}\Big(y^D y^{D\dagger}\Big) - 3\,\mathrm{Tr}\Big(y^E y^{E\dagger}\Big) - 6\,\mathrm{Tr}\Big(\kappa\kappa^\dagger\Big) \\
&- 4\,\mathrm{Tr}\Big(\tilde{\lambda}\tilde{\lambda}^\dagger\Big) - 3\,\mathrm{Tr}\Big(ff^\dagger\Big) - 3\,\mathrm{Tr}\Big(\tilde{f}\tilde{f}^\dagger\Big)\Big] - 3\,\mathrm{Tr}\Big(ff^\dagger ff^\dagger\Big) \\
&- 4\,\mathrm{Tr}\Big(ff^\dagger\tilde{f}\tilde{f}^\dagger\Big) - 3\,\mathrm{Tr}\Big(\tilde{f}\tilde{f}^\dagger\tilde{f}\tilde{f}^\dagger\Big) - \mathrm{Tr}\Big(\tilde{f}h^{E\dagger}h^E\tilde{f}^\dagger\Big) - 3\,\mathrm{Tr}\Big(\tilde{f}\tilde{\lambda}^\dagger\tilde{\lambda}\tilde{f}^\dagger\Big) \\
&- 3\,\mathrm{Tr}\Big(g^D g^{D\dagger} y^{DT} y^{D*}\Big) - 3\,\mathrm{Tr}\Big(g^D g^{D\dagger} y^{UT} y^{U*}\Big) - 6\,\mathrm{Tr}\Big(g^D\kappa^\dagger\kappa g^{D\dagger}\Big) \\
&- 2\,\mathrm{Tr}\Big(h^E h^{E\dagger} y^E y^{E\dagger}\Big) - 2\,\mathrm{Tr}\Big(h^E\tilde{\lambda}^\dagger\tilde{\lambda}h^{E\dagger}\Big) - 9\,\mathrm{Tr}\Big(y^D y^{D\dagger} y^D y^{D\dagger}\Big) \\
&- 6\,\mathrm{Tr}\Big(y^D y^{U\dagger} y^U y^{D\dagger}\Big) - 3\,\mathrm{Tr}\Big(y^E y^{E\dagger} y^E y^{E\dagger}\Big) - 9\,\mathrm{Tr}\Big(y^U y^{U\dagger} y^U y^{U\dagger}\Big) \\
&- 6\,\mathrm{Tr}\Big(\kappa\kappa^\dagger\kappa\kappa^\dagger\Big) - 4\,\mathrm{Tr}\Big(\tilde{\lambda}\tilde{\lambda}^\dagger\tilde{\lambda}\tilde{\lambda}^\dagger\Big) - 3\,\mathrm{Tr}\Big(\tilde{\lambda}\tilde{\lambda}^\dagger f^T f^*\Big)\Big\}\,, \qquad \text{(D.18)}
\end{aligned}
$$

$$
\begin{aligned}
\beta_{\tilde{\lambda}}^{(1)} &= \tilde{\lambda}\Big[2|\lambda|^2 + |\sigma|^2 - \frac{3}{5}g_1^2 - \frac{19}{10}g_1'^2 - 3g_2^2 + 2\,\mathrm{Tr}\Big(\tilde{\lambda}\tilde{\lambda}^\dagger\Big) + 3\,\mathrm{Tr}\Big(\kappa\kappa^\dagger\Big)\Big] \\
&\quad + \tilde{\lambda}\Big(\tilde{f}^\dagger\tilde{f} + h^{E\dagger}h^E + 2\tilde{\lambda}^\dagger\tilde{\lambda}\Big) + f^T f^*\tilde{\lambda}\,, \qquad \text{(D.19)}
\end{aligned}
$$

$$
\begin{aligned}
\beta_{\tilde{\lambda}}^{(2)} &= \tilde{\lambda}\Big\{\tilde{\lambda}^\dagger\tilde{\lambda}\Big[\frac{5}{2}g_1'^2 - 4|\lambda|^2 - 2|\sigma|^2 - 4\,\mathrm{Tr}\Big(\tilde{\lambda}\tilde{\lambda}^\dagger\Big) - 6\,\mathrm{Tr}\Big(\kappa\kappa^\dagger\Big)\Big] \\
&\quad + h^{E\dagger}h^E\Big[\frac{6}{5}g_1^2 - \frac{1}{5}g_1'^2 - |\tilde{\sigma}|^2 - 3\,\mathrm{Tr}\Big(g^D g^{D\dagger}\Big) - \mathrm{Tr}\Big(h^E h^{E\dagger}\Big)\Big] \\
&\quad + \tilde{f}^\dagger\tilde{f}\Big[g_1'^2 - |\lambda|^2 - 3\,\mathrm{Tr}\Big(y^U y^{U\dagger}\Big) - \mathrm{Tr}\Big(\tilde{f}\tilde{f}^\dagger\Big)\Big] - 2\tilde{f}^\dagger f f^\dagger\tilde{f} - 2\tilde{f}^\dagger\tilde{f}\tilde{f}^\dagger\tilde{f} \\
&\quad - \tilde{f}^\dagger\tilde{f}\tilde{\lambda}^\dagger\tilde{\lambda} - 2h^{E\dagger}h^E h^{E\dagger}h^E - h^{E\dagger}h^E\tilde{\lambda}^\dagger\tilde{\lambda} - 2h^{E\dagger}y^E y^{E\dagger}h^E - 2\tilde{\lambda}^\dagger\tilde{\lambda}\tilde{\lambda}^\dagger\tilde{\lambda}\Big\} \\
&\quad + \Big\{f^T f^*\Big[\frac{3}{2}g_1'^2 - |\lambda|^2 - 3\,\mathrm{Tr}\Big(y^D y^{D\dagger}\Big) - \mathrm{Tr}\Big(y^E y^{E\dagger}\Big) - \mathrm{Tr}\Big(ff^\dagger\Big)\Big] \\
&\quad - \tilde{\lambda}\tilde{\lambda}^\dagger f^T f^* - 2f^T f^* f^T f^* - 2f^T\tilde{f}^*\tilde{f}^T f^*\Big\}\tilde{\lambda} + \tilde{\lambda}\Big\{\frac{297}{50}g_1^4 + \frac{551}{25}g_1'^4 + \frac{33}{2}g_2^4 \\
&\quad + \frac{27}{100}g_1^2 g_1'^2 + \frac{9}{5}g_1^2 g_2^2 + \frac{39}{20}g_1'^2 g_2^2 - 4|\lambda|^4 - 2|\sigma|^2\Big(|\kappa_\phi|^2 + |\sigma|^2 + |\tilde{\sigma}|^2\Big) \\
&\quad + \frac{2}{5}g_1^2\Big[3\,\mathrm{Tr}\Big(\tilde{\lambda}\tilde{\lambda}^\dagger\Big) + 2\,\mathrm{Tr}\Big(\kappa\kappa^\dagger\Big)\Big] - \frac{3}{5}g_1'^2\Big[2\,\mathrm{Tr}\Big(\tilde{\lambda}\tilde{\lambda}^\dagger\Big) + 3\,\mathrm{Tr}\Big(\kappa\kappa^\dagger\Big)\Big] \\
&\quad + 6g_2^2\,\mathrm{Tr}\Big(\tilde{\lambda}\tilde{\lambda}^\dagger\Big) + 16g_3^2\,\mathrm{Tr}\Big(\kappa\kappa^\dagger\Big) + |\lambda|^2\Big[\frac{6}{5}g_1^2 - \frac{6}{5}g_1'^2 + 6g_2^2 - 6\,\mathrm{Tr}\Big(y^U y^{U\dagger}\Big)
\end{aligned}
$$

$$
\begin{aligned}
&- 6\,\mathrm{Tr}\Big(y^D y^{D\dagger}\Big) - 2\,\mathrm{Tr}\Big(y^E y^{E\dagger}\Big) - 2\,\mathrm{Tr}\Big(f f^\dagger\Big) - 2\,\mathrm{Tr}\Big(\tilde{f}\tilde{f}^\dagger\Big)\Big] \\
&- 2\,\mathrm{Tr}\Big(\tilde{f}\tilde{\lambda}^\dagger\tilde{\lambda}\tilde{f}^\dagger\Big) - 6\,\mathrm{Tr}\Big(g^D\kappa^\dagger\kappa g^{D\dagger}\Big) - 2\,\mathrm{Tr}\Big(h^E\tilde{\lambda}^\dagger\tilde{\lambda}h^{E\dagger}\Big) \\
&- 6\,\mathrm{Tr}\Big(\kappa\kappa^\dagger\kappa\kappa^\dagger\Big) - 4\,\mathrm{Tr}\Big(\tilde{\lambda}\tilde{\lambda}^\dagger\tilde{\lambda}\tilde{\lambda}^\dagger\Big) - 2\,\mathrm{Tr}\Big(\tilde{\lambda}\tilde{\lambda}^\dagger f^T f^*\Big)\Big\}, \qquad \text{(D.20)}
\end{aligned}
$$

$$
\begin{aligned}
\beta_\kappa^{(1)} = \kappa\Big[&2|\lambda|^2 + |\sigma|^2 - \frac{4}{15}g_1^2 - \frac{19}{10}g_1'^2 - \frac{16}{3}g_3^2 + 2\,\mathrm{Tr}\Big(\tilde{\lambda}\tilde{\lambda}^\dagger\Big) + 3\,\mathrm{Tr}\Big(\kappa\kappa^\dagger\Big)\Big] \\
&+ 2\kappa\Big(\kappa^\dagger\kappa + g^{D\dagger}g^D\Big), \qquad \text{(D.21)}
\end{aligned}
$$

$$
\begin{aligned}
\beta_\kappa^{(2)} = \kappa\Big\{&\kappa^\dagger\kappa\Big[\frac{5}{2}g_1'^2 - 4|\lambda|^2 - 2|\sigma|^2 - 4\,\mathrm{Tr}\Big(\tilde{\lambda}\tilde{\lambda}^\dagger\Big) - 6\,\mathrm{Tr}\Big(\kappa\kappa^\dagger\Big)\Big] \\
&+ g^{D\dagger}g^D\Big[\frac{2}{5}g_1^2 - \frac{2}{5}g_1'^2 + 6g_2^2 - 2|\tilde{\sigma}|^2 - 6\,\mathrm{Tr}\Big(g^D g^{D\dagger}\Big) - 2\,\mathrm{Tr}\Big(h^E h^{E\dagger}\Big)\Big] \\
&- 2g^{D\dagger}g^D g^{D\dagger}g^D - 2g^{D\dagger}g^D\kappa^\dagger\kappa - 2g^{D\dagger}y^{DT}y^{D*}g^D - 2g^{D\dagger}y^{UT}y^{U*}g^D \\
&- 2\kappa^\dagger\kappa\kappa^\dagger\kappa\Big\} + \kappa\Big\{\frac{584}{225}g_1^4 + \frac{551}{25}g_1'^4 + \frac{128}{9}g_3^4 + \frac{19}{75}g_1^2g_1'^2 + \frac{64}{45}g_1^2g_3^2 \\
&+ \frac{52}{15}g_1'^2g_3^2 - 4|\lambda|^4 - 2|\sigma|^2\Big(|\kappa_\phi|^2 + |\sigma|^2 + |\tilde{\sigma}|^2\Big) \\
&+ \frac{2}{5}g_1^2\Big[3\,\mathrm{Tr}\Big(\tilde{\lambda}\tilde{\lambda}^\dagger\Big) + 2\,\mathrm{Tr}\Big(\kappa\kappa^\dagger\Big)\Big] - \frac{3}{5}g_1'^2\Big[2\,\mathrm{Tr}\Big(\tilde{\lambda}\tilde{\lambda}^\dagger\Big) + 3\,\mathrm{Tr}\Big(\kappa\kappa^\dagger\Big)\Big] \\
&+ 6g_2^2\,\mathrm{Tr}\Big(\tilde{\lambda}\tilde{\lambda}^\dagger\Big) + 16g_3^2\,\mathrm{Tr}\Big(\kappa\kappa^\dagger\Big) + |\lambda|^2\Big[\frac{6}{5}g_1^2 - \frac{6}{5}g_1'^2 + 6g_2^2 - 6\,\mathrm{Tr}\Big(y^U y^{U\dagger}\Big) \\
&- 6\,\mathrm{Tr}\Big(y^D y^{D\dagger}\Big) - 2\,\mathrm{Tr}\Big(y^E y^{E\dagger}\Big) - 2\,\mathrm{Tr}\Big(f f^\dagger\Big) - 2\,\mathrm{Tr}\Big(\tilde{f}\tilde{f}^\dagger\Big)\Big] \\
&- 2\,\mathrm{Tr}\Big(\tilde{f}\tilde{\lambda}^\dagger\tilde{\lambda}\tilde{f}^\dagger\Big) - 6\,\mathrm{Tr}\Big(g^D\kappa^\dagger\kappa g^{D\dagger}\Big) - 2\,\mathrm{Tr}\Big(h^E\tilde{\lambda}^\dagger\tilde{\lambda}h^{E\dagger}\Big) \\
&- 6\,\mathrm{Tr}\Big(\kappa\kappa^\dagger\kappa\kappa^\dagger\Big) - 4\,\mathrm{Tr}\Big(\tilde{\lambda}\tilde{\lambda}^\dagger\tilde{\lambda}\tilde{\lambda}^\dagger\Big) - 2\,\mathrm{Tr}\Big(\tilde{\lambda}\tilde{\lambda}^\dagger f^T f^*\Big)\Big\}, \qquad \text{(D.22)}
\end{aligned}
$$

$$
\beta_\sigma^{(1)} = \sigma\Big[2|\kappa_\phi|^2 + 2|\lambda|^2 + 3|\sigma|^2 + 2|\tilde{\sigma}|^2 + 2\,\mathrm{Tr}\Big(\tilde{\lambda}\tilde{\lambda}^\dagger\Big) + 3\,\mathrm{Tr}\Big(\kappa\kappa^\dagger\Big) - \frac{5}{2}g_1'^2\Big], \qquad \text{(D.23)}
$$

$$
\begin{aligned}
\beta_\sigma^{(2)} = \sigma\Big\{&\frac{119}{4}g_1'^4 - 4|\lambda|^4 - 6|\sigma|^4 - 4|\tilde{\sigma}|^4 - 8|\kappa_\phi|^4 \\
&+ \frac{2}{5}g_1^2\Big[3\,\mathrm{Tr}\Big(\tilde{\lambda}\tilde{\lambda}^\dagger\Big) + 2\,\mathrm{Tr}\Big(\kappa\kappa^\dagger\Big)\Big] - \frac{3}{5}g_1'^2\Big[2\,\mathrm{Tr}\Big(\tilde{\lambda}\tilde{\lambda}^\dagger\Big) + 3\,\mathrm{Tr}\Big(\kappa\kappa^\dagger\Big)\Big] \\
&+ 6g_2^2\,\mathrm{Tr}\Big(\tilde{\lambda}\tilde{\lambda}^\dagger\Big) + 16g_3^2\,\mathrm{Tr}\Big(\kappa\kappa^\dagger\Big) + |\sigma|^2\Big[\frac{5}{2}g_1'^2 - 2|\tilde{\sigma}|^2 - 8|\kappa_\phi|^2 - 4\,\mathrm{Tr}\Big(\tilde{\lambda}\tilde{\lambda}^\dagger\Big) \\
&- 6\,\mathrm{Tr}\Big(\kappa\kappa^\dagger\Big)\Big] + |\tilde{\sigma}|^2\Big[\frac{6}{5}g_1^2 + \frac{4}{5}g_1'^2 + 6g_2^2 - 2|\sigma|^2 - 8|\kappa_\phi|^2 - 6\,\mathrm{Tr}\Big(g^D g^{D\dagger}\Big) \\
&- 2\,\mathrm{Tr}\Big(h^E h^{E\dagger}\Big)\Big] + |\lambda|^2\Big[\frac{6}{5}g_1^2 - \frac{6}{5}g_1'^2 + 6g_2^2 - 4|\sigma|^2 - 6\,\mathrm{Tr}\Big(y^U y^{U\dagger}\Big) \\
&- 6\,\mathrm{Tr}\Big(y^D y^{D\dagger}\Big) - 2\,\mathrm{Tr}\Big(y^E y^{E\dagger}\Big) - 2\,\mathrm{Tr}\Big(f f^\dagger\Big) - 2\,\mathrm{Tr}\Big(\tilde{f}\tilde{f}^\dagger\Big)\Big]
\end{aligned}
$$

$$
\begin{aligned}
&- 2\,\mathrm{Tr}\Big(\tilde{f}\tilde{\lambda}^\dagger\tilde{\lambda}\tilde{f}^\dagger\Big) - 6\,\mathrm{Tr}\Big(g^D\kappa^\dagger\kappa g^{D\dagger}\Big) - 2\,\mathrm{Tr}\Big(h^E\tilde{\lambda}^\dagger\tilde{\lambda}h^{E\dagger}\Big) - 6\,\mathrm{Tr}\Big(\kappa\kappa^\dagger\kappa\kappa^\dagger\Big) \\
&- 4\,\mathrm{Tr}\Big(\tilde{\lambda}\tilde{\lambda}^\dagger\tilde{\lambda}\tilde{\lambda}^\dagger\Big) - 2\,\mathrm{Tr}\Big(\tilde{\lambda}\tilde{\lambda}^\dagger f^T f^*\Big)\Big\}, \qquad \text{(D.24)}
\end{aligned}
$$

$$
\beta^{(1)}_{\kappa_\phi} = 3\kappa_\phi\Big(2|\kappa_\phi|^2 + 2|\tilde{\sigma}|^2 + |\sigma|^2\Big), \qquad \text{(D.25)}
$$

$$
\begin{aligned}
\beta^{(2)}_{\kappa_\phi} = \kappa_\phi\Big\{&-24|\kappa_\phi|^4 - 6|\sigma|^4 - 12|\tilde{\sigma}|^4 + |\sigma|^2\Big[\frac{15}{2}g_1'^2 - 6|\lambda|^2 - 12|\kappa_\phi|^2 \\
&- 6\,\mathrm{Tr}\Big(\tilde{\lambda}\tilde{\lambda}^\dagger\Big) - 9\,\mathrm{Tr}\Big(\kappa\kappa^\dagger\Big)\Big] + |\tilde{\sigma}|^2\Big[\frac{18}{5}g_1^2 + \frac{12}{5}g_1'^2 + 18g_2^2 - 24|\kappa_\phi|^2 \\
&- 18\,\mathrm{Tr}\Big(g^D g^{D\dagger}\Big) - 6\,\mathrm{Tr}\Big(h^E h^{E\dagger}\Big)\Big]\Big\}, \qquad \text{(D.26)}
\end{aligned}
$$

$$
\begin{aligned}
\beta^{(1)}_{\tilde{\sigma}} = \tilde{\sigma}\Big[&2|\kappa_\phi|^2 + |\sigma|^2 + 4|\tilde{\sigma}|^2 - \frac{3}{5}g_1^2 - \frac{2}{5}g_1'^2 - 3g_2^2 + 3\,\mathrm{Tr}\Big(g^D g^{D\dagger}\Big) \\
&+ \mathrm{Tr}\Big(h^E h^{E\dagger}\Big)\Big], \qquad \text{(D.27)}
\end{aligned}
$$

$$
\begin{aligned}
\beta^{(2)}_{\tilde{\sigma}} = \tilde{\sigma}\Big\{&\frac{297}{50}g_1^4 + \frac{217}{50}g_1'^4 + \frac{33}{2}g_2^4 + \frac{18}{25}g_1^2g_1'^2 + \frac{9}{5}g_1^2g_2^2 + \frac{6}{5}g_1'^2g_2^2 - 8|\kappa_\phi|^4 - 2|\sigma|^4 \\
&- 10|\tilde{\sigma}|^4 + \frac{2}{5}g_1^2\Big[-\mathrm{Tr}\Big(g^D g^{D\dagger}\Big) + 3\,\mathrm{Tr}\Big(h^E h^{E\dagger}\Big)\Big] + \frac{3}{10}g_1'^2\Big[3\,\mathrm{Tr}\Big(g^D g^{D\dagger}\Big) \\
&+ \mathrm{Tr}\Big(h^E h^{E\dagger}\Big)\Big] + 16g_3^2\,\mathrm{Tr}\Big(g^D g^{D\dagger}\Big) + |\tilde{\sigma}|^2\Big[\frac{6}{5}g_1^2 + \frac{4}{5}g_1'^2 + 6g_2^2 - 12|\kappa_\phi|^2 \\
&- 9\,\mathrm{Tr}\Big(g^D g^{D\dagger}\Big) - 3\,\mathrm{Tr}\Big(h^E h^{E\dagger}\Big)\Big] + |\sigma|^2\Big[\frac{5}{2}g_1'^2 - 2|\lambda|^2 - 4|\kappa_\phi|^2 - 2|\tilde{\sigma}|^2 \\
&- 2\,\mathrm{Tr}\Big(\tilde{\lambda}\tilde{\lambda}^\dagger\Big) - 3\,\mathrm{Tr}\Big(\kappa\kappa^\dagger\Big)\Big] - \mathrm{Tr}\Big(\tilde{f}h^{E\dagger}h^E\tilde{f}^\dagger\Big) - 9\,\mathrm{Tr}\Big(g^D g^{D\dagger}g^D g^{D\dagger}\Big) \\
&- 3\,\mathrm{Tr}\Big(g^D g^{D\dagger}y^{DT}y^{D*}\Big) - 3\,\mathrm{Tr}\Big(g^D g^{D\dagger}y^{UT}y^{U*}\Big) - 3\,\mathrm{Tr}\Big(g^D\kappa^\dagger\kappa g^{D\dagger}\Big) \\
&- 3\,\mathrm{Tr}\Big(h^E h^{E\dagger}h^E h^{E\dagger}\Big) - 2\,\mathrm{Tr}\Big(h^E h^{E\dagger}y^E y^{E\dagger}\Big) - \mathrm{Tr}\Big(h^E\tilde{\lambda}^\dagger\tilde{\lambda}h^{E\dagger}\Big)\Big\}, \qquad \text{(D.28)}
\end{aligned}
$$

$$
\begin{aligned}
\beta^{(1)}_{g^D} = g^D\Big[&|\tilde{\sigma}|^2 + 3\,\mathrm{Tr}\Big(g^D g^{D\dagger}\Big) + \mathrm{Tr}\Big(h^E h^{E\dagger}\Big) - \frac{7}{15}g_1^2 - \frac{7}{10}g_1'^2 - 3g_2^2 - \frac{16}{3}g_3^2\Big] \\
&+ g^D\Big(3g^{D\dagger}g^D + \kappa^\dagger\kappa\Big) + \Big(y^{DT}y^{D*} + y^{UT}y^{U*}\Big)g^D, \qquad \text{(D.29)}
\end{aligned}
$$

$$
\begin{aligned}
\beta^{(2)}_{g^D} = g^D\Big\{&\kappa^\dagger\kappa\Big[g_1'^2 - 2|\lambda|^2 - |\sigma|^2 - 2\,\mathrm{Tr}\Big(\tilde{\lambda}\tilde{\lambda}^\dagger\Big) - 3\,\mathrm{Tr}\Big(\kappa\kappa^\dagger\Big)\Big] \\
&+ g^{D\dagger}g^D\Big[\frac{4}{5}g_1^2 + \frac{1}{5}g_1'^2 + 6g_2^2 - 3|\tilde{\sigma}|^2 - 9\,\mathrm{Tr}\Big(g^D g^{D\dagger}\Big) - 3\,\mathrm{Tr}\Big(h^E h^{E\dagger}\Big)\Big] \\
&- 4g^{D\dagger}g^D g^{D\dagger}g^D - \kappa^\dagger\kappa g^{D\dagger}g^D - \kappa^\dagger\kappa\kappa^\dagger\kappa\Big\} + \Big\{y^{DT}y^{D*}\Big[\frac{2}{5}g_1^2 + \frac{3}{5}g_1'^2 - |\lambda|^2 \\
&- 3\,\mathrm{Tr}\Big(y^D y^{D\dagger}\Big) - \mathrm{Tr}\Big(y^E y^{E\dagger}\Big) - \mathrm{Tr}\Big(ff^\dagger\Big)\Big] + y^{UT}y^{U*}\Big[\frac{4}{5}g_1^2 + \frac{1}{5}g_1'^2 - |\lambda|^2 \\
&- 3\,\mathrm{Tr}\Big(y^U y^{U\dagger}\Big) - \mathrm{Tr}\Big(\tilde{f}\tilde{f}^\dagger\Big)\Big] - 2g^D g^{D\dagger}y^{DT}y^{D*} - 2g^D g^{D\dagger}y^{UT}y^{U*}
\end{aligned}
$$

$$
\begin{aligned}
&- 2y^{DT}y^{D*}y^{DT}y^{D*} - 2y^{UT}y^{U*}y^{UT}y^{U*}\Big\}g^D + g^D\Big\{\frac{413}{90}g_1^4 + \frac{77}{10}g_1'^4 + \frac{33}{2}g_2^4 \\
&+ \frac{128}{9}g_3^4 + \frac{41}{60}g_1^2g_1'^2 + g_1^2g_2^2 + \frac{8}{9}g_1^2g_3^2 + \frac{3}{4}g_1'^2g_2^2 + \frac{8}{3}g_1'^2g_3^2 + 8g_2^2g_3^2 \\
&- |\tilde{\sigma}|^2\Big(2|\kappa_\phi|^2 + |\sigma|^2 + 3|\tilde{\sigma}|^2\Big) + \frac{2}{5}g_1^2\Big[-\mathrm{Tr}\Big(g^Dg^{D\dagger}\Big) + 3\,\mathrm{Tr}\Big(h^Eh^{E\dagger}\Big)\Big] \\
&+ \frac{3}{10}g_1'^2\Big[3\,\mathrm{Tr}\Big(g^Dg^{D\dagger}\Big) + \mathrm{Tr}\Big(h^Eh^{E\dagger}\Big)\Big] + 16g_3^2\,\mathrm{Tr}\Big(g^Dg^{D\dagger}\Big) \\
&- \mathrm{Tr}\Big(\tilde{f}h^{E\dagger}h^E\tilde{f}^\dagger\Big) - 9\,\mathrm{Tr}\Big(g^Dg^{D\dagger}g^Dg^{D\dagger}\Big) - 3\,\mathrm{Tr}\Big(g^Dg^{D\dagger}y^{DT}y^{D*}\Big) \\
&- 3\,\mathrm{Tr}\Big(g^Dg^{D\dagger}y^{UT}y^{U*}\Big) - 3\,\mathrm{Tr}\Big(g^D\kappa^\dagger\kappa g^{D\dagger}\Big) - 3\,\mathrm{Tr}\Big(h^Eh^{E\dagger}h^Eh^{E\dagger}\Big) \\
&- 2\,\mathrm{Tr}\Big(h^Eh^{E\dagger}y^Ey^{E\dagger}\Big) - \mathrm{Tr}\Big(h^E\tilde{\lambda}^\dagger\tilde{\lambda}h^{E\dagger}\Big)\Big\}, \qquad \text{(D.30)}
\end{aligned}
$$

$$
\begin{aligned}
\beta_{h^E}^{(1)} = {}& h^E\Big[|\tilde{\sigma}|^2 + 3\,\mathrm{Tr}\Big(g^Dg^{D\dagger}\Big) + \mathrm{Tr}\Big(h^Eh^{E\dagger}\Big) - \frac{9}{5}g_1^2 - \frac{7}{10}g_1'^2 - 3g_2^2\Big] \\
&+ h^E\Big(\tilde{f}^\dagger\tilde{f} + 3h^{E\dagger}h^E + \tilde{\lambda}^\dagger\tilde{\lambda}\Big) + 2y^Ey^{E\dagger}h^E, \qquad \text{(D.31)}
\end{aligned}
$$

$$
\begin{aligned}
\beta_{h^E}^{(2)} = {}& h^E\Big\{h^{E\dagger}h^E\Big[g_1'^2 + 6g_2^2 - 3|\tilde{\sigma}|^2 - 9\,\mathrm{Tr}\Big(g^Dg^{D\dagger}\Big) - 3\,\mathrm{Tr}\Big(h^Eh^{E\dagger}\Big)\Big] \\
&+ \tilde{\lambda}^\dagger\tilde{\lambda}\Big[g_1'^2 - 2|\lambda|^2 - |\sigma|^2 - 2\,\mathrm{Tr}\Big(\tilde{\lambda}\tilde{\lambda}^\dagger\Big) - 3\,\mathrm{Tr}\Big(\kappa\kappa^\dagger\Big)\Big] \\
&+ \tilde{f}^\dagger\tilde{f}\Big[g_1'^2 - |\lambda|^2 - 3\,\mathrm{Tr}\Big(y^Uy^{U\dagger}\Big) - \mathrm{Tr}\Big(\tilde{f}\tilde{f}^\dagger\Big)\Big] - 2\tilde{f}^\dagger ff^\dagger\tilde{f} - 2\tilde{f}^\dagger\tilde{f}\tilde{f}^\dagger\tilde{f} \\
&- 2\tilde{f}^\dagger\tilde{f}h^{E\dagger}h^E - 4h^{E\dagger}h^Eh^{E\dagger}h^E - 2\tilde{\lambda}^\dagger\tilde{\lambda}h^{E\dagger}h^E - \tilde{\lambda}^\dagger\tilde{\lambda}\tilde{\lambda}^\dagger\tilde{\lambda} - \tilde{\lambda}^\dagger f^Tf^*\tilde{\lambda}\Big\} \\
&+ \Big\{y^Ey^{E\dagger}\Big[-\frac{6}{5}g_1^2 + \frac{6}{5}g_1'^2 + 6g_2^2 - 2|\lambda|^2 - 6\,\mathrm{Tr}\Big(y^Dy^{D\dagger}\Big) - 2\,\mathrm{Tr}\Big(y^Ey^{E\dagger}\Big) \\
&- 2\,\mathrm{Tr}\Big(ff^\dagger\Big)\Big] - 2h^Eh^{E\dagger}y^Ey^{E\dagger} - 2y^Ey^{E\dagger}y^Ey^{E\dagger}\Big\}h^E + h^E\Big\{\frac{189}{10}g_1^4 + \frac{77}{10}g_1'^4 \\
&+ \frac{33}{2}g_2^4 + \frac{3}{20}g_1^2g_1'^2 + \frac{9}{5}g_1^2g_2^2 + \frac{39}{20}g_1'^2g_2^2 - |\tilde{\sigma}|^2\Big(2|\kappa_\phi|^2 + 2|\sigma|^2 + 3|\tilde{\sigma}|^2\Big) \\
&+ \frac{2}{5}g_1^2\Big[3\,\mathrm{Tr}\Big(h^Eh^{E\dagger}\Big) - \mathrm{Tr}\Big(g^Dg^{D\dagger}\Big)\Big] + \frac{3}{10}g_1'^2\Big[3\,\mathrm{Tr}\Big(g^Dg^{D\dagger}\Big) + \mathrm{Tr}\Big(h^Eh^{E\dagger}\Big)\Big] \\
&+ 16g_3^2\,\mathrm{Tr}\Big(g^Dg^{D\dagger}\Big) - \mathrm{Tr}\Big(\tilde{f}h^{E\dagger}h^E\tilde{f}^\dagger\Big) - 9\,\mathrm{Tr}\Big(g^Dg^{D\dagger}g^Dg^{D\dagger}\Big) \\
&- 3\,\mathrm{Tr}\Big(g^Dg^{D\dagger}y^{DT}y^{D*}\Big) - 3\,\mathrm{Tr}\Big(g^Dg^{D\dagger}y^{UT}y^{U*}\Big) - 3\,\mathrm{Tr}\Big(g^D\kappa^\dagger\kappa g^{D\dagger}\Big) \\
&- 3\,\mathrm{Tr}\Big(h^Eh^{E\dagger}h^Eh^{E\dagger}\Big) - 2\,\mathrm{Tr}\Big(h^Eh^{E\dagger}y^Ey^{E\dagger}\Big) - \mathrm{Tr}\Big(h^E\tilde{\lambda}^\dagger\tilde{\lambda}h^{E\dagger}\Big)\Big\}, \qquad \text{(D.32)}
\end{aligned}
$$

$$
\begin{aligned}
\beta_{\tilde{f}}^{(1)} = {}& \tilde{f}\Big[|\lambda|^2 + 3\,\mathrm{Tr}\Big(y^Uy^{U\dagger}\Big) + \mathrm{Tr}\Big(\tilde{f}\tilde{f}^\dagger\Big) - \frac{3}{5}g_1^2 - \frac{19}{10}g_1'^2 - 3g_2^2\Big] \\
&+ \Big(2ff^\dagger + 3\tilde{f}\tilde{f}^\dagger\Big)\tilde{f} + \tilde{f}\Big(h^{E\dagger}h^E + \tilde{\lambda}^\dagger\tilde{\lambda}\Big), \qquad \text{(D.33)}
\end{aligned}
$$

$$
\begin{aligned}
\beta^{(2)}_{\tilde{f}} = &\Big\{\tilde{f}\tilde{f}^\dagger\Big[\frac{6}{5}g_1^2 - \frac{1}{5}g_1'^2 + 6g_2^2 - 3|\lambda|^2 - 9\,\mathrm{Tr}\Big(y^U y^{U\dagger}\Big) - 3\,\mathrm{Tr}\Big(\tilde{f}\tilde{f}^\dagger\Big)\Big] \\
&+ ff^\dagger\Big[\frac{6}{5}g_1^2 - \frac{6}{5}g_1'^2 + 6g_2^2 - 2|\lambda|^2 - 6\,\mathrm{Tr}\Big(y^D y^{D\dagger}\Big) - 2\,\mathrm{Tr}\Big(y^E y^{E\dagger}\Big) \\
&- 2\,\mathrm{Tr}\Big(ff^\dagger\Big)\Big] - 2ff^\dagger ff^\dagger - 2f\tilde{\lambda}^*\tilde{\lambda}^T f^\dagger - 2\tilde{f}\tilde{f}^\dagger ff^\dagger - 4\tilde{f}\tilde{f}^\dagger\tilde{f}\tilde{f}^\dagger\Big\}\tilde{f} \\
&+ \tilde{f}\Big\{h^{E\dagger}h^E\Big[\frac{6}{5}g_1^2 - \frac{1}{5}g_1'^2 - |\tilde{\sigma}|^2 - 3\,\mathrm{Tr}\Big(g^D g^{D\dagger}\Big) - \mathrm{Tr}\Big(h^E h^{E\dagger}\Big)\Big] \\
&+ \tilde{\lambda}^\dagger\tilde{\lambda}\Big[g_1'^2 - 2|\lambda|^2 - |\sigma|^2 - 2\,\mathrm{Tr}\Big(\tilde{\lambda}\tilde{\lambda}^\dagger\Big) - 3\,\mathrm{Tr}\Big(\kappa\kappa^\dagger\Big)\Big] - 2h^{E\dagger}h^E\tilde{f}^\dagger\tilde{f} \\
&- 2h^{E\dagger}h^E h^{E\dagger}h^E - 2h^{E\dagger}y^E y^{E\dagger}h^E - 2\tilde{\lambda}^\dagger\tilde{\lambda}\tilde{f}^\dagger\tilde{f} - \tilde{\lambda}^\dagger\tilde{\lambda}\tilde{\lambda}^\dagger\tilde{\lambda} - \tilde{\lambda}^\dagger f^T f^*\tilde{\lambda}\Big\} \\
&+ \tilde{f}\Big\{\frac{297}{50}g_1^4 + \frac{551}{25}g_1'^4 + \frac{33}{2}g_2^4 + \frac{27}{100}g_1^2 g_1'^2 + \frac{9}{5}g_1^2 g_2^2 + \frac{39}{20}g_1'^2 g_2^2 - 3|\lambda|^4 \\
&+ \frac{4}{5}g_1^2\,\mathrm{Tr}\Big(y^U y^{U\dagger}\Big) + \frac{3}{2}g_1'^2\Big[-\frac{1}{5}\,\mathrm{Tr}\Big(y^U y^{U\dagger}\Big) + \mathrm{Tr}\Big(\tilde{f}\tilde{f}^\dagger\Big)\Big] + 16g_3^2\,\mathrm{Tr}\Big(y^U y^{U\dagger}\Big) \\
&+ |\lambda|^2\Big[\frac{3}{2}g_1'^2 - |\sigma|^2 - 3\,\mathrm{Tr}\Big(y^D y^{D\dagger}\Big) - \mathrm{Tr}\Big(y^E y^{E\dagger}\Big) - 2\,\mathrm{Tr}\Big(\tilde{\lambda}\tilde{\lambda}^\dagger\Big) \\
&- 3\,\mathrm{Tr}\Big(\kappa\kappa^\dagger\Big) - \mathrm{Tr}\Big(ff^\dagger\Big)\Big] - 2\,\mathrm{Tr}\Big(ff^\dagger\tilde{f}\tilde{f}^\dagger\Big) - 3\,\mathrm{Tr}\Big(\tilde{f}\tilde{f}^\dagger\tilde{f}\tilde{f}^\dagger\Big) \\
&- \mathrm{Tr}\Big(\tilde{f}h^{E\dagger}h^E\tilde{f}^\dagger\Big) - \mathrm{Tr}\Big(\tilde{f}\tilde{\lambda}^\dagger\tilde{\lambda}\tilde{f}^\dagger\Big) - 3\,\mathrm{Tr}\Big(g^D g^{D\dagger}y^{UT}y^{U*}\Big) \\
&- 3\,\mathrm{Tr}\Big(y^D y^{U\dagger}y^U y^{D\dagger}\Big) - 9\,\mathrm{Tr}\Big(y^U y^{U\dagger}y^U y^{U\dagger}\Big)\Big\}, \qquad \text{(D.34)}
\end{aligned}
$$

$$
\begin{aligned}
\beta^{(1)}_f = &f\Big[|\lambda|^2 + 3\,\mathrm{Tr}\Big(y^D y^{D\dagger}\Big) + \mathrm{Tr}\Big(y^E y^{E\dagger}\Big) + \mathrm{Tr}\Big(ff^\dagger\Big) - \frac{3}{5}g_1^2 - \frac{19}{10}g_1'^2 - 3g_2^2\Big] \\
&+ \Big(3ff^\dagger + 2\tilde{f}\tilde{f}^\dagger\Big)f + f\tilde{\lambda}^*\tilde{\lambda}^T, \qquad \text{(D.35)}
\end{aligned}
$$

$$
\begin{aligned}
\beta^{(2)}_f = &f\Big\{\tilde{\lambda}^*\tilde{\lambda}^T\Big[\frac{3}{2}g_1'^2 - 2|\lambda|^2 - |\sigma|^2 - 2\,\mathrm{Tr}\Big(\tilde{\lambda}\tilde{\lambda}^\dagger\Big) - 3\,\mathrm{Tr}\Big(\kappa\kappa^\dagger\Big)\Big] \\
&- \tilde{\lambda}^*\tilde{f}^T\tilde{f}^*\tilde{\lambda}^T - \tilde{\lambda}^* h^{ET}h^{E*}\tilde{\lambda}^T - 2\tilde{\lambda}^*\tilde{\lambda}^T f^\dagger f - \tilde{\lambda}^*\tilde{\lambda}^T\tilde{\lambda}^*\tilde{\lambda}^T\Big\} \\
&+ \Big\{\tilde{f}\tilde{f}^\dagger\Big[\frac{6}{5}g_1^2 - \frac{6}{5}g_1'^2 + 6g_2^2 - 2|\lambda|^2 - 6\,\mathrm{Tr}\Big(y^U y^{U\dagger}\Big) - 2\,\mathrm{Tr}\Big(\tilde{f}\tilde{f}^\dagger\Big)\Big] \\
&+ ff^\dagger\Big[\frac{6}{5}g_1^2 + \frac{3}{10}g_1'^2 + 6g_2^2 - 3|\lambda|^2 - 9\,\mathrm{Tr}\Big(y^D y^{D\dagger}\Big) - 3\,\mathrm{Tr}\Big(y^E y^{E\dagger}\Big) \\
&- 3\,\mathrm{Tr}\Big(ff^\dagger\Big)\Big] - 4ff^\dagger ff^\dagger - 2ff^\dagger\tilde{f}\tilde{f}^\dagger - 2\tilde{f}\tilde{f}^\dagger\tilde{f}\tilde{f}^\dagger - 2\tilde{f}h^{E\dagger}h^E\tilde{f}^\dagger \\
&- 2\tilde{f}\tilde{\lambda}^\dagger\tilde{\lambda}\tilde{f}^\dagger\Big\}f + f\Big\{\frac{297}{50}g_1^4 + \frac{551}{25}g_1'^4 + \frac{33}{2}g_2^4 + \frac{27}{100}g_1^2 g_1'^2 + \frac{9}{5}g_1^2 g_2^2 + \frac{39}{20}g_1'^2 g_2^2 \\
&- 3|\lambda|^4 + \frac{2}{5}g_1^2\Big[-\mathrm{Tr}\Big(y^D y^{D\dagger}\Big) + 3\,\mathrm{Tr}\Big(y^E y^{E\dagger}\Big)\Big] + g_1'^2\Big[-\frac{3}{5}\,\mathrm{Tr}\Big(y^D y^{D\dagger}\Big) \\
&- \frac{1}{5}\,\mathrm{Tr}\Big(y^E y^{E\dagger}\Big) + \mathrm{Tr}\Big(ff^\dagger\Big)\Big] + 16g_3^2\,\mathrm{Tr}\Big(y^D y^{D\dagger}\Big) + |\lambda|^2\Big[g_1'^2 - |\sigma|^2
\end{aligned}
$$

$$
\begin{aligned}
&- 3\,\mathrm{Tr}\Big(y^U y^{U\dagger}\Big) - 2\,\mathrm{Tr}\Big(\tilde{\lambda}\tilde{\lambda}^\dagger\Big) - 3\,\mathrm{Tr}\Big(\kappa\kappa^\dagger\Big) - \mathrm{Tr}\Big(\tilde{f}\tilde{f}^\dagger\Big)\Big] - 3\,\mathrm{Tr}\Big(ff^\dagger ff^\dagger\Big) \\
&- 2\,\mathrm{Tr}\Big(ff^\dagger\tilde{f}\tilde{f}^\dagger\Big) - 3\,\mathrm{Tr}\Big(g^D g^{D\dagger} y^{DT} y^{D*}\Big) - 2\,\mathrm{Tr}\Big(h^E h^{E\dagger} y^E y^{E\dagger}\Big) \\
&- 9\,\mathrm{Tr}\Big(y^D y^{D\dagger} y^D y^{D\dagger}\Big) - 3\,\mathrm{Tr}\Big(y^D y^{U\dagger} y^U y^{D\dagger}\Big) - 3\,\mathrm{Tr}\Big(y^E y^{E\dagger} y^E y^{E\dagger}\Big) \\
&- \mathrm{Tr}\Big(\tilde{\lambda}\tilde{\lambda}^\dagger f^T f^*\Big)\Big\}. \qquad \text{(D.36)}
\end{aligned}
$$

D.3 Superpotential Bilinear and Linear Couplings

The β functions of the bilinear superpotential parameters μ_ϕ and μ_L read

$$
\begin{aligned}
\beta^{(1)}_{\mu_\phi} &= 2\mu_\phi\Big(2|\kappa_\phi|^2 + 2|\tilde{\sigma}|^2 + |\sigma|^2\Big), \qquad \text{(D.37)} \\
\beta^{(2)}_{\mu_\phi} &= \mu_\phi\Big\{-16|\kappa_\phi|^4 - 8|\tilde{\sigma}|^4 - 4|\sigma|^4 + |\tilde{\sigma}|^2\Big[\frac{12}{5}g_1^2 + \frac{8}{5}g_1'^2 + 12g_2^2 - 16|\kappa_\phi|^2 \\
&\quad - 12\,\mathrm{Tr}\Big(g^D g^{D\dagger}\Big) - 4\,\mathrm{Tr}\Big(h^E h^{E\dagger}\Big)\Big] + |\sigma|^2\Big[5g_1'^2 - 4|\lambda|^2 - 8|\kappa_\phi|^2 \\
&\quad - 4\,\mathrm{Tr}\Big(\tilde{\lambda}\tilde{\lambda}^\dagger\Big) - 6\,\mathrm{Tr}\Big(\kappa\kappa^\dagger\Big)\Big]\Big\}, \qquad \text{(D.38)} \\
\beta^{(1)}_{\mu_L} &= \mu_L\Big[2|\tilde{\sigma}|^2 + 3\,\mathrm{Tr}\Big(g^D g^{D\dagger}\Big) + \mathrm{Tr}\Big(h^E h^{E\dagger}\Big) - \frac{3}{5}g_1^2 - \frac{2}{5}g_1'^2 - 3g_2^2\Big], \qquad \text{(D.39)} \\
\beta^{(2)}_{\mu_L} &= \mu_L\Big\{\frac{297}{50}g_1^4 + \frac{217}{50}g_1'^4 + \frac{33}{2}g_2^4 + \frac{18}{25}g_1^2 g_1'^2 + \frac{9}{5}g_1^2 g_2^2 + \frac{6}{5}g_1'^2 g_2^2 \\
&\quad - 2|\tilde{\sigma}|^2\Big(2|\kappa_\phi|^2 + 3|\tilde{\sigma}|^2 + |\sigma|^2\Big) + \frac{2}{5}g_1^2\Big[-\mathrm{Tr}\Big(g^D g^{D\dagger}\Big) + 3\,\mathrm{Tr}\Big(h^E h^{E\dagger}\Big)\Big] \\
&\quad + \Big(\frac{3}{10}g_1'^2 - |\tilde{\sigma}|^2\Big)\Big[3\,\mathrm{Tr}\Big(g^D g^{D\dagger}\Big) + \mathrm{Tr}\Big(h^E h^{E\dagger}\Big)\Big] + 16g_3^2\,\mathrm{Tr}\Big(g^D g^{D\dagger}\Big) \\
&\quad - \mathrm{Tr}\Big(\tilde{f}h^{E\dagger}h^E\tilde{f}^\dagger\Big) - 9\,\mathrm{Tr}\Big(g^D g^{D\dagger} g^D g^{D\dagger}\Big) - 3\,\mathrm{Tr}\Big(g^D g^{D\dagger} y^{DT} y^{D*}\Big) \\
&\quad - 3\,\mathrm{Tr}\Big(g^D g^{D\dagger} y^{UT} y^{U*}\Big) - 3\,\mathrm{Tr}\Big(g^D \kappa^\dagger \kappa g^{D\dagger}\Big) - 3\,\mathrm{Tr}\Big(h^E h^{E\dagger} h^E h^{E\dagger}\Big) \\
&\quad - 2\,\mathrm{Tr}\Big(h^E h^{E\dagger} y^E y^{E\dagger}\Big) - \mathrm{Tr}\Big(h^E \tilde{\lambda}^\dagger \tilde{\lambda} h^{E\dagger}\Big)\Big\}, \qquad \text{(D.40)}
\end{aligned}
$$

while that for the linear superpotential parameter Λ_F is

$$
\begin{aligned}
\beta^{(1)}_{\Lambda_F} &= \Lambda_F\Big(2|\kappa_\phi|^2 + 2|\tilde{\sigma}|^2 + |\sigma|^2\Big), \qquad \text{(D.41)} \\
\beta^{(2)}_{\Lambda_F} &= \Lambda_F\Big\{-8|\kappa_\phi|^4 - 4|\tilde{\sigma}|^2 - 2|\sigma|^4 + |\tilde{\sigma}|^2\Big[\frac{6}{5}g_1^2 + \frac{4}{5}g_1'^2 + 6g_2^2 - 8|\kappa_\phi|^2 \\
&\quad - 6\,\mathrm{Tr}\Big(g^D g^{D\dagger}\Big) - 2\,\mathrm{Tr}\Big(h^E h^{E\dagger}\Big)\Big] + |\sigma|^2\Big[\frac{5}{2}g_1'^2 - 2|\lambda|^2 - 4|\kappa_\phi|^2
\end{aligned}
$$

$$- 2\,\mathrm{Tr}\Big(\tilde{\lambda}\tilde{\lambda}^\dagger\Big) - 3\,\mathrm{Tr}\Big(\kappa\kappa^\dagger\Big)\Big]\Big\}\,. \tag{D.42}$$

D.4 Gaugino Masses

The two-loop β functions for the soft gaugino masses are

$$\beta_{M_1}^{(1)} = \frac{96}{5} g_1^2 M_1\,, \tag{D.43}$$

$$\begin{aligned}\beta_{M_1}^{(2)} = g_1^2\Big[&\frac{936}{25} g_1^2 M_1 + \frac{162}{25} g_1'^2 (M_1 + M_1') + \frac{108}{5} g_2^2 (M_1 + M_2) + 48 g_3^2 (M_1 + M_3) \\ &- \frac{52}{5}\,\mathrm{Tr}\Big(M_1 y^U y^{U\dagger} - y^{U\dagger} T^U\Big) - \frac{28}{5}\,\mathrm{Tr}\Big(M_1 y^D y^{D\dagger} - y^{D\dagger} T^D\Big) \\ &- \frac{36}{5}\,\mathrm{Tr}\Big(M_1 y^E y^{E\dagger} - y^{E\dagger} T^E\Big) - \frac{12}{5}\lambda^*\Big(M_1\lambda - T_\lambda\Big) \\ &- \frac{12}{5}\,\mathrm{Tr}\Big(M_1 \tilde{\lambda}\tilde{\lambda}^\dagger - \tilde{\lambda}^\dagger T^{\tilde{\lambda}}\Big) - \frac{8}{5}\,\mathrm{Tr}\Big(M_1 \kappa\kappa^\dagger - \kappa^\dagger T^\kappa\Big) - \frac{12}{5}\tilde{\sigma}^*\Big(M_1\tilde{\sigma} - T_{\tilde{\sigma}}\Big) \\ &- \frac{12}{5}\,\mathrm{Tr}\Big(M_1 f f^\dagger - f^\dagger T^f\Big) - \frac{12}{5}\,\mathrm{Tr}\Big(M_1 \tilde{f}\tilde{f}^\dagger - \tilde{f}^\dagger T^{\tilde{f}}\Big) \\ &- \frac{28}{5}\,\mathrm{Tr}\Big(M_1 g^D g^{D\dagger} - g^{D\dagger} T^{g^D}\Big) - \frac{36}{5}\,\mathrm{Tr}\Big(M_1 h^E h^{E\dagger} - h^{E\dagger} T^{h^E}\Big)\Big]\,,\end{aligned} \tag{D.44}$$

$$\beta_{M_2}^{(1)} = 8 g_2^2 M_2\,, \tag{D.45}$$

$$\begin{aligned}\beta_{M_2}^{(2)} = g_2^2\Big[&\frac{36}{5} g_1^2 (M_1 + M_2) + \frac{34}{5} g_1'^2 (M_1' + M_2) + \frac{184}{5} g_2^2 M_2 + 48 g_3^2 (M_2 + M_3) \\ &- 12\,\mathrm{Tr}\Big(M_2 y^U y^{U\dagger} - y^{U\dagger} T^U\Big) - 12\,\mathrm{Tr}\Big(M_2 y^D y^{D\dagger} - y^{D\dagger} T^D\Big) \\ &- 4\,\mathrm{Tr}\Big(M_2 y^E y^{E\dagger} - y^{E\dagger} T^E\Big) - 4\lambda^*\Big(M_2\lambda - T_\lambda\Big) - 4\,\mathrm{Tr}\Big(M_2 \tilde{\lambda}\tilde{\lambda}^\dagger - \tilde{\lambda}^\dagger T^{\tilde{\lambda}}\Big) \\ &- 4\tilde{\sigma}^*\Big(M_2\tilde{\sigma} - T_{\tilde{\sigma}}\Big) - 4\,\mathrm{Tr}\Big(M_2 f f^\dagger - f^\dagger T^f\Big) - 4\,\mathrm{Tr}\Big(M_2 \tilde{f}\tilde{f}^\dagger - \tilde{f}^\dagger T^{\tilde{f}}\Big) \\ &- 12\,\mathrm{Tr}\Big(M_2 g^D g^{D\dagger} - g^{D\dagger} T^{g^D}\Big) - 4\,\mathrm{Tr}\Big(M_2 h^E h^{E\dagger} - h^{E\dagger} T^{h^E}\Big)\Big]\,,\end{aligned} \tag{D.46}$$

$$\beta_{M_3}^{(1)} = 0\,, \tag{D.47}$$

$$\begin{aligned}\beta_{M_3}^{(2)} = g_3^2\Big[&6 g_1^2 (M_1 + M_3) + 6 g_1'^2 (M_1' + M_3) + 18 g_2^2 (M_2 + M_3) + 192 g_3^2 M_3 \\ &- 8\,\mathrm{Tr}\Big(M_3 y^U y^{U\dagger} - y^{U\dagger} T^U\Big) - 8\,\mathrm{Tr}\Big(M_3 y^D y^{D\dagger} - y^{D\dagger} T^D\Big) \\ &- 4\,\mathrm{Tr}\Big(M_3 \kappa\kappa^\dagger - \kappa^\dagger T^\kappa\Big) - 8\,\mathrm{Tr}\Big(M_3 g^D g^{D\dagger} - g^{D\dagger} T^{g^D}\Big)\Big]\,,\end{aligned} \tag{D.48}$$

$$\beta_{M_1'}^{(1)} = \frac{213}{10} g_1'^2 M_1'\,, \tag{D.49}$$

$$\beta_{M_1'}^{(2)} = g_1'^2\Big[\frac{162}{25} g_1^2 (M_1 + M_1') + \frac{2457}{50} g_1'^2 M_1' + \frac{102}{5} g_2^2 (M_1' + M_2) + 48 g_3^2 (M_1' + M_3)$$

$$
\begin{aligned}
&- \frac{18}{5}\,\mathrm{Tr}\Big(M_1' y^U y^{U\dagger} - y^{U\dagger} T^U\Big) - \frac{42}{5}\,\mathrm{Tr}\Big(M_1' y^D y^{D\dagger} - y^{D\dagger} T^D\Big) \\
&- \frac{14}{5}\,\mathrm{Tr}\Big(M_1' y^E y^{E\dagger} - y^{E\dagger} T^E\Big) - \frac{38}{5}\lambda^*\Big(M_1'\lambda - T_\lambda\Big) \\
&- \frac{38}{5}\,\mathrm{Tr}\Big(M_1' \tilde{\lambda}\tilde{\lambda}^\dagger - \tilde{\lambda}^\dagger T^{\tilde{\lambda}}\Big) - \frac{57}{5}\,\mathrm{Tr}\Big(M_1' \kappa\kappa^\dagger - \kappa^\dagger T^\kappa\Big) - \frac{8}{5}\tilde{\sigma}^*\Big(M_1'\tilde{\sigma} - T_{\tilde{\sigma}}\Big) \\
&- 5\sigma^*\Big(M_1'\sigma - T_\sigma\Big) - \frac{38}{5}\,\mathrm{Tr}\Big(M_1' f f^\dagger - f^\dagger T^f\Big) - \frac{38}{5}\,\mathrm{Tr}\Big(M_1' \tilde{f}\tilde{f}^\dagger - \tilde{f}^\dagger T^{\tilde{f}}\Big) \\
&- \frac{42}{5}\,\mathrm{Tr}\Big(M_1' g^D g^{D\dagger} - g^{D\dagger} T^{g^D}\Big) - \frac{14}{5}\,\mathrm{Tr}\Big(M_1' h^E h^{E\dagger} - h^{E\dagger} T^{h^E}\Big)\Big]\,. \qquad \text{(D.50)}
\end{aligned}
$$

As mentioned above, kinetic mixing in this class of E_6 inspired models is small and so we neglect the mixed gaugino mass M_{11}.

D.5 Soft-breaking Trilinear Scalar Couplings

The two-loop RGEs for the soft scalar trilinear couplings read

$$
\begin{aligned}
\beta^{(1)}_{T^D} &= 4y^D y^{D\dagger} T^D + 2y^D y^{U\dagger} T^U + 2y^D g^{D*} T^{g^D T} + 5T^D y^{D\dagger} y^D + T^D y^{U\dagger} y^U \\
&+ T^D g^{D*} g^{DT} - \frac{7}{15} g_1^2 T^D - \frac{7}{10} g_1'^2 T^D - 3g_2^2 T^D - \frac{16}{3} g_3^2 T^D + |\lambda|^2 T^D \\
&+ T^D\,\mathrm{Tr}\Big(f f^\dagger\Big) + 3T^D\,\mathrm{Tr}\Big(y^D y^{D\dagger}\Big) + T^D\,\mathrm{Tr}\Big(y^E y^{E\dagger}\Big) + y^D\Big[2\lambda^* T_\lambda \\
&+ 2\,\mathrm{Tr}\Big(f^\dagger T^f\Big) + 2\,\mathrm{Tr}\Big(y^{E\dagger} T^E\Big) + 6g_2^2 M_2 + 6\,\mathrm{Tr}\Big(y^{D\dagger} T^D\Big) + \frac{14}{15} g_1^2 M_1 \\
&+ \frac{32}{3} g_3^2 M_3 + \frac{7}{5} g_1'^2 M_1'\Big]\,, \qquad \text{(D.51)} \\
\beta^{(2)}_{T^D} &= \frac{6}{5} g_1^2 y^D y^{D\dagger} T^D + \frac{9}{5} g_1'^2 y^D y^{D\dagger} T^D + 6g_2^2 y^D y^{D\dagger} T^D - 4|\lambda|^2 y^D y^{D\dagger} T^D \\
&- \frac{8}{5} g_1^2 M_1 y^D y^{U\dagger} y^U - \frac{2}{5} g_1'^2 M_1' y^D y^{U\dagger} y^U + \frac{8}{5} g_1^2 y^D y^{U\dagger} T^U + \frac{2}{5} g_1'^2 y^D y^{U\dagger} T^U \\
&- 2|\lambda|^2 y^D y^{U\dagger} T^U - \frac{4}{5} g_1^2 M_1 y^D g^{D*} g^{DT} - \frac{6}{5} g_1'^2 M_1' y^D g^{D*} g^{DT} \\
&+ \frac{4}{5} g_1^2 y^D g^{D*} T^{g^D T} + \frac{6}{5} g_1'^2 y^D g^{D*} T^{g^D T} - 2|\tilde{\sigma}|^2 y^D g^{D*} T^{g^D T} + \frac{6}{5} g_1^2 T^D y^{D\dagger} y^D \\
&+ \frac{9}{5} g_1'^2 T^D y^{D\dagger} y^D + 12 g_2^2 T^D y^{D\dagger} y^D - 5|\lambda|^2 T^D y^{D\dagger} y^D + \frac{4}{5} g_1^2 T^D y^{U\dagger} y^U \\
&+ \frac{1}{5} g_1'^2 T^D y^{U\dagger} y^U - |\lambda|^2 T^D y^{U\dagger} y^U + \frac{2}{5} g_1^2 T^D g^{D*} g^{DT} + \frac{3}{5} g_1'^2 T^D g^{D*} g^{DT} \\
&- |\tilde{\sigma}|^2 T^D g^{D*} g^{DT} - 6 y^D y^{D\dagger} y^D y^{D\dagger} T^D - 8 y^D y^{D\dagger} T^D y^{D\dagger} y^D \\
&- 2 y^D y^{U\dagger} y^U y^{D\dagger} T^D - 4 y^D y^{U\dagger} y^U y^{U\dagger} T^U - 4 y^D y^{U\dagger} T^U y^{D\dagger} y^D \\
&- 4 y^D y^{U\dagger} T^U y^{U\dagger} y^U - 2 y^D g^{D*} g^{DT} y^{D\dagger} T^D - 4 y^D g^{D*} g^{DT} g^{D*} T^{g^D T}
\end{aligned}
$$

$$
\begin{aligned}
&- 2y^D g^{D*}\kappa^T\kappa^* T^{g^D T} - 4y^D g^{D*} T^{g^D T} y^{D\dagger} y^D - 4y^D g^{D*} T^{g^D T} g^{D*} g^{DT} \\
&- 2y^D g^{D*} T^{\kappa T}\kappa^* g^{DT} - 6T^D y^{D\dagger} y^D y^{D\dagger} y^D - 4T^D y^{U\dagger} y^U y^{D\dagger} y^D \\
&- 2T^D y^{U\dagger} y^U y^{U\dagger} y^U - 4T^D g^{D*} g^{DT} y^{D\dagger} y^D - 2T^D g^{D*} g^{DT} g^{D*} g^{DT} \\
&- T^D g^{D*}\kappa^T\kappa^* g^{DT} + \frac{413}{90} g_1^4 T^D - \frac{7}{30} g_1^2 g_1'^2 T^D + \frac{77}{10} g_1'^4 T^D + g_1^2 g_2^2 T^D \\
&+ \frac{3}{2} g_1'^2 g_2^2 T^D + \frac{33}{2} g_2^4 T^D + \frac{8}{9} g_1^2 g_3^2 T^D + \frac{4}{3} g_1'^2 g_3^2 T^D + 8 g_2^2 g_3^2 T^D + \frac{128}{9} g_3^4 T^D \\
&+ g_1'^2 |\lambda|^2 T^D - 3|\lambda|^4 T^D - |\sigma|^2 |\lambda|^2 T^D - 2\lambda^* y^D y^{U\dagger} y^U T_\lambda \\
&- 2\tilde{\sigma}^* y^D g^{D*} g^{DT} T_{\tilde{\sigma}} - 4y^D y^{D\dagger} T^D \operatorname{Tr}\Big(f f^\dagger\Big) - 5T^D y^{D\dagger} y^D \operatorname{Tr}\Big(f f^\dagger\Big) \\
&+ g_1'^2 T^D \operatorname{Tr}\Big(f f^\dagger\Big) - 2y^D y^{U\dagger} T^U \operatorname{Tr}\Big(\tilde{f}\tilde{f}^\dagger\Big) - T^D y^{U\dagger} y^U \operatorname{Tr}\Big(\tilde{f}\tilde{f}^\dagger\Big) \\
&- |\lambda|^2 T^D \operatorname{Tr}\Big(\tilde{f}\tilde{f}^\dagger\Big) - 6y^D g^{D*} T^{g^D T} \operatorname{Tr}\Big(g^D g^{D\dagger}\Big) - 3T^D g^{D*} g^{DT} \operatorname{Tr}\Big(g^D g^{D\dagger}\Big) \\
&- 2y^D g^{D*} T^{g^D T} \operatorname{Tr}\Big(h^E h^{E\dagger}\Big) - T^D g^{D*} g^{DT} \operatorname{Tr}\Big(h^E h^{E\dagger}\Big) \\
&- 12 y^D y^{D\dagger} T^D \operatorname{Tr}\Big(y^D y^{D\dagger}\Big) - 15 T^D y^{D\dagger} y^D \operatorname{Tr}\Big(y^D y^{D\dagger}\Big) - \frac{2}{5} g_1^2 T^D \operatorname{Tr}\Big(y^D y^{D\dagger}\Big) \\
&- \frac{3}{5} g_1'^2 T^D \operatorname{Tr}\Big(y^D y^{D\dagger}\Big) + 16 g_3^2 T^D \operatorname{Tr}\Big(y^D y^{D\dagger}\Big) - 4 y^D y^{D\dagger} T^D \operatorname{Tr}\Big(y^E y^{E\dagger}\Big) \\
&- 5 T^D y^{D\dagger} y^D \operatorname{Tr}\Big(y^E y^{E\dagger}\Big) + \frac{6}{5} g_1^2 T^D \operatorname{Tr}\Big(y^E y^{E\dagger}\Big) - \frac{1}{5} g_1'^2 T^D \operatorname{Tr}\Big(y^E y^{E\dagger}\Big) \\
&- 6 y^D y^{U\dagger} T^U \operatorname{Tr}\Big(y^U y^{U\dagger}\Big) - 3 T^D y^{U\dagger} y^U \operatorname{Tr}\Big(y^U y^{U\dagger}\Big) - 3|\lambda|^2 T^D \operatorname{Tr}\Big(y^U y^{U\dagger}\Big) \\
&- 3|\lambda|^2 T^D \operatorname{Tr}\Big(\kappa\kappa^\dagger\Big) - 2|\lambda|^2 T^D \operatorname{Tr}\Big(\tilde{\lambda}\tilde{\lambda}^\dagger\Big) - 2 y^D y^{U\dagger} y^U \operatorname{Tr}\Big(\tilde{f}^\dagger T^{\tilde{f}}\Big) \\
&- 6 y^D g^{D*} g^{DT} \operatorname{Tr}\Big(g^{D\dagger} T^{g^D}\Big) - 2 y^D g^{D*} g^{DT} \operatorname{Tr}\Big(h^{E\dagger} T^{h^E}\Big) \\
&- \frac{2}{5} y^D y^{D\dagger} y^D \Big[15\lambda^* T_\lambda + 15 \operatorname{Tr}\Big(f^\dagger T^f\Big) + 15 \operatorname{Tr}\Big(y^{E\dagger} T^E\Big) + 30 g_2^2 M_2 \\
&+ 45 \operatorname{Tr}\Big(y^{D\dagger} T^D\Big) + 4 g_1^2 M_1 + 6 g_1'^2 M_1'\Big] - 6 y^D y^{U\dagger} y^U \operatorname{Tr}\Big(y^{U\dagger} T^U\Big) \\
&- 3 T^D \operatorname{Tr}\Big(f f^\dagger f f^\dagger\Big) - 2 T^D \operatorname{Tr}\Big(f f^\dagger \tilde{f}\tilde{f}^\dagger\Big) - 3 T^D \operatorname{Tr}\Big(g^D g^{D\dagger} y^{DT} y^{D*}\Big) \\
&- 2 T^D \operatorname{Tr}\Big(h^E h^{E\dagger} y^E y^{E\dagger}\Big) - 9 T^D \operatorname{Tr}\Big(y^D y^{D\dagger} y^D y^{D\dagger}\Big) - 3 T^D \operatorname{Tr}\Big(y^D y^{U\dagger} y^U y^{D\dagger}\Big) \\
&- 3 T^D \operatorname{Tr}\Big(y^E y^{E\dagger} y^E y^{E\dagger}\Big) - T^D \operatorname{Tr}\Big(\tilde{\lambda}\tilde{\lambda}^\dagger f^T f^*\Big) - \frac{1}{45} y^D \Big(826 g_1^4 M_1 - 21 g_1^2 g_1'^2 M_1 \\
&+ 90 g_1^2 g_2^2 M_1 + 80 g_1^2 g_3^2 M_1 - 21 g_1^2 g_1'^2 M_1' + 1386 g_1'^4 M_1' + 135 g_1'^2 g_2^2 M_1' \\
&+ 120 g_1'^2 g_3^2 M_1' + 80 g_1^2 g_3^2 M_3 + 120 g_1'^2 g_3^2 M_3 + 720 g_2^2 g_3^2 M_3 + 2560 g_3^4 M_3 \\
&+ 90 g_1^2 g_2^2 M_2 + 135 g_1'^2 g_2^2 M_2 + 2970 g_2^4 M_2 + 720 g_2^2 g_3^2 M_2 + 540\lambda^* |\lambda|^2 T_\lambda
\end{aligned}
$$

$$
\begin{aligned}
&+ 90g_1'^2 M_1' \operatorname{Tr}\Big(ff^\dagger\Big) - 36g_1^2 M_1 \operatorname{Tr}\Big(y^D y^{D\dagger}\Big) - 54g_1'^2 M_1' \operatorname{Tr}\Big(y^D y^{D\dagger}\Big) \\
&+ 1440g_3^2 M_3 \operatorname{Tr}\Big(y^D y^{D\dagger}\Big) + 108g_1^2 M_1 \operatorname{Tr}\Big(y^E y^{E\dagger}\Big) - 18g_1'^2 M_1' \operatorname{Tr}\Big(y^E y^{E\dagger}\Big) \\
&- 90g_1'^2 \operatorname{Tr}\Big(f^\dagger T^f\Big) + 36g_1^2 \operatorname{Tr}\Big(y^{D\dagger} T^D\Big) + 54g_1'^2 \operatorname{Tr}\Big(y^{D\dagger} T^D\Big) \\
&- 1440g_3^2 \operatorname{Tr}\Big(y^{D\dagger} T^D\Big) - 108g_1^2 \operatorname{Tr}\Big(y^{E\dagger} T^E\Big) + 18g_1'^2 \operatorname{Tr}\Big(y^{E\dagger} T^E\Big) \\
&+ 90\lambda^*\Big\{T_\lambda\Big[2\operatorname{Tr}\Big(\tilde{\lambda}\tilde{\lambda}^\dagger\Big) + 3\operatorname{Tr}\Big(\kappa\kappa^\dagger\Big) + 3\operatorname{Tr}\Big(y^U y^{U\dagger}\Big) - g_1'^2 + |\sigma|^2 \\
&+ \operatorname{Tr}\Big(\tilde{f}\tilde{f}^\dagger\Big)\Big] + \lambda\Big[2\operatorname{Tr}\Big(\tilde{\lambda}^\dagger T^{\tilde{\lambda}}\Big) + 3\operatorname{Tr}\Big(\kappa^\dagger T^\kappa\Big) + 3\operatorname{Tr}\Big(y^{U\dagger} T^U\Big) + g_1'^2 M_1' \\
&+ \sigma^* T_\sigma + \operatorname{Tr}\Big(\tilde{f}^\dagger T^{\tilde{f}}\Big)\Big]\Big\} + 540\operatorname{Tr}\Big(ff^\dagger T^f f^\dagger\Big) + 180\operatorname{Tr}\Big(ff^\dagger T^{\tilde{f}}\tilde{f}^\dagger\Big) \\
&+ 180\operatorname{Tr}\Big(\tilde{f}\tilde{f}^\dagger T^f f^\dagger\Big) + 180\operatorname{Tr}\Big(h^E h^{E\dagger} T^E y^{E\dagger}\Big) + 1620\operatorname{Tr}\Big(y^D y^{D\dagger} T^D y^{D\dagger}\Big) \\
&+ 270\operatorname{Tr}\Big(y^D y^{U\dagger} T^U y^{D\dagger}\Big) + 180\operatorname{Tr}\Big(y^E y^{E\dagger} T^{h^E} h^{E\dagger}\Big) + 540\operatorname{Tr}\Big(y^E y^{E\dagger} T^E y^{E\dagger}\Big) \\
&+ 270\operatorname{Tr}\Big(y^U y^{D\dagger} T^D y^{U\dagger}\Big) + 90\operatorname{Tr}\Big(f^\dagger T^f \tilde{\lambda}^* \tilde{\lambda}^T\Big) + 270\operatorname{Tr}\Big(g^{D\dagger} y^{DT} y^{D*} T^{g^D}\Big) \\
&+ 270\operatorname{Tr}\Big(y^{D\dagger} T^D g^{D*} g^{DT}\Big) + 90\operatorname{Tr}\Big(\tilde{\lambda}^\dagger f^T f^* T^{\tilde{\lambda}}\Big)\Big), \qquad \text{(D.52)}
\end{aligned}
$$

$$
\begin{aligned}
\beta^{(1)}_{T^{h^E}} &= 2h^E \tilde{f}^\dagger T^{\tilde{f}} + 4h^E h^{E\dagger} T^{h^E} + 2h^E \tilde{\lambda}^\dagger T^{\tilde{\lambda}} + 2y^E y^{E\dagger} T^{h^E} + T^{h^E} \tilde{f}^\dagger \tilde{f} \\
&+ 5T^{h^E} h^{E\dagger} h^E + T^{h^E} \tilde{\lambda}^\dagger \tilde{\lambda} + 4T^E y^{E\dagger} h^E - \frac{9}{5} g_1^2 T^{h^E} - \frac{7}{10} g_1'^2 T^{h^E} - 3g_2^2 T^{h^E} \\
&+ |\tilde{\sigma}|^2 T^{h^E} + 3T^{h^E} \operatorname{Tr}\Big(g^D g^{D\dagger}\Big) + T^{h^E} \operatorname{Tr}\Big(h^E h^{E\dagger}\Big) + h^E\Big[2\operatorname{Tr}\Big(h^{E\dagger} T^{h^E}\Big) \\
&+ 2\tilde{\sigma}^* T_{\tilde{\sigma}} + 6g_2^2 M_2 + 6\operatorname{Tr}\Big(g^{D\dagger} T^{g^D}\Big) + \frac{18}{5} g_1^2 M_1 + \frac{7}{5} g_1'^2 M_1'\Big], \qquad \text{(D.53)}
\end{aligned}
$$

$$
\begin{aligned}
\beta^{(2)}_{T^{h^E}} &= 2g_1'^2 h^E \tilde{f}^\dagger T^{\tilde{f}} - 2|\lambda|^2 h^E \tilde{f}^\dagger T^{\tilde{f}} - 2g_1'^2 M_1' h^E h^{E\dagger} h^E - 12g_2^2 M_2 h^E h^{E\dagger} h^E \\
&+ \frac{6}{5} g_1^2 h^E h^{E\dagger} T^{h^E} + \frac{4}{5} g_1'^2 h^E h^{E\dagger} T^{h^E} + 6g_2^2 h^E h^{E\dagger} T^{h^E} - 4|\tilde{\sigma}|^2 h^E h^{E\dagger} T^{h^E} \\
&- 2g_1'^2 M_1' h^E \tilde{\lambda}^\dagger \tilde{\lambda} + 2g_1'^2 h^E \tilde{\lambda}^\dagger T^{\tilde{\lambda}} - 4|\lambda|^2 h^E \tilde{\lambda}^\dagger T^{\tilde{\lambda}} - 2|\sigma|^2 h^E \tilde{\lambda}^\dagger T^{\tilde{\lambda}} \\
&+ \frac{12}{5} g_1^2 M_1 y^E y^{E\dagger} h^E - \frac{12}{5} g_1'^2 M_1' y^E y^{E\dagger} h^E - 12g_2^2 M_2 y^E y^{E\dagger} h^E \\
&- \frac{6}{5} g_1^2 y^E y^{E\dagger} T^{h^E} + \frac{6}{5} g_1'^2 y^E y^{E\dagger} T^{h^E} + 6g_2^2 y^E y^{E\dagger} T^{h^E} - 2|\lambda|^2 y^E y^{E\dagger} T^{h^E} \\
&+ g_1'^2 T^{h^E} \tilde{f}^\dagger \tilde{f} - |\lambda|^2 T^{h^E} \tilde{f}^\dagger \tilde{f} - \frac{6}{5} g_1^2 T^{h^E} h^{E\dagger} h^E + \frac{11}{5} g_1'^2 T^{h^E} h^{E\dagger} h^E \\
&+ 12g_2^2 T^{h^E} h^{E\dagger} h^E - 5|\tilde{\sigma}|^2 T^{h^E} h^{E\dagger} h^E + g_1'^2 T^{h^E} \tilde{\lambda}^\dagger \tilde{\lambda} - 2|\lambda|^2 T^{h^E} \tilde{\lambda}^\dagger \tilde{\lambda} \\
&- |\sigma|^2 T^{h^E} \tilde{\lambda}^\dagger \tilde{\lambda} - \frac{12}{5} g_1^2 T^E y^{E\dagger} h^E + \frac{12}{5} g_1'^2 T^E y^{E\dagger} h^E + 12g_2^2 T^E y^{E\dagger} h^E \\
&- 4|\lambda|^2 T^E y^{E\dagger} h^E - 4h^E \tilde{f}^\dagger f f^\dagger T^{\tilde{f}} - 4h^E \tilde{f}^\dagger \tilde{f} \tilde{f}^\dagger T^{\tilde{f}} - 2h^E \tilde{f}^\dagger \tilde{f} h^{E\dagger} T^{h^E}
\end{aligned}
$$

$$
\begin{aligned}
&- 4h^E \tilde{f}^\dagger T^f f^\dagger \tilde{f} - 4h^E \tilde{f}^\dagger T^{\tilde{f}} \tilde{f}^\dagger \tilde{f} - 4h^E \tilde{f}^\dagger T^{\tilde{f}} h^{E\dagger} h^E - 6h^E h^{E\dagger} h^E h^{E\dagger} T^{h^E} \\
&- 4h^E h^{E\dagger} y^E y^{E\dagger} T^{h^E} - 8h^E h^{E\dagger} T^{h^E} h^{E\dagger} h^E - 4h^E h^{E\dagger} T^E y^{E\dagger} h^E \\
&- 2h^E \tilde{\lambda}^\dagger \tilde{\lambda} h^{E\dagger} T^{h^E} - 2h^E \tilde{\lambda}^\dagger \tilde{\lambda} \tilde{\lambda}^\dagger T^{\tilde{\lambda}} - 4h^E \tilde{\lambda}^\dagger T^{\tilde{\lambda}} h^{E\dagger} h^E - 2h^E \tilde{\lambda}^\dagger T^{\tilde{\lambda}} \tilde{\lambda}^\dagger \tilde{\lambda} \\
&- 2h^E \tilde{\lambda}^\dagger f^T f^* T^{\tilde{\lambda}} - 2h^E \tilde{\lambda}^\dagger T^{fT} f^* \tilde{\lambda} - 2y^E y^{E\dagger} y^E y^{E\dagger} T^{h^E} - 4y^E y^{E\dagger} T^E y^{E\dagger} h^E \\
&- 2T^{h^E} \tilde{f}^\dagger f f^\dagger \tilde{f} - 2T^{h^E} \tilde{f}^\dagger \tilde{f} \tilde{f}^\dagger \tilde{f} - 4T^{h^E} \tilde{f}^\dagger \tilde{f} h^{E\dagger} h^E - 6T^{h^E} h^{E\dagger} h^E h^{E\dagger} h^E \\
&- 2T^{h^E} h^{E\dagger} y^E y^{E\dagger} h^E - 4T^{h^E} \tilde{\lambda}^\dagger \tilde{\lambda} h^{E\dagger} h^E - T^{h^E} \tilde{\lambda}^\dagger \tilde{\lambda} \tilde{\lambda}^\dagger \tilde{\lambda} - T^{h^E} \tilde{\lambda}^\dagger f^T f^* \tilde{\lambda} \\
&- 4T^E y^{E\dagger} y^E y^{E\dagger} h^E + \frac{189}{10} g_1^4 T^{h^E} + \frac{3}{20} g_1^2 g_1'^2 T^{h^E} + \frac{77}{10} g_1'^4 T^{h^E} + \frac{9}{5} g_1^2 g_2^2 T^{h^E} \\
&+ \frac{39}{20} g_1'^2 g_2^2 T^{h^E} + \frac{33}{2} g_2^4 T^{h^E} - 2|\tilde{\sigma}|^2 |\kappa_\phi|^2 T^{h^E} - |\tilde{\sigma}|^2 |\sigma|^2 T^{h^E} - 3|\tilde{\sigma}|^4 T^{h^E} \\
&- 4\lambda^* h^E \tilde{\lambda}^\dagger \tilde{\lambda} T_\lambda - 4\lambda^* y^E y^{E\dagger} h^E T_\lambda - 2\sigma^* h^E \tilde{\lambda}^\dagger \tilde{\lambda} T_\sigma - 6\tilde{\sigma}^* h^E h^{E\dagger} h^E T_{\tilde{\sigma}} \\
&- 2y^E y^{E\dagger} T^{h^E} \operatorname{Tr}\Big(f f^\dagger \Big) - 4T^E y^{E\dagger} h^E \operatorname{Tr}\Big(f f^\dagger \Big) - 2h^E \tilde{f}^\dagger T^{\tilde{f}} \operatorname{Tr}\Big(\tilde{f} \tilde{f}^\dagger \Big) \\
&- T^{h^E} \tilde{f}^\dagger \tilde{f} \operatorname{Tr}\Big(\tilde{f} \tilde{f}^\dagger \Big) - 12h^E h^{E\dagger} T^{h^E} \operatorname{Tr}\Big(g^D g^{D\dagger} \Big) - 15T^{h^E} h^{E\dagger} h^E \operatorname{Tr}\Big(g^D g^{D\dagger} \Big) \\
&- \frac{2}{5} g_1^2 T^{h^E} \operatorname{Tr}\Big(g^D g^{D\dagger} \Big) + \frac{9}{10} g_1'^2 T^{h^E} \operatorname{Tr}\Big(g^D g^{D\dagger} \Big) + 16 g_3^2 T^{h^E} \operatorname{Tr}\Big(g^D g^{D\dagger} \Big) \\
&- 4h^E h^{E\dagger} T^{h^E} \operatorname{Tr}\Big(h^E h^{E\dagger} \Big) - 5T^{h^E} h^{E\dagger} h^E \operatorname{Tr}\Big(h^E h^{E\dagger} \Big) + \frac{6}{5} g_1^2 T^{h^E} \operatorname{Tr}\Big(h^E h^{E\dagger} \Big) \\
&+ \frac{3}{10} g_1'^2 T^{h^E} \operatorname{Tr}\Big(h^E h^{E\dagger} \Big) - 6y^E y^{E\dagger} T^{h^E} \operatorname{Tr}\Big(y^D y^{D\dagger} \Big) - 12T^E y^{E\dagger} h^E \operatorname{Tr}\Big(y^D y^{D\dagger} \Big) \\
&- 2y^E y^{E\dagger} T^{h^E} \operatorname{Tr}\Big(y^E y^{E\dagger} \Big) - 4T^E y^{E\dagger} h^E \operatorname{Tr}\Big(y^E y^{E\dagger} \Big) - 6h^E \tilde{f}^\dagger T^{\tilde{f}} \operatorname{Tr}\Big(y^U y^{U\dagger} \Big) \\
&- 3T^{h^E} \tilde{f}^\dagger \tilde{f} \operatorname{Tr}\Big(y^U y^{U\dagger} \Big) - 6h^E \tilde{\lambda}^\dagger T^{\tilde{\lambda}} \operatorname{Tr}\Big(\kappa \kappa^\dagger \Big) - 3T^{h^E} \tilde{\lambda}^\dagger \tilde{\lambda} \operatorname{Tr}\Big(\kappa \kappa^\dagger \Big) \\
&- 4h^E \tilde{\lambda}^\dagger T^{\tilde{\lambda}} \operatorname{Tr}\Big(\tilde{\lambda} \tilde{\lambda}^\dagger \Big) - 2T^{h^E} \tilde{\lambda}^\dagger \tilde{\lambda} \operatorname{Tr}\Big(\tilde{\lambda} \tilde{\lambda}^\dagger \Big) - 4y^E y^{E\dagger} h^E \operatorname{Tr}\Big(f^\dagger T^f \Big) \\
&- 18h^E h^{E\dagger} h^E \operatorname{Tr}\Big(g^{D\dagger} T^{g^D} \Big) - 6h^E h^{E\dagger} h^E \operatorname{Tr}\Big(h^{E\dagger} T^{h^E} \Big) \\
&- 12y^E y^{E\dagger} h^E \operatorname{Tr}\Big(y^{D\dagger} T^D \Big) - 4y^E y^{E\dagger} h^E \operatorname{Tr}\Big(y^{E\dagger} T^E \Big) - 2h^E \tilde{f}^\dagger \tilde{f} \Big[3 \operatorname{Tr}\Big(y^{U\dagger} T^U \Big) \\
&+ g_1'^2 M_1' + \lambda^* T_\lambda + \operatorname{Tr}\Big(\tilde{f}^\dagger T^{\tilde{f}} \Big) \Big] - 6h^E \tilde{\lambda}^\dagger \tilde{\lambda} \operatorname{Tr}\Big(\kappa^\dagger T^\kappa \Big) - 4h^E \tilde{\lambda}^\dagger \tilde{\lambda} \operatorname{Tr}\Big(\tilde{\lambda}^\dagger T^{\tilde{\lambda}} \Big) \\
&- T^{h^E} \operatorname{Tr}\Big(\tilde{f} h^{E\dagger} h^E \tilde{f}^\dagger \Big) - 9T^{h^E} \operatorname{Tr}\Big(g^D g^{D\dagger} g^D g^{D\dagger} \Big) - 3T^{h^E} \operatorname{Tr}\Big(g^D g^{D\dagger} y^{DT} y^{D*} \Big) \\
&- 3T^{h^E} \operatorname{Tr}\Big(g^D g^{D\dagger} y^{UT} y^{U*} \Big) - 3T^{h^E} \operatorname{Tr}\Big(g^D \kappa^\dagger \kappa g^{D\dagger} \Big) - 3T^{h^E} \operatorname{Tr}\Big(h^E h^{E\dagger} h^E h^{E\dagger} \Big) \\
&- 2T^{h^E} \operatorname{Tr}\Big(h^E h^{E\dagger} y^E y^{E\dagger} \Big) - T^{h^E} \operatorname{Tr}\Big(h^E \tilde{\lambda}^\dagger \tilde{\lambda} h^{E\dagger} \Big) - \frac{1}{10} h^E \Big[756 g_1^4 M_1 \\
&+ 3g_1^2 g_1'^2 M_1 + 36 g_1^2 g_2^2 M_1 + 3g_1^2 g_1'^2 M_1' + 308 g_1'^4 M_1' + 39 g_1'^2 g_2^2 M_1' + 36 g_1^2 g_2^2 M_2
\end{aligned}
$$

$$
\begin{aligned}
&+ 39g_1'^2g_2^2M_2 + 660g_2^4M_2 + 120\tilde{\sigma}^*|\tilde{\sigma}|^2T_{\tilde{\sigma}} + 40\kappa_\phi^*\tilde{\sigma}^*\Big(\kappa_\phi T_{\tilde{\sigma}} + \tilde{\sigma}T_{\kappa_\phi}\Big)\\
&+ 20\sigma^*\tilde{\sigma}^*\Big(\sigma T_{\tilde{\sigma}} + \tilde{\sigma}T_\sigma\Big) - 8g_1^2M_1\,\mathrm{Tr}\Big(g^Dg^{D\dagger}\Big) + 18g_1'^2M_1'\,\mathrm{Tr}\Big(g^Dg^{D\dagger}\Big)\\
&+ 320g_3^2M_3\,\mathrm{Tr}\Big(g^Dg^{D\dagger}\Big) + 24g_1^2M_1\,\mathrm{Tr}\Big(h^Eh^{E\dagger}\Big) + 6g_1'^2M_1'\,\mathrm{Tr}\Big(h^Eh^{E\dagger}\Big)\\
&+ 8g_1^2\,\mathrm{Tr}\Big(g^{D\dagger}T^{g^D}\Big) - 18g_1'^2\,\mathrm{Tr}\Big(g^{D\dagger}T^{g^D}\Big) - 320g_3^2\,\mathrm{Tr}\Big(g^{D\dagger}T^{g^D}\Big)\\
&- 24g_1^2\,\mathrm{Tr}\Big(h^{E\dagger}T^{h^E}\Big) - 6g_1'^2\,\mathrm{Tr}\Big(h^{E\dagger}T^{h^E}\Big) + 20\,\mathrm{Tr}\Big(\tilde{f}h^{E\dagger}T^{h^E}\tilde{f}^\dagger\Big)\\
&+ 360\,\mathrm{Tr}\Big(g^Dg^{D\dagger}T^{g^D}g^{D\dagger}\Big) + 60\,\mathrm{Tr}\Big(g^D\kappa^\dagger T^\kappa g^{D\dagger}\Big) + 20\,\mathrm{Tr}\Big(h^E\tilde{f}^\dagger T^{\tilde{f}}h^{E\dagger}\Big)\\
&+ 120\,\mathrm{Tr}\Big(h^Eh^{E\dagger}T^{h^E}h^{E\dagger}\Big) + 40\,\mathrm{Tr}\Big(h^Eh^{E\dagger}T^Ey^{E\dagger}\Big) + 20\,\mathrm{Tr}\Big(h^E\tilde{\lambda}^\dagger T^{\tilde{\lambda}}h^{E\dagger}\Big)\\
&+ 40\,\mathrm{Tr}\Big(y^Ey^{E\dagger}T^{h^E}h^{E\dagger}\Big) + 60\,\mathrm{Tr}\Big(\kappa g^{D\dagger}T^{g^D}\kappa^\dagger\Big) + 20\,\mathrm{Tr}\Big(\tilde{\lambda}h^{E\dagger}T^{h^E}\tilde{\lambda}^\dagger\Big)\\
&+ 60\,\mathrm{Tr}\Big(g^{D\dagger}y^{DT}y^{D*}T^{g^D}\Big) + 60\,\mathrm{Tr}\Big(g^{D\dagger}y^{UT}y^{U*}T^{g^D}\Big)\\
&+ 60\,\mathrm{Tr}\Big(y^{D\dagger}T^Dg^{D*}g^{DT}\Big) + 60\,\mathrm{Tr}\Big(y^{U\dagger}T^Ug^{D*}g^{DT}\Big)\Big], \qquad \text{(D.54)}
\end{aligned}
$$

$$
\begin{aligned}
\beta_{T^E}^{(1)} = {}& 2h^Eh^{E\dagger}T^E + 4y^Ey^{E\dagger}T^E + 4T^{h^E}h^{E\dagger}y^E + 5T^Ey^{E\dagger}y^E - \frac{9}{5}g_1^2T^E\\
&- \frac{7}{10}g_1'^2T^E - 3g_2^2T^E + |\lambda|^2T^E + T^E\,\mathrm{Tr}\Big(ff^\dagger\Big) + 3T^E\,\mathrm{Tr}\Big(y^Dy^{D\dagger}\Big)\\
&+ T^E\,\mathrm{Tr}\Big(y^Ey^{E\dagger}\Big) + y^E\Big[2\lambda^*T_\lambda + 2\,\mathrm{Tr}\Big(f^\dagger T^f\Big) + 2\,\mathrm{Tr}\Big(y^{E\dagger}T^E\Big) + 6g_2^2M_2\\
&+ 6\,\mathrm{Tr}\Big(y^{D\dagger}T^D\Big) + \frac{18}{5}g_1^2M_1 + \frac{7}{5}g_1'^2M_1'\Big], \qquad \text{(D.55)}
\end{aligned}
$$

$$
\begin{aligned}
\beta_{T^E}^{(2)} = {}& -\frac{6}{5}g_1^2h^Eh^{E\dagger}T^E + \frac{6}{5}g_1'^2h^Eh^{E\dagger}T^E + 6g_2^2h^Eh^{E\dagger}T^E - 2|\tilde{\sigma}|^2h^Eh^{E\dagger}T^E\\
&- 3g_1'^2M_1'y^Ey^{E\dagger}y^E - 12g_2^2M_2y^Ey^{E\dagger}y^E + \frac{6}{5}g_1^2y^Ey^{E\dagger}T^E + \frac{9}{5}g_1'^2y^Ey^{E\dagger}T^E\\
&+ 6g_2^2y^Ey^{E\dagger}T^E - 4|\lambda|^2y^Ey^{E\dagger}T^E - \frac{12}{5}g_1^2T^{h^E}h^{E\dagger}y^E + \frac{12}{5}g_1'^2T^{h^E}h^{E\dagger}y^E\\
&+ 12g_2^2T^{h^E}h^{E\dagger}y^E - 4|\tilde{\sigma}|^2T^{h^E}h^{E\dagger}y^E - \frac{6}{5}g_1^2T^Ey^{E\dagger}y^E + \frac{27}{10}g_1'^2T^Ey^{E\dagger}y^E\\
&+ 12g_2^2T^Ey^{E\dagger}y^E - 5|\lambda|^2T^Ey^{E\dagger}y^E - 2h^E\tilde{f}^\dagger\tilde{f}h^{E\dagger}T^E - 4h^E\tilde{f}^\dagger T^{\tilde{f}}h^{E\dagger}y^E\\
&- 2h^Eh^{E\dagger}h^Eh^{E\dagger}T^E - 4h^Eh^{E\dagger}T^{h^E}h^{E\dagger}y^E - 2h^E\tilde{\lambda}^\dagger\tilde{\lambda}h^{E\dagger}T^E\\
&- 4h^E\tilde{\lambda}^\dagger T^{\tilde{\lambda}}h^{E\dagger}y^E - 4y^Ey^{E\dagger}h^Eh^{E\dagger}T^E - 6y^Ey^{E\dagger}y^Ey^{E\dagger}T^E\\
&- 4y^Ey^{E\dagger}T^{h^E}h^{E\dagger}y^E - 8y^Ey^{E\dagger}T^Ey^{E\dagger}y^E - 4T^{h^E}\tilde{f}^\dagger\tilde{f}h^{E\dagger}y^E\\
&- 4T^{h^E}h^{E\dagger}h^Eh^{E\dagger}y^E - 4T^{h^E}\tilde{\lambda}^\dagger\tilde{\lambda}h^{E\dagger}y^E - 2T^Ey^{E\dagger}h^Eh^{E\dagger}y^E\\
&- 6T^Ey^{E\dagger}y^Ey^{E\dagger}y^E + \frac{189}{10}g_1^4T^E + \frac{3}{20}g_1^2g_1'^2T^E + \frac{77}{10}g_1'^4T^E + \frac{9}{5}g_1^2g_2^2T^E
\end{aligned}
$$

$$
\begin{aligned}
&+\frac{39}{20}g_1'^2g_2^2T^E+\frac{33}{2}g_2^4T^E+g_1'^2|\lambda|^2T^E-3|\lambda|^4T^E-|\sigma|^2|\lambda|^2T^E\\
&-6\lambda^*y^Ey^{E\dagger}y^ET_\lambda-4y^Ey^{E\dagger}T^E\,\mathrm{Tr}\Big(ff^\dagger\Big)-5T^Ey^{E\dagger}y^E\,\mathrm{Tr}\Big(ff^\dagger\Big)\\
&+g_1'^2T^E\,\mathrm{Tr}\Big(ff^\dagger\Big)-|\lambda|^2T^E\,\mathrm{Tr}\Big(\tilde f\tilde f^\dagger\Big)-6h^Eh^{E\dagger}T^E\,\mathrm{Tr}\Big(g^Dg^{D\dagger}\Big)\\
&-12T^{h^E}h^{E\dagger}y^E\,\mathrm{Tr}\Big(g^Dg^{D\dagger}\Big)-2h^Eh^{E\dagger}T^E\,\mathrm{Tr}\Big(h^Eh^{E\dagger}\Big)\\
&-4T^{h^E}h^{E\dagger}y^E\,\mathrm{Tr}\Big(h^Eh^{E\dagger}\Big)-12y^Ey^{E\dagger}T^E\,\mathrm{Tr}\Big(y^Dy^{D\dagger}\Big)\\
&-15T^Ey^{E\dagger}y^E\,\mathrm{Tr}\Big(y^Dy^{D\dagger}\Big)-\frac{2}{5}g_1^2T^E\,\mathrm{Tr}\Big(y^Dy^{D\dagger}\Big)-\frac{3}{5}g_1'^2T^E\,\mathrm{Tr}\Big(y^Dy^{D\dagger}\Big)\\
&+16g_3^2T^E\,\mathrm{Tr}\Big(y^Dy^{D\dagger}\Big)-4y^Ey^{E\dagger}T^E\,\mathrm{Tr}\Big(y^Ey^{E\dagger}\Big)-5T^Ey^{E\dagger}y^E\,\mathrm{Tr}\Big(y^Ey^{E\dagger}\Big)\\
&+\frac{6}{5}g_1^2T^E\,\mathrm{Tr}\Big(y^Ey^{E\dagger}\Big)-\frac{1}{5}g_1'^2T^E\,\mathrm{Tr}\Big(y^Ey^{E\dagger}\Big)-3|\lambda|^2T^E\,\mathrm{Tr}\Big(y^Uy^{U\dagger}\Big)\\
&-3|\lambda|^2T^E\,\mathrm{Tr}\Big(\kappa\kappa^\dagger\Big)-2|\lambda|^2T^E\,\mathrm{Tr}\Big(\tilde\lambda\tilde\lambda^\dagger\Big)-6y^Ey^{E\dagger}y^E\,\mathrm{Tr}\Big(f^\dagger T^f\Big)\\
&+\frac{4}{5}h^Eh^{E\dagger}y^E\Big[-15g_2^2M_2-15\,\mathrm{Tr}\Big(g^{D\dagger}T^{g^D}\Big)+3g_1^2M_1-3g_1'^2M_1'\\
&-5\,\mathrm{Tr}\Big(h^{E\dagger}T^{h^E}\Big)-5\tilde\sigma^*T_{\tilde\sigma}\Big]-18y^Ey^{E\dagger}y^E\,\mathrm{Tr}\Big(y^{D\dagger}T^D\Big)\\
&-6y^Ey^{E\dagger}y^E\,\mathrm{Tr}\Big(y^{E\dagger}T^E\Big)-3T^E\,\mathrm{Tr}\Big(ff^\dagger ff^\dagger\Big)-2T^E\,\mathrm{Tr}\Big(ff^\dagger\tilde f\tilde f^\dagger\Big)\\
&-3T^E\,\mathrm{Tr}\Big(g^Dg^{D\dagger}y^{DT}y^{D*}\Big)-2T^E\,\mathrm{Tr}\Big(h^Eh^{E\dagger}y^Ey^{E\dagger}\Big)\\
&-9T^E\,\mathrm{Tr}\Big(y^Dy^{D\dagger}y^Dy^{D\dagger}\Big)-3T^E\,\mathrm{Tr}\Big(y^Dy^{U\dagger}y^Uy^{D\dagger}\Big)\\
&-3T^E\,\mathrm{Tr}\Big(y^Ey^{E\dagger}y^Ey^{E\dagger}\Big)-T^E\,\mathrm{Tr}\Big(\tilde\lambda\tilde\lambda^\dagger f^Tf^*\Big)-\frac{1}{10}y^E\Big(756g_1^4M_1\\
&+3g_1^2g_1'^2M_1+36g_1^2g_2^2M_1+3g_1^2g_1'^2M_1'+308g_1'^4M_1'+39g_1'^2g_2^2M_1'\\
&+36g_1^2g_2^2M_2+39g_1'^2g_2^2M_2+660g_2^4M_2+120\lambda^*|\lambda|^2T_\lambda+20g_1'^2M_1'\,\mathrm{Tr}\Big(ff^\dagger\Big)\\
&-8g_1^2M_1\,\mathrm{Tr}\Big(y^Dy^{D\dagger}\Big)-12g_1'^2M_1'\,\mathrm{Tr}\Big(y^Dy^{D\dagger}\Big)+320g_3^2M_3\,\mathrm{Tr}\Big(y^Dy^{D\dagger}\Big)\\
&+24g_1^2M_1\,\mathrm{Tr}\Big(y^Ey^{E\dagger}\Big)-4g_1'^2M_1'\,\mathrm{Tr}\Big(y^Ey^{E\dagger}\Big)-20g_1'^2\,\mathrm{Tr}\Big(f^\dagger T^f\Big)\\
&+8g_1^2\,\mathrm{Tr}\Big(y^{D\dagger}T^D\Big)+12g_1'^2\,\mathrm{Tr}\Big(y^{D\dagger}T^D\Big)-320g_3^2\,\mathrm{Tr}\Big(y^{D\dagger}T^D\Big)\\
&-24g_1^2\,\mathrm{Tr}\Big(y^{E\dagger}T^E\Big)+4g_1'^2\,\mathrm{Tr}\Big(y^{E\dagger}T^E\Big)+20\lambda^*\Big\{T_\lambda\Big[2\,\mathrm{Tr}\Big(\tilde\lambda\tilde\lambda^\dagger\Big)\\
&+3\,\mathrm{Tr}\Big(\kappa\kappa^\dagger\Big)+3\,\mathrm{Tr}\Big(y^Uy^{U\dagger}\Big)-g_1'^2+|\sigma|^2+\mathrm{Tr}\Big(\tilde f\tilde f^\dagger\Big)\Big]+\lambda\Big[2\,\mathrm{Tr}\Big(\tilde\lambda^\dagger T^{\tilde\lambda}\Big)\\
&+3\,\mathrm{Tr}\Big(\kappa^\dagger T^\kappa\Big)+3\,\mathrm{Tr}\Big(y^{U\dagger}T^U\Big)+g_1'^2M_1'+\sigma^*T_\sigma+\mathrm{Tr}\Big(\tilde f^\dagger T^{\tilde f}\Big)\Big]\Big\}
\end{aligned}
$$

$$
\begin{aligned}
&+ 120\,\mathrm{Tr}\Big(ff^\dagger T^f f^\dagger\Big) + 40\,\mathrm{Tr}\Big(ff^\dagger T^{\tilde{f}}\tilde{f}^\dagger\Big) + 40\,\mathrm{Tr}\Big(\tilde{f}\tilde{f}^\dagger T^f f^\dagger\Big)\\
&+ 40\,\mathrm{Tr}\Big(h^E h^{E\dagger} T^E y^{E\dagger}\Big) + 360\,\mathrm{Tr}\Big(y^D y^{D\dagger} T^D y^{D\dagger}\Big) + 60\,\mathrm{Tr}\Big(y^D y^{U\dagger} T^U y^{D\dagger}\Big)\\
&+ 40\,\mathrm{Tr}\Big(y^E y^{E\dagger} T^{h^E} h^{E\dagger}\Big) + 120\,\mathrm{Tr}\Big(y^E y^{E\dagger} T^E y^{E\dagger}\Big) + 60\,\mathrm{Tr}\Big(y^U y^{D\dagger} T^D y^{U\dagger}\Big)\\
&+ 20\,\mathrm{Tr}\Big(f^\dagger T^f \tilde{\lambda}^* \tilde{\lambda}^T\Big) + 60\,\mathrm{Tr}\Big(g^{D\dagger} y^{DT} y^{D*} T^{g^D}\Big) + 60\,\mathrm{Tr}\Big(y^{D\dagger} T^D g^{D*} g^{DT}\Big)\\
&+ 20\,\mathrm{Tr}\Big(\tilde{\lambda}^\dagger f^T f^* T^{\tilde{\lambda}}\Big)\Big), \qquad \text{(D.56)}
\end{aligned}
$$

$$
\begin{aligned}
\beta^{(1)}_{T_{\tilde{\sigma}}} =\ & \frac{6}{5}g_1^2 M_1 \tilde{\sigma} + \frac{4}{5}g_1'^2 M_1' \tilde{\sigma} + 6g_2^2 M_2 \tilde{\sigma} - \frac{3}{5}g_1^2 T_{\tilde{\sigma}} - \frac{2}{5}g_1'^2 T_{\tilde{\sigma}} - 3g_2^2 T_{\tilde{\sigma}} + 12|\tilde{\sigma}|^2 T_{\tilde{\sigma}}\\
&+ 2\kappa_\phi^*\Big(2\tilde{\sigma}T_{\kappa_\phi} + \kappa_\phi T_{\tilde{\sigma}}\Big) + \sigma^*\Big(2\tilde{\sigma}T_\sigma + \sigma T_{\tilde{\sigma}}\Big) + 3T_{\tilde{\sigma}}\,\mathrm{Tr}\Big(g^D g^{D\dagger}\Big)\\
&+ T_{\tilde{\sigma}}\,\mathrm{Tr}\Big(h^E h^{E\dagger}\Big) + 6\tilde{\sigma}\,\mathrm{Tr}\Big(g^{D\dagger} T^{g^D}\Big) + 2\tilde{\sigma}\,\mathrm{Tr}\Big(h^{E\dagger} T^{h^E}\Big), \qquad \text{(D.57)}
\end{aligned}
$$

$$
\begin{aligned}
\beta^{(2)}_{T_{\tilde{\sigma}}} =\ & -\frac{594}{25}g_1^4 M_1 \tilde{\sigma} - \frac{36}{25}g_1^2 g_1'^2 M_1 \tilde{\sigma} - \frac{18}{5}g_1^2 g_2^2 M_1 \tilde{\sigma} - \frac{36}{25}g_1^2 g_1'^2 M_1' \tilde{\sigma} - \frac{434}{25}g_1'^4 M_1' \tilde{\sigma}\\
&- \frac{12}{5}g_1'^2 g_2^2 M_1' \tilde{\sigma} - \frac{18}{5}g_1^2 g_2^2 M_2 \tilde{\sigma} - \frac{12}{5}g_1'^2 g_2^2 M_2 \tilde{\sigma} - 66 g_2^4 M_2 \tilde{\sigma} - 32\kappa_\phi^* \tilde{\sigma} |\kappa_\phi|^2 T_{\kappa_\phi}\\
&+ \frac{297}{50}g_1^4 T_{\tilde{\sigma}} + \frac{18}{25}g_1^2 g_1'^2 T_{\tilde{\sigma}} + \frac{217}{50}g_1'^4 T_{\tilde{\sigma}} + \frac{9}{5}g_1^2 g_2^2 T_{\tilde{\sigma}} + \frac{6}{5}g_1'^2 g_2^2 T_{\tilde{\sigma}} + \frac{33}{2}g_2^4 T_{\tilde{\sigma}}\\
&- 8|\kappa_\phi|^4 T_{\tilde{\sigma}} - 50|\tilde{\sigma}|^4 T_{\tilde{\sigma}} - 2\sigma^*|\sigma|^2\Big(4\tilde{\sigma}T_\sigma + \sigma T_{\tilde{\sigma}}\Big) + \frac{4}{5}g_1^2 M_1 \tilde{\sigma}\,\mathrm{Tr}\Big(g^D g^{D\dagger}\Big)\\
&- \frac{9}{5}g_1'^2 M_1' \tilde{\sigma}\,\mathrm{Tr}\Big(g^D g^{D\dagger}\Big) - 32 g_3^2 M_3 \tilde{\sigma}\,\mathrm{Tr}\Big(g^D g^{D\dagger}\Big) - \frac{2}{5}g_1^2 T_{\tilde{\sigma}}\,\mathrm{Tr}\Big(g^D g^{D\dagger}\Big)\\
&+ \frac{9}{10}g_1'^2 T_{\tilde{\sigma}}\,\mathrm{Tr}\Big(g^D g^{D\dagger}\Big) + 16 g_3^2 T_{\tilde{\sigma}}\,\mathrm{Tr}\Big(g^D g^{D\dagger}\Big) - \frac{12}{5}g_1^2 M_1 \tilde{\sigma}\,\mathrm{Tr}\Big(h^E h^{E\dagger}\Big)\\
&- \frac{3}{5}g_1'^2 M_1' \tilde{\sigma}\,\mathrm{Tr}\Big(h^E h^{E\dagger}\Big) + \frac{6}{5}g_1^2 T_{\tilde{\sigma}}\,\mathrm{Tr}\Big(h^E h^{E\dagger}\Big) + \frac{3}{10}g_1'^2 T_{\tilde{\sigma}}\,\mathrm{Tr}\Big(h^E h^{E\dagger}\Big)\\
&- \frac{4}{5}g_1^2 \tilde{\sigma}\,\mathrm{Tr}\Big(g^{D\dagger} T^{g^D}\Big) + \frac{9}{5}g_1'^2 \tilde{\sigma}\,\mathrm{Tr}\Big(g^{D\dagger} T^{g^D}\Big) + 32 g_3^2 \tilde{\sigma}\,\mathrm{Tr}\Big(g^{D\dagger} T^{g^D}\Big)\\
&+ \frac{12}{5}g_1^2 \tilde{\sigma}\,\mathrm{Tr}\Big(h^{E\dagger} T^{h^E}\Big) + \frac{3}{5}g_1'^2 \tilde{\sigma}\,\mathrm{Tr}\Big(h^{E\dagger} T^{h^E}\Big) - \frac{1}{5}|\tilde{\sigma}|^2\Big\{60\kappa_\phi^*\Big(2\tilde{\sigma}T_{\kappa_\phi}\\
&+ 3\kappa_\phi T_{\tilde{\sigma}}\Big) - 3T_{\tilde{\sigma}}\Big[-15\,\mathrm{Tr}\Big(h^E h^{E\dagger}\Big) + 30 g_2^2 - 45\,\mathrm{Tr}\Big(g^D g^{D\dagger}\Big) + 4g_1'^2 + 6g_1^2\Big]\\
&+ 2\tilde{\sigma}\Big[15\,\mathrm{Tr}\Big(h^{E\dagger} T^{h^E}\Big) + 30 g_2^2 M_2 + 45\,\mathrm{Tr}\Big(g^{D\dagger} T^{g^D}\Big) + 4g_1'^2 M_1' + 6g_1^2 M_1\Big]\Big\}\\
&- \frac{1}{2}\sigma^*\Big[10 g_1'^2 M_1' \sigma\tilde{\sigma} - 10 g_1'^2 \tilde{\sigma} T_\sigma + 8\tilde{\sigma}|\tilde{\sigma}|^2 T_\sigma - 5 g_1'^2 \sigma T_{\tilde{\sigma}} + 12\sigma|\tilde{\sigma}|^2 T_{\tilde{\sigma}}\\
&+ 8\kappa_\phi^*\Big(2\kappa_\phi \tilde{\sigma} T_\sigma + 2\sigma\tilde{\sigma}T_{\kappa_\phi} + \kappa_\phi \sigma T_{\tilde{\sigma}}\Big) + 4\lambda^*\Big(2\lambda\tilde{\sigma}T_\sigma + 2\sigma\tilde{\sigma}T_\lambda + \lambda\sigma T_{\tilde{\sigma}}\Big)\\
&+ 12\tilde{\sigma}T_\sigma\,\mathrm{Tr}\Big(\kappa\kappa^\dagger\Big) + 6\sigma T_{\tilde{\sigma}}\,\mathrm{Tr}\Big(\kappa\kappa^\dagger\Big) + 8\tilde{\sigma}T_\sigma\,\mathrm{Tr}\Big(\tilde{\lambda}\tilde{\lambda}^\dagger\Big) + 4\sigma T_{\tilde{\sigma}}\,\mathrm{Tr}\Big(\tilde{\lambda}\tilde{\lambda}^\dagger\Big)
\end{aligned}
$$

$$
\begin{aligned}
&+ 12\sigma\tilde{\sigma}\,\mathrm{Tr}\Big(\kappa^\dagger T^\kappa\Big) + 8\sigma\tilde{\sigma}\,\mathrm{Tr}\Big(\tilde{\lambda}^\dagger T^{\tilde{\lambda}}\Big)\Big] - T_{\tilde{\sigma}}\,\mathrm{Tr}\Big(\tilde{f}h^{E\dagger}h^E\tilde{f}^\dagger\Big)\\
&- 2\tilde{\sigma}\,\mathrm{Tr}\Big(\tilde{f}h^{E\dagger}T^{h^E}\tilde{f}^\dagger\Big) - 9T_{\tilde{\sigma}}\,\mathrm{Tr}\Big(g^D g^{D\dagger}g^D g^{D\dagger}\Big) - 36\tilde{\sigma}\,\mathrm{Tr}\Big(g^D g^{D\dagger}T^{g^D}g^{D\dagger}\Big)\\
&- 3T_{\tilde{\sigma}}\,\mathrm{Tr}\Big(g^D g^{D\dagger}y^{DT}y^{D*}\Big) - 3T_{\tilde{\sigma}}\,\mathrm{Tr}\Big(g^D g^{D\dagger}y^{UT}y^{U*}\Big) - 3T_{\tilde{\sigma}}\,\mathrm{Tr}\Big(g^D\kappa^\dagger\kappa g^{D\dagger}\Big)\\
&- 6\tilde{\sigma}\,\mathrm{Tr}\Big(g^D\kappa^\dagger T^\kappa g^{D\dagger}\Big) - 2\tilde{\sigma}\,\mathrm{Tr}\Big(h^E\tilde{f}^\dagger T^{\tilde{f}}h^{E\dagger}\Big) - 3T_{\tilde{\sigma}}\,\mathrm{Tr}\Big(h^E h^{E\dagger}h^E h^{E\dagger}\Big)\\
&- 2T_{\tilde{\sigma}}\,\mathrm{Tr}\Big(h^E h^{E\dagger}y^E y^{E\dagger}\Big) - 12\tilde{\sigma}\,\mathrm{Tr}\Big(h^E h^{E\dagger}T^{h^E}h^{E\dagger}\Big) - 4\tilde{\sigma}\,\mathrm{Tr}\Big(h^E h^{E\dagger}T^E y^{E\dagger}\Big)\\
&- T_{\tilde{\sigma}}\,\mathrm{Tr}\Big(h^E\tilde{\lambda}^\dagger\tilde{\lambda}h^{E\dagger}\Big) - 2\tilde{\sigma}\,\mathrm{Tr}\Big(h^E\tilde{\lambda}^\dagger T^{\tilde{\lambda}}h^{E\dagger}\Big) - 4\tilde{\sigma}\,\mathrm{Tr}\Big(y^E y^{E\dagger}T^{h^E}h^{E\dagger}\Big)\\
&- 6\tilde{\sigma}\,\mathrm{Tr}\Big(\kappa g^{D\dagger}T^{g^D}\kappa^\dagger\Big) - 2\tilde{\sigma}\,\mathrm{Tr}\Big(\tilde{\lambda}h^{E\dagger}T^{h^E}\tilde{\lambda}^\dagger\Big) - 6\tilde{\sigma}\,\mathrm{Tr}\Big(g^{D\dagger}y^{DT}y^{D*}T^{g^D}\Big)\\
&- 6\tilde{\sigma}\,\mathrm{Tr}\Big(g^{D\dagger}y^{UT}y^{U*}T^{g^D}\Big) - 6\tilde{\sigma}\,\mathrm{Tr}\Big(y^{D\dagger}T^D g^{D*}g^{DT}\Big)\\
&- 6\tilde{\sigma}\,\mathrm{Tr}\Big(y^{U\dagger}T^U g^{D*}g^{DT}\Big),
\end{aligned}
\tag{D.58}
$$

$$
\beta^{(1)}_{T_{\kappa_\phi}} = 3\Big[2\tilde{\sigma}^*\Big(2\kappa_\phi T_{\tilde{\sigma}} + \tilde{\sigma}T_{\kappa_\phi}\Big) + 6|\kappa_\phi|^2 T_{\kappa_\phi} + \sigma^*\Big(2\kappa_\phi T_\sigma + \sigma T_{\kappa_\phi}\Big)\Big], \tag{D.59}
$$

$$
\begin{aligned}
\beta^{(2)}_{T_{\kappa_\phi}} = &-\frac{3}{10}\Big\{20\sigma^*|\sigma|^2\Big(4\kappa_\phi T_\sigma + \sigma T_{\kappa_\phi}\Big) + 4\Big[100|\kappa_\phi|^4 T_{\kappa_\phi} + 10\tilde{\sigma}^*|\tilde{\sigma}|^2\Big(4\kappa_\phi T_{\tilde{\sigma}}\\
&+ \tilde{\sigma}T_{\kappa_\phi}\Big) + \tilde{\sigma}^*\Big(\tilde{\sigma}T_{\kappa_\phi}\Big[-15g_2^2 + 15\,\mathrm{Tr}\Big(g^D g^{D\dagger}\Big) - 2g_1'^2 - 3g_1^2\\
&+ 5\,\mathrm{Tr}\Big(h^E h^{E\dagger}\Big) + 60|\kappa_\phi|^2\Big] + 2\kappa_\phi\Big\{T_{\tilde{\sigma}}\Big[-15g_2^2 + 15\,\mathrm{Tr}\Big(g^D g^{D\dagger}\Big) + 20|\kappa_\phi|^2\\
&- 2g_1'^2 - 3g_1^2 + 5\,\mathrm{Tr}\Big(h^E h^{E\dagger}\Big)\Big] + \tilde{\sigma}\Big[15g_2^2 M_2 + 15\,\mathrm{Tr}\Big(g^{D\dagger}T^{g^D}\Big) + 2g_1'^2 M_1'\\
&+ 3g_1^2 M_1 + 5\,\mathrm{Tr}\Big(h^{E\dagger}T^{h^E}\Big)\Big]\Big\}\Big)\Big] + 5\sigma^*\Big(\sigma T_{\kappa_\phi}\Big[24|\kappa_\phi|^2 + 4|\lambda|^2 + 4\,\mathrm{Tr}\Big(\tilde{\lambda}\tilde{\lambda}^\dagger\Big)\\
&- 5g_1'^2 + 6\,\mathrm{Tr}\Big(\kappa\kappa^\dagger\Big)\Big] + 2\kappa_\phi\Big\{4\lambda^*\Big(\lambda T_\sigma + \sigma T_\lambda\Big) + T_\sigma\Big[4\,\mathrm{Tr}\Big(\tilde{\lambda}\tilde{\lambda}^\dagger\Big) - 5g_1'^2\\
&+ 6\,\mathrm{Tr}\Big(\kappa\kappa^\dagger\Big) + 8|\kappa_\phi|^2\Big] + \sigma\Big[4\,\mathrm{Tr}\Big(\tilde{\lambda}^\dagger T^{\tilde{\lambda}}\Big) + 5g_1'^2 M_1' + 6\,\mathrm{Tr}\Big(\kappa^\dagger T^\kappa\Big)\Big]\Big\}\Big)\Big\},
\end{aligned}
\tag{D.60}
$$

$$
\begin{aligned}
\beta^{(1)}_{T_\sigma} = &\,5g_1'^2 M_1'\sigma - \frac{5}{2}g_1'^2 T_\sigma + 9|\sigma|^2 T_\sigma + 2|\tilde{\sigma}|^2 T_\sigma + 2\kappa_\phi^*\Big(2\sigma T_{\kappa_\phi} + \kappa_\phi T_\sigma\Big)\\
&+ 2\lambda^*\Big(2\sigma T_\lambda + \lambda T_\sigma\Big) + 4\sigma\tilde{\sigma}^* T_{\tilde{\sigma}} + 3T_\sigma\,\mathrm{Tr}\Big(\kappa\kappa^\dagger\Big) + 2T_\sigma\,\mathrm{Tr}\Big(\tilde{\lambda}\tilde{\lambda}^\dagger\Big)\\
&+ 6\sigma\,\mathrm{Tr}\Big(\kappa^\dagger T^\kappa\Big) + 4\sigma\,\mathrm{Tr}\Big(\tilde{\lambda}^\dagger T^{\tilde{\lambda}}\Big),
\end{aligned}
\tag{D.61}
$$

$$
\begin{aligned}
\beta^{(2)}_{T_\sigma} = &-119g_1'^4 M_1'\sigma - \frac{12}{5}g_1^2 M_1\sigma|\tilde{\sigma}|^2 - \frac{8}{5}g_1'^2 M_1'\sigma|\tilde{\sigma}|^2 - 12g_2^2 M_2\sigma|\tilde{\sigma}|^2\\
&- 16\sigma|\tilde{\sigma}|^2\kappa_\phi^* T_{\kappa_\phi} - 32\kappa_\phi^*\sigma|\kappa_\phi|^2 T_{\kappa_\phi} + \frac{119}{4}g_1'^4 T_\sigma + \frac{6}{5}g_1^2|\tilde{\sigma}|^2 T_\sigma + \frac{4}{5}g_1'^2|\tilde{\sigma}|^2 T_\sigma
\end{aligned}
$$

$$
\begin{aligned}
&+ 6g_2^2|\tilde{\sigma}|^2T_\sigma - 8|\kappa_\phi|^4T_\sigma - 30|\sigma|^4T_\sigma - 8|\tilde{\sigma}|^2|\kappa_\phi|^2T_\sigma - 4|\tilde{\sigma}|^4T_\sigma \\
&- 4\lambda^*|\lambda|^2\Big(4\sigma T_\lambda + \lambda T_\sigma\Big) + \frac{12}{5}g_1^2\sigma\tilde{\sigma}^*T_{\tilde{\sigma}} + \frac{8}{5}g_1'^2\sigma\tilde{\sigma}^*T_{\tilde{\sigma}} + 12g_2^2\sigma\tilde{\sigma}^*T_{\tilde{\sigma}} \\
&- 16\sigma|\kappa_\phi|^2\tilde{\sigma}^*T_{\tilde{\sigma}} - 16\sigma\tilde{\sigma}^*|\tilde{\sigma}|^2T_{\tilde{\sigma}} - 6|\tilde{\sigma}|^2T_\sigma \operatorname{Tr}\Big(g^Dg^{D\dagger}\Big) \\
&- 12\sigma\tilde{\sigma}^*T_{\tilde{\sigma}} \operatorname{Tr}\Big(g^Dg^{D\dagger}\Big) - 2|\tilde{\sigma}|^2T_\sigma \operatorname{Tr}\Big(h^Eh^{E\dagger}\Big) - 4\sigma\tilde{\sigma}^*T_{\tilde{\sigma}} \operatorname{Tr}\Big(h^Eh^{E\dagger}\Big) \\
&- \frac{8}{5}g_1^2M_1\sigma \operatorname{Tr}\Big(\kappa\kappa^\dagger\Big) + \frac{18}{5}g_1'^2M_1'\sigma \operatorname{Tr}\Big(\kappa\kappa^\dagger\Big) - 32g_3^2M_3\sigma \operatorname{Tr}\Big(\kappa\kappa^\dagger\Big) \\
&+ \frac{4}{5}g_1^2T_\sigma \operatorname{Tr}\Big(\kappa\kappa^\dagger\Big) - \frac{9}{5}g_1'^2T_\sigma \operatorname{Tr}\Big(\kappa\kappa^\dagger\Big) + 16g_3^2T_\sigma \operatorname{Tr}\Big(\kappa\kappa^\dagger\Big) \\
&- \frac{12}{5}g_1^2M_1\sigma \operatorname{Tr}\Big(\tilde{\lambda}\tilde{\lambda}^\dagger\Big) + \frac{12}{5}g_1'^2M_1'\sigma \operatorname{Tr}\Big(\tilde{\lambda}\tilde{\lambda}^\dagger\Big) - 12g_2^2M_2\sigma \operatorname{Tr}\Big(\tilde{\lambda}\tilde{\lambda}^\dagger\Big) \\
&+ \frac{6}{5}g_1^2T_\sigma \operatorname{Tr}\Big(\tilde{\lambda}\tilde{\lambda}^\dagger\Big) - \frac{6}{5}g_1'^2T_\sigma \operatorname{Tr}\Big(\tilde{\lambda}\tilde{\lambda}^\dagger\Big) + 6g_2^2T_\sigma \operatorname{Tr}\Big(\tilde{\lambda}\tilde{\lambda}^\dagger\Big) \\
&- 12\sigma|\tilde{\sigma}|^2 \operatorname{Tr}\Big(g^{D\dagger}T^{g^D}\Big) - 4\sigma|\tilde{\sigma}|^2 \operatorname{Tr}\Big(h^{E\dagger}T^{h^E}\Big) - \frac{2}{5}\lambda^*\Big(2\sigma T_\lambda\Big[-3g_1^2 \\
&+ 3g_1'^2 - 15g_2^2 + 10|\sigma|^2 + 5\operatorname{Tr}\Big(ff^\dagger\Big) + 5\operatorname{Tr}\Big(\tilde{f}\tilde{f}^\dagger\Big) + 15\operatorname{Tr}\Big(y^Dy^{D\dagger}\Big) \\
&+ 5\operatorname{Tr}\Big(y^Ey^{E\dagger}\Big) + 15\operatorname{Tr}\Big(y^Uy^{U\dagger}\Big)\Big] + \lambda\Big\{T_\sigma\Big[-3g_1^2 + 3g_1'^2 - 15g_2^2 + 30|\sigma|^2 \\
&+ 5\operatorname{Tr}\Big(ff^\dagger\Big) + 5\operatorname{Tr}\Big(\tilde{f}\tilde{f}^\dagger\Big) + 15\operatorname{Tr}\Big(y^Dy^{D\dagger}\Big) + 5\operatorname{Tr}\Big(y^Ey^{E\dagger}\Big) + 15\operatorname{Tr}\Big(y^Uy^{U\dagger}\Big)\Big] \\
&+ 2\sigma\Big[3g_1^2M_1 - 3g_1'^2M_1' + 15g_2^2M_2 + 5\operatorname{Tr}\Big(f^\dagger T^f\Big) + 5\operatorname{Tr}\Big(\tilde{f}^\dagger T^{\tilde{f}}\Big) \\
&+ 15\operatorname{Tr}\Big(y^{D\dagger}T^D\Big) + 5\operatorname{Tr}\Big(y^{E\dagger}T^E\Big) + 15\operatorname{Tr}\Big(y^{U\dagger}T^U\Big)\Big]\Big\}\Big) + \frac{8}{5}g_1^2\sigma \operatorname{Tr}\Big(\kappa^\dagger T^\kappa\Big) \\
&- \frac{18}{5}g_1'^2\sigma \operatorname{Tr}\Big(\kappa^\dagger T^\kappa\Big) + 32g_3^2\sigma \operatorname{Tr}\Big(\kappa^\dagger T^\kappa\Big) + \frac{12}{5}g_1^2\sigma \operatorname{Tr}\Big(\tilde{\lambda}^\dagger T^{\tilde{\lambda}}\Big) \\
&- \frac{12}{5}g_1'^2\sigma \operatorname{Tr}\Big(\tilde{\lambda}^\dagger T^{\tilde{\lambda}}\Big) + 12g_2^2\sigma \operatorname{Tr}\Big(\tilde{\lambda}^\dagger T^{\tilde{\lambda}}\Big) - \frac{1}{2}|\sigma|^2\Big\{16\kappa_\phi^*\Big(2\sigma T_{\kappa_\phi} + 3\kappa_\phi T_\sigma\Big) \\
&+ 3T_\sigma\Big[12\operatorname{Tr}\Big(\kappa\kappa^\dagger\Big) - 5g_1'^2 + 8\operatorname{Tr}\Big(\tilde{\lambda}\tilde{\lambda}^\dagger\Big) + 8|\tilde{\sigma}|^2\Big] + 2\sigma\Big[12\operatorname{Tr}\Big(\kappa^\dagger T^\kappa\Big) \\
&+ 5g_1'^2M_1' + 8\operatorname{Tr}\Big(\tilde{\lambda}^\dagger T^{\tilde{\lambda}}\Big) + 8\tilde{\sigma}^*T_{\tilde{\sigma}}\Big]\Big\} - 2T_\sigma \operatorname{Tr}\Big(\tilde{f}\tilde{\lambda}^\dagger\tilde{\lambda}\tilde{f}^\dagger\Big) - 4\sigma \operatorname{Tr}\Big(\tilde{f}\tilde{\lambda}^\dagger T^{\tilde{\lambda}}\tilde{f}^\dagger\Big) \\
&- 6T_\sigma \operatorname{Tr}\Big(g^D\kappa^\dagger\kappa g^{D\dagger}\Big) - 12\sigma \operatorname{Tr}\Big(g^D\kappa^\dagger T^\kappa g^{D\dagger}\Big) - 2T_\sigma \operatorname{Tr}\Big(h^E\tilde{\lambda}^\dagger\tilde{\lambda}h^{E\dagger}\Big) \\
&- 4\sigma \operatorname{Tr}\Big(h^E\tilde{\lambda}^\dagger T^{\tilde{\lambda}}h^{E\dagger}\Big) - 12\sigma \operatorname{Tr}\Big(\kappa g^{D\dagger}T^{g^D}\kappa^\dagger\Big) - 6T_\sigma \operatorname{Tr}\Big(\kappa\kappa^\dagger\kappa\kappa^\dagger\Big) \\
&- 24\sigma \operatorname{Tr}\Big(\kappa\kappa^\dagger T^\kappa\kappa^\dagger\Big) - 4\sigma \operatorname{Tr}\Big(\tilde{\lambda}\tilde{f}^\dagger T^{\tilde{f}}\tilde{\lambda}^\dagger\Big) - 4\sigma \operatorname{Tr}\Big(\tilde{\lambda}h^{E\dagger}T^{h^E}\tilde{\lambda}^\dagger\Big) \\
&- 4T_\sigma \operatorname{Tr}\Big(\tilde{\lambda}\tilde{\lambda}^\dagger\tilde{\lambda}\tilde{\lambda}^\dagger\Big) - 16\sigma \operatorname{Tr}\Big(\tilde{\lambda}\tilde{\lambda}^\dagger T^{\tilde{\lambda}}\tilde{\lambda}^\dagger\Big) - 2T_\sigma \operatorname{Tr}\Big(\tilde{\lambda}\tilde{\lambda}^\dagger f^Tf^*\Big) \\
&- 4\sigma \operatorname{Tr}\Big(f^\dagger T^f\tilde{\lambda}^*\tilde{\lambda}^T\Big) - 4\sigma \operatorname{Tr}\Big(\tilde{\lambda}^\dagger f^Tf^*T^{\tilde{\lambda}}\Big),
\end{aligned}
\tag{D.62}
$$

$$
\begin{aligned}
\beta^{(1)}_{T^{g^D}} &= 5g^D g^{D\dagger} T^{g^D} + 2g^D \kappa^\dagger T^\kappa + 4T^{g^D} g^{D\dagger} g^D + T^{g^D} \kappa^\dagger \kappa + y^{DT} y^{D*} T^{g^D} \\
&+ y^{UT} y^{U*} T^{g^D} + 2T^{DT} y^{D*} g^D + 2T^{UT} y^{U*} g^D - \frac{7}{15} g_1^2 T^{g^D} - \frac{7}{10} g_1'^2 T^{g^D} \\
&- 3g_2^2 T^{g^D} - \frac{16}{3} g_3^2 T^{g^D} + |\tilde{\sigma}|^2 T^{g^D} + 3T^{g^D} \operatorname{Tr}\Big(g^D g^{D\dagger}\Big) + T^{g^D} \operatorname{Tr}\Big(h^E h^{E\dagger}\Big) \\
&+ g^D \Big[2 \operatorname{Tr}\Big(h^{E\dagger} T^{h^E}\Big) + 2\tilde{\sigma}^* T_{\tilde{\sigma}} + 6g_2^2 M_2 + 6 \operatorname{Tr}\Big(g^{D\dagger} T^{g^D}\Big) + \frac{14}{15} g_1^2 M_1 \\
&+ \frac{32}{3} g_3^2 M_3 + \frac{7}{5} g_1'^2 M_1'\Big], \qquad \text{(D.63)} \\
\beta^{(2)}_{T^{g^D}} &= \frac{6}{5} g_1^2 g^D g^{D\dagger} T^{g^D} - \frac{1}{5} g_1'^2 g^D g^{D\dagger} T^{g^D} + 12 g_2^2 g^D g^{D\dagger} T^{g^D} - 5|\tilde{\sigma}|^2 g^D g^{D\dagger} T^{g^D} \\
&- 2g_1'^2 M_1' g^D \kappa^\dagger \kappa + 2g_1'^2 g^D \kappa^\dagger T^\kappa - 4|\lambda|^2 g^D \kappa^\dagger T^\kappa - 2|\sigma|^2 g^D \kappa^\dagger T^\kappa \\
&+ \frac{6}{5} g_1^2 T^{g^D} g^{D\dagger} g^D + \frac{4}{5} g_1'^2 T^{g^D} g^{D\dagger} g^D + 6g_2^2 T^{g^D} g^{D\dagger} g^D - 4|\tilde{\sigma}|^2 T^{g^D} g^{D\dagger} g^D \\
&+ g_1'^2 T^{g^D} \kappa^\dagger \kappa - 2|\lambda|^2 T^{g^D} \kappa^\dagger \kappa - |\sigma|^2 T^{g^D} \kappa^\dagger \kappa - \frac{4}{5} g_1^2 M_1 y^{DT} y^{D*} g^D \\
&- \frac{6}{5} g_1'^2 M_1' y^{DT} y^{D*} g^D + \frac{2}{5} g_1^2 y^{DT} y^{D*} T^{g^D} + \frac{3}{5} g_1'^2 y^{DT} y^{D*} T^{g^D} \\
&- |\lambda|^2 y^{DT} y^{D*} T^{g^D} - \frac{8}{5} g_1^2 M_1 y^{UT} y^{U*} g^D - \frac{2}{5} g_1'^2 M_1' y^{UT} y^{U*} g^D \\
&+ \frac{4}{5} g_1^2 y^{UT} y^{U*} T^{g^D} + \frac{1}{5} g_1'^2 y^{UT} y^{U*} T^{g^D} - |\lambda|^2 y^{UT} y^{U*} T^{g^D} + \frac{4}{5} g_1^2 T^{DT} y^{D*} g^D \\
&+ \frac{6}{5} g_1'^2 T^{DT} y^{D*} g^D - 2|\lambda|^2 T^{DT} y^{D*} g^D + \frac{8}{5} g_1^2 T^{UT} y^{U*} g^D + \frac{2}{5} g_1'^2 T^{UT} y^{U*} g^D \\
&- 2|\lambda|^2 T^{UT} y^{U*} g^D - 6g^D g^{D\dagger} g^D g^{D\dagger} T^{g^D} - 8g^D g^{D\dagger} T^{g^D} g^{D\dagger} g^D \\
&- 4g^D g^{D\dagger} y^{DT} y^{D*} T^{g^D} - 4g^D g^{D\dagger} y^{UT} y^{U*} T^{g^D} - 4g^D g^{D\dagger} T^{DT} y^{D*} g^D \\
&- 4g^D g^{D\dagger} T^{UT} y^{U*} g^D - g^D \kappa^\dagger \kappa g^{D\dagger} T^{g^D} - 2g^D \kappa^\dagger \kappa \kappa^\dagger T^\kappa - 2g^D \kappa^\dagger T^\kappa g^{D\dagger} g^D \\
&- 2g^D \kappa^\dagger T^\kappa \kappa^\dagger \kappa - 6T^{g^D} g^{D\dagger} g^D g^{D\dagger} g^D - 2T^{g^D} g^{D\dagger} y^{DT} y^{D*} g^D \\
&- 2T^{g^D} g^{D\dagger} y^{UT} y^{U*} g^D - 2T^{g^D} \kappa^\dagger \kappa g^{D\dagger} g^D - T^{g^D} \kappa^\dagger \kappa \kappa^\dagger \kappa \\
&- 2y^{DT} y^{D*} y^{DT} y^{D*} T^{g^D} - 4y^{DT} y^{D*} T^{DT} y^{D*} g^D - 2y^{UT} y^{U*} y^{UT} y^{U*} T^{g^D} \\
&- 4y^{UT} y^{U*} T^{UT} y^{U*} g^D - 4T^{DT} y^{D*} y^{DT} y^{D*} g^D - 4T^{UT} y^{U*} y^{UT} y^{U*} g^D \\
&+ \frac{413}{90} g_1^4 T^{g^D} + \frac{41}{60} g_1^2 g_1'^2 T^{g^D} + \frac{77}{10} g_1'^4 T^{g^D} + g_1^2 g_2^2 T^{g^D} + \frac{3}{4} g_1'^2 g_2^2 T^{g^D} \\
&+ \frac{33}{2} g_2^4 T^{g^D} + \frac{8}{9} g_1^2 g_3^2 T^{g^D} + \frac{8}{3} g_1'^2 g_3^2 T^{g^D} + 8g_2^2 g_3^2 T^{g^D} + \frac{128}{9} g_3^4 T^{g^D} \\
&- 2|\tilde{\sigma}|^2 |\kappa_\phi|^2 T^{g^D} - |\tilde{\sigma}|^2 |\sigma|^2 T^{g^D} - 3|\tilde{\sigma}|^4 T^{g^D} - 4\lambda^* g^D \kappa^\dagger \kappa T_\lambda \\
&- 2\lambda^* y^{DT} y^{D*} g^D T_\lambda - 2\lambda^* y^{UT} y^{U*} g^D T_\lambda - 2\sigma^* g^D \kappa^\dagger \kappa T_\sigma \\
&- y^{DT} y^{D*} T^{g^D} \operatorname{Tr}\Big(f f^\dagger\Big) - 2T^{DT} y^{D*} g^D \operatorname{Tr}\Big(f f^\dagger\Big) - y^{UT} y^{U*} T^{g^D} \operatorname{Tr}\Big(\tilde{f} \tilde{f}^\dagger\Big)
\end{aligned}
$$

$$
\begin{aligned}
&- 2T^{UT} y^{U*} g^D \operatorname{Tr}\Big(\tilde{f}\tilde{f}^\dagger\Big) - 15 g^D g^{D\dagger} T^{g^D} \operatorname{Tr}\Big(g^D g^{D\dagger}\Big) \\
&- 12 T^{g^D} g^{D\dagger} g^D \operatorname{Tr}\Big(g^D g^{D\dagger}\Big) - \frac{2}{5} g_1^2 T^{g^D} \operatorname{Tr}\Big(g^D g^{D\dagger}\Big) + \frac{9}{10} g_1'^2 T^{g^D} \operatorname{Tr}\Big(g^D g^{D\dagger}\Big) \\
&+ 16 g_3^2 T^{g^D} \operatorname{Tr}\Big(g^D g^{D\dagger}\Big) - 5 g^D g^{D\dagger} T^{g^D} \operatorname{Tr}\Big(h^E h^{E\dagger}\Big) - 4 T^{g^D} g^{D\dagger} g^D \operatorname{Tr}\Big(h^E h^{E\dagger}\Big) \\
&+ \frac{6}{5} g_1^2 T^{g^D} \operatorname{Tr}\Big(h^E h^{E\dagger}\Big) + \frac{3}{10} g_1'^2 T^{g^D} \operatorname{Tr}\Big(h^E h^{E\dagger}\Big) - 3 y^{DT} y^{D*} T^{g^D} \operatorname{Tr}\Big(y^D y^{D\dagger}\Big) \\
&- 6 T^{DT} y^{D*} g^D \operatorname{Tr}\Big(y^D y^{D\dagger}\Big) - y^{DT} y^{D*} T^{g^D} \operatorname{Tr}\Big(y^E y^{E\dagger}\Big) \\
&- 2 T^{DT} y^{D*} g^D \operatorname{Tr}\Big(y^E y^{E\dagger}\Big) - 3 y^{UT} y^{U*} T^{g^D} \operatorname{Tr}\Big(y^U y^{U\dagger}\Big) \\
&- 6 T^{UT} y^{U*} g^D \operatorname{Tr}\Big(y^U y^{U\dagger}\Big) - 6 g^D \kappa^\dagger T^\kappa \operatorname{Tr}\Big(\kappa\kappa^\dagger\Big) - 3 T^{g^D} \kappa^\dagger \kappa \operatorname{Tr}\Big(\kappa\kappa^\dagger\Big) \\
&- 4 g^D \kappa^\dagger T^\kappa \operatorname{Tr}\Big(\tilde{\lambda}\tilde{\lambda}^\dagger\Big) - 2 T^{g^D} \kappa^\dagger \kappa \operatorname{Tr}\Big(\tilde{\lambda}\tilde{\lambda}^\dagger\Big) - 2 y^{DT} y^{D*} g^D \operatorname{Tr}\Big(f^\dagger T^f\Big) \\
&- 2 y^{UT} y^{U*} g^D \operatorname{Tr}\Big(\tilde{f}^\dagger T^{\tilde{f}}\Big) - \frac{2}{5} g^D g^{D\dagger} g^D \Big[15 \operatorname{Tr}\Big(h^{E\dagger} T^{h^E}\Big) + 15 \tilde{\sigma}^* T_{\tilde{\sigma}} \\
&+ 30 g_2^2 M_2 + 45 \operatorname{Tr}\Big(g^{D\dagger} T^{g^D}\Big) + 4 g_1^2 M_1 + g_1'^2 M_1'\Big] - 6 y^{DT} y^{D*} g^D \operatorname{Tr}\Big(y^{D\dagger} T^D\Big) \\
&- 2 y^{DT} y^{D*} g^D \operatorname{Tr}\Big(y^{E\dagger} T^E\Big) - 6 y^{UT} y^{U*} g^D \operatorname{Tr}\Big(y^{U\dagger} T^U\Big) - 6 g^D \kappa^\dagger \kappa \operatorname{Tr}\Big(\kappa^\dagger T^\kappa\Big) \\
&- 4 g^D \kappa^\dagger \kappa \operatorname{Tr}\Big(\tilde{\lambda}^\dagger T^{\tilde{\lambda}}\Big) - T^{g^D} \operatorname{Tr}\Big(\tilde{f} h^{E\dagger} h^E \tilde{f}^\dagger\Big) - 9 T^{g^D} \operatorname{Tr}\Big(g^D g^{D\dagger} g^D g^{D\dagger}\Big) \\
&- 3 T^{g^D} \operatorname{Tr}\Big(g^D g^{D\dagger} y^{DT} y^{D*}\Big) - 3 T^{g^D} \operatorname{Tr}\Big(g^D g^{D\dagger} y^{UT} y^{U*}\Big) \\
&- 3 T^{g^D} \operatorname{Tr}\Big(g^D \kappa^\dagger \kappa g^{D\dagger}\Big) - 3 T^{g^D} \operatorname{Tr}\Big(h^E h^{E\dagger} h^E h^{E\dagger}\Big) - 2 T^{g^D} \operatorname{Tr}\Big(h^E h^{E\dagger} y^E y^{E\dagger}\Big) \\
&- T^{g^D} \operatorname{Tr}\Big(h^E \tilde{\lambda}^\dagger \tilde{\lambda} h^{E\dagger}\Big) - \frac{1}{90} g^D \Big[1652 g_1^4 M_1 + 123 g_1^2 g_1'^2 M_1 + 180 g_1^2 g_2^2 M_1 \\
&+ 160 g_1^2 g_3^2 M_1 + 123 g_1^2 g_1'^2 M_1' + 2772 g_1'^4 M_1' + 135 g_1'^2 g_2^2 M_1' + 480 g_1'^2 g_3^2 M_1' \\
&+ 160 g_1^2 g_3^2 M_3 + 480 g_1'^2 g_3^2 M_3 + 1440 g_2^2 g_3^2 M_3 + 5120 g_3^4 M_3 + 180 g_1^2 g_2^2 M_2 \\
&+ 135 g_1'^2 g_2^2 M_2 + 5940 g_2^4 M_2 + 1440 g_2^2 g_3^2 M_2 + 1080 \tilde{\sigma}^* |\tilde{\sigma}|^2 T_{\tilde{\sigma}} \\
&+ 360 \kappa_\phi^* \tilde{\sigma}^* \Big(\kappa_\phi T_{\tilde{\sigma}} + \tilde{\sigma} T_{\kappa_\phi}\Big) + 180 \sigma^* \tilde{\sigma}^* \Big(\sigma T_{\tilde{\sigma}} + \tilde{\sigma} T_\sigma\Big) - 72 g_1^2 M_1 \operatorname{Tr}\Big(g^D g^{D\dagger}\Big) \\
&+ 162 g_1'^2 M_1' \operatorname{Tr}\Big(g^D g^{D\dagger}\Big) + 2880 g_3^2 M_3 \operatorname{Tr}\Big(g^D g^{D\dagger}\Big) + 216 g_1^2 M_1 \operatorname{Tr}\Big(h^E h^{E\dagger}\Big) \\
&+ 54 g_1'^2 M_1' \operatorname{Tr}\Big(h^E h^{E\dagger}\Big) + 72 g_1^2 \operatorname{Tr}\Big(g^{D\dagger} T^{g^D}\Big) - 162 g_1'^2 \operatorname{Tr}\Big(g^{D\dagger} T^{g^D}\Big) \\
&- 2880 g_3^2 \operatorname{Tr}\Big(g^{D\dagger} T^{g^D}\Big) - 216 g_1^2 \operatorname{Tr}\Big(h^{E\dagger} T^{h^E}\Big) - 54 g_1'^2 \operatorname{Tr}\Big(h^{E\dagger} T^{h^E}\Big) \\
&+ 180 \operatorname{Tr}\Big(\tilde{f} h^{E\dagger} T^{h^E} \tilde{f}^\dagger\Big) + 3240 \operatorname{Tr}\Big(g^D g^{D\dagger} T^{g^D} g^{D\dagger}\Big) + 540 \operatorname{Tr}\Big(g^D \kappa^\dagger T^\kappa g^{D\dagger}\Big)
\end{aligned}
$$

$$
\begin{aligned}
&+ 180\,\mathrm{Tr}\Big(h^E \tilde{f}^\dagger T^{\tilde{f}} h^{E\dagger}\Big) + 1080\,\mathrm{Tr}\Big(h^E h^{E\dagger} T^{h^E} h^{E\dagger}\Big) + 360\,\mathrm{Tr}\Big(h^E h^{E\dagger} T^E y^{E\dagger}\Big) \\
&+ 180\,\mathrm{Tr}\Big(h^E \tilde{\lambda}^\dagger T^{\tilde{\lambda}} h^{E\dagger}\Big) + 360\,\mathrm{Tr}\Big(y^E y^{E\dagger} T^{h^E} h^{E\dagger}\Big) + 540\,\mathrm{Tr}\Big(\kappa g^{D\dagger} T^{g^D} \kappa^\dagger\Big) \\
&+ 180\,\mathrm{Tr}\Big(\tilde{\lambda} h^{E\dagger} T^{h^E} \tilde{\lambda}^\dagger\Big) + 540\,\mathrm{Tr}\Big(g^{D\dagger} y^{DT} y^{D*} T^{g^D}\Big) \\
&+ 540\,\mathrm{Tr}\Big(g^{D\dagger} y^{UT} y^{U*} T^{g^D}\Big) + 540\,\mathrm{Tr}\Big(y^{D\dagger} T^D g^{D*} g^{DT}\Big) \\
&+ 540\,\mathrm{Tr}\Big(y^{U\dagger} T^U g^{D*} g^{DT}\Big)\Big], \qquad \text{(D.64)}
\end{aligned}
$$

$$
\begin{aligned}
\beta^{(1)}_{T^\kappa} = {}& 4\kappa g^{D\dagger} T^{g^D} + 3\kappa\kappa^\dagger T^\kappa + 2T^\kappa g^{D\dagger} g^D + 3T^\kappa \kappa^\dagger \kappa - \frac{4}{15} g_1^2 T^\kappa - \frac{19}{10} g_1'^2 T^\kappa \\
&- \frac{16}{3} g_3^2 T^\kappa + 2|\lambda|^2 T^\kappa + |\sigma|^2 T^\kappa + 3T^\kappa\,\mathrm{Tr}\Big(\kappa\kappa^\dagger\Big) + 2T^\kappa\,\mathrm{Tr}\Big(\tilde{\lambda}\tilde{\lambda}^\dagger\Big) \\
&+ \kappa\Big[2\sigma^* T_\sigma + 4\lambda^* T_\lambda + 4\,\mathrm{Tr}\Big(\tilde{\lambda}^\dagger T^{\tilde{\lambda}}\Big) + 6\,\mathrm{Tr}\Big(\kappa^\dagger T^\kappa\Big) + \frac{19}{5} g_1'^2 M_1' \\
&+ \frac{32}{3} g_3^2 M_3 + \frac{8}{15} g_1^2 M_1\Big], \qquad \text{(D.65)}
\end{aligned}
$$

$$
\begin{aligned}
\beta^{(2)}_{T^\kappa} = {}& \frac{4}{5} g_1^2 \kappa g^{D\dagger} T^{g^D} - \frac{4}{5} g_1'^2 \kappa g^{D\dagger} T^{g^D} + 12 g_2^2 \kappa g^{D\dagger} T^{g^D} - 4|\tilde{\sigma}|^2 \kappa g^{D\dagger} T^{g^D} \\
&- 5 g_1'^2 M_1' \kappa\kappa^\dagger \kappa + \frac{7}{2} g_1'^2 \kappa\kappa^\dagger T^\kappa - 6|\lambda|^2 \kappa\kappa^\dagger T^\kappa - 3|\sigma|^2 \kappa\kappa^\dagger T^\kappa + \frac{2}{5} g_1^2 T^\kappa g^{D\dagger} g^D \\
&- \frac{2}{5} g_1'^2 T^\kappa g^{D\dagger} g^D + 6 g_2^2 T^\kappa g^{D\dagger} g^D - 2|\tilde{\sigma}|^2 T^\kappa g^{D\dagger} g^D + 4 g_1'^2 T^\kappa \kappa^\dagger \kappa \\
&- 6|\lambda|^2 T^\kappa \kappa^\dagger \kappa - 3|\sigma|^2 T^\kappa \kappa^\dagger \kappa - 4\kappa g^{D\dagger} g^D g^{D\dagger} T^{g^D} - 2\kappa g^{D\dagger} g^D \kappa^\dagger T^\kappa \\
&- 4\kappa g^{D\dagger} T^{g^D} g^{D\dagger} g^D - 4\kappa g^{D\dagger} T^{g^D} \kappa^\dagger \kappa - 4\kappa g^{D\dagger} y^{DT} y^{D*} T^{g^D} \\
&- 4\kappa g^{D\dagger} y^{UT} y^{U*} T^{g^D} - 4\kappa g^{D\dagger} T^{DT} y^{D*} g^D - 4\kappa g^{D\dagger} T^{UT} y^{U*} g^D - 3\kappa\kappa^\dagger \kappa\kappa^\dagger T^\kappa \\
&- 4\kappa\kappa^\dagger T^\kappa \kappa^\dagger \kappa - 2T^\kappa g^{D\dagger} g^D g^{D\dagger} g^D - 4T^\kappa g^{D\dagger} g^D \kappa^\dagger \kappa - 2T^\kappa g^{D\dagger} y^{DT} y^{D*} g^D \\
&- 2T^\kappa g^{D\dagger} y^{UT} y^{U*} g^D - 3T^\kappa \kappa^\dagger \kappa\kappa^\dagger \kappa + \frac{584}{225} g_1^4 T^\kappa + \frac{19}{75} g_1^2 g_1'^2 T^\kappa + \frac{551}{25} g_1'^4 T^\kappa \\
&+ \frac{64}{45} g_1^2 g_3^2 T^\kappa + \frac{52}{15} g_1'^2 g_3^2 T^\kappa + \frac{128}{9} g_3^4 T^\kappa + \frac{6}{5} g_1^2 |\lambda|^2 T^\kappa - \frac{6}{5} g_1'^2 |\lambda|^2 T^\kappa \\
&+ 6 g_2^2 |\lambda|^2 T^\kappa - 4|\lambda|^4 T^\kappa - 2|\sigma|^2 |\kappa_\phi|^2 T^\kappa - 2|\sigma|^4 T^\kappa - 2|\tilde{\sigma}|^2 |\sigma|^2 T^\kappa \\
&- 8\lambda^* \kappa\kappa^\dagger \kappa T_\lambda - 4\sigma^* \kappa\kappa^\dagger \kappa T_\sigma - 2|\lambda|^2 T^\kappa\,\mathrm{Tr}\Big(f f^\dagger\Big) - 2|\lambda|^2 T^\kappa\,\mathrm{Tr}\Big(\tilde{f}\tilde{f}^\dagger\Big) \\
&- 12\kappa g^{D\dagger} T^{g^D}\,\mathrm{Tr}\Big(g^D g^{D\dagger}\Big) - 6T^\kappa g^{D\dagger} g^D\,\mathrm{Tr}\Big(g^D g^{D\dagger}\Big) \\
&- 4\kappa g^{D\dagger} T^{g^D}\,\mathrm{Tr}\Big(h^E h^{E\dagger}\Big) - 2T^\kappa g^{D\dagger} g^D\,\mathrm{Tr}\Big(h^E h^{E\dagger}\Big) - 6|\lambda|^2 T^\kappa\,\mathrm{Tr}\Big(y^D y^{D\dagger}\Big) \\
&- 2|\lambda|^2 T^\kappa\,\mathrm{Tr}\Big(y^E y^{E\dagger}\Big) - 6|\lambda|^2 T^\kappa\,\mathrm{Tr}\Big(y^U y^{U\dagger}\Big) - 9\kappa\kappa^\dagger T^\kappa\,\mathrm{Tr}\Big(\kappa\kappa^\dagger\Big) \\
&- 9T^\kappa \kappa^\dagger \kappa\,\mathrm{Tr}\Big(\kappa\kappa^\dagger\Big) + \frac{4}{5} g_1^2 T^\kappa\,\mathrm{Tr}\Big(\kappa\kappa^\dagger\Big) - \frac{9}{5} g_1'^2 T^\kappa\,\mathrm{Tr}\Big(\kappa\kappa^\dagger\Big) + 16 g_3^2 T^\kappa\,\mathrm{Tr}\Big(\kappa\kappa^\dagger\Big)
\end{aligned}
$$

$$
\begin{aligned}
&- 6\kappa\kappa^\dagger T^\kappa \operatorname{Tr}\Big(\tilde{\lambda}\tilde{\lambda}^\dagger\Big) - 6T^\kappa\kappa^\dagger\kappa \operatorname{Tr}\Big(\tilde{\lambda}\tilde{\lambda}^\dagger\Big) + \frac{6}{5}g_1^2T^\kappa \operatorname{Tr}\Big(\tilde{\lambda}\tilde{\lambda}^\dagger\Big) - \frac{6}{5}g_1'^2T^\kappa \operatorname{Tr}\Big(\tilde{\lambda}\tilde{\lambda}^\dagger\Big)\\
&+ 6g_2^2T^\kappa \operatorname{Tr}\Big(\tilde{\lambda}\tilde{\lambda}^\dagger\Big) - \frac{4}{5}\kappa g^{D\dagger}g^D\Big[15g_2^2M_2 + 15\operatorname{Tr}\Big(g^{D\dagger}T^{g^D}\Big) + 5\operatorname{Tr}\Big(h^{E\dagger}T^{h^E}\Big)\\
&+ 5\tilde{\sigma}^*T_{\tilde{\sigma}} + g_1^2M_1 - g_1'^2M_1'\Big] - 12\kappa\kappa^\dagger\kappa \operatorname{Tr}\Big(\kappa^\dagger T^\kappa\Big) - 8\kappa\kappa^\dagger\kappa \operatorname{Tr}\Big(\tilde{\lambda}^\dagger T^{\tilde{\lambda}}\Big)\\
&- 2T^\kappa \operatorname{Tr}\Big(\tilde{f}\tilde{\lambda}^\dagger\tilde{\lambda}\tilde{f}^\dagger\Big) - 6T^\kappa \operatorname{Tr}\Big(g^D\kappa^\dagger\kappa g^{D\dagger}\Big) - 2T^\kappa \operatorname{Tr}\Big(h^E\tilde{\lambda}^\dagger\tilde{\lambda}h^{E\dagger}\Big)\\
&- 6T^\kappa \operatorname{Tr}\Big(\kappa\kappa^\dagger\kappa\kappa^\dagger\Big) - 4T^\kappa \operatorname{Tr}\Big(\tilde{\lambda}\tilde{\lambda}^\dagger\tilde{\lambda}\tilde{\lambda}^\dagger\Big) - 2T^\kappa \operatorname{Tr}\Big(\tilde{\lambda}\tilde{\lambda}^\dagger f^Tf^*\Big)\\
&- \frac{2}{225}\kappa\Big(1168g_1^4M_1 + 57g_1^2g_1'^2M_1 + 320g_1^2g_3^2M_1 + 57g_1^2g_1'^2M_1' + 9918g_1'^4M_1'\\
&+ 780g_1'^2g_3^2M_1' + 320g_1^2g_3^2M_3 + 780g_1'^2g_3^2M_3 + 6400g_3^4M_3 + 1800\lambda^*|\lambda|^2T_\lambda\\
&+ 450|\tilde{\sigma}|^2\sigma^*T_\sigma + 900\sigma^*|\sigma|^2T_\sigma + 450\kappa_\phi^*\sigma^*\Big(\kappa_\phi T_\sigma + \sigma T_{\kappa_\phi}\Big) + 450|\sigma|^2\tilde{\sigma}^*T_{\tilde{\sigma}}\\
&+ 180g_1^2M_1 \operatorname{Tr}\Big(\kappa\kappa^\dagger\Big) - 405g_1'^2M_1' \operatorname{Tr}\Big(\kappa\kappa^\dagger\Big) + 3600g_3^2M_3 \operatorname{Tr}\Big(\kappa\kappa^\dagger\Big)\\
&+ 270g_1^2M_1 \operatorname{Tr}\Big(\tilde{\lambda}\tilde{\lambda}^\dagger\Big) - 270g_1'^2M_1' \operatorname{Tr}\Big(\tilde{\lambda}\tilde{\lambda}^\dagger\Big) + 1350g_2^2M_2 \operatorname{Tr}\Big(\tilde{\lambda}\tilde{\lambda}^\dagger\Big)\\
&+ 90\lambda^*\Big\{T_\lambda\Big[-15g_2^2 + 15\operatorname{Tr}\Big(y^Dy^{D\dagger}\Big) + 15\operatorname{Tr}\Big(y^Uy^{U\dagger}\Big) - 3g_1^2 + 3g_1'^2\\
&+ 5\operatorname{Tr}\Big(ff^\dagger\Big) + 5\operatorname{Tr}\Big(\tilde{f}\tilde{f}^\dagger\Big) + 5\operatorname{Tr}\Big(y^Ey^{E\dagger}\Big)\Big] + \lambda\Big[3g_1^2M_1 - 3g_1'^2M_1'\\
&+ 15g_2^2M_2 + 5\operatorname{Tr}\Big(f^\dagger T^f\Big) + 5\operatorname{Tr}\Big(\tilde{f}^\dagger T^{\tilde{f}}\Big) + 15\operatorname{Tr}\Big(y^{D\dagger}T^D\Big) + 5\operatorname{Tr}\Big(y^{E\dagger}T^E\Big)\\
&+ 15\operatorname{Tr}\Big(y^{U\dagger}T^U\Big)\Big]\Big\} - 180g_1^2 \operatorname{Tr}\Big(\kappa^\dagger T^\kappa\Big) + 405g_1'^2 \operatorname{Tr}\Big(\kappa^\dagger T^\kappa\Big)\\
&- 3600g_3^2 \operatorname{Tr}\Big(\kappa^\dagger T^\kappa\Big) - 270g_1^2 \operatorname{Tr}\Big(\tilde{\lambda}^\dagger T^{\tilde{\lambda}}\Big) + 270g_1'^2 \operatorname{Tr}\Big(\tilde{\lambda}^\dagger T^{\tilde{\lambda}}\Big)\\
&- 1350g_2^2 \operatorname{Tr}\Big(\tilde{\lambda}^\dagger T^{\tilde{\lambda}}\Big) + 450\operatorname{Tr}\Big(\tilde{f}\tilde{\lambda}^\dagger T^{\tilde{\lambda}}\tilde{f}^\dagger\Big) + 1350\operatorname{Tr}\Big(g^D\kappa^\dagger T^\kappa g^{D\dagger}\Big)\\
&+ 450\operatorname{Tr}\Big(h^E\tilde{\lambda}^\dagger T^{\tilde{\lambda}}h^{E\dagger}\Big) + 1350\operatorname{Tr}\Big(\kappa g^{D\dagger}T^{g^D}\kappa^\dagger\Big) + 2700\operatorname{Tr}\Big(\kappa\kappa^\dagger T^\kappa\kappa^\dagger\Big)\\
&+ 450\operatorname{Tr}\Big(\tilde{\lambda}\tilde{f}^\dagger T^{\tilde{f}}\tilde{\lambda}^\dagger\Big) + 450\operatorname{Tr}\Big(\tilde{\lambda}h^{E\dagger}T^{h^E}\tilde{\lambda}^\dagger\Big) + 1800\operatorname{Tr}\Big(\tilde{\lambda}\tilde{\lambda}^\dagger T^{\tilde{\lambda}}\tilde{\lambda}^\dagger\Big)\\
&+ 450\operatorname{Tr}\Big(f^\dagger T^f\tilde{\lambda}^*\tilde{\lambda}^T\Big) + 450\operatorname{Tr}\Big(\tilde{\lambda}^\dagger f^Tf^*T^{\tilde{\lambda}}\Big)\Big), \qquad \text{(D.66)}
\end{aligned}
$$

$$
\begin{aligned}
\beta_{T^{\tilde{\lambda}}}^{(1)} &= 2\tilde{\lambda}\tilde{f}^\dagger T^{\tilde{f}} + 2\tilde{\lambda}h^{E\dagger}T^{h^E} + 3\tilde{\lambda}\tilde{\lambda}^\dagger T^{\tilde{\lambda}} + T^{\tilde{\lambda}}\tilde{f}^\dagger\tilde{f} + T^{\tilde{\lambda}}h^{E\dagger}h^E + 3T^{\tilde{\lambda}}\tilde{\lambda}^\dagger\tilde{\lambda}\\
&+ f^Tf^*T^{\tilde{\lambda}} + 2T^{fT}f^*\tilde{\lambda} - \frac{3}{5}g_1^2T^{\tilde{\lambda}} - \frac{19}{10}g_1'^2T^{\tilde{\lambda}} - 3g_2^2T^{\tilde{\lambda}} + 2|\lambda|^2T^{\tilde{\lambda}} + |\sigma|^2T^{\tilde{\lambda}}\\
&+ 3T^{\tilde{\lambda}} \operatorname{Tr}\Big(\kappa\kappa^\dagger\Big) + 2T^{\tilde{\lambda}} \operatorname{Tr}\Big(\tilde{\lambda}\tilde{\lambda}^\dagger\Big) + \tilde{\lambda}\Big[2\sigma^*T_\sigma + 4\lambda^*T_\lambda + 4\operatorname{Tr}\Big(\tilde{\lambda}^\dagger T^{\tilde{\lambda}}\Big)\\
&+ 6g_2^2M_2 + 6\operatorname{Tr}\Big(\kappa^\dagger T^\kappa\Big) + \frac{19}{5}g_1'^2M_1' + \frac{6}{5}g_1^2M_1\Big], \qquad \text{(D.67)}
\end{aligned}
$$

$$
\begin{aligned}
\beta^{(2)}_{T^{\tilde\lambda}} = {} & 2g_1'^2\tilde\lambda\tilde f^\dagger T^{\tilde f} - 2|\lambda|^2\tilde\lambda\tilde f^\dagger T^{\tilde f} - \frac{12}{5}g_1^2M_1\tilde\lambda h^{E\dagger}h^E + \frac{2}{5}g_1'^2M_1'\tilde\lambda h^{E\dagger}h^E \\
& + \frac{12}{5}g_1^2\tilde\lambda h^{E\dagger}T^{h^E} - \frac{2}{5}g_1'^2\tilde\lambda h^{E\dagger}T^{h^E} - 2|\tilde\sigma|^2\tilde\lambda h^{E\dagger}T^{h^E} - 5g_1'^2M_1'\tilde\lambda\tilde\lambda^\dagger\tilde\lambda \\
& + \frac{7}{2}g_1'^2\tilde\lambda\tilde\lambda^\dagger T^{\tilde\lambda} - 6|\lambda|^2\tilde\lambda\tilde\lambda^\dagger T^{\tilde\lambda} - 3|\sigma|^2\tilde\lambda\tilde\lambda^\dagger T^{\tilde\lambda} + g_1'^2T^{\tilde\lambda}\tilde f^\dagger\tilde f \\
& - |\lambda|^2T^{\tilde\lambda}\tilde f^\dagger\tilde f + \frac{6}{5}g_1^2T^{\tilde\lambda}h^{E\dagger}h^E - \frac{1}{5}g_1'^2T^{\tilde\lambda}h^{E\dagger}h^E - |\tilde\sigma|^2T^{\tilde\lambda}h^{E\dagger}h^E \\
& + 4g_1'^2T^{\tilde\lambda}\tilde\lambda^\dagger\tilde\lambda - 6|\lambda|^2T^{\tilde\lambda}\tilde\lambda^\dagger\tilde\lambda - 3|\sigma|^2T^{\tilde\lambda}\tilde\lambda^\dagger\tilde\lambda - 3g_1'^2M_1'f^Tf^*\tilde\lambda \\
& + \frac{3}{2}g_1'^2f^Tf^*T^{\tilde\lambda} - |\lambda|^2f^Tf^*T^{\tilde\lambda} + 3g_1'^2T^{fT}f^*\tilde\lambda - 2|\lambda|^2T^{fT}f^*\tilde\lambda \\
& - 4\tilde\lambda\tilde f^\dagger ff^\dagger T^{\tilde f} - 4\tilde\lambda\tilde f^\dagger\tilde f\tilde f^\dagger T^{\tilde f} - \tilde\lambda\tilde f^\dagger\tilde f\tilde\lambda^\dagger T^{\tilde\lambda} - 4\tilde\lambda\tilde f^\dagger T^ff^\dagger\tilde f \\
& - 4\tilde\lambda\tilde f^\dagger T^{\tilde f}\tilde f^\dagger\tilde f - 2\tilde\lambda\tilde f^\dagger T^{\tilde f}\tilde\lambda^\dagger\tilde\lambda - 4\tilde\lambda h^{E\dagger}h^Eh^{E\dagger}T^{h^E} - \tilde\lambda h^{E\dagger}h^E\tilde\lambda^\dagger T^{\tilde\lambda} \\
& - 4\tilde\lambda h^{E\dagger}y^Ey^{E\dagger}T^{h^E} - 4\tilde\lambda h^{E\dagger}T^{h^E}h^{E\dagger}h^E - 2\tilde\lambda h^{E\dagger}T^{h^E}\tilde\lambda^\dagger\tilde\lambda \\
& - 4\tilde\lambda h^{E\dagger}T^Ey^{E\dagger}h^E - 3\tilde\lambda\tilde\lambda^\dagger\tilde\lambda\tilde\lambda^\dagger T^{\tilde\lambda} - 4\tilde\lambda\tilde\lambda^\dagger T^{\tilde\lambda}\tilde\lambda^\dagger\tilde\lambda - 2\tilde\lambda\tilde\lambda^\dagger f^Tf^*T^{\tilde\lambda} \\
& - 2\tilde\lambda\tilde\lambda^\dagger T^{fT}f^*\tilde\lambda - 2T^{\tilde\lambda}\tilde f^\dagger ff^\dagger\tilde f - 2T^{\tilde\lambda}\tilde f^\dagger\tilde f\tilde f^\dagger\tilde f - 2T^{\tilde\lambda}\tilde f^\dagger\tilde f\tilde\lambda^\dagger\tilde\lambda \\
& - 2T^{\tilde\lambda}h^{E\dagger}h^Eh^{E\dagger}h^E - 2T^{\tilde\lambda}h^{E\dagger}h^E\tilde\lambda^\dagger\tilde\lambda - 2T^{\tilde\lambda}h^{E\dagger}y^Ey^{E\dagger}h^E \\
& - 3T^{\tilde\lambda}\tilde\lambda^\dagger\tilde\lambda\tilde\lambda^\dagger\tilde\lambda - T^{\tilde\lambda}\tilde\lambda^\dagger f^Tf^*\tilde\lambda - 2f^Tf^*f^Tf^*T^{\tilde\lambda} - 4f^Tf^*T^{fT}f^*\tilde\lambda \\
& - 2f^T\tilde f^*\tilde f^Tf^*T^{\tilde\lambda} - 4f^T\tilde f^*T^{\tilde fT}f^*\tilde\lambda - 4T^{fT}f^*f^Tf^*\tilde\lambda - 4T^{fT}\tilde f^*\tilde f^Tf^*\tilde\lambda \\
& - 8\lambda^*\tilde\lambda\tilde\lambda^\dagger\tilde\lambda T_\lambda - 2\lambda^*f^Tf^*\tilde\lambda T_\lambda + \frac{297}{50}g_1^4T^{\tilde\lambda} + \frac{27}{100}g_1^2g_1'^2T^{\tilde\lambda} + \frac{551}{25}g_1'^4T^{\tilde\lambda} \\
& + \frac{9}{5}g_1^2g_2^2T^{\tilde\lambda} + \frac{39}{20}g_1'^2g_2^2T^{\tilde\lambda} + \frac{33}{2}g_2^4T^{\tilde\lambda} + \frac{6}{5}g_1^2|\lambda|^2T^{\tilde\lambda} - \frac{6}{5}g_1'^2|\lambda|^2T^{\tilde\lambda} \\
& + 6g_2^2|\lambda|^2T^{\tilde\lambda} - 4|\lambda|^4T^{\tilde\lambda} - 2|\sigma|^2|\kappa_\phi|^2T^{\tilde\lambda} - 2|\sigma|^4T^{\tilde\lambda} - 2|\tilde\sigma|^2|\sigma|^2T^{\tilde\lambda} \\
& - 4\sigma^*\tilde\lambda\tilde\lambda^\dagger\tilde\lambda T_\sigma - 2\tilde\sigma^*\tilde\lambda h^{E\dagger}h^ET_{\tilde\sigma} - f^Tf^*T^{\tilde\lambda}\,\mathrm{Tr}\Big(ff^\dagger\Big) - 2T^{fT}f^*\tilde\lambda\,\mathrm{Tr}\Big(ff^\dagger\Big) \\
& - 2|\lambda|^2T^{\tilde\lambda}\,\mathrm{Tr}\Big(ff^\dagger\Big) - 2\tilde\lambda\tilde f^\dagger T^{\tilde f}\,\mathrm{Tr}\Big(\tilde f\tilde f^\dagger\Big) - T^{\tilde\lambda}\tilde f^\dagger\tilde f\,\mathrm{Tr}\Big(\tilde f\tilde f^\dagger\Big) \\
& - 2|\lambda|^2T^{\tilde\lambda}\,\mathrm{Tr}\Big(\tilde f\tilde f^\dagger\Big) - 6\tilde\lambda h^{E\dagger}T^{h^E}\,\mathrm{Tr}\Big(g^Dg^{D\dagger}\Big) - 3T^{\tilde\lambda}h^{E\dagger}h^E\,\mathrm{Tr}\Big(g^Dg^{D\dagger}\Big) \\
& - 2\tilde\lambda h^{E\dagger}T^{h^E}\,\mathrm{Tr}\Big(h^Eh^{E\dagger}\Big) - T^{\tilde\lambda}h^{E\dagger}h^E\,\mathrm{Tr}\Big(h^Eh^{E\dagger}\Big) - 3f^Tf^*T^{\tilde\lambda}\,\mathrm{Tr}\Big(y^Dy^{D\dagger}\Big) \\
& - 6T^{fT}f^*\tilde\lambda\,\mathrm{Tr}\Big(y^Dy^{D\dagger}\Big) - 6|\lambda|^2T^{\tilde\lambda}\,\mathrm{Tr}\Big(y^Dy^{D\dagger}\Big) - f^Tf^*T^{\tilde\lambda}\,\mathrm{Tr}\Big(y^Ey^{E\dagger}\Big) \\
& - 2T^{fT}f^*\tilde\lambda\,\mathrm{Tr}\Big(y^Ey^{E\dagger}\Big) - 2|\lambda|^2T^{\tilde\lambda}\,\mathrm{Tr}\Big(y^Ey^{E\dagger}\Big) - 6\tilde\lambda\tilde f^\dagger T^{\tilde f}\,\mathrm{Tr}\Big(y^Uy^{U\dagger}\Big) \\
& - 3T^{\tilde\lambda}\tilde f^\dagger\tilde f\,\mathrm{Tr}\Big(y^Uy^{U\dagger}\Big) - 6|\lambda|^2T^{\tilde\lambda}\,\mathrm{Tr}\Big(y^Uy^{U\dagger}\Big) - 9\tilde\lambda\tilde\lambda^\dagger T^{\tilde\lambda}\,\mathrm{Tr}\Big(\kappa\kappa^\dagger\Big) \\
& - 9T^{\tilde\lambda}\tilde\lambda^\dagger\tilde\lambda\,\mathrm{Tr}\Big(\kappa\kappa^\dagger\Big) + \frac{4}{5}g_1^2T^{\tilde\lambda}\,\mathrm{Tr}\Big(\kappa\kappa^\dagger\Big) - \frac{9}{5}g_1'^2T^{\tilde\lambda}\,\mathrm{Tr}\Big(\kappa\kappa^\dagger\Big)
\end{aligned}
$$

$$
\begin{aligned}
&+ 16 g_3^2 T^{\tilde{\lambda}} \operatorname{Tr}\Big(\kappa\kappa^\dagger\Big) - 6\tilde{\lambda}\tilde{\lambda}^\dagger T^{\tilde{\lambda}} \operatorname{Tr}\Big(\tilde{\lambda}\tilde{\lambda}^\dagger\Big) - 6 T^{\tilde{\lambda}} \tilde{\lambda}\tilde{\lambda}^\dagger \tilde{\lambda} \operatorname{Tr}\Big(\tilde{\lambda}\tilde{\lambda}^\dagger\Big) \\
&+ \frac{6}{5} g_1^2 T^{\tilde{\lambda}} \operatorname{Tr}\Big(\tilde{\lambda}\tilde{\lambda}^\dagger\Big) - \frac{6}{5} g_1'^2 T^{\tilde{\lambda}} \operatorname{Tr}\Big(\tilde{\lambda}\tilde{\lambda}^\dagger\Big) + 6 g_2^2 T^{\tilde{\lambda}} \operatorname{Tr}\Big(\tilde{\lambda}\tilde{\lambda}^\dagger\Big) \\
&- 2 f^T f^* \tilde{\lambda} \operatorname{Tr}\Big(f^\dagger T^f\Big) - 6\tilde{\lambda} h^{E\dagger} h^E \operatorname{Tr}\Big(g^{D\dagger} T^{g^D}\Big) - 2\tilde{\lambda} h^{E\dagger} h^E \operatorname{Tr}\Big(h^{E\dagger} T^{h^E}\Big) \\
&- 6 f^T f^* \tilde{\lambda} \operatorname{Tr}\Big(y^{D\dagger} T^D\Big) - 2 f^T f^* \tilde{\lambda} \operatorname{Tr}\Big(y^{E\dagger} T^E\Big) - 2\tilde{\lambda}\tilde{f}^\dagger \tilde{f} \Big[3 \operatorname{Tr}\Big(y^{U\dagger} T^U\Big) \\
&+ g_1'^2 M_1' + \lambda^* T_\lambda + \operatorname{Tr}\Big(\tilde{f}^\dagger T^{\tilde{f}}\Big)\Big] - 12\tilde{\lambda}\tilde{\lambda}^\dagger\tilde{\lambda} \operatorname{Tr}\Big(\kappa^\dagger T^\kappa\Big) - 8\tilde{\lambda}\tilde{\lambda}^\dagger\tilde{\lambda} \operatorname{Tr}\Big(\tilde{\lambda}^\dagger T^{\tilde{\lambda}}\Big) \\
&- 2 T^{\tilde{\lambda}} \operatorname{Tr}\Big(\tilde{f}\tilde{\lambda}^\dagger\tilde{\lambda}\tilde{f}^\dagger\Big) - 6 T^{\tilde{\lambda}} \operatorname{Tr}\Big(g^D \kappa^\dagger \kappa g^{D\dagger}\Big) - 2 T^{\tilde{\lambda}} \operatorname{Tr}\Big(h^E \tilde{\lambda}^\dagger \tilde{\lambda} h^{E\dagger}\Big) \\
&- 6 T^{\tilde{\lambda}} \operatorname{Tr}\Big(\kappa\kappa^\dagger\kappa\kappa^\dagger\Big) - 4 T^{\tilde{\lambda}} \operatorname{Tr}\Big(\tilde{\lambda}\tilde{\lambda}^\dagger\tilde{\lambda}\tilde{\lambda}^\dagger\Big) - 2 T^{\tilde{\lambda}} \operatorname{Tr}\Big(\tilde{\lambda}\tilde{\lambda}^\dagger f^T f^*\Big) \\
&- \frac{1}{50}\tilde{\lambda}\Big(1188 g_1^4 M_1 + 27 g_1^2 g_1'^2 M_1 + 180 g_1^2 g_2^2 M_1 + 27 g_1^2 g_1'^2 M_1' + 4408 g_1'^4 M_1' \\
&+ 195 g_1'^2 g_2^2 M_1' + 180 g_1^2 g_2^2 M_2 + 195 g_1'^2 g_2^2 M_2 + 3300 g_2^4 M_2 + 800\lambda^*|\lambda|^2 T_\lambda \\
&+ 200|\tilde{\sigma}|^2 \sigma^* T_\sigma + 400\sigma^*|\sigma|^2 T_\sigma + 200\kappa_\phi^* \sigma^* \Big(\kappa_\phi T_\sigma + \sigma T_{\kappa_\phi}\Big) + 200|\sigma|^2 \tilde{\sigma}^* T_{\tilde{\sigma}} \\
&+ 80 g_1^2 M_1 \operatorname{Tr}\Big(\kappa\kappa^\dagger\Big) - 180 g_1'^2 M_1' \operatorname{Tr}\Big(\kappa\kappa^\dagger\Big) + 1600 g_3^2 M_3 \operatorname{Tr}\Big(\kappa\kappa^\dagger\Big) \\
&+ 120 g_1^2 M_1 \operatorname{Tr}\Big(\tilde{\lambda}\tilde{\lambda}^\dagger\Big) - 120 g_1'^2 M_1' \operatorname{Tr}\Big(\tilde{\lambda}\tilde{\lambda}^\dagger\Big) + 600 g_2^2 M_2 \operatorname{Tr}\Big(\tilde{\lambda}\tilde{\lambda}^\dagger\Big) \\
&+ 40\lambda^* \Big\{ T_\lambda \Big[-15 g_2^2 + 15 \operatorname{Tr}\Big(y^D y^{D\dagger}\Big) + 15 \operatorname{Tr}\Big(y^U y^{U\dagger}\Big) - 3 g_1^2 + 3 g_1'^2 \\
&+ 5 \operatorname{Tr}\Big(f f^\dagger\Big) + 5 \operatorname{Tr}\Big(\tilde{f}\tilde{f}^\dagger\Big) + 5 \operatorname{Tr}\Big(y^E y^{E\dagger}\Big)\Big] + \lambda\Big[3 g_1^2 M_1 - 3 g_1'^2 M_1' \\
&+ 15 g_2^2 M_2 + 5 \operatorname{Tr}\Big(f^\dagger T^f\Big) + 5 \operatorname{Tr}\Big(\tilde{f}^\dagger T^{\tilde{f}}\Big) + 15 \operatorname{Tr}\Big(y^{D\dagger} T^D\Big) \\
&+ 5 \operatorname{Tr}\Big(y^{E\dagger} T^E\Big) + 15 \operatorname{Tr}\Big(y^{U\dagger} T^U\Big)\Big]\Big\} - 80 g_1^2 \operatorname{Tr}\Big(\kappa^\dagger T^\kappa\Big) + 180 g_1'^2 \operatorname{Tr}\Big(\kappa^\dagger T^\kappa\Big) \\
&- 1600 g_3^2 \operatorname{Tr}\Big(\kappa^\dagger T^\kappa\Big) - 120 g_1^2 \operatorname{Tr}\Big(\tilde{\lambda}^\dagger T^{\tilde{\lambda}}\Big) + 120 g_1'^2 \operatorname{Tr}\Big(\tilde{\lambda}^\dagger T^{\tilde{\lambda}}\Big) \\
&- 600 g_2^2 \operatorname{Tr}\Big(\tilde{\lambda}^\dagger T^{\tilde{\lambda}}\Big) + 200 \operatorname{Tr}\Big(\tilde{f}\tilde{\lambda}^\dagger T^{\tilde{\lambda}} \tilde{f}^\dagger\Big) + 600 \operatorname{Tr}\Big(g^D \kappa^\dagger T^\kappa g^{D\dagger}\Big) \\
&+ 200 \operatorname{Tr}\Big(h^E \tilde{\lambda}^\dagger T^{\tilde{\lambda}} h^{E\dagger}\Big) + 600 \operatorname{Tr}\Big(\kappa g^{D\dagger} T^{g^D} \kappa^\dagger\Big) + 1200 \operatorname{Tr}\Big(\kappa\kappa^\dagger T^\kappa \kappa^\dagger\Big) \\
&+ 200 \operatorname{Tr}\Big(\tilde{\lambda}\tilde{f}^\dagger T^{\tilde{f}} \tilde{\lambda}^\dagger\Big) + 200 \operatorname{Tr}\Big(\tilde{\lambda} h^{E\dagger} T^{h^E} \tilde{\lambda}^\dagger\Big) + 800 \operatorname{Tr}\Big(\tilde{\lambda}\tilde{\lambda}^\dagger T^{\tilde{\lambda}} \tilde{\lambda}^\dagger\Big) \\
&+ 200 \operatorname{Tr}\Big(f^\dagger T^f \tilde{\lambda}^* \tilde{\lambda}^T\Big) + 200 \operatorname{Tr}\Big(\tilde{\lambda}^\dagger f^T f^* T^{\tilde{\lambda}}\Big)\Big), \qquad \text{(D.68)}
\end{aligned}
$$

$$
\begin{aligned}
\beta_{T_\lambda}^{(1)} = T_\lambda \Big[&-\frac{3}{5} g_1^2 - \frac{19}{10} g_1'^2 - 3 g_2^2 + 12|\lambda|^2 + |\sigma|^2 + \operatorname{Tr}\Big(f f^\dagger\Big) + \operatorname{Tr}\Big(\tilde{f}\tilde{f}^\dagger\Big) \\
&+ 3 \operatorname{Tr}\Big(y^D y^{D\dagger}\Big) + \operatorname{Tr}\Big(y^E y^{E\dagger}\Big) + 3 \operatorname{Tr}\Big(y^U y^{U\dagger}\Big) + 3 \operatorname{Tr}\Big(\kappa\kappa^\dagger\Big) + 2 \operatorname{Tr}\Big(\tilde{\lambda}\tilde{\lambda}^\dagger\Big)\Big]
\end{aligned}
$$

$$
\begin{aligned}
&+\frac{1}{5}\lambda\Big[6g_1^2M_1+19g_1'^2M_1'+30g_2^2M_2+10\sigma^*T_\sigma+10\,\mathrm{Tr}\Big(f^\dagger T^f\Big)\\
&+10\,\mathrm{Tr}\Big(\tilde{f}^\dagger T^{\tilde{f}}\Big)+30\,\mathrm{Tr}\Big(y^{D\dagger}T^D\Big)+10\,\mathrm{Tr}\Big(y^{E\dagger}T^E\Big)+30\,\mathrm{Tr}\Big(y^{U\dagger}T^U\Big)\\
&+30\,\mathrm{Tr}\Big(\kappa^\dagger T^\kappa\Big)+20\,\mathrm{Tr}\Big(\tilde{\lambda}^\dagger T^{\tilde{\lambda}}\Big)\Big], \qquad \text{(D.69)}\\
\beta_{T_\lambda}^{(2)} =& -\frac{594}{25}g_1^4M_1\lambda-\frac{27}{50}g_1^2g_1'^2M_1\lambda-\frac{18}{5}g_1^2g_2^2M_1\lambda-\frac{27}{50}g_1^2g_1'^2M_1'\lambda-\frac{2204}{25}g_1'^4M_1'\lambda\\
&-\frac{39}{10}g_1'^2g_2^2M_1'\lambda-\frac{18}{5}g_1^2g_2^2M_2\lambda-\frac{39}{10}g_1'^2g_2^2M_2\lambda-66g_2^4M_2\lambda+\frac{297}{50}g_1^4T_\lambda\\
&+\frac{27}{100}g_1^2g_1'^2T_\lambda+\frac{551}{25}g_1'^4T_\lambda+\frac{9}{5}g_1^2g_2^2T_\lambda+\frac{39}{20}g_1'^2g_2^2T_\lambda+\frac{33}{2}g_2^4T_\lambda-50|\lambda|^4T_\lambda\\
&-2|\sigma|^4T_\lambda-2|\tilde{\sigma}|^2|\sigma|^2T_\lambda-4\lambda|\tilde{\sigma}|^2\sigma^*T_\sigma-8\lambda\sigma^*|\sigma|^2T_\sigma-2\kappa_\phi^*\sigma^*\Big(2\kappa_\phi\lambda T_\sigma\\
&+2\lambda\sigma T_{\kappa_\phi}+\kappa_\phi\sigma T_\lambda\Big)-4\lambda|\sigma|^2\tilde{\sigma}^*T_{\tilde{\sigma}}-2g_1'^2M_1'\lambda\,\mathrm{Tr}\Big(ff^\dagger\Big)+g_1'^2T_\lambda\,\mathrm{Tr}\Big(ff^\dagger\Big)\\
&-3g_1'^2M_1'\lambda\,\mathrm{Tr}\Big(\tilde{f}\tilde{f}^\dagger\Big)+\frac{3}{2}g_1'^2T_\lambda\,\mathrm{Tr}\Big(\tilde{f}\tilde{f}^\dagger\Big)+\frac{4}{5}g_1^2M_1\lambda\,\mathrm{Tr}\Big(y^Dy^{D\dagger}\Big)\\
&+\frac{6}{5}g_1'^2M_1'\lambda\,\mathrm{Tr}\Big(y^Dy^{D\dagger}\Big)-32g_3^2M_3\lambda\,\mathrm{Tr}\Big(y^Dy^{D\dagger}\Big)-\frac{2}{5}g_1^2T_\lambda\,\mathrm{Tr}\Big(y^Dy^{D\dagger}\Big)\\
&-\frac{3}{5}g_1'^2T_\lambda\,\mathrm{Tr}\Big(y^Dy^{D\dagger}\Big)+16g_3^2T_\lambda\,\mathrm{Tr}\Big(y^Dy^{D\dagger}\Big)-\frac{12}{5}g_1^2M_1\lambda\,\mathrm{Tr}\Big(y^Ey^{E\dagger}\Big)\\
&+\frac{2}{5}g_1'^2M_1'\lambda\,\mathrm{Tr}\Big(y^Ey^{E\dagger}\Big)+\frac{6}{5}g_1^2T_\lambda\,\mathrm{Tr}\Big(y^Ey^{E\dagger}\Big)-\frac{1}{5}g_1'^2T_\lambda\,\mathrm{Tr}\Big(y^Ey^{E\dagger}\Big)\\
&-\frac{8}{5}g_1^2M_1\lambda\,\mathrm{Tr}\Big(y^Uy^{U\dagger}\Big)+\frac{3}{5}g_1'^2M_1'\lambda\,\mathrm{Tr}\Big(y^Uy^{U\dagger}\Big)-32g_3^2M_3\lambda\,\mathrm{Tr}\Big(y^Uy^{U\dagger}\Big)\\
&+\frac{4}{5}g_1^2T_\lambda\,\mathrm{Tr}\Big(y^Uy^{U\dagger}\Big)-\frac{3}{10}g_1'^2T_\lambda\,\mathrm{Tr}\Big(y^Uy^{U\dagger}\Big)+16g_3^2T_\lambda\,\mathrm{Tr}\Big(y^Uy^{U\dagger}\Big)\\
&-\frac{8}{5}g_1^2M_1\lambda\,\mathrm{Tr}\Big(\kappa\kappa^\dagger\Big)+\frac{18}{5}g_1'^2M_1'\lambda\,\mathrm{Tr}\Big(\kappa\kappa^\dagger\Big)-32g_3^2M_3\lambda\,\mathrm{Tr}\Big(\kappa\kappa^\dagger\Big)\\
&+\frac{4}{5}g_1^2T_\lambda\,\mathrm{Tr}\Big(\kappa\kappa^\dagger\Big)-\frac{9}{5}g_1'^2T_\lambda\,\mathrm{Tr}\Big(\kappa\kappa^\dagger\Big)+16g_3^2T_\lambda\,\mathrm{Tr}\Big(\kappa\kappa^\dagger\Big)-\frac{12}{5}g_1^2M_1\lambda\,\mathrm{Tr}\Big(\tilde{\lambda}\tilde{\lambda}^\dagger\Big)\\
&+\frac{12}{5}g_1'^2M_1'\lambda\,\mathrm{Tr}\Big(\tilde{\lambda}\tilde{\lambda}^\dagger\Big)-12g_2^2M_2\lambda\,\mathrm{Tr}\Big(\tilde{\lambda}\tilde{\lambda}^\dagger\Big)+\frac{6}{5}g_1^2T_\lambda\,\mathrm{Tr}\Big(\tilde{\lambda}\tilde{\lambda}^\dagger\Big)\\
&-\frac{6}{5}g_1'^2T_\lambda\,\mathrm{Tr}\Big(\tilde{\lambda}\tilde{\lambda}^\dagger\Big)+6g_2^2T_\lambda\,\mathrm{Tr}\Big(\tilde{\lambda}\tilde{\lambda}^\dagger\Big)+2g_1'^2\lambda\,\mathrm{Tr}\Big(f^\dagger T^f\Big)+3g_1'^2\lambda\,\mathrm{Tr}\Big(\tilde{f}^\dagger T^{\tilde{f}}\Big)\\
&-\frac{4}{5}g_1^2\lambda\,\mathrm{Tr}\Big(y^{D\dagger}T^D\Big)-\frac{6}{5}g_1'^2\lambda\,\mathrm{Tr}\Big(y^{D\dagger}T^D\Big)+32g_3^2\lambda\,\mathrm{Tr}\Big(y^{D\dagger}T^D\Big)\\
&+\frac{12}{5}g_1^2\lambda\,\mathrm{Tr}\Big(y^{E\dagger}T^E\Big)-\frac{2}{5}g_1'^2\lambda\,\mathrm{Tr}\Big(y^{E\dagger}T^E\Big)+\frac{8}{5}g_1^2\lambda\,\mathrm{Tr}\Big(y^{U\dagger}T^U\Big)\\
&-\frac{3}{5}g_1'^2\lambda\,\mathrm{Tr}\Big(y^{U\dagger}T^U\Big)+32g_3^2\lambda\,\mathrm{Tr}\Big(y^{U\dagger}T^U\Big)+\frac{8}{5}g_1^2\lambda\,\mathrm{Tr}\Big(\kappa^\dagger T^\kappa\Big)\\
&-\frac{18}{5}g_1'^2\lambda\,\mathrm{Tr}\Big(\kappa^\dagger T^\kappa\Big)+32g_3^2\lambda\,\mathrm{Tr}\Big(\kappa^\dagger T^\kappa\Big)+\frac{12}{5}g_1^2\lambda\,\mathrm{Tr}\Big(\tilde{\lambda}^\dagger T^{\tilde{\lambda}}\Big)
\end{aligned}
$$

$$
\begin{aligned}
&- \frac{12}{5}g_1'^2\lambda\,\mathrm{Tr}\Big(\tilde{\lambda}^\dagger T^{\tilde{\lambda}}\Big) + 12g_2^2\lambda\,\mathrm{Tr}\Big(\tilde{\lambda}^\dagger T^{\tilde{\lambda}}\Big) - \frac{1}{10}|\lambda|^2\Big\{3T_\lambda\Big[-12g_1^2 - 13g_1'^2 \\
&- 60g_2^2 + 20|\sigma|^2 + 30\,\mathrm{Tr}\Big(ff^\dagger\Big) + 30\,\mathrm{Tr}\Big(\tilde{f}\tilde{f}^\dagger\Big) + 90\,\mathrm{Tr}\Big(y^D y^{D\dagger}\Big) \\
&+ 30\,\mathrm{Tr}\Big(y^E y^{E\dagger}\Big) + 90\,\mathrm{Tr}\Big(y^U y^{U\dagger}\Big) + 60\,\mathrm{Tr}\Big(\kappa\kappa^\dagger\Big) + 40\,\mathrm{Tr}\Big(\tilde{\lambda}\tilde{\lambda}^\dagger\Big)\Big] \\
&+ 2\lambda\Big[12g_1^2M_1 + 13g_1'^2M_1' + 60g_2^2M_2 + 20\sigma^*T_\sigma + 30\,\mathrm{Tr}\Big(f^\dagger T^f\Big) \\
&+ 30\,\mathrm{Tr}\Big(\tilde{f}^\dagger T^{\tilde{f}}\Big) + 90\,\mathrm{Tr}\Big(y^{D\dagger}T^D\Big) + 30\,\mathrm{Tr}\Big(y^{E\dagger}T^E\Big) + 90\,\mathrm{Tr}\Big(y^{U\dagger}T^U\Big) \\
&+ 60\,\mathrm{Tr}\Big(\kappa^\dagger T^\kappa\Big) + 40\,\mathrm{Tr}\Big(\tilde{\lambda}^\dagger T^{\tilde{\lambda}}\Big)\Big]\Big\} - 3T_\lambda\,\mathrm{Tr}\Big(ff^\dagger ff^\dagger\Big) - 4T_\lambda\,\mathrm{Tr}\Big(ff^\dagger\tilde{f}\tilde{f}^\dagger\Big) \\
&- 12\lambda\,\mathrm{Tr}\Big(ff^\dagger T^f f^\dagger\Big) - 8\lambda\,\mathrm{Tr}\Big(ff^\dagger T^{\tilde{f}}\tilde{f}^\dagger\Big) - 3T_\lambda\,\mathrm{Tr}\Big(\tilde{f}\tilde{f}^\dagger\tilde{f}\tilde{f}^\dagger\Big) \\
&- 8\lambda\,\mathrm{Tr}\Big(\tilde{f}\tilde{f}^\dagger T^f f^\dagger\Big) - 12\lambda\,\mathrm{Tr}\Big(\tilde{f}\tilde{f}^\dagger T^{\tilde{f}}\tilde{f}^\dagger\Big) - T_\lambda\,\mathrm{Tr}\Big(\tilde{f}h^{E\dagger}h^E\tilde{f}^\dagger\Big) \\
&- 2\lambda\,\mathrm{Tr}\Big(\tilde{f}h^{E\dagger}T^{h^E}\tilde{f}^\dagger\Big) - 3T_\lambda\,\mathrm{Tr}\Big(\tilde{f}\tilde{\lambda}^\dagger\tilde{\lambda}\tilde{f}^\dagger\Big) - 6\lambda\,\mathrm{Tr}\Big(\tilde{f}\tilde{\lambda}^\dagger T^{\tilde{\lambda}}\tilde{f}^\dagger\Big) \\
&- 3T_\lambda\,\mathrm{Tr}\Big(g^D g^{D\dagger}y^{DT}y^{D*}\Big) - 3T_\lambda\,\mathrm{Tr}\Big(g^D g^{D\dagger}y^{UT}y^{U*}\Big) - 6T_\lambda\,\mathrm{Tr}\Big(g^D\kappa^\dagger\kappa g^{D\dagger}\Big) \\
&- 12\lambda\,\mathrm{Tr}\Big(g^D\kappa^\dagger T^\kappa g^{D\dagger}\Big) - 2\lambda\,\mathrm{Tr}\Big(h^E\tilde{f}^\dagger T^{\tilde{f}}h^{E\dagger}\Big) - 2T_\lambda\,\mathrm{Tr}\Big(h^E h^{E\dagger}y^E y^{E\dagger}\Big) \\
&- 4\lambda\,\mathrm{Tr}\Big(h^E h^{E\dagger}T^E y^{E\dagger}\Big) - 2T_\lambda\,\mathrm{Tr}\Big(h^E\tilde{\lambda}^\dagger\tilde{\lambda}h^{E\dagger}\Big) - 4\lambda\,\mathrm{Tr}\Big(h^E\tilde{\lambda}^\dagger T^{\tilde{\lambda}}h^{E\dagger}\Big) \\
&- 9T_\lambda\,\mathrm{Tr}\Big(y^D y^{D\dagger}y^D y^{D\dagger}\Big) - 36\lambda\,\mathrm{Tr}\Big(y^D y^{D\dagger}T^D y^{D\dagger}\Big) - 6T_\lambda\,\mathrm{Tr}\Big(y^D y^{U\dagger}y^U y^{D\dagger}\Big) \\
&- 12\lambda\,\mathrm{Tr}\Big(y^D y^{U\dagger}T^U y^{D\dagger}\Big) - 3T_\lambda\,\mathrm{Tr}\Big(y^E y^{E\dagger}y^E y^{E\dagger}\Big) - 4\lambda\,\mathrm{Tr}\Big(y^E y^{E\dagger}T^{h^E}h^{E\dagger}\Big) \\
&- 12\lambda\,\mathrm{Tr}\Big(y^E y^{E\dagger}T^E y^{E\dagger}\Big) - 12\lambda\,\mathrm{Tr}\Big(y^U y^{D\dagger}T^D y^{U\dagger}\Big) - 9T_\lambda\,\mathrm{Tr}\Big(y^U y^{U\dagger}y^U y^{U\dagger}\Big) \\
&- 36\lambda\,\mathrm{Tr}\Big(y^U y^{U\dagger}T^U y^{U\dagger}\Big) - 12\lambda\,\mathrm{Tr}\Big(\kappa g^{D\dagger}T^{g^D}\kappa^\dagger\Big) - 6T_\lambda\,\mathrm{Tr}\Big(\kappa\kappa^\dagger\kappa\kappa^\dagger\Big) \\
&- 24\lambda\,\mathrm{Tr}\Big(\kappa\kappa^\dagger T^\kappa\kappa^\dagger\Big) - 6\lambda\,\mathrm{Tr}\Big(\tilde{\lambda}\tilde{f}^\dagger T^{\tilde{f}}\tilde{\lambda}^\dagger\Big) - 4\lambda\,\mathrm{Tr}\Big(\tilde{\lambda}h^{E\dagger}T^{h^E}\tilde{\lambda}^\dagger\Big) \\
&- 4T_\lambda\,\mathrm{Tr}\Big(\tilde{\lambda}\tilde{\lambda}^\dagger\tilde{\lambda}\tilde{\lambda}^\dagger\Big) - 16\lambda\,\mathrm{Tr}\Big(\tilde{\lambda}\tilde{\lambda}^\dagger T^{\tilde{\lambda}}\tilde{\lambda}^\dagger\Big) - 3T_\lambda\,\mathrm{Tr}\Big(\tilde{\lambda}\tilde{\lambda}^\dagger f^T f^*\Big) \\
&- 6\lambda\,\mathrm{Tr}\Big(f^\dagger T^f\tilde{\lambda}^*\tilde{\lambda}^T\Big) - 6\lambda\,\mathrm{Tr}\Big(g^{D\dagger}y^{DT}y^{D*}T^{g^D}\Big) - 6\lambda\,\mathrm{Tr}\Big(g^{D\dagger}y^{UT}y^{U*}T^{g^D}\Big) \\
&- 6\lambda\,\mathrm{Tr}\Big(y^{D\dagger}T^D g^{D*}g^{DT}\Big) - 6\lambda\,\mathrm{Tr}\Big(y^{U\dagger}T^U g^{D*}g^{DT}\Big) - 6\lambda\,\mathrm{Tr}\Big(\tilde{\lambda}^\dagger f^T f^* T^{\tilde{\lambda}}\Big),
\end{aligned}
\tag{D.70}
$$

$$
\begin{aligned}
\beta^{(1)}_{T^{\tilde{f}}} = {} & 2ff^\dagger T^{\tilde{f}} + 4\tilde{f}\tilde{f}^\dagger T^{\tilde{f}} + 2\tilde{f}h^{E\dagger}T^{h^E} + 2\tilde{f}\tilde{\lambda}^\dagger T^{\tilde{\lambda}} + 4T^f f^\dagger\tilde{f} + 5T^{\tilde{f}}\tilde{f}^\dagger\tilde{f} \\
& + T^{\tilde{f}}h^{E\dagger}h^E + T^{\tilde{f}}\tilde{\lambda}^\dagger\tilde{\lambda} - \frac{3}{5}g_1^2T^{\tilde{f}} - \frac{19}{10}g_1'^2T^{\tilde{f}} - 3g_2^2T^{\tilde{f}} + |\lambda|^2T^{\tilde{f}}
\end{aligned}
$$

$$
\begin{aligned}
&+ T^{\tilde{f}}\,\mathrm{Tr}\Big(\tilde{f}\tilde{f}^\dagger\Big) + 3T^{\tilde{f}}\,\mathrm{Tr}\Big(y^U y^{U\dagger}\Big) + \tilde{f}\Big[2\lambda^* T_\lambda + 2\,\mathrm{Tr}\Big(\tilde{f}^\dagger T^{\tilde{f}}\Big) + 6g_2^2 M_2 \\
&+ 6\,\mathrm{Tr}\Big(y^{U\dagger}T^U\Big) + \frac{19}{5}g_1'^2 M_1' + \frac{6}{5}g_1^2 M_1\Big], \qquad \text{(D.71)}\\
\beta^{(2)}_{T^{\tilde{f}}} = &\frac{6}{5}g_1^2 f f^\dagger T^{\tilde{f}} - \frac{6}{5}g_1'^2 f f^\dagger T^{\tilde{f}} + 6g_2^2 f f^\dagger T^{\tilde{f}} - 2|\lambda|^2 f f^\dagger T^{\tilde{f}} \\
&- \frac{12}{5}g_1^2 M_1 \tilde{f}\tilde{f}^\dagger\tilde{f} + \frac{2}{5}g_1'^2 M_1' \tilde{f}\tilde{f}^\dagger\tilde{f} - 12g_2^2 M_2 \tilde{f}\tilde{f}^\dagger\tilde{f} + \frac{6}{5}g_1^2 \tilde{f}\tilde{f}^\dagger T^{\tilde{f}} \\
&+ \frac{4}{5}g_1'^2 \tilde{f}\tilde{f}^\dagger T^{\tilde{f}} + 6g_2^2 \tilde{f}\tilde{f}^\dagger T^{\tilde{f}} - 4|\lambda|^2 \tilde{f}\tilde{f}^\dagger T^{\tilde{f}} - \frac{12}{5}g_1^2 M_1 \tilde{f} h^{E\dagger} h^E \\
&+ \frac{2}{5}g_1'^2 M_1' \tilde{f} h^{E\dagger} h^E + \frac{12}{5}g_1^2 \tilde{f} h^{E\dagger} T^{h^E} - \frac{2}{5}g_1'^2 \tilde{f} h^{E\dagger} T^{h^E} - 2|\tilde{\sigma}|^2 \tilde{f} h^{E\dagger} T^{h^E} \\
&- 2g_1'^2 M_1' \tilde{f}\tilde{\lambda}^\dagger\tilde{\lambda} + 2g_1'^2 \tilde{f}\tilde{\lambda}^\dagger T^{\tilde{\lambda}} - 4|\lambda|^2 \tilde{f}\tilde{\lambda}^\dagger T^{\tilde{\lambda}} - 2|\sigma|^2 \tilde{f}\tilde{\lambda}^\dagger T^{\tilde{\lambda}} \\
&+ \frac{12}{5}g_1^2 T^f f^\dagger \tilde{f} - \frac{12}{5}g_1'^2 T^f f^\dagger \tilde{f} + 12g_2^2 T^f f^\dagger \tilde{f} - 4|\lambda|^2 T^f f^\dagger \tilde{f} \\
&+ \frac{12}{5}g_1^2 T^{\tilde{f}} \tilde{f}^\dagger \tilde{f} - \frac{7}{5}g_1'^2 T^{\tilde{f}} \tilde{f}^\dagger \tilde{f} + 12g_2^2 T^{\tilde{f}} \tilde{f}^\dagger \tilde{f} - 5|\lambda|^2 T^{\tilde{f}} \tilde{f}^\dagger \tilde{f} \\
&+ \frac{6}{5}g_1^2 T^{\tilde{f}} h^{E\dagger} h^E - \frac{1}{5}g_1'^2 T^{\tilde{f}} h^{E\dagger} h^E - |\tilde{\sigma}|^2 T^{\tilde{f}} h^{E\dagger} h^E + g_1'^2 T^{\tilde{f}} \tilde{\lambda}^\dagger\tilde{\lambda} \\
&- 2|\lambda|^2 T^{\tilde{f}} \tilde{\lambda}^\dagger\tilde{\lambda} - |\sigma|^2 T^{\tilde{f}} \tilde{\lambda}^\dagger\tilde{\lambda} - 2 f f^\dagger f f^\dagger T^{\tilde{f}} - 4 f f^\dagger T^f f^\dagger \tilde{f} \\
&- 2f\tilde{\lambda}^*\tilde{\lambda}^T f^\dagger T^{\tilde{f}} - 4f\tilde{\lambda}^* T^{\tilde{\lambda}T} f^\dagger \tilde{f} - 4\tilde{f}\tilde{f}^\dagger f f^\dagger T^{\tilde{f}} - 6\tilde{f}\tilde{f}^\dagger \tilde{f}\tilde{f}^\dagger T^{\tilde{f}} \\
&- 4\tilde{f}\tilde{f}^\dagger T^f f^\dagger \tilde{f} - 8\tilde{f}\tilde{f}^\dagger T^{\tilde{f}} \tilde{f}^\dagger \tilde{f} - 2\tilde{f} h^{E\dagger} h^E \tilde{f}^\dagger T^{\tilde{f}} - 4\tilde{f} h^{E\dagger} h^E h^{E\dagger} T^{h^E} \\
&- 4\tilde{f} h^{E\dagger} y^E y^{E\dagger} T^{h^E} - 4\tilde{f} h^{E\dagger} T^{h^E} \tilde{f}^\dagger \tilde{f} - 4\tilde{f} h^{E\dagger} T^{h^E} h^{E\dagger} h^E - 4\tilde{f} h^{E\dagger} T^E y^{E\dagger} h^E \\
&- 2\tilde{f}\tilde{\lambda}^\dagger\tilde{\lambda}\tilde{f}^\dagger T^{\tilde{f}} - 2\tilde{f}\tilde{\lambda}^\dagger\tilde{\lambda}\tilde{\lambda}^\dagger T^{\tilde{\lambda}} - 4\tilde{f}\tilde{\lambda}^\dagger T^{\tilde{\lambda}} \tilde{f}^\dagger \tilde{f} - 2\tilde{f}\tilde{\lambda}^\dagger T^{\tilde{\lambda}} \tilde{\lambda}^\dagger\tilde{\lambda} \\
&- 2\tilde{f}\tilde{\lambda}^\dagger f^T f^* T^{\tilde{\lambda}} - 2\tilde{f}\tilde{\lambda}^\dagger T^{fT} f^* \tilde{\lambda} - 4T^f f^\dagger f f^\dagger \tilde{f} - 4T^f \tilde{\lambda}^*\tilde{\lambda}^T f^\dagger \tilde{f} \\
&- 2T^{\tilde{f}} \tilde{f}^\dagger f f^\dagger \tilde{f} - 6T^{\tilde{f}} \tilde{f}^\dagger \tilde{f}\tilde{f}^\dagger \tilde{f} - 4T^{\tilde{f}} h^{E\dagger} h^E \tilde{f}^\dagger \tilde{f} - 2T^{\tilde{f}} h^{E\dagger} h^E h^{E\dagger} h^E \\
&- 2T^{\tilde{f}} h^{E\dagger} y^E y^{E\dagger} h^E - 4T^{\tilde{f}} \tilde{\lambda}^\dagger\tilde{\lambda}\tilde{f}^\dagger \tilde{f} - T^{\tilde{f}} \tilde{\lambda}^\dagger\tilde{\lambda}\tilde{\lambda}^\dagger\tilde{\lambda} - T^{\tilde{f}} \tilde{\lambda}^\dagger f^T f^* \tilde{\lambda} \\
&+ \frac{297}{50}g_1^4 T^{\tilde{f}} + \frac{27}{100}g_1^2 g_1'^2 T^{\tilde{f}} + \frac{551}{25}g_1'^4 T^{\tilde{f}} + \frac{9}{5}g_1^2 g_2^2 T^{\tilde{f}} + \frac{39}{20}g_1'^2 g_2^2 T^{\tilde{f}} \\
&+ \frac{33}{2}g_2^4 T^{\tilde{f}} + \frac{3}{2}g_1'^2 |\lambda|^2 T^{\tilde{f}} - 3|\lambda|^4 T^{\tilde{f}} - |\sigma|^2 |\lambda|^2 T^{\tilde{f}} - 6\lambda^* \tilde{f}\tilde{f}^\dagger \tilde{f} T_\lambda \\
&- 4\lambda^* \tilde{f}\tilde{\lambda}^\dagger\tilde{\lambda} T_\lambda - 2\sigma^* \tilde{f}\tilde{\lambda}^\dagger\tilde{\lambda} T_\sigma - 2\tilde{\sigma}^* \tilde{f} h^{E\dagger} h^E T_{\tilde{\sigma}} - 2 f f^\dagger T^{\tilde{f}}\,\mathrm{Tr}\Big(f f^\dagger\Big) \\
&- 4T^f f^\dagger \tilde{f}\,\mathrm{Tr}\Big(f f^\dagger\Big) - |\lambda|^2 T^{\tilde{f}}\,\mathrm{Tr}\Big(f f^\dagger\Big) - 4\tilde{f}\tilde{f}^\dagger T^{\tilde{f}}\,\mathrm{Tr}\Big(\tilde{f}\tilde{f}^\dagger\Big) \\
&- 5T^{\tilde{f}} \tilde{f}^\dagger \tilde{f}\,\mathrm{Tr}\Big(\tilde{f}\tilde{f}^\dagger\Big) + \frac{3}{2}g_1'^2 T^{\tilde{f}}\,\mathrm{Tr}\Big(\tilde{f}\tilde{f}^\dagger\Big) - 6\tilde{f} h^{E\dagger} T^{h^E}\,\mathrm{Tr}\Big(g^D g^{D\dagger}\Big) \\
&- 3T^{\tilde{f}} h^{E\dagger} h^E\,\mathrm{Tr}\Big(g^D g^{D\dagger}\Big) - 2\tilde{f} h^{E\dagger} T^{h^E}\,\mathrm{Tr}\Big(h^E h^{E\dagger}\Big) \\
&- T^{\tilde{f}} h^{E\dagger} h^E\,\mathrm{Tr}\Big(h^E h^{E\dagger}\Big) - 6 f f^\dagger T^{\tilde{f}}\,\mathrm{Tr}\Big(y^D y^{D\dagger}\Big) - 12T^f f^\dagger \tilde{f}\,\mathrm{Tr}\Big(y^D y^{D\dagger}\Big)
\end{aligned}
$$

$$
\begin{aligned}
&- 3|\lambda|^2 T^{\tilde{f}} \operatorname{Tr}\Big(y^D y^{D\dagger}\Big) - 2 f f^\dagger T^{\tilde{f}} \operatorname{Tr}\Big(y^E y^{E\dagger}\Big) - 4 T^f f^\dagger \tilde{f} \operatorname{Tr}\Big(y^E y^{E\dagger}\Big) \\
&- |\lambda|^2 T^{\tilde{f}} \operatorname{Tr}\Big(y^E y^{E\dagger}\Big) - 12 \tilde{f} \tilde{f}^\dagger T^{\tilde{f}} \operatorname{Tr}\Big(y^U y^{U\dagger}\Big) - 15 T^{\tilde{f}} \tilde{f}^\dagger \tilde{f} \operatorname{Tr}\Big(y^U y^{U\dagger}\Big) \\
&+ \frac{4}{5} g_1^2 T^{\tilde{f}} \operatorname{Tr}\Big(y^U y^{U\dagger}\Big) - \frac{3}{10} g_1'^2 T^{\tilde{f}} \operatorname{Tr}\Big(y^U y^{U\dagger}\Big) + 16 g_3^2 T^{\tilde{f}} \operatorname{Tr}\Big(y^U y^{U\dagger}\Big) \\
&- 6 \tilde{f} \tilde{\lambda}^\dagger T^{\tilde{\lambda}} \operatorname{Tr}\Big(\kappa \kappa^\dagger\Big) - 3 T^{\tilde{f}} \tilde{\lambda}^\dagger \tilde{\lambda} \operatorname{Tr}\Big(\kappa \kappa^\dagger\Big) - 3|\lambda|^2 T^{\tilde{f}} \operatorname{Tr}\Big(\kappa \kappa^\dagger\Big) \\
&- 4 \tilde{f} \tilde{\lambda}^\dagger T^{\tilde{\lambda}} \operatorname{Tr}\Big(\tilde{\lambda} \tilde{\lambda}^\dagger\Big) - 2 T^{\tilde{f}} \tilde{\lambda}^\dagger \tilde{\lambda} \operatorname{Tr}\Big(\tilde{\lambda} \tilde{\lambda}^\dagger\Big) - 2|\lambda|^2 T^{\tilde{f}} \operatorname{Tr}\Big(\tilde{\lambda} \tilde{\lambda}^\dagger\Big) \\
&- 6 \tilde{f} \tilde{f}^\dagger \tilde{f} \operatorname{Tr}\Big(\tilde{f}^\dagger T^{\tilde{f}}\Big) - 6 \tilde{f} h^{E\dagger} h^E \operatorname{Tr}\Big(g^{D\dagger} T^{g^D}\Big) - 2 \tilde{f} h^{E\dagger} h^E \operatorname{Tr}\Big(h^{E\dagger} T^{h^E}\Big) \\
&- \frac{4}{5} f f^\dagger \tilde{f} \Big[15 g_2^2 M_2 + 15 \operatorname{Tr}\Big(y^{D\dagger} T^D\Big) + 3 g_1^2 M_1 - 3 g_1'^2 M_1' + 5 \lambda^* T_\lambda \\
&+ 5 \operatorname{Tr}\Big(f^\dagger T^f\Big) + 5 \operatorname{Tr}\Big(y^{E\dagger} T^E\Big)\Big] - 18 \tilde{f} \tilde{f}^\dagger \tilde{f} \operatorname{Tr}\Big(y^{U\dagger} T^U\Big) - 6 \tilde{f} \tilde{\lambda}^\dagger \tilde{\lambda} \operatorname{Tr}\Big(\kappa^\dagger T^\kappa\Big) \\
&- 4 \tilde{f} \tilde{\lambda}^\dagger \tilde{\lambda} \operatorname{Tr}\Big(\tilde{\lambda}^\dagger T^{\tilde{\lambda}}\Big) - 2 T^{\tilde{f}} \operatorname{Tr}\Big(f f^\dagger \tilde{f} \tilde{f}^\dagger\Big) - 3 T^{\tilde{f}} \operatorname{Tr}\Big(\tilde{f} \tilde{f}^\dagger \tilde{f} \tilde{f}^\dagger\Big) \\
&- T^{\tilde{f}} \operatorname{Tr}\Big(\tilde{f} h^{E\dagger} h^E \tilde{f}^\dagger\Big) - T^{\tilde{f}} \operatorname{Tr}\Big(\tilde{f} \tilde{\lambda}^\dagger \tilde{\lambda} \tilde{f}^\dagger\Big) - 3 T^{\tilde{f}} \operatorname{Tr}\Big(g^D g^{D\dagger} y^{UT} y^{U*}\Big) \\
&- 3 T^{\tilde{f}} \operatorname{Tr}\Big(y^D y^{U\dagger} y^U y^{D\dagger}\Big) - 9 T^{\tilde{f}} \operatorname{Tr}\Big(y^U y^{U\dagger} y^U y^{U\dagger}\Big) \\
&- \frac{1}{50} \tilde{f} \Big(1188 g_1^4 M_1 + 27 g_1^2 g_1'^2 M_1 + 180 g_1^2 g_2^2 M_1 + 27 g_1^2 g_1'^2 M_1' + 4408 g_1'^4 M_1' \\
&+ 195 g_1'^2 g_2^2 M_1' + 180 g_1^2 g_2^2 M_2 + 195 g_1'^2 g_2^2 M_2 + 3300 g_2^4 M_2 + 600 \lambda^* |\lambda|^2 T_\lambda \\
&+ 150 g_1'^2 M_1' \operatorname{Tr}\Big(\tilde{f} \tilde{f}^\dagger\Big) + 80 g_1^2 M_1 \operatorname{Tr}\Big(y^U y^{U\dagger}\Big) - 30 g_1'^2 M_1' \operatorname{Tr}\Big(y^U y^{U\dagger}\Big) \\
&+ 1600 g_3^2 M_3 \operatorname{Tr}\Big(y^U y^{U\dagger}\Big) - 150 g_1'^2 \operatorname{Tr}\Big(\tilde{f}^\dagger T^{\tilde{f}}\Big) - 80 g_1^2 \operatorname{Tr}\Big(y^{U\dagger} T^U\Big) \\
&+ 30 g_1'^2 \operatorname{Tr}\Big(y^{U\dagger} T^U\Big) - 1600 g_3^2 \operatorname{Tr}\Big(y^{U\dagger} T^U\Big) + 50 \lambda^* \Big\{ T_\lambda \Big[2 \operatorname{Tr}\Big(f f^\dagger\Big) \\
&+ 2 \operatorname{Tr}\Big(y^E y^{E\dagger}\Big) + 2|\sigma|^2 - 3 g_1'^2 + 4 \operatorname{Tr}\Big(\tilde{\lambda} \tilde{\lambda}^\dagger\Big) + 6 \operatorname{Tr}\Big(\kappa \kappa^\dagger\Big) + 6 \operatorname{Tr}\Big(y^D y^{D\dagger}\Big)\Big] \\
&+ \lambda \Big[2 \operatorname{Tr}\Big(f^\dagger T^f\Big) + 2 \operatorname{Tr}\Big(y^{E\dagger} T^E\Big) + 2 \sigma^* T_\sigma + 3 g_1'^2 M_1' + 4 \operatorname{Tr}\Big(\tilde{\lambda}^\dagger T^{\tilde{\lambda}}\Big) \\
&+ 6 \operatorname{Tr}\Big(\kappa^\dagger T^\kappa\Big) + 6 \operatorname{Tr}\Big(y^{D\dagger} T^D\Big)\Big]\Big\} + 200 \operatorname{Tr}\Big(f f^\dagger T^{\tilde{f}} \tilde{f}^\dagger\Big) + 200 \operatorname{Tr}\Big(\tilde{f} \tilde{f}^\dagger T^f f^\dagger\Big) \\
&+ 600 \operatorname{Tr}\Big(\tilde{f} \tilde{f}^\dagger T^{\tilde{f}} \tilde{f}^\dagger\Big) + 100 \operatorname{Tr}\Big(\tilde{f} h^{E\dagger} T^{h^E} \tilde{f}^\dagger\Big) + 100 \operatorname{Tr}\Big(\tilde{f} \tilde{\lambda}^\dagger T^{\tilde{\lambda}} \tilde{f}^\dagger\Big) \\
&+ 100 \operatorname{Tr}\Big(h^E \tilde{f}^\dagger T^{\tilde{f}} h^{E\dagger}\Big) + 300 \operatorname{Tr}\Big(y^D y^{U\dagger} T^U y^{D\dagger}\Big) + 300 \operatorname{Tr}\Big(y^U y^{D\dagger} T^D y^{U\dagger}\Big) \\
&+ 1800 \operatorname{Tr}\Big(y^U y^{U\dagger} T^U y^{U\dagger}\Big) + 100 \operatorname{Tr}\Big(\tilde{\lambda} \tilde{f}^\dagger T^{\tilde{f}} \tilde{\lambda}^\dagger\Big) + 300 \operatorname{Tr}\Big(g^{D\dagger} y^{UT} y^{U*} T^{g^D}\Big) \\
&+ 300 \operatorname{Tr}\Big(y^{U\dagger} T^U g^{D*} g^{DT}\Big)\Big), \qquad \text{(D.72)}
\end{aligned}
$$

$$
\begin{aligned}
\beta_{T^f}^{(1)} &= 4ff^\dagger T^f + 2f\tilde{\lambda}^* T^{\tilde{\lambda}T} + 2\tilde{f}\tilde{f}^\dagger T^f + 5T^f f^\dagger f + T^f \tilde{\lambda}^* \tilde{\lambda}^T + 4T^{\tilde{f}} \tilde{f}^\dagger f \\
&\quad - \frac{3}{5} g_1^2 T^f - \frac{19}{10} g_1'^2 T^f - 3g_2^2 T^f + |\lambda|^2 T^f + T^f \operatorname{Tr}\Big(ff^\dagger\Big) + 3T^f \operatorname{Tr}\Big(y^D y^{D\dagger}\Big) \\
&\quad + T^f \operatorname{Tr}\Big(y^E y^{E\dagger}\Big) + f\Big[2\lambda^* T_\lambda + 2\operatorname{Tr}\Big(f^\dagger T^f\Big) + 2\operatorname{Tr}\Big(y^{E\dagger} T^E\Big) + 6g_2^2 M_2 \\
&\quad + 6\operatorname{Tr}\Big(y^{D\dagger} T^D\Big) + \frac{19}{5} g_1'^2 M_1' + \frac{6}{5} g_1^2 M_1\Big], \qquad \text{(D.73)} \\
\beta_{T^f}^{(2)} &= \frac{6}{5} g_1^2 ff^\dagger T^f + \frac{9}{5} g_1'^2 ff^\dagger T^f + 6g_2^2 ff^\dagger T^f - 4|\lambda|^2 ff^\dagger T^f \\
&\quad - 3g_1'^2 M_1' f\tilde{\lambda}^* \tilde{\lambda}^T + 3g_1'^2 f\tilde{\lambda}^* T^{\tilde{\lambda}T} - 4|\lambda|^2 f\tilde{\lambda}^* T^{\tilde{\lambda}T} - 2|\sigma|^2 f\tilde{\lambda}^* T^{\tilde{\lambda}T} \\
&\quad - \frac{12}{5} g_1^2 M_1 \tilde{f}\tilde{f}^\dagger f + \frac{12}{5} g_1'^2 M_1' \tilde{f}\tilde{f}^\dagger f - 12g_2^2 M_2 \tilde{f}\tilde{f}^\dagger f + \frac{6}{5} g_1^2 \tilde{f}\tilde{f}^\dagger T^f \\
&\quad - \frac{6}{5} g_1'^2 \tilde{f}\tilde{f}^\dagger T^f + 6g_2^2 \tilde{f}\tilde{f}^\dagger T^f - 2|\lambda|^2 \tilde{f}\tilde{f}^\dagger T^f + \frac{12}{5} g_1^2 T^f f^\dagger f \\
&\quad - \frac{9}{10} g_1'^2 T^f f^\dagger f + 12g_2^2 T^f f^\dagger f - 5|\lambda|^2 T^f f^\dagger f + \frac{3}{2} g_1'^2 T^f \tilde{\lambda}^* \tilde{\lambda}^T \\
&\quad - 2|\lambda|^2 T^f \tilde{\lambda}^* \tilde{\lambda}^T - |\sigma|^2 T^f \tilde{\lambda}^* \tilde{\lambda}^T + \frac{12}{5} g_1^2 T^{\tilde{f}} \tilde{f}^\dagger f - \frac{12}{5} g_1'^2 T^{\tilde{f}} \tilde{f}^\dagger f \\
&\quad + 12g_2^2 T^{\tilde{f}} \tilde{f}^\dagger f - 4|\lambda|^2 T^{\tilde{f}} \tilde{f}^\dagger f - 6ff^\dagger ff^\dagger T^f - 4ff^\dagger \tilde{f}\tilde{f}^\dagger T^f \\
&\quad - 8ff^\dagger T^f f^\dagger f - 4ff^\dagger T^{\tilde{f}} \tilde{f}^\dagger f - 2f\tilde{\lambda}^* \tilde{f}^T \tilde{f}^* T^{\tilde{\lambda}T} - 2f\tilde{\lambda}^* h^{ET} h^{E*} T^{\tilde{\lambda}T} \\
&\quad - 2f\tilde{\lambda}^* \tilde{\lambda}^T f^\dagger T^f - 2f\tilde{\lambda}^* \tilde{\lambda}^T \tilde{\lambda}^* T^{\tilde{\lambda}T} - 2f\tilde{\lambda}^* T^{\tilde{f}T} \tilde{f}^* \tilde{\lambda}^T - 2f\tilde{\lambda}^* T^{h^E T} h^{E*} \tilde{\lambda}^T \\
&\quad - 4f\tilde{\lambda}^* T^{\tilde{\lambda}T} f^\dagger f - 2f\tilde{\lambda}^* T^{\tilde{\lambda}T} \tilde{\lambda}^* \tilde{\lambda}^T - 2\tilde{f}\tilde{f}^\dagger \tilde{f}\tilde{f}^\dagger T^f - 4\tilde{f}\tilde{f}^\dagger T^{\tilde{f}} \tilde{f}^\dagger f \\
&\quad - 2\tilde{f} h^{E\dagger} h^E \tilde{f}^\dagger T^f - 4\tilde{f} h^{E\dagger} T^{h^E} \tilde{f}^\dagger f - 2\tilde{f}\tilde{\lambda}^\dagger \tilde{\lambda} \tilde{f}^\dagger T^f - 4\tilde{f}\tilde{\lambda}^\dagger T^{\tilde{\lambda}} \tilde{f}^\dagger f \\
&\quad - 6T^f f^\dagger ff^\dagger f - 2T^f f^\dagger \tilde{f}\tilde{f}^\dagger f - T^f \tilde{\lambda}^* \tilde{f}^T \tilde{f}^* \tilde{\lambda}^T - T^f \tilde{\lambda}^* h^{ET} h^{E*} \tilde{\lambda}^T \\
&\quad - 4T^f \tilde{\lambda}^* \tilde{\lambda}^T f^\dagger f - T^f \tilde{\lambda}^* \tilde{\lambda}^T \tilde{\lambda}^* \tilde{\lambda}^T - 4T^{\tilde{f}} \tilde{f}^\dagger \tilde{f}\tilde{f}^\dagger f - 4T^{\tilde{f}} h^{E\dagger} h^E \tilde{f}^\dagger f \\
&\quad - 4T^{\tilde{f}} \tilde{\lambda}^\dagger \tilde{\lambda} \tilde{f}^\dagger f + \frac{297}{50} g_1^4 T^f + \frac{27}{100} g_1^2 g_1'^2 T^f + \frac{551}{25} g_1'^4 T^f + \frac{9}{5} g_1^2 g_2^2 T^f \\
&\quad + \frac{39}{20} g_1'^2 g_2^2 T^f + \frac{33}{2} g_2^4 T^f + g_1'^2 |\lambda|^2 T^f - 3|\lambda|^4 T^f - |\sigma|^2 |\lambda|^2 T^f \\
&\quad - 4\lambda^* f\tilde{\lambda}^* \tilde{\lambda}^T T_\lambda - 4\lambda^* \tilde{f}\tilde{f}^\dagger f T_\lambda - 2\sigma^* f\tilde{\lambda}^* \tilde{\lambda}^T T_\sigma - 4ff^\dagger T^f \operatorname{Tr}\Big(ff^\dagger\Big) \\
&\quad - 5T^f f^\dagger f \operatorname{Tr}\Big(ff^\dagger\Big) + g_1'^2 T^f \operatorname{Tr}\Big(ff^\dagger\Big) - 2\tilde{f}\tilde{f}^\dagger T^f \operatorname{Tr}\Big(\tilde{f}\tilde{f}^\dagger\Big) \\
&\quad - 4T^{\tilde{f}} \tilde{f}^\dagger f \operatorname{Tr}\Big(\tilde{f}\tilde{f}^\dagger\Big) - |\lambda|^2 T^f \operatorname{Tr}\Big(\tilde{f}\tilde{f}^\dagger\Big) - 12ff^\dagger T^f \operatorname{Tr}\Big(y^D y^{D\dagger}\Big) \\
&\quad - 15T^f f^\dagger f \operatorname{Tr}\Big(y^D y^{D\dagger}\Big) - \frac{2}{5} g_1^2 T^f \operatorname{Tr}\Big(y^D y^{D\dagger}\Big) - \frac{3}{5} g_1'^2 T^f \operatorname{Tr}\Big(y^D y^{D\dagger}\Big) \\
&\quad + 16g_3^2 T^f \operatorname{Tr}\Big(y^D y^{D\dagger}\Big) - 4ff^\dagger T^f \operatorname{Tr}\Big(y^E y^{E\dagger}\Big) - 5T^f f^\dagger f \operatorname{Tr}\Big(y^E y^{E\dagger}\Big) \\
&\quad + \frac{6}{5} g_1^2 T^f \operatorname{Tr}\Big(y^E y^{E\dagger}\Big) - \frac{1}{5} g_1'^2 T^f \operatorname{Tr}\Big(y^E y^{E\dagger}\Big) - 6\tilde{f}\tilde{f}^\dagger T^f \operatorname{Tr}\Big(y^U y^{U\dagger}\Big)
\end{aligned}
$$

$$
\begin{aligned}
&- 12T^{\tilde{f}}\tilde{f}^{\dagger}f\,\mathrm{Tr}\Big(y^{U}y^{U\dagger}\Big) - 3|\lambda|^2T^{f}\,\mathrm{Tr}\Big(y^{U}y^{U\dagger}\Big) - 6f\tilde{\lambda}^{*}T^{\tilde{\lambda}T}\,\mathrm{Tr}\Big(\kappa\kappa^{\dagger}\Big)\\
&- 3T^{f}\tilde{\lambda}^{*}\tilde{\lambda}^{T}\,\mathrm{Tr}\Big(\kappa\kappa^{\dagger}\Big) - 3|\lambda|^2T^{f}\,\mathrm{Tr}\Big(\kappa\kappa^{\dagger}\Big) - 4f\tilde{\lambda}^{*}T^{\tilde{\lambda}T}\,\mathrm{Tr}\Big(\tilde{\lambda}\tilde{\lambda}^{\dagger}\Big)\\
&- 2T^{f}\tilde{\lambda}^{*}\tilde{\lambda}^{T}\,\mathrm{Tr}\Big(\tilde{\lambda}\tilde{\lambda}^{\dagger}\Big) - 2|\lambda|^2T^{f}\,\mathrm{Tr}\Big(\tilde{\lambda}\tilde{\lambda}^{\dagger}\Big) - 4\tilde{f}\tilde{f}^{\dagger}f\,\mathrm{Tr}\Big(\tilde{f}^{\dagger}T^{\tilde{f}}\Big)\\
&- \frac{3}{5}ff^{\dagger}f\Big[10\lambda^{*}T_{\lambda} + 10\,\mathrm{Tr}\Big(f^{\dagger}T^{f}\Big) + 10\,\mathrm{Tr}\Big(y^{E\dagger}T^{E}\Big) + 20g_2^2M_2\\
&+ 30\,\mathrm{Tr}\Big(y^{D\dagger}T^{D}\Big) + 4g_1^2M_1 + g_1'^2M_1'\Big] - 12\tilde{f}\tilde{f}^{\dagger}f\,\mathrm{Tr}\Big(y^{U\dagger}T^{U}\Big)\\
&- 6f\tilde{\lambda}^{*}\tilde{\lambda}^{T}\,\mathrm{Tr}\Big(\kappa^{\dagger}T^{\kappa}\Big) - 4f\tilde{\lambda}^{*}\tilde{\lambda}^{T}\,\mathrm{Tr}\Big(\tilde{\lambda}^{\dagger}T^{\tilde{\lambda}}\Big) - 3T^{f}\,\mathrm{Tr}\Big(ff^{\dagger}ff^{\dagger}\Big)\\
&- 2T^{f}\,\mathrm{Tr}\Big(ff^{\dagger}\tilde{f}\tilde{f}^{\dagger}\Big) - 3T^{f}\,\mathrm{Tr}\Big(g^{D}g^{D\dagger}y^{DT}y^{D*}\Big) - 2T^{f}\,\mathrm{Tr}\Big(h^{E}h^{E\dagger}y^{E}y^{E\dagger}\Big)\\
&- 9T^{f}\,\mathrm{Tr}\Big(y^{D}y^{D\dagger}y^{D}y^{D\dagger}\Big) - 3T^{f}\,\mathrm{Tr}\Big(y^{D}y^{U\dagger}y^{U}y^{D\dagger}\Big) - 3T^{f}\,\mathrm{Tr}\Big(y^{E}y^{E\dagger}y^{E}y^{E\dagger}\Big)\\
&- T^{f}\,\mathrm{Tr}\Big(\tilde{\lambda}\tilde{\lambda}^{\dagger}f^{T}f^{*}\Big) - \frac{1}{50}f\Big(1188g_1^4M_1 + 27g_1^2g_1'^2M_1 + 180g_1^2g_2^2M_1\\
&+ 27g_1^2g_1'^2M_1' + 4408g_1'^4M_1' + 195g_1'^2g_2^2M_1' + 180g_1^2g_2^2M_2 + 195g_1'^2g_2^2M_2\\
&+ 3300g_2^4M_2 + 600\lambda^{*}|\lambda|^2T_{\lambda} + 100g_1'^2M_1'\,\mathrm{Tr}\Big(ff^{\dagger}\Big) - 40g_1^2M_1\,\mathrm{Tr}\Big(y^{D}y^{D\dagger}\Big)\\
&- 60g_1'^2M_1'\,\mathrm{Tr}\Big(y^{D}y^{D\dagger}\Big) + 1600g_3^2M_3\,\mathrm{Tr}\Big(y^{D}y^{D\dagger}\Big) + 120g_1^2M_1\,\mathrm{Tr}\Big(y^{E}y^{E\dagger}\Big)\\
&- 20g_1'^2M_1'\,\mathrm{Tr}\Big(y^{E}y^{E\dagger}\Big) - 100g_1'^2\,\mathrm{Tr}\Big(f^{\dagger}T^{f}\Big) + 40g_1^2\,\mathrm{Tr}\Big(y^{D\dagger}T^{D}\Big)\\
&+ 60g_1'^2\,\mathrm{Tr}\Big(y^{D\dagger}T^{D}\Big) - 1600g_3^2\,\mathrm{Tr}\Big(y^{D\dagger}T^{D}\Big) - 120g_1^2\,\mathrm{Tr}\Big(y^{E\dagger}T^{E}\Big)\\
&+ 20g_1'^2\,\mathrm{Tr}\Big(y^{E\dagger}T^{E}\Big) + 100\lambda^{*}\Big\{T_{\lambda}\Big[2\,\mathrm{Tr}\Big(\tilde{\lambda}\tilde{\lambda}^{\dagger}\Big) + 3\,\mathrm{Tr}\Big(\kappa\kappa^{\dagger}\Big) + 3\,\mathrm{Tr}\Big(y^{U}y^{U\dagger}\Big)\\
&- g_1'^2 + |\sigma|^2 + \mathrm{Tr}\Big(\tilde{f}\tilde{f}^{\dagger}\Big)\Big] + \lambda\Big[2\,\mathrm{Tr}\Big(\tilde{\lambda}^{\dagger}T^{\tilde{\lambda}}\Big) + 3\,\mathrm{Tr}\Big(\kappa^{\dagger}T^{\kappa}\Big) + 3\,\mathrm{Tr}\Big(y^{U\dagger}T^{U}\Big)\\
&+ g_1'^2M_1' + \sigma^{*}T_{\sigma} + \mathrm{Tr}\Big(\tilde{f}^{\dagger}T^{\tilde{f}}\Big)\Big]\Big\} + 600\,\mathrm{Tr}\Big(ff^{\dagger}T^{f}f^{\dagger}\Big)\\
&+ 200\,\mathrm{Tr}\Big(ff^{\dagger}T^{\tilde{f}}\tilde{f}^{\dagger}\Big) + 200\,\mathrm{Tr}\Big(\tilde{f}\tilde{f}^{\dagger}T^{f}f^{\dagger}\Big) + 200\,\mathrm{Tr}\Big(h^{E}h^{E\dagger}T^{E}y^{E\dagger}\Big)\\
&+ 1800\,\mathrm{Tr}\Big(y^{D}y^{D\dagger}T^{D}y^{D\dagger}\Big) + 300\,\mathrm{Tr}\Big(y^{D}y^{U\dagger}T^{U}y^{D\dagger}\Big) + 200\,\mathrm{Tr}\Big(y^{E}y^{E\dagger}T^{h^{E}}h^{E\dagger}\Big)\\
&+ 600\,\mathrm{Tr}\Big(y^{E}y^{E\dagger}T^{E}y^{E\dagger}\Big) + 300\,\mathrm{Tr}\Big(y^{U}y^{D\dagger}T^{D}y^{U\dagger}\Big) + 100\,\mathrm{Tr}\Big(f^{\dagger}T^{f}\tilde{\lambda}^{*}\tilde{\lambda}^{T}\Big)\\
&+ 300\,\mathrm{Tr}\Big(g^{D\dagger}y^{DT}y^{D*}T^{g^{D}}\Big) + 300\,\mathrm{Tr}\Big(y^{D\dagger}T^{D}g^{D*}g^{DT}\Big)\\
&+ 100\,\mathrm{Tr}\Big(\tilde{\lambda}^{\dagger}f^{T}f^{*}T^{\tilde{\lambda}}\Big)\Big), \qquad \text{(D.74)}
\end{aligned}
$$

$$
\beta_{T^U}^{(1)} = 2y^{U}y^{D\dagger}T^{D} + 4y^{U}y^{U\dagger}T^{U} + 2y^{U}g^{D*}T^{g^{D}T} + T^{U}y^{D\dagger}y^{D} + 5T^{U}y^{U\dagger}y^{U}
$$

$$
\begin{aligned}
&+ T^U g^{D*} g^{DT} - \frac{13}{15} g_1^2 T^U - \frac{3}{10} g_1'^2 T^U - 3 g_2^2 T^U - \frac{16}{3} g_3^2 T^U + |\lambda|^2 T^U \\
&+ T^U \operatorname{Tr}\Big(\tilde{f}\tilde{f}^\dagger\Big) + 3 T^U \operatorname{Tr}\Big(y^U y^{U\dagger}\Big) + y^U \Big[2\lambda^* T_\lambda + 2 \operatorname{Tr}\Big(\tilde{f}^\dagger T^{\tilde{f}}\Big) + 6 g_2^2 M_2 \\
&+ 6 \operatorname{Tr}\Big(y^{U\dagger} T^U\Big) + \frac{26}{15} g_1^2 M_1 + \frac{32}{3} g_3^2 M_3 + \frac{3}{5} g_1'^2 M_1'\Big], \qquad \text{(D.75)} \\
\beta_{T^U}^{(2)} = &\frac{4}{5} g_1^2 y^U y^{D\dagger} T^D + \frac{6}{5} g_1'^2 y^U y^{D\dagger} T^D - 2|\lambda|^2 y^U y^{D\dagger} T^D - \frac{4}{5} g_1^2 M_1 y^U y^{U\dagger} y^U \\
&- \frac{6}{5} g_1'^2 M_1' y^U y^{U\dagger} y^U - 12 g_2^2 M_2 y^U y^{U\dagger} y^U + \frac{6}{5} g_1^2 y^U y^{U\dagger} T^U + \frac{4}{5} g_1'^2 y^U y^{U\dagger} T^U \\
&+ 6 g_2^2 y^U y^{U\dagger} T^U - 4|\lambda|^2 y^U y^{U\dagger} T^U - \frac{4}{5} g_1^2 M_1 y^U g^{D*} g^{DT} - \frac{6}{5} g_1'^2 M_1' y^U g^{D*} g^{DT} \\
&+ \frac{4}{5} g_1^2 y^U g^{D*} T^{g^D T} + \frac{6}{5} g_1'^2 y^U g^{D*} T^{g^D T} - 2|\tilde{\sigma}|^2 y^U g^{D*} T^{g^D T} + \frac{2}{5} g_1^2 T^U y^{D\dagger} y^D \\
&+ \frac{3}{5} g_1'^2 T^U y^{D\dagger} y^D - |\lambda|^2 T^U y^{D\dagger} y^D + g_1'^2 T^U y^{U\dagger} y^U + 12 g_2^2 T^U y^{U\dagger} y^U \\
&- 5|\lambda|^2 T^U y^{U\dagger} y^U + \frac{2}{5} g_1^2 T^U g^{D*} g^{DT} + \frac{3}{5} g_1'^2 T^U g^{D*} g^{DT} - |\tilde{\sigma}|^2 T^U g^{D*} g^{DT} \\
&- 4 y^U y^{D\dagger} y^D y^{D\dagger} T^D - 2 y^U y^{D\dagger} y^D y^{U\dagger} T^U - 4 y^U y^{D\dagger} T^D y^{D\dagger} y^D \\
&- 4 y^U y^{D\dagger} T^D y^{U\dagger} y^U - 6 y^U y^{U\dagger} y^U y^{U\dagger} T^U - 8 y^U y^{U\dagger} T^U y^{U\dagger} y^U \\
&- 2 y^U g^{D*} g^{DT} y^{U\dagger} T^U - 4 y^U g^{D*} g^{DT} g^{D*} T^{g^D T} - 2 y^U g^{D*} \kappa^T \kappa^* T^{g^D T} \\
&- 4 y^U g^{D*} T^{g^D T} y^{U\dagger} y^U - 4 y^U g^{D*} T^{g^D T} g^{D*} g^{DT} - 2 y^U g^{D*} T^{\kappa T} \kappa^* g^{DT} \\
&- 2 T^U y^{D\dagger} y^D y^{D\dagger} y^D - 4 T^U y^{D\dagger} y^D y^{U\dagger} y^U - 6 T^U y^{U\dagger} y^U y^{U\dagger} y^U \\
&- 4 T^U g^{D*} g^{DT} y^{U\dagger} y^U - 2 T^U g^{D*} g^{DT} g^{D*} g^{DT} - T^U g^{D*} \kappa^T \kappa^* g^{DT} + \frac{3913}{450} g_1^4 T^U \\
&+ \frac{161}{300} g_1^2 g_1'^2 T^U + \frac{81}{25} g_1'^4 T^U + g_1^2 g_2^2 T^U + \frac{3}{4} g_1'^2 g_2^2 T^U + \frac{33}{2} g_2^4 T^U + \frac{136}{45} g_1^2 g_3^2 T^U \\
&+ \frac{8}{15} g_1'^2 g_3^2 T^U + 8 g_2^2 g_3^2 T^U + \frac{128}{9} g_3^4 T^U + \frac{3}{2} g_1'^2 |\lambda|^2 T^U - 3|\lambda|^4 T^U \\
&- |\sigma|^2 |\lambda|^2 T^U - 6\lambda^* y^U y^{U\dagger} y^U T_\lambda - 2\tilde{\sigma}^* y^U g^{D*} g^{DT} T_{\tilde{\sigma}} - 2 y^U y^{D\dagger} T^D \operatorname{Tr}\Big(f f^\dagger\Big) \\
&- T^U y^{D\dagger} y^D \operatorname{Tr}\Big(f f^\dagger\Big) - |\lambda|^2 T^U \operatorname{Tr}\Big(f f^\dagger\Big) - 4 y^U y^{U\dagger} T^U \operatorname{Tr}\Big(\tilde{f}\tilde{f}^\dagger\Big) \\
&- 5 T^U y^{U\dagger} y^U \operatorname{Tr}\Big(\tilde{f}\tilde{f}^\dagger\Big) + \frac{3}{2} g_1'^2 T^U \operatorname{Tr}\Big(\tilde{f}\tilde{f}^\dagger\Big) - 6 y^U g^{D*} T^{g^D T} \operatorname{Tr}\Big(g^D g^{D\dagger}\Big) \\
&- 3 T^U g^{D*} g^{DT} \operatorname{Tr}\Big(g^D g^{D\dagger}\Big) - 2 y^U g^{D*} T^{g^D T} \operatorname{Tr}\Big(h^E h^{E\dagger}\Big) \\
&- T^U g^{D*} g^{DT} \operatorname{Tr}\Big(h^E h^{E\dagger}\Big) - 6 y^U y^{D\dagger} T^D \operatorname{Tr}\Big(y^D y^{D\dagger}\Big) \\
&- 3 T^U y^{D\dagger} y^D \operatorname{Tr}\Big(y^D y^{D\dagger}\Big) - 3|\lambda|^2 T^U \operatorname{Tr}\Big(y^D y^{D\dagger}\Big) - 2 y^U y^{D\dagger} T^D \operatorname{Tr}\Big(y^E y^{E\dagger}\Big) \\
&- T^U y^{D\dagger} y^D \operatorname{Tr}\Big(y^E y^{E\dagger}\Big) - |\lambda|^2 T^U \operatorname{Tr}\Big(y^E y^{E\dagger}\Big) - 12 y^U y^{U\dagger} T^U \operatorname{Tr}\Big(y^U y^{U\dagger}\Big)
\end{aligned}
$$

$$
\begin{aligned}
&- 15T^U y^{U\dagger} y^U \operatorname{Tr}\Big(y^U y^{U\dagger}\Big) + \frac{4}{5} g_1^2 T^U \operatorname{Tr}\Big(y^U y^{U\dagger}\Big) - \frac{3}{10} g_1'^2 T^U \operatorname{Tr}\Big(y^U y^{U\dagger}\Big) \\
&+ 16 g_3^2 T^U \operatorname{Tr}\Big(y^U y^{U\dagger}\Big) - 3|\lambda|^2 T^U \operatorname{Tr}\Big(\kappa\kappa^\dagger\Big) - 2|\lambda|^2 T^U \operatorname{Tr}\Big(\tilde{\lambda}\tilde{\lambda}^\dagger\Big) \\
&- 6 y^U y^{U\dagger} y^U \operatorname{Tr}\Big(\tilde{f}^\dagger T^{\tilde{f}}\Big) - 6 y^U g^{D*} g^{DT} \operatorname{Tr}\Big(g^{D\dagger} T^{g^D}\Big) - 2 y^U g^{D*} g^{DT} \operatorname{Tr}\Big(h^{E\dagger} T^{h^E}\Big) \\
&- \frac{2}{5} y^U y^{D\dagger} y^D \Big[15 \operatorname{Tr}\Big(y^{D\dagger} T^D\Big) + 2 g_1^2 M_1 + 3 g_1'^2 M_1' + 5\lambda^* T_\lambda + 5 \operatorname{Tr}\Big(f^\dagger T^f\Big) \\
&+ 5 \operatorname{Tr}\Big(y^{E\dagger} T^E\Big)\Big] - 18 y^U y^{U\dagger} y^U \operatorname{Tr}\Big(y^{U\dagger} T^U\Big) - 2T^U \operatorname{Tr}\Big(f f^\dagger \tilde{f} \tilde{f}^\dagger\Big) \\
&- 3T^U \operatorname{Tr}\Big(\tilde{f} \tilde{f}^\dagger \tilde{f} \tilde{f}^\dagger\Big) - T^U \operatorname{Tr}\Big(\tilde{f} h^{E\dagger} h^E \tilde{f}^\dagger\Big) - T^U \operatorname{Tr}\Big(\tilde{f} \tilde{\lambda}^\dagger \tilde{\lambda} \tilde{f}^\dagger\Big) \\
&- 3T^U \operatorname{Tr}\Big(g^D g^{D\dagger} y^{UT} y^{U*}\Big) - 3T^U \operatorname{Tr}\Big(y^D y^{U\dagger} y^U y^{D\dagger}\Big) - 9T^U \operatorname{Tr}\Big(y^U y^{U\dagger} y^U y^{U\dagger}\Big) \\
&- \frac{1}{450} y^U \Big(15652 g_1^4 M_1 + 483 g_1^2 g_1'^2 M_1 + 900 g_1^2 g_2^2 M_1 + 2720 g_1^2 g_3^2 M_1 \\
&+ 483 g_1^2 g_1'^2 M_1' + 5832 g_1'^4 M_1' + 675 g_1'^2 g_2^2 M_1' + 480 g_1'^2 g_3^2 M_1' + 2720 g_1^2 g_3^2 M_3 \\
&+ 480 g_1'^2 g_3^2 M_3 + 7200 g_2^2 g_3^2 M_3 + 25600 g_3^4 M_3 + 900 g_1^2 g_2^2 M_2 + 675 g_1'^2 g_2^2 M_2 \\
&+ 29700 g_2^4 M_2 + 7200 g_2^2 g_3^2 M_2 + 5400 \lambda^* |\lambda|^2 T_\lambda + 1350 g_1'^2 M_1' \operatorname{Tr}\Big(\tilde{f} \tilde{f}^\dagger\Big) \\
&+ 720 g_1^2 M_1 \operatorname{Tr}\Big(y^U y^{U\dagger}\Big) - 270 g_1'^2 M_1' \operatorname{Tr}\Big(y^U y^{U\dagger}\Big) + 14400 g_3^2 M_3 \operatorname{Tr}\Big(y^U y^{U\dagger}\Big) \\
&- 1350 g_1'^2 \operatorname{Tr}\Big(\tilde{f}^\dagger T^{\tilde{f}}\Big) - 720 g_1^2 \operatorname{Tr}\Big(y^{U\dagger} T^U\Big) + 270 g_1'^2 \operatorname{Tr}\Big(y^{U\dagger} T^U\Big) \\
&- 14400 g_3^2 \operatorname{Tr}\Big(y^{U\dagger} T^U\Big) + 450 \lambda^* \Big\{ T_\lambda \Big[2 \operatorname{Tr}\Big(f f^\dagger\Big) + 2 \operatorname{Tr}\Big(y^E y^{E\dagger}\Big) + 2|\sigma|^2 \\
&- 3 g_1'^2 + 4 \operatorname{Tr}\Big(\tilde{\lambda}\tilde{\lambda}^\dagger\Big) + 6 \operatorname{Tr}\Big(\kappa\kappa^\dagger\Big) + 6 \operatorname{Tr}\Big(y^D y^{D\dagger}\Big)\Big] + \lambda \Big[2 \operatorname{Tr}\Big(f^\dagger T^f\Big) \\
&+ 2 \operatorname{Tr}\Big(y^{E\dagger} T^E\Big) + 2\sigma^* T_\sigma + 3 g_1'^2 M_1' + 4 \operatorname{Tr}\Big(\tilde{\lambda}^\dagger T^{\tilde{\lambda}}\Big) + 6 \operatorname{Tr}\Big(\kappa^\dagger T^\kappa\Big) \\
&+ 6 \operatorname{Tr}\Big(y^{D\dagger} T^D\Big)\Big]\Big\} + 1800 \operatorname{Tr}\Big(f f^\dagger T^{\tilde{f}} \tilde{f}^\dagger\Big) + 1800 \operatorname{Tr}\Big(\tilde{f} \tilde{f}^\dagger T^f f^\dagger\Big) \\
&+ 5400 \operatorname{Tr}\Big(\tilde{f} \tilde{f}^\dagger T^{\tilde{f}} \tilde{f}^\dagger\Big) + 900 \operatorname{Tr}\Big(\tilde{f} h^{E\dagger} T^{h^E} \tilde{f}^\dagger\Big) + 900 \operatorname{Tr}\Big(\tilde{f} \tilde{\lambda}^\dagger T^{\tilde{\lambda}} \tilde{f}^\dagger\Big) \\
&+ 900 \operatorname{Tr}\Big(h^E \tilde{f}^\dagger T^{\tilde{f}} h^{E\dagger}\Big) + 2700 \operatorname{Tr}\Big(y^D y^{U\dagger} T^U y^{D\dagger}\Big) + 2700 \operatorname{Tr}\Big(y^U y^{D\dagger} T^D y^{U\dagger}\Big) \\
&+ 16200 \operatorname{Tr}\Big(y^U y^{U\dagger} T^U y^{U\dagger}\Big) + 900 \operatorname{Tr}\Big(\tilde{\lambda} \tilde{f}^\dagger T^{\tilde{f}} \tilde{\lambda}^\dagger\Big) \\
&+ 2700 \operatorname{Tr}\Big(g^{D\dagger} y^{UT} y^{U*} T^{g^D}\Big) + 2700 \operatorname{Tr}\Big(y^{U\dagger} T^U g^{D*} g^{DT}\Big)\Big) . \qquad \text{(D.76)}
\end{aligned}
$$

D.6 Soft-breaking Bilinear and Linear Couplings

The β functions for the soft-breaking bilinears are given by

$$\begin{aligned}
\beta^{(1)}_{B_\phi\mu_\phi} &= 2B_\phi\mu_\phi\Big(2|\tilde\sigma|^2+4|\kappa_\phi|^2+|\sigma|^2\Big)+4\mu_\phi\Big(2\kappa_\phi^* T_{\kappa_\phi}+2\tilde\sigma^* T_{\tilde\sigma}+\sigma^* T_\sigma\Big)\\
&\quad -8\tilde\sigma^*\kappa_\phi B_L\mu_L\,, \qquad\qquad (D.77)\\
\beta^{(2)}_{B_\phi\mu_\phi} &= B_\phi\mu_\phi\Big\{-32|\kappa_\phi|^4-8|\tilde\sigma|^4-4|\sigma|^4+|\tilde\sigma|^2\Big[\frac{12}{5}g_1^2+\frac{8}{5}g_1'^2+12g_2^2-32|\kappa_\phi|^2\\
&\quad -12\,\mathrm{Tr}\Big(g^D g^{D\dagger}\Big)-4\,\mathrm{Tr}\Big(h^E h^{E\dagger}\Big)\Big]+|\sigma|^2\Big[5g_1'^2-4|\lambda|^2-16|\kappa_\phi|^2\\
&\quad -4\,\mathrm{Tr}\Big(\tilde\lambda\tilde\lambda^\dagger\Big)-6\,\mathrm{Tr}\Big(\kappa\kappa^\dagger\Big)\Big]\Big\}-\mu_\phi\Big\{16|\sigma|^2\sigma^* T_\sigma+80|\kappa_\phi|^2\kappa_\phi^* T_{\kappa_\phi}\\
&\quad +32|\tilde\sigma|^2\tilde\sigma^* T_{\tilde\sigma}+\frac{24}{5}g_1^2\tilde\sigma^*(\tilde\sigma M_1-T_{\tilde\sigma})+\frac{16}{5}g_1'^2\tilde\sigma^*(\tilde\sigma M_1'-T_{\tilde\sigma})\\
&\quad +24g_2^2\tilde\sigma^*(\tilde\sigma M_2-T_{\tilde\sigma})+10g_1'^2\sigma^*(M_1'\sigma-T_\sigma)+16\tilde\sigma^*\kappa_\phi^*\Big(2\tilde\sigma T_{\kappa_\phi}+3\kappa_\phi T_{\tilde\sigma}\Big)\\
&\quad +8\sigma^*\kappa_\phi^*\Big(2\sigma T_{\kappa_\phi}+3\kappa_\phi T_\sigma\Big)+8\lambda^*\sigma^*\Big(\lambda T_\sigma+\sigma T_\lambda\Big)\\
&\quad +12\sigma^*\Big[T_\sigma\,\mathrm{Tr}\Big(\kappa\kappa^\dagger\Big)+\sigma\,\mathrm{Tr}\Big(\kappa^\dagger T^\kappa\Big)\Big]+8\sigma^*\Big[T_\sigma\,\mathrm{Tr}\Big(\tilde\lambda\tilde\lambda^\dagger\Big)+\sigma\,\mathrm{Tr}\Big(\tilde\lambda^\dagger T^{\tilde\lambda}\Big)\Big]\\
&\quad +24\tilde\sigma^*\Big[T_{\tilde\sigma}\,\mathrm{Tr}\Big(g^D g^{D\dagger}\Big)+\tilde\sigma\,\mathrm{Tr}\Big(g^{D\dagger}T^{g^D}\Big)\Big]\\
&\quad +8\tilde\sigma^*\Big[T_{\tilde\sigma}\,\mathrm{Tr}\Big(h^E h^{E\dagger}\Big)+\tilde\sigma\,\mathrm{Tr}\Big(h^{E\dagger}T^{h^E}\Big)\Big]\Big\}+8\kappa_\phi\tilde\sigma^* B_L\mu_L\Big[2|\tilde\sigma|^2\\
&\quad +3\,\mathrm{Tr}\Big(g^D g^{D\dagger}\Big)+\mathrm{Tr}\Big(h^E h^{E\dagger}\Big)-\frac{12}{5}g_1^2-\frac{8}{5}g_1'^2-12g_2^2\Big]+8\kappa_\phi\tilde\sigma^*\mu_L\Big[2\tilde\sigma^* T_{\tilde\sigma}\\
&\quad +3\,\mathrm{Tr}\Big(g^{D\dagger}T^{g^D}\Big)+\mathrm{Tr}\Big(h^{E\dagger}T^{h^E}\Big)+\frac{12}{5}g_1^2M_1+\frac{8}{5}g_1'^2M_1'+12g_2^2M_2\Big]\,, \qquad (D.78)\\
\beta^{(1)}_{B_L\mu_L} &= B_L\mu_L\Big[6|\tilde\sigma|^2+3\,\mathrm{Tr}\Big(g^D g^{D\dagger}\Big)+\mathrm{Tr}\Big(h^E h^{E\dagger}\Big)-\frac{3}{5}g_1^2-\frac{2}{5}g_1'^2-3g_2^2\Big]\\
&\quad +\mu_L\Big[4\tilde\sigma^* T_{\tilde\sigma}+6\,\mathrm{Tr}\Big(g^{D\dagger}T^{g^D}\Big)+2\,\mathrm{Tr}\Big(h^{E\dagger}T^{h^E}\Big)+\frac{6}{5}g_1^2M_1+\frac{4}{5}g_1'^2M_1'\\
&\quad +6g_2^2M_2\Big]-2\tilde\sigma\kappa_\phi^* B_\phi\mu_\phi\,, \qquad\qquad (D.79)\\
\beta^{(2)}_{B_L\mu_L} &= B_L\mu_L\Big\{\frac{297}{50}g_1^4+\frac{217}{50}g_1'^4+\frac{33}{2}g_2^4+\frac{18}{25}g_1^2g_1'^2+\frac{9}{5}g_1^2g_2^2+\frac{6}{5}g_1'^2g_2^2\\
&\quad -14|\tilde\sigma|^4+\frac{2}{5}g_1^2\Big[-\mathrm{Tr}\Big(g^D g^{D\dagger}\Big)+3\,\mathrm{Tr}\Big(h^E h^{E\dagger}\Big)\Big]+\frac{3}{10}g_1'^2\Big[3\,\mathrm{Tr}\Big(g^D g^{D\dagger}\Big)\\
&\quad +\mathrm{Tr}\Big(h^E h^{E\dagger}\Big)\Big]+16g_3^2\,\mathrm{Tr}\Big(g^D g^{D\dagger}\Big)+|\tilde\sigma|^2\Big[\frac{48}{5}g_1^2+\frac{32}{5}g_1'^2+48g_2^2\\
&\quad -2|\sigma|^2-4|\kappa_\phi|^2-15\,\mathrm{Tr}\Big(g^D g^{D\dagger}\Big)-5\,\mathrm{Tr}\Big(h^E h^{E\dagger}\Big)\Big]-\mathrm{Tr}\Big(\tilde f h^{E\dagger}h^E\tilde f^\dagger\Big)
\end{aligned}$$

$$
\begin{aligned}
&- 9\,\mathrm{Tr}\Big(g^D g^{D\dagger} g^D g^{D\dagger}\Big) - 3\,\mathrm{Tr}\Big(g^D g^{D\dagger} y^{DT} y^{D*}\Big) - 3\,\mathrm{Tr}\Big(g^D g^{D\dagger} y^{UT} y^{U*}\Big) \\
&- 3\,\mathrm{Tr}\Big(g^D \kappa^\dagger \kappa g^{D\dagger}\Big) - 3\,\mathrm{Tr}\Big(h^E h^{E\dagger} h^E h^{E\dagger}\Big) - 2\,\mathrm{Tr}\Big(h^E h^{E\dagger} y^E y^{E\dagger}\Big) \\
&- \mathrm{Tr}\Big(h^E \tilde{\lambda}^\dagger \tilde{\lambda} h^{E\dagger}\Big)\Big\} - \mu_L\Big\{\frac{594}{25} g_1^4 M_1 + \frac{434}{25} g_1'^4 M_1' + 66 g_2^4 M_2 \\
&+ \frac{36}{25} g_1^2 g_1'^2 (M_1 + M_1') + \frac{18}{5} g_1^2 g_2^2 (M_1 + M_2) + \frac{12}{5} g_1'^2 g_2^2 (M_1' + M_2) \\
&- \frac{4}{5} g_1^2\,\mathrm{Tr}\Big(M_1 g^D g^{D\dagger} - g^{D\dagger} T^{g^D}\Big) + \frac{9}{5} g_1'^2\,\mathrm{Tr}\Big(M_1' g^D g^{D\dagger} - g^{D\dagger} T^{g^D}\Big) \\
&+ 32 g_3^2\,\mathrm{Tr}\Big(M_3 g^D g^{D\dagger} - g^{D\dagger} T^{g^D}\Big) + \frac{12}{5} g_1^2\,\mathrm{Tr}\Big(M_1 h^E h^{E\dagger} - h^{E\dagger} T^{h^E}\Big) \\
&+ \frac{3}{5} g_1'^2\,\mathrm{Tr}\Big(M_1' h^E h^{E\dagger} - h^{E\dagger} T^{h^E}\Big) + |\tilde{\sigma}|^2\Big[\frac{48}{5} g_1^2 M_1 + \frac{32}{5} g_1'^2 M_1' \\
&+ 48 g_2^2 M_2 + 8\kappa_\phi^* T_{\kappa_\phi} + 4\sigma^* T_\sigma + 18\,\mathrm{Tr}\Big(g^{D\dagger} T^{g^D}\Big) + 6\,\mathrm{Tr}\Big(h^{E\dagger} T^{h^E}\Big)\Big] \\
&+ \tilde{\sigma}^* T_{\tilde{\sigma}}\Big[8|\kappa_\phi|^2 + 4|\sigma|^2 + 32|\tilde{\sigma}|^2 + 6\,\mathrm{Tr}\Big(g^D g^{D\dagger}\Big) + 2\,\mathrm{Tr}\Big(h^E h^{E\dagger}\Big)\Big] \\
&+ 2\,\mathrm{Tr}\Big(\tilde{f} h^{E\dagger} T^{h^E} \tilde{f}^\dagger\Big) + 36\,\mathrm{Tr}\Big(g^D g^{D\dagger} T^{g^D} g^{D\dagger}\Big) + 6\,\mathrm{Tr}\Big(g^D \kappa^\dagger T^\kappa g^{D\dagger}\Big) \\
&+ 2\,\mathrm{Tr}\Big(h^E \tilde{f}^\dagger T^{\tilde{f}} h^{E\dagger}\Big) + 12\,\mathrm{Tr}\Big(h^E h^{E\dagger} T^{h^E} h^{E\dagger}\Big) + 4\,\mathrm{Tr}\Big(h^E h^{E\dagger} T^E y^{E\dagger}\Big) \\
&+ 2\,\mathrm{Tr}\Big(h^E \tilde{\lambda}^\dagger T^{\tilde{\lambda}} h^{E\dagger}\Big) + 4\,\mathrm{Tr}\Big(y^E y^{E\dagger} T^{h^E} h^{E\dagger}\Big) + 6\,\mathrm{Tr}\Big(\kappa g^{D\dagger} T^{g^D} \kappa^\dagger\Big) \\
&+ 2\,\mathrm{Tr}\Big(\tilde{\lambda} h^{E\dagger} T^{h^E} \tilde{\lambda}^\dagger\Big) + 6\,\mathrm{Tr}\Big(g^{D\dagger} y^{DT} y^{D*} T^{g^D}\Big) + 6\,\mathrm{Tr}\Big(g^{D\dagger} y^{UT} y^{U*} T^{g^D}\Big) \\
&+ 6\,\mathrm{Tr}\Big(y^{D\dagger} T^D g^{D*} g^{DT}\Big) + 6\,\mathrm{Tr}\Big(y^{U\dagger} T^U g^{D*} g^{DT}\Big)\Big\} \\
&+ 4\tilde{\sigma}\kappa_\phi^*\Big[B_\phi \mu_\phi\Big(2|\kappa_\phi|^2 + 2|\tilde{\sigma}|^2 + |\sigma|^2\Big) \\
&+ \mu_\phi\Big(2\kappa_\phi^* T_{\kappa_\phi} + 2\tilde{\sigma}^* T_{\tilde{\sigma}} + \sigma^* T_\sigma\Big)\Big]\,. \qquad \text{(D.80)}
\end{aligned}
$$

The two-loop β function for the soft-breaking linear coupling Λ_S is

$$
\begin{aligned}
\beta_{\Lambda_S}^{(1)} &= \Lambda_S\Big(2|\kappa_\phi|^2 + 2|\tilde{\sigma}|^2 + |\sigma|^2\Big) + 2\Lambda_F\Big(2\kappa_\phi^* T_{\kappa_\phi} + 2\tilde{\sigma}^* T_{\tilde{\sigma}} + \sigma^* T_\sigma\Big) \\
&\quad + 2(B_\phi \mu_\phi)\mu_\phi \kappa_\phi^* + 2(B_\phi \mu_\phi)^* T_{\kappa_\phi} - 4(B_L \mu_L)\mu_\phi \tilde{\sigma}^* - 4(B_L \mu_L)^* T_{\tilde{\sigma}} \\
&\quad - 4\Big(m_{L_4}^2 + m_{\bar{L}_4}^2\Big)\tilde{\sigma}\mu_L^* + 4 m_\phi^2 \kappa_\phi \mu_\phi^*\,, \qquad \text{(D.81)} \\
\beta_{\Lambda_S}^{(2)} &= \Lambda_S\Big\{|\sigma|^2\Big[\frac{5}{2} g_1'^2 - 4|\kappa_\phi|^2 - 2|\lambda|^2 - 2|\sigma|^2 - 3\,\mathrm{Tr}\Big(\kappa\kappa^\dagger\Big) - 2\,\mathrm{Tr}\Big(\tilde{\lambda}\tilde{\lambda}^\dagger\Big)\Big] \\
&\quad + |\tilde{\sigma}|^2\Big[\frac{6}{5} g_1^2 + \frac{4}{5} g_1'^2 + 6 g_2^2 - 8|\kappa_\phi|^2 - 4|\tilde{\sigma}|^2 - 6\,\mathrm{Tr}\Big(g^D g^{D\dagger}\Big) - 2\,\mathrm{Tr}\Big(h^E h^{E\dagger}\Big)\Big]
\end{aligned}
$$

$$
\begin{aligned}
&- 8|\kappa_\phi|^4\Big\} + \Lambda_F\Big\{\sigma^* T_\sigma\Big[5g_1'^2 - 8|\kappa_\phi|^2 - 4|\lambda|^2 - 4|\sigma|^2 - 6\,\mathrm{Tr}\Big(\kappa\kappa^\dagger\Big) \\
&- 4\,\mathrm{Tr}\Big(\tilde\lambda\tilde\lambda^\dagger\Big)\Big] - |\sigma|^2\Big[5g_1'^2 M_1' + 8\kappa_\phi^* T_{\kappa_\phi} + 4\lambda^* T_\lambda + 4\sigma^* T_\sigma + 6\,\mathrm{Tr}\Big(\kappa^\dagger T^\kappa\Big) \\
&+ 4\,\mathrm{Tr}\Big(\tilde\lambda^\dagger T^{\tilde\lambda}\Big)\Big] + \tilde\sigma^* T_{\tilde\sigma}\Big[\frac{12}{5}g_1^2 + \frac{8}{5}g_1'^2 + 12g_2^2 - 16|\kappa_\phi|^2 - 8|\tilde\sigma|^2 \\
&- 12\,\mathrm{Tr}\Big(g^D g^{D\dagger}\Big) - 4\,\mathrm{Tr}\Big(h^E h^{E\dagger}\Big)\Big] - |\tilde\sigma|^2\Big[\frac{12}{5}g_1^2 M_1 + \frac{8}{5}g_1'^2 M_1' + 12g_2^2 M_2 \\
&+ 16\kappa_\phi^* T_{\kappa_\phi} + 8\tilde\sigma^* T_{\tilde\sigma} + 12\,\mathrm{Tr}\Big(g^{D\dagger} T^{g^D}\Big) + 4\,\mathrm{Tr}\Big(h^{E\dagger} T^{h^E}\Big)\Big] - 32|\kappa_\phi|^2\kappa_\phi^* T_{\kappa_\phi}\Big\} \\
&- 4(B_\phi\mu_\phi)^*\Big[T_{\kappa_\phi}\Big(4|\kappa_\phi|^2 + 2|\tilde\sigma|^2 + |\sigma|^2\Big) + \kappa_\phi\sigma^* T_\sigma + 2\kappa_\phi\tilde\sigma^* T_{\tilde\sigma}\Big] \\
&+ (B_L\mu_L)^*\Big\{\frac{12}{5}g_1^2\Big(\tilde\sigma M_1 - T_{\tilde\sigma}\Big) + \frac{8}{5}g_1'^2\Big(\tilde\sigma M_1' - T_{\tilde\sigma}\Big) + 12g_2^2\Big(\tilde\sigma M_2 - T_{\tilde\sigma}\Big) \\
&+ 16|\tilde\sigma|^2 T_{\tilde\sigma} + 12\Big[T_{\tilde\sigma}\,\mathrm{Tr}\Big(g^D g^{D\dagger}\Big) + \tilde\sigma\,\mathrm{Tr}\Big(g^{D\dagger} T^{g^D}\Big)\Big] + 4\Big[T_{\tilde\sigma}\,\mathrm{Tr}\Big(h^E h^{E\dagger}\Big) \\
&+ \tilde\sigma\,\mathrm{Tr}\Big(h^{E\dagger} T^{h^E}\Big)\Big]\Big\} - 4\kappa_\phi^*\mu_\phi(B_\phi\mu_\phi)\Big(2|\kappa_\phi|^2 + 2|\tilde\sigma|^2 + |\sigma|^2\Big) \\
&+ \tilde\sigma^*\mu_\phi B_L\mu_L\Big[8|\tilde\sigma|^2 + 12\,\mathrm{Tr}\Big(g^D g^{D\dagger}\Big) + 4\,\mathrm{Tr}\Big(h^E h^{E\dagger}\Big) - \frac{12}{5}g_1^2 - \frac{8}{5}g_1'^2 \\
&- 12g_2^2\Big] + \tilde\sigma^*\mu_L\mu_\phi\Big[\frac{12}{5}g_1^2 M_1 + \frac{8}{5}g_1'^2 M_1' + 12g_2^2 M_2 + 8\tilde\sigma^* T_{\tilde\sigma} \\
&+ 12\,\mathrm{Tr}\Big(g^{D\dagger} T^{g^D}\Big) + 4\,\mathrm{Tr}\Big(h^{E\dagger} T^{h^E}\Big)\Big] - 4\kappa_\phi^*\mu_\phi^2\Big[2\kappa_\phi^* T_{\kappa_\phi} + 2\tilde\sigma^* T_{\tilde\sigma} + \sigma^* T_\sigma\Big] \\
&- 4\mu_\phi^*\Big[\kappa_\phi|\sigma|^2\Big(3m_\phi^2 + m_S^2 + m_{\tilde S}^2\Big) + 2\kappa_\phi|\tilde\sigma|^2\Big(3m_\phi^2 + m_{L_4}^2 + m_{\bar L_4}^2\Big) \\
&+ \kappa_\phi\Big(10m_\phi^2|\kappa_\phi|^2 + 4|T_{\kappa_\phi}|^2 + |T_\sigma|^2 + 2|T_{\tilde\sigma}|^2\Big) + \sigma T_\sigma^* T_{\kappa_\phi} + 2\tilde\sigma T_{\tilde\sigma}^* T_{\kappa_\phi}\Big] \\
&+ \mu_L^*\Big\{\tilde\sigma\Big[16|T_{\tilde\sigma}|^2 + 16m_{L_4}^2|\tilde\sigma|^2 + 16m_{\bar L_4}^2|\tilde\sigma|^2 + 8m_\phi^2|\tilde\sigma|^2 + 24m_{L_4}^2\,\mathrm{Tr}\Big(g^D g^{D\dagger}\Big) \\
&+ 12m_{\bar L_4}^2\,\mathrm{Tr}\Big(g^D g^{D\dagger}\Big) + 8m_{L_4}^2\,\mathrm{Tr}\Big(h^E h^{E\dagger}\Big) + 4m_{\bar L_4}^2\,\mathrm{Tr}\Big(h^E h^{E\dagger}\Big) \\
&+ 12\,\mathrm{Tr}\Big(T^{g^D *} T^{g^D T}\Big) + \mathrm{Tr}\Big(T^{h^E *} T^{h^E T}\Big) + 12\,\mathrm{Tr}\Big(g^D m_{\bar D}^2 g^{D\dagger}\Big) \\
&+ 12\,\mathrm{Tr}\Big(g^D g^{D\dagger} m_Q^2\Big) + \mathrm{Tr}\Big(h^E h^{E\dagger} m_{e^c}^{2*}\Big) + \mathrm{Tr}\Big(h^E m_{H_1}^{2*} h^{E\dagger}\Big)\Big] \\
&+ T_{\tilde\sigma}\Big[12\,\mathrm{Tr}\Big(T^{g^D *} g^{DT}\Big) + \mathrm{Tr}\Big(T^{h^E *} h^{ET}\Big)\Big] \\
&- \frac{12}{5}g_1^2\Big(\tilde\sigma m_{L_4}^2 + \tilde\sigma m_{\bar L_4}^2 + 2\tilde\sigma|M_1|^2 - M_1 T_{\tilde\sigma}\Big) \\
&- \frac{8}{5}g_1'^2\Big(\tilde\sigma m_{L_4}^2 + \tilde\sigma m_{\bar L_4}^2 + 2\tilde\sigma|M_1'|^2 - M_1' T_{\tilde\sigma}\Big) \\
&- 12g_2^2\Big(\tilde\sigma m_{L_4}^2 + \tilde\sigma m_{\bar L_4}^2 + 2\tilde\sigma|M_2|^2 - M_2 T_{\tilde\sigma}\Big)\Big\}. \qquad \text{(D.82)}
\end{aligned}
$$

D.7 Soft Scalar Masses

In writing down the two-loop β functions for the soft scalar masses, the following quantities are defined,

$$\begin{aligned}
\Sigma_{1,1} = \sqrt{\frac{3}{5}}g_1\Big[&-m_{H_d}^2 - m_{L_4}^2 + m_{\bar{L}_4}^2 + m_{H_u}^2 + \mathrm{Tr}\Big(m_{d^c}^2\Big) - \mathrm{Tr}\Big(m_D^2\Big) \\
&+ \mathrm{Tr}\Big(m_{\bar{D}}^2\Big) + \mathrm{Tr}\Big(m_{e^c}^2\Big) - \mathrm{Tr}\Big(m_{H_1}^2\Big) + \mathrm{Tr}\Big(m_{H_2}^2\Big) - \mathrm{Tr}\Big(m_L^2\Big) \\
&+ \mathrm{Tr}\Big(m_Q^2\Big) - 2\,\mathrm{Tr}\Big(m_{u^c}^2\Big)\Big], \qquad \text{(D.83)} \\
\Sigma_{1,4} = \frac{1}{\sqrt{40}}g_1'\Big[&-6m_{H_d}^2 + 4m_{L_4}^2 - 4m_{\bar{L}_4}^2 - 4m_{H_u}^2 + 5m_S^2 - 5m_{\bar{S}}^2 \\
&+ 6\,\mathrm{Tr}\Big(m_{d^c}^2\Big) - 6\,\mathrm{Tr}\Big(m_D^2\Big) - 9\,\mathrm{Tr}\Big(m_{\bar{D}}^2\Big) + \mathrm{Tr}\Big(m_{e^c}^2\Big) - 6\,\mathrm{Tr}\Big(m_{H_1}^2\Big) \\
&- 4\,\mathrm{Tr}\Big(m_{H_2}^2\Big) + 4\,\mathrm{Tr}\Big(m_L^2\Big) + 6\,\mathrm{Tr}\Big(m_Q^2\Big) + 5\,\mathrm{Tr}\Big(m_\Sigma^2\Big) + 3\,\mathrm{Tr}\Big(m_{u^c}^2\Big)\Big], \qquad \text{(D.84)} \\
\Sigma_{2,11} = \frac{1}{10}g_1^2\Big[&3m_{H_d}^2 + 3m_{L_4}^2 + 3m_{\bar{L}_4}^2 + 3m_{H_u}^2 + 2\,\mathrm{Tr}\Big(m_{d^c}^2\Big) + 2\,\mathrm{Tr}\Big(m_D^2\Big) \\
&+ 2\,\mathrm{Tr}\Big(m_{\bar{D}}^2\Big) + 6\,\mathrm{Tr}\Big(m_{e^c}^2\Big) + 3\,\mathrm{Tr}\Big(m_{H_1}^2\Big) + 3\,\mathrm{Tr}\Big(m_{H_2}^2\Big) + 3\,\mathrm{Tr}\Big(m_L^2\Big) \\
&+ \mathrm{Tr}\Big(m_Q^2\Big) + 8\,\mathrm{Tr}\Big(m_{u^c}^2\Big)\Big], \qquad \text{(D.85)} \\
\Sigma_{2,14} = \frac{1}{10}\sqrt{\frac{3}{2}}g_1g_1'\Big[&3m_{H_d}^2 - 2m_{L_4}^2 - 2m_{\bar{L}_4}^2 - 2m_{H_u}^2 + 2\,\mathrm{Tr}\Big(m_{d^c}^2\Big) + 2\,\mathrm{Tr}\Big(m_D^2\Big) \\
&- 3\,\mathrm{Tr}\Big(m_{\bar{D}}^2\Big) + \mathrm{Tr}\Big(m_{e^c}^2\Big) + 3\,\mathrm{Tr}\Big(m_{H_1}^2\Big) - 2\,\mathrm{Tr}\Big(m_{H_2}^2\Big) - 2\,\mathrm{Tr}\Big(m_L^2\Big) \\
&+ \mathrm{Tr}\Big(m_Q^2\Big) - 2\,\mathrm{Tr}\Big(m_{u^c}^2\Big)\Big], \qquad \text{(D.86)} \\
\Sigma_{3,1} = \frac{1}{40\sqrt{15}}g_1\Big[&-18g_1^2m_{H_d}^2 - 27g_1'^2m_{H_d}^2 - 90g_2^2m_{H_d}^2 - 18g_1^2m_{L_4}^2 - 12g_1'^2m_{L_4}^2 \\
&- 90g_2^2m_{L_4}^2 + 18g_1^2m_{\bar{L}_4}^2 + 12g_1'^2m_{\bar{L}_4}^2 + 90g_2^2m_{\bar{L}_4}^2 + 18g_1^2m_{H_u}^2 + 12g_1'^2m_{H_u}^2 \\
&+ 90g_2^2m_{H_u}^2 + 60\Big(-m_{H_u}^2 + m_{H_d}^2\Big)|\lambda|^2 + 60\Big(-m_{\bar{L}_4}^2 + m_{L_4}^2\Big)|\tilde{\sigma}|^2 \\
&+ 8g_1^2\,\mathrm{Tr}\Big(m_{d^c}^2\Big) + 12g_1'^2\,\mathrm{Tr}\Big(m_{d^c}^2\Big) + 160g_3^2\,\mathrm{Tr}\Big(m_{d^c}^2\Big) - 8g_1^2\,\mathrm{Tr}\Big(m_D^2\Big) \\
&- 12g_1'^2\,\mathrm{Tr}\Big(m_D^2\Big) - 160g_3^2\,\mathrm{Tr}\Big(m_D^2\Big) + 8g_1^2\,\mathrm{Tr}\Big(m_{\bar{D}}^2\Big) + 27g_1'^2\,\mathrm{Tr}\Big(m_{\bar{D}}^2\Big) \\
&+ 160g_3^2\,\mathrm{Tr}\Big(m_{\bar{D}}^2\Big) + 72g_1^2\,\mathrm{Tr}\Big(m_{e^c}^2\Big) + 3g_1'^2\,\mathrm{Tr}\Big(m_{e^c}^2\Big) - 18g_1^2\,\mathrm{Tr}\Big(m_{H_1}^2\Big) \\
&- 27g_1'^2\,\mathrm{Tr}\Big(m_{H_1}^2\Big) - 90g_2^2\,\mathrm{Tr}\Big(m_{H_1}^2\Big) + 18g_1^2\,\mathrm{Tr}\Big(m_{H_2}^2\Big) + 12g_1'^2\,\mathrm{Tr}\Big(m_{H_2}^2\Big)
\end{aligned}$$

$$
\begin{aligned}
&+ 90g_2^2 \operatorname{Tr}\Big(m_{H_2}^2\Big) - 18g_1^2 \operatorname{Tr}\Big(m_L^2\Big) - 12g_1'^2 \operatorname{Tr}\Big(m_L^2\Big) - 90g_2^2 \operatorname{Tr}\Big(m_L^2\Big) \\
&+ 2g_1^2 \operatorname{Tr}\Big(m_Q^2\Big) + 3g_1'^2 \operatorname{Tr}\Big(m_Q^2\Big) + 90g_2^2 \operatorname{Tr}\Big(m_Q^2\Big) + 160g_3^2 \operatorname{Tr}\Big(m_Q^2\Big) \\
&- 64g_1^2 \operatorname{Tr}\Big(m_{u^c}^2\Big) - 6g_1'^2 \operatorname{Tr}\Big(m_{u^c}^2\Big) - 320g_3^2 \operatorname{Tr}\Big(m_{u^c}^2\Big) + 60m_{H_d}^2 \operatorname{Tr}\Big(ff^\dagger\Big) \\
&- 60m_{H_u}^2 \operatorname{Tr}\Big(\tilde{f}\tilde{f}^\dagger\Big) + 180m_{L_4}^2 \operatorname{Tr}\Big(g^D g^{D\dagger}\Big) + 60m_{L_4}^2 \operatorname{Tr}\Big(h^E h^{E\dagger}\Big) \\
&+ 180m_{H_d}^2 \operatorname{Tr}\Big(y^D y^{D\dagger}\Big) + 60m_{H_d}^2 \operatorname{Tr}\Big(y^E y^{E\dagger}\Big) - 180m_{H_u}^2 \operatorname{Tr}\Big(y^U y^{U\dagger}\Big) \\
&- 60 \operatorname{Tr}\Big(f m_{H_2}^{2*} f^\dagger\Big) + 60 \operatorname{Tr}\Big(\tilde{f} m_{H_1}^{2*} \tilde{f}^\dagger\Big) - 120 \operatorname{Tr}\Big(g^D m_{\bar{D}}^2 g^{D\dagger}\Big) \\
&- 60 \operatorname{Tr}\Big(g^D g^{D\dagger} m_Q^2\Big) - 120 \operatorname{Tr}\Big(h^E h^{E\dagger} m_{e^c}^{2*}\Big) + 60 \operatorname{Tr}\Big(h^E m_{H_1}^{2*} h^{E\dagger}\Big) \\
&+ 60 \operatorname{Tr}\Big(m_D^2 \kappa\kappa^\dagger\Big) - 60 \operatorname{Tr}\Big(m_{\bar{D}}^2 \kappa^\dagger\kappa\Big) - 60 \operatorname{Tr}\Big(m_{H_2}^2 \tilde{\lambda}\tilde{\lambda}^\dagger\Big) \\
&- 120 \operatorname{Tr}\Big(y^D y^{D\dagger} m_{d^c}^{2*}\Big) - 60 \operatorname{Tr}\Big(y^D m_Q^{2*} y^{D\dagger}\Big) - 120 \operatorname{Tr}\Big(y^E y^{E\dagger} m_{e^c}^{2*}\Big) \\
&+ 60 \operatorname{Tr}\Big(y^E m_L^{2*} y^{E\dagger}\Big) + 240 \operatorname{Tr}\Big(y^U y^{U\dagger} m_{u^c}^{2*}\Big) - 60 \operatorname{Tr}\Big(y^U m_Q^{2*} y^{U\dagger}\Big) \\
&+ 60 \operatorname{Tr}\Big(\tilde{\lambda} m_{H_1}^{2*} \tilde{\lambda}^\dagger\Big)\Big], \qquad \text{(D.87)}
\end{aligned}
$$

$$
\begin{aligned}
\Sigma_{2,2} = \frac{1}{2}\Big[&3 \operatorname{Tr}\Big(m_Q^2\Big) + m_{H_d}^2 + m_{L_4}^2 + m_{\bar{L}_4}^2 + m_{H_u}^2 + \operatorname{Tr}\Big(m_{H_1}^2\Big) + \operatorname{Tr}\Big(m_{H_2}^2\Big) \\
&+ \operatorname{Tr}\Big(m_L^2\Big)\Big], \qquad \text{(D.88)}
\end{aligned}
$$

$$
\Sigma_{2,3} = \frac{1}{2}\Big[2 \operatorname{Tr}\Big(m_Q^2\Big) + \operatorname{Tr}\Big(m_{d^c}^2\Big) + \operatorname{Tr}\Big(m_D^2\Big) + \operatorname{Tr}\Big(m_{\bar{D}}^2\Big) + \operatorname{Tr}\Big(m_{u^c}^2\Big)\Big], \qquad \text{(D.89)}
$$

$$
\begin{aligned}
\Sigma_{2,41} = \frac{1}{10}\sqrt{\frac{3}{2}} g_1 g_1' \Big[&3m_{H_d}^2 - 2m_{L_4}^2 - 2m_{\bar{L}_4}^2 - 2m_{H_u}^2 + 2 \operatorname{Tr}\Big(m_{d^c}^2\Big) + 2 \operatorname{Tr}\Big(m_D^2\Big) \\
&- 3 \operatorname{Tr}\Big(m_{\bar{D}}^2\Big) + \operatorname{Tr}\Big(m_{e^c}^2\Big) + 3 \operatorname{Tr}\Big(m_{H_1}^2\Big) - 2 \operatorname{Tr}\Big(m_{H_2}^2\Big) - 2 \operatorname{Tr}\Big(m_L^2\Big) \\
&+ \operatorname{Tr}\Big(m_Q^2\Big) - 2 \operatorname{Tr}\Big(m_{u^c}^2\Big)\Big], \qquad \text{(D.90)}
\end{aligned}
$$

$$
\begin{aligned}
\Sigma_{2,44} = \frac{1}{40} g_1'^2 \Big[&18m_{H_d}^2 + 8m_{L_4}^2 + 8m_{\bar{L}_4}^2 + 8m_{H_u}^2 + 25m_S^2 + 25m_{\bar{S}}^2 + 12 \operatorname{Tr}\Big(m_{d^c}^2\Big) \\
&+ 12 \operatorname{Tr}\Big(m_D^2\Big) + 27 \operatorname{Tr}\Big(m_{\bar{D}}^2\Big) + \operatorname{Tr}\Big(m_{e^c}^2\Big) + 18 \operatorname{Tr}\Big(m_{H_1}^2\Big) + 8 \operatorname{Tr}\Big(m_{H_2}^2\Big) \\
&+ 8 \operatorname{Tr}\Big(m_L^2\Big) + 6 \operatorname{Tr}\Big(m_Q^2\Big) + 25 \operatorname{Tr}\Big(m_\Sigma^2\Big) + 3 \operatorname{Tr}\Big(m_{u^c}^2\Big)\Big], \qquad \text{(D.91)}
\end{aligned}
$$

$$
\begin{aligned}
\Sigma_{3,4} = -\frac{1}{80\sqrt{10}} g_1' \Big[&36g_1^2 m_{H_d}^2 + 54g_1'^2 m_{H_d}^2 + 180g_2^2 m_{H_d}^2 - 24g_1^2 m_{L_4}^2 - 16g_1'^2 m_{L_4}^2 \\
&- 120g_2^2 m_{L_4}^2 + 24g_1^2 m_{\bar{L}_4}^2 + 16g_1'^2 m_{\bar{L}_4}^2 + 120g_2^2 m_{\bar{L}_4}^2 + 24g_1^2 m_{H_u}^2 + 16g_1'^2 m_{H_u}^2
\end{aligned}
$$

$$
\begin{aligned}
&+ 120g_2^2 m_{H_u}^2 - 125g_1'^2 m_S^2 + 125g_1'^2 m_{\bar{S}}^2 - 40\Big(2m_{H_u}^2 + 3m_{H_d}^2 - 5m_S^2\Big)|\lambda|^2 \\
&+ 100\Big(-m_{\bar{S}}^2 + m_S^2\Big)|\sigma|^2 + 80m_{L_4}^2|\tilde{\sigma}|^2 - 80m_{\bar{L}_4}^2|\tilde{\sigma}|^2 - 16g_1^2\,\mathrm{Tr}\Big(m_{d^c}^2\Big) \\
&- 24g_1'^2\,\mathrm{Tr}\Big(m_{d^c}^2\Big) - 320g_3^2\,\mathrm{Tr}\Big(m_{d^c}^2\Big) + 16g_1^2\,\mathrm{Tr}\Big(m_D^2\Big) + 24g_1'^2\,\mathrm{Tr}\Big(m_D^2\Big) \\
&+ 320g_3^2\,\mathrm{Tr}\Big(m_D^2\Big) + 24g_1^2\,\mathrm{Tr}\Big(m_{\bar{D}}^2\Big) + 81g_1'^2\,\mathrm{Tr}\Big(m_{\bar{D}}^2\Big) + 480g_3^2\,\mathrm{Tr}\Big(m_{\bar{D}}^2\Big) \\
&- 24g_1^2\,\mathrm{Tr}\Big(m_{e^c}^2\Big) - g_1'^2\,\mathrm{Tr}\Big(m_{e^c}^2\Big) + 36g_1^2\,\mathrm{Tr}\Big(m_{H_1}^2\Big) + 54g_1'^2\,\mathrm{Tr}\Big(m_{H_1}^2\Big) \\
&+ 180g_2^2\,\mathrm{Tr}\Big(m_{H_1}^2\Big) + 24g_1^2\,\mathrm{Tr}\Big(m_{H_2}^2\Big) + 16g_1'^2\,\mathrm{Tr}\Big(m_{H_2}^2\Big) + 120g_2^2\,\mathrm{Tr}\Big(m_{H_2}^2\Big) \\
&- 24g_1^2\,\mathrm{Tr}\Big(m_L^2\Big) - 16g_1'^2\,\mathrm{Tr}\Big(m_L^2\Big) - 120g_2^2\,\mathrm{Tr}\Big(m_L^2\Big) - 4g_1^2\,\mathrm{Tr}\Big(m_Q^2\Big) \\
&- 6g_1'^2\,\mathrm{Tr}\Big(m_Q^2\Big) - 180g_2^2\,\mathrm{Tr}\Big(m_Q^2\Big) - 320g_3^2\,\mathrm{Tr}\Big(m_Q^2\Big) - 125g_1'^2\,\mathrm{Tr}\Big(m_\Sigma^2\Big) \\
&- 32g_1^2\,\mathrm{Tr}\Big(m_{u^c}^2\Big) - 3g_1'^2\,\mathrm{Tr}\Big(m_{u^c}^2\Big) - 160g_3^2\,\mathrm{Tr}\Big(m_{u^c}^2\Big) - 120m_{H_d}^2\,\mathrm{Tr}\Big(ff^\dagger\Big) \\
&- 80m_{H_u}^2\,\mathrm{Tr}\Big(\tilde{f}\tilde{f}^\dagger\Big) + 240m_{L_4}^2\,\mathrm{Tr}\Big(g^D g^{D\dagger}\Big) + 80m_{L_4}^2\,\mathrm{Tr}\Big(h^E h^{E\dagger}\Big) \\
&- 360m_{H_d}^2\,\mathrm{Tr}\Big(y^D y^{D\dagger}\Big) - 120m_{H_d}^2\,\mathrm{Tr}\Big(y^E y^{E\dagger}\Big) - 240m_{H_u}^2\,\mathrm{Tr}\Big(y^U y^{U\dagger}\Big) \\
&+ 300m_S^2\,\mathrm{Tr}\Big(\kappa\kappa^\dagger\Big) + 200m_S^2\,\mathrm{Tr}\Big(\tilde{\lambda}\tilde{\lambda}^\dagger\Big) + 200\,\mathrm{Tr}\Big(ff^\dagger m_\Sigma^2\Big) \\
&- 80\,\mathrm{Tr}\Big(fm_{H_2}^{2*}f^\dagger\Big) + 200\,\mathrm{Tr}\Big(\tilde{f}\tilde{f}^\dagger m_\Sigma^2\Big) - 120\,\mathrm{Tr}\Big(\tilde{f}m_{H_1}^{2*}\tilde{f}^\dagger\Big) \\
&- 360\,\mathrm{Tr}\Big(g^D m_{\bar{D}}^2 g^{D\dagger}\Big) + 120\,\mathrm{Tr}\Big(g^D g^{D\dagger} m_Q^2\Big) + 40\,\mathrm{Tr}\Big(h^E h^{E\dagger} m_{e^c}^{2*}\Big) \\
&- 120\,\mathrm{Tr}\Big(h^E m_{H_1}^{2*} h^{E\dagger}\Big) - 120\,\mathrm{Tr}\Big(m_{\bar{D}}^2\kappa\kappa^\dagger\Big) - 180\,\mathrm{Tr}\Big(m_{\bar{D}}^2\kappa^\dagger\kappa\Big) \\
&- 80\,\mathrm{Tr}\Big(m_{H_2}^2\tilde{\lambda}\tilde{\lambda}^\dagger\Big) + 240\,\mathrm{Tr}\Big(y^D y^{D\dagger} m_{d^c}^{2*}\Big) + 120\,\mathrm{Tr}\Big(y^D m_Q^{2*} y^{D\dagger}\Big) \\
&+ 40\,\mathrm{Tr}\Big(y^E y^{E\dagger} m_{e^c}^{2*}\Big) + 80\,\mathrm{Tr}\Big(y^E m_L^{2*} y^{E\dagger}\Big) + 120\,\mathrm{Tr}\Big(y^U y^{U\dagger} m_{u^c}^{2*}\Big) \\
&+ 120\,\mathrm{Tr}\Big(y^U m_Q^{2*} y^{U\dagger}\Big) - 120\,\mathrm{Tr}\Big(\tilde{\lambda}m_{H_1}^{2*}\tilde{\lambda}^\dagger\Big)\Big]\,. \qquad \text{(D.92)}
\end{aligned}
$$

In the following, $\mathbf{1}$ denotes an identity matrix of the appropriate dimensions. The RGEs are then given by

$$
\begin{aligned}
\beta_{m_Q^2}^{(1)} = &-\frac{2}{15}g_1^2\mathbf{1}|M_1|^2 - \frac{1}{5}g_1'^2\mathbf{1}|M_1'|^2 - \frac{32}{3}g_3^2\mathbf{1}|M_3|^2 - 6g_2^2\mathbf{1}|M_2|^2 + 2m_{H_d}^2 y^{D\dagger}y^D \\
&+ 2m_{H_u}^2 y^{U\dagger}y^U + 2T^{D\dagger}T^D + 2T^{U\dagger}T^U + 2m_{L_4}^2 g^{D*}g^{DT} + 2T^{g^{D}*}T^{g^{D}T} \\
&+ m_Q^2 y^{D\dagger}y^D + m_Q^2 y^{U\dagger}y^U + m_Q^2 g^{D*}g^{DT} + 2y^{D\dagger}m_{d^c}^2 y^D + y^{D\dagger}y^D m_Q^2
\end{aligned}
$$

$$
\begin{aligned}
&+ 2y^{U\dagger}m_{u^c}^2 y^U + y^{U\dagger}y^U m_Q^2 + 2g^{D*}m_{\bar{D}}^2 g^{DT} + g^{D*}g^{DT}m_Q^2 + \frac{1}{\sqrt{15}}g_1\mathbf{1}\Sigma_{1,1} \\
&+ \frac{1}{\sqrt{10}}g_1'\mathbf{1}\Sigma_{1,4}\,, \qquad \text{(D.93)} \\
\beta_{m_Q^2}^{(2)} = &\frac{32}{45}g_1^2g_3^2\mathbf{1}|M_3|^2 + \frac{16}{15}g_1'^2g_3^2\mathbf{1}|M_3|^2 + 32g_2^2g_3^2\mathbf{1}|M_3|^2 + \frac{160}{3}g_3^4\mathbf{1}|M_3|^2 \\
&+ \frac{2}{5}g_1^2g_2^2\mathbf{1}|M_2|^2 + \frac{3}{5}g_1'^2g_2^2\mathbf{1}|M_2|^2 + 87g_2^4\mathbf{1}|M_2|^2 + 32g_2^2g_3^2\mathbf{1}|M_2|^2 \\
&+ \frac{16}{45}g_1^2g_3^2M_1\mathbf{1}M_3^* + \frac{8}{15}g_1'^2g_3^2M_1'\mathbf{1}M_3^* + 16g_2^2g_3^2M_2\mathbf{1}M_3^* + \frac{1}{5}g_1^2g_2^2M_1\mathbf{1}M_2^* \\
&+ \frac{3}{10}g_1'^2g_2^2M_1'\mathbf{1}M_2^* + 16g_2^2g_3^2M_3\mathbf{1}M_2^* + \frac{4}{5}g_1^2m_{H_d}^2y^{D\dagger}y^D + \frac{6}{5}g_1'^2m_{H_d}^2y^{D\dagger}y^D \\
&- 4m_{H_d}^2|\lambda|^2y^{D\dagger}y^D - 2m_{H_u}^2|\lambda|^2y^{D\dagger}y^D - 2m_S^2|\lambda|^2y^{D\dagger}y^D - 2|T_\lambda|^2y^{D\dagger}y^D \\
&- 2\lambda T_\lambda^*y^{D\dagger}T^D + \frac{8}{5}g_1^2m_{H_u}^2y^{U\dagger}y^U + \frac{2}{5}g_1'^2m_{H_u}^2y^{U\dagger}y^U - 2m_{H_d}^2|\lambda|^2y^{U\dagger}y^U \\
&- 4m_{H_u}^2|\lambda|^2y^{U\dagger}y^U - 2m_S^2|\lambda|^2y^{U\dagger}y^U - 2|T_\lambda|^2y^{U\dagger}y^U - 2\lambda T_\lambda^*y^{U\dagger}T^U \\
&- \frac{4}{5}g_1^2M_1T^{D\dagger}y^D - \frac{6}{5}g_1'^2M_1'T^{D\dagger}y^D + \frac{4}{5}g_1^2T^{D\dagger}T^D + \frac{6}{5}g_1'^2T^{D\dagger}T^D \\
&- 2|\lambda|^2T^{D\dagger}T^D - \frac{8}{5}g_1^2M_1T^{U\dagger}y^U - \frac{2}{5}g_1'^2M_1'T^{U\dagger}y^U + \frac{8}{5}g_1^2T^{U\dagger}T^U \\
&+ \frac{2}{5}g_1'^2T^{U\dagger}T^U - 2|\lambda|^2T^{U\dagger}T^U + \frac{4}{5}g_1^2m_{L_4}^2g^{D*}g^{DT} + \frac{6}{5}g_1'^2m_{L_4}^2g^{D*}g^{DT} \\
&- 4m_{L_4}^2|\tilde{\sigma}|^2g^{D*}g^{DT} - 2m_{\bar{L}_4}^2|\tilde{\sigma}|^2g^{D*}g^{DT} - 2m_\phi^2|\tilde{\sigma}|^2g^{D*}g^{DT} - 2|T_{\tilde{\sigma}}|^2g^{D*}g^{DT} \\
&+ \frac{1}{150}g_1'^2\Big\{\Big[-11g_1^2\Big(2M_1' + M_1\Big) + 160g_3^2M_1' + 45g_2^2M_2 + 80g_3^2M_3 \\
&+ 90g_2^2M_1' + 963g_1'^2M_1'\Big]\mathbf{1} + 60\Big(2M_1'y^{U\dagger}y^U - 3g^{D*}T^{g^DT} - 3y^{D\dagger}T^D \\
&+ 6M_1'g^{D*}g^{DT} + 6M_1'y^{D\dagger}y^D - y^{U\dagger}T^U\Big)\Big\}M_1'^* + \frac{1}{450}g_1^2\Big(\Big\{10\Big[16g_3^2\Big(2M_1 \\
&+ M_3\Big) + 9g_2^2\Big(2M_1 + M_2\Big)\Big] + 1734g_1^2M_1 - 33g_1'^2\Big(2M_1 + M_1'\Big)\Big\}\mathbf{1} \\
&+ 360\Big(2M_1g^{D*}g^{DT} + 2M_1y^{D\dagger}y^D - 2y^{U\dagger}T^U + 4M_1y^{U\dagger}y^U - g^{D*}T^{g^DT} \\
&- y^{D\dagger}T^D\Big)\Big)M_1^* - 2\tilde{\sigma}T_{\tilde{\sigma}}^*g^{D*}T^{g^DT} - \frac{4}{5}g_1^2M_1T^{g^D*}g^{DT} - \frac{6}{5}g_1'^2M_1'T^{g^D*}g^{DT} \\
&+ \frac{4}{5}g_1^2T^{g^D*}T^{g^DT} + \frac{6}{5}g_1'^2T^{g^D*}T^{g^DT} - 2|\tilde{\sigma}|^2T^{g^D*}T^{g^DT} + \frac{2}{5}g_1^2m_Q^2y^{D\dagger}y^D \\
&+ \frac{3}{5}g_1'^2m_Q^2y^{D\dagger}y^D - |\lambda|^2m_Q^2y^{D\dagger}y^D + \frac{4}{5}g_1^2m_Q^2y^{U\dagger}y^U + \frac{1}{5}g_1'^2m_Q^2y^{U\dagger}y^U \\
&- |\lambda|^2m_Q^2y^{U\dagger}y^U + \frac{2}{5}g_1^2m_Q^2g^{D*}g^{DT} + \frac{3}{5}g_1'^2m_Q^2g^{D*}g^{DT} - |\tilde{\sigma}|^2m_Q^2g^{D*}g^{DT} \\
&+ \frac{4}{5}g_1^2y^{D\dagger}m_{d^c}^2y^D + \frac{6}{5}g_1'^2y^{D\dagger}m_{d^c}^2y^D - 2|\lambda|^2y^{D\dagger}m_{d^c}^2y^D + \frac{2}{5}g_1^2y^{D\dagger}y^Dm_Q^2
\end{aligned}
$$

$$
\begin{aligned}
&+ \frac{3}{5}g_1'^2 y^{D\dagger} y^D m_Q^2 - |\lambda|^2 y^{D\dagger} y^D m_Q^2 + \frac{8}{5}g_1^2 y^{U\dagger} m_{u^c}^2 y^U + \frac{2}{5}g_1'^2 y^{U\dagger} m_{u^c}^2 y^U \\
&- 2|\lambda|^2 y^{U\dagger} m_{u^c}^2 y^U + \frac{4}{5}g_1^2 y^{U\dagger} y^U m_Q^2 + \frac{1}{5}g_1'^2 y^{U\dagger} y^U m_Q^2 - |\lambda|^2 y^{U\dagger} y^U m_Q^2 \\
&+ \frac{4}{5}g_1^2 g^{D*} m_{\bar{D}}^2 g^{DT} + \frac{6}{5}g_1'^2 g^{D*} m_{\bar{D}}^2 g^{DT} - 2|\tilde{\sigma}|^2 g^{D*} m_{\bar{D}}^2 g^{DT} + \frac{2}{5}g_1^2 g^{D*} g^{DT} m_Q^2 \\
&+ \frac{3}{5}g_1'^2 g^{D*} g^{DT} m_Q^2 - |\tilde{\sigma}|^2 g^{D*} g^{DT} m_Q^2 - 8m_{H_d}^2 y^{D\dagger} y^D y^{D\dagger} y^D - 4y^{D\dagger} y^D T^{D\dagger} T^D \\
&- 4y^{D\dagger} T^D T^{D\dagger} y^D - 8m_{H_u}^2 y^{U\dagger} y^U y^{U\dagger} y^U - 4y^{U\dagger} y^U T^{U\dagger} T^U - 4y^{U\dagger} T^U T^{U\dagger} y^U \\
&- 4T^{D\dagger} y^D y^{D\dagger} T^D - 4T^{D\dagger} T^D y^{D\dagger} y^D - 4T^{U\dagger} y^U y^{U\dagger} T^U - 4T^{U\dagger} T^U y^{U\dagger} y^U \\
&- 8m_{L_4}^2 g^{D*} g^{DT} g^{D*} g^{DT} - 4g^{D*} g^{DT} T^{g^D *} T^{g^D T} - 2m_{L_4}^2 g^{D*} \kappa^T \kappa^* g^{DT} \\
&- 2m_S^2 g^{D*} \kappa^T \kappa^* g^{DT} - 2g^{D*} \kappa^T T^{\kappa *} T^{g^D T} - 4g^{D*} T^{g^D T} T^{g^D *} g^{DT} \\
&- 2g^{D*} T^{\kappa T} T^{\kappa *} g^{DT} - 4T^{g^D *} g^{DT} g^{D*} T^{g^D T} - 2T^{g^D *} \kappa^T \kappa^* T^{g^D T} \\
&- 4T^{g^D *} T^{g^D T} g^{D*} g^{DT} - 2T^{g^D *} T^{\kappa T} \kappa^* g^{DT} - 2m_Q^2 y^{D\dagger} y^D y^{D\dagger} y^D \\
&- 2m_Q^2 y^{U\dagger} y^U y^{U\dagger} y^U - 2m_Q^2 g^{D*} g^{DT} g^{D*} g^{DT} - m_Q^2 g^{D*} \kappa^T \kappa^* g^{DT} \\
&- 4y^{D\dagger} m_{d^c}^2 y^D y^{D\dagger} y^D - 4y^{D\dagger} y^D m_Q^2 y^{D\dagger} y^D - 4y^{D\dagger} y^D y^{D\dagger} m_{d^c}^2 y^D \\
&- 2y^{D\dagger} y^D y^{D\dagger} y^D m_Q^2 - 4y^{U\dagger} m_{u^c}^2 y^U y^{U\dagger} y^U - 4y^{U\dagger} y^U m_Q^2 y^{U\dagger} y^U \\
&- 4y^{U\dagger} y^U y^{U\dagger} m_{u^c}^2 y^U - 2y^{U\dagger} y^U y^{U\dagger} y^U m_Q^2 - 4g^{D*} m_{\bar{D}}^2 g^{DT} g^{D*} g^{DT} \\
&- 2g^{D*} m_{\bar{D}}^2 \kappa^T \kappa^* g^{DT} - 4g^{D*} g^{DT} m_Q^2 g^{D*} g^{DT} - 4g^{D*} g^{DT} g^{D*} m_{\bar{D}}^2 g^{DT} \\
&- 2g^{D*} g^{DT} g^{D*} g^{DT} m_Q^2 - 2g^{D*} \kappa^T m_D^2 \kappa^* g^{DT} - 2g^{D*} \kappa^T \kappa^* m_{\bar{D}}^2 g^{DT} \\
&- g^{D*} \kappa^T \kappa^* g^{DT} m_Q^2 - 2\lambda^* T^{D\dagger} y^D T_\lambda - 2\lambda^* T^{U\dagger} y^U T_\lambda - 2\tilde{\sigma}^* T^{g^D *} g^{DT} T_{\tilde{\sigma}} \\
&+ 6g_2^4 \mathbf{1} \Sigma_{2,2} + \frac{32}{3}g_3^4 \mathbf{1} \Sigma_{2,3} + \frac{2}{15}g_1^2 \mathbf{1} \Sigma_{2,11} + \frac{1}{5}\sqrt{\frac{2}{3}} g_1 g_1' \mathbf{1} \Sigma_{2,14} \\
&+ \frac{1}{5}\sqrt{\frac{2}{3}} g_1 g_1' \mathbf{1} \Sigma_{2,41} + \frac{1}{5}g_1'^2 \mathbf{1} \Sigma_{2,44} + \frac{4}{\sqrt{15}} g_1 \mathbf{1} \Sigma_{3,1} + 2\sqrt{\frac{2}{5}} g_1' \mathbf{1} \Sigma_{3,4} \\
&- 4m_{H_d}^2 y^{D\dagger} y^D \operatorname{Tr}\Big(f f^\dagger\Big) - 2T^{D\dagger} T^D \operatorname{Tr}\Big(f f^\dagger\Big) - m_Q^2 y^{D\dagger} y^D \operatorname{Tr}\Big(f f^\dagger\Big) \\
&- 2y^{D\dagger} m_{d^c}^2 y^D \operatorname{Tr}\Big(f f^\dagger\Big) - y^{D\dagger} y^D m_Q^2 \operatorname{Tr}\Big(f f^\dagger\Big) - 4m_{H_u}^2 y^{U\dagger} y^U \operatorname{Tr}\Big(\tilde{f} \tilde{f}^\dagger\Big) \\
&- 2T^{U\dagger} T^U \operatorname{Tr}\Big(\tilde{f} \tilde{f}^\dagger\Big) - m_Q^2 y^{U\dagger} y^U \operatorname{Tr}\Big(\tilde{f} \tilde{f}^\dagger\Big) - 2y^{U\dagger} m_{u^c}^2 y^U \operatorname{Tr}\Big(\tilde{f} \tilde{f}^\dagger\Big) \\
&- y^{U\dagger} y^U m_Q^2 \operatorname{Tr}\Big(\tilde{f} \tilde{f}^\dagger\Big) - 12m_{L_4}^2 g^{D*} g^{DT} \operatorname{Tr}\Big(g^D g^{D\dagger}\Big) \\
&- 6T^{g^D *} T^{g^D T} \operatorname{Tr}\Big(g^D g^{D\dagger}\Big) - 3m_Q^2 g^{D*} g^{DT} \operatorname{Tr}\Big(g^D g^{D\dagger}\Big) \\
&- 6g^{D*} m_{\bar{D}}^2 g^{DT} \operatorname{Tr}\Big(g^D g^{D\dagger}\Big) - 3g^{D*} g^{DT} m_Q^2 \operatorname{Tr}\Big(g^D g^{D\dagger}\Big) \\
&- 4m_{L_4}^2 g^{D*} g^{DT} \operatorname{Tr}\Big(h^E h^{E\dagger}\Big) - 2T^{g^D *} T^{g^D T} \operatorname{Tr}\Big(h^E h^{E\dagger}\Big)
\end{aligned}
$$

$$
\begin{aligned}
&- m_Q^2 g^{D*} g^{DT} \operatorname{Tr}\Big(h^E h^{E\dagger}\Big) - 2 g^{D*} m_{\bar{D}}^2 g^{DT} \operatorname{Tr}\Big(h^E h^{E\dagger}\Big) \\
&- g^{D*} g^{DT} m_Q^2 \operatorname{Tr}\Big(h^E h^{E\dagger}\Big) - 12 m_{H_d}^2 y^{D\dagger} y^D \operatorname{Tr}\Big(y^D y^{D\dagger}\Big) \\
&- 6 T^{D\dagger} T^D \operatorname{Tr}\Big(y^D y^{D\dagger}\Big) - 3 m_Q^2 y^{D\dagger} y^D \operatorname{Tr}\Big(y^D y^{D\dagger}\Big) - 6 y^{D\dagger} m_{d^c}^2 y^D \operatorname{Tr}\Big(y^D y^{D\dagger}\Big) \\
&- 3 y^{D\dagger} y^D m_Q^2 \operatorname{Tr}\Big(y^D y^{D\dagger}\Big) - 4 m_{H_d}^2 y^{D\dagger} y^D \operatorname{Tr}\Big(y^E y^{E\dagger}\Big) - 2 T^{D\dagger} T^D \operatorname{Tr}\Big(y^E y^{E\dagger}\Big) \\
&- m_Q^2 y^{D\dagger} y^D \operatorname{Tr}\Big(y^E y^{E\dagger}\Big) - 2 y^{D\dagger} m_{d^c}^2 y^D \operatorname{Tr}\Big(y^E y^{E\dagger}\Big) - y^{D\dagger} y^D m_Q^2 \operatorname{Tr}\Big(y^E y^{E\dagger}\Big) \\
&- 12 m_{H_u}^2 y^{U\dagger} y^U \operatorname{Tr}\Big(y^U y^{U\dagger}\Big) - 6 T^{U\dagger} T^U \operatorname{Tr}\Big(y^U y^{U\dagger}\Big) - 3 m_Q^2 y^{U\dagger} y^U \operatorname{Tr}\Big(y^U y^{U\dagger}\Big) \\
&- 6 y^{U\dagger} m_{u^c}^2 y^U \operatorname{Tr}\Big(y^U y^{U\dagger}\Big) - 3 y^{U\dagger} y^U m_Q^2 \operatorname{Tr}\Big(y^U y^{U\dagger}\Big) - 2 T^{D\dagger} y^D \operatorname{Tr}\Big(f^\dagger T^f\Big) \\
&- 2 T^{U\dagger} y^U \operatorname{Tr}\Big(\tilde{f}^\dagger T^{\tilde{f}}\Big) - 6 T^{g^D *} g^{DT} \operatorname{Tr}\Big(g^{D\dagger} T^{g^D}\Big) - 2 T^{g^D *} g^{DT} \operatorname{Tr}\Big(h^{E\dagger} T^{h^E}\Big) \\
&- 6 T^{D\dagger} y^D \operatorname{Tr}\Big(y^{D\dagger} T^D\Big) - 2 T^{D\dagger} y^D \operatorname{Tr}\Big(y^{E\dagger} T^E\Big) - 6 T^{U\dagger} y^U \operatorname{Tr}\Big(y^{U\dagger} T^U\Big) \\
&- 2 y^{D\dagger} T^D \operatorname{Tr}\Big(T^{f*} f^T\Big) - 2 y^{D\dagger} y^D \operatorname{Tr}\Big(T^{f*} T^{fT}\Big) - 2 y^{U\dagger} T^U \operatorname{Tr}\Big(T^{\tilde{f}*} \tilde{f}^T\Big) \\
&- 2 y^{U\dagger} y^U \operatorname{Tr}\Big(T^{\tilde{f}*} T^{\tilde{f}T}\Big) - 6 g^{D*} T^{g^D T} \operatorname{Tr}\Big(T^{g^D *} g^{DT}\Big) \\
&- 6 g^{D*} g^{DT} \operatorname{Tr}\Big(T^{g^D *} T^{g^D T}\Big) - 2 g^{D*} T^{g^D T} \operatorname{Tr}\Big(T^{h^E *} h^{ET}\Big) \\
&- 2 g^{D*} g^{DT} \operatorname{Tr}\Big(T^{h^E *} T^{h^E T}\Big) - 6 y^{D\dagger} T^D \operatorname{Tr}\Big(T^{D*} y^{DT}\Big) \\
&- 6 y^{D\dagger} y^D \operatorname{Tr}\Big(T^{D*} T^{DT}\Big) - 2 y^{D\dagger} T^D \operatorname{Tr}\Big(T^{E*} y^{ET}\Big) - 2 y^{D\dagger} y^D \operatorname{Tr}\Big(T^{E*} T^{ET}\Big) \\
&- 6 y^{U\dagger} T^U \operatorname{Tr}\Big(T^{U*} y^{UT}\Big) - 6 y^{U\dagger} y^U \operatorname{Tr}\Big(T^{U*} T^{UT}\Big) - 2 y^{D\dagger} y^D \operatorname{Tr}\Big(f m_{H_2}^2 f^\dagger\Big) \\
&- 2 y^{D\dagger} y^D \operatorname{Tr}\Big(f f^\dagger m_\Sigma^{2*}\Big) - 2 y^{U\dagger} y^U \operatorname{Tr}\Big(\tilde{f} m_{H_1}^2 \tilde{f}^\dagger\Big) - 2 y^{U\dagger} y^U \operatorname{Tr}\Big(\tilde{f} \tilde{f}^\dagger m_\Sigma^{2*}\Big) \\
&- 6 g^{D*} g^{DT} \operatorname{Tr}\Big(g^D g^{D\dagger} m_Q^{2*}\Big) - 6 g^{D*} g^{DT} \operatorname{Tr}\Big(g^D m_{\bar{D}}^{2*} g^{D\dagger}\Big) \\
&- 2 g^{D*} g^{DT} \operatorname{Tr}\Big(h^E m_{H_1}^2 h^{E\dagger}\Big) - 2 g^{D*} g^{DT} \operatorname{Tr}\Big(h^E h^{E\dagger} m_{e^c}^2\Big) \\
&- 6 y^{D\dagger} y^D \operatorname{Tr}\Big(m_{d^c}^2 y^D y^{D\dagger}\Big) - 2 y^{D\dagger} y^D \operatorname{Tr}\Big(m_{e^c}^2 y^E y^{E\dagger}\Big) \\
&- 2 y^{D\dagger} y^D \operatorname{Tr}\Big(m_L^2 y^{E\dagger} y^E\Big) - 6 y^{D\dagger} y^D \operatorname{Tr}\Big(m_Q^2 y^{D\dagger} y^D\Big) \\
&- 6 y^{U\dagger} y^U \operatorname{Tr}\Big(m_Q^2 y^{U\dagger} y^U\Big) - 6 y^{U\dagger} y^U \operatorname{Tr}\Big(m_{u^c}^2 y^U y^{U\dagger}\Big),
\end{aligned}
\tag{D.94}
$$

$$
\beta_{m_L^2}^{(1)} = -\frac{6}{5} g_1^2 \mathbf{1} |M_1|^2 - \frac{4}{5} g_1'^2 \mathbf{1} |M_1'|^2 - 6 g_2^2 \mathbf{1} |M_2|^2 + 2 m_{H_d}^2 y^{E\dagger} y^E + 2 T^{E\dagger} T^E
$$

$$+ m_L^2 y^{E\dagger} y^E + 2 y^{E\dagger} m_{e^c}^2 y^E + y^{E\dagger} y^E m_L^2 - \sqrt{\frac{3}{5}} g_1 \mathbf{1} \Sigma_{1,1} + \sqrt{\frac{2}{5}} g_1' \mathbf{1} \Sigma_{1,4} \,, \tag{D.95}$$

$$\begin{aligned}
\beta_{m_L^2}^{(2)} = {} & \frac{18}{5} g_1^2 g_2^2 \mathbf{1} |M_2|^2 + \frac{12}{5} g_1'^2 g_2^2 \mathbf{1} |M_2|^2 + 87 g_2^4 \mathbf{1} |M_2|^2 + \frac{9}{5} g_1^2 g_2^2 M_1 \mathbf{1} M_2^* \\
& + \frac{6}{5} g_1'^2 g_2^2 M_1' \mathbf{1} M_2^* + \frac{12}{5} g_1^2 m_{H_d}^2 y^{E\dagger} y^E + \frac{3}{5} g_1'^2 m_{H_d}^2 y^{E\dagger} y^E - 4 m_{H_d}^2 |\lambda|^2 y^{E\dagger} y^E \\
& - 2 m_{H_u}^2 |\lambda|^2 y^{E\dagger} y^E - 2 m_S^2 |\lambda|^2 y^{E\dagger} y^E - 2 |T_\lambda|^2 y^{E\dagger} y^E \\
& + \frac{3}{25} g_1^2 \Big\{ -20 y^{E\dagger} T^E + 3 \Big[2 g_1'^2 \Big(2 M_1 + M_1' \Big) + 5 g_2^2 \Big(2 M_1 + M_2 \Big) \\
& + 99 g_1^2 M_1 \Big] \mathbf{1} + 40 M_1 y^{E\dagger} y^E \Big\} M_1^* + \frac{3}{25} g_1'^2 \Big\{ \Big[10 g_2^2 \Big(2 M_1' + M_2 \Big) \\
& + 217 g_1'^2 M_1' + 6 g_1^2 \Big(2 M_1' + M_1 \Big) \Big] \mathbf{1} + 10 M_1' y^{E\dagger} y^E - 5 y^{E\dagger} T^E \Big\} M_1'^* \\
& - 2 \lambda T_\lambda^* y^{E\dagger} T^E - \frac{12}{5} g_1^2 M_1 T^{E\dagger} y^E - \frac{3}{5} g_1'^2 M_1' T^{E\dagger} y^E + \frac{12}{5} g_1^2 T^{E\dagger} T^E \\
& + \frac{3}{5} g_1'^2 T^{E\dagger} T^E - 2 |\lambda|^2 T^{E\dagger} T^E + \frac{6}{5} g_1^2 m_L^2 y^{E\dagger} y^E + \frac{3}{10} g_1'^2 m_L^2 y^{E\dagger} y^E \\
& - |\lambda|^2 m_L^2 y^{E\dagger} y^E + \frac{12}{5} g_1^2 y^{E\dagger} m_{e^c}^2 y^E + \frac{3}{5} g_1'^2 y^{E\dagger} m_{e^c}^2 y^E - 2 |\lambda|^2 y^{E\dagger} m_{e^c}^2 y^E \\
& + \frac{6}{5} g_1^2 y^{E\dagger} y^E m_L^2 + \frac{3}{10} g_1'^2 y^{E\dagger} y^E m_L^2 - |\lambda|^2 y^{E\dagger} y^E m_L^2 \\
& - 4 m_{H_d}^2 y^{E\dagger} h^E h^{E\dagger} y^E - 4 m_{L_4}^2 y^{E\dagger} h^E h^{E\dagger} y^E - 4 y^{E\dagger} h^E T^{h^E\dagger} T^E \\
& - 8 m_{H_d}^2 y^{E\dagger} y^E y^{E\dagger} y^E - 4 y^{E\dagger} y^E T^{E\dagger} T^E - 4 y^{E\dagger} T^{h^E} T^{h^E\dagger} y^E - 4 y^{E\dagger} T^E T^{E\dagger} y^E \\
& - 4 T^{E\dagger} h^E h^{E\dagger} T^E - 4 T^{E\dagger} y^E y^{E\dagger} T^E - 4 T^{E\dagger} T^{h^E} h^{E\dagger} y^E - 4 T^{E\dagger} T^E y^{E\dagger} y^E \\
& - 2 m_L^2 y^{E\dagger} h^E h^{E\dagger} y^E - 2 m_L^2 y^{E\dagger} y^E y^{E\dagger} y^E - 4 y^{E\dagger} h^E m_{H_1}^2 h^{E\dagger} y^E \\
& - 4 y^{E\dagger} h^E h^{E\dagger} m_{e^c}^2 y^E - 2 y^{E\dagger} h^E h^{E\dagger} y^E m_L^2 - 4 y^{E\dagger} m_{e^c}^2 h^E h^{E\dagger} y^E \\
& - 4 y^{E\dagger} m_{e^c}^2 y^E y^{E\dagger} y^E - 4 y^{E\dagger} y^E m_L^2 y^{E\dagger} y^E - 4 y^{E\dagger} y^E y^{E\dagger} m_{e^c}^2 y^E \\
& - 2 y^{E\dagger} y^E y^{E\dagger} y^E m_L^2 - 2 \lambda^* T^{E\dagger} y^E T_\lambda + 6 g_2^4 \mathbf{1} \Sigma_{2,2} + \frac{6}{5} g_1^2 \mathbf{1} \Sigma_{2,11} \\
& - \frac{2}{5} \sqrt{6} g_1 g_1' \mathbf{1} \Sigma_{2,14} - \frac{2}{5} \sqrt{6} g_1 g_1' \mathbf{1} \Sigma_{2,41} + \frac{4}{5} g_1'^2 \mathbf{1} \Sigma_{2,44} - 4 \sqrt{\frac{3}{5}} g_1 \mathbf{1} \Sigma_{3,1} \\
& + 4 \sqrt{\frac{2}{5}} g_1' \mathbf{1} \Sigma_{3,4} - 4 m_{H_d}^2 y^{E\dagger} y^E \operatorname{Tr}\Big(f f^\dagger \Big) - 2 T^{E\dagger} T^E \operatorname{Tr}\Big(f f^\dagger \Big) \\
& - m_L^2 y^{E\dagger} y^E \operatorname{Tr}\Big(f f^\dagger \Big) - 2 y^{E\dagger} m_{e^c}^2 y^E \operatorname{Tr}\Big(f f^\dagger \Big) - y^{E\dagger} y^E m_L^2 \operatorname{Tr}\Big(f f^\dagger \Big) \\
& - 12 m_{H_d}^2 y^{E\dagger} y^E \operatorname{Tr}\Big(y^D y^{D\dagger} \Big) - 6 T^{E\dagger} T^E \operatorname{Tr}\Big(y^D y^{D\dagger} \Big) \\
& - 3 m_L^2 y^{E\dagger} y^E \operatorname{Tr}\Big(y^D y^{D\dagger} \Big) - 6 y^{E\dagger} m_{e^c}^2 y^E \operatorname{Tr}\Big(y^D y^{D\dagger} \Big) \\
& - 3 y^{E\dagger} y^E m_L^2 \operatorname{Tr}\Big(y^D y^{D\dagger} \Big) - 4 m_{H_d}^2 y^{E\dagger} y^E \operatorname{Tr}\Big(y^E y^{E\dagger} \Big)
\end{aligned}$$

$$
\begin{aligned}
&- 2T^{E\dagger}T^{E}\,\mathrm{Tr}\Big(y^{E}y^{E\dagger}\Big) - m_L^2 y^{E\dagger}y^{E}\,\mathrm{Tr}\Big(y^{E}y^{E\dagger}\Big) - 2y^{E\dagger}m_{e^c}^2 y^{E}\,\mathrm{Tr}\Big(y^{E}y^{E\dagger}\Big)\\
&- y^{E\dagger}y^{E}m_L^2\,\mathrm{Tr}\Big(y^{E}y^{E\dagger}\Big) - 2T^{E\dagger}y^{E}\,\mathrm{Tr}\Big(f^{\dagger}T^{f}\Big) - 6T^{E\dagger}y^{E}\,\mathrm{Tr}\Big(y^{D\dagger}T^{D}\Big)\\
&- 2T^{E\dagger}y^{E}\,\mathrm{Tr}\Big(y^{E\dagger}T^{E}\Big) - 2y^{E\dagger}T^{E}\,\mathrm{Tr}\Big(T^{f*}f^{T}\Big) - 2y^{E\dagger}y^{E}\,\mathrm{Tr}\Big(T^{f*}T^{fT}\Big)\\
&- 6y^{E\dagger}T^{E}\,\mathrm{Tr}\Big(T^{D*}y^{DT}\Big) - 6y^{E\dagger}y^{E}\,\mathrm{Tr}\Big(T^{D*}T^{DT}\Big) - 2y^{E\dagger}T^{E}\,\mathrm{Tr}\Big(T^{E*}y^{ET}\Big)\\
&- 2y^{E\dagger}y^{E}\,\mathrm{Tr}\Big(T^{E*}T^{ET}\Big) - 2y^{E\dagger}y^{E}\,\mathrm{Tr}\Big(fm_{H_2}^2 f^{\dagger}\Big) - 2y^{E\dagger}y^{E}\,\mathrm{Tr}\Big(ff^{\dagger}m_{\Sigma}^{2*}\Big)\\
&- 6y^{E\dagger}y^{E}\,\mathrm{Tr}\Big(m_{d^c}^2 y^{D}y^{D\dagger}\Big) - 2y^{E\dagger}y^{E}\,\mathrm{Tr}\Big(m_{e^c}^2 y^{E}y^{E\dagger}\Big)\\
&- 2y^{E\dagger}y^{E}\,\mathrm{Tr}\Big(m_L^2 y^{E\dagger}y^{E}\Big) - 6y^{E\dagger}y^{E}\,\mathrm{Tr}\Big(m_Q^2 y^{D\dagger}y^{D}\Big),
\end{aligned}
\tag{D.96}
$$

$$
\begin{aligned}
\beta^{(1)}_{m_{H_d}^2} = &-\frac{6}{5}g_1^2|M_1|^2 - \frac{9}{5}g_1'^2|M_1'|^2 - 6g_2^2|M_2|^2 + 2m_{H_d}^2|\lambda|^2 + 2m_{H_u}^2|\lambda|^2\\
&+ 2m_S^2|\lambda|^2 + 2|T_\lambda|^2 - \sqrt{\frac{3}{5}}g_1\Sigma_{1,1} - \frac{3}{\sqrt{10}}g_1'\Sigma_{1,4} + 2m_{H_d}^2\,\mathrm{Tr}\Big(ff^{\dagger}\Big)\\
&+ 6m_{H_d}^2\,\mathrm{Tr}\Big(y^{D}y^{D\dagger}\Big) + 2m_{H_d}^2\,\mathrm{Tr}\Big(y^{E}y^{E\dagger}\Big) + 2\,\mathrm{Tr}\Big(T^{f*}T^{fT}\Big)\\
&+ 6\,\mathrm{Tr}\Big(T^{D*}T^{DT}\Big) + 2\,\mathrm{Tr}\Big(T^{E*}T^{ET}\Big) + 2\,\mathrm{Tr}\Big(fm_{H_2}^2 f^{\dagger}\Big) + 2\,\mathrm{Tr}\Big(ff^{\dagger}m_{\Sigma}^{2*}\Big)\\
&+ 6\,\mathrm{Tr}\Big(m_{d^c}^2 y^{D}y^{D\dagger}\Big) + 2\,\mathrm{Tr}\Big(m_{e^c}^2 y^{E}y^{E\dagger}\Big) + 2\,\mathrm{Tr}\Big(m_L^2 y^{E\dagger}y^{E}\Big)\\
&+ 6\,\mathrm{Tr}\Big(m_Q^2 y^{D\dagger}y^{D}\Big),
\end{aligned}
\tag{D.97}
$$

$$
\begin{aligned}
\beta^{(2)}_{m_{H_d}^2} = &\frac{18}{5}g_1^2g_2^2|M_2|^2 + \frac{27}{5}g_1'^2g_2^2|M_2|^2 + 87g_2^4|M_2|^2 + 2g_1'^2m_{H_d}^2|\lambda|^2 + 2g_1'^2m_{H_u}^2|\lambda|^2\\
&+ 2g_1'^2m_S^2|\lambda|^2 + 2g_1'^2|T_\lambda|^2 + \frac{9}{5}g_1^2g_2^2M_1M_2^* + \frac{27}{10}g_1'^2g_2^2M_1'M_2^* - 12m_{H_d}^2|\lambda|^4\\
&- 12m_{H_u}^2|\lambda|^4 - 12m_S^2|\lambda|^4 - 2m_{H_d}^2|\sigma|^2|\lambda|^2 - 2m_{H_u}^2|\sigma|^2|\lambda|^2 - 2m_\phi^2|\sigma|^2|\lambda|^2\\
&- 4m_S^2|\sigma|^2|\lambda|^2 - 2m_S^2|\sigma|^2|\lambda|^2 - 2g_1'^2M_1'\lambda T_\lambda^* - 24|\lambda|^2|T_\lambda|^2 - 2|\sigma|^2|T_\lambda|^2\\
&- 2\sigma\lambda^*T_\sigma^*T_\lambda - 2\lambda\sigma^*T_\lambda^*T_\sigma - 2|\lambda|^2|T_\sigma|^2 + 6g_2^4\Sigma_{2,2} + \frac{6}{5}g_1^2\Sigma_{2,11}\\
&+ \frac{3}{5}\sqrt{6}g_1g_1'\Sigma_{2,14} + \frac{3}{5}\sqrt{6}g_1g_1'\Sigma_{2,41} + \frac{9}{5}g_1'^2\Sigma_{2,44} - 4\sqrt{\frac{3}{5}}g_1\Sigma_{3,1}\\
&- 6\sqrt{\frac{2}{5}}g_1'\Sigma_{3,4} + 2g_1'^2m_{H_d}^2\,\mathrm{Tr}\Big(ff^{\dagger}\Big) - 2m_{H_d}^2|\lambda|^2\,\mathrm{Tr}\Big(\tilde{f}\tilde{f}^{\dagger}\Big)\\
&- 4m_{H_u}^2|\lambda|^2\,\mathrm{Tr}\Big(\tilde{f}\tilde{f}^{\dagger}\Big) - 2m_S^2|\lambda|^2\,\mathrm{Tr}\Big(\tilde{f}\tilde{f}^{\dagger}\Big) - 2|T_\lambda|^2\,\mathrm{Tr}\Big(\tilde{f}\tilde{f}^{\dagger}\Big)\\
&- \frac{4}{5}g_1^2m_{H_d}^2\,\mathrm{Tr}\Big(y^{D}y^{D\dagger}\Big) - \frac{6}{5}g_1'^2m_{H_d}^2\,\mathrm{Tr}\Big(y^{D}y^{D\dagger}\Big) + 32g_3^2m_{H_d}^2\,\mathrm{Tr}\Big(y^{D}y^{D\dagger}\Big)
\end{aligned}
$$

$$
\begin{aligned}
&+ 64 g_3^2 |M_3|^2 \operatorname{Tr}\Big(y^D y^{D\dagger}\Big) + \frac{12}{5} g_1^2 m_{H_d}^2 \operatorname{Tr}\Big(y^E y^{E\dagger}\Big) - \frac{2}{5} g_1'^2 m_{H_d}^2 \operatorname{Tr}\Big(y^E y^{E\dagger}\Big) \\
&- 6 m_{H_d}^2 |\lambda|^2 \operatorname{Tr}\Big(y^U y^{U\dagger}\Big) - 12 m_{H_u}^2 |\lambda|^2 \operatorname{Tr}\Big(y^U y^{U\dagger}\Big) - 6 m_S^2 |\lambda|^2 \operatorname{Tr}\Big(y^U y^{U\dagger}\Big) \\
&- 6 |T_\lambda|^2 \operatorname{Tr}\Big(y^U y^{U\dagger}\Big) - 6 m_{H_d}^2 |\lambda|^2 \operatorname{Tr}\Big(\kappa \kappa^\dagger\Big) - 6 m_{H_u}^2 |\lambda|^2 \operatorname{Tr}\Big(\kappa \kappa^\dagger\Big) \\
&- 12 m_S^2 |\lambda|^2 \operatorname{Tr}\Big(\kappa \kappa^\dagger\Big) - 6 |T_\lambda|^2 \operatorname{Tr}\Big(\kappa \kappa^\dagger\Big) - 4 m_{H_d}^2 |\lambda|^2 \operatorname{Tr}\Big(\tilde{\lambda} \tilde{\lambda}^\dagger\Big) \\
&- 4 m_{H_u}^2 |\lambda|^2 \operatorname{Tr}\Big(\tilde{\lambda} \tilde{\lambda}^\dagger\Big) - 8 m_S^2 |\lambda|^2 \operatorname{Tr}\Big(\tilde{\lambda} \tilde{\lambda}^\dagger\Big) - 4 |T_\lambda|^2 \operatorname{Tr}\Big(\tilde{\lambda} \tilde{\lambda}^\dagger\Big) \\
&- 2 \lambda T_\lambda^* \operatorname{Tr}\Big(\tilde{f}^\dagger T^{\tilde{f}}\Big) - 32 g_3^2 M_3^* \operatorname{Tr}\Big(y^{D\dagger} T^D\Big) + \frac{1}{50} g_1^2 M_1^* \Big[1782 g_1^2 M_1 \\
&- 18 g_1'^2 M_1 + 180 g_2^2 M_1 - 9 g_1'^2 M_1' + 90 g_2^2 M_2 - 80 M_1 \operatorname{Tr}\Big(y^D y^{D\dagger}\Big) \\
&+ 240 M_1 \operatorname{Tr}\Big(y^E y^{E\dagger}\Big) + 40 \operatorname{Tr}\Big(y^{D\dagger} T^D\Big) - 120 \operatorname{Tr}\Big(y^{E\dagger} T^E\Big)\Big] \\
&+ \frac{1}{50} g_1'^2 M_1'^* \Big[-9 g_1^2 M_1 - 18 g_1^2 M_1' + 2997 g_1'^2 M_1' + 270 g_2^2 M_1' + 135 g_2^2 M_2 \\
&+ 100 \lambda^* \Big(2 M_1' \lambda - T_\lambda\Big) + 200 M_1' \operatorname{Tr}\Big(f f^\dagger\Big) - 120 M_1' \operatorname{Tr}\Big(y^D y^{D\dagger}\Big) \\
&- 40 M_1' \operatorname{Tr}\Big(y^E y^{E\dagger}\Big) - 100 \operatorname{Tr}\Big(f^\dagger T^f\Big) + 60 \operatorname{Tr}\Big(y^{D\dagger} T^D\Big) + 20 \operatorname{Tr}\Big(y^{E\dagger} T^E\Big)\Big] \\
&- 6 \lambda T_\lambda^* \operatorname{Tr}\Big(y^{U\dagger} T^U\Big) - 6 \lambda T_\lambda^* \operatorname{Tr}\Big(\kappa^\dagger T^\kappa\Big) - 4 \lambda T_\lambda^* \operatorname{Tr}\Big(\tilde{\lambda}^\dagger T^{\tilde{\lambda}}\Big) \\
&- 2 g_1'^2 M_1' \operatorname{Tr}\Big(T^{f*} f^T\Big) + 2 g_1'^2 \operatorname{Tr}\Big(T^{f*} T^{fT}\Big) - 2 \lambda^* T_\lambda \operatorname{Tr}\Big(T^{\tilde{f}*} \tilde{f}^T\Big) \\
&- 2 |\lambda|^2 \operatorname{Tr}\Big(T^{\tilde{f}*} T^{\tilde{f}T}\Big) + \frac{4}{5} g_1^2 M_1 \operatorname{Tr}\Big(T^{D*} y^{DT}\Big) + \frac{6}{5} g_1'^2 M_1' \operatorname{Tr}\Big(T^{D*} y^{DT}\Big) \\
&- 32 g_3^2 M_3 \operatorname{Tr}\Big(T^{D*} y^{DT}\Big) - \frac{4}{5} g_1^2 \operatorname{Tr}\Big(T^{D*} T^{DT}\Big) - \frac{6}{5} g_1'^2 \operatorname{Tr}\Big(T^{D*} T^{DT}\Big) \\
&+ 32 g_3^2 \operatorname{Tr}\Big(T^{D*} T^{DT}\Big) - \frac{12}{5} g_1^2 M_1 \operatorname{Tr}\Big(T^{E*} y^{ET}\Big) + \frac{2}{5} g_1'^2 M_1' \operatorname{Tr}\Big(T^{E*} y^{ET}\Big) \\
&+ \frac{12}{5} g_1^2 \operatorname{Tr}\Big(T^{E*} T^{ET}\Big) - \frac{2}{5} g_1'^2 \operatorname{Tr}\Big(T^{E*} T^{ET}\Big) - 6 \lambda^* T_\lambda \operatorname{Tr}\Big(T^{U*} y^{UT}\Big) \\
&- 6 |\lambda|^2 \operatorname{Tr}\Big(T^{U*} T^{UT}\Big) - 6 \lambda^* T_\lambda \operatorname{Tr}\Big(T^{\kappa*} \kappa^T\Big) - 6 |\lambda|^2 \operatorname{Tr}\Big(T^{\kappa*} T^{\kappa T}\Big) \\
&- 4 \lambda^* T_\lambda \operatorname{Tr}\Big(T^{\tilde{\lambda}*} \tilde{\lambda}^T\Big) - 4 |\lambda|^2 \operatorname{Tr}\Big(T^{\tilde{\lambda}*} T^{\tilde{\lambda}T}\Big) + 2 g_1'^2 \operatorname{Tr}\Big(f m_{H_2}^2 f^\dagger\Big) \\
&+ 2 g_1'^2 \operatorname{Tr}\Big(f f^\dagger m_\Sigma^{2*}\Big) - 2 |\lambda|^2 \operatorname{Tr}\Big(\tilde{f} m_{H_1}^2 \tilde{f}^\dagger\Big) - 2 |\lambda|^2 \operatorname{Tr}\Big(\tilde{f} \tilde{f}^\dagger m_\Sigma^{2*}\Big) \\
&- \frac{4}{5} g_1^2 \operatorname{Tr}\Big(m_{d^c}^2 y^D y^{D\dagger}\Big) - \frac{6}{5} g_1'^2 \operatorname{Tr}\Big(m_{d^c}^2 y^D y^{D\dagger}\Big) + 32 g_3^2 \operatorname{Tr}\Big(m_{d^c}^2 y^D y^{D\dagger}\Big) \\
&+ \frac{12}{5} g_1^2 \operatorname{Tr}\Big(m_{e^c}^2 y^E y^{E\dagger}\Big) - \frac{2}{5} g_1'^2 \operatorname{Tr}\Big(m_{e^c}^2 y^E y^{E\dagger}\Big) - 4 |\lambda|^2 \operatorname{Tr}\Big(m_{H_1}^2 \tilde{\lambda}^\dagger \tilde{\lambda}\Big)
\end{aligned}
$$

$$
\begin{aligned}
&+ \frac{12}{5} g_1^2 \operatorname{Tr}\Big(m_L^2 y^{E\dagger} y^E \Big) - \frac{2}{5} g_1'^2 \operatorname{Tr}\Big(m_L^2 y^{E\dagger} y^E \Big) - \frac{4}{5} g_1^2 \operatorname{Tr}\Big(m_Q^2 y^{D\dagger} y^D \Big) \\
&- \frac{6}{5} g_1'^2 \operatorname{Tr}\Big(m_Q^2 y^{D\dagger} y^D \Big) + 32 g_3^2 \operatorname{Tr}\Big(m_Q^2 y^{D\dagger} y^D \Big) - 6|\lambda|^2 \operatorname{Tr}\Big(m_Q^2 y^{U\dagger} y^U \Big) \\
&- 6|\lambda|^2 \operatorname{Tr}\Big(m_{u^c}^2 y^U y^{U\dagger} \Big) - 6|\lambda|^2 \operatorname{Tr}\Big(\kappa \kappa^\dagger m_D^{2*} \Big) - 6|\lambda|^2 \operatorname{Tr}\Big(\kappa m_{\bar{D}}^{2*} \kappa^\dagger \Big) \\
&- 4|\lambda|^2 \operatorname{Tr}\Big(\tilde{\lambda} \tilde{\lambda}^\dagger m_{H_2}^{2*} \Big) - 12 m_{H_d}^2 \operatorname{Tr}\Big(f f^\dagger f f^\dagger \Big) - 4 m_{H_d}^2 \operatorname{Tr}\Big(f f^\dagger \tilde{f} \tilde{f}^\dagger \Big) \\
&- 4 m_{H_u}^2 \operatorname{Tr}\Big(f f^\dagger \tilde{f} \tilde{f}^\dagger \Big) - 12 \operatorname{Tr}\Big(f f^\dagger T^f T^{f\dagger} \Big) - 4 \operatorname{Tr}\Big(f f^\dagger T^{\tilde{f}} T^{\tilde{f}\dagger} \Big) \\
&- 12 \operatorname{Tr}\Big(f T^{f\dagger} T^f f^\dagger \Big) - 4 \operatorname{Tr}\Big(f T^{f\dagger} T^{\tilde{f}} \tilde{f}^\dagger \Big) - 2 \operatorname{Tr}\Big(f T^{\tilde{\lambda}*} T^{\tilde{\lambda}T} f^\dagger \Big) \\
&- 4 \operatorname{Tr}\Big(\tilde{f} \tilde{f}^\dagger T^f T^{f\dagger} \Big) - 4 \operatorname{Tr}\Big(\tilde{f} T^{\tilde{f}\dagger} T^f f^\dagger \Big) - 6 m_{H_d}^2 \operatorname{Tr}\Big(g^D g^{D\dagger} y^{DT} y^{D*} \Big) \\
&- 6 m_{L_4}^2 \operatorname{Tr}\Big(g^D g^{D\dagger} y^{DT} y^{D*} \Big) - 6 \operatorname{Tr}\Big(g^D g^{D\dagger} T^{DT} T^{D*} \Big) \\
&- 4 m_{H_d}^2 \operatorname{Tr}\Big(h^E h^{E\dagger} y^E y^{E\dagger} \Big) - 4 m_{L_4}^2 \operatorname{Tr}\Big(h^E h^{E\dagger} y^E y^{E\dagger} \Big) \\
&- 4 \operatorname{Tr}\Big(h^E h^{E\dagger} T^E T^{E\dagger} \Big) - 4 \operatorname{Tr}\Big(h^E T^{h^E\dagger} T^E y^{E\dagger} \Big) \\
&- 36 m_{H_d}^2 \operatorname{Tr}\Big(y^D y^{D\dagger} y^D y^{D\dagger} \Big) - 36 \operatorname{Tr}\Big(y^D y^{D\dagger} T^D T^{D\dagger} \Big) \\
&- 6 m_{H_d}^2 \operatorname{Tr}\Big(y^D y^{U\dagger} y^U y^{D\dagger} \Big) - 6 m_{H_u}^2 \operatorname{Tr}\Big(y^D y^{U\dagger} y^U y^{D\dagger} \Big) \\
&- 6 \operatorname{Tr}\Big(y^D y^{U\dagger} T^U T^{D\dagger} \Big) - 36 \operatorname{Tr}\Big(y^D T^{D\dagger} T^D y^{D\dagger} \Big) \\
&- 6 \operatorname{Tr}\Big(y^D T^{U\dagger} T^U y^{D\dagger} \Big) - 6 \operatorname{Tr}\Big(y^D T^{g^D *} T^{g^D T} y^{D\dagger} \Big) \\
&- 12 m_{H_d}^2 \operatorname{Tr}\Big(y^E y^{E\dagger} y^E y^{E\dagger} \Big) - 4 \operatorname{Tr}\Big(y^E y^{E\dagger} T^{h^E} T^{h^E\dagger} \Big) \\
&- 12 \operatorname{Tr}\Big(y^E y^{E\dagger} T^E T^{E\dagger} \Big) - 4 \operatorname{Tr}\Big(y^E T^{E\dagger} T^{h^E} h^{E\dagger} \Big) - 12 \operatorname{Tr}\Big(y^E T^{E\dagger} T^E y^{E\dagger} \Big) \\
&- 6 \operatorname{Tr}\Big(y^U y^{D\dagger} T^D T^{U\dagger} \Big) - 6 \operatorname{Tr}\Big(y^U T^{D\dagger} T^D y^{U\dagger} \Big) - 2 m_{H_d}^2 \operatorname{Tr}\Big(\tilde{\lambda} \tilde{\lambda}^\dagger f^T f^* \Big) \\
&- 2 m_S^2 \operatorname{Tr}\Big(\tilde{\lambda} \tilde{\lambda}^\dagger f^T f^* \Big) - 2 \operatorname{Tr}\Big(\tilde{\lambda} \tilde{\lambda}^\dagger T^{fT} T^{f*} \Big) - 2 \operatorname{Tr}\Big(f^\dagger T^f T^{\tilde{\lambda}*} \tilde{\lambda}^T \Big) \\
&- 6 \operatorname{Tr}\Big(g^{D\dagger} y^{DT} T^{D*} T^{g^D} \Big) - 6 \operatorname{Tr}\Big(y^{D\dagger} T^D T^{g^D *} g^{DT} \Big) - 2 \operatorname{Tr}\Big(\tilde{\lambda}^\dagger f^T T^{f*} T^{\tilde{\lambda}} \Big) \\
&- 6 \operatorname{Tr}\Big(f m_{H_2}^2 f^\dagger f f^\dagger \Big) - 4 \operatorname{Tr}\Big(f m_{H_2}^2 f^\dagger \tilde{f} \tilde{f}^\dagger \Big) - 6 \operatorname{Tr}\Big(f f^\dagger f m_{H_2}^2 f^\dagger \Big) \\
&- 4 \operatorname{Tr}\Big(f f^\dagger \tilde{f} m_{H_1}^2 \tilde{f}^\dagger \Big) - 4 \operatorname{Tr}\Big(f f^\dagger \tilde{f} \tilde{f}^\dagger m_\Sigma^{2*} \Big) - 12 \operatorname{Tr}\Big(f f^\dagger m_\Sigma^{2*} f f^\dagger \Big) \\
&- 4 \operatorname{Tr}\Big(f f^\dagger m_\Sigma^{2*} \tilde{f} \tilde{f}^\dagger \Big) - 2 \operatorname{Tr}\Big(f \tilde{\lambda}^* \tilde{\lambda}^T f^\dagger m_\Sigma^{2*} \Big) - 6 \operatorname{Tr}\Big(g^D g^{D\dagger} m_Q^{2*} y^{DT} y^{D*} \Big)
\end{aligned}
$$

$$
\begin{aligned}
&- 6\,\mathrm{Tr}\Big(g^D g^{D\dagger} y^{DT} m^{2*}_{d^c} y^{D*}\Big) - 6\,\mathrm{Tr}\Big(g^D g^{D\dagger} y^{DT} y^{D*} m^{2*}_{Q}\Big)\\
&- 6\,\mathrm{Tr}\Big(g^D m^{2*}_{D} g^{D\dagger} y^{DT} y^{D*}\Big) - 4\,\mathrm{Tr}\Big(h^E m^2_{H_1} h^{E\dagger} y^E y^{E\dagger}\Big)\\
&- 4\,\mathrm{Tr}\Big(h^E h^{E\dagger} m^2_{e^c} y^E y^{E\dagger}\Big) - 4\,\mathrm{Tr}\Big(h^E h^{E\dagger} y^E m^2_{L} y^{E\dagger}\Big)\\
&- 4\,\mathrm{Tr}\Big(h^E h^{E\dagger} y^E y^{E\dagger} m^2_{e^c}\Big) - 36\,\mathrm{Tr}\Big(m^2_{d^c} y^D y^{D\dagger} y^D y^{D\dagger}\Big)\\
&- 6\,\mathrm{Tr}\Big(m^2_{d^c} y^D y^{U\dagger} y^U y^{D\dagger}\Big) - 12\,\mathrm{Tr}\Big(m^2_{e^c} y^E y^{E\dagger} y^E y^{E\dagger}\Big)\\
&- 2\,\mathrm{Tr}\Big(m^2_{H_1} \tilde{\lambda}^\dagger f^T f^* \tilde{\lambda}\Big) - 12\,\mathrm{Tr}\Big(m^2_{L} y^{E\dagger} y^E y^{E\dagger} y^E\Big)\\
&- 36\,\mathrm{Tr}\Big(m^2_{Q} y^{D\dagger} y^D y^{D\dagger} y^D\Big) - 6\,\mathrm{Tr}\Big(m^2_{Q} y^{D\dagger} y^D y^{U\dagger} y^U\Big)\\
&- 6\,\mathrm{Tr}\Big(m^2_{Q} y^{U\dagger} y^U y^{D\dagger} y^D\Big) - 6\,\mathrm{Tr}\Big(m^2_{u^c} y^U y^{D\dagger} y^D y^{U\dagger}\Big)\\
&- 2\,\mathrm{Tr}\Big(\tilde{\lambda}\tilde{\lambda}^\dagger m^{2*}_{H_2} f^T f^*\Big) - 2\,\mathrm{Tr}\Big(\tilde{\lambda}\tilde{\lambda}^\dagger f^T f^* m^{2*}_{H_2}\Big),
\end{aligned}
\tag{D.98}
$$

$$
\begin{aligned}
\beta^{(1)}_{m^2_{H_u}} = &-\frac{6}{5} g_1^2 |M_1|^2 - \frac{4}{5} g_1'^2 |M_1'|^2 - 6 g_2^2 |M_2|^2 + 2 m^2_{H_d} |\lambda|^2 + 2 m^2_{H_u} |\lambda|^2\\
&+ 2 m_S^2 |\lambda|^2 + 2 |T_\lambda|^2 + \sqrt{\frac{3}{5}} g_1 \Sigma_{1,1} - \sqrt{\frac{2}{5}} g_1' \Sigma_{1,4} + 2 m^2_{H_u}\,\mathrm{Tr}\Big(\tilde{f}\tilde{f}^\dagger\Big)\\
&+ 6 m^2_{H_u}\,\mathrm{Tr}\Big(y^U y^{U\dagger}\Big) + 2\,\mathrm{Tr}\Big(T^{\tilde{f}*} T^{\tilde{f}T}\Big) + 6\,\mathrm{Tr}\Big(T^{U*} T^{UT}\Big)\\
&+ 2\,\mathrm{Tr}\Big(\tilde{f} m^2_{H_1} \tilde{f}^\dagger\Big) + 2\,\mathrm{Tr}\Big(\tilde{f}\tilde{f}^\dagger m^{2*}_{\Sigma}\Big) + 6\,\mathrm{Tr}\Big(m^2_{Q} y^{U\dagger} y^U\Big)\\
&+ 6\,\mathrm{Tr}\Big(m^2_{u^c} y^U y^{U\dagger}\Big),
\end{aligned}
\tag{D.99}
$$

$$
\begin{aligned}
\beta^{(2)}_{m^2_{H_u}} = &\frac{18}{5} g_1^2 g_2^2 |M_2|^2 + \frac{12}{5} g_1'^2 g_2^2 |M_2|^2 + 87 g_2^4 |M_2|^2 + 3 g_1'^2 m^2_{H_d} |\lambda|^2\\
&+ 3 g_1'^2 m^2_{H_u} |\lambda|^2 + 3 g_1'^2 m_S^2 |\lambda|^2 + 3 g_1'^2 |T_\lambda|^2 + \frac{9}{5} g_1^2 g_2^2 M_1 M_2^* + \frac{6}{5} g_1'^2 g_2^2 M_1' M_2^*\\
&- 12 m^2_{H_d} |\lambda|^4 - 12 m^2_{H_u} |\lambda|^4 - 12 m_S^2 |\lambda|^4 - 2 m^2_{H_d} |\sigma|^2 |\lambda|^2 - 2 m^2_{H_u} |\sigma|^2 |\lambda|^2\\
&- 2 m_\phi^2 |\sigma|^2 |\lambda|^2 - 4 m_S^2 |\sigma|^2 |\lambda|^2 - 2 m_{\bar{S}}^2 |\sigma|^2 |\lambda|^2 - 3 g_1'^2 M_1' \lambda T_\lambda^* - 24 |\lambda|^2 |T_\lambda|^2\\
&- 2 |\sigma|^2 |T_\lambda|^2 - 2\sigma \lambda^* T_\sigma^* T_\lambda - 2\lambda\sigma^* T_\lambda^* T_\sigma - 2 |\lambda|^2 |T_\sigma|^2 + 6 g_2^4 \Sigma_{2,2} + \frac{6}{5} g_1^2 \Sigma_{2,11}\\
&- \frac{2}{5}\sqrt{6} g_1 g_1' \Sigma_{2,14} - \frac{2}{5}\sqrt{6} g_1 g_1' \Sigma_{2,41} + \frac{4}{5} g_1'^2 \Sigma_{2,44} + 4\sqrt{\frac{3}{5}} g_1 \Sigma_{3,1} - 4\sqrt{\frac{2}{5}} g_1' \Sigma_{3,4}\\
&- 4 m^2_{H_d} |\lambda|^2\,\mathrm{Tr}\Big(f f^\dagger\Big) - 2 m^2_{H_u} |\lambda|^2\,\mathrm{Tr}\Big(f f^\dagger\Big) - 2 m_S^2 |\lambda|^2\,\mathrm{Tr}\Big(f f^\dagger\Big)\\
&- 2 |T_\lambda|^2\,\mathrm{Tr}\Big(f f^\dagger\Big) + 3 g_1'^2 m^2_{H_u}\,\mathrm{Tr}\Big(\tilde{f}\tilde{f}^\dagger\Big) - 12 m^2_{H_d} |\lambda|^2\,\mathrm{Tr}\Big(y^D y^{D\dagger}\Big)\\
&- 6 m^2_{H_u} |\lambda|^2\,\mathrm{Tr}\Big(y^D y^{D\dagger}\Big) - 6 m_S^2 |\lambda|^2\,\mathrm{Tr}\Big(y^D y^{D\dagger}\Big) - 6 |T_\lambda|^2\,\mathrm{Tr}\Big(y^D y^{D\dagger}\Big)
\end{aligned}
$$

$$
\begin{aligned}
&- 4m_{H_d}^2|\lambda|^2\,\mathrm{Tr}\Big(y^E y^{E\dagger}\Big) - 2m_{H_u}^2|\lambda|^2\,\mathrm{Tr}\Big(y^E y^{E\dagger}\Big) - 2m_S^2|\lambda|^2\,\mathrm{Tr}\Big(y^E y^{E\dagger}\Big)\\
&- 2|T_\lambda|^2\,\mathrm{Tr}\Big(y^E y^{E\dagger}\Big) + \frac{8}{5}g_1^2 m_{H_u}^2\,\mathrm{Tr}\Big(y^U y^{U\dagger}\Big) - \frac{3}{5}g_1'^2 m_{H_u}^2\,\mathrm{Tr}\Big(y^U y^{U\dagger}\Big)\\
&+ 32g_3^2 m_{H_u}^2\,\mathrm{Tr}\Big(y^U y^{U\dagger}\Big) + 64g_3^2|M_3|^2\,\mathrm{Tr}\Big(y^U y^{U\dagger}\Big) - 6m_{H_d}^2|\lambda|^2\,\mathrm{Tr}\Big(\kappa\kappa^\dagger\Big)\\
&- 6m_{H_u}^2|\lambda|^2\,\mathrm{Tr}\Big(\kappa\kappa^\dagger\Big) - 12m_S^2|\lambda|^2\,\mathrm{Tr}\Big(\kappa\kappa^\dagger\Big) - 6|T_\lambda|^2\,\mathrm{Tr}\Big(\kappa\kappa^\dagger\Big)\\
&- 4m_{H_d}^2|\lambda|^2\,\mathrm{Tr}\Big(\tilde\lambda\tilde\lambda^\dagger\Big) - 4m_{H_u}^2|\lambda|^2\,\mathrm{Tr}\Big(\tilde\lambda\tilde\lambda^\dagger\Big) - 8m_S^2|\lambda|^2\,\mathrm{Tr}\Big(\tilde\lambda\tilde\lambda^\dagger\Big)\\
&- 4|T_\lambda|^2\,\mathrm{Tr}\Big(\tilde\lambda\tilde\lambda^\dagger\Big) - 2\lambda T_\lambda^*\,\mathrm{Tr}\Big(f^\dagger T^f\Big) - 6\lambda T_\lambda^*\,\mathrm{Tr}\Big(y^{D\dagger}T^D\Big)\\
&- 2\lambda T_\lambda^*\,\mathrm{Tr}\Big(y^{E\dagger}T^E\Big) + \frac{1}{25}g_1^2 M_1^*\Big\{-40\,\mathrm{Tr}\Big(y^{U\dagger}T^U\Big) + 80M_1\,\mathrm{Tr}\Big(y^U y^{U\dagger}\Big)\\
&+ 9\Big[2g_1'^2\Big(2M_1 + M_1'\Big) + 5g_2^2\Big(2M_1 + M_2\Big) + 99g_1^2 M_1\Big]\Big\}\\
&- 32g_3^2 M_3^*\,\mathrm{Tr}\Big(y^{U\dagger}T^U\Big) + \frac{3}{25}g_1'^2 M_1'^*\Big[6g_1^2 M_1 + 12g_1^2 M_1' + 217g_1'^2 M_1'\\
&+ 20g_2^2 M_1' + 10g_2^2 M_2 + 25\lambda^*\Big(2M_1'\lambda - T_\lambda\Big) + 50M_1'\,\mathrm{Tr}\Big(\tilde f\tilde f^\dagger\Big)\\
&- 10M_1'\,\mathrm{Tr}\Big(y^U y^{U\dagger}\Big) - 25\,\mathrm{Tr}\Big(\tilde f^\dagger T^{\tilde f}\Big) + 5\,\mathrm{Tr}\Big(y^{U\dagger}T^U\Big)\Big]\\
&- 6\lambda T_\lambda^*\,\mathrm{Tr}\Big(\kappa^\dagger T^\kappa\Big) - 4\lambda T_\lambda^*\,\mathrm{Tr}\Big(\tilde\lambda^\dagger T^{\tilde\lambda}\Big) - 2\lambda^* T_\lambda\,\mathrm{Tr}\Big(T^{f*}f^T\Big)\\
&- 2|\lambda|^2\,\mathrm{Tr}\Big(T^{f*}T^{fT}\Big) - 3g_1'^2 M_1'\,\mathrm{Tr}\Big(T^{\tilde f*}\tilde f^T\Big) + 3g_1'^2\,\mathrm{Tr}\Big(T^{\tilde f*}T^{\tilde fT}\Big)\\
&- 6\lambda^* T_\lambda\,\mathrm{Tr}\Big(T^{D*}y^{DT}\Big) - 6|\lambda|^2\,\mathrm{Tr}\Big(T^{D*}T^{DT}\Big) - 2\lambda^* T_\lambda\,\mathrm{Tr}\Big(T^{E*}y^{ET}\Big)\\
&- 2|\lambda|^2\,\mathrm{Tr}\Big(T^{E*}T^{ET}\Big) - \frac{8}{5}g_1^2 M_1\,\mathrm{Tr}\Big(T^{U*}y^{UT}\Big) + \frac{3}{5}g_1'^2 M_1'\,\mathrm{Tr}\Big(T^{U*}y^{UT}\Big)\\
&- 32g_3^2 M_3\,\mathrm{Tr}\Big(T^{U*}y^{UT}\Big) + \frac{8}{5}g_1^2\,\mathrm{Tr}\Big(T^{U*}T^{UT}\Big) - \frac{3}{5}g_1'^2\,\mathrm{Tr}\Big(T^{U*}T^{UT}\Big)\\
&+ 32g_3^2\,\mathrm{Tr}\Big(T^{U*}T^{UT}\Big) - 6\lambda^* T_\lambda\,\mathrm{Tr}\Big(T^{\kappa*}\kappa^T\Big) - 6|\lambda|^2\,\mathrm{Tr}\Big(T^{\kappa*}T^{\kappa T}\Big)\\
&- 4\lambda^* T_\lambda\,\mathrm{Tr}\Big(T^{\tilde\lambda*}\tilde\lambda^T\Big) - 4|\lambda|^2\,\mathrm{Tr}\Big(T^{\tilde\lambda*}T^{\tilde\lambda T}\Big) - 2|\lambda|^2\,\mathrm{Tr}\Big(f m_{H_2}^2 f^\dagger\Big)\\
&- 2|\lambda|^2\,\mathrm{Tr}\Big(f f^\dagger m_\Sigma^{2*}\Big) + 3g_1'^2\,\mathrm{Tr}\Big(\tilde f m_{H_1}^2\tilde f^\dagger\Big) + 3g_1'^2\,\mathrm{Tr}\Big(\tilde f\tilde f^\dagger m_\Sigma^{2*}\Big)\\
&- 6|\lambda|^2\,\mathrm{Tr}\Big(m_{d^c}^2 y^D y^{D\dagger}\Big) - 2|\lambda|^2\,\mathrm{Tr}\Big(m_{e^c}^2 y^E y^{E\dagger}\Big) - 4|\lambda|^2\,\mathrm{Tr}\Big(m_{H_1}^2\tilde\lambda^\dagger\tilde\lambda\Big)\\
&- 2|\lambda|^2\,\mathrm{Tr}\Big(m_L^2 y^{E\dagger}y^E\Big) - 6|\lambda|^2\,\mathrm{Tr}\Big(m_Q^2 y^{D\dagger}y^D\Big) + \frac{8}{5}g_1^2\,\mathrm{Tr}\Big(m_Q^2 y^{U\dagger}y^U\Big)\\
&- \frac{3}{5}g_1'^2\,\mathrm{Tr}\Big(m_Q^2 y^{U\dagger}y^U\Big) + 32g_3^2\,\mathrm{Tr}\Big(m_Q^2 y^{U\dagger}y^U\Big) + \frac{8}{5}g_1^2\,\mathrm{Tr}\Big(m_{u^c}^2 y^U y^{U\dagger}\Big)
\end{aligned}
$$

$$
\begin{aligned}
&- \frac{3}{5}g_1'^2 \operatorname{Tr}\Big(m_{u^c}^2 y^U y^{U\dagger}\Big) + 32 g_3^2 \operatorname{Tr}\Big(m_{u^c}^2 y^U y^{U\dagger}\Big) - 6|\lambda|^2 \operatorname{Tr}\Big(\kappa\kappa^\dagger m_D^{2*}\Big) \\
&- 6|\lambda|^2 \operatorname{Tr}\Big(\kappa m_{\bar{D}}^{2*}\kappa^\dagger\Big) - 4|\lambda|^2 \operatorname{Tr}\Big(\tilde{\lambda}\tilde{\lambda}^\dagger m_{H_2}^{2*}\Big) - 4m_{H_d}^2 \operatorname{Tr}\Big(f f^\dagger \tilde{f}\tilde{f}^\dagger\Big) \\
&- 4m_{H_u}^2 \operatorname{Tr}\Big(f f^\dagger \tilde{f}\tilde{f}^\dagger\Big) - 4 \operatorname{Tr}\Big(f f^\dagger T^{\tilde{f}} T^{\tilde{f}\dagger}\Big) - 4 \operatorname{Tr}\Big(f T^{f\dagger} T^{\tilde{f}} \tilde{f}^\dagger\Big) \\
&- 12 m_{H_u}^2 \operatorname{Tr}\Big(\tilde{f}\tilde{f}^\dagger \tilde{f}\tilde{f}^\dagger\Big) - 4 \operatorname{Tr}\Big(\tilde{f}\tilde{f}^\dagger T^f T^{f\dagger}\Big) - 12 \operatorname{Tr}\Big(\tilde{f}\tilde{f}^\dagger T^{\tilde{f}} T^{\tilde{f}\dagger}\Big) \\
&- 2m_{L_4}^2 \operatorname{Tr}\Big(\tilde{f} h^{E\dagger} h^E \tilde{f}^\dagger\Big) - 2m_{H_u}^2 \operatorname{Tr}\Big(\tilde{f} h^{E\dagger} h^E \tilde{f}^\dagger\Big) - 2 \operatorname{Tr}\Big(\tilde{f} h^{E\dagger} T^{h^E} T^{\tilde{f}\dagger}\Big) \\
&- 2m_{H_u}^2 \operatorname{Tr}\Big(\tilde{f}\tilde{\lambda}^\dagger \tilde{\lambda}\tilde{f}^\dagger\Big) - 2m_S^2 \operatorname{Tr}\Big(\tilde{f}\tilde{\lambda}^\dagger \tilde{\lambda}\tilde{f}^\dagger\Big) - 2 \operatorname{Tr}\Big(\tilde{f}\tilde{\lambda}^\dagger T^{\tilde{\lambda}} T^{\tilde{f}\dagger}\Big) \\
&- 4 \operatorname{Tr}\Big(\tilde{f} T^{\tilde{f}\dagger} T^f f^\dagger\Big) - 12 \operatorname{Tr}\Big(\tilde{f} T^{\tilde{f}\dagger} T^{\tilde{f}} \tilde{f}^\dagger\Big) - 2 \operatorname{Tr}\Big(\tilde{f} T^{h^E\dagger} T^{h^E} \tilde{f}^\dagger\Big) \\
&- 2 \operatorname{Tr}\Big(\tilde{f} T^{\tilde{\lambda}\dagger} T^{\tilde{\lambda}} \tilde{f}^\dagger\Big) - 6m_{L_4}^2 \operatorname{Tr}\Big(g^D g^{D\dagger} y^{UT} y^{U*}\Big) \\
&- 6m_{H_u}^2 \operatorname{Tr}\Big(g^D g^{D\dagger} y^{UT} y^{U*}\Big) - 6 \operatorname{Tr}\Big(g^D g^{D\dagger} T^{UT} T^{U*}\Big) \\
&- 2 \operatorname{Tr}\Big(h^E \tilde{f}^\dagger T^{\tilde{f}} T^{h^E\dagger}\Big) - 2 \operatorname{Tr}\Big(h^E T^{\tilde{f}\dagger} T^{\tilde{f}} h^{E\dagger}\Big) - 6m_{H_d}^2 \operatorname{Tr}\Big(y^D y^{U\dagger} y^U y^{D\dagger}\Big) \\
&- 6m_{H_u}^2 \operatorname{Tr}\Big(y^D y^{U\dagger} y^U y^{D\dagger}\Big) - 6 \operatorname{Tr}\Big(y^D y^{U\dagger} T^U T^{D\dagger}\Big) - 6 \operatorname{Tr}\Big(y^D T^{U\dagger} T^U y^{D\dagger}\Big) \\
&- 6 \operatorname{Tr}\Big(y^U y^{D\dagger} T^D T^{U\dagger}\Big) - 36 m_{H_u}^2 \operatorname{Tr}\Big(y^U y^{U\dagger} y^U y^{U\dagger}\Big) \\
&- 36 \operatorname{Tr}\Big(y^U y^{U\dagger} T^U T^{U\dagger}\Big) - 6 \operatorname{Tr}\Big(y^U T^{D\dagger} T^D y^{U\dagger}\Big) - 36 \operatorname{Tr}\Big(y^U T^{U\dagger} T^U y^{U\dagger}\Big) \\
&- 6 \operatorname{Tr}\Big(y^U T^{g^D *} T^{g^D T} y^{U\dagger}\Big) - 2 \operatorname{Tr}\Big(\tilde{\lambda}\tilde{f}^\dagger T^{\tilde{f}} T^{\tilde{\lambda}\dagger}\Big) - 2 \operatorname{Tr}\Big(\tilde{\lambda} T^{\tilde{f}\dagger} T^{\tilde{f}} \tilde{\lambda}^\dagger\Big) \\
&- 6 \operatorname{Tr}\Big(g^{D\dagger} y^{UT} T^{U*} T^{g^D}\Big) - 6 \operatorname{Tr}\Big(y^{U\dagger} T^U T^{g^D *} g^{DT}\Big) - 4 \operatorname{Tr}\Big(f m_{H_2}^2 f^\dagger \tilde{f}\tilde{f}^\dagger\Big) \\
&- 4 \operatorname{Tr}\Big(f f^\dagger \tilde{f} m_{H_1}^2 \tilde{f}^\dagger\Big) - 4 \operatorname{Tr}\Big(f f^\dagger \tilde{f}\tilde{f}^\dagger m_\Sigma^{2*}\Big) - 4 \operatorname{Tr}\Big(f f^\dagger m_\Sigma^{2*} \tilde{f}\tilde{f}^\dagger\Big) \\
&- 6 \operatorname{Tr}\Big(\tilde{f} m_{H_1}^2 \tilde{f}^\dagger \tilde{f}\tilde{f}^\dagger\Big) - 2 \operatorname{Tr}\Big(\tilde{f} m_{H_1}^2 h^{E\dagger} h^E \tilde{f}^\dagger\Big) - 2 \operatorname{Tr}\Big(\tilde{f} m_{H_1}^2 \tilde{\lambda}^\dagger \tilde{\lambda}\tilde{f}^\dagger\Big) \\
&- 6 \operatorname{Tr}\Big(\tilde{f}\tilde{f}^\dagger \tilde{f} m_{H_1}^2 \tilde{f}^\dagger\Big) - 12 \operatorname{Tr}\Big(\tilde{f}\tilde{f}^\dagger m_\Sigma^{2*} \tilde{f}\tilde{f}^\dagger\Big) - 2 \operatorname{Tr}\Big(\tilde{f} h^{E\dagger} h^E m_{H_1}^2 \tilde{f}^\dagger\Big) \\
&- 2 \operatorname{Tr}\Big(\tilde{f} h^{E\dagger} h^E \tilde{f}^\dagger m_\Sigma^{2*}\Big) - 2 \operatorname{Tr}\Big(\tilde{f} h^{E\dagger} m_{e^c}^2 h^E \tilde{f}^\dagger\Big) - 2 \operatorname{Tr}\Big(\tilde{f}\tilde{\lambda}^\dagger \tilde{\lambda} m_{H_1}^2 \tilde{f}^\dagger\Big) \\
&- 2 \operatorname{Tr}\Big(\tilde{f}\tilde{\lambda}^\dagger \tilde{\lambda}\tilde{f}^\dagger m_\Sigma^{2*}\Big) - 2 \operatorname{Tr}\Big(\tilde{f}\tilde{\lambda}^\dagger m_{H_2}^{2*} \tilde{\lambda}\tilde{f}^\dagger\Big) - 6 \operatorname{Tr}\Big(g^D g^{D\dagger} m_Q^{2*} y^{UT} y^{U*}\Big) \\
&- 6 \operatorname{Tr}\Big(g^D g^{D\dagger} y^{UT} m_{u^c}^{2*} y^{U*}\Big) - 6 \operatorname{Tr}\Big(g^D g^{D\dagger} y^{UT} y^{U*} m_Q^{2*}\Big) \\
&- 6 \operatorname{Tr}\Big(g^D m_{\bar{D}}^{2*} g^{D\dagger} y^{UT} y^{U*}\Big) - 6 \operatorname{Tr}\Big(m_{d^c}^2 y^D y^{U\dagger} y^U y^{D\dagger}\Big)
\end{aligned}
$$

$$
\begin{aligned}
&- 6\,\mathrm{Tr}\Big(m_Q^2 y^{D\dagger} y^D y^{U\dagger} y^U\Big) - 6\,\mathrm{Tr}\Big(m_Q^2 y^{U\dagger} y^U y^{D\dagger} y^D\Big) \\
&- 36\,\mathrm{Tr}\Big(m_Q^2 y^{U\dagger} y^U y^{U\dagger} y^U\Big) - 6\,\mathrm{Tr}\Big(m_{u^c}^2 y^U y^{D\dagger} y^D y^{U\dagger}\Big) \\
&- 36\,\mathrm{Tr}\Big(m_{u^c}^2 y^U y^{U\dagger} y^U y^{U\dagger}\Big)\,, \qquad \text{(D.100)}
\end{aligned}
$$

$$
\begin{aligned}
\beta^{(1)}_{m_{d^c}^2} =& -\frac{8}{15} g_1^2 \mathbf{1} |M_1|^2 - \frac{4}{5} g_1'^2 \mathbf{1} |M_1'|^2 - \frac{32}{3} g_3^2 \mathbf{1} |M_3|^2 + 4 m_{H_d}^2 y^D y^{D\dagger} + 4 T^D T^{D\dagger} \\
&+ 2 m_{d^c}^2 y^D y^{D\dagger} + 4 y^D m_Q^2 y^{D\dagger} + 2 y^D y^{D\dagger} m_{d^c}^2 + \frac{2}{\sqrt{15}} g_1 \mathbf{1} \Sigma_{1,1} \\
&+ \sqrt{\frac{2}{5}} g_1' \mathbf{1} \Sigma_{1,4}\,, \qquad \text{(D.101)}
\end{aligned}
$$

$$
\begin{aligned}
\beta^{(2)}_{m_{d^c}^2} =& \frac{128}{45} g_1^2 g_3^2 \mathbf{1} |M_3|^2 + \frac{64}{15} g_1'^2 g_3^2 \mathbf{1} |M_3|^2 + \frac{160}{3} g_3^4 \mathbf{1} |M_3|^2 + \frac{64}{45} g_1^2 g_3^2 M_1 \mathbf{1} M_3^* \\
&+ \frac{32}{15} g_1'^2 g_3^2 M_1' \mathbf{1} M_3^* + \frac{4}{5} g_1^2 m_{H_d}^2 y^D y^{D\dagger} + \frac{6}{5} g_1'^2 m_{H_d}^2 y^D y^{D\dagger} + 12 g_2^2 m_{H_d}^2 y^D y^{D\dagger} \\
&+ 24 g_2^2 |M_2|^2 y^D y^{D\dagger} - 8 m_{H_d}^2 |\lambda|^2 y^D y^{D\dagger} - 4 m_{H_u}^2 |\lambda|^2 y^D y^{D\dagger} \\
&- 4 m_S^2 |\lambda|^2 y^D y^{D\dagger} - 4 |T_\lambda|^2 y^D y^{D\dagger} - \frac{4}{5} g_1^2 M_1 y^D T^{D\dagger} - \frac{6}{5} g_1'^2 M_1' y^D T^{D\dagger} \\
&- 12 g_2^2 M_2 y^D T^{D\dagger} + \frac{1}{75} g_1'^2 \Big\{ \Big[160 g_3^2 \Big(2 M_1' + M_3 \Big) - 16 g_1^2 \Big(2 M_1' + M_1 \Big) \\
&+ 1953 g_1'^2 M_1' \Big] \mathbf{1} + 90 \Big(2 M_1' y^D y^{D\dagger} - T^D y^{D\dagger} \Big) \Big\} M_1'^* \\
&+ \frac{4}{225} g_1^2 \Big\{ 4 \Big[20 g_3^2 \Big(2 M_1 + M_3 \Big) + 219 g_1^2 M_1 - 3 g_1'^2 \Big(2 M_1 + M_1' \Big) \Big] \mathbf{1} \\
&- 45 T^D y^{D\dagger} + 90 M_1 y^D y^{D\dagger} \Big\} M_1^* - 12 g_2^2 M_2^* T^D y^{D\dagger} - 4 \lambda T_\lambda^* T^D y^{D\dagger} \\
&+ \frac{4}{5} g_1^2 T^D T^{D\dagger} + \frac{6}{5} g_1'^2 T^D T^{D\dagger} + 12 g_2^2 T^D T^{D\dagger} - 4 |\lambda|^2 T^D T^{D\dagger} \\
&+ \frac{2}{5} g_1^2 m_{d^c}^2 y^D y^{D\dagger} + \frac{3}{5} g_1'^2 m_{d^c}^2 y^D y^{D\dagger} + 6 g_2^2 m_{d^c}^2 y^D y^{D\dagger} - 2 |\lambda|^2 m_{d^c}^2 y^D y^{D\dagger} \\
&+ \frac{4}{5} g_1^2 y^D m_Q^2 y^{D\dagger} + \frac{6}{5} g_1'^2 y^D m_Q^2 y^{D\dagger} + 12 g_2^2 y^D m_Q^2 y^{D\dagger} - 4 |\lambda|^2 y^D m_Q^2 y^{D\dagger} \\
&+ \frac{2}{5} g_1^2 y^D y^{D\dagger} m_{d^c}^2 + \frac{3}{5} g_1'^2 y^D y^{D\dagger} m_{d^c}^2 + 6 g_2^2 y^D y^{D\dagger} m_{d^c}^2 - 2 |\lambda|^2 y^D y^{D\dagger} m_{d^c}^2 \\
&- 8 m_{H_d}^2 y^D y^{D\dagger} y^D y^{D\dagger} - 4 y^D y^{D\dagger} T^D T^{D\dagger} - 4 m_{H_d}^2 y^D y^{U\dagger} y^U y^{D\dagger} \\
&- 4 m_{H_u}^2 y^D y^{U\dagger} y^U y^{D\dagger} - 4 y^D y^{U\dagger} T^U T^{D\dagger} - 4 y^D T^{D\dagger} T^D y^{D\dagger} \\
&- 4 y^D T^{U\dagger} T^U y^{D\dagger} - 4 m_{H_d}^2 y^D g^{D*} g^{DT} y^{D\dagger} - 4 m_{L_4}^2 y^D g^{D*} g^{DT} y^{D\dagger} \\
&- 4 y^D g^{D*} T^{g^D T} T^{D\dagger} - 4 y^D T^{g^D *} T^{g^D T} y^{D\dagger} - 4 T^D y^{D\dagger} y^D T^{D\dagger} \\
&- 4 T^D y^{U\dagger} y^U T^{D\dagger} - 4 T^D T^{D\dagger} y^D y^{D\dagger} - 4 T^D T^{U\dagger} y^U y^{D\dagger} - 4 T^D g^{D*} g^{DT} T^{D\dagger} \\
&- 4 T^D T^{g^D *} g^{DT} y^{D\dagger} - 2 m_{d^c}^2 y^D y^{D\dagger} y^D y^{D\dagger} - 2 m_{d^c}^2 y^D y^{U\dagger} y^U y^{D\dagger}
\end{aligned}
$$

$$
\begin{aligned}
&- 2m_{d^c}^2 y^D g^{D*} g^{DT} y^{D\dagger} - 4y^D m_Q^2 y^{D\dagger} y^D y^{D\dagger} - 4y^D m_Q^2 y^{U\dagger} y^U y^{D\dagger} \\
&- 4y^D m_Q^2 g^{D*} g^{DT} y^{D\dagger} - 4y^D y^{D\dagger} m_{d^c}^2 y^D y^{D\dagger} - 4y^D y^{D\dagger} y^D m_Q^2 y^{D\dagger} \\
&- 2y^D y^{D\dagger} y^D y^{D\dagger} m_{d^c}^2 - 4y^D y^{U\dagger} m_{u^c}^2 y^U y^{D\dagger} - 4y^D y^{U\dagger} y^U m_Q^2 y^{D\dagger} \\
&- 2y^D y^{U\dagger} y^U y^{D\dagger} m_{d^c}^2 - 4y^D g^{D*} m_{\bar{D}}^2 g^{DT} y^{D\dagger} - 4y^D g^{D*} g^{DT} m_Q^2 y^{D\dagger} \\
&- 2y^D g^{D*} g^{DT} y^{D\dagger} m_{d^c}^2 - 4\lambda^* y^D T^{D\dagger} T_\lambda + \frac{32}{3} g_3^4 \mathbf{1} \Sigma_{2,3} + \frac{8}{15} g_1^2 \mathbf{1} \Sigma_{2,11} \\
&+ \frac{4}{5}\sqrt{\frac{2}{3}} g_1 g_1' \mathbf{1} \Sigma_{2,14} + \frac{4}{5}\sqrt{\frac{2}{3}} g_1 g_1' \mathbf{1} \Sigma_{2,41} + \frac{4}{5} g_1'^2 \mathbf{1} \Sigma_{2,44} + \frac{8}{\sqrt{15}} g_1 \mathbf{1} \Sigma_{3,1} \\
&+ 4\sqrt{\frac{2}{5}} g_1' \mathbf{1} \Sigma_{3,4} - 8m_{H_d}^2 y^D y^{D\dagger} \operatorname{Tr}\Big(f f^\dagger\Big) - 4T^D T^{D\dagger} \operatorname{Tr}\Big(f f^\dagger\Big) \\
&- 2m_{d^c}^2 y^D y^{D\dagger} \operatorname{Tr}\Big(f f^\dagger\Big) - 4y^D m_Q^2 y^{D\dagger} \operatorname{Tr}\Big(f f^\dagger\Big) - 2y^D y^{D\dagger} m_{d^c}^2 \operatorname{Tr}\Big(f f^\dagger\Big) \\
&- 24m_{H_d}^2 y^D y^{D\dagger} \operatorname{Tr}\Big(y^D y^{D\dagger}\Big) - 12T^D T^{D\dagger} \operatorname{Tr}\Big(y^D y^{D\dagger}\Big) \\
&- 6m_{d^c}^2 y^D y^{D\dagger} \operatorname{Tr}\Big(y^D y^{D\dagger}\Big) - 12y^D m_Q^2 y^{D\dagger} \operatorname{Tr}\Big(y^D y^{D\dagger}\Big) \\
&- 6y^D y^{D\dagger} m_{d^c}^2 \operatorname{Tr}\Big(y^D y^{D\dagger}\Big) - 8m_{H_d}^2 y^D y^{D\dagger} \operatorname{Tr}\Big(y^E y^{E\dagger}\Big) \\
&- 4T^D T^{D\dagger} \operatorname{Tr}\Big(y^E y^{E\dagger}\Big) - 2m_{d^c}^2 y^D y^{D\dagger} \operatorname{Tr}\Big(y^E y^{E\dagger}\Big) \\
&- 4y^D m_Q^2 y^{D\dagger} \operatorname{Tr}\Big(y^E y^{E\dagger}\Big) - 2y^D y^{D\dagger} m_{d^c}^2 \operatorname{Tr}\Big(y^E y^{E\dagger}\Big) - 4y^D T^{D\dagger} \operatorname{Tr}\Big(f^\dagger T^f\Big) \\
&- 12y^D T^{D\dagger} \operatorname{Tr}\Big(y^{D\dagger} T^D\Big) - 4y^D T^{D\dagger} \operatorname{Tr}\Big(y^{E\dagger} T^E\Big) - 4T^D y^{D\dagger} \operatorname{Tr}\Big(T^{f*} f^T\Big) \\
&- 4y^D y^{D\dagger} \operatorname{Tr}\Big(T^{f*} T^{fT}\Big) - 12T^D y^{D\dagger} \operatorname{Tr}\Big(T^{D*} y^{DT}\Big) \\
&- 12y^D y^{D\dagger} \operatorname{Tr}\Big(T^{D*} T^{DT}\Big) - 4T^D y^{D\dagger} \operatorname{Tr}\Big(T^{E*} y^{ET}\Big) \\
&- 4y^D y^{D\dagger} \operatorname{Tr}\Big(T^{E*} T^{ET}\Big) - 4y^D y^{D\dagger} \operatorname{Tr}\Big(f m_{H_2}^2 f^\dagger\Big) - 4y^D y^{D\dagger} \operatorname{Tr}\Big(f f^\dagger m_\Sigma^{2*}\Big) \\
&- 12y^D y^{D\dagger} \operatorname{Tr}\Big(m_{d^c}^2 y^D y^{D\dagger}\Big) - 4y^D y^{D\dagger} \operatorname{Tr}\Big(m_{e^c}^2 y^E y^{E\dagger}\Big) \\
&- 4y^D y^{D\dagger} \operatorname{Tr}\Big(m_L^2 y^{E\dagger} y^E\Big) - 12y^D y^{D\dagger} \operatorname{Tr}\Big(m_Q^2 y^{D\dagger} y^D\Big), \qquad \text{(D.102)}
\end{aligned}
$$

$$
\begin{aligned}
\beta_{m_{u^c}^2}^{(1)} = &- \frac{32}{15} g_1^2 \mathbf{1} |M_1|^2 - \frac{1}{5} g_1'^2 \mathbf{1} |M_1'|^2 - \frac{32}{3} g_3^2 \mathbf{1} |M_3|^2 + 4m_{H_u}^2 y^U y^{U\dagger} + 4T^U T^{U\dagger} \\
&+ 2m_{u^c}^2 y^U y^{U\dagger} + 4y^U m_Q^2 y^{U\dagger} + 2y^U y^{U\dagger} m_{u^c}^2 - \frac{4}{\sqrt{15}} g_1 \mathbf{1} \Sigma_{1,1} \\
&+ \frac{1}{\sqrt{10}} g_1' \mathbf{1} \Sigma_{1,4}, \qquad \text{(D.103)} \\
\beta_{m_{u^c}^2}^{(2)} = &\frac{512}{45} g_1^2 g_3^2 \mathbf{1} |M_3|^2 + \frac{16}{15} g_1'^2 g_3^2 \mathbf{1} |M_3|^2 + \frac{160}{3} g_3^4 \mathbf{1} |M_3|^2 + \frac{256}{45} g_1^2 g_3^2 M_1 \mathbf{1} M_3^*
\end{aligned}
$$

$$
\begin{aligned}
&+\frac{8}{15}g_1'^2 g_3^2 M_1' \mathbf{1} M_3^* - \frac{4}{5}g_1^2 m_{H_u}^2 y^U y^{U\dagger} + \frac{4}{5}g_1'^2 m_{H_u}^2 y^U y^{U\dagger} + 12 g_2^2 m_{H_u}^2 y^U y^{U\dagger} \\
&+ 24 g_2^2 |M_2|^2 y^U y^{U\dagger} - 4 m_{H_d}^2 |\lambda|^2 y^U y^{U\dagger} - 8 m_{H_u}^2 |\lambda|^2 y^U y^{U\dagger} \\
&- 4 m_S^2 |\lambda|^2 y^U y^{U\dagger} - 4 |T_\lambda|^2 y^U y^{U\dagger} + \frac{4}{5}g_1^2 M_1 y^U T^{U\dagger} - \frac{4}{5}g_1'^2 M_1' y^U T^{U\dagger} \\
&- 12 g_2^2 M_2 y^U T^{U\dagger} + \frac{1}{150}g_1'^2 \Big\{ 120 \Big(2 M_1' y^U y^{U\dagger} - T^U y^{U\dagger} \Big) \\
&+ \Big[64 g_1^2 \Big(2M_1' + M_1 \Big) + 80 g_3^2 \Big(2M_1' + M_3 \Big) + 963 g_1'^2 M_1' \Big] \mathbf{1} \Big\} M_1'^* \\
&- 12 g_2^2 M_2^* T^U y^{U\dagger} - 4 \lambda T_\lambda^* T^U y^{U\dagger} + \frac{4}{225}g_1^2 \Big\{ 45 \Big(-2 M_1 y^U y^{U\dagger} + T^U y^{U\dagger} \Big) \\
&+ 8 \Big[3 g_1'^2 \Big(2M_1 + M_1' \Big) + 40 g_3^2 \Big(2M_1 + M_3 \Big) + 456 g_1^2 M_1 \Big] \mathbf{1} \Big\} M_1^* \\
&- \frac{4}{5}g_1^2 T^U T^{U\dagger} + \frac{4}{5}g_1'^2 T^U T^{U\dagger} + 12 g_2^2 T^U T^{U\dagger} - 4 |\lambda|^2 T^U T^{U\dagger} \\
&- \frac{2}{5}g_1^2 m_{u^c}^2 y^U y^{U\dagger} + \frac{2}{5}g_1'^2 m_{u^c}^2 y^U y^{U\dagger} + 6 g_2^2 m_{u^c}^2 y^U y^{U\dagger} - 2 |\lambda|^2 m_{u^c}^2 y^U y^{U\dagger} \\
&- \frac{4}{5}g_1^2 y^U m_Q^2 y^{U\dagger} + \frac{4}{5}g_1'^2 y^U m_Q^2 y^{U\dagger} + 12 g_2^2 y^U m_Q^2 y^{U\dagger} - 4 |\lambda|^2 y^U m_Q^2 y^{U\dagger} \\
&- \frac{2}{5}g_1^2 y^U y^{U\dagger} m_{u^c}^2 + \frac{2}{5}g_1'^2 y^U y^{U\dagger} m_{u^c}^2 + 6 g_2^2 y^U y^{U\dagger} m_{u^c}^2 - 2 |\lambda|^2 y^U y^{U\dagger} m_{u^c}^2 \\
&- 4 m_{H_d}^2 y^U y^{D\dagger} y^D y^{U\dagger} - 4 m_{H_u}^2 y^U y^{D\dagger} y^D y^{U\dagger} - 4 y^U y^{D\dagger} T^D T^{U\dagger} \\
&- 8 m_{H_u}^2 y^U y^{U\dagger} y^U y^{U\dagger} - 4 y^U y^{U\dagger} T^U T^{U\dagger} - 4 y^U T^{D\dagger} T^D y^{U\dagger} - 4 y^U T^{U\dagger} T^U y^{U\dagger} \\
&- 4 m_{L_4}^2 y^U g^{D*} g^{DT} y^{U\dagger} - 4 m_{H_u}^2 y^U g^{D*} g^{DT} y^{U\dagger} - 4 y^U g^{D*} T^{g^D T} T^{U\dagger} \\
&- 4 y^U T^{g^D *} T^{g^D T} y^{U\dagger} - 4 T^U y^{D\dagger} y^D T^{U\dagger} - 4 T^U y^{U\dagger} y^U T^{U\dagger} - 4 T^U T^{D\dagger} y^D y^{U\dagger} \\
&- 4 T^U T^{U\dagger} y^U y^{U\dagger} - 4 T^U g^{D*} g^{DT} T^{U\dagger} - 4 T^U T^{g^D *} g^{DT} y^{U\dagger} \\
&- 2 m_{u^c}^2 y^U y^{D\dagger} y^D y^{U\dagger} - 2 m_{u^c}^2 y^U y^{U\dagger} y^U y^{U\dagger} - 2 m_{u^c}^2 y^U g^{D*} g^{DT} y^{U\dagger} \\
&- 4 y^U m_Q^2 y^{D\dagger} y^D y^{U\dagger} - 4 y^U m_Q^2 y^{U\dagger} y^U y^{U\dagger} - 4 y^U m_Q^2 g^{D*} g^{DT} y^{U\dagger} \\
&- 4 y^U y^{D\dagger} m_{d^c}^2 y^D y^{U\dagger} - 4 y^U y^{D\dagger} y^D m_Q^2 y^{U\dagger} - 2 y^U y^{D\dagger} y^D y^{U\dagger} m_{u^c}^2 \\
&- 4 y^U y^{U\dagger} m_{u^c}^2 y^U y^{U\dagger} - 4 y^U y^{U\dagger} y^U m_Q^2 y^{U\dagger} - 2 y^U y^{U\dagger} y^U y^{U\dagger} m_{u^c}^2 \\
&- 4 y^U g^{D*} m_{\bar{D}}^2 g^{DT} y^{U\dagger} - 4 y^U g^{D*} g^{DT} m_Q^2 y^{U\dagger} - 2 y^U g^{D*} g^{DT} y^{U\dagger} m_{u^c}^2 \\
&- 4 \lambda^* y^U T^{U\dagger} T_\lambda + \frac{32}{3}g_3^4 \mathbf{1} \Sigma_{2,3} + \frac{32}{15}g_1^2 \mathbf{1} \Sigma_{2,11} - \frac{4}{5}\sqrt{\frac{2}{3}} g_1 g_1' \mathbf{1} \Sigma_{2,14} \\
&- \frac{4}{5}\sqrt{\frac{2}{3}} g_1 g_1' \mathbf{1} \Sigma_{2,41} + \frac{1}{5}g_1'^2 \mathbf{1} \Sigma_{2,44} - \frac{16}{\sqrt{15}} g_1 \mathbf{1} \Sigma_{3,1} + 2\sqrt{\frac{2}{5}} g_1' \mathbf{1} \Sigma_{3,4} \\
&- 8 m_{H_u}^2 y^U y^{U\dagger} \operatorname{Tr}\Big(\tilde{f} \tilde{f}^\dagger \Big) - 4 T^U T^{U\dagger} \operatorname{Tr}\Big(\tilde{f} \tilde{f}^\dagger \Big) - 2 m_{u^c}^2 y^U y^{U\dagger} \operatorname{Tr}\Big(\tilde{f} \tilde{f}^\dagger \Big) \\
&- 4 y^U m_Q^2 y^{U\dagger} \operatorname{Tr}\Big(\tilde{f} \tilde{f}^\dagger \Big) - 2 y^U y^{U\dagger} m_{u^c}^2 \operatorname{Tr}\Big(\tilde{f} \tilde{f}^\dagger \Big) - 24 m_{H_u}^2 y^U y^{U\dagger} \operatorname{Tr}\Big(y^U y^{U\dagger} \Big)
\end{aligned}
$$

$$
\begin{aligned}
&- 12T^U T^{U\dagger}\,\mathrm{Tr}\Big(y^U y^{U\dagger}\Big) - 6m^2_{u^c} y^U y^{U\dagger}\,\mathrm{Tr}\Big(y^U y^{U\dagger}\Big)\\
&- 12y^U m^2_Q y^{U\dagger}\,\mathrm{Tr}\Big(y^U y^{U\dagger}\Big) - 6y^U y^{U\dagger} m^2_{u^c}\,\mathrm{Tr}\Big(y^U y^{U\dagger}\Big)\\
&- 4y^U T^{U\dagger}\,\mathrm{Tr}\Big(\tilde{f}^\dagger T^{\tilde{f}}\Big) - 12y^U T^{U\dagger}\,\mathrm{Tr}\Big(y^{U\dagger} T^U\Big)\\
&- 4T^U y^{U\dagger}\,\mathrm{Tr}\Big(T^{\tilde{f}*}\tilde{f}^T\Big) - 4y^U y^{U\dagger}\,\mathrm{Tr}\Big(T^{\tilde{f}*} T^{\tilde{f}T}\Big) - 12T^U y^{U\dagger}\,\mathrm{Tr}\Big(T^{U*} y^{UT}\Big)\\
&- 12y^U y^{U\dagger}\,\mathrm{Tr}\Big(T^{U*} T^{UT}\Big) - 4y^U y^{U\dagger}\,\mathrm{Tr}\Big(\tilde{f} m^2_{H_1}\tilde{f}^\dagger\Big) - 4y^U y^{U\dagger}\,\mathrm{Tr}\Big(\tilde{f}\tilde{f}^\dagger m^{2*}_\Sigma\Big)\\
&- 12y^U y^{U\dagger}\,\mathrm{Tr}\Big(m^2_Q y^{U\dagger} y^U\Big) - 12y^U y^{U\dagger}\,\mathrm{Tr}\Big(m^2_{u^c} y^U y^{U\dagger}\Big)\,, \qquad \text{(D.104)}
\end{aligned}
$$

$$
\begin{aligned}
\beta^{(1)}_{m^2_{e^c}} =& -\frac{24}{5}g_1^2\mathbf{1}|M_1|^2 - \frac{1}{5}g_1'^2\mathbf{1}|M_1'|^2 + 4m^2_{L_4}h^E h^{E\dagger} + 4m^2_{H_d}y^E y^{E\dagger} + 4T^{h^E}T^{h^E\dagger}\\
&+ 4T^E T^{E\dagger} + 4h^E m^2_{H_1}h^{E\dagger} + 2h^E h^{E\dagger}m^2_{e^c} + 2m^2_{e^c}h^E h^{E\dagger} + 2m^2_{e^c}y^E y^{E\dagger}\\
&+ 4y^E m^2_L y^{E\dagger} + 2y^E y^{E\dagger}m^2_{e^c} + 2\sqrt{\frac{3}{5}}g_1\mathbf{1}\Sigma_{1,1} + \frac{1}{\sqrt{10}}g_1'\mathbf{1}\Sigma_{1,4}\,, \qquad \text{(D.105)}
\end{aligned}
$$

$$
\begin{aligned}
\beta^{(2)}_{m^2_{e^c}} =& -\frac{12}{5}g_1^2 m^2_{L_4}h^E h^{E\dagger} + \frac{12}{5}g_1'^2 m^2_{L_4}h^E h^{E\dagger} + 12g_2^2 m^2_{L_4}h^E h^{E\dagger}\\
&+ 24g_2^2|M_2|^2 h^E h^{E\dagger} - 8m^2_{L_4}|\tilde{\sigma}|^2 h^E h^{E\dagger} - 4m^2_{\bar{L}_4}|\tilde{\sigma}|^2 h^E h^{E\dagger}\\
&- 4m^2_\phi|\tilde{\sigma}|^2 h^E h^{E\dagger} - 4|T_{\tilde{\sigma}}|^2 h^E h^{E\dagger} + \frac{12}{5}g_1^2 M_1 h^E T^{h^E\dagger} - \frac{12}{5}g_1'^2 M_1' h^E T^{h^E\dagger}\\
&- 12g_2^2 M_2 h^E T^{h^E\dagger} - \frac{12}{5}g_1^2 m^2_{H_d}y^E y^{E\dagger} + \frac{12}{5}g_1'^2 m^2_{H_d}y^E y^{E\dagger}\\
&+ 12g_2^2 m^2_{H_d}y^E y^{E\dagger} + 24g_2^2|M_2|^2 y^E y^{E\dagger} - 8m^2_{H_d}|\lambda|^2 y^E y^{E\dagger} - 4m^2_{H_u}|\lambda|^2 y^E y^{E\dagger}\\
&- 4m^2_S|\lambda|^2 y^E y^{E\dagger} - 4|T_\lambda|^2 y^E y^{E\dagger} + \frac{12}{5}g_1^2 M_1 y^E T^{E\dagger} - \frac{12}{5}g_1'^2 M_1' y^E T^{E\dagger}\\
&- 12g_2^2 M_2 y^E T^{E\dagger} - 12g_2^2 M_2^* T^{h^E} h^{E\dagger} - 4\tilde{\sigma}T^*_{\tilde{\sigma}}T^{h^E}h^{E\dagger} - \frac{12}{5}g_1^2 T^{h^E}T^{h^E\dagger}\\
&+ \frac{12}{5}g_1'^2 T^{h^E}T^{h^E\dagger} + 12g_2^2 T^{h^E}T^{h^E\dagger} - 4|\tilde{\sigma}|^2 T^{h^E}T^{h^E\dagger}\\
&+ \frac{3}{50}g_1'^2\Big\{\Big[107g_1'^2 M_1' - 4g_1^2\Big(2M_1' + M_1\Big)\Big]\mathbf{1} + 40\Big(2M_1' h^E h^{E\dagger}\\
&+ 2M_1' y^E y^{E\dagger} - T^E y^{E\dagger} - T^{h^E}h^{E\dagger}\Big)\Big\}M_1'^* - 12g_2^2 M_2^* T^E y^{E\dagger} - 4\lambda T^*_\lambda T^E y^{E\dagger}\\
&+ \frac{6}{25}g_1^2\Big\{10\Big(-2M_1 h^E h^{E\dagger} - 2M_1 y^E y^{E\dagger} + T^{h^E}h^{E\dagger} + T^E y^{E\dagger}\Big)\\
&+ \Big[648g_1^2 M_1 - g_1'^2\Big(2M_1 + M_1'\Big)\Big]\mathbf{1}\Big\}M_1^* - \frac{12}{5}g_1^2 T^E T^{E\dagger} + \frac{12}{5}g_1'^2 T^E T^{E\dagger}\\
&+ 12g_2^2 T^E T^{E\dagger} - 4|\lambda|^2 T^E T^{E\dagger} - \frac{12}{5}g_1^2 h^E m^2_{H_1}h^{E\dagger} + \frac{12}{5}g_1'^2 h^E m^2_{H_1}h^{E\dagger}\\
&+ 12g_2^2 h^E m^2_{H_1}h^{E\dagger} - 4|\tilde{\sigma}|^2 h^E m^2_{H_1}h^{E\dagger} - \frac{6}{5}g_1^2 h^E h^{E\dagger}m^2_{e^c} + \frac{6}{5}g_1'^2 h^E h^{E\dagger}m^2_{e^c}
\end{aligned}
$$

$$
\begin{aligned}
&+ 6g_2^2 h^E h^{E\dagger} m_{e^c}^2 - 2|\tilde{\sigma}|^2 h^E h^{E\dagger} m_{e^c}^2 - \frac{6}{5} g_1^2 m_{e^c}^2 h^E h^{E\dagger} + \frac{6}{5} g_1'^2 m_{e^c}^2 h^E h^{E\dagger} \\
&+ 6g_2^2 m_{e^c}^2 h^E h^{E\dagger} - 2|\tilde{\sigma}|^2 m_{e^c}^2 h^E h^{E\dagger} - \frac{6}{5} g_1^2 m_{e^c}^2 y^E y^{E\dagger} + \frac{6}{5} g_1'^2 m_{e^c}^2 y^E y^{E\dagger} \\
&+ 6g_2^2 m_{e^c}^2 y^E y^{E\dagger} - 2|\lambda|^2 m_{e^c}^2 y^E y^{E\dagger} - \frac{12}{5} g_1^2 y^E m_L^2 y^{E\dagger} + \frac{12}{5} g_1'^2 y^E m_L^2 y^{E\dagger} \\
&+ 12g_2^2 y^E m_L^2 y^{E\dagger} - 4|\lambda|^2 y^E m_L^2 y^{E\dagger} - \frac{6}{5} g_1^2 y^E y^{E\dagger} m_{e^c}^2 + \frac{6}{5} g_1'^2 y^E y^{E\dagger} m_{e^c}^2 \\
&+ 6g_2^2 y^E y^{E\dagger} m_{e^c}^2 - 2|\lambda|^2 y^E y^{E\dagger} m_{e^c}^2 - 4m_{L_4}^2 h^E \tilde{f}^\dagger \tilde{f} h^{E\dagger} - 4m_{H_u}^2 h^E \tilde{f}^\dagger \tilde{f} h^{E\dagger} \\
&- 4h^E \tilde{f}^\dagger T^{\tilde{f}} T^{h^E\dagger} - 8m_{L_4}^2 h^E h^{E\dagger} h^E h^{E\dagger} - 4h^E h^{E\dagger} T^{h^E} T^{h^E\dagger} \\
&- 4m_{L_4}^2 h^E \tilde{\lambda}^\dagger \tilde{\lambda} h^{E\dagger} - 4m_S^2 h^E \tilde{\lambda}^\dagger \tilde{\lambda} h^{E\dagger} - 4h^E \tilde{\lambda}^\dagger T^{\tilde{\lambda}} T^{h^E\dagger} - 4h^E T^{\tilde{f}\dagger} T^{\tilde{f}} h^{E\dagger} \\
&- 4h^E T^{h^E\dagger} T^{h^E} h^{E\dagger} - 4h^E T^{\tilde{\lambda}\dagger} T^{\tilde{\lambda}} h^{E\dagger} - 8m_{H_d}^2 y^E y^{E\dagger} y^E y^{E\dagger} \\
&- 4y^E y^{E\dagger} T^E T^{E\dagger} - 4y^E T^{E\dagger} T^E y^{E\dagger} - 4T^{h^E} \tilde{f}^\dagger \tilde{f} T^{h^E\dagger} \\
&- 4T^{h^E} h^{E\dagger} h^E T^{h^E\dagger} - 4T^{h^E} \tilde{\lambda}^\dagger \tilde{\lambda} T^{h^E\dagger} - 4T^{h^E} T^{\tilde{f}\dagger} \tilde{f} h^{E\dagger} - 4T^{h^E} T^{h^E\dagger} h^E h^{E\dagger} \\
&- 4T^{h^E} T^{\tilde{\lambda}\dagger} \tilde{\lambda} h^{E\dagger} - 4T^E y^{E\dagger} y^E T^{E\dagger} - 4T^E T^{E\dagger} y^E y^{E\dagger} - 4h^E m_{H_1}^2 \tilde{f}^\dagger \tilde{f} h^{E\dagger} \\
&- 4h^E m_{H_1}^2 h^{E\dagger} h^E h^{E\dagger} - 4h^E m_{H_1}^2 \tilde{\lambda}^\dagger \tilde{\lambda} h^{E\dagger} - 4h^E \tilde{f}^\dagger \tilde{f} m_{H_1}^2 h^{E\dagger} \\
&- 2h^E \tilde{f}^\dagger \tilde{f} h^{E\dagger} m_{e^c}^2 - 4h^E \tilde{f}^\dagger m_\Sigma^{2*} \tilde{f} h^{E\dagger} - 4h^E h^{E\dagger} h^E m_{H_1}^2 h^{E\dagger} \\
&- 2h^E h^{E\dagger} h^E h^{E\dagger} m_{e^c}^2 - 4h^E h^{E\dagger} m_{e^c}^2 h^E h^{E\dagger} - 4h^E \tilde{\lambda}^\dagger \tilde{\lambda} m_{H_1}^2 h^{E\dagger} \\
&- 2h^E \tilde{\lambda}^\dagger \tilde{\lambda} h^{E\dagger} m_{e^c}^2 - 4h^E \tilde{\lambda}^\dagger m_{H_2}^{2*} \tilde{\lambda} h^{E\dagger} - 2m_{e^c}^2 h^E \tilde{f}^\dagger \tilde{f} h^{E\dagger} \\
&- 2m_{e^c}^2 h^E h^{E\dagger} h^E h^{E\dagger} - 2m_{e^c}^2 h^E \tilde{\lambda}^\dagger \tilde{\lambda} h^{E\dagger} - 2m_{e^c}^2 y^E y^{E\dagger} y^E y^{E\dagger} \\
&- 4y^E m_L^2 y^{E\dagger} y^E y^{E\dagger} - 4y^E y^{E\dagger} m_{e^c}^2 y^E y^{E\dagger} - 4y^E y^{E\dagger} y^E m_L^2 y^{E\dagger} \\
&- 2y^E y^{E\dagger} y^E y^{E\dagger} m_{e^c}^2 - 4\lambda^* y^E T^{E\dagger} T_\lambda - 4\tilde{\sigma}^* h^E T^{h^E\dagger} T_{\tilde{\sigma}} + \frac{24}{5} g_1^2 \mathbf{1} \Sigma_{2,11} \\
&+ \frac{2}{5}\sqrt{6} g_1 g_1' \mathbf{1} \Sigma_{2,14} + \frac{2}{5}\sqrt{6} g_1 g_1' \mathbf{1} \Sigma_{2,41} + \frac{1}{5} g_1'^2 \mathbf{1} \Sigma_{2,44} + 8\sqrt{\frac{3}{5}} g_1 \mathbf{1} \Sigma_{3,1} \\
&+ 2\sqrt{\frac{2}{5}} g_1' \mathbf{1} \Sigma_{3,4} - 8m_{H_d}^2 y^E y^{E\dagger} \operatorname{Tr}\Big(f f^\dagger\Big) - 4T^E T^{E\dagger} \operatorname{Tr}\Big(f f^\dagger\Big) \\
&- 2m_{e^c}^2 y^E y^{E\dagger} \operatorname{Tr}\Big(f f^\dagger\Big) - 4y^E m_L^2 y^{E\dagger} \operatorname{Tr}\Big(f f^\dagger\Big) - 2y^E y^{E\dagger} m_{e^c}^2 \operatorname{Tr}\Big(f f^\dagger\Big) \\
&- 24m_{L_4}^2 h^E h^{E\dagger} \operatorname{Tr}\Big(g^D g^{D\dagger}\Big) - 12T^{h^E} T^{h^E\dagger} \operatorname{Tr}\Big(g^D g^{D\dagger}\Big) \\
&- 12h^E m_{H_1}^2 h^{E\dagger} \operatorname{Tr}\Big(g^D g^{D\dagger}\Big) - 6h^E h^{E\dagger} m_{e^c}^2 \operatorname{Tr}\Big(g^D g^{D\dagger}\Big) \\
&- 6m_{e^c}^2 h^E h^{E\dagger} \operatorname{Tr}\Big(g^D g^{D\dagger}\Big) - 8m_{L_4}^2 h^E h^{E\dagger} \operatorname{Tr}\Big(h^E h^{E\dagger}\Big) \\
&- 4T^{h^E} T^{h^E\dagger} \operatorname{Tr}\Big(h^E h^{E\dagger}\Big) - 4h^E m_{H_1}^2 h^{E\dagger} \operatorname{Tr}\Big(h^E h^{E\dagger}\Big)
\end{aligned}
$$

$$
\begin{aligned}
&- 2h^E h^{E\dagger} m^2_{e^c} \operatorname{Tr}\Big(h^E h^{E\dagger}\Big) - 2m^2_{e^c} h^E h^{E\dagger} \operatorname{Tr}\Big(h^E h^{E\dagger}\Big) \\
&- 24 m^2_{H_d} y^E y^{E\dagger} \operatorname{Tr}\Big(y^D y^{D\dagger}\Big) - 12 T^E T^{E\dagger} \operatorname{Tr}\Big(y^D y^{D\dagger}\Big) \\
&- 6 m^2_{e^c} y^E y^{E\dagger} \operatorname{Tr}\Big(y^D y^{D\dagger}\Big) - 12 y^E m^2_L y^{E\dagger} \operatorname{Tr}\Big(y^D y^{D\dagger}\Big) \\
&- 6 y^E y^{E\dagger} m^2_{e^c} \operatorname{Tr}\Big(y^D y^{D\dagger}\Big) - 8 m^2_{H_d} y^E y^{E\dagger} \operatorname{Tr}\Big(y^E y^{E\dagger}\Big) \\
&- 4 T^E T^{E\dagger} \operatorname{Tr}\Big(y^E y^{E\dagger}\Big) - 2 m^2_{e^c} y^E y^{E\dagger} \operatorname{Tr}\Big(y^E y^{E\dagger}\Big) \\
&- 4 y^E m^2_L y^{E\dagger} \operatorname{Tr}\Big(y^E y^{E\dagger}\Big) - 2 y^E y^{E\dagger} m^2_{e^c} \operatorname{Tr}\Big(y^E y^{E\dagger}\Big) \\
&- 4 y^E T^{E\dagger} \operatorname{Tr}\Big(f^\dagger T^f\Big) - 12 h^E T^{h^E\dagger} \operatorname{Tr}\Big(g^{D\dagger} T^{g^D}\Big) \\
&- 4 h^E T^{h^E\dagger} \operatorname{Tr}\Big(h^{E\dagger} T^{h^E}\Big) - 12 y^E T^{E\dagger} \operatorname{Tr}\Big(y^{D\dagger} T^D\Big) - 4 y^E T^{E\dagger} \operatorname{Tr}\Big(y^{E\dagger} T^E\Big) \\
&- 4 T^E y^{E\dagger} \operatorname{Tr}\Big(T^{f*} f^T\Big) - 4 y^E y^{E\dagger} \operatorname{Tr}\Big(T^{f*} T^{fT}\Big) - 12 T^{h^E} h^{E\dagger} \operatorname{Tr}\Big(T^{g^D *} g^{DT}\Big) \\
&- 12 h^E h^{E\dagger} \operatorname{Tr}\Big(T^{g^D *} T^{g^D T}\Big) - 4 T^{h^E} h^{E\dagger} \operatorname{Tr}\Big(T^{h^E *} h^{ET}\Big) \\
&- 4 h^E h^{E\dagger} \operatorname{Tr}\Big(T^{h^E *} T^{h^E T}\Big) - 12 T^E y^{E\dagger} \operatorname{Tr}\Big(T^{D*} y^{DT}\Big) \\
&- 12 y^E y^{E\dagger} \operatorname{Tr}\Big(T^{D*} T^{DT}\Big) - 4 T^E y^{E\dagger} \operatorname{Tr}\Big(T^{E*} y^{ET}\Big) \\
&- 4 y^E y^{E\dagger} \operatorname{Tr}\Big(T^{E*} T^{ET}\Big) - 4 y^E y^{E\dagger} \operatorname{Tr}\Big(f m^2_{H_2} f^\dagger\Big) \\
&- 4 y^E y^{E\dagger} \operatorname{Tr}\Big(f f^\dagger m^{2*}_\Sigma\Big) - 12 h^E h^{E\dagger} \operatorname{Tr}\Big(g^D g^{D\dagger} m^{2*}_Q\Big) \\
&- 12 h^E h^{E\dagger} \operatorname{Tr}\Big(g^D m^{2*}_{\bar{D}} g^{D\dagger}\Big) - 4 h^E h^{E\dagger} \operatorname{Tr}\Big(h^E m^2_{H_1} h^{E\dagger}\Big) \\
&- 4 h^E h^{E\dagger} \operatorname{Tr}\Big(h^E h^{E\dagger} m^2_{e^c}\Big) - 12 y^E y^{E\dagger} \operatorname{Tr}\Big(m^2_{d^c} y^D y^{D\dagger}\Big) \\
&- 4 y^E y^{E\dagger} \operatorname{Tr}\Big(m^2_{e^c} y^E y^{E\dagger}\Big) - 4 y^E y^{E\dagger} \operatorname{Tr}\Big(m^2_L y^{E\dagger} y^E\Big) \\
&- 12 y^E y^{E\dagger} \operatorname{Tr}\Big(m^2_Q y^{D\dagger} y^D\Big), \qquad \text{(D.106)}
\end{aligned}
$$

$$
\begin{aligned}
\beta^{(1)}_{m^2_S} = &-5 g'^2_1 |M'_1|^2 + 4\Big(m^2_{H_d} + m^2_{H_u} + m^2_S\Big)|\lambda|^2 + 2 m^2_\phi |\sigma|^2 + 2 m^2_S |\sigma|^2 \\
&+ 2 m^2_{\bar{S}} |\sigma|^2 + 4|T_\lambda|^2 + 2|T_\sigma|^2 + \sqrt{\frac{5}{2}} g'_1 \Sigma_{1,4} + 6 m^2_S \operatorname{Tr}\Big(\kappa \kappa^\dagger\Big) \\
&+ 4 m^2_S \operatorname{Tr}\Big(\tilde{\lambda} \tilde{\lambda}^\dagger\Big) + 6 \operatorname{Tr}\Big(T^{\kappa *} T^{\kappa T}\Big) + 4 \operatorname{Tr}\Big(T^{\tilde{\lambda} *} T^{\tilde{\lambda} T}\Big) + 4 \operatorname{Tr}\Big(m^2_{H_1} \tilde{\lambda}^\dagger \tilde{\lambda}\Big) \\
&+ 6 \operatorname{Tr}\Big(\kappa \kappa^\dagger m^{2*}_D\Big) + 6 \operatorname{Tr}\Big(\kappa m^{2*}_{\bar{D}} \kappa^\dagger\Big) + 4 \operatorname{Tr}\Big(\tilde{\lambda} \tilde{\lambda}^\dagger m^{2*}_{H_2}\Big), \qquad \text{(D.107)}
\end{aligned}
$$

$$
\begin{aligned}
\beta^{(2)}_{m_S^2} = {} & \frac{12}{5} g_1^2 |T_\lambda|^2 - \frac{12}{5} g_1'^2 |T_\lambda|^2 + 12 g_2^2 |T_\lambda|^2 - 16 \Big(m_{H_d}^2 + m_{H_u}^2 + m_S^2 \Big) |\lambda|^4 \\
& - 16 m_\phi^2 |\sigma|^2 |\kappa_\phi|^2 - 4 m_S^2 |\sigma|^2 |\kappa_\phi|^2 - 4 m_{\tilde{S}}^2 |\sigma|^2 |\kappa_\phi|^2 - 8 m_\phi^2 |\sigma|^4 \\
& - 8 m_S^2 |\sigma|^4 - 8 m_{\tilde{S}}^2 |\sigma|^4 - 4 m_{L_4}^2 |\tilde{\sigma}|^2 |\sigma|^2 - 4 m_{\tilde{L}_4}^2 |\tilde{\sigma}|^2 |\sigma|^2 - 8 m_\phi^2 |\tilde{\sigma}|^2 |\sigma|^2 \\
& - 4 m_S^2 |\tilde{\sigma}|^2 |\sigma|^2 - 4 m_{\tilde{S}}^2 |\tilde{\sigma}|^2 |\sigma|^2 - \frac{12}{5} g_1^2 M_1 \lambda T_\lambda^* + \frac{12}{5} g_1'^2 M_1' \lambda T_\lambda^* \\
& - 12 g_2^2 M_2 \lambda T_\lambda^* - 4 |\sigma|^2 |T_{\kappa_\phi}|^2 - 4 \sigma \kappa_\phi^* T_\sigma^* T_{\kappa_\phi} - 4 \kappa_\phi \sigma^* T_{\kappa_\phi}^* T_\sigma - 4 |\kappa_\phi|^2 |T_\sigma|^2 \\
& - 16 |\sigma|^2 |T_\sigma|^2 - 4 |\tilde{\sigma}|^2 |T_\sigma|^2 - 4 \tilde{\sigma} \sigma^* T_{\tilde{\sigma}}^* T_\sigma - 4 \sigma \tilde{\sigma}^* T_\sigma^* T_{\tilde{\sigma}} - 4 |\sigma|^2 |T_{\tilde{\sigma}}|^2 \\
& + 5 g_1'^2 \Sigma_{2,44} + 2 \sqrt{10} g_1' \Sigma_{3,4} - 4 |T_\lambda|^2 \operatorname{Tr}\Big(f f^\dagger \Big) - 4 |T_\lambda|^2 \operatorname{Tr}\Big(\tilde{f} \tilde{f}^\dagger \Big) \\
& - 12 |T_\lambda|^2 \operatorname{Tr}\Big(y^D y^{D\dagger} \Big) - 4 |T_\lambda|^2 \operatorname{Tr}\Big(y^E y^{E\dagger} \Big) - 12 |T_\lambda|^2 \operatorname{Tr}\Big(y^U y^{U\dagger} \Big) \\
& + \frac{8}{5} g_1^2 m_S^2 \operatorname{Tr}\Big(\kappa \kappa^\dagger \Big) - \frac{18}{5} g_1'^2 m_S^2 \operatorname{Tr}\Big(\kappa \kappa^\dagger \Big) + 32 g_3^2 m_S^2 \operatorname{Tr}\Big(\kappa \kappa^\dagger \Big) \\
& + \frac{16}{5} g_1^2 |M_1|^2 \operatorname{Tr}\Big(\kappa \kappa^\dagger \Big) + 64 g_3^2 |M_3|^2 \operatorname{Tr}\Big(\kappa \kappa^\dagger \Big) + \frac{12}{5} g_1^2 m_S^2 \operatorname{Tr}\Big(\tilde{\lambda} \tilde{\lambda}^\dagger \Big) \\
& - \frac{12}{5} g_1'^2 m_S^2 \operatorname{Tr}\Big(\tilde{\lambda} \tilde{\lambda}^\dagger \Big) + 12 g_2^2 m_S^2 \operatorname{Tr}\Big(\tilde{\lambda} \tilde{\lambda}^\dagger \Big) + \frac{24}{5} g_1^2 |M_1|^2 \operatorname{Tr}\Big(\tilde{\lambda} \tilde{\lambda}^\dagger \Big) \\
& + 24 g_2^2 |M_2|^2 \operatorname{Tr}\Big(\tilde{\lambda} \tilde{\lambda}^\dagger \Big) - 4 \lambda T_\lambda^* \operatorname{Tr}\Big(f^\dagger T^f \Big) - 4 \lambda T_\lambda^* \operatorname{Tr}\Big(\tilde{f}^\dagger T^{\tilde{f}} \Big) \\
& - 12 \lambda T_\lambda^* \operatorname{Tr}\Big(y^{D\dagger} T^D \Big) - 4 \lambda T_\lambda^* \operatorname{Tr}\Big(y^{E\dagger} T^E \Big) - 12 \lambda T_\lambda^* \operatorname{Tr}\Big(y^{U\dagger} T^U \Big) \\
& - \frac{8}{5} g_1^2 M_1^* \operatorname{Tr}\Big(\kappa^\dagger T^\kappa \Big) - 32 g_3^2 M_3^* \operatorname{Tr}\Big(\kappa^\dagger T^\kappa \Big) - \frac{12}{5} g_1^2 M_1^* \operatorname{Tr}\Big(\tilde{\lambda}^\dagger T^{\tilde{\lambda}} \Big) \\
& - 12 g_2^2 M_2^* \operatorname{Tr}\Big(\tilde{\lambda}^\dagger T^{\tilde{\lambda}} \Big) + \frac{3}{10} g_1'^2 M_1'^* \Big[12 \operatorname{Tr}\Big(\kappa^\dagger T^\kappa \Big) - 16 M_1' \operatorname{Tr}\Big(\tilde{\lambda} \tilde{\lambda}^\dagger \Big) \\
& - 24 M_1' \operatorname{Tr}\Big(\kappa \kappa^\dagger \Big) + 595 g_1'^2 M_1' + 8 \lambda^* \Big(-2 M_1' \lambda + T_\lambda \Big) + 8 \operatorname{Tr}\Big(\tilde{\lambda}^\dagger T^{\tilde{\lambda}} \Big) \Big] \\
& - \frac{8}{5} g_1^2 M_1 \operatorname{Tr}\Big(T^{\kappa *} \kappa^T \Big) + \frac{18}{5} g_1'^2 M_1' \operatorname{Tr}\Big(T^{\kappa *} \kappa^T \Big) - 32 g_3^2 M_3 \operatorname{Tr}\Big(T^{\kappa *} \kappa^T \Big) \\
& + \frac{8}{5} g_1^2 \operatorname{Tr}\Big(T^{\kappa *} T^{\kappa T} \Big) - \frac{18}{5} g_1'^2 \operatorname{Tr}\Big(T^{\kappa *} T^{\kappa T} \Big) + 32 g_3^2 \operatorname{Tr}\Big(T^{\kappa *} T^{\kappa T} \Big) \\
& - \frac{12}{5} g_1^2 M_1 \operatorname{Tr}\Big(T^{\tilde{\lambda} *} \tilde{\lambda}^T \Big) + \frac{12}{5} g_1'^2 M_1' \operatorname{Tr}\Big(T^{\tilde{\lambda} *} \tilde{\lambda}^T \Big) - 12 g_2^2 M_2 \operatorname{Tr}\Big(T^{\tilde{\lambda} *} \tilde{\lambda}^T \Big) \\
& + \frac{12}{5} g_1^2 \operatorname{Tr}\Big(T^{\tilde{\lambda} *} T^{\tilde{\lambda} T} \Big) - \frac{12}{5} g_1'^2 \operatorname{Tr}\Big(T^{\tilde{\lambda} *} T^{\tilde{\lambda} T} \Big) + 12 g_2^2 \operatorname{Tr}\Big(T^{\tilde{\lambda} *} T^{\tilde{\lambda} T} \Big) \\
& + \frac{12}{5} g_1^2 \operatorname{Tr}\Big(m_{H_1}^2 \tilde{\lambda}^\dagger \tilde{\lambda} \Big) - \frac{12}{5} g_1'^2 \operatorname{Tr}\Big(m_{H_1}^2 \tilde{\lambda}^\dagger \tilde{\lambda} \Big) + 12 g_2^2 \operatorname{Tr}\Big(m_{H_1}^2 \tilde{\lambda}^\dagger \tilde{\lambda} \Big) \\
& + \frac{4}{5} \lambda^* \Big[3 g_1^2 m_{H_d}^2 \lambda - 3 g_1'^2 m_{H_d}^2 \lambda + 15 g_2^2 m_{H_d}^2 \lambda + 3 g_1^2 m_{H_u}^2 \lambda - 3 g_1'^2 m_{H_u}^2 \lambda \\
& + 15 g_2^2 m_{H_u}^2 \lambda + 3 g_1^2 m_S^2 \lambda - 3 g_1'^2 m_S^2 \lambda + 15 g_2^2 m_S^2 \lambda - 40 \lambda |T_\lambda|^2
\end{aligned}
$$

$$
\begin{aligned}
&+ 3g_1^2 M_1^* \Big(2M_1\lambda - T_\lambda\Big) + 15g_2^2 M_2^* \Big(2M_2\lambda - T_\lambda\Big) - 10m_{H_d}^2 \lambda \,\mathrm{Tr}\Big(f f^\dagger\Big) \\
&- 5m_{H_u}^2 \lambda \,\mathrm{Tr}\Big(f f^\dagger\Big) - 5m_S^2 \lambda \,\mathrm{Tr}\Big(f f^\dagger\Big) - 5m_{H_d}^2 \lambda \,\mathrm{Tr}\Big(\tilde{f}\tilde{f}^\dagger\Big) \\
&- 10m_{H_u}^2 \lambda \,\mathrm{Tr}\Big(\tilde{f}\tilde{f}^\dagger\Big) - 5m_S^2 \lambda \,\mathrm{Tr}\Big(\tilde{f}\tilde{f}^\dagger\Big) - 30m_{H_d}^2 \lambda \,\mathrm{Tr}\Big(y^D y^{D\dagger}\Big) \\
&- 15m_{H_u}^2 \lambda \,\mathrm{Tr}\Big(y^D y^{D\dagger}\Big) - 15m_S^2 \lambda \,\mathrm{Tr}\Big(y^D y^{D\dagger}\Big) - 10m_{H_d}^2 \lambda \,\mathrm{Tr}\Big(y^E y^{E\dagger}\Big) \\
&- 5m_{H_u}^2 \lambda \,\mathrm{Tr}\Big(y^E y^{E\dagger}\Big) - 5m_S^2 \lambda \,\mathrm{Tr}\Big(y^E y^{E\dagger}\Big) - 15m_{H_d}^2 \lambda \,\mathrm{Tr}\Big(y^U y^{U\dagger}\Big) \\
&- 30m_{H_u}^2 \lambda \,\mathrm{Tr}\Big(y^U y^{U\dagger}\Big) - 15m_S^2 \lambda \,\mathrm{Tr}\Big(y^U y^{U\dagger}\Big) - 5T_\lambda \,\mathrm{Tr}\Big(T^{f*} f^T\Big) \\
&- 5\lambda \,\mathrm{Tr}\Big(T^{f*} T^{fT}\Big) - 5T_\lambda \,\mathrm{Tr}\Big(T^{\tilde{f}*} \tilde{f}^T\Big) - 5\lambda \,\mathrm{Tr}\Big(T^{\tilde{f}*} T^{\tilde{f}T}\Big) \\
&- 15T_\lambda \,\mathrm{Tr}\Big(T^{D*} y^{DT}\Big) - 15\lambda \,\mathrm{Tr}\Big(T^{D*} T^{DT}\Big) - 5T_\lambda \,\mathrm{Tr}\Big(T^{E*} y^{ET}\Big) \\
&- 5\lambda \,\mathrm{Tr}\Big(T^{E*} T^{ET}\Big) - 15T_\lambda \,\mathrm{Tr}\Big(T^{U*} y^{UT}\Big) - 15\lambda \,\mathrm{Tr}\Big(T^{U*} T^{UT}\Big) \\
&- 5\lambda \,\mathrm{Tr}\Big(f m_{H_2}^2 f^\dagger\Big) - 5\lambda \,\mathrm{Tr}\Big(f f^\dagger m_\Sigma^{2*}\Big) - 5\lambda \,\mathrm{Tr}\Big(\tilde{f} m_{H_1}^2 \tilde{f}^\dagger\Big) \\
&- 5\lambda \,\mathrm{Tr}\Big(\tilde{f}\tilde{f}^\dagger m_\Sigma^{2*}\Big) - 15\lambda \,\mathrm{Tr}\Big(m_{d^c}^2 y^D y^{D\dagger}\Big) - 5\lambda \,\mathrm{Tr}\Big(m_{e^c}^2 y^E y^{E\dagger}\Big) \\
&- 5\lambda \,\mathrm{Tr}\Big(m_L^2 y^{E\dagger} y^E\Big) - 15\lambda \,\mathrm{Tr}\Big(m_Q^2 y^{D\dagger} y^D\Big) - 15\lambda \,\mathrm{Tr}\Big(m_Q^2 y^{U\dagger} y^U\Big) \\
&- 15\lambda \,\mathrm{Tr}\Big(m_{u^c}^2 y^U y^{U\dagger}\Big)\Big] + \frac{8}{5} g_1^2 \,\mathrm{Tr}\Big(\kappa\kappa^\dagger m_D^{2*}\Big) - \frac{18}{5} g_1'^2 \,\mathrm{Tr}\Big(\kappa\kappa^\dagger m_D^{2*}\Big) \\
&+ 32g_3^2 \,\mathrm{Tr}\Big(\kappa\kappa^\dagger m_D^{2*}\Big) + \frac{8}{5} g_1^2 \,\mathrm{Tr}\Big(\kappa m_{\bar{D}}^{2*} \kappa^\dagger\Big) - \frac{18}{5} g_1'^2 \,\mathrm{Tr}\Big(\kappa m_{\bar{D}}^{2*} \kappa^\dagger\Big) \\
&+ 32g_3^2 \,\mathrm{Tr}\Big(\kappa m_{\bar{D}}^{2*} \kappa^\dagger\Big) + \frac{12}{5} g_1^2 \,\mathrm{Tr}\Big(\tilde{\lambda}\tilde{\lambda}^\dagger m_{H_2}^{2*}\Big) - \frac{12}{5} g_1'^2 \,\mathrm{Tr}\Big(\tilde{\lambda}\tilde{\lambda}^\dagger m_{H_2}^{2*}\Big) \\
&+ 12g_2^2 \,\mathrm{Tr}\Big(\tilde{\lambda}\tilde{\lambda}^\dagger m_{H_2}^{2*}\Big) - 4 \,\mathrm{Tr}\Big(f T^{\tilde{\lambda}*} T^{\tilde{\lambda}T} f^\dagger\Big) - 4m_{H_u}^2 \,\mathrm{Tr}\Big(\tilde{f}\tilde{\lambda}^\dagger \tilde{\lambda}\tilde{f}^\dagger\Big) \\
&- 4m_S^2 \,\mathrm{Tr}\Big(\tilde{f}\tilde{\lambda}^\dagger \tilde{\lambda}\tilde{f}^\dagger\Big) - 4 \,\mathrm{Tr}\Big(\tilde{f}\tilde{\lambda}^\dagger T^{\tilde{\lambda}} T^{\tilde{f}\dagger}\Big) - 4 \,\mathrm{Tr}\Big(\tilde{f} T^{\tilde{\lambda}\dagger} T^{\tilde{\lambda}} \tilde{f}^\dagger\Big) \\
&- 12m_{L_4}^2 \,\mathrm{Tr}\Big(g^D \kappa^\dagger \kappa g^{D\dagger}\Big) - 12m_S^2 \,\mathrm{Tr}\Big(g^D \kappa^\dagger \kappa g^{D\dagger}\Big) - 12 \,\mathrm{Tr}\Big(g^D \kappa^\dagger T^\kappa T^{g^D\dagger}\Big) \\
&- 12 \,\mathrm{Tr}\Big(g^D T^{\kappa\dagger} T^\kappa g^{D\dagger}\Big) - 4m_{L_4}^2 \,\mathrm{Tr}\Big(h^E \tilde{\lambda}^\dagger \tilde{\lambda} h^{E\dagger}\Big) - 4m_S^2 \,\mathrm{Tr}\Big(h^E \tilde{\lambda}^\dagger \tilde{\lambda} h^{E\dagger}\Big) \\
&- 4 \,\mathrm{Tr}\Big(h^E \tilde{\lambda}^\dagger T^{\tilde{\lambda}} T^{h^E\dagger}\Big) - 4 \,\mathrm{Tr}\Big(h^E T^{\tilde{\lambda}\dagger} T^{\tilde{\lambda}} h^{E\dagger}\Big) - 12 \,\mathrm{Tr}\Big(\kappa g^{D\dagger} T^{g^D} T^{\kappa\dagger}\Big) \\
&- 24m_S^2 \,\mathrm{Tr}\Big(\kappa\kappa^\dagger \kappa\kappa^\dagger\Big) - 24 \,\mathrm{Tr}\Big(\kappa\kappa^\dagger T^\kappa T^{\kappa\dagger}\Big) - 12 \,\mathrm{Tr}\Big(\kappa T^{g^D\dagger} T^{g^D} \kappa^\dagger\Big) \\
&- 24 \,\mathrm{Tr}\Big(\kappa T^{\kappa\dagger} T^\kappa \kappa^\dagger\Big) - 4 \,\mathrm{Tr}\Big(\tilde{\lambda}\tilde{f}^\dagger T^{\tilde{f}} T^{\tilde{\lambda}\dagger}\Big) - 4 \,\mathrm{Tr}\Big(\tilde{\lambda} h^{E\dagger} T^{h^E} T^{\tilde{\lambda}\dagger}\Big)
\end{aligned}
$$

$$
\begin{aligned}
&- 16m_S^2\,\mathrm{Tr}\Big(\tilde{\lambda}\tilde{\lambda}^\dagger\tilde{\lambda}\tilde{\lambda}^\dagger\Big) - 16\,\mathrm{Tr}\Big(\tilde{\lambda}\tilde{\lambda}^\dagger T^{\tilde{\lambda}} T^{\tilde{\lambda}\dagger}\Big) - 4m_{H_d}^2\,\mathrm{Tr}\Big(\tilde{\lambda}\tilde{\lambda}^\dagger f^T f^*\Big)\\
&- 4m_S^2\,\mathrm{Tr}\Big(\tilde{\lambda}\tilde{\lambda}^\dagger f^T f^*\Big) - 4\,\mathrm{Tr}\Big(\tilde{\lambda}\tilde{\lambda}^\dagger T^{fT} T^{f*}\Big) - 4\,\mathrm{Tr}\Big(\tilde{\lambda} T^{\tilde{f}\dagger} T^{\tilde{f}}\tilde{\lambda}^\dagger\Big)\\
&- 4\,\mathrm{Tr}\Big(\tilde{\lambda} T^{h^E\dagger} T^{h^E}\tilde{\lambda}^\dagger\Big) - 16\,\mathrm{Tr}\Big(\tilde{\lambda} T^{\tilde{\lambda}\dagger} T^{\tilde{\lambda}}\tilde{\lambda}^\dagger\Big) - 4\,\mathrm{Tr}\Big(f^\dagger T^f T^{\tilde{\lambda}*}\tilde{\lambda}^T\Big)\\
&- 4\,\mathrm{Tr}\Big(\tilde{\lambda}^\dagger f^T T^{f*} T^{\tilde{\lambda}}\Big) - 4\,\mathrm{Tr}\Big(f\tilde{\lambda}^*\tilde{\lambda}^T f^\dagger m_\Sigma^{2*}\Big) - 4\,\mathrm{Tr}\Big(\tilde{f} m_{H_1}^2\tilde{\lambda}^\dagger\tilde{\lambda}\tilde{f}^\dagger\Big)\\
&- 4\,\mathrm{Tr}\Big(\tilde{f}\tilde{\lambda}^\dagger\tilde{\lambda} m_{H_1}^2\tilde{f}^\dagger\Big) - 4\,\mathrm{Tr}\Big(\tilde{f}\tilde{\lambda}^\dagger\tilde{\lambda}\tilde{f}^\dagger m_\Sigma^{2*}\Big) - 4\,\mathrm{Tr}\Big(\tilde{f}\tilde{\lambda}^\dagger m_{H_2}^{2*}\tilde{\lambda}\tilde{f}^\dagger\Big)\\
&- 12\,\mathrm{Tr}\Big(g^D\kappa^\dagger\kappa g^{D\dagger} m_Q^{2*}\Big) - 12\,\mathrm{Tr}\Big(g^D\kappa^\dagger\kappa m_{\bar{D}}^{2*} g^{D\dagger}\Big) - 12\,\mathrm{Tr}\Big(g^D\kappa^\dagger m_D^{2*}\kappa g^{D\dagger}\Big)\\
&- 12\,\mathrm{Tr}\Big(g^D m_{\bar{D}}^{2*}\kappa^\dagger\kappa g^{D\dagger}\Big) - 4\,\mathrm{Tr}\Big(h^E m_{H_1}^2\tilde{\lambda}^\dagger\tilde{\lambda} h^{E\dagger}\Big) - 4\,\mathrm{Tr}\Big(h^E\tilde{\lambda}^\dagger\tilde{\lambda} m_{H_1}^2 h^{E\dagger}\Big)\\
&- 4\,\mathrm{Tr}\Big(h^E\tilde{\lambda}^\dagger\tilde{\lambda} h^{E\dagger} m_{e^c}^2\Big) - 4\,\mathrm{Tr}\Big(h^E\tilde{\lambda}^\dagger m_{H_2}^{2*}\tilde{\lambda} h^{E\dagger}\Big) - 16\,\mathrm{Tr}\Big(m_{H_1}^2\tilde{\lambda}^\dagger\tilde{\lambda}\tilde{\lambda}^\dagger\tilde{\lambda}\Big)\\
&- 4\,\mathrm{Tr}\Big(m_{H_1}^2\tilde{\lambda}^\dagger f^T f^*\tilde{\lambda}\Big) - 12\,\mathrm{Tr}\Big(\kappa\kappa^\dagger\kappa\kappa^\dagger m_D^{2*}\Big) - 12\,\mathrm{Tr}\Big(\kappa\kappa^\dagger\kappa m_{\bar{D}}^{2*}\kappa^\dagger\Big)\\
&- 12\,\mathrm{Tr}\Big(\kappa\kappa^\dagger m_D^{2*}\kappa\kappa^\dagger\Big) - 12\,\mathrm{Tr}\Big(\kappa m_{\bar{D}}^{2*}\kappa^\dagger\kappa\kappa^\dagger\Big) - 8\,\mathrm{Tr}\Big(\tilde{\lambda}\tilde{\lambda}^\dagger\tilde{\lambda}\tilde{\lambda}^\dagger m_{H_2}^{2*}\Big)\\
&- 8\,\mathrm{Tr}\Big(\tilde{\lambda}\tilde{\lambda}^\dagger m_{H_2}^{2*}\tilde{\lambda}\tilde{\lambda}^\dagger\Big) - 4\,\mathrm{Tr}\Big(\tilde{\lambda}\tilde{\lambda}^\dagger m_{H_2}^{2*} f^T f^*\Big)\\
&- 4\,\mathrm{Tr}\Big(\tilde{\lambda}\tilde{\lambda}^\dagger f^T f^* m_{H_2}^{2*}\Big),
\end{aligned}
\tag{D.108}
$$

$$
\beta^{(1)}_{m_{\bar{S}}^2} = 2\Big(m_\phi^2 + m_S^2 + m_{\bar{S}}^2\Big)|\sigma|^2 + 2|T_\sigma|^2 - 5g_1'^2|M_1'|^2 - \sqrt{\frac{5}{2}}g_1'\Sigma_{1,4}\,,
\tag{D.109}
$$

$$
\begin{aligned}
\beta^{(2)}_{m_{\bar{S}}^2} = {}& \frac{357}{2}g_1'^4|M_1'|^2 - 4m_{H_d}^2|\sigma|^2|\lambda|^2 - 4m_{H_u}^2|\sigma|^2|\lambda|^2 - 4m_\phi^2|\sigma|^2|\lambda|^2\\
&- 8m_S^2|\sigma|^2|\lambda|^2 - 4m_{\bar{S}}^2|\sigma|^2|\lambda|^2 - 8m_\phi^2|\sigma|^4 - 8m_S^2|\sigma|^4 - 8m_{\bar{S}}^2|\sigma|^4\\
&- 4m_{L_4}^2|\tilde{\sigma}|^2|\sigma|^2 - 4m_{\bar{L}_4}^2|\tilde{\sigma}|^2|\sigma|^2 - 8m_\phi^2|\tilde{\sigma}|^2|\sigma|^2 - 4m_S^2|\tilde{\sigma}|^2|\sigma|^2\\
&- 4m_{\bar{S}}^2|\tilde{\sigma}|^2|\sigma|^2 - 4|\sigma|^2|T_{\kappa_\phi}|^2 - 4|\sigma|^2|T_\lambda|^2 - 4\sigma\lambda^* T_\sigma^* T_\lambda - 4\kappa_\phi\sigma^* T_{\kappa_\phi}^* T_\sigma\\
&- 4\lambda\sigma^* T_\lambda^* T_\sigma - 4|\lambda|^2|T_\sigma|^2 - 16|\sigma|^2|T_\sigma|^2 - 4|\tilde{\sigma}|^2|T_\sigma|^2 - 4\tilde{\sigma}\sigma^* T_{\tilde{\sigma}}^* T_\sigma\\
&- 4\kappa_\phi^*\Big[\Big(4m_\phi^2 + m_S^2 + m_{\bar{S}}^2\Big)\kappa_\phi|\sigma|^2 + T_\sigma^*\Big(\kappa_\phi T_\sigma + \sigma T_{\kappa_\phi}\Big)\Big] - 4\sigma\tilde{\sigma}^* T_\sigma^* T_{\tilde{\sigma}}\\
&- 4|\sigma|^2|T_{\tilde{\sigma}}|^2 + 5g_1'^2\Sigma_{2,44} - 2\sqrt{10}g_1'\Sigma_{3,4} - 6m_\phi^2|\sigma|^2\,\mathrm{Tr}\Big(\kappa\kappa^\dagger\Big)\\
&- 12m_S^2|\sigma|^2\,\mathrm{Tr}\Big(\kappa\kappa^\dagger\Big) - 6m_{\bar{S}}^2|\sigma|^2\,\mathrm{Tr}\Big(\kappa\kappa^\dagger\Big) - 6|T_\sigma|^2\,\mathrm{Tr}\Big(\kappa\kappa^\dagger\Big)\\
&- 4m_\phi^2|\sigma|^2\,\mathrm{Tr}\Big(\tilde{\lambda}\tilde{\lambda}^\dagger\Big) - 8m_S^2|\sigma|^2\,\mathrm{Tr}\Big(\tilde{\lambda}\tilde{\lambda}^\dagger\Big) - 4m_{\bar{S}}^2|\sigma|^2\,\mathrm{Tr}\Big(\tilde{\lambda}\tilde{\lambda}^\dagger\Big)\\
&- 4|T_\sigma|^2\,\mathrm{Tr}\Big(\tilde{\lambda}\tilde{\lambda}^\dagger\Big) - 6\sigma T_\sigma^*\,\mathrm{Tr}\Big(\kappa^\dagger T^\kappa\Big) - 4\sigma T_\sigma^*\,\mathrm{Tr}\Big(\tilde{\lambda}^\dagger T^{\tilde{\lambda}}\Big)
\end{aligned}
$$

$$
\begin{aligned}
&- 6\sigma^* T_\sigma \operatorname{Tr}\Big(T^{\kappa *}\kappa^T\Big) - 6|\sigma|^2 \operatorname{Tr}\Big(T^{\kappa *}T^{\kappa T}\Big) - 4\sigma^* T_\sigma \operatorname{Tr}\Big(T^{\tilde{\lambda} *}\tilde{\lambda}^T\Big) \\
&- 4|\sigma|^2 \operatorname{Tr}\Big(T^{\tilde{\lambda} *}T^{\tilde{\lambda} T}\Big) - 4|\sigma|^2 \operatorname{Tr}\Big(m^2_{H_1}\tilde{\lambda}^\dagger\tilde{\lambda}\Big) - 6|\sigma|^2 \operatorname{Tr}\Big(\kappa\kappa^\dagger m^{2*}_D\Big) \\
&- 6|\sigma|^2 \operatorname{Tr}\Big(\kappa m^{2*}_{\bar{D}}\kappa^\dagger\Big) - 4|\sigma|^2 \operatorname{Tr}\Big(\tilde{\lambda}\tilde{\lambda}^\dagger m^{2*}_{H_2}\Big), \qquad \text{(D.110)}
\end{aligned}
$$

$$
\begin{aligned}
\beta^{(1)}_{m^2_{H_1}} =& -\frac{6}{5}g_1^2\mathbf{1}|M_1|^2 - \frac{9}{5}g_1'^2\mathbf{1}|M_1'|^2 - 6g_2^2\mathbf{1}|M_2|^2 + 2m^2_{H_u}\tilde{f}^\dagger\tilde{f} + 2m^2_{L_4}h^{E\dagger}h^E \\
&+ 2m^2_S\tilde{\lambda}^\dagger\tilde{\lambda} + 2T^{\tilde{f}\dagger}T^{\tilde{f}} + 2T^{h^{E\dagger}}T^{h^E} + 2T^{\tilde{\lambda}\dagger}T^{\tilde{\lambda}} + m^2_{H_1}\tilde{f}^\dagger\tilde{f} + m^2_{H_1}h^{E\dagger}h^E \\
&+ m^2_{H_1}\tilde{\lambda}^\dagger\tilde{\lambda} + \tilde{f}^\dagger\tilde{f}m^2_{H_1} + 2\tilde{f}^\dagger m^{2*}_\Sigma\tilde{f} + h^{E\dagger}h^E m^2_{H_1} + 2h^{E\dagger}m^2_{\bar{e}^c}h^E + \tilde{\lambda}^\dagger\tilde{\lambda}m^2_{H_1} \\
&+ 2\tilde{\lambda}^\dagger m^{2*}_{H_2}\tilde{\lambda} - \sqrt{\frac{3}{5}}g_1\mathbf{1}\Sigma_{1,1} - \frac{3}{\sqrt{10}}g_1'\mathbf{1}\Sigma_{1,4}\,, \qquad \text{(D.111)}
\end{aligned}
$$

$$
\begin{aligned}
\beta^{(2)}_{m^2_{H_1}} =& \frac{18}{5}g_1^2g_2^2\mathbf{1}|M_2|^2 + \frac{27}{5}g_1'^2g_2^2\mathbf{1}|M_2|^2 + 87g_2^4\mathbf{1}|M_2|^2 + \frac{9}{5}g_1^2g_2^2M_1\mathbf{1}M_2^* \\
&+ \frac{27}{10}g_1'^2g_2^2M_1'\mathbf{1}M_2^* + 2g_1'^2m^2_{H_u}\tilde{f}^\dagger\tilde{f} - 2m^2_{H_d}|\lambda|^2\tilde{f}^\dagger\tilde{f} - 4m^2_{H_u}|\lambda|^2\tilde{f}^\dagger\tilde{f} \\
&- 2m^2_S|\lambda|^2\tilde{f}^\dagger\tilde{f} - 2|T_\lambda|^2\tilde{f}^\dagger\tilde{f} - 2\lambda T^*_\lambda\tilde{f}^\dagger T^{\tilde{f}} + \frac{12}{5}g_1^2m^2_{L_4}h^{E\dagger}h^E \\
&- \frac{2}{5}g_1'^2m^2_{L_4}h^{E\dagger}h^E - 4m^2_{L_4}|\tilde{\sigma}|^2h^{E\dagger}h^E - 2m^2_{\bar{L}_4}|\tilde{\sigma}|^2h^{E\dagger}h^E - 2m^2_\phi|\tilde{\sigma}|^2h^{E\dagger}h^E \\
&- 2|T_{\tilde{\sigma}}|^2h^{E\dagger}h^E + \frac{3}{50}g_1^2\Big\{\Big[30g_2^2\Big(2M_1 + M_2\Big) - 3g_1'^2\Big(2M_1 + M_1'\Big) \\
&+ 594g_1^2M_1\Big]\mathbf{1} - 40h^{E\dagger}T^{h^E} + 80M_1h^{E\dagger}h^E\Big\}M_1^* - 2\tilde{\sigma}T^*_{\tilde{\sigma}}h^{E\dagger}T^{h^E} \\
&+ 2g_1'^2m^2_S\tilde{\lambda}^\dagger\tilde{\lambda} - 4m^2_{H_d}|\lambda|^2\tilde{\lambda}^\dagger\tilde{\lambda} - 4m^2_{H_u}|\lambda|^2\tilde{\lambda}^\dagger\tilde{\lambda} - 8m^2_S|\lambda|^2\tilde{\lambda}^\dagger\tilde{\lambda} \\
&- 2m^2_\phi|\sigma|^2\tilde{\lambda}^\dagger\tilde{\lambda} - 4m^2_S|\sigma|^2\tilde{\lambda}^\dagger\tilde{\lambda} - 2m^2_{\bar{S}}|\sigma|^2\tilde{\lambda}^\dagger\tilde{\lambda} - 4|T_\lambda|^2\tilde{\lambda}^\dagger\tilde{\lambda} - 2|T_\sigma|^2\tilde{\lambda}^\dagger\tilde{\lambda} \\
&+ \frac{1}{50}g_1'^2\Big(-9\Big\{-3\Big[111g_1'^2M_1' + 5g_2^2\Big(2M_1' + M_2\Big)\Big] + g_1^2\Big(2M_1' \\
&+ M_1\Big)\Big\}\mathbf{1} + 20\Big(10M_1'\tilde{f}^\dagger\tilde{f} + 10M_1'\tilde{\lambda}^\dagger\tilde{\lambda} - 2M_1'h^{E\dagger}h^E - 5\tilde{f}^\dagger T^{\tilde{f}} \\
&- 5\tilde{\lambda}^\dagger T^{\tilde{\lambda}} + h^{E\dagger}T^{h^E}\Big)\Big)M_1'^* - 4\lambda T^*_\lambda\tilde{\lambda}^\dagger T^{\tilde{\lambda}} - 2\sigma T^*_\sigma\tilde{\lambda}^\dagger T^{\tilde{\lambda}} - 2g_1'^2M_1'T^{\tilde{f}\dagger}\tilde{f} \\
&+ 2g_1'^2T^{\tilde{f}\dagger}T^{\tilde{f}} - 2|\lambda|^2T^{\tilde{f}\dagger}T^{\tilde{f}} - \frac{12}{5}g_1^2M_1T^{h^{E}\dagger}h^E + \frac{2}{5}g_1'^2M_1'T^{h^{E}\dagger}h^E \\
&+ \frac{12}{5}g_1^2T^{h^{E}\dagger}T^{h^E} - \frac{2}{5}g_1'^2T^{h^{E}\dagger}T^{h^E} - 2|\tilde{\sigma}|^2T^{h^{E}\dagger}T^{h^E} - 2g_1'^2M_1'T^{\tilde{\lambda}\dagger}\tilde{\lambda} \\
&+ 2g_1'^2T^{\tilde{\lambda}\dagger}T^{\tilde{\lambda}} - 4|\lambda|^2T^{\tilde{\lambda}\dagger}T^{\tilde{\lambda}} - 2|\sigma|^2T^{\tilde{\lambda}\dagger}T^{\tilde{\lambda}} + g_1'^2m^2_{H_1}\tilde{f}^\dagger\tilde{f} - |\lambda|^2m^2_{H_1}\tilde{f}^\dagger\tilde{f} \\
&+ \frac{6}{5}g_1^2m^2_{H_1}h^{E\dagger}h^E - \frac{1}{5}g_1'^2m^2_{H_1}h^{E\dagger}h^E - |\tilde{\sigma}|^2m^2_{H_1}h^{E\dagger}h^E + g_1'^2m^2_{H_1}\tilde{\lambda}^\dagger\tilde{\lambda} \\
&- 2|\lambda|^2m^2_{H_1}\tilde{\lambda}^\dagger\tilde{\lambda} - |\sigma|^2m^2_{H_1}\tilde{\lambda}^\dagger\tilde{\lambda} + g_1'^2\tilde{f}^\dagger\tilde{f}m^2_{H_1} - |\lambda|^2\tilde{f}^\dagger\tilde{f}m^2_{H_1} \\
&+ 2g_1'^2\tilde{f}^\dagger m^{2*}_\Sigma\tilde{f} - 2|\lambda|^2\tilde{f}^\dagger m^{2*}_\Sigma\tilde{f} + \frac{6}{5}g_1^2h^{E\dagger}h^Em^2_{H_1} - \frac{1}{5}g_1'^2h^{E\dagger}h^Em^2_{H_1}
\end{aligned}
$$

$$
\begin{aligned}
&- |\tilde{\sigma}|^2 h^{E\dagger} h^E m_{H_1}^2 + \frac{12}{5} g_1^2 h^{E\dagger} m_{e^c}^2 h^E - \frac{2}{5} g_1'^2 h^{E\dagger} m_{e^c}^2 h^E \\
&- 2|\tilde{\sigma}|^2 h^{E\dagger} m_{e^c}^2 h^E + g_1'^2 \tilde{\lambda}^\dagger \tilde{\lambda} m_{H_1}^2 - 2|\lambda|^2 \tilde{\lambda}^\dagger \tilde{\lambda} m_{H_1}^2 - |\sigma|^2 \tilde{\lambda}^\dagger \tilde{\lambda} m_{H_1}^2 \\
&+ 2 g_1'^2 \tilde{\lambda}^\dagger m_{H_2}^{2*} \tilde{\lambda} - 4|\lambda|^2 \tilde{\lambda}^\dagger m_{H_2}^{2*} \tilde{\lambda} - 2|\sigma|^2 \tilde{\lambda}^\dagger m_{H_2}^{2*} \tilde{\lambda} - 4 m_{H_d}^2 \tilde{f}^\dagger f f^\dagger \tilde{f} \\
&- 4 m_{H_u}^2 \tilde{f}^\dagger f f^\dagger \tilde{f} - 4 \tilde{f}^\dagger f T^{f\dagger} T^{\tilde{f}} - 8 m_{H_u}^2 \tilde{f}^\dagger \tilde{f} \tilde{f}^\dagger \tilde{f} - 4 \tilde{f}^\dagger \tilde{f} T^{\tilde{f}\dagger} T^{\tilde{f}} \\
&- 4 \tilde{f}^\dagger T^f T^{f\dagger} \tilde{f} - 4 \tilde{f}^\dagger T^{\tilde{f}} T^{\tilde{f}\dagger} \tilde{f} - 8 m_{L_4}^2 h^{E\dagger} h^E h^{E\dagger} h^E - 4 h^{E\dagger} h^E T^{h^E\dagger} T^{h^E} \\
&- 4 m_{H_d}^2 h^{E\dagger} y^E y^{E\dagger} h^E - 4 m_{L_4}^2 h^{E\dagger} y^E y^{E\dagger} h^E - 4 h^{E\dagger} y^E T^{E\dagger} T^{h^E} \\
&- 4 h^{E\dagger} T^{h^E} T^{h^E\dagger} h^E - 4 h^{E\dagger} T^E T^{E\dagger} h^E - 4 m_S^2 \tilde{\lambda}^\dagger \tilde{\lambda} \tilde{\lambda}^\dagger \tilde{\lambda} - 2 \tilde{\lambda}^\dagger \tilde{\lambda} T^{\tilde{\lambda}\dagger} T^{\tilde{\lambda}} \\
&- 2 \tilde{\lambda}^\dagger T^{\tilde{\lambda}} T^{\tilde{\lambda}\dagger} \tilde{\lambda} - 2 m_{H_d}^2 \tilde{\lambda}^\dagger f^T f^* \tilde{\lambda} - 2 m_S^2 \tilde{\lambda}^\dagger f^T f^* \tilde{\lambda} - 2 \tilde{\lambda}^\dagger f^T T^{f*} T^{\tilde{\lambda}} \\
&- 2 \tilde{\lambda}^\dagger T^{fT} T^{f*} \tilde{\lambda} - 4 T^{\tilde{f}\dagger} f f^\dagger T^{\tilde{f}} - 4 T^{\tilde{f}\dagger} \tilde{f} \tilde{f}^\dagger T^{\tilde{f}} - 4 T^{\tilde{f}\dagger} T^f f^\dagger \tilde{f} \\
&- 4 T^{\tilde{f}\dagger} T^{\tilde{f}} \tilde{f}^\dagger \tilde{f} - 4 T^{h^E\dagger} h^E h^{E\dagger} T^{h^E} - 4 T^{h^E\dagger} y^E y^{E\dagger} T^{h^E} - 4 T^{h^E\dagger} T^{h^E} h^{E\dagger} h^E \\
&- 4 T^{h^E\dagger} T^E y^{E\dagger} h^E - 2 T^{\tilde{\lambda}\dagger} \tilde{\lambda} \tilde{\lambda}^\dagger T^{\tilde{\lambda}} - 2 T^{\tilde{\lambda}\dagger} T^{\tilde{\lambda}} \tilde{\lambda}^\dagger \tilde{\lambda} - 2 T^{\tilde{\lambda}\dagger} f^T f^* T^{\tilde{\lambda}} \\
&- 2 T^{\tilde{\lambda}\dagger} T^{fT} f^* \tilde{\lambda} - 2 m_{H_1}^2 \tilde{f}^\dagger f f^\dagger \tilde{f} - 2 m_{H_1}^2 \tilde{f}^\dagger \tilde{f} \tilde{f}^\dagger \tilde{f} - 2 m_{H_1}^2 h^{E\dagger} h^E h^{E\dagger} h^E \\
&- 2 m_{H_1}^2 h^{E\dagger} y^E y^{E\dagger} h^E - m_{H_1}^2 \tilde{\lambda}^\dagger \tilde{\lambda} \tilde{\lambda}^\dagger \tilde{\lambda} - m_{H_1}^2 \tilde{\lambda}^\dagger f^T f^* \tilde{\lambda} - 4 \tilde{f}^\dagger f m_{H_2}^2 f^\dagger \tilde{f} \\
&- 2 \tilde{f}^\dagger f f^\dagger \tilde{f} m_{H_1}^2 - 4 \tilde{f}^\dagger f f^\dagger m_\Sigma^{2*} \tilde{f} - 4 \tilde{f}^\dagger \tilde{f} m_{H_1}^2 \tilde{f}^\dagger \tilde{f} - 2 \tilde{f}^\dagger \tilde{f} \tilde{f}^\dagger \tilde{f} m_{H_1}^2 \\
&- 4 \tilde{f}^\dagger \tilde{f} \tilde{f}^\dagger m_\Sigma^{2*} \tilde{f} - 4 \tilde{f}^\dagger m_\Sigma^{2*} f f^\dagger \tilde{f} - 4 \tilde{f}^\dagger m_\Sigma^{2*} \tilde{f} \tilde{f}^\dagger \tilde{f} - 4 h^{E\dagger} h^E m_{H_1}^2 h^{E\dagger} h^E \\
&- 2 h^{E\dagger} h^E h^{E\dagger} h^E m_{H_1}^2 - 4 h^{E\dagger} h^E h^{E\dagger} m_{e^c}^2 h^E - 4 h^{E\dagger} m_{e^c}^2 h^E h^{E\dagger} h^E \\
&- 4 h^{E\dagger} m_{e^c}^2 y^E y^{E\dagger} h^E - 4 h^{E\dagger} y^E m_L^2 y^{E\dagger} h^E - 2 h^{E\dagger} y^E y^{E\dagger} h^E m_{H_1}^2 \\
&- 4 h^{E\dagger} y^E y^{E\dagger} m_{e^c}^2 h^E - 2 \tilde{\lambda}^\dagger \tilde{\lambda} m_{H_1}^2 \tilde{\lambda}^\dagger \tilde{\lambda} - \tilde{\lambda}^\dagger \tilde{\lambda} \tilde{\lambda}^\dagger \tilde{\lambda} m_{H_1}^2 - 2 \tilde{\lambda}^\dagger \tilde{\lambda} \tilde{\lambda}^\dagger m_{H_2}^{2*} \tilde{\lambda} \\
&- 2 \tilde{\lambda}^\dagger m_{H_2}^{2*} \tilde{\lambda} \tilde{\lambda}^\dagger \tilde{\lambda} - 2 \tilde{\lambda}^\dagger m_{H_2}^{2*} f^T f^* \tilde{\lambda} - 2 \tilde{\lambda}^\dagger f^T m_\Sigma^2 f^* \tilde{\lambda} - \tilde{\lambda}^\dagger f^T f^* \tilde{\lambda} m_{H_1}^2 \\
&- 2 \tilde{\lambda}^\dagger f^T f^* m_{H_2}^{2*} \tilde{\lambda} - 2 \lambda^* T^{\tilde{f}\dagger} \tilde{f} T_\lambda - 4 \lambda^* T^{\tilde{\lambda}\dagger} \tilde{\lambda} T_\lambda - 2 \sigma^* T^{\tilde{\lambda}\dagger} \tilde{\lambda} T_\sigma \\
&- 2 \tilde{\sigma}^* T^{h^E\dagger} h^E T_{\tilde{\sigma}} + 6 g_2^4 \mathbf{1} \Sigma_{2,2} + \frac{6}{5} g_1^2 \mathbf{1} \Sigma_{2,11} + \frac{3}{5} \sqrt{6} g_1 g_1' \mathbf{1} \Sigma_{2,14} \\
&+ \frac{3}{5} \sqrt{6} g_1 g_1' \mathbf{1} \Sigma_{2,41} + \frac{9}{5} g_1'^2 \mathbf{1} \Sigma_{2,44} - 4 \sqrt{\frac{3}{5}} g_1 \mathbf{1} \Sigma_{3,1} - 6 \sqrt{\frac{2}{5}} g_1' \mathbf{1} \Sigma_{3,4} \\
&- 4 m_{H_u}^2 \tilde{f}^\dagger \tilde{f} \operatorname{Tr}\Big(\tilde{f} \tilde{f}^\dagger \Big) - 2 T^{\tilde{f}\dagger} T^{\tilde{f}} \operatorname{Tr}\Big(\tilde{f} \tilde{f}^\dagger \Big) - m_{H_1}^2 \tilde{f}^\dagger \tilde{f} \operatorname{Tr}\Big(\tilde{f} \tilde{f}^\dagger \Big) \\
&- \tilde{f}^\dagger \tilde{f} m_{H_1}^2 \operatorname{Tr}\Big(\tilde{f} \tilde{f}^\dagger \Big) - 2 \tilde{f}^\dagger m_\Sigma^{2*} \tilde{f} \operatorname{Tr}\Big(\tilde{f} \tilde{f}^\dagger \Big) - 12 m_{L_4}^2 h^{E\dagger} h^E \operatorname{Tr}\Big(g^D g^{D\dagger} \Big) \\
&- 6 T^{h^E\dagger} T^{h^E} \operatorname{Tr}\Big(g^D g^{D\dagger} \Big) - 3 m_{H_1}^2 h^{E\dagger} h^E \operatorname{Tr}\Big(g^D g^{D\dagger} \Big) \\
&- 3 h^{E\dagger} h^E m_{H_1}^2 \operatorname{Tr}\Big(g^D g^{D\dagger} \Big) - 6 h^{E\dagger} m_{e^c}^2 h^E \operatorname{Tr}\Big(g^D g^{D\dagger} \Big) \\
&- 4 m_{L_4}^2 h^{E\dagger} h^E \operatorname{Tr}\Big(h^E h^{E\dagger} \Big) - 2 T^{h^E\dagger} T^{h^E} \operatorname{Tr}\Big(h^E h^{E\dagger} \Big)
\end{aligned}
$$

$$
\begin{aligned}
&- m_{H_1}^2 h^{E\dagger} h^E \operatorname{Tr}\Big(h^E h^{E\dagger}\Big) - h^{E\dagger} h^E m_{H_1}^2 \operatorname{Tr}\Big(h^E h^{E\dagger}\Big) \\
&- 2 h^{E\dagger} m_{e^c}^2 h^E \operatorname{Tr}\Big(h^E h^{E\dagger}\Big) - 12 m_{H_u}^2 \tilde{f}^\dagger \tilde{f} \operatorname{Tr}\Big(y^U y^{U\dagger}\Big) - 6 T^{\tilde{f}\dagger} T^{\tilde{f}} \operatorname{Tr}\Big(y^U y^{U\dagger}\Big) \\
&- 3 m_{H_1}^2 \tilde{f}^\dagger \tilde{f} \operatorname{Tr}\Big(y^U y^{U\dagger}\Big) - 3 \tilde{f}^\dagger \tilde{f} m_{H_1}^2 \operatorname{Tr}\Big(y^U y^{U\dagger}\Big) - 6 \tilde{f}^\dagger m_\Sigma^{2*} \tilde{f} \operatorname{Tr}\Big(y^U y^{U\dagger}\Big) \\
&- 12 m_S^2 \tilde{\lambda}^\dagger \tilde{\lambda} \operatorname{Tr}\Big(\kappa \kappa^\dagger\Big) - 6 T^{\tilde{\lambda}\dagger} T^{\tilde{\lambda}} \operatorname{Tr}\Big(\kappa \kappa^\dagger\Big) - 3 m_{H_1}^2 \tilde{\lambda}^\dagger \tilde{\lambda} \operatorname{Tr}\Big(\kappa \kappa^\dagger\Big) \\
&- 3 \tilde{\lambda}^\dagger \tilde{\lambda} m_{H_1}^2 \operatorname{Tr}\Big(\kappa \kappa^\dagger\Big) - 6 \tilde{\lambda}^\dagger m_{H_2}^{2*} \tilde{\lambda} \operatorname{Tr}\Big(\kappa \kappa^\dagger\Big) - 8 m_S^2 \tilde{\lambda}^\dagger \tilde{\lambda} \operatorname{Tr}\Big(\tilde{\lambda} \tilde{\lambda}^\dagger\Big) \\
&- 4 T^{\tilde{\lambda}\dagger} T^{\tilde{\lambda}} \operatorname{Tr}\Big(\tilde{\lambda} \tilde{\lambda}^\dagger\Big) - 2 m_{H_1}^2 \tilde{\lambda}^\dagger \tilde{\lambda} \operatorname{Tr}\Big(\tilde{\lambda} \tilde{\lambda}^\dagger\Big) - 2 \tilde{\lambda}^\dagger \tilde{\lambda} m_{H_1}^2 \operatorname{Tr}\Big(\tilde{\lambda} \tilde{\lambda}^\dagger\Big) \\
&- 4 \tilde{\lambda}^\dagger m_{H_2}^{2*} \tilde{\lambda} \operatorname{Tr}\Big(\tilde{\lambda} \tilde{\lambda}^\dagger\Big) - 2 T^{\tilde{f}\dagger} \tilde{f} \operatorname{Tr}\Big(\tilde{f}^\dagger T^{\tilde{f}}\Big) - 6 T^{h^E\dagger} h^E \operatorname{Tr}\Big(g^{D\dagger} T^{g^D}\Big) \\
&- 2 T^{h^E\dagger} h^E \operatorname{Tr}\Big(h^{E\dagger} T^{h^E}\Big) - 6 T^{\tilde{f}\dagger} \tilde{f} \operatorname{Tr}\Big(y^{U\dagger} T^U\Big) - 6 T^{\tilde{\lambda}\dagger} \tilde{\lambda} \operatorname{Tr}\Big(\kappa^\dagger T^\kappa\Big) \\
&- 4 T^{\tilde{\lambda}\dagger} \tilde{\lambda} \operatorname{Tr}\Big(\tilde{\lambda}^\dagger T^{\tilde{\lambda}}\Big) - 2 \tilde{f}^\dagger T^{\tilde{f}} \operatorname{Tr}\Big(T^{\tilde{f}*} \tilde{f}^T\Big) - 2 \tilde{f}^\dagger \tilde{f} \operatorname{Tr}\Big(T^{\tilde{f}*} T^{\tilde{f}T}\Big) \\
&- 6 h^{E\dagger} T^{h^E} \operatorname{Tr}\Big(T^{g^D *} g^{DT}\Big) - 6 h^{E\dagger} h^E \operatorname{Tr}\Big(T^{g^D *} T^{g^D T}\Big) \\
&- 2 h^{E\dagger} T^{h^E} \operatorname{Tr}\Big(T^{h^E *} h^{ET}\Big) - 2 h^{E\dagger} h^E \operatorname{Tr}\Big(T^{h^E *} T^{h^E T}\Big) \\
&- 6 \tilde{f}^\dagger T^{\tilde{f}} \operatorname{Tr}\Big(T^{U*} y^{UT}\Big) - 6 \tilde{f}^\dagger \tilde{f} \operatorname{Tr}\Big(T^{U*} T^{UT}\Big) - 6 \tilde{\lambda}^\dagger T^{\tilde{\lambda}} \operatorname{Tr}\Big(T^{\kappa *} \kappa^T\Big) \\
&- 6 \tilde{\lambda}^\dagger \tilde{\lambda} \operatorname{Tr}\Big(T^{\kappa *} T^{\kappa T}\Big) - 4 \tilde{\lambda}^\dagger T^{\tilde{\lambda}} \operatorname{Tr}\Big(T^{\tilde{\lambda}*} \tilde{\lambda}^T\Big) - 4 \tilde{\lambda}^\dagger \tilde{\lambda} \operatorname{Tr}\Big(T^{\tilde{\lambda}*} T^{\tilde{\lambda}T}\Big) \\
&- 2 \tilde{f}^\dagger \tilde{f} \operatorname{Tr}\Big(\tilde{f} m_{H_1}^2 \tilde{f}^\dagger\Big) - 2 \tilde{f}^\dagger \tilde{f} \operatorname{Tr}\Big(\tilde{f} \tilde{f}^\dagger m_\Sigma^{2*}\Big) - 6 h^{E\dagger} h^E \operatorname{Tr}\Big(g^D g^{D\dagger} m_Q^{2*}\Big) \\
&- 6 h^{E\dagger} h^E \operatorname{Tr}\Big(g^D m_{\bar{D}}^{2*} g^{D\dagger}\Big) - 2 h^{E\dagger} h^E \operatorname{Tr}\Big(h^E m_{H_1}^2 h^{E\dagger}\Big) \\
&- 2 h^{E\dagger} h^E \operatorname{Tr}\Big(h^E h^{E\dagger} m_{e^c}^2\Big) - 4 \tilde{\lambda}^\dagger \tilde{\lambda} \operatorname{Tr}\Big(m_{H_1}^2 \tilde{\lambda}^\dagger \tilde{\lambda}\Big) - 6 \tilde{f}^\dagger \tilde{f} \operatorname{Tr}\Big(m_Q^2 y^{U\dagger} y^U\Big) \\
&- 6 \tilde{f}^\dagger \tilde{f} \operatorname{Tr}\Big(m_{u^c}^2 y^U y^{U\dagger}\Big) - 6 \tilde{\lambda}^\dagger \tilde{\lambda} \operatorname{Tr}\Big(\kappa \kappa^\dagger m_D^{2*}\Big) - 6 \tilde{\lambda}^\dagger \tilde{\lambda} \operatorname{Tr}\Big(\kappa m_{\bar{D}}^{2*} \kappa^\dagger\Big) \\
&- 4 \tilde{\lambda}^\dagger \tilde{\lambda} \operatorname{Tr}\Big(\tilde{\lambda} \tilde{\lambda}^\dagger m_{H_2}^{2*}\Big), \qquad \text{(D.112)}
\end{aligned}
$$

$$
\begin{aligned}
\beta_{m_{H_2}^2}^{(1)} = &- \frac{6}{5} g_1^2 \mathbf{1} |M_1|^2 - \frac{4}{5} g_1'^2 \mathbf{1} |M_1'|^2 - 6 g_2^2 \mathbf{1} |M_2|^2 + 2 m_{H_d}^2 f^\dagger f + 2 T^{f\dagger} T^f \\
&+ 2 m_S^2 \tilde{\lambda}^* \tilde{\lambda}^T + 2 T^{\tilde{\lambda}*} T^{\tilde{\lambda}T} + m_{H_2}^2 f^\dagger f + m_{H_2}^2 \tilde{\lambda}^* \tilde{\lambda}^T + f^\dagger f m_{H_2}^2 + 2 f^\dagger m_\Sigma^{2*} f \\
&+ 2 \tilde{\lambda}^* m_{H_1}^{2*} \tilde{\lambda}^T + \tilde{\lambda}^* \tilde{\lambda}^T m_{H_2}^2 + \sqrt{\frac{3}{5}} g_1 \mathbf{1} \Sigma_{1,1} - \sqrt{\frac{2}{5}} g_1' \mathbf{1} \Sigma_{1,4}, \qquad \text{(D.113)}
\end{aligned}
$$

$$
\beta_{m_{H_2}^2}^{(2)} = \frac{18}{5} g_1^2 g_2^2 \mathbf{1} |M_2|^2 + \frac{12}{5} g_1'^2 g_2^2 \mathbf{1} |M_2|^2 + 87 g_2^4 \mathbf{1} |M_2|^2
$$

$$
\begin{aligned}
&+\frac{9}{25}g_1^2\Big[2g_1'^2\Big(2M_1+M_1'\Big)+5g_2^2\Big(2M_1+M_2\Big)+99g_1^2M_1\Big]\mathbf{1}M_1^*\\
&+\frac{9}{5}g_1^2g_2^2M_1\mathbf{1}M_2^*+\frac{6}{5}g_1'^2g_2^2M_1'\mathbf{1}M_2^*+3g_1'^2m_{H_d}^2f^\dagger f-4m_{H_d}^2|\lambda|^2f^\dagger f\\
&-2m_{H_u}^2|\lambda|^2f^\dagger f-2m_S^2|\lambda|^2f^\dagger f-2|T_\lambda|^2f^\dagger f-2\lambda T_\lambda^*f^\dagger T^f\\
&-3g_1'^2M_1'T^{f\dagger}f+3g_1'^2T^{f\dagger}T^f-2|\lambda|^2T^{f\dagger}T^f+3g_1'^2m_S^2\tilde\lambda^*\tilde\lambda^T\\
&-4m_{H_d}^2|\lambda|^2\tilde\lambda^*\tilde\lambda^T-4m_{H_u}^2|\lambda|^2\tilde\lambda^*\tilde\lambda^T-8m_S^2|\lambda|^2\tilde\lambda^*\tilde\lambda^T-2m_\phi^2|\sigma|^2\tilde\lambda^*\tilde\lambda^T\\
&-4m_S^2|\sigma|^2\tilde\lambda^*\tilde\lambda^T-2m_{\bar S}^2|\sigma|^2\tilde\lambda^*\tilde\lambda^T-4|T_\lambda|^2\tilde\lambda^*\tilde\lambda^T-2|T_\sigma|^2\tilde\lambda^*\tilde\lambda^T\\
&+\frac{3}{25}g_1'^2\Big\{\Big[10g_2^2\Big(2M_1'+M_2\Big)+217g_1'^2M_1'+6g_1^2\Big(2M_1'+M_1\Big)\Big]\mathbf{1}\\
&+25\Big(2M_1'f^\dagger f+2M_1'\tilde\lambda^*\tilde\lambda^T-f^\dagger T^f-\tilde\lambda^*T^{\tilde\lambda T}\Big)\Big\}M_1'^*-4\lambda T_\lambda^*\tilde\lambda^*T^{\tilde\lambda T}\\
&-2\sigma T_\sigma^*\tilde\lambda^*T^{\tilde\lambda T}-3g_1'^2M_1'T^{\tilde\lambda*}\tilde\lambda^T+3g_1'^2T^{\tilde\lambda*}T^{\tilde\lambda T}-4|\lambda|^2T^{\tilde\lambda*}T^{\tilde\lambda T}\\
&-2|\sigma|^2T^{\tilde\lambda*}T^{\tilde\lambda T}+\frac{3}{2}g_1'^2m_{H_2}^2f^\dagger f-|\lambda|^2m_{H_2}^2f^\dagger f+\frac{3}{2}g_1'^2m_{H_2}^2\tilde\lambda^*\tilde\lambda^T\\
&-2|\lambda|^2m_{H_2}^2\tilde\lambda^*\tilde\lambda^T-|\sigma|^2m_{H_2}^2\tilde\lambda^*\tilde\lambda^T+\frac{3}{2}g_1'^2f^\dagger fm_{H_2}^2-|\lambda|^2f^\dagger fm_{H_2}^2\\
&+3g_1'^2f^\dagger m_\Sigma^{2*}f-2|\lambda|^2f^\dagger m_\Sigma^{2*}f+3g_1'^2\tilde\lambda^*m_{H_1}^{2*}\tilde\lambda^T-4|\lambda|^2\tilde\lambda^*m_{H_1}^{2*}\tilde\lambda^T\\
&-2|\sigma|^2\tilde\lambda^*m_{H_1}^{2*}\tilde\lambda^T+\frac{3}{2}g_1'^2\tilde\lambda^*\tilde\lambda^Tm_{H_2}^2-2|\lambda|^2\tilde\lambda^*\tilde\lambda^Tm_{H_2}^2\\
&-|\sigma|^2\tilde\lambda^*\tilde\lambda^Tm_{H_2}^2-8m_{H_d}^2f^\dagger ff^\dagger f-4f^\dagger fT^{f\dagger}T^f-4m_{H_d}^2f^\dagger\tilde f\tilde f^\dagger f\\
&-4m_{H_u}^2f^\dagger\tilde f\tilde f^\dagger f-4f^\dagger\tilde fT^{\tilde f\dagger}T^f-4f^\dagger T^fT^{f\dagger}f-4f^\dagger T^{\tilde f}T^{\tilde f\dagger}f\\
&-4T^{f\dagger}ff^\dagger T^f-4T^{f\dagger}\tilde f\tilde f^\dagger T^f-4T^{f\dagger}T^ff^\dagger f-4T^{f\dagger}T^{\tilde f}\tilde f^\dagger f\\
&-2m_{H_u}^2\tilde\lambda^*\tilde f^T\tilde f^*\tilde\lambda^T-2m_S^2\tilde\lambda^*\tilde f^T\tilde f^*\tilde\lambda^T-2\tilde\lambda^*\tilde f^TT^{\tilde f*}T^{\tilde\lambda T}\\
&-2m_{L_4}^2\tilde\lambda^*h^{ET}h^{E*}\tilde\lambda^T-2m_S^2\tilde\lambda^*h^{ET}h^{E*}\tilde\lambda^T-2\tilde\lambda^*h^{ET}T^{h^E*}T^{\tilde\lambda T}\\
&-4m_S^2\tilde\lambda^*\tilde\lambda^T\tilde\lambda^*\tilde\lambda^T-2\tilde\lambda^*\tilde\lambda^TT^{\tilde\lambda*}T^{\tilde\lambda T}-2\tilde\lambda^*T^{\tilde fT}T^{\tilde f*}\tilde\lambda^T\\
&-2\tilde\lambda^*T^{h^ET}T^{h^E*}\tilde\lambda^T-2\tilde\lambda^*T^{\tilde\lambda T}T^{\tilde\lambda*}\tilde\lambda^T-2T^{\tilde\lambda*}\tilde f^T\tilde f^*T^{\tilde\lambda T}\\
&-2T^{\tilde\lambda*}h^{ET}h^{E*}T^{\tilde\lambda T}-2T^{\tilde\lambda*}\tilde\lambda^T\tilde\lambda^*T^{\tilde\lambda T}-2T^{\tilde\lambda*}T^{\tilde fT}\tilde f^*\tilde\lambda^T-2T^{\tilde\lambda*}T^{h^ET}h^{E*}\tilde\lambda^T\\
&-2T^{\tilde\lambda*}T^{\tilde\lambda T}\tilde\lambda^*\tilde\lambda^T-2m_{H_2}^2f^\dagger ff^\dagger f-2m_{H_2}^2f^\dagger\tilde f\tilde f^\dagger f-m_{H_2}^2\tilde\lambda^*\tilde f^T\tilde f^*\tilde\lambda^T\\
&-m_{H_2}^2\tilde\lambda^*h^{ET}h^{E*}\tilde\lambda^T-m_{H_2}^2\tilde\lambda^*\tilde\lambda^T\tilde\lambda^*\tilde\lambda^T-4f^\dagger fm_{H_2}^2f^\dagger f-2f^\dagger ff^\dagger fm_{H_2}^2\\
&-4f^\dagger ff^\dagger m_\Sigma^{2*}f-4f^\dagger\tilde fm_{H_1}^2\tilde f^\dagger f-2f^\dagger\tilde f\tilde f^\dagger fm_{H_2}^2-4f^\dagger\tilde f\tilde f^\dagger m_\Sigma^{2*}f\\
&-4f^\dagger m_\Sigma^{2*}ff^\dagger f-4f^\dagger m_\Sigma^{2*}\tilde f\tilde f^\dagger f-2\tilde\lambda^*m_{H_1}^{2*}\tilde f^T\tilde f^*\tilde\lambda^T\\
&-2\tilde\lambda^*m_{H_1}^{2*}h^{ET}h^{E*}\tilde\lambda^T-2\tilde\lambda^*m_{H_1}^{2*}\tilde\lambda^T\tilde\lambda^*\tilde\lambda^T-2\tilde\lambda^*\tilde f^Tm_\Sigma^2\tilde f^*\tilde\lambda^T\\
&-2\tilde\lambda^*\tilde f^T\tilde f^*m_{H_1}^{2*}\tilde\lambda^T-\tilde\lambda^*\tilde f^T\tilde f^*\tilde\lambda^Tm_{H_2}^2-2\tilde\lambda^*h^{ET}h^{E*}m_{H_1}^{2*}\tilde\lambda^T\\
&-\tilde\lambda^*h^{ET}h^{E*}\tilde\lambda^Tm_{H_2}^2-2\tilde\lambda^*h^{ET}m_{e^c}^{2*}h^{E*}\tilde\lambda^T-2\tilde\lambda^*\tilde\lambda^Tm_{H_2}^2\tilde\lambda^*\tilde\lambda^T
\end{aligned}
$$

$$
\begin{aligned}
&- 2\tilde{\lambda}^*\tilde{\lambda}^T\tilde{\lambda}^* m^{2*}_{H_1}\tilde{\lambda}^T - \tilde{\lambda}^*\tilde{\lambda}^T\tilde{\lambda}^*\tilde{\lambda}^T m^2_{H_2} - 2\lambda^* T^{f\dagger} f T_\lambda - 4\lambda^* T^{\tilde{\lambda}*}\tilde{\lambda}^T T_\lambda \\
&- 2\sigma^* T^{\tilde{\lambda}*}\tilde{\lambda}^T T_\sigma + 6g_2^4\mathbf{1}\Sigma_{2,2} + \frac{6}{5}g_1^2\mathbf{1}\Sigma_{2,11} - \frac{2}{5}\sqrt{6}g_1 g_1'\mathbf{1}\Sigma_{2,14} \\
&- \frac{2}{5}\sqrt{6}g_1 g_1'\mathbf{1}\Sigma_{2,41} + \frac{4}{5}g_1'^2\mathbf{1}\Sigma_{2,44} + 4\sqrt{\frac{3}{5}}g_1\mathbf{1}\Sigma_{3,1} - 4\sqrt{\frac{2}{5}}g_1'\mathbf{1}\Sigma_{3,4} \\
&- 4m^2_{H_d} f^\dagger f \,\mathrm{Tr}\Big(ff^\dagger\Big) - 2T^{f\dagger}T^f \,\mathrm{Tr}\Big(ff^\dagger\Big) - m^2_{H_2} f^\dagger f \,\mathrm{Tr}\Big(ff^\dagger\Big) \\
&- f^\dagger f m^2_{H_2} \,\mathrm{Tr}\Big(ff^\dagger\Big) - 2f^\dagger m^{2*}_\Sigma f \,\mathrm{Tr}\Big(ff^\dagger\Big) - 12m^2_{H_d} f^\dagger f \,\mathrm{Tr}\Big(y^D y^{D\dagger}\Big) \\
&- 6T^{f\dagger}T^f \,\mathrm{Tr}\Big(y^D y^{D\dagger}\Big) - 3m^2_{H_2} f^\dagger f \,\mathrm{Tr}\Big(y^D y^{D\dagger}\Big) - 3f^\dagger f m^2_{H_2} \,\mathrm{Tr}\Big(y^D y^{D\dagger}\Big) \\
&- 6f^\dagger m^{2*}_\Sigma f \,\mathrm{Tr}\Big(y^D y^{D\dagger}\Big) - 4m^2_{H_d} f^\dagger f \,\mathrm{Tr}\Big(y^E y^{E\dagger}\Big) - 2T^{f\dagger}T^f \,\mathrm{Tr}\Big(y^E y^{E\dagger}\Big) \\
&- m^2_{H_2} f^\dagger f \,\mathrm{Tr}\Big(y^E y^{E\dagger}\Big) - f^\dagger f m^2_{H_2} \,\mathrm{Tr}\Big(y^E y^{E\dagger}\Big) - 2f^\dagger m^{2*}_\Sigma f \,\mathrm{Tr}\Big(y^E y^{E\dagger}\Big) \\
&- 12m^2_S \tilde{\lambda}^*\tilde{\lambda}^T \,\mathrm{Tr}\Big(\kappa\kappa^\dagger\Big) - 6T^{\tilde{\lambda}*}T^{\tilde{\lambda}T} \,\mathrm{Tr}\Big(\kappa\kappa^\dagger\Big) - 3m^2_{H_2}\tilde{\lambda}^*\tilde{\lambda}^T \,\mathrm{Tr}\Big(\kappa\kappa^\dagger\Big) \\
&- 6\tilde{\lambda}^* m^{2*}_{H_1}\tilde{\lambda}^T \,\mathrm{Tr}\Big(\kappa\kappa^\dagger\Big) - 3\tilde{\lambda}^*\tilde{\lambda}^T m^2_{H_2} \,\mathrm{Tr}\Big(\kappa\kappa^\dagger\Big) - 8m^2_S\tilde{\lambda}^*\tilde{\lambda}^T \,\mathrm{Tr}\Big(\tilde{\lambda}\tilde{\lambda}^\dagger\Big) \\
&- 4T^{\tilde{\lambda}*}T^{\tilde{\lambda}T} \,\mathrm{Tr}\Big(\tilde{\lambda}\tilde{\lambda}^\dagger\Big) - 2m^2_{H_2}\tilde{\lambda}^*\tilde{\lambda}^T \,\mathrm{Tr}\Big(\tilde{\lambda}\tilde{\lambda}^\dagger\Big) - 4\tilde{\lambda}^* m^{2*}_{H_1}\tilde{\lambda}^T \,\mathrm{Tr}\Big(\tilde{\lambda}\tilde{\lambda}^\dagger\Big) \\
&- 2\tilde{\lambda}^*\tilde{\lambda}^T m^2_{H_2} \,\mathrm{Tr}\Big(\tilde{\lambda}\tilde{\lambda}^\dagger\Big) - 2T^{f\dagger} f \,\mathrm{Tr}\Big(f^\dagger T^f\Big) - 6T^{f\dagger} f \,\mathrm{Tr}\Big(y^{D\dagger}T^D\Big) \\
&- 2T^{f\dagger} f \,\mathrm{Tr}\Big(y^{E\dagger}T^E\Big) - 6T^{\tilde{\lambda}*}\tilde{\lambda}^T \,\mathrm{Tr}\Big(\kappa^\dagger T^\kappa\Big) - 4T^{\tilde{\lambda}*}\tilde{\lambda}^T \,\mathrm{Tr}\Big(\tilde{\lambda}^\dagger T^{\tilde{\lambda}}\Big) \\
&- 2f^\dagger T^f \,\mathrm{Tr}\Big(T^{f*}f^T\Big) - 2f^\dagger f \,\mathrm{Tr}\Big(T^{f*}T^{fT}\Big) - 6f^\dagger T^f \,\mathrm{Tr}\Big(T^{D*}y^{DT}\Big) \\
&- 6f^\dagger f \,\mathrm{Tr}\Big(T^{D*}T^{DT}\Big) - 2f^\dagger T^f \,\mathrm{Tr}\Big(T^{E*}y^{ET}\Big) - 2f^\dagger f \,\mathrm{Tr}\Big(T^{E*}T^{ET}\Big) \\
&- 6\tilde{\lambda}^* T^{\tilde{\lambda}T} \,\mathrm{Tr}\Big(T^{\kappa*}\kappa^T\Big) - 6\tilde{\lambda}^*\tilde{\lambda}^T \,\mathrm{Tr}\Big(T^{\kappa*}T^{\kappa T}\Big) - 4\tilde{\lambda}^* T^{\tilde{\lambda}T} \,\mathrm{Tr}\Big(T^{\tilde{\lambda}*}\tilde{\lambda}^T\Big) \\
&- 4\tilde{\lambda}^*\tilde{\lambda}^T \,\mathrm{Tr}\Big(T^{\tilde{\lambda}*}T^{\tilde{\lambda}T}\Big) - 2f^\dagger f \,\mathrm{Tr}\Big(f m^2_{H_2} f^\dagger\Big) - 2f^\dagger f \,\mathrm{Tr}\Big(ff^\dagger m^{2*}_\Sigma\Big) \\
&- 6f^\dagger f \,\mathrm{Tr}\Big(m^2_{d^c} y^D y^{D\dagger}\Big) - 2f^\dagger f \,\mathrm{Tr}\Big(m^2_{e^c} y^E y^{E\dagger}\Big) - 4\tilde{\lambda}^*\tilde{\lambda}^T \,\mathrm{Tr}\Big(m^2_{H_1}\tilde{\lambda}^\dagger\tilde{\lambda}\Big) \\
&- 2f^\dagger f \,\mathrm{Tr}\Big(m^2_L y^{E\dagger} y^E\Big) - 6f^\dagger f \,\mathrm{Tr}\Big(m^2_Q y^{D\dagger} y^D\Big) - 6\tilde{\lambda}^*\tilde{\lambda}^T \,\mathrm{Tr}\Big(\kappa\kappa^\dagger m^{2*}_D\Big) \\
&- 6\tilde{\lambda}^*\tilde{\lambda}^T \,\mathrm{Tr}\Big(\kappa m^{2*}_{\bar{D}}\kappa^\dagger\Big) - 4\tilde{\lambda}^*\tilde{\lambda}^T \,\mathrm{Tr}\Big(\tilde{\lambda}\tilde{\lambda}^\dagger m^{2*}_{H_2}\Big)\,, \qquad \text{(D.114)}
\end{aligned}
$$

$$
\begin{aligned}
\beta^{(1)}_{m^2_\Sigma} = &-5g_1'^2\mathbf{1}|M_1'|^2 + 2\Big(2m^2_{H_d} f^* f^T + 2m^2_{H_u}\tilde{f}^*\tilde{f}^T + 2T^{f*}T^{fT} + 2T^{\tilde{f}*}T^{\tilde{f}T} \\
&+ m^2_\Sigma f^* f^T + m^2_\Sigma\tilde{f}^*\tilde{f}^T + 2f^* m^{2*}_{H_2} f^T + f^* f^T m^2_\Sigma + 2\tilde{f}^* m^{2*}_{H_1}\tilde{f}^T \\
&+ \tilde{f}^*\tilde{f}^T m^2_\Sigma\Big) + \sqrt{\frac{5}{2}}g_1'\mathbf{1}\Sigma_{1,4}\,, \qquad \text{(D.115)}
\end{aligned}
$$

$$
\begin{aligned}
\beta^{(2)}_{m^2_\Sigma} = {} & \frac{12}{5}g_1^2 m_{H_d}^2 f^* f^T - \frac{12}{5}g_1'^2 m_{H_d}^2 f^* f^T + 12 g_2^2 m_{H_d}^2 f^* f^T + \frac{24}{5}g_1^2 |M_1|^2 f^* f^T \\
& + 24 g_2^2 |M_2|^2 f^* f^T - 8 m_{H_d}^2 |\lambda|^2 f^* f^T - 4 m_{H_u}^2 |\lambda|^2 f^* f^T - 4 m_S^2 |\lambda|^2 f^* f^T \\
& - 4|T_\lambda|^2 f^* f^T - \frac{12}{5}g_1^2 M_1^* f^* T^{fT} - 12 g_2^2 M_2^* f^* T^{fT} - 4\lambda T_\lambda^* f^* T^{fT} \\
& + \frac{12}{5}g_1^2 m_{H_u}^2 \tilde{f}^* \tilde{f}^T - \frac{12}{5}g_1'^2 m_{H_u}^2 \tilde{f}^* \tilde{f}^T + 12 g_2^2 m_{H_u}^2 \tilde{f}^* \tilde{f}^T + \frac{24}{5}g_1^2 |M_1|^2 \tilde{f}^* \tilde{f}^T \\
& + 24 g_2^2 |M_2|^2 \tilde{f}^* \tilde{f}^T - 4 m_{H_d}^2 |\lambda|^2 \tilde{f}^* \tilde{f}^T - 8 m_{H_u}^2 |\lambda|^2 \tilde{f}^* \tilde{f}^T - 4 m_S^2 |\lambda|^2 \tilde{f}^* \tilde{f}^T \\
& - 4|T_\lambda|^2 \tilde{f}^* \tilde{f}^T - \frac{12}{5}g_1^2 M_1^* \tilde{f}^* T^{\tilde{f}T} - 12 g_2^2 M_2^* \tilde{f}^* T^{\tilde{f}T} - 4\lambda T_\lambda^* \tilde{f}^* T^{\tilde{f}T} \\
& + \frac{3}{10}g_1'^2 \Big[595 g_1'^2 M_1' \mathbf{1} + 8 \Big(-2 M_1' f^* f^T - 2 M_1' \tilde{f}^* \tilde{f}^T + f^* T^{fT} \\
& + \tilde{f}^* T^{\tilde{f}T} \Big) \Big] M_1'^* - \frac{12}{5}g_1^2 M_1 T^{f*} f^T + \frac{12}{5}g_1'^2 M_1' T^{f*} f^T - 12 g_2^2 M_2 T^{f*} f^T \\
& + \frac{12}{5}g_1^2 T^{f*} T^{fT} - \frac{12}{5}g_1'^2 T^{f*} T^{fT} + 12 g_2^2 T^{f*} T^{fT} - 4|\lambda|^2 T^{f*} T^{fT} \\
& - \frac{12}{5}g_1^2 M_1 T^{\tilde{f}*} \tilde{f}^T + \frac{12}{5}g_1'^2 M_1' T^{\tilde{f}*} \tilde{f}^T - 12 g_2^2 M_2 T^{\tilde{f}*} \tilde{f}^T + \frac{12}{5}g_1^2 T^{\tilde{f}*} T^{\tilde{f}T} \\
& - \frac{12}{5}g_1'^2 T^{\tilde{f}*} T^{\tilde{f}T} + 12 g_2^2 T^{\tilde{f}*} T^{\tilde{f}T} - 4|\lambda|^2 T^{\tilde{f}*} T^{\tilde{f}T} + \frac{6}{5}g_1^2 m_\Sigma^2 f^* f^T \\
& - \frac{6}{5}g_1'^2 m_\Sigma^2 f^* f^T + 6 g_2^2 m_\Sigma^2 f^* f^T - 2|\lambda|^2 m_\Sigma^2 f^* f^T + \frac{6}{5}g_1^2 m_\Sigma^2 \tilde{f}^* \tilde{f}^T \\
& - \frac{6}{5}g_1'^2 m_\Sigma^2 \tilde{f}^* \tilde{f}^T + 6 g_2^2 m_\Sigma^2 \tilde{f}^* \tilde{f}^T - 2|\lambda|^2 m_\Sigma^2 \tilde{f}^* \tilde{f}^T + \frac{12}{5}g_1^2 f^* m_{H_2}^{2*} f^T \\
& - \frac{12}{5}g_1'^2 f^* m_{H_2}^{2*} f^T + 12 g_2^2 f^* m_{H_2}^{2*} f^T - 4|\lambda|^2 f^* m_{H_2}^{2*} f^T + \frac{6}{5}g_1^2 f^* f^T m_\Sigma^2 \\
& - \frac{6}{5}g_1'^2 f^* f^T m_\Sigma^2 + 6 g_2^2 f^* f^T m_\Sigma^2 - 2|\lambda|^2 f^* f^T m_\Sigma^2 + \frac{12}{5}g_1^2 \tilde{f}^* m_{H_1}^{2*} \tilde{f}^T \\
& - \frac{12}{5}g_1'^2 \tilde{f}^* m_{H_1}^{2*} \tilde{f}^T + 12 g_2^2 \tilde{f}^* m_{H_1}^{2*} \tilde{f}^T - 4|\lambda|^2 \tilde{f}^* m_{H_1}^{2*} \tilde{f}^T + \frac{6}{5}g_1^2 \tilde{f}^* \tilde{f}^T m_\Sigma^2 \\
& - \frac{6}{5}g_1'^2 \tilde{f}^* \tilde{f}^T m_\Sigma^2 + 6 g_2^2 \tilde{f}^* \tilde{f}^T m_\Sigma^2 - 2|\lambda|^2 \tilde{f}^* \tilde{f}^T m_\Sigma^2 - 4 m_{H_d}^2 f^* \tilde{\lambda} \tilde{\lambda}^\dagger f^T \\
& - 4 m_S^2 f^* \tilde{\lambda} \tilde{\lambda}^\dagger f^T - 4 f^* \tilde{\lambda} T^{\tilde{\lambda}\dagger} T^{fT} - 4 f^* T^{\tilde{\lambda}} T^{\tilde{\lambda}\dagger} f^T - 8 m_{H_d}^2 f^* f^T f^* f^T \\
& - 4 f^* f^T T^{f*} T^{fT} - 4 f^* T^{fT} T^{f*} f^T - 8 m_{H_u}^2 \tilde{f}^* \tilde{f}^T \tilde{f}^* \tilde{f}^T - 4 \tilde{f}^* \tilde{f}^T T^{\tilde{f}*} T^{\tilde{f}T} \\
& - 4 m_{L_4}^2 \tilde{f}^* h^{ET} h^{E*} \tilde{f}^T - 4 m_{H_u}^2 \tilde{f}^* h^{ET} h^{E*} \tilde{f}^T - 4 \tilde{f}^* h^{ET} T^{h^E *} T^{\tilde{f}T} \\
& - 4 m_{H_u}^2 \tilde{f}^* \tilde{\lambda}^T \tilde{\lambda}^* \tilde{f}^T - 4 m_S^2 \tilde{f}^* \tilde{\lambda}^T \tilde{\lambda}^* \tilde{f}^T - 4 \tilde{f}^* \tilde{\lambda}^T T^{\tilde{\lambda}*} T^{\tilde{f}T} - 4 \tilde{f}^* T^{\tilde{f}T} T^{\tilde{f}*} \tilde{f}^T \\
& - 4 \tilde{f}^* T^{h^E T} T^{h^E *} \tilde{f}^T - 4 \tilde{f}^* T^{\tilde{\lambda}T} T^{\tilde{\lambda}*} \tilde{f}^T - 4 T^{f*} \tilde{\lambda} \tilde{\lambda}^\dagger T^{fT} - 4 T^{f*} T^{\tilde{\lambda}} \tilde{\lambda}^\dagger f^T \\
& - 4 T^{f*} f^T f^* T^{fT} - 4 T^{f*} T^{fT} f^* f^T - 4 T^{\tilde{f}*} \tilde{f}^T \tilde{f}^* T^{\tilde{f}T} - 4 T^{\tilde{f}*} h^{ET} h^{E*} T^{\tilde{f}T} \\
& - 4 T^{\tilde{f}*} \tilde{\lambda}^T \tilde{\lambda}^* T^{\tilde{f}T} - 4 T^{\tilde{f}*} T^{\tilde{f}T} \tilde{f}^* \tilde{f}^T - 4 T^{\tilde{f}*} T^{h^E T} h^{E*} \tilde{f}^T - 4 T^{\tilde{f}*} T^{\tilde{\lambda}T} \tilde{\lambda}^* \tilde{f}^T \\
& - 2 m_\Sigma^2 f^* \tilde{\lambda} \tilde{\lambda}^\dagger f^T - 2 m_\Sigma^2 f^* f^T f^* f^T - 2 m_\Sigma^2 \tilde{f}^* \tilde{f}^T \tilde{f}^* \tilde{f}^T - 2 m_\Sigma^2 \tilde{f}^* h^{ET} h^{E*} \tilde{f}^T
\end{aligned}
$$

$$
\begin{aligned}
&- 2m_{\Sigma}^2 \tilde{f}^* \tilde{\lambda}^T \tilde{\lambda}^* \tilde{f}^T - 4f^* \tilde{\lambda} m_{H_1}^2 \tilde{\lambda}^\dagger f^T - 4f^* \tilde{\lambda} \tilde{\lambda}^\dagger m_{H_2}^{2*} f^T - 2f^* \tilde{\lambda} \tilde{\lambda}^\dagger f^T m_{\Sigma}^2 \\
&- 4f^* m_{H_2}^{2*} \tilde{\lambda} \tilde{\lambda}^\dagger f^T - 4f^* m_{H_2}^{2*} f^T f^* f^T - 4f^* f^T m_{\Sigma}^2 f^* f^T - 4f^* f^T f^* m_{H_2}^{2*} f^T \\
&- 2f^* f^T f^* f^T m_{\Sigma}^2 - 4\tilde{f}^* m_{H_1}^{2*} \tilde{f}^T \tilde{f}^* \tilde{f}^T - 4\tilde{f}^* m_{H_1}^{2*} h^{ET} h^{E*} \tilde{f}^T \\
&- 4\tilde{f}^* m_{H_1}^{2*} \tilde{\lambda}^T \tilde{\lambda}^* \tilde{f}^T - 4\tilde{f}^* \tilde{f}^T m_{\Sigma}^2 \tilde{f}^* \tilde{f}^T - 4\tilde{f}^* \tilde{f}^T \tilde{f}^* m_{H_1}^{2*} \tilde{f}^T \\
&- 2\tilde{f}^* \tilde{f}^T \tilde{f}^* \tilde{f}^T m_{\Sigma}^2 - 4\tilde{f}^* h^{ET} h^{E*} m_{H_1}^{2*} \tilde{f}^T - 2\tilde{f}^* h^{ET} h^{E*} \tilde{f}^T m_{\Sigma}^2 \\
&- 4\tilde{f}^* h^{ET} m_{e^c}^{2*} h^{E*} \tilde{f}^T - 4\tilde{f}^* \tilde{\lambda}^T m_{H_2}^2 \tilde{\lambda}^* \tilde{f}^T - 4\tilde{f}^* \tilde{\lambda}^T \tilde{\lambda}^* m_{H_1}^{2*} \tilde{f}^T \\
&- 2\tilde{f}^* \tilde{\lambda}^T \tilde{\lambda}^* \tilde{f}^T m_{\Sigma}^2 - 4\lambda^* T^{f*} f^T T_\lambda - 4\lambda^* T^{\tilde{f}*} \tilde{f}^T T_\lambda + g_1' \mathbf{1} \Big(2\sqrt{10} \Sigma_{3,4} \\
&+ 5g_1' \Sigma_{2,44} \Big) - 8m_{H_d}^2 f^* f^T \operatorname{Tr}\Big(f f^\dagger \Big) - 4T^{f*} T^{fT} \operatorname{Tr}\Big(f f^\dagger \Big) \\
&- 2m_{\Sigma}^2 f^* f^T \operatorname{Tr}\Big(f f^\dagger \Big) - 4f^* m_{H_2}^{2*} f^T \operatorname{Tr}\Big(f f^\dagger \Big) - 2f^* f^T m_{\Sigma}^2 \operatorname{Tr}\Big(f f^\dagger \Big) \\
&- 8m_{H_u}^2 \tilde{f}^* \tilde{f}^T \operatorname{Tr}\Big(\tilde{f} \tilde{f}^\dagger \Big) - 4T^{\tilde{f}*} T^{\tilde{f}T} \operatorname{Tr}\Big(\tilde{f} \tilde{f}^\dagger \Big) - 2m_{\Sigma}^2 \tilde{f}^* \tilde{f}^T \operatorname{Tr}\Big(\tilde{f} \tilde{f}^\dagger \Big) \\
&- 4\tilde{f}^* m_{H_1}^{2*} \tilde{f}^T \operatorname{Tr}\Big(\tilde{f} \tilde{f}^\dagger \Big) - 2\tilde{f}^* \tilde{f}^T m_{\Sigma}^2 \operatorname{Tr}\Big(\tilde{f} \tilde{f}^\dagger \Big) - 24m_{H_d}^2 f^* f^T \operatorname{Tr}\Big(y^D y^{D\dagger} \Big) \\
&- 12T^{f*} T^{fT} \operatorname{Tr}\Big(y^D y^{D\dagger} \Big) - 6m_{\Sigma}^2 f^* f^T \operatorname{Tr}\Big(y^D y^{D\dagger} \Big) - 12f^* m_{H_2}^{2*} f^T \operatorname{Tr}\Big(y^D y^{D\dagger} \Big) \\
&- 6f^* f^T m_{\Sigma}^2 \operatorname{Tr}\Big(y^D y^{D\dagger} \Big) - 8m_{H_d}^2 f^* f^T \operatorname{Tr}\Big(y^E y^{E\dagger} \Big) - 4T^{f*} T^{fT} \operatorname{Tr}\Big(y^E y^{E\dagger} \Big) \\
&- 2m_{\Sigma}^2 f^* f^T \operatorname{Tr}\Big(y^E y^{E\dagger} \Big) - 4f^* m_{H_2}^{2*} f^T \operatorname{Tr}\Big(y^E y^{E\dagger} \Big) - 2f^* f^T m_{\Sigma}^2 \operatorname{Tr}\Big(y^E y^{E\dagger} \Big) \\
&- 24m_{H_u}^2 \tilde{f}^* \tilde{f}^T \operatorname{Tr}\Big(y^U y^{U\dagger} \Big) - 12T^{\tilde{f}*} T^{\tilde{f}T} \operatorname{Tr}\Big(y^U y^{U\dagger} \Big) - 6m_{\Sigma}^2 \tilde{f}^* \tilde{f}^T \operatorname{Tr}\Big(y^U y^{U\dagger} \Big) \\
&- 12\tilde{f}^* m_{H_1}^{2*} \tilde{f}^T \operatorname{Tr}\Big(y^U y^{U\dagger} \Big) - 6\tilde{f}^* \tilde{f}^T m_{\Sigma}^2 \operatorname{Tr}\Big(y^U y^{U\dagger} \Big) - 4T^{f*} f^T \operatorname{Tr}\Big(f^\dagger T^f \Big) \\
&- 4T^{\tilde{f}*} \tilde{f}^T \operatorname{Tr}\Big(\tilde{f}^\dagger T^{\tilde{f}} \Big) - 12T^{f*} f^T \operatorname{Tr}\Big(y^{D\dagger} T^D \Big) - 4T^{f*} f^T \operatorname{Tr}\Big(y^{E\dagger} T^E \Big) \\
&- 12T^{\tilde{f}*} \tilde{f}^T \operatorname{Tr}\Big(y^{U\dagger} T^U \Big) - 4f^* T^{fT} \operatorname{Tr}\Big(T^{f*} f^T \Big) - 4f^* f^T \operatorname{Tr}\Big(T^{f*} T^{fT} \Big) \\
&- 4\tilde{f}^* T^{\tilde{f}T} \operatorname{Tr}\Big(T^{\tilde{f}*} \tilde{f}^T \Big) - 4\tilde{f}^* \tilde{f}^T \operatorname{Tr}\Big(T^{\tilde{f}*} T^{\tilde{f}T} \Big) - 12f^* T^{fT} \operatorname{Tr}\Big(T^{D*} y^{DT} \Big) \\
&- 12f^* f^T \operatorname{Tr}\Big(T^{D*} T^{DT} \Big) - 4f^* T^{fT} \operatorname{Tr}\Big(T^{E*} y^{ET} \Big) - 4f^* f^T \operatorname{Tr}\Big(T^{E*} T^{ET} \Big) \\
&- 12\tilde{f}^* T^{\tilde{f}T} \operatorname{Tr}\Big(T^{U*} y^{UT} \Big) - 12\tilde{f}^* \tilde{f}^T \operatorname{Tr}\Big(T^{U*} T^{UT} \Big) - 4f^* f^T \operatorname{Tr}\Big(f m_{H_2}^2 f^\dagger \Big) \\
&- 4f^* f^T \operatorname{Tr}\Big(f f^\dagger m_{\Sigma}^{2*} \Big) - 4\tilde{f}^* \tilde{f}^T \operatorname{Tr}\Big(\tilde{f} m_{H_1}^2 \tilde{f}^\dagger \Big) - 4\tilde{f}^* \tilde{f}^T \operatorname{Tr}\Big(\tilde{f} \tilde{f}^\dagger m_{\Sigma}^{2*} \Big) \\
&- 12f^* f^T \operatorname{Tr}\Big(m_{d^c}^2 y^D y^{D\dagger} \Big) - 4f^* f^T \operatorname{Tr}\Big(m_{e^c}^2 y^E y^{E\dagger} \Big) \\
&- 4f^* f^T \operatorname{Tr}\Big(m_L^2 y^{E\dagger} y^E \Big) - 12f^* f^T \operatorname{Tr}\Big(m_Q^2 y^{D\dagger} y^D \Big)
\end{aligned}
$$

$$- 12\tilde{f}^* \tilde{f}^T \operatorname{Tr}\Big(m_Q^2 y^{U\dagger} y^U\Big) - 12\tilde{f}^* \tilde{f}^T \operatorname{Tr}\Big(m_{u^c}^2 y^U y^{U\dagger}\Big)\,, \tag{D.116}$$

$$\begin{aligned}
\beta^{(1)}_{m_D^2} =& -\frac{8}{15} g_1^2 \mathbf{1} |M_1|^2 - \frac{4}{5} g_1'^2 \mathbf{1} |M_1'|^2 - \frac{32}{3} g_3^2 \mathbf{1} |M_3|^2 + 2 m_S^2 \kappa^* \kappa^T + 2 T^{\kappa *} T^{\kappa T} \\
&+ m_D^2 \kappa^* \kappa^T + 2 \kappa^* m_{\bar{D}}^2 \kappa^T + \kappa^* \kappa^T m_D^2 - \frac{2}{\sqrt{15}} g_1 \mathbf{1} \Sigma_{1,1} - \sqrt{\frac{2}{5}} g_1' \mathbf{1} \Sigma_{1,4}\,,
\end{aligned} \tag{D.117}$$

$$\begin{aligned}
\beta^{(2)}_{m_D^2} =& \frac{128}{45} g_1^2 g_3^2 \mathbf{1} |M_3|^2 + \frac{64}{15} g_1'^2 g_3^2 \mathbf{1} |M_3|^2 + \frac{160}{3} g_3^4 \mathbf{1} |M_3|^2 \\
&+ \frac{16}{225} g_1^2 \Big[20 g_3^2 \Big(2M_1 + M_3 \Big) + 219 g_1^2 M_1 - 3 g_1'^2 \Big(2M_1 + M_1' \Big) \Big] \mathbf{1} M_1^* \\
&+ \frac{64}{45} g_1^2 g_3^2 M_1 \mathbf{1} M_3^* + \frac{32}{15} g_1'^2 g_3^2 M_1' \mathbf{1} M_3^* + 3 g_1'^2 m_S^2 \kappa^* \kappa^T - 4 m_{H_d}^2 |\lambda|^2 \kappa^* \kappa^T \\
&- 4 m_{H_u}^2 |\lambda|^2 \kappa^* \kappa^T - 8 m_S^2 |\lambda|^2 \kappa^* \kappa^T - 2 m_\phi^2 |\sigma|^2 \kappa^* \kappa^T - 4 m_S^2 |\sigma|^2 \kappa^* \kappa^T \\
&- 2 m_{\bar{S}}^2 |\sigma|^2 \kappa^* \kappa^T - 4 |T_\lambda|^2 \kappa^* \kappa^T - 2 |T_\sigma|^2 \kappa^* \kappa^T \\
&+ \frac{1}{75} g_1'^2 \Big\{ \Big[160 g_3^2 \Big(2M_1' + M_3 \Big) - 16 g_1^2 \Big(2M_1' + M_1 \Big) + 1953 g_1'^2 M_1' \Big] \mathbf{1} \\
&+ 225 \Big(2M_1' \kappa^* \kappa^T - \kappa^* T^{\kappa T} \Big) \Big\} M_1'^* - 4 \lambda T_\lambda^* \kappa^* T^{\kappa T} - 2 \sigma T_\sigma^* \kappa^* T^{\kappa T} \\
&- 3 g_1'^2 M_1' T^{\kappa *} \kappa^T + 3 g_1'^2 T^{\kappa *} T^{\kappa T} - 4 |\lambda|^2 T^{\kappa *} T^{\kappa T} - 2 |\sigma|^2 T^{\kappa *} T^{\kappa T} \\
&+ \frac{3}{2} g_1'^2 m_D^2 \kappa^* \kappa^T - 2 |\lambda|^2 m_D^2 \kappa^* \kappa^T - |\sigma|^2 m_D^2 \kappa^* \kappa^T + 3 g_1'^2 \kappa^* m_{\bar{D}}^2 \kappa^T \\
&- 4 |\lambda|^2 \kappa^* m_{\bar{D}}^2 \kappa^T - 2 |\sigma|^2 \kappa^* m_{\bar{D}}^2 \kappa^T + \frac{3}{2} g_1'^2 \kappa^* \kappa^T m_D^2 - 2 |\lambda|^2 \kappa^* \kappa^T m_D^2 \\
&- |\sigma|^2 \kappa^* \kappa^T m_D^2 - 4 m_{L_4}^2 \kappa^* g^{DT} g^{D*} \kappa^T - 4 m_S^2 \kappa^* g^{DT} g^{D*} \kappa^T \\
&- 4 \kappa^* g^{DT} T^{g^D *} T^{\kappa T} - 4 m_S^2 \kappa^* \kappa^T \kappa^* \kappa^T - 2 \kappa^* \kappa^T T^{\kappa *} T^{\kappa T} \\
&- 4 \kappa^* T^{g^D T} T^{g^D *} \kappa^T - 2 \kappa^* T^{\kappa T} T^{\kappa *} \kappa^T - 4 T^{\kappa *} g^{DT} g^{D*} T^{\kappa T} \\
&- 2 T^{\kappa *} \kappa^T \kappa^* T^{\kappa T} - 4 T^{\kappa *} T^{g^D T} g^{D*} \kappa^T - 2 T^{\kappa *} T^{\kappa T} \kappa^* \kappa^T \\
&- 2 m_D^2 \kappa^* g^{DT} g^{D*} \kappa^T - m_D^2 \kappa^* \kappa^T \kappa^* \kappa^T - 4 \kappa^* m_{\bar{D}}^2 g^{DT} g^{D*} \kappa^T \\
&- 2 \kappa^* m_{\bar{D}}^2 \kappa^T \kappa^* \kappa^T - 4 \kappa^* g^{DT} m_Q^2 g^{D*} \kappa^T - 4 \kappa^* g^{DT} g^{D*} m_{\bar{D}}^2 \kappa^T \\
&- 2 \kappa^* g^{DT} g^{D*} \kappa^T m_D^2 - 2 \kappa^* \kappa^T m_D^2 \kappa^* \kappa^T - 2 \kappa^* \kappa^T \kappa^* m_{\bar{D}}^2 \kappa^T \\
&- \kappa^* \kappa^T \kappa^* \kappa^T m_D^2 - 4 \lambda^* T^{\kappa *} \kappa^T T_\lambda - 2 \sigma^* T^{\kappa *} \kappa^T T_\sigma + \frac{32}{3} g_3^4 \mathbf{1} \Sigma_{2,3} \\
&+ \frac{8}{15} g_1^2 \mathbf{1} \Sigma_{2,11} + \frac{4}{5} \sqrt{\frac{2}{3}} g_1 g_1' \mathbf{1} \Sigma_{2,14} + \frac{4}{5} \sqrt{\frac{2}{3}} g_1 g_1' \mathbf{1} \Sigma_{2,41} + \frac{4}{5} g_1'^2 \mathbf{1} \Sigma_{2,44} \\
&- \frac{8}{\sqrt{15}} g_1 \mathbf{1} \Sigma_{3,1} - 4 \sqrt{\frac{2}{5}} g_1' \mathbf{1} \Sigma_{3,4} - 12 m_S^2 \kappa^* \kappa^T \operatorname{Tr}\Big(\kappa \kappa^\dagger \Big) \\
&- 6 T^{\kappa *} T^{\kappa T} \operatorname{Tr}\Big(\kappa \kappa^\dagger \Big) - 3 m_D^2 \kappa^* \kappa^T \operatorname{Tr}\Big(\kappa \kappa^\dagger \Big) - 6 \kappa^* m_{\bar{D}}^2 \kappa^T \operatorname{Tr}\Big(\kappa \kappa^\dagger \Big)
\end{aligned}$$

$$
\begin{aligned}
&- 3\kappa^{*}\kappa^{T}m_{D}^{2}\,\mathrm{Tr}\Big(\kappa\kappa^{\dagger}\Big) - 8m_{S}^{2}\kappa^{*}\kappa^{T}\,\mathrm{Tr}\Big(\tilde{\lambda}\tilde{\lambda}^{\dagger}\Big) - 4T^{\kappa *}T^{\kappa T}\,\mathrm{Tr}\Big(\tilde{\lambda}\tilde{\lambda}^{\dagger}\Big)\\
&- 2m_{\bar{D}}^{2}\kappa^{*}\kappa^{T}\,\mathrm{Tr}\Big(\tilde{\lambda}\tilde{\lambda}^{\dagger}\Big) - 4\kappa^{*}m_{\bar{D}}^{2}\kappa^{T}\,\mathrm{Tr}\Big(\tilde{\lambda}\tilde{\lambda}^{\dagger}\Big) - 2\kappa^{*}\kappa^{T}m_{D}^{2}\,\mathrm{Tr}\Big(\tilde{\lambda}\tilde{\lambda}^{\dagger}\Big)\\
&- 6T^{\kappa *}\kappa^{T}\,\mathrm{Tr}\Big(\kappa^{\dagger}T^{\kappa}\Big) - 4T^{\kappa *}\kappa^{T}\,\mathrm{Tr}\Big(\tilde{\lambda}^{\dagger}T^{\tilde{\lambda}}\Big) - 6\kappa^{*}T^{\kappa T}\,\mathrm{Tr}\Big(T^{\kappa *}\kappa^{T}\Big)\\
&- 6\kappa^{*}\kappa^{T}\,\mathrm{Tr}\Big(T^{\kappa *}T^{\kappa T}\Big) - 4\kappa^{*}T^{\kappa T}\,\mathrm{Tr}\Big(T^{\tilde{\lambda}*}\tilde{\lambda}^{T}\Big) - 4\kappa^{*}\kappa^{T}\,\mathrm{Tr}\Big(T^{\tilde{\lambda}*}T^{\tilde{\lambda}T}\Big)\\
&- 4\kappa^{*}\kappa^{T}\,\mathrm{Tr}\Big(m_{H_1}^{2}\tilde{\lambda}^{\dagger}\tilde{\lambda}\Big) - 6\kappa^{*}\kappa^{T}\,\mathrm{Tr}\Big(\kappa\kappa^{\dagger}m_{D}^{2*}\Big) - 6\kappa^{*}\kappa^{T}\,\mathrm{Tr}\Big(\kappa m_{\bar{D}}^{2*}\kappa^{\dagger}\Big)\\
&- 4\kappa^{*}\kappa^{T}\,\mathrm{Tr}\Big(\tilde{\lambda}\tilde{\lambda}^{\dagger}m_{H_2}^{2*}\Big)\,, \qquad \text{(D.118)}
\end{aligned}
$$

$$
\begin{aligned}
\beta^{(1)}_{m^2_{\bar{D}}} =& -\frac{8}{15}g_1^2\mathbf{1}|M_1|^2 - \frac{9}{5}g_1'^2\mathbf{1}|M_1'|^2 - \frac{32}{3}g_3^2\mathbf{1}|M_3|^2 + 4m_{L_4}^2 g^{DT}g^{D*}\\
&+ 2m_S^2\kappa^T\kappa^* + 4T^{g^{D}T}T^{g^{D}*} + 2T^{\kappa T}T^{\kappa *} + 2m_{\bar{D}}^2 g^{DT}g^{D*} + m_{\bar{D}}^2\kappa^T\kappa^*\\
&+ 4g^{DT}m_Q^2 g^{D*} + 2g^{DT}g^{D*}m_{\bar{D}}^2 + 2\kappa^T m_D^2\kappa^* + \kappa^T\kappa^* m_{\bar{D}}^2\\
&+ \frac{2}{\sqrt{15}}g_1\mathbf{1}\Sigma_{1,1} - \frac{3}{\sqrt{10}}g_1'\mathbf{1}\Sigma_{1,4}\,, \qquad \text{(D.119)}\\
\beta^{(2)}_{m^2_{\bar{D}}} =& \frac{128}{45}g_1^2g_3^2\mathbf{1}|M_3|^2 + \frac{48}{5}g_1'^2g_3^2\mathbf{1}|M_3|^2 + \frac{160}{3}g_3^4\mathbf{1}|M_3|^2 + \frac{64}{45}g_1^2g_3^2M_1\mathbf{1}M_3^*\\
&+ \frac{24}{5}g_1'^2g_3^2M_1'\mathbf{1}M_3^* + \frac{4}{5}g_1^2m_{L_4}^2g^{DT}g^{D*} - \frac{4}{5}g_1'^2m_{L_4}^2g^{DT}g^{D*}\\
&+ 12g_2^2m_{L_4}^2g^{DT}g^{D*} + 24g_2^2|M_2|^2g^{DT}g^{D*} - 8m_{L_4}^2|\tilde{\sigma}|^2g^{DT}g^{D*}\\
&- 4m_{\bar{L}_4}^2|\tilde{\sigma}|^2g^{DT}g^{D*} - 4m_{\phi}^2|\tilde{\sigma}|^2g^{DT}g^{D*} - 4|T_{\tilde{\sigma}}|^2g^{DT}g^{D*} - \frac{4}{5}g_1^2M_1g^{DT}T^{g^{D}*}\\
&+ \frac{4}{5}g_1'^2M_1'g^{DT}T^{g^{D}*} - 12g_2^2M_2g^{DT}T^{g^{D}*} + 2g_1'^2m_S^2\kappa^T\kappa^* - 4m_{H_d}^2|\lambda|^2\kappa^T\kappa^*\\
&- 4m_{H_u}^2|\lambda|^2\kappa^T\kappa^* - 8m_S^2|\lambda|^2\kappa^T\kappa^* - 2m_{\phi}^2|\sigma|^2\kappa^T\kappa^* - 4m_S^2|\sigma|^2\kappa^T\kappa^*\\
&- 2m_{\tilde{S}}^2|\sigma|^2\kappa^T\kappa^* - 4|T_{\lambda}|^2\kappa^T\kappa^* - 2|T_{\sigma}|^2\kappa^T\kappa^* - 2g_1'^2M_1'\kappa^TT^{\kappa *}\\
&+ \frac{2}{225}g_1^2\Big\{\Big[160g_3^2\Big(2M_1 + M_3\Big) + 1752g_1^2M_1 + 81g_1'^2\Big(2M_1 + M_1'\Big)\Big]\mathbf{1}\\
&+ 90\Big(2M_1g^{DT}g^{D*} - T^{g^{D}T}g^{D*}\Big)\Big\}M_1^* - 12g_2^2M_2^*T^{g^{D}T}g^{D*} - 4\tilde{\sigma}T_{\tilde{\sigma}}^*T^{g^{D}T}g^{D*}\\
&+ \frac{4}{5}g_1^2T^{g^{D}T}T^{g^{D}*} - \frac{4}{5}g_1'^2T^{g^{D}T}T^{g^{D}*} + 12g_2^2T^{g^{D}T}T^{g^{D}*} - 4|\tilde{\sigma}|^2T^{g^{D}T}T^{g^{D}*}\\
&- 4\lambda T_{\lambda}^*T^{\kappa T}\kappa^* - 2\sigma T_{\sigma}^*T^{\kappa T}\kappa^* + \frac{1}{50}g_1'^2\Big\{3\Big[12g_1^2\Big(2M_1' + M_1\Big)\\
&+ 80g_3^2\Big(2M_1' + M_3\Big) + 999g_1'^2M_1'\Big]\mathbf{1} - 20\Big(-10M_1'\kappa^T\kappa^* - 2T^{g^{D}T}g^{D*}\\
&+ 4M_1'g^{DT}g^{D*} + 5T^{\kappa T}\kappa^*\Big)\Big\}M_1'^* + 2g_1'^2T^{\kappa T}T^{\kappa *} - 4|\lambda|^2T^{\kappa T}T^{\kappa *}\\
&- 2|\sigma|^2T^{\kappa T}T^{\kappa *} + \frac{2}{5}g_1^2m_{\bar{D}}^2g^{DT}g^{D*} - \frac{2}{5}g_1'^2m_{\bar{D}}^2g^{DT}g^{D*} + 6g_2^2m_{\bar{D}}^2g^{DT}g^{D*}
\end{aligned}
$$

$$
\begin{aligned}
&- 2|\tilde{\sigma}|^2 m_{\bar{D}}^2 g^{DT} g^{D*} + g_1'^2 m_{\bar{D}}^2 \kappa^T \kappa^* - 2|\lambda|^2 m_{\bar{D}}^2 \kappa^T \kappa^* - |\sigma|^2 m_{\bar{D}}^2 \kappa^T \kappa^* \\
&+ \frac{4}{5} g_1^2 g^{DT} m_Q^2 g^{D*} - \frac{4}{5} g_1'^2 g^{DT} m_Q^2 g^{D*} + 12 g_2^2 g^{DT} m_Q^2 g^{D*} - 4|\tilde{\sigma}|^2 g^{DT} m_Q^2 g^{D*} \\
&+ \frac{2}{5} g_1^2 g^{DT} g^{D*} m_{\bar{D}}^2 - \frac{2}{5} g_1'^2 g^{DT} g^{D*} m_{\bar{D}}^2 + 6 g_2^2 g^{DT} g^{D*} m_{\bar{D}}^2 - 2|\tilde{\sigma}|^2 g^{DT} g^{D*} m_{\bar{D}}^2 \\
&+ 2 g_1'^2 \kappa^T m_D^2 \kappa^* - 4|\lambda|^2 \kappa^T m_D^2 \kappa^* - 2|\sigma|^2 \kappa^T m_D^2 \kappa^* + g_1'^2 \kappa^T \kappa^* m_{\bar{D}}^2 \\
&- 2|\lambda|^2 \kappa^T \kappa^* m_{\bar{D}}^2 - |\sigma|^2 \kappa^T \kappa^* m_{\bar{D}}^2 - 4 m_{H_d}^2 g^{DT} y^{D\dagger} y^D g^{D*} \\
&- 4 m_{L_4}^2 g^{DT} y^{D\dagger} y^D g^{D*} - 4 g^{DT} y^{D\dagger} T^D T^{g^D *} - 4 m_{L_4}^2 g^{DT} y^{U\dagger} y^U g^{D*} \\
&- 4 m_{H_u}^2 g^{DT} y^{U\dagger} y^U g^{D*} - 4 g^{DT} y^{U\dagger} T^U T^{g^D *} - 4 g^{DT} T^{D\dagger} T^D g^{D*} \\
&- 4 g^{DT} T^{U\dagger} T^U g^{D*} - 8 m_{L_4}^2 g^{DT} g^{D*} g^{DT} g^{D*} - 4 g^{DT} g^{D*} T^{g^D T} T^{g^D *} \\
&- 4 g^{DT} T^{g^D *} T^{g^D T} g^{D*} - 4 m_S^2 \kappa^T \kappa^* \kappa^T \kappa^* - 2 \kappa^T \kappa^* T^{\kappa T} T^{\kappa *} - 2 \kappa^T T^{\kappa *} T^{\kappa T} \kappa^* \\
&- 4 T^{g^D T} y^{D\dagger} y^D T^{g^D *} - 4 T^{g^D T} y^{U\dagger} y^U T^{g^D *} - 4 T^{g^D T} T^{D\dagger} y^D g^{D*} \\
&- 4 T^{g^D T} T^{U\dagger} y^U g^{D*} - 4 T^{g^D T} g^{D*} g^{DT} T^{g^D *} - 4 T^{g^D T} T^{g^D *} g^{DT} g^{D*} \\
&- 2 T^{\kappa T} \kappa^* \kappa^T T^{\kappa *} - 2 T^{\kappa T} T^{\kappa *} \kappa^T \kappa^* - 2 m_{\bar{D}}^2 g^{DT} y^{D\dagger} y^D g^{D*} \\
&- 2 m_{\bar{D}}^2 g^{DT} y^{U\dagger} y^U g^{D*} - 2 m_{\bar{D}}^2 g^{DT} g^{D*} g^{DT} g^{D*} - m_{\bar{D}}^2 \kappa^T \kappa^* \kappa^T \kappa^* \\
&- 4 g^{DT} m_Q^2 y^{D\dagger} y^D g^{D*} - 4 g^{DT} m_Q^2 y^{U\dagger} y^U g^{D*} - 4 g^{DT} m_Q^2 g^{D*} g^{DT} g^{D*} \\
&- 4 g^{DT} y^{D\dagger} m_{d^c}^2 y^D g^{D*} - 4 g^{DT} y^{D\dagger} y^D m_Q^2 g^{D*} - 2 g^{DT} y^{D\dagger} y^D g^{D*} m_{\bar{D}}^2 \\
&- 4 g^{DT} y^{U\dagger} m_{u^c}^2 y^U g^{D*} - 4 g^{DT} y^{U\dagger} y^U m_Q^2 g^{D*} - 2 g^{DT} y^{U\dagger} y^U g^{D*} m_{\bar{D}}^2 \\
&- 4 g^{DT} g^{D*} m_{\bar{D}}^2 g^{DT} g^{D*} - 4 g^{DT} g^{D*} g^{DT} m_Q^2 g^{D*} - 2 g^{DT} g^{D*} g^{DT} g^{D*} m_{\bar{D}}^2 \\
&- 2 \kappa^T m_D^2 \kappa^* \kappa^T \kappa^* - 2 \kappa^T \kappa^* m_{\bar{D}}^2 \kappa^T \kappa^* - 2 \kappa^T \kappa^* \kappa^T m_D^2 \kappa^* - \kappa^T \kappa^* \kappa^T \kappa^* m_{\bar{D}}^2 \\
&- 4 \lambda^* \kappa^T T^{\kappa *} T_\lambda - 2 \sigma^* \kappa^T T^{\kappa *} T_\sigma - 4 \tilde{\sigma}^* g^{DT} T^{g^D *} T_{\tilde{\sigma}} + \frac{32}{3} g_3^4 \mathbf{1} \Sigma_{2,3} \\
&+ \frac{8}{15} g_1^2 \mathbf{1} \Sigma_{2,11} - \frac{2}{5} \sqrt{6} g_1 g_1' \mathbf{1} \Sigma_{2,14} - \frac{2}{5} \sqrt{6} g_1 g_1' \mathbf{1} \Sigma_{2,41} + \frac{9}{5} g_1'^2 \mathbf{1} \Sigma_{2,44} \\
&+ \frac{8}{\sqrt{15}} g_1 \mathbf{1} \Sigma_{3,1} - 6 \sqrt{\frac{2}{5}} g_1' \mathbf{1} \Sigma_{3,4} - 24 m_{L_4}^2 g^{DT} g^{D*} \operatorname{Tr}\Big(g^D g^{D\dagger} \Big) \\
&- 12 T^{g^D T} T^{g^D *} \operatorname{Tr}\Big(g^D g^{D\dagger} \Big) - 6 m_{\bar{D}}^2 g^{DT} g^{D*} \operatorname{Tr}\Big(g^D g^{D\dagger} \Big) \\
&- 12 g^{DT} m_Q^2 g^{D*} \operatorname{Tr}\Big(g^D g^{D\dagger} \Big) - 6 g^{DT} g^{D*} m_{\bar{D}}^2 \operatorname{Tr}\Big(g^D g^{D\dagger} \Big) \\
&- 8 m_{L_4}^2 g^{DT} g^{D*} \operatorname{Tr}\Big(h^E h^{E\dagger} \Big) - 4 T^{g^D T} T^{g^D *} \operatorname{Tr}\Big(h^E h^{E\dagger} \Big) \\
&- 2 m_{\bar{D}}^2 g^{DT} g^{D*} \operatorname{Tr}\Big(h^E h^{E\dagger} \Big) - 4 g^{DT} m_Q^2 g^{D*} \operatorname{Tr}\Big(h^E h^{E\dagger} \Big) \\
&- 2 g^{DT} g^{D*} m_{\bar{D}}^2 \operatorname{Tr}\Big(h^E h^{E\dagger} \Big) - 12 m_S^2 \kappa^T \kappa^* \operatorname{Tr}\Big(\kappa \kappa^\dagger \Big) \\
&- 6 T^{\kappa T} T^{\kappa *} \operatorname{Tr}\Big(\kappa \kappa^\dagger \Big) - 3 m_{\bar{D}}^2 \kappa^T \kappa^* \operatorname{Tr}\Big(\kappa \kappa^\dagger \Big) - 6 \kappa^T m_D^2 \kappa^* \operatorname{Tr}\Big(\kappa \kappa^\dagger \Big)
\end{aligned}
$$

$$
\begin{aligned}
&- 3\kappa^T\kappa^* m_{\bar{D}}^2 \operatorname{Tr}\Big(\kappa\kappa^\dagger\Big) - 8m_S^2\kappa^T\kappa^* \operatorname{Tr}\Big(\tilde{\lambda}\tilde{\lambda}^\dagger\Big) - 4T^{\kappa T}T^{\kappa *} \operatorname{Tr}\Big(\tilde{\lambda}\tilde{\lambda}^\dagger\Big) \\
&- 2m_{\bar{D}}^2\kappa^T\kappa^* \operatorname{Tr}\Big(\tilde{\lambda}\tilde{\lambda}^\dagger\Big) - 4\kappa^T m_D^2\kappa^* \operatorname{Tr}\Big(\tilde{\lambda}\tilde{\lambda}^\dagger\Big) - 2\kappa^T\kappa^* m_{\bar{D}}^2 \operatorname{Tr}\Big(\tilde{\lambda}\tilde{\lambda}^\dagger\Big) \\
&- 12g^{DT}T^{g^D *} \operatorname{Tr}\Big(g^{D\dagger}T^{g^D}\Big) - 4g^{DT}T^{g^D *} \operatorname{Tr}\Big(h^{E\dagger}T^{h^E}\Big) \\
&- 6\kappa^T T^{\kappa *} \operatorname{Tr}\Big(\kappa^\dagger T^\kappa\Big) - 4\kappa^T T^{\kappa *} \operatorname{Tr}\Big(\tilde{\lambda}^\dagger T^{\tilde{\lambda}}\Big) - 12T^{g^D T}g^{D*} \operatorname{Tr}\Big(T^{g^D *}g^{DT}\Big) \\
&- 12g^{DT}g^{D*} \operatorname{Tr}\Big(T^{g^D *}T^{g^D T}\Big) - 4T^{g^D T}g^{D*} \operatorname{Tr}\Big(T^{h^E *}h^{ET}\Big) \\
&- 4g^{DT}g^{D*} \operatorname{Tr}\Big(T^{h^E *}T^{h^E T}\Big) - 6T^{\kappa T}\kappa^* \operatorname{Tr}\Big(T^{\kappa *}\kappa^T\Big) \\
&- 6\kappa^T\kappa^* \operatorname{Tr}\Big(T^{\kappa *}T^{\kappa T}\Big) - 4T^{\kappa T}\kappa^* \operatorname{Tr}\Big(T^{\tilde{\lambda}*}\tilde{\lambda}^T\Big) - 4\kappa^T\kappa^* \operatorname{Tr}\Big(T^{\tilde{\lambda}*}T^{\tilde{\lambda}T}\Big) \\
&- 12g^{DT}g^{D*} \operatorname{Tr}\Big(g^D g^{D\dagger}m_Q^{2*}\Big) - 12g^{DT}g^{D*} \operatorname{Tr}\Big(g^D m_{\bar{D}}^{2*}g^{D\dagger}\Big) \\
&- 4g^{DT}g^{D*} \operatorname{Tr}\Big(h^E m_{H_1}^2 h^{E\dagger}\Big) - 4g^{DT}g^{D*} \operatorname{Tr}\Big(h^E h^{E\dagger}m_{e^c}^2\Big) \\
&- 4\kappa^T\kappa^* \operatorname{Tr}\Big(m_{H_1}^2\tilde{\lambda}^\dagger\tilde{\lambda}\Big) - 6\kappa^T\kappa^* \operatorname{Tr}\Big(\kappa\kappa^\dagger m_D^{2*}\Big) \\
&- 6\kappa^T\kappa^* \operatorname{Tr}\Big(\kappa m_{\bar{D}}^{2*}\kappa^\dagger\Big) - 4\kappa^T\kappa^* \operatorname{Tr}\Big(\tilde{\lambda}\tilde{\lambda}^\dagger m_{H_2}^{2*}\Big), \qquad \text{(D.120)}
\end{aligned}
$$

$$
\begin{aligned}
\beta_{m_{L_4}^2}^{(1)} = &-\frac{6}{5}g_1^2|M_1|^2 - \frac{4}{5}g_1'^2|M_1'|^2 - 6g_2^2|M_2|^2 + 2m_{L_4}^2|\tilde{\sigma}|^2 + 2m_{\bar{L}_4}^2|\tilde{\sigma}|^2 \\
&+ 2m_\phi^2|\tilde{\sigma}|^2 + 2|T_{\tilde{\sigma}}|^2 - \sqrt{\frac{3}{5}}g_1\Sigma_{1,1} + \sqrt{\frac{2}{5}}g_1'\Sigma_{1,4} + 6m_{L_4}^2 \operatorname{Tr}\Big(g^D g^{D\dagger}\Big) \\
&+ 2m_{L_4}^2 \operatorname{Tr}\Big(h^E h^{E\dagger}\Big) + 6 \operatorname{Tr}\Big(T^{g^D *}T^{g^D T}\Big) + 2 \operatorname{Tr}\Big(T^{h^E *}T^{h^E T}\Big) \\
&+ 6 \operatorname{Tr}\Big(g^D g^{D\dagger}m_Q^{2*}\Big) + 6 \operatorname{Tr}\Big(g^D m_{\bar{D}}^{2*}g^{D\dagger}\Big) + 2 \operatorname{Tr}\Big(h^E m_{H_1}^2 h^{E\dagger}\Big) \\
&+ 2 \operatorname{Tr}\Big(h^E h^{E\dagger}m_{e^c}^2\Big), \qquad \text{(D.121)}
\end{aligned}
$$

$$
\begin{aligned}
\beta_{m_{L_4}^2}^{(2)} = &\frac{18}{5}g_1^2g_2^2|M_2|^2 + \frac{12}{5}g_1'^2g_2^2|M_2|^2 + 87g_2^4|M_2|^2 + \frac{9}{5}g_1^2g_2^2M_1M_2^* \\
&+ \frac{6}{5}g_1'^2g_2^2M_1'M_2^* - 4m_{L_4}^2|\tilde{\sigma}|^2|\kappa_\phi|^2 - 4m_{\bar{L}_4}^2|\tilde{\sigma}|^2|\kappa_\phi|^2 - 16m_\phi^2|\tilde{\sigma}|^2|\kappa_\phi|^2 \\
&- 2m_{L_4}^2|\tilde{\sigma}|^2|\sigma|^2 - 2m_{\bar{L}_4}^2|\tilde{\sigma}|^2|\sigma|^2 - 4m_\phi^2|\tilde{\sigma}|^2|\sigma|^2 - 2m_S^2|\tilde{\sigma}|^2|\sigma|^2 \\
&- 2m_{\bar{S}}^2|\tilde{\sigma}|^2|\sigma|^2 - 12m_{L_4}^2|\tilde{\sigma}|^4 - 12m_{\bar{L}_4}^2|\tilde{\sigma}|^4 - 12m_\phi^2|\tilde{\sigma}|^4 - 4|\tilde{\sigma}|^2|T_{\kappa_\phi}|^2 \\
&- 4\tilde{\sigma}\kappa_\phi^* T_{\tilde{\sigma}}^* T_{\kappa_\phi} - 2|\tilde{\sigma}|^2|T_\sigma|^2 - 2\tilde{\sigma}\sigma^* T_{\tilde{\sigma}}^* T_\sigma - 4\kappa_\phi\tilde{\sigma}^* T_{\kappa_\phi}^* T_{\tilde{\sigma}} - 2\sigma\tilde{\sigma}^* T_\sigma^* T_{\tilde{\sigma}} \\
&- 4|\kappa_\phi|^2|T_{\tilde{\sigma}}|^2 - 2|\sigma|^2|T_{\tilde{\sigma}}|^2 - 24|\tilde{\sigma}|^2|T_{\tilde{\sigma}}|^2 + 6g_2^4\Sigma_{2,2} + \frac{6}{5}g_1^2\Sigma_{2,11} \\
&- \frac{2}{5}\sqrt{6}g_1g_1'\Sigma_{2,14} - \frac{2}{5}\sqrt{6}g_1g_1'\Sigma_{2,41} + \frac{4}{5}g_1'^2\Sigma_{2,44} - 4\sqrt{\frac{3}{5}}g_1\Sigma_{3,1} + 4\sqrt{\frac{2}{5}}g_1'\Sigma_{3,4}
\end{aligned}
$$

$$
\begin{aligned}
&- \frac{4}{5}g_1^2 m_{L_4}^2 \operatorname{Tr}\Big(g^D g^{D\dagger}\Big) + \frac{9}{5}g_1'^2 m_{L_4}^2 \operatorname{Tr}\Big(g^D g^{D\dagger}\Big) + 32 g_3^2 m_{L_4}^2 \operatorname{Tr}\Big(g^D g^{D\dagger}\Big) \\
&+ 64 g_3^2 |M_3|^2 \operatorname{Tr}\Big(g^D g^{D\dagger}\Big) + \frac{12}{5}g_1^2 m_{L_4}^2 \operatorname{Tr}\Big(h^E h^{E\dagger}\Big) + \frac{3}{5}g_1'^2 m_{L_4}^2 \operatorname{Tr}\Big(h^E h^{E\dagger}\Big) \\
&- 32 g_3^2 M_3^* \operatorname{Tr}\Big(g^{D\dagger} T^{g^D}\Big) + \frac{1}{25}g_1^2 M_1^* \Big[891 g_1^2 M_1 + 36 g_1'^2 M_1 + 90 g_2^2 M_1 \\
&+ 18 g_1'^2 M_1' + 45 g_2^2 M_2 - 40 M_1 \operatorname{Tr}\Big(g^D g^{D\dagger}\Big) + 120 M_1 \operatorname{Tr}\Big(h^E h^{E\dagger}\Big) \\
&+ 20 \operatorname{Tr}\Big(g^{D\dagger} T^{g^D}\Big) - 60 \operatorname{Tr}\Big(h^{E\dagger} T^{h^E}\Big)\Big] + \frac{3}{25}g_1'^2 M_1'^* \Big[6 g_1^2 M_1 + 12 g_1^2 M_1' \\
&+ 217 g_1'^2 M_1' + 20 g_2^2 M_1' + 10 g_2^2 M_2 + 30 M_1' \operatorname{Tr}\Big(g^D g^{D\dagger}\Big) + 10 M_1' \operatorname{Tr}\Big(h^E h^{E\dagger}\Big) \\
&- 15 \operatorname{Tr}\Big(g^{D\dagger} T^{g^D}\Big) - 5 \operatorname{Tr}\Big(h^{E\dagger} T^{h^E}\Big)\Big] + \frac{4}{5}g_1^2 M_1 \operatorname{Tr}\Big(T^{g^D *} g^{DT}\Big) \\
&- \frac{9}{5}g_1'^2 M_1' \operatorname{Tr}\Big(T^{g^D *} g^{DT}\Big) - 32 g_3^2 M_3 \operatorname{Tr}\Big(T^{g^D *} g^{DT}\Big) - \frac{4}{5}g_1^2 \operatorname{Tr}\Big(T^{g^D *} T^{g^D T}\Big) \\
&+ \frac{9}{5}g_1'^2 \operatorname{Tr}\Big(T^{g^D *} T^{g^D T}\Big) + 32 g_3^2 \operatorname{Tr}\Big(T^{g^D *} T^{g^D T}\Big) - \frac{12}{5}g_1^2 M_1 \operatorname{Tr}\Big(T^{h^E *} h^{ET}\Big) \\
&- \frac{3}{5}g_1'^2 M_1' \operatorname{Tr}\Big(T^{h^E *} h^{ET}\Big) + \frac{12}{5}g_1^2 \operatorname{Tr}\Big(T^{h^E *} T^{h^E T}\Big) + \frac{3}{5}g_1'^2 \operatorname{Tr}\Big(T^{h^E *} T^{h^E T}\Big) \\
&- \frac{4}{5}g_1^2 \operatorname{Tr}\Big(g^D g^{D\dagger} m_Q^{2*}\Big) + \frac{9}{5}g_1'^2 \operatorname{Tr}\Big(g^D g^{D\dagger} m_Q^{2*}\Big) + 32 g_3^2 \operatorname{Tr}\Big(g^D g^{D\dagger} m_Q^{2*}\Big) \\
&- \frac{4}{5}g_1^2 \operatorname{Tr}\Big(g^D m_{\bar{D}}^{2*} g^{D\dagger}\Big) + \frac{9}{5}g_1'^2 \operatorname{Tr}\Big(g^D m_{\bar{D}}^{2*} g^{D\dagger}\Big) + 32 g_3^2 \operatorname{Tr}\Big(g^D m_{\bar{D}}^{2*} g^{D\dagger}\Big) \\
&+ \frac{12}{5}g_1^2 \operatorname{Tr}\Big(h^E m_{H_1}^2 h^{E\dagger}\Big) + \frac{3}{5}g_1'^2 \operatorname{Tr}\Big(h^E m_{H_1}^2 h^{E\dagger}\Big) + \frac{12}{5}g_1^2 \operatorname{Tr}\Big(h^E h^{E\dagger} m_{e^c}^2\Big) \\
&+ \frac{3}{5}g_1'^2 \operatorname{Tr}\Big(h^E h^{E\dagger} m_{e^c}^2\Big) - 2 m_{L_4}^2 \operatorname{Tr}\Big(\tilde{f} h^{E\dagger} h^E \tilde{f}^\dagger\Big) - 2 m_{H_u}^2 \operatorname{Tr}\Big(\tilde{f} h^{E\dagger} h^E \tilde{f}^\dagger\Big) \\
&- 2 \operatorname{Tr}\Big(\tilde{f} h^{E\dagger} T^{h^E} T^{\tilde{f}\dagger}\Big) - 2 \operatorname{Tr}\Big(\tilde{f} T^{h^E\dagger} T^{h^E} \tilde{f}^\dagger\Big) - 36 m_{L_4}^2 \operatorname{Tr}\Big(g^D g^{D\dagger} g^D g^{D\dagger}\Big) \\
&- 36 \operatorname{Tr}\Big(g^D g^{D\dagger} T^{g^D} T^{g^D\dagger}\Big) - 6 m_{H_d}^2 \operatorname{Tr}\Big(g^D g^{D\dagger} y^{DT} y^{D*}\Big) \\
&- 6 m_{L_4}^2 \operatorname{Tr}\Big(g^D g^{D\dagger} y^{DT} y^{D*}\Big) - 6 m_{L_4}^2 \operatorname{Tr}\Big(g^D g^{D\dagger} y^{UT} y^{U*}\Big) \\
&- 6 m_{H_u}^2 \operatorname{Tr}\Big(g^D g^{D\dagger} y^{UT} y^{U*}\Big) - 6 \operatorname{Tr}\Big(g^D g^{D\dagger} T^{DT} T^{D*}\Big) \\
&- 6 \operatorname{Tr}\Big(g^D g^{D\dagger} T^{UT} T^{U*}\Big) - 6 m_{L_4}^2 \operatorname{Tr}\Big(g^D \kappa^\dagger \kappa g^{D\dagger}\Big) - 6 m_S^2 \operatorname{Tr}\Big(g^D \kappa^\dagger \kappa g^{D\dagger}\Big) \\
&- 6 \operatorname{Tr}\Big(g^D \kappa^\dagger T^\kappa T^{g^D\dagger}\Big) - 36 \operatorname{Tr}\Big(g^D T^{g^D\dagger} T^{g^D} g^{D\dagger}\Big) - 6 \operatorname{Tr}\Big(g^D T^{\kappa\dagger} T^\kappa g^{D\dagger}\Big) \\
&- 2 \operatorname{Tr}\Big(h^E \tilde{f}^\dagger T^{\tilde{f}} T^{h^E\dagger}\Big) - 12 m_{L_4}^2 \operatorname{Tr}\Big(h^E h^{E\dagger} h^E h^{E\dagger}\Big) \\
&- 4 m_{H_d}^2 \operatorname{Tr}\Big(h^E h^{E\dagger} y^E y^{E\dagger}\Big) - 4 m_{L_4}^2 \operatorname{Tr}\Big(h^E h^{E\dagger} y^E y^{E\dagger}\Big)
\end{aligned}
$$

$$
\begin{aligned}
&- 12\,\mathrm{Tr}\Big(h^E h^{E\dagger} T^{h^E} T^{h^E\dagger}\Big) - 4\,\mathrm{Tr}\Big(h^E h^{E\dagger} T^E T^{E\dagger}\Big) \\
&- 2m_{L_4}^2\,\mathrm{Tr}\Big(h^E \tilde{\lambda}^\dagger \tilde{\lambda} h^{E\dagger}\Big) - 2m_S^2\,\mathrm{Tr}\Big(h^E \tilde{\lambda}^\dagger \tilde{\lambda} h^{E\dagger}\Big) - 2\,\mathrm{Tr}\Big(h^E \tilde{\lambda}^\dagger T^{\tilde{\lambda}} T^{h^E\dagger}\Big) \\
&- 2\,\mathrm{Tr}\Big(h^E T^{\tilde{f}\dagger} T^{\tilde{f}} h^{E\dagger}\Big) - 12\,\mathrm{Tr}\Big(h^E T^{h^E\dagger} T^{h^E} h^{E\dagger}\Big) - 4\,\mathrm{Tr}\Big(h^E T^{h^E\dagger} T^E y^{E\dagger}\Big) \\
&- 2\,\mathrm{Tr}\Big(h^E T^{\tilde{\lambda}\dagger} T^{\tilde{\lambda}} h^{E\dagger}\Big) - 6\,\mathrm{Tr}\Big(y^D T^{g^D *} T^{g^D T} y^{D\dagger}\Big) - 4\,\mathrm{Tr}\Big(y^E y^{E\dagger} T^{h^E} T^{h^E\dagger}\Big) \\
&- 4\,\mathrm{Tr}\Big(y^E T^{E\dagger} T^{h^E} h^{E\dagger}\Big) - 6\,\mathrm{Tr}\Big(y^U T^{g^D *} T^{g^D T} y^{U\dagger}\Big) - 6\,\mathrm{Tr}\Big(\kappa g^{D\dagger} T^{g^D} T^{\kappa\dagger}\Big) \\
&- 6\,\mathrm{Tr}\Big(\kappa T^{g^D\dagger} T^{g^D} \kappa^\dagger\Big) - 2\,\mathrm{Tr}\Big(\tilde{\lambda} h^{E\dagger} T^{h^E} T^{\tilde{\lambda}\dagger}\Big) - 2\,\mathrm{Tr}\Big(\tilde{\lambda} T^{h^E\dagger} T^{h^E} \tilde{\lambda}^\dagger\Big) \\
&- 6\,\mathrm{Tr}\Big(g^{D\dagger} y^{DT} T^{D*} T^{g^D}\Big) - 6\,\mathrm{Tr}\Big(g^{D\dagger} y^{UT} T^{U*} T^{g^D}\Big) \\
&- 6\,\mathrm{Tr}\Big(y^{D\dagger} T^D T^{g^D *} g^{DT}\Big) - 6\,\mathrm{Tr}\Big(y^{U\dagger} T^U T^{g^D *} g^{DT}\Big) \\
&- 2\,\mathrm{Tr}\Big(\tilde{f} m_{H_1}^2 h^{E\dagger} h^E \tilde{f}^\dagger\Big) - 2\,\mathrm{Tr}\Big(\tilde{f} h^{E\dagger} h^E m_{H_1}^2 \tilde{f}^\dagger\Big) - 2\,\mathrm{Tr}\Big(\tilde{f} h^{E\dagger} h^E \tilde{f}^\dagger m_\Sigma^{2*}\Big) \\
&- 2\,\mathrm{Tr}\Big(\tilde{f} h^{E\dagger} m_{e^c}^2 h^E \tilde{f}^\dagger\Big) - 18\,\mathrm{Tr}\Big(g^D g^{D\dagger} g^D m_{\bar{D}}^{2*} g^{D\dagger}\Big) \\
&- 36\,\mathrm{Tr}\Big(g^D g^{D\dagger} m_Q^{2*} g^D g^{D\dagger}\Big) - 6\,\mathrm{Tr}\Big(g^D g^{D\dagger} m_Q^{2*} y^{DT} y^{D*}\Big) \\
&- 6\,\mathrm{Tr}\Big(g^D g^{D\dagger} m_Q^{2*} y^{UT} y^{U*}\Big) - 6\,\mathrm{Tr}\Big(g^D g^{D\dagger} y^{DT} m_{d^c}^{2*} y^{D*}\Big) \\
&- 6\,\mathrm{Tr}\Big(g^D g^{D\dagger} y^{DT} y^{D*} m_Q^{2*}\Big) - 6\,\mathrm{Tr}\Big(g^D g^{D\dagger} y^{UT} m_{u^c}^{2*} y^{U*}\Big) \\
&- 6\,\mathrm{Tr}\Big(g^D g^{D\dagger} y^{UT} y^{U*} m_Q^{2*}\Big) - 6\,\mathrm{Tr}\Big(g^D \kappa^\dagger \kappa g^{D\dagger} m_Q^{2*}\Big) \\
&- 6\,\mathrm{Tr}\Big(g^D \kappa^\dagger \kappa m_{\bar{D}}^{2*} g^{D\dagger}\Big) - 6\,\mathrm{Tr}\Big(g^D \kappa^\dagger m_D^{2*} \kappa g^{D\dagger}\Big) \\
&- 18\,\mathrm{Tr}\Big(g^D m_{\bar{D}}^{2*} g^{D\dagger} g^D g^{D\dagger}\Big) - 6\,\mathrm{Tr}\Big(g^D m_{\bar{D}}^{2*} g^{D\dagger} y^{DT} y^{D*}\Big) \\
&- 6\,\mathrm{Tr}\Big(g^D m_{\bar{D}}^{2*} g^{D\dagger} y^{UT} y^{U*}\Big) - 6\,\mathrm{Tr}\Big(g^D m_{\bar{D}}^{2*} \kappa^\dagger \kappa g^{D\dagger}\Big) \\
&- 6\,\mathrm{Tr}\Big(h^E m_{H_1}^2 h^{E\dagger} h^E h^{E\dagger}\Big) - 4\,\mathrm{Tr}\Big(h^E m_{H_1}^2 h^{E\dagger} y^E y^{E\dagger}\Big) \\
&- 2\,\mathrm{Tr}\Big(h^E m_{H_1}^2 \tilde{\lambda}^\dagger \tilde{\lambda} h^{E\dagger}\Big) - 6\,\mathrm{Tr}\Big(h^E h^{E\dagger} h^E m_{H_1}^2 h^{E\dagger}\Big) \\
&- 6\,\mathrm{Tr}\Big(h^E h^{E\dagger} h^E h^{E\dagger} m_{e^c}^2\Big) - 6\,\mathrm{Tr}\Big(h^E h^{E\dagger} m_{e^c}^2 h^E h^{E\dagger}\Big) \\
&- 4\,\mathrm{Tr}\Big(h^E h^{E\dagger} m_{e^c}^2 y^E y^{E\dagger}\Big) - 4\,\mathrm{Tr}\Big(h^E h^{E\dagger} y^E m_L^2 y^{E\dagger}\Big) \\
&- 4\,\mathrm{Tr}\Big(h^E h^{E\dagger} y^E y^{E\dagger} m_{e^c}^2\Big) - 2\,\mathrm{Tr}\Big(h^E \tilde{\lambda}^\dagger \tilde{\lambda} m_{H_1}^2 h^{E\dagger}\Big)
\end{aligned}
$$

$$- 2\,\mathrm{Tr}\Big(h^E\tilde{\lambda}^\dagger\tilde{\lambda}h^{E\dagger}m^2_{e^c}\Big) - 2\,\mathrm{Tr}\Big(h^E\tilde{\lambda}^\dagger m^{2*}_{H_2}\tilde{\lambda}h^{E\dagger}\Big)\,, \tag{D.122}$$

$$\begin{aligned}\beta^{(1)}_{m^2_{\tilde{L}_4}} &= -\frac{6}{5}g_1^2|M_1|^2 - \frac{4}{5}g_1'^2|M_1'|^2 - 6g_2^2|M_2|^2 + 2m^2_{L_4}|\tilde{\sigma}|^2 + 2m^2_{\tilde{L}_4}|\tilde{\sigma}|^2 \\ &\quad + 2m^2_\phi|\tilde{\sigma}|^2 + 2|T_{\tilde{\sigma}}|^2 + \sqrt{\frac{3}{5}}g_1\Sigma_{1,1} - \sqrt{\frac{2}{5}}g_1'\Sigma_{1,4}\,,\end{aligned} \tag{D.123}$$

$$\begin{aligned}\beta^{(2)}_{m^2_{\tilde{L}_4}} &= \frac{18}{5}g_1^2g_2^2|M_2|^2 + \frac{12}{5}g_1'^2g_2^2|M_2|^2 + 87g_2^4|M_2|^2 \\ &\quad + \frac{9}{25}g_1^2\Big[2g_1'^2\Big(2M_1 + M_1'\Big) + 5g_2^2\Big(2M_1 + M_2\Big) + 99g_1^2M_1\Big]M_1^* \\ &\quad + \frac{3}{25}g_1'^2\Big[10g_2^2\Big(2M_1' + M_2\Big) + 217g_1'^2M_1' + 6g_1^2\Big(2M_1' + M_1\Big)\Big]M_1'^* \\ &\quad + \frac{9}{5}g_1^2g_2^2M_1M_2^* + \frac{6}{5}g_1'^2g_2^2M_1'M_2^* - 4m^2_{L_4}|\tilde{\sigma}|^2|\kappa_\phi|^2 - 4m^2_{\tilde{L}_4}|\tilde{\sigma}|^2|\kappa_\phi|^2 \\ &\quad - 16m^2_\phi|\tilde{\sigma}|^2|\kappa_\phi|^2 - 2m^2_{L_4}|\tilde{\sigma}|^2|\sigma|^2 - 2m^2_{\tilde{L}_4}|\tilde{\sigma}|^2|\sigma|^2 - 4m^2_\phi|\tilde{\sigma}|^2|\sigma|^2 \\ &\quad - 2m^2_S|\tilde{\sigma}|^2|\sigma|^2 - 2m^2_{\tilde{S}}|\tilde{\sigma}|^2|\sigma|^2 - 12m^2_{L_4}|\tilde{\sigma}|^4 - 12m^2_{\tilde{L}_4}|\tilde{\sigma}|^4 \\ &\quad - 12m^2_\phi|\tilde{\sigma}|^4 - 4|\tilde{\sigma}|^2|T_{\kappa_\phi}|^2 - 4\tilde{\sigma}\kappa_\phi^*T^*_{\tilde{\sigma}}T_{\kappa_\phi} - 2|\tilde{\sigma}|^2|T_\sigma|^2 - 2\tilde{\sigma}\sigma^*T^*_{\tilde{\sigma}}T_\sigma \\ &\quad - 4\kappa_\phi\tilde{\sigma}^*T^*_{\kappa_\phi}T_{\tilde{\sigma}} - 2\sigma\tilde{\sigma}^*T^*_\sigma T_{\tilde{\sigma}} - 4|\kappa_\phi|^2|T_{\tilde{\sigma}}|^2 - 2|\sigma|^2|T_{\tilde{\sigma}}|^2 - 24|\tilde{\sigma}|^2|T_{\tilde{\sigma}}|^2 \\ &\quad + 6g_2^4\Sigma_{2,2} + \frac{6}{5}g_1^2\Sigma_{2,11} - \frac{2}{5}\sqrt{6}g_1g_1'\Sigma_{2,14} - \frac{2}{5}\sqrt{6}g_1g_1'\Sigma_{2,41} \\ &\quad + \frac{4}{5}g_1'^2\Sigma_{2,44} + 4\sqrt{\frac{3}{5}}g_1\Sigma_{3,1} - 4\sqrt{\frac{2}{5}}g_1'\Sigma_{3,4} - 12m^2_{L_4}|\tilde{\sigma}|^2\,\mathrm{Tr}\Big(g^Dg^{D\dagger}\Big) \\ &\quad - 6m^2_{\tilde{L}_4}|\tilde{\sigma}|^2\,\mathrm{Tr}\Big(g^Dg^{D\dagger}\Big) - 6m^2_\phi|\tilde{\sigma}|^2\,\mathrm{Tr}\Big(g^Dg^{D\dagger}\Big) - 6|T_{\tilde{\sigma}}|^2\,\mathrm{Tr}\Big(g^Dg^{D\dagger}\Big) \\ &\quad - 4m^2_{L_4}|\tilde{\sigma}|^2\,\mathrm{Tr}\Big(h^Eh^{E\dagger}\Big) - 2m^2_{\tilde{L}_4}|\tilde{\sigma}|^2\,\mathrm{Tr}\Big(h^Eh^{E\dagger}\Big) - 2m^2_\phi|\tilde{\sigma}|^2\,\mathrm{Tr}\Big(h^Eh^{E\dagger}\Big) \\ &\quad - 2|T_{\tilde{\sigma}}|^2\,\mathrm{Tr}\Big(h^Eh^{E\dagger}\Big) - 6\tilde{\sigma}T^*_{\tilde{\sigma}}\,\mathrm{Tr}\Big(g^{D\dagger}T^{g^D}\Big) - 2\tilde{\sigma}T^*_{\tilde{\sigma}}\,\mathrm{Tr}\Big(h^{E\dagger}T^{h^E}\Big) \\ &\quad - 6\tilde{\sigma}^*T_{\tilde{\sigma}}\,\mathrm{Tr}\Big(T^{g^{D}*}g^{DT}\Big) - 6|\tilde{\sigma}|^2\,\mathrm{Tr}\Big(T^{g^{D}*}T^{g^{D}T}\Big) - 2\tilde{\sigma}^*T_{\tilde{\sigma}}\,\mathrm{Tr}\Big(T^{h^{E}*}h^{ET}\Big) \\ &\quad - 2|\tilde{\sigma}|^2\,\mathrm{Tr}\Big(T^{h^{E}*}T^{h^{E}T}\Big) - 6|\tilde{\sigma}|^2\,\mathrm{Tr}\Big(g^Dg^{D\dagger}m^{2*}_Q\Big) - 6|\tilde{\sigma}|^2\,\mathrm{Tr}\Big(g^Dm^{2*}_{\bar{D}}g^{D\dagger}\Big) \\ &\quad - 2|\tilde{\sigma}|^2\,\mathrm{Tr}\Big(h^Em^2_{H_1}h^{E\dagger}\Big) - 2|\tilde{\sigma}|^2\,\mathrm{Tr}\Big(h^Eh^{E\dagger}m^2_{e^c}\Big)\,,\end{aligned} \tag{D.124}$$

$$\begin{aligned}\beta^{(1)}_{m^2_\phi} &= 2\Big[2m^2_{\tilde{L}_4}|\tilde{\sigma}|^2 + 2m^2_{L_4}|\tilde{\sigma}|^2 + 2m^2_\phi|\tilde{\sigma}|^2 + 2|T_{\kappa_\phi}|^2 + 2|T_{\tilde{\sigma}}|^2 + 6m^2_\phi|\kappa_\phi|^2 \\ &\quad + \Big(m^2_\phi + m^2_S + m^2_{\tilde{S}}\Big)|\sigma|^2 + |T_\sigma|^2\Big]\,,\end{aligned} \tag{D.125}$$

$$\begin{aligned}\beta^{(2)}_{m^2_\phi} &= -96m^2_\phi|\kappa_\phi|^4 - 8\Big(m^2_\phi + m^2_S + m^2_{\tilde{S}}\Big)|\sigma|^4 - 8\kappa_\phi^*\Big[\Big(4m^2_\phi + m^2_S + m^2_{\tilde{S}}\Big)\kappa_\phi|\sigma|^2 \\ &\quad + 2\Big(4m^2_\phi + m^2_{L_4} + m^2_{\tilde{L}_4}\Big)\kappa_\phi|\tilde{\sigma}|^2 + 8\kappa_\phi|T_{\kappa_\phi}|^2 + \kappa_\phi|T_\sigma|^2 + 2\kappa_\phi|T_{\tilde{\sigma}}|^2\end{aligned}$$

$$
\begin{aligned}
&+ \sigma T_\sigma^* T_{\kappa_\phi} + 2\tilde{\sigma} T_{\tilde{\sigma}}^* T_{\kappa_\phi}\Big] + \frac{1}{5}\Big(-80\Big(m_{L_4}^2 + m_{\bar{L}_4}^2 + m_\phi^2\Big)|\tilde{\sigma}|^4 \\
&- 4T_{\tilde{\sigma}}^*\Big\{T_{\tilde{\sigma}}\Big[-15g_2^2 + 15\,\mathrm{Tr}\Big(g^D g^{D\dagger}\Big) - 2g_1'^2 - 3g_1^2 + 5\,\mathrm{Tr}\Big(h^E h^{E\dagger}\Big)\Big] \\
&+ \tilde{\sigma}\Big[15g_2^2 M_2 + 15\,\mathrm{Tr}\Big(g^{D\dagger} T^{g^D}\Big) + 2g_1'^2 M_1' + 3g_1^2 M_1 + 5\,\mathrm{Tr}\Big(h^{E\dagger} T^{h^E}\Big)\Big]\Big\} \\
&- 5T_\sigma^*\Big\{4\lambda^*\Big(\lambda T_\sigma + \sigma T_\lambda\Big) + \sigma\Big[4\,\mathrm{Tr}\Big(\tilde{\lambda}^\dagger T^{\tilde{\lambda}}\Big) + 5g_1'^2 M_1' + 6\,\mathrm{Tr}\Big(\kappa^\dagger T^\kappa\Big)\Big] \\
&+ T_\sigma\Big[4\,\mathrm{Tr}\Big(\tilde{\lambda}\tilde{\lambda}^\dagger\Big) - 5g_1'^2 + 6\,\mathrm{Tr}\Big(\kappa\kappa^\dagger\Big)\Big]\Big\} + 4\tilde{\sigma}^*\Big[3g_1^2 m_{L_4}^2\tilde{\sigma} + 2g_1'^2 m_{L_4}^2\tilde{\sigma} \\
&+ 15g_2^2 m_{L_4}^2\tilde{\sigma} + 3g_1^2 m_{\bar{L}_4}^2\tilde{\sigma} + 2g_1'^2 m_{\bar{L}_4}^2\tilde{\sigma} + 15g_2^2 m_{\bar{L}_4}^2\tilde{\sigma} + 3g_1^2 m_\phi^2\tilde{\sigma} \\
&+ 2g_1'^2 m_\phi^2\tilde{\sigma} + 15g_2^2 m_\phi^2\tilde{\sigma} + 30g_2^2\tilde{\sigma}|M_2|^2 - 20\tilde{\sigma}|T_{\kappa_\phi}|^2 - 40\tilde{\sigma}|T_{\tilde{\sigma}}|^2 \\
&+ 3g_1^2 M_1^*\Big(2M_1\tilde{\sigma} - T_{\tilde{\sigma}}\Big) + 2g_1'^2 M_1'^*\Big(2M_1'\tilde{\sigma} - T_{\tilde{\sigma}}\Big) - 15g_2^2 M_2^* T_{\tilde{\sigma}} \\
&- 20\kappa_\phi T_{\kappa_\phi}^* T_{\tilde{\sigma}} - 30m_{L_4}^2\tilde{\sigma}\,\mathrm{Tr}\Big(g^D g^{D\dagger}\Big) - 15m_{\bar{L}_4}^2\tilde{\sigma}\,\mathrm{Tr}\Big(g^D g^{D\dagger}\Big) \\
&- 15m_\phi^2\tilde{\sigma}\,\mathrm{Tr}\Big(g^D g^{D\dagger}\Big) - 10m_{L_4}^2\tilde{\sigma}\,\mathrm{Tr}\Big(h^E h^{E\dagger}\Big) - 5m_{\bar{L}_4}^2\tilde{\sigma}\,\mathrm{Tr}\Big(h^E h^{E\dagger}\Big) \\
&- 5m_\phi^2\tilde{\sigma}\,\mathrm{Tr}\Big(h^E h^{E\dagger}\Big) - 15T_{\tilde{\sigma}}\,\mathrm{Tr}\Big(T^{g^D *} g^{DT}\Big) - 15\tilde{\sigma}\,\mathrm{Tr}\Big(T^{g^D *} T^{g^D T}\Big) \\
&- 5T_{\tilde{\sigma}}\,\mathrm{Tr}\Big(T^{h^E *} h^{ET}\Big) - 5\tilde{\sigma}\,\mathrm{Tr}\Big(T^{h^E *} T^{h^E T}\Big) - 15\tilde{\sigma}\,\mathrm{Tr}\Big(g^D g^{D\dagger} m_Q^{2*}\Big) \\
&- 15\tilde{\sigma}\,\mathrm{Tr}\Big(g^D m_D^{2*} g^{D\dagger}\Big) - 5\tilde{\sigma}\,\mathrm{Tr}\Big(h^E m_{H_1}^2 h^{E\dagger}\Big) - 5\tilde{\sigma}\,\mathrm{Tr}\Big(h^E h^{E\dagger} m_{e^c}^2\Big)\Big]\Big) \\
&+ \sigma^*\Big[5g_1'^2 m_\phi^2\sigma + 5g_1'^2 m_S^2\sigma + 5g_1'^2 m_{\bar{S}}^2\sigma - 4\Big(2m_S^2 + m_{H_d}^2 + m_{H_u}^2 \\
&+ m_\phi^2 + m_{\bar{S}}^2\Big)\sigma|\lambda|^2 - 8\sigma|T_{\kappa_\phi}|^2 - 4\sigma|T_\lambda|^2 - 16\sigma|T_\sigma|^2 \\
&+ 5g_1'^2 M_1'^*\Big(2M_1'\sigma - T_\sigma\Big) - 8\kappa_\phi T_{\kappa_\phi}^* T_\sigma - 4\lambda T_\lambda^* T_\sigma - 6m_\phi^2\sigma\,\mathrm{Tr}\Big(\kappa\kappa^\dagger\Big) \\
&- 12m_S^2\sigma\,\mathrm{Tr}\Big(\kappa\kappa^\dagger\Big) - 6m_{\bar{S}}^2\sigma\,\mathrm{Tr}\Big(\kappa\kappa^\dagger\Big) - 4m_\phi^2\sigma\,\mathrm{Tr}\Big(\tilde{\lambda}\tilde{\lambda}^\dagger\Big) \\
&- 8m_S^2\sigma\,\mathrm{Tr}\Big(\tilde{\lambda}\tilde{\lambda}^\dagger\Big) - 4m_{\bar{S}}^2\sigma\,\mathrm{Tr}\Big(\tilde{\lambda}\tilde{\lambda}^\dagger\Big) - 6T_\sigma\,\mathrm{Tr}\Big(T^{\kappa *}\kappa^T\Big) \\
&- 6\sigma\,\mathrm{Tr}\Big(T^{\kappa *} T^{\kappa T}\Big) - 4T_\sigma\,\mathrm{Tr}\Big(T^{\tilde{\lambda}*}\tilde{\lambda}^T\Big) - 4\sigma\,\mathrm{Tr}\Big(T^{\tilde{\lambda}*} T^{\tilde{\lambda}T}\Big) \\
&- 4\sigma\,\mathrm{Tr}\Big(m_{H_1}^2\tilde{\lambda}^\dagger\tilde{\lambda}\Big) - 6\sigma\,\mathrm{Tr}\Big(\kappa\kappa^\dagger m_D^{2*}\Big) - 6\sigma\,\mathrm{Tr}\Big(\kappa m_D^{2*}\kappa^\dagger\Big) \\
&- 4\sigma\,\mathrm{Tr}\Big(\tilde{\lambda}\tilde{\lambda}^\dagger m_{H_2}^{2*}\Big)\Big]. \qquad \text{(D.126)}
\end{aligned}
$$

Bibliography

[1] S. L. Glashow, Nucl. Phys. **22**, 579 (1961).

[2] M. Gell-Mann, Phys. Lett. **8**, 214 (1964).

[3] G. Zweig, "An $SU(3)$ model for strong interaction symmetry and its breaking. Version 1," (1964), CERN-TH-401.

[4] G. Zweig, in *Developments in the Quark Theory of Hadrons. Vol. 1. 1964 - 1978*, edited by D. Lichtenberg and S. P. Rosen (Hadronic Press, 1980) pp. 22–101.

[5] S. Weinberg, Phys. Rev. Lett. **19**, 1264 (1967).

[6] A. Salam, in *Proceedings of the 8th Nobel Symposium, Lerum, 1968*, edited by N. Svartholm (Almqvist and Wiksell, Stockholm, 1968) pp. 367–377.

[7] W. J. Marciano and H. Pagels, Phys. Rept. **36**, 137 (1978).

[8] J. J. Thomson, Phil. Mag. Ser.5 **44**, 293 (1897).

[9] J. C. Street and E. C. Stevenson, Phys. Rev. **52**, 1003 (1937).

[10] F. Reines and C. L. Cowan, Phys. Rev. **92**, 830 (1953).

[11] G. Danby, J. M. Gaillard, K. A. Goulianos, L. M. Lederman, N. B. Mistry, M. Schwartz, and J. Steinberger, Phys. Rev. Lett. **9**, 36 (1962).

[12] E. D. Bloom *et al.*, Phys. Rev. Lett. **23**, 930 (1969).

[13] M. Breidenbach, J. I. Friedman, H. W. Kendall, E. D. Bloom, D. H. Coward, H. C. DeStaebler, J. Drees, L. W. Mo, and R. E. Taylor, Phys. Rev. Lett. **23**, 935 (1969).

[14] J. E. Augustin *et al.* (SLAC-SP-017), Phys. Rev. Lett. **33**, 1406 (1974), [Adv. Exp. Phys. 5, 141 (1976)].

[15] J. J. Aubert *et al.* (E598), Phys. Rev. Lett. **33**, 1404 (1974).

[16] M. L. Perl *et al.*, Phys. Rev. Lett. **35**, 1489 (1975).

[17] S. W. Herb *et al.*, Phys. Rev. Lett. **39**, 252 (1977).

[18] F. Abe *et al.* (CDF), Phys. Rev. Lett. **73**, 225 (1994), arXiv:hep-ex/9405005 [hep-ex].

[19] K. Kodama *et al.*, Nucl. Instrum. Meth. **A493**, 45 (2002).

[20] P. W. Higgs, Phys. Lett. **12**, 132 (1964).

[21] P. W. Higgs, Phys. Rev. Lett. **13**, 508 (1964).

[22] P. W. Higgs, Phys. Rev. **145**, 1156 (1966).

[23] F. Englert and R. Brout, Phys. Rev. Lett. **13**, 321 (1964).

[24] G. S. Guralnik, C. R. Hagen, and T. W. B. Kibble, Phys. Rev. Lett. **13**, 585 (1964).

[25] T. W. B. Kibble, Phys. Rev. **155**, 1554 (1967).

[26] G. Aad *et al.* (ATLAS), Phys. Lett. **B716**, 1 (2012), arXiv:1207.7214 [hep-ex].

[27] S. Chatrchyan *et al.* (CMS), Phys. Lett. **B716**, 30 (2012), arXiv:1207.7235 [hep-ex].

[28] G. Aad *et al.* (ATLAS, CMS), Phys. Rev. Lett. **114**, 191803 (2015), arXiv:1503.07589 [hep-ex].

[29] V. Khachatryan *et al.* (CMS), Eur. Phys. J. **C75**, 212 (2015), arXiv:1412.8662 [hep-ex].

[30] G. Aad *et al.* (ATLAS), Eur. Phys. J. **C75**, 476 (2015), [Erratum: Eur. Phys. J. **C76**, no.3, 152 (2016)], arXiv:1506.05669 [hep-ex].

[31] G. Aad *et al.* (ATLAS, CMS), JHEP **08**, 045 (2016), arXiv:1606.02266 [hep-ex].

[32] B. T. Cleveland, T. Daily, R. Davis, Jr., J. R. Distel, K. Lande, C. K. Lee, P. S. Wildenhain, and J. Ullman, Astrophys. J. **496**, 505 (1998).

[33] Y. Fukuda *et al.* (Kamiokande), Phys. Rev. Lett. **77**, 1683 (1996).

[34] J. N. Abdurashitov *et al.* (SAGE), Phys. Rev. **C80**, 015807 (2009), arXiv:0901.2200 [nucl-ex].

[35] P. Anselmann *et al.* (GALLEX), Phys. Lett. **B285**, 376 (1992).

[36] W. Hampel *et al.* (GALLEX), Phys. Lett. **B447**, 127 (1999).

[37] M. Altmann *et al.* (GNO), Phys. Lett. **B616**, 174 (2005), arXiv:hep-ex/0504037 [hep-ex].

[38] S. Fukuda *et al.* (Super-Kamiokande), Phys. Lett. **B539**, 179 (2002), arXiv:hep-ex/0205075 [hep-ex].

[39] Q. R. Ahmad *et al.* (SNO), Phys. Rev. Lett. **87**, 071301 (2001), arXiv:nucl-ex/0106015 [nucl-ex].

[40] Q. R. Ahmad *et al.* (SNO), Phys. Rev. Lett. **89**, 011302 (2002), arXiv:nucl-ex/0204009 [nucl-ex].

[41] K. Eguchi *et al.* (KamLAND), Phys. Rev. Lett. **90**, 021802 (2003), arXiv:hep-ex/0212021 [hep-ex].

[42] T. Araki *et al.* (KamLAND), Phys. Rev. Lett. **94**, 081801 (2005), arXiv:hep-ex/0406035 [hep-ex].

[43] Y. Fukuda *et al.* (Super-Kamiokande), Phys. Rev. Lett. **81**, 1562 (1998), arXiv:hep-ex/9807003 [hep-ex].

[44] Y. Ashie *et al.* (Super-Kamiokande), Phys. Rev. Lett. **93**, 101801 (2004), arXiv:hep-ex/0404034 [hep-ex].

[45] M. H. Ahn *et al.* (K2K), Phys. Rev. **D74**, 072003 (2006), arXiv:hep-ex/0606032 [hep-ex].

[46] D. G. Michael *et al.* (MINOS), Phys. Rev. Lett. **97**, 191801 (2006), arXiv:hep-ex/0607088 [hep-ex].

[47] P. Adamson *et al.* (MINOS), Phys. Rev. Lett. **101**, 131802 (2008), arXiv:0806.2237 [hep-ex].

[48] P. Adamson *et al.* (MINOS), Phys. Rev. Lett. **106**, 181801 (2011), arXiv:1103.0340 [hep-ex].

[49] K. Abe *et al.* (Super-Kamiokande), Phys. Rev. Lett. **110**, 181802 (2013), arXiv:1206.0328 [hep-ex].

[50] K. Abe *et al.* (T2K), Phys. Rev. **D85**, 031103 (2012), arXiv:1201.1386 [hep-ex].

[51] K. Abe *et al.* (T2K), Phys. Rev. Lett. **111**, 211803 (2013), arXiv:1308.0465 [hep-ex].

[52] B. Pontecorvo, Sov. Phys. JETP **6**, 429 (1957), [Zh. Eksp. Teor. Fiz.33, 549 (1957)].

[53] B. Pontecorvo, Sov. Phys. JETP **7**, 172 (1958), [Zh. Eksp. Teor. Fiz.34, 247 (1957)].

[54] Z. Maki, M. Nakagawa, and S. Sakata, Prog. Theor. Phys. **28**, 870 (1962).

[55] P. Minkowski, Phys. Lett. **B67**, 421 (1977).

[56] R. N. Mohapatra and G. Senjanovic, Phys. Rev. Lett. **44**, 912 (1980).

[57] T. Yanagida, in *Proceedings: Workshop on the Unified Theories and the Baryon Number in the Universe: Tsukuba, 1979*, edited by O. Sawada and A. Sugamoto (1979) pp. 95–99.

[58] M. Gell-Mann, P. Ramond, and R. Slansky, in *Supergravity Workshop Stony Brook, New York, 1979*, edited by P. Van Nieuwenhuizen and D. Z. Freedman (1979) pp. 315–321, arXiv:1306.4669 [hep-th].

[59] R. N. Mohapatra and G. Senjanovic, Phys. Rev. **D23**, 165 (1981).

[60] F. Zwicky, Helv. Phys. Acta **6**, 110 (1933), [Gen. Rel. Grav. 41, 207 (2009)].

[61] V. C. Rubin and W. K. Ford, Jr., Astrophys. J. **159**, 379 (1970).

[62] M. S. Roberts and R. N. Whitehurst, Astrophys. J. **201**, 327 (1975).

[63] V. C. Rubin, N. Thonnard, and W. K. Ford, Jr., Astrophys. J. **238**, 471 (1980).

[64] A. Bosma, Astron. J. **86**, 1825 (1981).

[65] M. Persic, P. Salucci, and F. Stel, Mon. Not. Roy. Astron. Soc. **281**, 27 (1996), arXiv:astro-ph/9506004 [astro-ph].

[66] D. Clowe, M. Bradac, A. H. Gonzalez, M. Markevitch, S. W. Randall, C. Jones, and D. Zaritsky, Astrophys. J. **648**, L109 (2006), arXiv:astro-ph/0608407 [astro-ph].

[67] G. F. Smoot *et al.* (COBE), Astrophys. J. **396**, L1 (1992).

[68] E. Komatsu *et al.* (WMAP), Astrophys. J. Suppl. **192**, 18 (2011), arXiv:1001.4538 [astro-ph.CO].

[69] C. L. Bennett *et al.*, Astrophys. J. Suppl. **208**, 20 (2013), arXiv:1212.5225 [astro-ph.CO].

[70] P. A. R. Ade *et al.* (Planck), Astron. Astrophys. **594**, A13 (2016), arXiv:1502.01589 [astro-ph.CO].

[71] L. Bergström, Rept. Prog. Phys. **63**, 793 (2000), arXiv:hep-ph/0002126 [hep-ph].

[72] G. Bertone, D. Hooper, and J. Silk, Phys. Rept. **405**, 279 (2005), arXiv:hep-ph/0404175 [hep-ph].

[73] T. Clifton, P. G. Ferreira, A. Padilla, and C. Skordis, Phys. Rept. **513**, 1 (2012), arXiv:1106.2476 [astro-ph.CO].

[74] M. Milgrom, Astrophys. J. **270**, 365 (1983).

[75] K. Freese, in *14th Marcel Grossmann Meeting on Recent Developments in Theoretical and Experimental General Relativity, Astrophysics, and Relativistic Field Theories (MG14), Rome, 2015* (2017) arXiv:1701.01840 [astro-ph.CO].

[76] P. A. R. Ade *et al.* (Planck), Astron. Astrophys. **594**, A14 (2016), arXiv:1502.01590 [astro-ph.CO].

[77] S. Weinberg, Phys. Rev. **D13**, 974 (1976).

[78] S. Weinberg, Phys. Rev. **D19**, 1277 (1979).

[79] E. Gildener, Phys. Rev. **D14**, 1667 (1976).

[80] L. Susskind, Phys. Rev. **D20**, 2619 (1979).

[81] G. 't Hooft, in *Recent Developments in Gauge Theories. Proceedings, Nato Advanced Study Institute, Cargese, 1979*, Vol. 59, edited by G. 't Hooft, C. Itzykson, A. Jaffe, H. Lehmann, P. K. Mitter, I. M. Singer, and R. Stora (Springer US, Boston, MA, 1980) pp. 135–157.

[82] M. E. Peskin and D. V. Schroeder, *An Introduction to Quantum Field Theory* (Addison-Wesley, 1995).

[83] H. Georgi and S. L. Glashow, Phys. Rev. Lett. **32**, 438 (1974).

[84] S. P. Martin, "A Supersymmetry Primer," in *Perspectives on Supersymmetry II*, edited by G. L. Kane (World Scientific, 2011) pp. 1–153, arXiv:hep-ph/9709356 [hep-ph].

[85] J. Wess and B. Zumino, Nucl. Phys. **B70**, 39 (1974).

[86] J. Wess and B. Zumino, Phys. Lett. **49B**, 52 (1974).

[87] A. Salam and J. A. Strathdee, Nucl. Phys. **B76**, 477 (1974).

[88] R. Haag, J. T. Łopuszański, and M. Sohnius, Nucl. Phys. **B88**, 257 (1975).

[89] S. R. Coleman and J. Mandula, Phys. Rev. **159**, 1251 (1967).

[90] E. Witten, Nucl. Phys. **B188**, 513 (1981).

[91] S. Dimopoulos and H. Georgi, Nucl. Phys. **B193**, 150 (1981).

[92] N. Sakai, Z. Phys. **C11**, 153 (1981).

[93] R. K. Kaul, Phys. Lett. **B109**, 19 (1982).

[94] R. K. Kaul and P. Majumdar, Nucl. Phys. **B199**, 36 (1982).

[95] C. Patrignani *et al.* (Particle Data Group), Chin. Phys. **C40**, 100001 (2016).

[96] L. Girardello and M. T. Grisaru, Nucl. Phys. **B194**, 65 (1982).

[97] P. Athron, M. Bach, D. Harries, J.-h. Park, D. Stöckinger, A. Voigt, and J. Ziebell, in preparation .

[98] F. Staub, P. Athron, L. Basso, M. D. Goodsell, D. Harries, M. E. Krauss, K. Nickel, T. Opferkuch, L. Ubaldi, A. Vicente, and A. Voigt, Eur. Phys. J. **C76**, 516 (2016), arXiv:1602.05581 [hep-ph].

[99] P. Athron, D. Harries, and A. G. Williams, Phys. Rev. **D91**, 115024 (2015), arXiv:1503.08929 [hep-ph].

[100] P. Athron, D. Harries, R. Nevzorov, and A. G. Williams, Phys. Lett. **B760**, 19 (2016), arXiv:1512.07040 [hep-ph].

[101] P. Athron, D. Harries, R. Nevzorov, and A. G. Williams, JHEP **12**, 128 (2016), arXiv:1610.03374 [hep-ph].

[102] P. Fayet, Phys. Lett. **B64**, 159 (1976).

[103] H. P. Nilles, Phys. Rept. **110**, 1 (1984).

[104] M. Drees, R. M. Godbole, and P. Roy, *Theory and phenomenology of sparticles: An account of four-dimensional N=1 supersymmetry in high energy physics* (World Scientific Publishing Co. Pte. Ltd., 2004).

[105] H. E. Haber and G. L. Kane, Phys. Rept. **117**, 75 (1985).

[106] B. A. Dobrescu and P. J. Fox, Eur. Phys. J. **C70**, 263 (2010), arXiv:1001.3147 [hep-ph].

[107] W. Altmannshofer and D. M. Straub, JHEP **09**, 078 (2010), arXiv:1004.1993 [hep-ph].

[108] J. R. Ellis and F. Zwirner, Nucl. Phys. **B338**, 317 (1990).

[109] L. J. Hall and M. Suzuki, Nucl. Phys. **B231**, 419 (1984).

[110] J. R. Ellis, G. Gelmini, C. Jarlskog, G. G. Ross, and J. W. F. Valle, Phys. Lett. **B150**, 142 (1985).

[111] M. Miura *et al.* (Super-Kamiokande), Phys. Rev. **D95**, 012004 (2017), arXiv:1610.03597 [hep-ex].

[112] A. Yu. Smirnov and F. Vissani, Phys. Lett. **B380**, 317 (1996), arXiv:hep-ph/9601387 [hep-ph].

[113] G. Bhattacharyya and P. B. Pal, Phys. Rev. **D59**, 097701 (1999), arXiv:hep-ph/9809493 [hep-ph].

[114] S. Weinberg, Phys. Rev. **D26**, 287 (1982).

[115] N. Sakai and T. Yanagida, Nucl. Phys. **B197**, 533 (1982).

[116] S. Dimopoulos, S. Raby, and F. Wilczek, Phys. Lett. **B112**, 133 (1982).

[117] G. R. Farrar and P. Fayet, Phys. Lett. **B76**, 575 (1978).

[118] G. G. Ross and J. W. F. Valle, Phys. Lett. **B151**, 375 (1985).

[119] V. D. Barger, G. F. Giudice, and T. Han, Phys. Rev. **D40**, 2987 (1989).

[120] L. E. Ibáñez and G. G. Ross, Nucl. Phys. **B368**, 3 (1992).

[121] H. Dreiner, "An Introduction to Explicit R–Parity Violation," in *Perspectives on Supersymmetry II*, edited by G. L. Kane (World Scientific, 2011) pp. 565–583, arXiv:hep-ph/9707435 [hep-ph].

[122] R. Barbier *et al.*, Phys. Rept. **420**, 1 (2005), arXiv:hep-ph/0406039 [hep-ph].

[123] R. N. Mohapatra, Phys. Scripta **90**, 088004 (2015), arXiv:1503.06478 [hep-ph].

[124] C. Csaki, E. Kuflik, S. Lombardo, O. Slone, and T. Volansky, JHEP **08**, 016 (2015), arXiv:1505.00784 [hep-ph].

[125] G. Jungman, M. Kamionkowski, and K. Griest, Phys. Rept. **267**, 195 (1996), arXiv:hep-ph/9506380 [hep-ph].

[126] K. Griest and M. Kamionkowski, Phys. Rev. Lett. **64**, 615 (1990).

[127] S. Ferrara, L. Girardello, and F. Palumbo, Phys. Rev. **D20**, 403 (1979).

[128] A. H. Chamseddine, R. L. Arnowitt, and P. Nath, Phys. Rev. Lett. **49**, 970 (1982).

[129] R. Barbieri, S. Ferrara, and C. A. Savoy, Phys. Lett. **B119**, 343 (1982).

[130] L. E. Ibáñez, Phys. Lett. **B118**, 73 (1982).

[131] L. J. Hall, J. D. Lykken, and S. Weinberg, Phys. Rev. **D27**, 2359 (1983).

[132] N. Ohta, Prog. Theor. Phys. **70**, 542 (1983).

[133] J. R. Ellis, D. V. Nanopoulos, and K. Tamvakis, Phys. Lett. **B121**, 123 (1983).

[134] L. Alvarez-Gaume, J. Polchinski, and M. B. Wise, Nucl. Phys. **B221**, 495 (1983).

[135] M. Dine and W. Fischler, Phys. Lett. **B110**, 227 (1982).

[136] C. R. Nappi and B. A. Ovrut, Phys. Lett. **B113**, 175 (1982).

[137] L. Alvarez-Gaume, M. Claudson, and M. B. Wise, Nucl. Phys. **B207**, 96 (1982).

[138] M. Dine and A. E. Nelson, Phys. Rev. **D48**, 1277 (1993), arXiv:hep-ph/9303230 [hep-ph].

[139] M. Dine, A. E. Nelson, and Y. Shirman, Phys. Rev. **D51**, 1362 (1995), arXiv:hep-ph/9408384 [hep-ph].

[140] M. Dine, A. E. Nelson, Y. Nir, and Y. Shirman, Phys. Rev. **D53**, 2658 (1996), arXiv:hep-ph/9507378 [hep-ph].

[141] M. Dine and D. MacIntire, Phys. Rev. **D46**, 2594 (1992), arXiv:hep-ph/9205227 [hep-ph].

[142] G. F. Giudice, M. A. Luty, H. Murayama, and R. Rattazzi, JHEP **12**, 027 (1998), arXiv:hep-ph/9810442 [hep-ph].

[143] L. Randall and R. Sundrum, Nucl. Phys. **B557**, 79 (1999), arXiv:hep-th/9810155 [hep-th].

[144] A. Pomarol and R. Rattazzi, JHEP **05**, 013 (1999), arXiv:hep-ph/9903448 [hep-ph].

[145] J. A. Bagger, T. Moroi, and E. Poppitz, JHEP **04**, 009 (2000), arXiv:hep-th/9911029 [hep-th].

[146] P. Binetruy, M. K. Gaillard, and B. D. Nelson, Nucl. Phys. **B604**, 32 (2001), arXiv:hep-ph/0011081 [hep-ph].

[147] S. Dimopoulos and D. W. Sutter, Nucl. Phys. **B452**, 496 (1995), arXiv:hep-ph/9504415 [hep-ph].

[148] J. Baron *et al.* (ACME), Science **343**, 269 (2014), arXiv:1310.7534 [physics.atom-ph].

[149] G. W. Bennett *et al.* (Muon (g-2)), Phys. Rev. **D80**, 052008 (2009), arXiv:0811.1207 [hep-ex].

[150] K. Inami *et al.* (Belle), Phys. Lett. **B551**, 16 (2003), arXiv:hep-ex/0210066 [hep-ex].

[151] J. M. Pendlebury *et al.*, Phys. Rev. **D92**, 092003 (2015), arXiv:1509.04411 [hep-ex].

[152] A. J. Bevan *et al.* (Belle, BaBar), Eur. Phys. J. **C74**, 3026 (2014), arXiv:1406.6311 [hep-ex].

[153] S. L. Glashow, J. Iliopoulos, and L. Maiani, Phys. Rev. **D2**, 1285 (1970).

[154] R. Aaij *et al.* (LHCb), Eur. Phys. J. **C73**, 2373 (2013), arXiv:1208.3355 [hep-ex].

[155] G. D'Ambrosio, G. F. Giudice, G. Isidori, and A. Strumia, Nucl. Phys. **B645**, 155 (2002), arXiv:hep-ph/0207036 [hep-ph].

[156] M. Misiak, S. Pokorski, and J. Rosiek, Adv. Ser. Direct. High Energy Phys. **15**, 795 (1998), arXiv:hep-ph/9703442 [hep-ph].

[157] A. Djouadi *et al.* (MSSM Working Group), *The Minimal Supersymmetric Standard Model: Group Summary Report*, (1998), arXiv:hep-ph/9901246 [hep-ph].

[158] C. F. Berger, J. S. Gainer, J. L. Hewett, and T. G. Rizzo, JHEP **02**, 023 (2009), arXiv:0812.0980 [hep-ph].

[159] S. S. AbdusSalam, B. C. Allanach, F. Quevedo, F. Feroz, and M. Hobson, Phys. Rev. **D81**, 095012 (2010), arXiv:0904.2548 [hep-ph].

[160] S. Sekmen, S. Kraml, J. Lykken, F. Moortgat, S. Padhi, L. Pape, M. Pierini, H. B. Prosper, and M. Spiropulu, JHEP **02**, 075 (2012), arXiv:1109.5119 [hep-ph].

[161] A. Arbey, M. Battaglia, and F. Mahmoudi, Eur. Phys. J. **C72**, 1906 (2012), arXiv:1112.3032 [hep-ph].

[162] P. Bechtle, S. Heinemeyer, O. Stal, T. Stefaniak, G. Weiglein, and L. Zeune, Eur. Phys. J. **C73**, 2354 (2013), arXiv:1211.1955 [hep-ph].

[163] D. Alves (LHC New Physics Working Group), J. Phys. **G39**, 105005 (2012), arXiv:1105.2838 [hep-ph].

[164] B. Zumino, Nucl. Phys. **B89**, 535 (1975).

[165] I. Affleck, M. Dine, and N. Seiberg, Phys. Rev. Lett. **51**, 1026 (1983).

[166] I. Affleck, M. Dine, and N. Seiberg, Phys. Lett. **B137**, 187 (1984).

[167] I. Affleck, M. Dine, and N. Seiberg, Nucl. Phys. **B256**, 557 (1985).

[168] E. Poppitz and S. P. Trivedi, Ann. Rev. Nucl. Part. Sci. **48**, 307 (1998), arXiv:hep-th/9803107 [hep-th].

[169] P. Fayet and J. Iliopoulos, Phys. Lett. **B51**, 461 (1974).

[170] P. Fayet, Nucl. Phys. **B90**, 104 (1975).

[171] L. O'Raifeartaigh, Nucl. Phys. **B96**, 331 (1975).

[172] P. Nath and R. L. Arnowitt, Phys. Lett. **B56**, 177 (1975).

[173] R. L. Arnowitt, P. Nath, and B. Zumino, Phys. Lett. **56B**, 81 (1975).

[174] D. Z. Freedman, P. van Nieuwenhuizen, and S. Ferrara, Phys. Rev. **D13**, 3214 (1976).

[175] S. Deser and B. Zumino, Phys. Lett. **62B**, 335 (1976).

[176] D. Z. Freedman and P. van Nieuwenhuizen, Phys. Rev. **D14**, 912 (1976).

[177] E. Cremmer, B. Julia, J. Scherk, S. Ferrara, L. Girardello, and P. van Nieuwenhuizen, Nucl. Phys. **B147**, 105 (1979).

[178] J. A. Bagger, Nucl. Phys. **B211**, 302 (1983).

[179] E. Cremmer, B. Julia, J. Scherk, P. van Nieuwenhuizen, S. Ferrara, and L. Girardello, Phys. Lett. **79B**, 231 (1978).

[180] S. J. Gates, M. T. Grisaru, M. Rocek, and W. Siegel, Front. Phys. **58**, 1 (1983), arXiv:hep-th/0108200 [hep-th].

[181] S. Deser and B. Zumino, Phys. Rev. Lett. **38**, 1433 (1977).

[182] V. S. Kaplunovsky and J. Louis, Phys. Lett. **B306**, 269 (1993), arXiv:hep-th/9303040 [hep-th].

[183] A. Brignole, L. E. Ibáñez, and C. Muñoz, Nucl. Phys. **B422**, 125 (1994), [Erratum: Nucl. Phys. **B436**, 747 (1995)], arXiv:hep-ph/9308271 [hep-ph].

[184] R. Barbieri, J. Louis, and M. Moretti, Phys. Lett. **B312**, 451 (1993), [Erratum: Phys. Lett. **B316**, 632 (1993)], arXiv:hep-ph/9305262 [hep-ph].

[185] J. R. Ellis, A. B. Lahanas, D. V. Nanopoulos, and K. Tamvakis, Phys. Lett. **134B**, 429 (1984).

[186] A. B. Lahanas and D. V. Nanopoulos, Phys. Rept. **145**, 1 (1987).

[187] F. Gabbiani and A. Masiero, Nucl. Phys. **B322**, 235 (1989).

[188] J. R. Ellis, S. Ferrara, and D. V. Nanopoulos, Phys. Lett. **B114**, 231 (1982).

[189] J. Polchinski and M. B. Wise, Phys. Lett. **B125**, 393 (1983).

[190] F. del Aguila, M. B. Gavela, J. A. Grifols, and A. Mendez, Phys. Lett. **B126**, 71 (1983), [Erratum: Phys. Lett. **B129**, 473 (1983)].

[191] G. F. Giudice and A. Masiero, Phys. Lett. **B206**, 480 (1988).

[192] G. C. Branco, P. M. Ferreira, L. Lavoura, M. N. Rebelo, M. Sher, and J. P. Silva, Phys. Rept. **516**, 1 (2012), arXiv:1106.0034 [hep-ph].

[193] J. F. Gunion and H. E. Haber, Nucl. Phys. **B272**, 1 (1986), [Erratum: Nucl. Phys. **B402**, 567 (1993)].

[194] J. A. Casas, A. Lleyda, and C. Muñoz, Nucl. Phys. **B471**, 3 (1996), arXiv:hep-ph/9507294 [hep-ph].

[195] S. P. Martin, Phys. Rev. **D66**, 096001 (2002), arXiv:hep-ph/0206136 [hep-ph].

[196] S. P. Martin, Phys. Rev. **D65**, 116003 (2002), arXiv:hep-ph/0111209 [hep-ph].

[197] N. Cabibbo, Phys. Rev. Lett. **10**, 531 (1963).

[198] M. Kobayashi and T. Maskawa, Prog. Theor. Phys. **49**, 652 (1973).

[199] B. Pontecorvo, Sov. Phys. JETP **26**, 984 (1968), [Zh. Eksp. Teor. Fiz.53, 1717 (1967)].

[200] P. Z. Skands *et al.*, JHEP **07**, 036 (2004), arXiv:hep-ph/0311123 [hep-ph].

[201] B. C. Allanach *et al.*, Comput. Phys. Commun. **180**, 8 (2009), arXiv:0801.0045 [hep-ph].

[202] H. E. Haber and R. Hempfling, Phys. Rev. Lett. **66**, 1815 (1991).

[203] Y. Okada, M. Yamaguchi, and T. Yanagida, Prog. Theor. Phys. **85**, 1 (1991).

[204] J. R. Ellis, G. Ridolfi, and F. Zwirner, Phys. Lett. **B257**, 83 (1991).

[205] P. Draper and H. Rzehak, Phys. Rept. **619**, 1 (2016), arXiv:1601.01890 [hep-ph].

[206] M. M. El Kheishen, A. A. Aboshousha, and A. A. Shafik, Phys. Rev. **D45**, 4345 (1992).

[207] M. Guchait, Z. Phys. **C57**, 157 (1993), [Erratum: Z. Phys. **C61**, 178 (1994)].

[208] V. D. Barger, M. S. Berger, and P. Ohmann, Phys. Rev. **D49**, 4908 (1994), arXiv:hep-ph/9311269 [hep-ph].

[209] R. L. Arnowitt and P. Nath, Phys. Rev. **D54**, 2374 (1996), arXiv:hep-ph/9509260 [hep-ph].

[210] L. Hofer, U. Nierste, and D. Scherer, JHEP **10**, 081 (2009), arXiv:0907.5408 [hep-ph].

[211] A. Crivellin, L. Hofer, and J. Rosiek, JHEP **07**, 017 (2011), arXiv:1103.4272 [hep-ph].

[212] D. M. Pierce, J. A. Bagger, K. T. Matchev, and R.-j. Zhang, Nucl. Phys. **B491**, 3 (1997), arXiv:hep-ph/9606211 [hep-ph].

[213] M. Aaboud *et al.* (ATLAS), Eur. Phys. J. **C76**, 547 (2016), arXiv:1606.08772 [hep-ex].

[214] M. Aaboud *et al.* (ATLAS), Phys. Rev. **D94**, 052009 (2016), arXiv:1606.03903 [hep-ex].

[215] A. M. Sirunyan *et al.* (CMS), (2016), arXiv:1612.03877 [hep-ex].

[216] V. Khachatryan *et al.* (CMS), Phys. Lett. **B767**, 403 (2017), arXiv:1605.08993 [hep-ex].

[217] M. Carena and H. E. Haber, Prog. Part. Nucl. Phys. **50**, 63 (2003), arXiv:hep-ph/0208209 [hep-ph].

[218] M. Carena, M. Quiros, and C. E. M. Wagner, Nucl. Phys. **B461**, 407 (1996), arXiv:hep-ph/9508343 [hep-ph].

[219] R. Barbieri, M. Frigeni, and F. Caravaglios, Phys. Lett. **B258**, 167 (1991).

[220] Y. Okada, M. Yamaguchi, and T. Yanagida, Phys. Lett. **B262**, 54 (1991).

[221] H. E. Haber and R. Hempfling, Phys. Rev. **D48**, 4280 (1993), arXiv:hep-ph/9307201 [hep-ph].

[222] J. A. Casas, J. R. Espinosa, M. Quiros, and A. Riotto, Nucl. Phys. **B436**, 3 (1995), [Erratum: Nucl. Phys. **B439**, 466 (1995)], arXiv:hep-ph/9407389 [hep-ph].

[223] M. Carena, J. R. Espinosa, M. Quiros, and C. E. M. Wagner, Phys. Lett. **B355**, 209 (1995), arXiv:hep-ph/9504316 [hep-ph].

[224] H. E. Haber, R. Hempfling, and A. H. Hoang, Z. Phys. **C75**, 539 (1997), arXiv:hep-ph/9609331 [hep-ph].

[225] H. Baer, V. Barger, and D. Mickelson, Phys. Rev. **D88**, 095013 (2013), arXiv:1309.2984 [hep-ph].

[226] G. Aad *et al.* (ATLAS), JHEP **10**, 054 (2015), arXiv:1507.05525 [hep-ex].

[227] A. Arvanitaki, M. Baryakhtar, X. Huang, K. van Tilburg, and G. Villadoro, JHEP **03**, 022 (2014), arXiv:1309.3568 [hep-ph].

[228] D. J. H. Chung, L. L. Everett, G. L. Kane, S. F. King, J. D. Lykken, and L.-T. Wang, Phys. Rept. **407**, 1 (2005), arXiv:hep-ph/0312378 [hep-ph].

[229] J. R. Ellis, K. Enqvist, D. V. Nanopoulos, and F. Zwirner, Mod. Phys. Lett. **A1**, 57 (1986).

[230] R. Barbieri and G. F. Giudice, Nucl. Phys. **B306**, 63 (1988).

[231] S. Cassel and D. M. Ghilencea, Mod. Phys. Lett. **A27**, 1230003 (2012), arXiv:1103.4793 [hep-ph].

[232] D. M. Ghilencea, H. M. Lee, and M. Park, JHEP **07**, 046 (2012), arXiv:1203.0569 [hep-ph].

[233] M. Maniatis, Int. J. Mod. Phys. **A25**, 3505 (2010), arXiv:0906.0777 [hep-ph].

[234] U. Ellwanger, C. Hugonie, and A. M. Teixeira, Phys. Rept. **496**, 1 (2010), arXiv:0910.1785 [hep-ph].

[235] L. Durand and J. L. Lopez, Phys. Lett. **B217**, 463 (1989).

[236] M. Drees, Int. J. Mod. Phys. **A4**, 3635 (1989).

[237] J. E. Kim and H. P. Nilles, Phys. Lett. **B138**, 150 (1984).

[238] A. Zee, Phys. Lett. **B93**, 389 (1980), [Erratum: Phys. Lett. **B95**, 461 (1980)].

[239] T. P. Cheng and L.-F. Li, Phys. Rev. **D22**, 2860 (1980).

[240] L. Wolfenstein, Nucl. Phys. **B175**, 93 (1980).

[241] E. Ma, Phys. Lett. **B380**, 286 (1996), arXiv:hep-ph/9507348 [hep-ph].

[242] J.-h. Kang, P. Langacker, and T.-j. Li, Phys. Rev. **D71**, 015012 (2005), arXiv:hep-ph/0411404 [hep-ph].

[243] M. Carena, G. Nardini, M. Quiros, and C. E. M. Wagner, JHEP **02**, 001 (2013), arXiv:1207.6330 [hep-ph].

[244] A. D. Sakharov, Pisma Zh. Eksp. Teor. Fiz. **5**, 32 (1967), [Usp. Fiz. Nauk 161, 61 (1991)].

[245] T. Hambye, E. Ma, M. Raidal, and U. Sarkar, Phys. Lett. **B512**, 373 (2001), arXiv:hep-ph/0011197 [hep-ph].

[246] S. F. King, R. Luo, D. J. Miller, and R. Nevzorov, JHEP **12**, 042 (2008), arXiv:0806.0330 [hep-ph].

[247] J. R. Ellis, S. Kelley, and D. V. Nanopoulos, Phys. Lett. **B249**, 441 (1990).

[248] J. R. Ellis, S. Kelley, and D. V. Nanopoulos, Phys. Lett. **B260**, 131 (1991).

[249] U. Amaldi, W. de Boer, and H. Furstenau, Phys. Lett. **B260**, 447 (1991).

[250] P. Langacker and M.-x. Luo, Phys. Rev. **D44**, 817 (1991).

[251] R. N. Mohapatra, in *Proceedings of the 1999 Summer School in Particle Physics, Trieste, 1999*, edited by G. Senjanovic and A. Y. Smirnov (World Scientific, Singapore, 1999) pp. 336–394, arXiv:hep-ph/9911272 [hep-ph].

[252] M. B. Green and J. H. Schwarz, Phys. Lett. **B149**, 117 (1984).

[253] M. B. Green, J. H. Schwarz, and E. Witten, *Superstring Theory* (Cambridge University Press, Cambridge, UK, 1987).

[254] H. P. Nilles, M. Srednicki, and D. Wyler, Phys. Lett. **B120**, 346 (1983).

[255] J. M. Frere, D. R. T. Jones, and S. Raby, Nucl. Phys. **B222**, 11 (1983).

[256] J. P. Derendinger and C. A. Savoy, Nucl. Phys. **B237**, 307 (1984).

[257] J. R. Ellis, J. F. Gunion, H. E. Haber, L. Roszkowski, and F. Zwirner, Phys. Rev. **D39**, 844 (1989).

[258] M. Carena, N. R. Shah, and C. E. M. Wagner, Phys. Rev. **D85**, 036003 (2012), arXiv:1110.4378 [hep-ph].

[259] C. Balázs, A. Mazumdar, E. Pukartas, and G. White, JHEP **01**, 073 (2014), arXiv:1309.5091 [hep-ph].

[260] J. Kozaczuk, S. Profumo, L. S. Haskins, and C. L. Wainwright, JHEP **01**, 144 (2015), arXiv:1407.4134 [hep-ph].

[261] A. Vilenkin, Phys. Rept. **121**, 263 (1985).

[262] S. A. Abel, S. Sarkar, and P. L. White, Nucl. Phys. **B454**, 663 (1995), arXiv:hep-ph/9506359 [hep-ph].

[263] H. P. Nilles, M. Srednicki, and D. Wyler, Phys. Lett. **B124**, 337 (1983).

[264] P. Langacker, Rev. Mod. Phys. **81**, 1199 (2009), arXiv:0801.1345 [hep-ph].

[265] P. Binetruy, S. Dawson, I. Hinchliffe, and M. Sher, Nucl. Phys. **B273**, 501 (1986).

[266] J. R. Ellis, K. Enqvist, D. V. Nanopoulos, and F. Zwirner, Nucl. Phys. **B276**, 14 (1986).

[267] L. E. Ibáñez and J. Mas, Nucl. Phys. **B286**, 107 (1987).

[268] J. F. Gunion, L. Roszkowski, and H. E. Haber, Phys. Lett. **B189**, 409 (1987).

[269] J. L. Hewett and T. G. Rizzo, Phys. Rept. **183**, 193 (1989).

[270] J. F. Gunion, H. E. Haber, G. L. Kane, and S. Dawson, *The Higgs Hunter's Guide* (Westview Press, Boulder, 2000) [Erratum: arXiv:hep-ph/9302272].

[271] H. E. Haber and M. Sher, Phys. Rev. **D35**, 2206 (1987).

[272] J. R. Ellis, D. V. Nanopoulos, S. T. Petcov, and F. Zwirner, Nucl. Phys. **B283**, 93 (1987).

[273] M. Drees, Phys. Rev. **D35**, 2910 (1987).

[274] H. Baer, D. Dicus, M. Drees, and X. Tata, Phys. Rev. **D36**, 1363 (1987).

[275] J. F. Gunion, L. Roszkowski, and H. E. Haber, Phys. Rev. **D38**, 105 (1988).

[276] M. Cvetič and P. Langacker, Phys. Rev. **D54**, 3570 (1996), arXiv:hep-ph/9511378 [hep-ph].

[277] M. Cvetič and P. Langacker, Mod. Phys. Lett. **A11**, 1247 (1996), arXiv:hep-ph/9602424 [hep-ph].

[278] S. F. King, S. Moretti, and R. Nevzorov, Phys. Rev. **D73**, 035009 (2006), arXiv:hep-ph/0510419 [hep-ph].

[279] M. Drees, Phys. Lett. **B181**, 279 (1986).

[280] J. S. Hagelin and S. Kelley, Nucl. Phys. **B342**, 95 (1990).

[281] P. Batra, A. Delgado, D. E. Kaplan, and T. M. P. Tait, JHEP **02**, 043 (2004), arXiv:hep-ph/0309149 [hep-ph].

[282] A. Maloney, A. Pierce, and J. G. Wacker, JHEP **06**, 034 (2006), arXiv:hep-ph/0409127 [hep-ph].

[283] M. Dine, N. Seiberg, and S. Thomas, Phys. Rev. **D76**, 095004 (2007), arXiv:0707.0005 [hep-ph].

[284] S. F. King, S. Moretti, and R. Nevzorov, Phys. Lett. **B634**, 278 (2006), arXiv:hep-ph/0511256 [hep-ph].

[285] S. F. King, S. Moretti, and R. Nevzorov, in *Particle physics at the year of 250th Anniversary of Moscow University. Proceedings, 12th Lomonosov Conference on Elementary Particle Physics, Moscow, 2006*, edited by I. Studenikin, A (2006) arXiv:hep-ph/0601269 [hep-ph].

[286] S. Kraml, G. Azuelos, D. Dominici, J. Ellis, G. Grenier, H. E. Haber, J. S. Lee, D. J. Miller, A. Pilaftsis, and W. Porod, eds., *Workshop on CP Studies and Non-Standard Higgs Physics* (CERN, Geneva, Switzerland, 2006) arXiv:hep-ph/0608079 [hep-ph].

[287] S. F. King, S. Moretti, and R. Nevzorov, in *Proceedings of the 33rd International Conference on High Energy Physics (ICHEP'06), Moscow, 2006*, edited by A. Sissakian, G. Kozlov, and E. Kolganova (2007) pp. 138–143, arXiv:hep-ph/0610002 [hep-ph].

[288] R. Howl and S. F. King, JHEP **01**, 030 (2008), arXiv:0708.1451 [hep-ph].

[289] P. Athron, J. P. Hall, R. Howl, S. F. King, D. J. Miller, S. Moretti, and R. Nevzorov, in *The International Workshop on Beyond the Standard Model Physics and LHC Signatures (BSM-LHC), Boston, USA, 2009*, edited by G. Alverson, P. Nath, and B. D. Nelson (2010) pp. 120–129.

[290] P. Athron, S. F. King, D. J. Miller, S. Moretti, and R. Nevzorov, Phys. Rev. **D84**, 055006 (2011), arXiv:1102.4363 [hep-ph].

[291] A. Belyaev, J. P. Hall, S. F. King, and P. Svantesson, Phys. Rev. **D86**, 031702 (2012), arXiv:1203.2495 [hep-ph].

[292] A. Belyaev, J. P. Hall, S. F. King, and P. Svantesson, Phys. Rev. **D87**, 035019 (2013), arXiv:1211.1962 [hep-ph].

[293] D. J. Gross, J. A. Harvey, E. J. Martinec, and R. Rohm, Phys. Rev. Lett. **54**, 502 (1985).

[294] E. Witten, Phys. Lett. **149B**, 351 (1984).

[295] D. J. Gross, J. A. Harvey, E. J. Martinec, and R. Rohm, Nucl. Phys. **B256**, 253 (1985).

[296] D. J. Gross, J. A. Harvey, E. J. Martinec, and R. Rohm, Nucl. Phys. **B267**, 75 (1986).

[297] P. Candelas, G. T. Horowitz, A. Strominger, and E. Witten, Nucl. Phys. **B258**, 46 (1985).

[298] E. Witten, Nucl. Phys. **B258**, 75 (1985).

[299] F. del Aguila, G. A. Blair, M. Daniel, and G. G. Ross, Nucl. Phys. **B272**, 413 (1986).

[300] R. Nevzorov, Phys. Rev. **D87**, 015029 (2013), arXiv:1205.5967 [hep-ph].

[301] R. Slansky, Phys. Rept. **79**, 1 (1981).

[302] P. Horava and E. Witten, Nucl. Phys. **B460**, 506 (1996), arXiv:hep-th/9510209 [hep-th].

[303] P. Horava and E. Witten, Nucl. Phys. **B475**, 94 (1996), arXiv:hep-th/9603142 [hep-th].

[304] E. Witten, Nucl. Phys. **B471**, 135 (1996), arXiv:hep-th/9602070 [hep-th].

[305] T. Banks and M. Dine, Nucl. Phys. **B479**, 173 (1996), arXiv:hep-th/9605136 [hep-th].

[306] K. Choi, H. B. Kim, and C. Muñoz, Phys. Rev. **D57**, 7521 (1998), arXiv:hep-th/9711158 [hep-th].

[307] Y. Hosotani, Phys. Lett. **B129**, 193 (1983).

[308] D. London and J. L. Rosner, Phys. Rev. **D34**, 1530 (1986).

[309] J. Kang, P. Langacker, and B. D. Nelson, Phys. Rev. **D77**, 035003 (2008), arXiv:0708.2701 [hep-ph].

[310] E. Accomando, A. Belyaev, L. Fedeli, S. F. King, and C. Shepherd-Themistocleous, Phys. Rev. **D83**, 075012 (2011), arXiv:1010.6058 [hep-ph].

[311] D. J. Miller, A. P. Morais, and P. N. Pandita, Phys. Rev. **D87**, 015007 (2013), arXiv:1208.5906 [hep-ph].

[312] Y. Daikoku and D. Suematsu, Phys. Rev. **D62**, 095006 (2000), arXiv:hep-ph/0003205 [hep-ph].

[313] V. Barger, P. Langacker, H.-S. Lee, and G. Shaughnessy, Phys. Rev. **D73**, 115010 (2006), arXiv:hep-ph/0603247 [hep-ph].

[314] V. Barger, P. Langacker, and G. Shaughnessy, New J. Phys. **9**, 333 (2007), arXiv:hep-ph/0702001 [HEP-PH].

[315] E. Keith and E. Ma, Phys. Rev. **D56**, 7155 (1997), arXiv:hep-ph/9704441 [hep-ph].

[316] D. Suematsu, Mod. Phys. Lett. **A12**, 1709 (1997), arXiv:hep-ph/9705412 [hep-ph].

[317] A. Gutierrez-Rodriguez, M. A. Hernandez-Ruiz, and M. A. Perez, Int. J. Mod. Phys. **A22**, 3493 (2007), arXiv:hep-ph/0611235 [hep-ph].

[318] D. Suematsu, Phys. Lett. **B416**, 108 (1998), arXiv:hep-ph/9705405 [hep-ph].

[319] D. Suematsu, Phys. Rev. **D57**, 1738 (1998), arXiv:hep-ph/9708413 [hep-ph].

[320] E. Keith and E. Ma, Phys. Rev. **D54**, 3587 (1996), arXiv:hep-ph/9603353 [hep-ph].

[321] S. Hesselbach, F. Franke, and H. Fraas, Eur. Phys. J. **C23**, 149 (2002), arXiv:hep-ph/0107080 [hep-ph].

[322] V. Barger, P. Langacker, and H.-S. Lee, Phys. Lett. **B630**, 85 (2005), arXiv:hep-ph/0508027 [hep-ph].

[323] S. Y. Choi, H. E. Haber, J. Kalinowski, and P. M. Zerwas, Nucl. Phys. **B778**, 85 (2007), arXiv:hep-ph/0612218 [hep-ph].

[324] V. Barger, P. Langacker, I. Lewis, M. McCaskey, G. Shaughnessy, and B. Yencho, Phys. Rev. **D75**, 115002 (2007), arXiv:hep-ph/0702036 [HEP-PH].

[325] T. Gherghetta, T. A. Kaeding, and G. L. Kane, Phys. Rev. **D57**, 3178 (1998), arXiv:hep-ph/9701343 [hep-ph].

[326] M. Asano, T. Kikuchi, and S.-G. Kim, (2008), arXiv:0807.5084 [hep-ph].

[327] B. Stech and Z. Tavartkiladze, Phys. Rev. **D77**, 076009 (2008), arXiv:0802.0894 [hep-ph].

[328] R. Howl and S. F. King, JHEP **05**, 008 (2008), arXiv:0802.1909 [hep-ph].

[329] R. Howl and S. F. King, Phys. Lett. **B687**, 355 (2010), arXiv:0908.2067 [hep-ph].

[330] J. E. Camargo-Molina, A. P. Morais, R. Pasechnik, and J. Wessén, (2016), arXiv:1606.03492 [hep-ph].

[331] D. Suematsu and Y. Yamagishi, Int. J. Mod. Phys. **A10**, 4521 (1995), arXiv:hep-ph/9411239 [hep-ph].

[332] M. Cvetič, D. A. Demir, J. R. Espinosa, L. L. Everett, and P. Langacker, Phys. Rev. **D56**, 2861 (1997), [Erratum: Phys. Rev. **D58**, 119905 (1998)], arXiv:hep-ph/9703317 [hep-ph].

[333] P. Langacker and J. Wang, Phys. Rev. **D58**, 115010 (1998), arXiv:hep-ph/9804428 [hep-ph].

[334] E. Ma and M. Raidal, J. Phys. **G28**, 95 (2002), arXiv:hep-ph/0012366 [hep-ph].

[335] J. Kang, P. Langacker, T.-j. Li, and T. Liu, Phys. Rev. Lett. **94**, 061801 (2005), arXiv:hep-ph/0402086 [hep-ph].

[336] J. A. Grifols, J. Solà, and A. Méndez, Phys. Rev. Lett. **57**, 2348 (1986).

[337] D. A. Morris, Phys. Rev. **D37**, 2012 (1988).

[338] S. W. Ham, J. O. Im, E. J. Yoo, and S. K. Oh, JHEP **12**, 017 (2008), arXiv:0810.4194 [hep-ph].

[339] R. W. Robinett and J. L. Rosner, Phys. Rev. **D26**, 2396 (1982).

[340] V. Barger, P. Langacker, and H.-S. Lee, Phys. Rev. **D67**, 075009 (2003), arXiv:hep-ph/0302066 [hep-ph].

[341] M. Fukugita and T. Yanagida, Phys. Lett. **B174**, 45 (1986).

[342] V. A. Kuzmin, V. A. Rubakov, and M. E. Shaposhnikov, Phys. Lett. **B155**, 36 (1985).

[343] R. Howl and S. F. King, Phys. Lett. **B652**, 331 (2007), arXiv:0705.0301 [hep-ph].

[344] J. P. Hall and S. F. King, JHEP **06**, 006 (2011), arXiv:1104.2259 [hep-ph].

[345] J. C. Callaghan and S. F. King, JHEP **04**, 034 (2013), arXiv:1210.6913 [hep-ph].

[346] J. C. Callaghan, S. F. King, and G. K. Leontaris, JHEP **12**, 037 (2013), arXiv:1307.4593 [hep-ph].

[347] P. Athron, M. Mühlleitner, R. Nevzorov, and A. G. Williams, JHEP **01**, 153 (2015), arXiv:1410.6288 [hep-ph].

[348] S. F. King and R. Nevzorov, JHEP **03**, 139 (2016), arXiv:1601.07242 [hep-ph].

[349] J. P. Hall and S. F. King, JHEP **08**, 088 (2009), arXiv:0905.2696 [hep-ph].

[350] S. F. King, S. Moretti, and R. Nevzorov, Phys. Lett. **B650**, 57 (2007), arXiv:hep-ph/0701064 [hep-ph].

[351] R. B. Nevzorov and M. A. Trusov, Phys. Atom. Nucl. **64**, 1299 (2001), [Yad. Fiz. 64, 1375 (2001)], arXiv:hep-ph/0110363 [hep-ph].

[352] R. Nevzorov, Phys. Rev. **D89**, 055010 (2014), arXiv:1309.4738 [hep-ph].

[353] R. Nevzorov, in *Proceedings, 2015 European Physical Society Conference on High Energy Physics (EPS-HEP 2015), Vienna, 2015* (SISSA, Trieste, Italy, 2015) p. 381, arXiv:1510.05387 [hep-ph].

[354] M. Sperling, D. Stöckinger, and A. Voigt, JHEP **07**, 132 (2013), arXiv:1305.1548 [hep-ph].

[355] M. Sperling, D. Stöckinger, and A. Voigt, JHEP **01**, 068 (2014), arXiv:1310.7629 [hep-ph].

[356] P. Athron, D. Stöckinger, and A. Voigt, Phys. Rev. **D86**, 095012 (2012), arXiv:1209.1470 [hep-ph].

[357] E. Ma, Phys. Rev. Lett. **60**, 1363 (1988).

[358] J. Rich, D. Lloyd Owen, and M. Spiro, Phys. Rept. **151**, 239 (1987).

[359] P. F. Smith, Contemp. Phys. **29**, 159 (1988).

[360] T. K. Hemmick *et al.*, Phys. Rev. **D41**, 2074 (1990).

[361] S. Wolfram, Phys. Lett. **B82**, 65 (1979).

[362] C. B. Dover, T. K. Gaisser, and G. Steigman, Phys. Rev. Lett. **42**, 1117 (1979).

[363] P. Athron, S. F. King, D. J. Miller, S. Moretti, and R. Nevzorov, Phys. Rev. **D80**, 035009 (2009), arXiv:0904.2169 [hep-ph].

[364] S. Hesselbach, D. J. Miller, G. Moortgat-Pick, R. Nevzorov, and M. Trusov, Phys. Lett. **B662**, 199 (2008), arXiv:0712.2001 [hep-ph].

[365] S. Hesselbach, D. J. Miller, G. Moortgat-Pick, R. Nevzorov, and M. Trusov, in *SUSY 2007 Proceedings, 15th International Conference on Supersymmetry and Unification of Fundamental Interactions, Karlsruhe, 2007*, edited by W. de Boer and I. Gebauer (2007) arXiv:0710.2550 [hep-ph].

[366] S. Hesselbach, G. Moortgat-Pick, D. J. Miller, R. Nevzorov, and M. Trusov, in *Proceedings of the 34th International Conference in High Energy Physics (ICHEP08), Philadelphia, 2008* (2008) arXiv:0810.0511 [hep-ph].

[367] J. P. Hall, S. F. King, R. Nevzorov, S. Pakvasa, and M. Sher, Phys. Rev. **D83**, 075013 (2011), arXiv:1012.5114 [hep-ph].

[368] J. P. Hall, S. F. King, R. Nevzorov, S. Pakvasa, and M. Sher, in *Proceedings, 19th International Workshop in Honoring and Celebrating the 100th Anniversary of Academician Sergey Nikolaevich Vernov on High Energy Physics and Quantum Field Theory (QFTHEP2010)*, edited by N. Nikitin (2010) p. 069, arXiv:1012.5365 [hep-ph].

[369] J. P. Hall, S. F. King, R. Nevzorov, S. Pakvasa, and M. Sher, in *Particles and fields. Proceedings, Meeting of the Division of the American Physical Society, DPF 2011, Providence, 2011*, edited by T. Speer (2011) arXiv:1109.4972 [hep-ph].

[370] E. Aprile *et al.* (XENON100), Phys. Rev. Lett. **107**, 131302 (2011), arXiv:1104.2549 [astro-ph.CO].

[371] E. Aprile *et al.* (XENON100), Phys. Rev. Lett. **109**, 181301 (2012), arXiv:1207.5988 [astro-ph.CO].

[372] D. S. Akerib *et al.* (LUX), Phys. Rev. Lett. **112**, 091303 (2014), arXiv:1310.8214 [astro-ph.CO].

[373] D. S. Akerib *et al.* (LUX), Phys. Rev. Lett. **116**, 161301 (2016), arXiv:1512.03506 [astro-ph.CO].

[374] D. S. Akerib *et al.* (LUX), Phys. Rev. Lett. **118**, 021303 (2017), arXiv:1608.07648 [astro-ph.CO].

[375] P. Athron, A. W. Thomas, S. J. Underwood, and M. J. White, Phys. Rev. **D95**, 035023 (2017), arXiv:1611.05966 [hep-ph].

[376] P. Athron, S. F. King, D. J. Miller, S. Moretti, and R. Nevzorov, Phys. Lett. **B681**, 448 (2009), arXiv:0901.1192 [hep-ph].

[377] J. A. Casas and C. Muñoz, Phys. Lett. **B306**, 288 (1993), arXiv:hep-ph/9302227 [hep-ph].

[378] P. Athron, S. F. King, D. J. Miller, S. Moretti, and R. Nevzorov, Phys. Rev. **D86**, 095003 (2012), arXiv:1206.5028 [hep-ph].

[379] B. Holdom, Phys. Lett. **B166**, 196 (1986).

[380] K. S. Babu, C. F. Kolda, and J. March-Russell, Phys. Rev. **D57**, 6788 (1998), arXiv:hep-ph/9710441 [hep-ph].

[381] F. del Aguila, J. A. Gonzalez, and M. Quiros, Nucl. Phys. **B307**, 571 (1988).

[382] F. del Aguila, G. D. Coughlan, and M. Quiros, Nucl. Phys. **B307**, 633 (1988), [Erratum: Nucl. Phys. **B312**, 751 (1989)].

[383] R. M. Fonseca, M. Malinský, W. Porod, and F. Staub, Nucl. Phys. **B854**, 28 (2012), arXiv:1107.2670 [hep-ph].

[384] T. G. Rizzo, Phys. Rev. **D59**, 015020 (1998), arXiv:hep-ph/9806397 [hep-ph].

[385] E. Salvioni, G. Villadoro, and F. Zwirner, JHEP **11**, 068 (2009), arXiv:0909.1320 [hep-ph].

[386] M. E. Krauss, B. O'Leary, W. Porod, and F. Staub, Phys. Rev. **D86**, 055017 (2012), arXiv:1206.3513 [hep-ph].

[387] J. Erler, P. Langacker, S. Munir, and E. Rojas, JHEP **08**, 017 (2009), arXiv:0906.2435 [hep-ph].

[388] *Search for new high-mass resonances in the dilepton final state using proton-proton collisions at $\sqrt{s}$ = 13 TeV with the ATLAS detector*, Tech. Rep. ATLAS-CONF-2016-045 (CERN, Geneva, Switzerland, 2016).

[389] P. Athron, M. Binjonaid, and S. F. King, Phys. Rev. **D87**, 115023 (2013), arXiv:1302.5291 [hep-ph].

[390] A. Belyaev, S. F. King, and P. Svantesson, Phys. Rev. **D88**, 035015 (2013), arXiv:1303.0770 [hep-ph].

[391] D. J. Miller, R. Nevzorov, and P. M. Zerwas, Nucl. Phys. **B681**, 3 (2004), arXiv:hep-ph/0304049 [hep-ph].

[392] D. J. Miller and R. Nevzorov, (2003), arXiv:hep-ph/0309143 [hep-ph].

[393] D. J. Miller, S. Moretti, and R. Nevzorov, in *High Energy Physics and Quantum Field Theory. Proceedings, 18th International Workshop, QFTHEP 2004, St. Petersburg, 2004*, edited by M. N. Dubinin and V. I. Savrin (2005) pp. 212–219, arXiv:hep-ph/0501139 [hep-ph].

[394] S. F. King, M. Mühlleitner, R. Nevzorov, and K. Walz, Phys. Rev. **D90**, 095014 (2014), arXiv:1408.1120 [hep-ph].

[395] R. Nevzorov and D. J. Miller, in *7th Workshop on What Comes Beyond the Standard Model, Bled, 2004*, edited by N. Mankoc Borstnik, D. Lukman, H. B. Nielsen, and C. Froggatt (2004) pp. 107–117, arXiv:hep-ph/0411275 [hep-ph].

[396] P. A. Kovalenko, R. B. Nevzorov, and K. A. Ter-Martirosian, Phys. Atom. Nucl. **61**, 812 (1998), [Yad. Fiz. 61, 898 (1998)].

[397] R. B. Nevzorov and M. A. Trusov, J. Exp. Theor. Phys. **91**, 1079 (2000), [Zh. Eksp. Teor. Fiz. 91, 1251 (2000)], arXiv:hep-ph/0106351 [hep-ph].

[398] R. B. Nevzorov, K. A. Ter-Martirosyan, and M. A. Trusov, in *Physics of Fundamental Interactions. Proceedings, Conference, Moscow, Russia, 2000*, edited by Y. G. Abov (2002) pp. 285–298, [Yad. Fiz. 65, 311 (2002)], arXiv:hep-ph/0105178 [hep-ph].

[399] R. Nevzorov and S. Pakvasa, Phys. Lett. **B728**, 210 (2014), arXiv:1308.1021 [hep-ph].

[400] R. Nevzorov and S. Pakvasa, in *Proceedings of the 37th International Conference on High Energy Physics (ICHEP 2014), Valencia, 2014*, edited by M. Aguilar-Benítez, J. Fuster, S. Martí-García, and A. Santamaría (2016) pp. 690–695, arXiv:1411.0386 [hep-ph].

[401] P. Athron, M. Mühlleitner, R. Nevzorov, and A. G. Williams, in *17th Lomonosov Conference on Elementary Particle Physics, Moscow, 2015* (2016) arXiv:1602.04453 [hep-ph].

[402] P. Athron, S. F. King, D. J. Miller, S. Moretti, and R. Nevzorov, in *Proceedings of the 34th International Conference in High Energy Physics (ICHEP08), Philadelphia, 2008* (2008) arXiv:0810.0617 [hep-ph].

[403] B. C. Allanach, Comput. Phys. Commun. **143**, 305 (2002), arXiv:hep-ph/0104145 [hep-ph].

[404] W. Porod, Comput. Phys. Commun. **153**, 275 (2003), arXiv:hep-ph/0301101 [hep-ph].

[405] H. Baer, F. E. Paige, S. D. Protopopescu, and X. Tata, (1999), arXiv:hep-ph/0001086 [hep-ph].

[406] A. Djouadi, J.-L. Kneur, and G. Moultaka, Comput. Phys. Commun. **176**, 426 (2007), arXiv:hep-ph/0211331 [hep-ph].

[407] B. C. Allanach, P. Athron, L. C. Tunstall, A. Voigt, and A. G. Williams, Comput. Phys. Commun. **185**, 2322 (2014), arXiv:1311.7659 [hep-ph].

[408] W. Porod and F. Staub, Comput. Phys. Commun. **183**, 2458 (2012), arXiv:1104.1573 [hep-ph].

[409] U. Ellwanger, J. F. Gunion, and C. Hugonie, JHEP **02**, 066 (2005), arXiv:hep-ph/0406215 [hep-ph].

[410] U. Ellwanger and C. Hugonie, Comput. Phys. Commun. **175**, 290 (2006), arXiv:hep-ph/0508022 [hep-ph].

[411] U. Ellwanger and C. Hugonie, Comput. Phys. Commun. **177**, 399 (2007), arXiv:hep-ph/0612134 [hep-ph].

[412] J. Baglio, R. Gröber, M. Mühlleitner, D. T. Nhung, H. Rzehak, M. Spira, J. Streicher, and K. Walz, Comput. Phys. Commun. **185**, 3372 (2014), arXiv:1312.4788 [hep-ph].

[413] A. Djouadi, J. Kalinowski, and M. Spira, Comput. Phys. Commun. **108**, 56 (1998), arXiv:hep-ph/9704448 [hep-ph].

[414] J. M. Butterworth *et al.*, in *Physics at TeV colliders. Proceedings, 6th Workshop, dedicated to Thomas Binoth, Les Houches, 2009*, edited by G. Bélanger, F. Boudjema, and J.-P. Guillet (2010) arXiv:1003.1643 [hep-ph].

[415] M. Mühlleitner, A. Djouadi, and Y. Mambrini, Comput. Phys. Commun. **168**, 46 (2005), arXiv:hep-ph/0311167 [hep-ph].

[416] D. Das, U. Ellwanger, and A. M. Teixeira, Comput. Phys. Commun. **183**, 774 (2012), arXiv:1106.5633 [hep-ph].

[417] A. Djouadi, M. M. Mühlleitner, and M. Spira, in *Physics at LHC. Proceedings, 3rd Conference, Cracow, 2006*, edited by K. Fialkowski and B. Muryn (2007) pp. 635–644, arXiv:hep-ph/0609292 [hep-ph].

[418] H. Hlucha, H. Eberl, and W. Frisch, Comput. Phys. Commun. **183**, 2307 (2012), arXiv:1104.2151 [hep-ph].

[419] B. Allanach, S. Kraml, and W. Porod, in *Supersymmetry and Unification of Fundamental Interactions. Proceedings, 10th International Conference, SUSY'02,*

Hamburg, 2002, edited by P. Nath and P. M. Zerwas (2002) pp. 904–910, arXiv:hep-ph/0207314 [hep-ph].

[420] B. C. Allanach, S. Kraml, and W. Porod, JHEP **03**, 016 (2003), arXiv:hep-ph/0302102 [hep-ph].

[421] B. C. Allanach, G. Bélanger, F. Boudjema, A. Pukhov, and W. Porod, (2004), arXiv:hep-ph/0402161 [hep-ph].

[422] F. Staub, P. Athron, U. Ellwanger, R. Gröber, M. Mühlleitner, P. Slavich, and A. Voigt, Comput. Phys. Commun. **202**, 113 (2016), arXiv:1507.05093 [hep-ph].

[423] F. Staub, (2008), arXiv:0806.0538 [hep-ph].

[424] F. Staub, Comput. Phys. Commun. **181**, 1077 (2010), arXiv:0909.2863 [hep-ph].

[425] F. Staub, Comput. Phys. Commun. **182**, 808 (2011), arXiv:1002.0840 [hep-ph].

[426] F. Staub, Comput. Phys. Commun. **184**, 1792 (2013), arXiv:1207.0906 [hep-ph].

[427] F. Staub, Comput. Phys. Commun. **185**, 1773 (2014), arXiv:1309.7223 [hep-ph].

[428] P. Athron, J.-h. Park, D. Stöckinger, and A. Voigt, Comput. Phys. Commun. **190**, 139 (2015), arXiv:1406.2319 [hep-ph].

[429] P. Athron, J.-h. Park, D. Stöckinger, and A. Voigt, in *Proceedings of the 37th International Conference on High Energy Physics (ICHEP 2014), Valencia, 2014*, edited by M. Aguilar-Benítez, J. Fuster, S. Martí-García, and A. Santamaría (2016) pp. 2424–2426, arXiv:1410.7385 [hep-ph].

[430] N. D. Christensen and C. Duhr, Comput. Phys. Commun. **180**, 1614 (2009), arXiv:0806.4194 [hep-ph].

[431] A. Alloul, N. D. Christensen, C. Degrande, C. Duhr, and B. Fuks, Comput. Phys. Commun. **185**, 2250 (2014), arXiv:1310.1921 [hep-ph].

[432] A. V. Semenov, (1996), arXiv:hep-ph/9608488 [hep-ph].

[433] A. Semenov, Comput. Phys. Commun. **115**, 124 (1998).

[434] A. V. Semenov, (2002), arXiv:hep-ph/0208011 [hep-ph].

[435] A. Semenov, Comput. Phys. Commun. **180**, 431 (2009), arXiv:0805.0555 [hep-ph].

[436] A. Semenov, (2010), arXiv:1005.1909 [hep-ph].

[437] E. E. Boos, M. N. Dubinin, V. A. Ilyin, A. E. Pukhov, and V. I. Savrin (1994) arXiv:hep-ph/9503280 [hep-ph].

[438] A. Belyaev, N. D. Christensen, and A. Pukhov, Comput. Phys. Commun. **184**, 1729 (2013), arXiv:1207.6082 [hep-ph].

[439] G. Bélanger, F. Boudjema, A. Pukhov, and A. Semenov, Comput. Phys. Commun. **149**, 103 (2002), arXiv:hep-ph/0112278 [hep-ph].

[440] G. Bélanger, F. Boudjema, A. Pukhov, and A. Semenov, Comput. Phys. Commun. **174**, 577 (2006), arXiv:hep-ph/0405253 [hep-ph].

[441] G. Bélanger, F. Boudjema, A. Pukhov, and A. Semenov, Comput. Phys. Commun. **176**, 367 (2007), arXiv:hep-ph/0607059 [hep-ph].

[442] G. Bélanger, F. Boudjema, A. Pukhov, and A. Semenov, Comput. Phys. Commun. **180**, 747 (2009), arXiv:0803.2360 [hep-ph].

[443] G. Bélanger, F. Boudjema, P. Brun, A. Pukhov, S. Rosier-Lees, P. Salati, and A. Semenov, Comput. Phys. Commun. **182**, 842 (2011), arXiv:1004.1092 [hep-ph].

[444] G. Bélanger, F. Boudjema, A. Pukhov, and A. Semenov, Comput. Phys. Commun. **185**, 960 (2014), arXiv:1305.0237 [hep-ph].

[445] G. Bélanger, F. Boudjema, A. Pukhov, and A. Semenov, Comput. Phys. Commun. **192**, 322 (2015), arXiv:1407.6129 [hep-ph].

[446] J. E. Camargo-Molina, B. O'Leary, W. Porod, and F. Staub, Eur. Phys. J. **C73**, 2588 (2013), arXiv:1307.1477 [hep-ph].

[447] J. Alwall, M. Herquet, F. Maltoni, O. Mattelaer, and T. Stelzer, JHEP **06**, 128 (2011), arXiv:1106.0522 [hep-ph].

[448] J. Alwall, R. Frederix, S. Frixione, V. Hirschi, F. Maltoni, O. Mattelaer, H. S. Shao, T. Stelzer, P. Torrielli, and M. Zaro, JHEP **07**, 079 (2014), arXiv:1405.0301 [hep-ph].

[449] P. Bechtle, O. Brein, S. Heinemeyer, G. Weiglein, and K. E. Williams, Comput. Phys. Commun. **181**, 138 (2010), arXiv:0811.4169 [hep-ph].

[450] P. Bechtle, O. Brein, S. Heinemeyer, G. Weiglein, and K. E. Williams, Comput. Phys. Commun. **182**, 2605 (2011), arXiv:1102.1898 [hep-ph].

[451] P. Bechtle, S. Heinemeyer, O. Stål, T. Stefaniak, and G. Weiglein, Eur. Phys. J. **C74**, 2711 (2014), arXiv:1305.1933 [hep-ph].

[452] M. Moretti, T. Ohl, and J. Reuter, in *Proceedings of the 2nd Workshop of the 2nd Joint ECFA/DESY Study on Physics and Detectors for a Linear Electron Positron Collider, 1998-2001, Vol. 1-3*, edited by T. Behnke, S. Bertolucci, R. D. Heuer, D. Miller, F. Richard, R. Settles, V. Telnov, and P. Zerwas (2001) pp. 1981–2009, arXiv:hep-ph/0102195 [hep-ph].

[453] W. Kilian, T. Ohl, and J. Reuter, Eur. Phys. J. **C71**, 1742 (2011), arXiv:0708.4233 [hep-ph].

[454] U. Ellwanger, M. Rausch de Traubenberg, and C. A. Savoy, Phys. Lett. **B315**, 331 (1993), arXiv:hep-ph/9307322 [hep-ph].

[455] U. Ellwanger, M. Rausch de Traubenberg, and C. A. Savoy, Z. Phys. **C67**, 665 (1995), arXiv:hep-ph/9502206 [hep-ph].

[456] U. Ellwanger, M. Rausch de Traubenberg, and C. A. Savoy, Nucl. Phys. **B492**, 21 (1997), arXiv:hep-ph/9611251 [hep-ph].

[457] B. C. Allanach, D. P. George, and B. Gripaios, JHEP **07**, 098 (2013), arXiv:1304.5462 [hep-ph].

[458] B. C. Allanach, D. P. George, and B. Nachman, JHEP **02**, 031 (2014), arXiv:1311.3960 [hep-ph].

[459] S. P. Martin and M. T. Vaughn, Phys. Rev. **D50**, 2282 (1994), [Erratum: Phys. Rev. **D78**, 039903 (2008)], arXiv:hep-ph/9311340 [hep-ph].

[460] Y. Yamada, Phys. Rev. **D50**, 3537 (1994), arXiv:hep-ph/9401241 [hep-ph].

[461] I. Jack, D. R. T. Jones, and A. Pickering, Phys. Lett. **B426**, 73 (1998), arXiv:hep-ph/9712542 [hep-ph].

[462] M. D. Goodsell, JHEP **01**, 066 (2013), arXiv:1206.6697 [hep-ph].

[463] J. Iliopoulos and B. Zumino, Nucl. Phys. **B76**, 310 (1974).

[464] S. Ferrara, J. Iliopoulos, and B. Zumino, Nucl. Phys. **B77**, 413 (1974).

[465] M. T. Grisaru, W. Siegel, and M. Roček, Nucl. Phys. **B159**, 429 (1979).

[466] P. Fayet, Phys. Lett. **B78**, 417 (1978).

[467] J. Polchinski and L. Susskind, Phys. Rev. **D26**, 3661 (1982).

[468] L. J. Hall and L. Randall, Nucl. Phys. **B352**, 289 (1991).

[469] P. J. Fox, A. E. Nelson, and N. Weiner, JHEP **08**, 035 (2002), arXiv:hep-ph/0206096 [hep-ph].

[470] M. E. Machacek and M. T. Vaughn, Nucl. Phys. **B222**, 83 (1983).

[471] M. E. Machacek and M. T. Vaughn, Nucl. Phys. **B236**, 221 (1984).

[472] M. E. Machacek and M. T. Vaughn, Nucl. Phys. **B249**, 70 (1985).

[473] M.-x. Luo, H.-w. Wang, and Y. Xiao, Phys. Rev. **D67**, 065019 (2003), arXiv:hep-ph/0211440 [hep-ph].

[474] R. M. Fonseca, M. Malinský, and F. Staub, Phys. Lett. **B726**, 882 (2013), arXiv:1308.1674 [hep-ph].

[475] J. A. Casas, J. R. Espinosa, and H. E. Haber, Nucl. Phys. **B526**, 3 (1998), arXiv:hep-ph/9801365 [hep-ph].

[476] M. Galassi, J. Davies, J. Theiler, B. Gough, G. Jungman, P. Alken, M. Booth, and F. Rossi, *GNU Scientific Library Reference Manual*, 3rd ed. (Network Theory Ltd., 2009).

[477] L. J. Hall, Nucl. Phys. **B178**, 75 (1981).

[478] S. P. Martin and M. T. Vaughn, Phys. Lett. **B318**, 331 (1993), arXiv:hep-ph/9308222 [hep-ph].

[479] "Boost C++ libraries," `http://www.boost.org/`.

[480] K. L. Chan, U. Chattopadhyay, and P. Nath, Phys. Rev. **D58**, 096004 (1998), arXiv:hep-ph/9710473 [hep-ph].

[481] J. L. Feng and T. Moroi, Phys. Rev. **D61**, 095004 (2000), arXiv:hep-ph/9907319 [hep-ph].

[482] J. L. Feng, K. T. Matchev, and T. Moroi, Phys. Rev. Lett. **84**, 2322 (2000), arXiv:hep-ph/9908309 [hep-ph].

[483] M. Aaboud *et al.* (ATLAS), JHEP **09**, 001 (2016), arXiv:1606.03833 [hep-ex].

[484] V. Khachatryan *et al.* (CMS), Phys. Rev. Lett. **117**, 051802 (2016), arXiv:1606.04093 [hep-ex].

[485] V. Khachatryan *et al.* (CMS), Phys. Lett. **B767**, 147 (2017), arXiv:1609.02507 [hep-ex].

[486] S. Catani, L. Cieri, D. de Florian, G. Ferrera, and M. Grazzini, Phys. Rev. Lett. **108**, 072001 (2012), [Erratum: Phys. Rev. Lett. **117**, no. 8, 089901 (2016)], arXiv:1110.2375 [hep-ph].

[487] P. Jain, S. Mitra, P. Sanyal, and R. K. Verma, (2016), arXiv:1605.07360 [hep-ph].

[488] M. Spira, A. Djouadi, D. Graudenz, and P. M. Zerwas, Nucl. Phys. **B453**, 17 (1995), arXiv:hep-ph/9504378 [hep-ph].

[489] A. Djouadi, Phys. Rept. **457**, 1 (2008), arXiv:hep-ph/0503172 [hep-ph].

[490] M. Kramer, E. Laenen, and M. Spira, Nucl. Phys. **B511**, 523 (1998), arXiv:hep-ph/9611272 [hep-ph].

[491] K. G. Chetyrkin, B. A. Kniehl, and M. Steinhauser, Phys. Rev. Lett. **79**, 353 (1997), arXiv:hep-ph/9705240 [hep-ph].

[492] K. G. Chetyrkin, J. H. Kuhn, and C. Sturm, Nucl. Phys. **B744**, 121 (2006), arXiv:hep-ph/0512060 [hep-ph].

[493] Y. Schröder and M. Steinhauser, JHEP **01**, 051 (2006), arXiv:hep-ph/0512058 [hep-ph].

[494] P. A. Baikov and K. G. Chetyrkin, Phys. Rev. Lett. **97**, 061803 (2006), arXiv:hep-ph/0604194 [hep-ph].

[495] S. Dawson, A. Djouadi, and M. Spira, Phys. Rev. Lett. **77**, 16 (1996), arXiv:hep-ph/9603423 [hep-ph].

[496] LHC Higgs Cross Section Working Group, *Handbook of LHC Higgs Cross Sections: 3. Higgs Properties*, edited by S. Heinemeyer, C. Mariotti, G. Passarino, and R. Tanaka (CERN, Geneva, Switzerland, 2013) arXiv:1307.1347 [hep-ph].

[497] M. Drees, N. K. Falck, and M. Gluck, Phys. Lett. B **167**, 187 (1986).

[498] J. L. Feng, K. T. Matchev, and T. Moroi, Phys. Rev. **D61**, 075005 (2000), arXiv:hep-ph/9909334 [hep-ph].

[499] J. L. Feng and K. T. Matchev, Phys. Rev. **D63**, 095003 (2001), arXiv:hep-ph/0011356 [hep-ph].

[500] S. Akula, M. Liu, P. Nath, and G. Peim, Phys. Lett. **B709**, 192 (2012), arXiv:1111.4589 [hep-ph].

[501] J. L. Feng, K. T. Matchev, and D. Sanford, Phys. Rev. **D85**, 075007 (2012), arXiv:1112.3021 [hep-ph].

[502] J. L. Feng and D. Sanford, Phys. Rev. **D86**, 055015 (2012), arXiv:1205.2372 [hep-ph].

[503] M. Liu and P. Nath, Phys. Rev. **D87**, 095012 (2013), arXiv:1303.7472 [hep-ph].

[504] R. Barbieri, L. J. Hall, Y. Nomura, and V. S. Rychkov, Phys. Rev. **D75**, 035007 (2007), arXiv:hep-ph/0607332 [hep-ph].

[505] L. J. Hall, D. Pinner, and J. T. Ruderman, JHEP **04**, 131 (2012), arXiv:1112.2703 [hep-ph].

[506] A. C. Kraan, in *Fundamental interactions. Proceedings, 20th Winter Institute, Lake Louise, 2005*, edited by A. Astbury, B. Campbell, F. Khanna, R. Moore, and M. Vincter (World Scientific, Hackensack, USA, 2005) pp. 189–193, arXiv:hep-ex/0505002 [hep-ex].

[507] G. W. Anderson and D. J. Castano, Phys. Lett. B **347**, 300 (1995), arXiv:hep-ph/9409419 [hep-ph].

[508] G. W. Anderson and D. J. Castano, Phys. Rev. D **52**, 1693 (1995), arXiv:hep-ph/9412322 [hep-ph].

[509] G. W. Anderson and D. J. Castano, Phys. Rev. D **53**, 2403 (1996), arXiv:hep-ph/9509212 [hep-ph].

[510] G. W. Anderson, D. J. Castano, and A. Riotto, Phys. Rev. D **55**, 2950 (1997), arXiv:hep-ph/9609463 [hep-ph].

[511] P. Ciafaloni and A. Strumia, Nucl. Phys. **B494**, 41 (1997), arXiv:hep-ph/9611204 [hep-ph].

[512] R. Barbieri and A. Strumia, Phys. Lett. B **433**, 63 (1998), arXiv:hep-ph/9801353 [hep-ph].

[513] L. Giusti, A. Romanino, and A. Strumia, Nucl. Phys. **B550**, 3 (1999), arXiv:hep-ph/9811386 [hep-ph].

[514] J. A. Casas, J. R. Espinosa, and I. Hidalgo, J. High Energy Phys. **0401**, 008 (2004), arXiv:hep-ph/0310137 [hep-ph].

[515] J. A. Casas, J. R. Espinosa, and I. Hidalgo, in *String Phenomenology 2003*, edited by V. Sanz, S. Abel, J. Santiago, and A. Fraraggi (World Scientific, Singapore, 2004) p. 76, arXiv:hep-ph/0402017 [hep-ph].

[516] J. A. Casas, J. R. Espinosa, and I. Hidalgo, J. High Energy Phys. **0411**, 057 (2004), arXiv:hep-ph/0410298 [hep-ph].

[517] J. A. Casas, J. R. Espinosa, and I. Hidalgo, Nucl. Phys. **B777**, 226 (2007), arXiv:hep-ph/0607279 [hep-ph].

[518] R. Kitano and Y. Nomura, Phys. Lett. B **631**, 58 (2005), arXiv:hep-ph/0509039 [hep-ph].

[519] P. Athron and D. J. Miller, Phys. Rev. D **76**, 075010 (2007), arXiv:0705.2241 [hep-ph].

[520] P. Athron and D. J. Miller, in *Proceedings of the 15th International Conference on Supersymmetry and the Unification of Fundamental Interactions*, edited by W. de Boer and I. Gebauer (University of Karlsruhe, Karlsruhe, 2007) p. 554, arXiv:0710.2486 [hep-ph].

[521] H. Baer, V. Barger, P. Huang, D. Mickelson, A. Mustafayev, and X. Tata, Phys. Rev. **D87**, 115028 (2013), arXiv:1212.2655 [hep-ph].

[522] H. Baer, V. Barger, P. Huang, A. Mustafayev, and X. Tata, Phys. Rev. Lett. **109**, 161802 (2012), arXiv:1207.3343 [hep-ph].

[523] H. Baer, V. Barger, P. Huang, D. Mickelson, A. Mustafayev, and X. Tata, Phys. Rev. **D87**, 035017 (2013), arXiv:1210.3019 [hep-ph].

[524] B. de Carlos and J. A. Casas, Phys. Lett. B **309**, 320 (1993), arXiv:hep-ph/9303291 [hep-ph].

[525] B. de Carlos and J. A. Casas, in *16th International Warsaw Meeting on Elementary Particle Physics: New Physics at New Experiments, Kazimierz, 1993*, edited by Z. Ajduk, S. Pokorski, and A. K. Wroblewski (1993) pp. 340–343, arXiv:hep-ph/9310232 [hep-ph].

[526] P. H. Chankowski, J. R. Ellis, and S. Pokorski, Phys. Lett. B **423**, 327 (1998), arXiv:hep-ph/9712234 [hep-ph].

[527] K. Agashe and M. Graesser, Nucl. Phys. **B507**, 3 (1997), arXiv:hep-ph/9704206 [hep-ph].

[528] D. Wright, (1998), arXiv:hep-ph/9801449 [hep-ph].

[529] G. L. Kane and S. F. King, Phys. Lett. B **451**, 113 (1999), arXiv:hep-ph/9810374 [hep-ph].

[530] M. Bastero-Gil, G. L. Kane, and S. F. King, Phys. Lett. B **474**, 103 (2000), arXiv:hep-ph/9910506 [hep-ph].

[531] B. C. Allanach, J. P. J. Hetherington, M. A. Parker, and B. R. Webber, J. High Energy Phys. **0008**, 017 (2000), arXiv:hep-ph/0005186 [hep-ph].

[532] R. Dermíšek and J. F. Gunion, Phys. Rev. Lett. **95**, 041801 (2005), arXiv:hep-ph/0502105 [hep-ph].

[533] R. Barbieri and L. J. Hall, (2005), arXiv:hep-ph/0510243 [hep-ph].

[534] B. C. Allanach, Phys. Lett. B **635**, 123 (2006), arXiv:hep-ph/0601089 [hep-ph].

[535] B. Gripaios and S. M. West, Phys. Rev. D **74**, 075002 (2006), arXiv:hep-ph/0603229 [hep-ph].

[536] R. Dermíšek, J. F. Gunion, and B. McElrath, Phys. Rev. D **76**, 051105 (2007), arXiv:hep-ph/0612031 [hep-ph].

[537] R. Barbieri, L. J. Hall, and V. S. Rychkov, Phys. Rev. D **74**, 015007 (2006), arXiv:hep-ph/0603188 [hep-ph].

[538] T. Kobayashi, H. Terao, and A. Tsuchiya, Phys. Rev. D **74**, 015002 (2006), arXiv:hep-ph/0604091 [hep-ph].

[539] M. Perelstein and B. Shakya, Phys. Rev. D **88**, 075003 (2013), arXiv:1208.0833 [hep-ph].

[540] S. Antusch, L. Calibbi, V. Maurer, M. Monaco, and M. Spinrath, J. High Energy Phys. **1301**, 187 (2013), arXiv:1207.7236.

[541] T. Cheng, J. Li, T. Li, X. Wan, Y. k. Wang, *et al.*, (2012), arXiv:1207.6392 [hep-ph].

[542] M. W. Cahill-Rowley, J. L. Hewett, A. Ismail, and T. G. Rizzo, Phys. Rev. D **86**, 075015 (2012), arXiv:1206.5800 [hep-ph].

[543] G. G. Ross, K. Schmidt-Hoberg, and F. Staub, J. High Energy Phys. **1208**, 074 (2012), arXiv:1205.1509 [hep-ph].

[544] T. Basak and S. Mohanty, Phys. Rev. D **86**, 075031 (2012), arXiv:1204.6592 [hep-ph].

[545] Z. Kang, J. Li, and T. Li, J. High Energy Phys. **1211**, 024 (2012), arXiv:1201.5305 [hep-ph].

[546] C. Boehm, P. S. B. Dev, A. Mazumdar, and E. Pukartas, J. High Energy Phys. **1306**, 113 (2013), arXiv:1303.5386 [hep-ph].

[547] D. J. Miller and A. P. Morais, J. High Energy Phys. **1310**, 226 (2013), arXiv:1307.1373 [hep-ph].

[548] M. Y. Binjonaid and S. F. King, Phys. Rev. D **90**, 055020 (2014), arXiv:1403.2088 [hep-ph].

[549] D. J. Miller and A. P. Morais, J. High Energy Phys. **1412**, 132 (2014), arXiv:1408.3013 [hep-ph].

[550] S. Fichet, Phys. Rev. D **86**, 125029 (2012), arXiv:1204.4940 [hep-ph].

[551] B. C. Allanach, K. Cranmer, C. G. Lester, and A. M. Weber, J. High Energy Phys. **0708**, 023 (2007), arXiv:0705.0487 [hep-ph].

[552] M. E. Cabrera, J. A. Casas, and R. Ruiz de Austri, J. High Energy Phys. **0903**, 075 (2009), arXiv:0812.0536 [hep-ph].

[553] D. M. Ghilencea and G. G. Ross, Nucl. Phys. **B868**, 65 (2013), arXiv:1208.0837 [hep-ph].

[554] D. Kim, P. Athron, C. Balázs, B. Farmer, and E. Hutchison, Phys. Rev. D **90**, 055008 (2014), arXiv:1312.4150 [hep-ph].

[555] A. Fowlie, Phys. Rev. **D90**, 015010 (2014), arXiv:1403.3407 [hep-ph].

[556] A. Fowlie, Eur. Phys. J. **C74**, 3105 (2014), arXiv:1407.7534 [hep-ph].

[557] S. Cassel, D. M. Ghilencea, and G. G. Ross, Nucl. Phys. **B835**, 110 (2010), arXiv:1001.3884 [hep-ph].

[558] U. Ellwanger, G. Espitalier-Noel, and C. Hugonie, JHEP **09**, 105 (2011), arXiv:1107.2472 [hep-ph].

[559] M. D. Goodsell, K. Nickel, and F. Staub, Eur. Phys. J. **C75**, 32 (2015), arXiv:1411.0675 [hep-ph].

[560] M. Goodsell, K. Nickel, and F. Staub, Eur. Phys. J. **C75**, 290 (2015), arXiv:1503.03098 [hep-ph].

[561] U. Ellwanger and C. Hugonie, Eur. Phys. J. **C25**, 297 (2002), arXiv:hep-ph/9909260 [hep-ph].

[562] G. Aad *et al.* (ATLAS Collaboration), Phys. Rev. D **90**, 052005 (2014), arXiv:1405.4123 [hep-ex].

[563] S. Godfrey and T. Martin, in *Proceedings, Community Summer Study 2013: Snowmass on the Mississippi (CSS2013), Minneapolis, 2013*, edited by N. A. Graf, M. E. Peskin, and J. L. Rosner (2013) arXiv:1309.1688 [hep-ph].

[564] V. Khachatryan *et al.* (CMS), Eur. Phys. J. **C74**, 3036 (2014), arXiv:1405.7570 [hep-ex].

[565] G. Aad *et al.* (ATLAS), Phys. Rev. **D93**, 052002 (2016), arXiv:1509.07152 [hep-ex].

[566] CMS Collaboration, *Search for electroweak production of charginos and neutralinos in multilepton final states in pp collision data at* $\sqrt{s} = 13$ TeV, Tech. Rep. CMS-PAS-SUS-16-039 (CERN, Geneva, Switzerland, 2017).

[567] G. Aad *et al.* (ATLAS), JHEP **10**, 024 (2014), arXiv:1407.0600 [hep-ex].

[568] R. Barate *et al.* (LEP Working Group for Higgs boson searches, ALEPH Collaboration, DELPHI Collaboration, L3 Collaboration, OPAL Collaboration), Phys. Lett. B **565**, 61 (2003), arXiv:hep-ex/0306033 [hep-ex].

[569] S. Schael *et al.* (ALEPH Collaboration, DELPHI Collaboration, L3 Collaboration, OPAL Collaboration, LEP Working Group for Higgs Boson Searches), Eur. Phys. J. C **47**, 547 (2006), arXiv:hep-ex/0602042 [hep-ex].

[570] L. J. Dixon, J. A. Harvey, C. Vafa, and E. Witten, Nucl. Phys. **B261**, 678 (1985).

[571] J. D. Breit, B. A. Ovrut, and G. C. Segre, Phys. Lett. **B158**, 33 (1985).

[572] A. Sen, Phys. Rev. Lett. **55**, 33 (1985).

[573] H. Kawai, D. C. Lewellen, and S. H. H. Tye, Phys. Rev. Lett. **57**, 1832 (1986), [Erratum: Phys. Rev. Lett. **58**, 429 (1987)].

[574] L. J. Dixon, J. A. Harvey, C. Vafa, and E. Witten, Nucl. Phys. **B274**, 285 (1986).

[575] K. S. Narain, M. H. Sarmadi, and C. Vafa, Nucl. Phys. **B288**, 551 (1987).

[576] H. Kawai, D. C. Lewellen, and S. H. H. Tye, Nucl. Phys. **B288**, 1 (1987).

[577] I. Antoniadis, C. P. Bachas, and C. Kounnas, Nucl. Phys. **B289**, 87 (1987).

[578] B. A. Campbell, J. R. Ellis, and D. V. Nanopoulos, Phys. Lett. **B181**, 283 (1986).

[579] L. E. Ibáñez, J. E. Kim, H. P. Nilles, and F. Quevedo, Phys. Lett. **B191**, 282 (1987).

[580] Y. Kawamura, Prog. Theor. Phys. **105**, 999 (2001), arXiv:hep-ph/0012125 [hep-ph].

[581] G. Altarelli and F. Feruglio, Phys. Lett. **B511**, 257 (2001), arXiv:hep-ph/0102301 [hep-ph].

[582] L. J. Hall and Y. Nomura, Phys. Rev. **D64**, 055003 (2001), arXiv:hep-ph/0103125 [hep-ph].

[583] A. Hebecker and J. March-Russell, Nucl. Phys. **B613**, 3 (2001), arXiv:hep-ph/0106166 [hep-ph].

[584] T. Asaka, W. Buchmuller, and L. Covi, Phys. Lett. **B523**, 199 (2001), arXiv:hep-ph/0108021 [hep-ph].

[585] L. J. Hall, Y. Nomura, T. Okui, and D. Tucker-Smith, Phys. Rev. **D65**, 035008 (2002), arXiv:hep-ph/0108071 [hep-ph].

[586] J. M. Frere, R. B. Nevzorov, and M. I. Vysotsky, Phys. Lett. **B394**, 127 (1997), arXiv:hep-ph/9608266 [hep-ph].

[587] V. Khachatryan *et al.* (CMS), (2017), arXiv:1701.01954 [hep-ex].

[588] N. Arkani-Hamed, A. Delgado, and G. F. Giudice, Nucl. Phys. **B741**, 108 (2006), arXiv:hep-ph/0601041 [hep-ph].

[589] M. Drees and M. M. Nojiri, Phys. Rev. **D47**, 376 (1993), arXiv:hep-ph/9207234 [hep-ph].

[590] L. Roszkowski, R. Ruiz de Austri, and T. Nihei, JHEP **08**, 024 (2001), arXiv:hep-ph/0106334 [hep-ph].

[591] A. Djouadi, M. Drees, and J.-L. Kneur, Phys. Lett. **B624**, 60 (2005), arXiv:hep-ph/0504090 [hep-ph].

[592] G. Steigman, Ann. Rev. Nucl. Part. Sci. **29**, 313 (1979).

[593] R. J. Scherrer and M. S. Turner, Phys. Rev. **D33**, 1585 (1986), [Erratum: Phys. Rev. **D34**, 3263 (1986)].

[594] E. W. Kolb and M. S. Turner, Front. Phys. **69**, 1 (1990).

[595] T. K. Gaisser, G. Steigman, and S. Tilav, Phys. Rev. **D34**, 2206 (1986).

[596] K. Griest and D. Seckel, Nucl. Phys. **B283**, 681 (1987), [Erratum: Nucl. Phys. **B296**, 1034 (1988)].

[597] B. W. Lee and S. Weinberg, Phys. Rev. Lett. **39**, 165 (1977).

[598] P. Binetruy, G. Girardi, and P. Salati, Nucl. Phys. **B237**, 285 (1984).

[599] M. Srednicki, R. Watkins, and K. A. Olive, Nucl. Phys. **B310**, 693 (1988).

[600] K. Griest and D. Seckel, Phys. Rev. **D43**, 3191 (1991).

[601] P. Gondolo and G. Gelmini, Nucl. Phys. **B360**, 145 (1991).

[602] M. W. Goodman and E. Witten, Phys. Rev. **D31**, 3059 (1985).

[603] J. D. Lewin and P. F. Smith, Astropart. Phys. **6**, 87 (1996).

[604] K. Freese, M. Lisanti, and C. Savage, Rev. Mod. Phys. **85**, 1561 (2013), arXiv:1209.3339 [astro-ph.CO].

[605] G. Duda, A. Kemper, and P. Gondolo, JCAP **0704**, 012 (2007), arXiv:hep-ph/0608035 [hep-ph].

[606] D. S. Akerib *et al.* (LUX), Phys. Rev. Lett. **116**, 161302 (2016), arXiv:1602.03489 [hep-ex].

[607] M. G. Aartsen *et al.* (IceCube), JCAP **1604**, 022 (2016), arXiv:1601.00653 [hep-ph].

[608] C. E. Yaguna, Phys. Rev. **D95**, 055015 (2017), arXiv:1610.08683 [hep-ph].

[609] A. Crivellin, M. Hoferichter, M. Procura, and L. C. Tunstall, JHEP **07**, 129 (2015), arXiv:1503.03478 [hep-ph].

[610] K. Griest, Phys. Rev. Lett. **61**, 666 (1988).

[611] A. W. Thomas, P. E. Shanahan, and R. D. Young, Nuovo Cim. **C035N04**, 3 (2012), arXiv:1202.6407 [nucl-th].

[612] J. M. Alarcon, J. Martin Camalich, and J. A. Oller, Phys. Rev. **D85**, 051503 (2012), arXiv:1110.3797 [hep-ph].

[613] J. M. Alarcon, L. S. Geng, J. Martin Camalich, and J. A. Oller, Phys. Lett. **B730**, 342 (2014), arXiv:1209.2870 [hep-ph].

[614] J. I. Read, J. Phys. **G41**, 063101 (2014), arXiv:1404.1938 [astro-ph.GA].

[615] M. Benito, N. Bernal, N. Bozorgnia, F. Calore, and F. Iocco, JCAP **1702**, 007 (2017), arXiv:1612.02010 [hep-ph].

[616] A. M. Green, (2017), arXiv:1703.10102 [astro-ph.CO].

[617] G. Degrassi and P. Slavich, Nucl. Phys. **B825**, 119 (2010), arXiv:0907.4682 [hep-ph].

[618] G. Degrassi, P. Slavich, and F. Zwirner, Nucl. Phys. **B611**, 403 (2001), arXiv:hep-ph/0105096 [hep-ph].

[619] A. Brignole, G. Degrassi, P. Slavich, and F. Zwirner, Nucl. Phys. **B631**, 195 (2002), arXiv:hep-ph/0112177 [hep-ph].

[620] A. Dedes and P. Slavich, Nucl. Phys. **B657**, 333 (2003), arXiv:hep-ph/0212132 [hep-ph].

[621] A. Brignole, G. Degrassi, P. Slavich, and F. Zwirner, Nucl. Phys. **B643**, 79 (2002), arXiv:hep-ph/0206101 [hep-ph].

[622] A. Dedes, G. Degrassi, and P. Slavich, Nucl. Phys. **B672**, 144 (2003), arXiv:hep-ph/0305127 [hep-ph].

[623] P. Athron, J.-h. Park, T. Steudtner, D. Stöckinger, and A. Voigt, JHEP **01**, 079 (2017), arXiv:1609.00371 [hep-ph].

[624] J. P. Vega and G. Villadoro, JHEP **07**, 159 (2015), arXiv:1504.05200 [hep-ph].

[625] M. Drees, H. Dreiner, D. Schmeier, J. Tattersall, and J. S. Kim, Comput. Phys. Commun. **187**, 227 (2015), arXiv:1312.2591 [hep-ph].

[626] E. Conte, B. Fuks, and G. Serret, Comput. Phys. Commun. **184**, 222 (2013), arXiv:1206.1599 [hep-ph].

[627] S. Kraml, S. Kulkarni, U. Laa, A. Lessa, W. Magerl, D. Proschofsky-Spindler, and W. Waltenberger, Eur. Phys. J. **C74**, 2868 (2014), arXiv:1312.4175 [hep-ph].

[628] M. Papucci, K. Sakurai, A. Weiler, and L. Zeune, Eur. Phys. J. **C74**, 3163 (2014), arXiv:1402.0492 [hep-ph].

[629] J. Edsjö and P. Gondolo, Phys. Rev. **D56**, 1879 (1997), arXiv:hep-ph/9704361 [hep-ph].

[630] G. Aad *et al.* (ATLAS), Phys. Rev. **D94**, 032003 (2016), arXiv:1605.09318 [hep-ex].

[631] M. Aaboud *et al.* (ATLAS), Eur. Phys. J. **C76**, 683 (2016), arXiv:1607.05979 [hep-ex].

[632] V. Khachatryan *et al.* (CMS), Submitted to: Eur. Phys. J. C (2016), arXiv:1611.00338 [hep-ex].

[633] A. M. Sirunyan *et al.* (CMS), (2017), arXiv:1704.07781 [hep-ex].

[634] ATLAS collaboration, ATL-PHYS-PUB **010** (2014).

[635] C. Cheung, L. J. Hall, D. Pinner, and J. T. Ruderman, JHEP **05**, 100 (2013), arXiv:1211.4873 [hep-ph].

[636] L. Roszkowski, E. M. Sessolo, and A. J. Williams, JHEP **08**, 067 (2014), arXiv:1405.4289 [hep-ph].

[637] E. A. Bagnaschi *et al.*, Eur. Phys. J. **C75**, 500 (2015), arXiv:1508.01173 [hep-ph].

[638] F. Rühr (ATLAS), in *Proceedings of the 37th International Conference on High Energy Physics (ICHEP 2014), Valencia, 2014*, edited by M. Aguilar-Benítez, J. Fuster, S. Martí-García, and A. Santamaría (2016) pp. 625–630.

[639] H. Baer, V. Barger, A. Lessa, and X. Tata, Phys. Rev. **D86**, 117701 (2012), arXiv:1207.4846 [hep-ph].

[640] M. E. Cabrera, J. A. Casas, A. Delgado, S. Robles, and R. Ruiz de Austri, JHEP **08**, 058 (2016), arXiv:1604.02102 [hep-ph].

[641] H. Baer, V. Barger, and H. Serce, (2016), arXiv:1609.06735 [hep-ph].

[642] E. Aprile *et al.* (XENON), JCAP **1604**, 027 (2016), arXiv:1512.07501 [physics.ins-det].

[643] K. Kowalska, L. Roszkowski, E. M. Sessolo, S. Trojanowski, and A. J. Williams, in *Proceedings, 50th Rencontres de Moriond, QCD and High Energy Interactions: La Thuile, 2015*, edited by E. Augé, J. Dumarchez, and J. Trân Thanh Vân (2015) pp. 195–198, arXiv:1507.07446 [hep-ph].

[644] B. J. Mount *et al.*, (2017), arXiv:1703.09144 [physics.ins-det].

[645] M. F. Sohnius, Phys. Rept. **128**, 39 (1985).

[646] H. K. Dreiner, H. E. Haber, and S. P. Martin, Phys. Rept. **494**, 1 (2010), arXiv:0812.1594 [hep-ph].

[647] A. Salam and J. A. Strathdee, Fortsch. Phys. **26**, 57 (1978).

[648] M. Drees, in *Current Topics in Physics. Proceedings, Inauguration Conference of the Asia-Pacific Center for Theoretical Physics (APCTP), Seoul, 1996, Vol. 1, 2*, edited by Y. M. Cho, J. B. Hong, and C. N. Yang (World Scientific, Singapore, 1998) arXiv:hep-ph/9611409 [hep-ph].

[649] A. Salam and J. A. Strathdee, Phys. Rev. **D11**, 1521 (1975).

[650] J. Wess and B. Zumino, Nucl. Phys. **B78**, 1 (1974).

[651] F. A. Berezin, *The method of second quantization* (New York Academic Press, 1966).

[652] S. Ferrara, J. Wess, and B. Zumino, Phys. Lett. **51B**, 239 (1974).

[653] A. Salam and J. A. Strathdee, Phys. Lett. **B51**, 353 (1974).

[654] S. Ferrara and B. Zumino, Nucl. Phys. **B79**, 413 (1974).